UNIVERSITY OF TRENTO

International PhD Program in Biomolecular Sciences

Department of Cellular, Computational and Integrative Biology – CIBIO

34th Cycle

"Achieving health promoting gut microbiome modulation through sustainable, nutritious and healthy foods"

Tutor:

Nicola SEGATA

University of Trento

Advisor

Francesca FAVA

Fondazione Edmund Mach

Ph.D. Thesis of

Giulia GAUDIOSO

University of Trento – Fondazione Edmund Mach

Academic Year 2020-2021

Declarations

I, Giulia Gaudioso, confirm that this is my own work and the use of all material from other sources has been properly and fully acknowledged.

The research work for this PhD thesis was carried out at and funded with support from Fondazione Edmund Mach.

Giulia Gaudioso

Table of contents

Abstract

The global pandemic of diet-related non-communicable diseases and the fact that global food production represents one of the largest contributors to greenhouse gas emissions, have identified unhealthy and unsustainably food chains as a major societal health challenge and a risk to ecosystem stability. This thesis aimed to investigate if digestion of nutritious, less highly processed foods could lead to health-promoting changes in the gut microbiota. Our modern Western-style diet (MWD) is characterized by high intake of extremely processed foods, which contain significant concentrations of inflammatory advanced glycation end-products (AGE) implicated in metabolic disease development. Novel observations in this thesis showed that chronic exposure to dietary AGE modulated gut microbiota (GM) community structure rendering it more similar to the GM previously observed in diabetic/obese mice. Further, I demonstrated that elevated systemic inflammatory markers could be mediated by AGE induced changes in GM composition. Measuring the potential of whole plant foods to improve gut health, a local broccoli ecotype (Broccolo of Torbole, BR) and *Moringa oleifera* were investigated using *in vitro* models of the human GM and intestinal epithelium. BR significantly reduced bacterial richness and evenness, increased *Escherichia-Shigella* relative abundance and decreased *Alistipes* and *Ruminococcus 1*. The GM extensively metabolized BR polyphenols and increased concentrations of short chain fatty acids. However, BR did not impact on intestinal permeability, using a Caco-2 monolayer model and trans-epithelial electrical resistance (TEER). This thesis provided novel insights on the fate of Moringa glucosinolates and polyphenols during faecal fermentation and on their potential beneficial activity on gut health, with glucomoringin significantly increasing TEER. Microbial communities are also involved in healthy and sustainable food production. Characterizing the successional development of local organic sauerkraut production, this thesis established a culture collection of sauerkraut lactic acid bacteria of potential future biotechnological evaluation and measured metabolite production during sauerkraut fermentation. Sauerkraut water improved immune response of a Caco-2-peripheral blood mononuclear cell (PBMC) *in vitro* model of the gut associated immune system upon inflammatory LPS challenge. Finally, since sustainable diets rely on sustainable and nutritious foods, I analyzed the role of the GM in improving the sustainability of farmed trout. Novel sustainable feeds containing poultry by-products (P) or insect protein (*Hermetia illucens* (H) meal), were investigated for their potential impact on fish growth performance, GM composition and inflammatory biomarkers. P increased the relative abundance of protein-degraders *Paeniclostridium*

and Bacteroidales, while H increased chitin-degraders *Actinomyces* and *Bacillus*. This study also provided evidence of feed-chain microbiome transmission of *Actinomyces* from insect H feed to trout GM. The analysis of gut microbiomes therefore represents an innovative strategy to define healthy reference diets, to characterize the potential health effects of local and traditionally produced foods, to identify new sustainable and nutritious crops, and to drive the urgently needed transformation of the global food system. In order to obtain more sustainable, healthy and nutritious food production systems a better understanding and management of microbiomes along the food chain has never been more important.

Chapter 1: Introduction

Giulia Gaudioso[1,2],

[1] Nutrition and Nutrigenomics Unit, Department of Food Quality and Nutrition, Research and Innovation Center, Fondazione Edmund Mach, 38098 Trento, Italy

[2] CIBIO – Department of Cellular, Computational and Integrative Biology, University of Trento, 38123 Trento, Italy

1. Diet, sustainability and health: starting from the EAT Lancet guidelines

In 2019, EAT-Lancet Commission defined the concept of a healthy diet and sustainable food systems (1). With more than 800 million people with currently insufficient food, 39% of adults being overweight or obese, 30% of food being wasted and pressing environmental challenges (2,3), sustainability and health concepts must be considered together. Global food production constitutes one of the largest environmental footprints caused by humans on the planet. Agriculture accounts for the 70% of global freshwater withdrawals (4), for 78% of ocean and freshwater eutrophication (5) and for using half the world's habitable land (4). Moreover, data from agricultural activity, food processing, packaging and retail revealed that food accounts for 26% of global greenhouse gas emissions (5). For these reasons, a sustainable diet cannot be separated from sustainable food production. Sustainable food production consists mainly in providing solutions to contain chemical pollution, reducing greenhouse gas emissions, freshwater use and over-exploitation of food sources.

As will be discussed later in detail, diet has a crucial role in determining human health. A nutritious and well balanced diet contains all the necessary elements for maintaining homeostasis, including substrates for energy production, essential amino acids, fatty acids, minerals and vitamins (1). Although healthy dietary guidelines have been known for several years and research is ongoing to further support healthy dietary models, such as the Mediterranean diet, global malnutrition persists, accounting for all people not receiving proper nutrition as a consequence of a lack or an excess of nutrients and energy (6). Alongside undernutrition, over-nutrition represents half of this so-called 'double burden of malnutrition', referring to chronic food intake in excess of dietary energy requirements, thus leading to overweight and/or obesity (6). Several studies reported a reduction in life expectancy associated to obesity, resulting from the wide spectrum of related-comorbidities, including diabetes, metabolic syndrome and cardiovascular disease (CVD) (7). Data resulting from the Framingham Heart observational cohort study suggested that obesity increases the risk of heart

failure (HF) (8). Framingham investigators analyzed 5881 participants during 14 years of follow-up, collecting data from physical examination (including anthropometric measurements and blood pressure data), from electrocardiogram and from questionnaires assessing risk factors for cardiovascular disease. A panel of physicians reviewed suspected cardiovascular events by examining hospital records, determining that obese subjects had double the risk of HF when compared with subjects with normal body-mass index (BMI 18.5-25 kg/m^2). The excess of body fat mass plays a central role in determining obesity-induced HF. In particular, visceral fat mass can stimulate production of pro-inflammatory cytokines (i.e. adipocytokines), thus driving chronic low-grade systemic inflammation observed in obese subjects (9). High levels of adipocytokines and the resulting chronic low-grade systemic inflammation have been associated with increased risk of developing insulin resistance and type 2 diabetes (T2DM), thus connecting obesity and T2DM. Boden and colleagues (2015) (10) observed that oxidative stress caused by over-nutrition results in the inactivation of the insulin-facilitated glucose transporter GLUT4, thus leading to insulin resistance which is a major cause of T2DM. On the other hand, weight loss usually improves these disorders. The Swedish Obese Subjects (SOS) prospective intervention study provided information about the effects of bariatric surgery on the incidence of obesity-related diseases. 2010 obese subjects underwent bariatric surgery were compared to 2037 obese control subjects. After 20 years of follow-up, bariatric surgery was associated with a long-term reduction in overall mortality and decreased incidences of diabetes, cardiovascular diseases and cancer, further confirming the role of weight in triggering obesity-related pathologies (11–15). Obesity itself, and these obesity associated diseases have chronic low-grade systemic inflammation as a defining characteristic, which in turn increases the risk of certain cancers (16). Considering direct and indirect factors, the burden of obesity and related diseases has a number of socio-economic implications and therefore represents one of the largest global public health challenges. A cohort study from Hiilamo and colleagues (2017) (17) observed a significant association between obesity and poverty, low household net income and low personal income in 5400 subjects of the Helsinki Health Study cohort. These socioeconomic disadvantages persisted during 12 years of follow-up. Previous studies reported higher healthcare costs due to treatment of obesity and comorbidities (18–20). In 2003, annual U.S. obesity-attributable medical expenditure were estimated at $75 billion dollars, with one-half of these expenditures being financed by Medicare and Medicaid services (20). Dick and colleagues (2021) (18) employed a Mendelian Randomization to estimate the impact of obesity on annual inpatient healthcare costs in the UK. Linking data from the UK Biobank and Hospital Episode Statistics (HES), the authors

predicted that obese subjects incurred from £201.58 to £205.53 greater costs than non-obese. Recently, Czernichow and colleagues (2020) (21) also revealed higher total costs of secondary care of COVID-19 associated with overweight and obesity in Europe. The authors applied a healthcare cost model screening pertinent and peer-reviewed papers published from January to June 2020. The excess costs were determined by higher probability of being hospitalized due to COVID-19, prolonged stay in the hospital and higher risk of severe outcomes. Risk of hospitalization was 1.88-2.77 times higher for people with BMI ≥ 40 when compared to normal weight people (BMI < 25).

The prevalence of obesity in elderly subjects is growing dramatically. The National Health and Nutrition Examination Surveys reported that obesity rates in adults aged ≥ 60 years reached 37.5% in males and 39.4% in females (22). Peralta and colleagues (2018) analyzed data from the Survey of Health, Ageing and Retirement in Europe, reporting that obesity prevalence increased in European subjects aged 60-79 years between 2005 and 2013 (23). Obese older adults are more likely to have a decreased quality of life, since the association between obesity and co-morbidities and mortality risk increases with age (24). On the other hand, lines of evidence from different studies predicted that obesity itself may accelerate the ageing process, because of the onset of metabolic imbalances and inflammation characterizing obese subjects (25). A significant correlation has been observed between higher BMI and ageing of human liver when considering epigenetic biomarker of ageing (26) and data from the Fels Longitudinal Study showed that high total and abdominal adiposity are directly related to decreased telomere length, reinforcing the idea that obesity may accelerate the ageing process (27).

A healthy and balanced diet is the first target to prevent obesity and related diseases, promoting healthy aging and improving health span. Considering the socio-economic impact of obesity epidemic, together with a rapidly aging population (28), a sustainable food production system cannot be separated from a nutritious food system.

One innovative approach to achieve all-round agri-food sustainability could be the modulation of environmental microbiomes along the food chain. The term 'microbiome' refers to all microbial communities and their genomes, including Bacteria, Archaea, viruses and some Eukarya (29). Microbial communities colonize the disparate habitats, from water sources, soil, food and several of human body surfaces (i.e. gastrointestinal and urinary tracts, skin, mouth and airways). Microbes are also implicated in food transformation, being involved in foods and beverages fermentation processes, and thus becoming a very promising tool in the food industries because they are a natural way of flavor enhancer and preservation (30). Moreover, microorganisms play a key role in food

spoilage, defined as the food deterioration process that 'renders a product unacceptable or undesirable for consumption' deriving from the 'biochemical activity of microbial populations that predominate the product' (31). The composition of these core ecosystems occupies a central role in determining food safety, final product quality and, in the case of mutualistic relationship with their host, in modulating health and bodily functions (32).

Changing our dietary habits and food wasting by retailers, providers and consumers, reaching a healthy and sustainable diet, is one of the biggest challenges, but still the only possibility to ensure a secure future for next generations. In line with this, the present introduction aim to discuss the existing relationship between diet, microbes along the food chain and human health, describing how sustainable, health-promoting and nutritious diets could be obtained through food chain microbiome modulation, with special attention to animal and human gastrointestinal microbiomes.

2. Diet

2.1 Healthy dietary guidelines: what is a healthy diet?

A healthy diet could be defined as a diet rich in fruit and vegetables, whole grains, legumes, unsaturated oils, with low levels of red meat, simple sugars, saturated fats, alcoholic beverages and highly processed food (33). Also, a healthy diet is related to lower incidence of metabolic and inflammatory diseases, with a protective role against obesity, diabetes, cardiovascular diseases and some types of cancer (1).

Early evidence for healthy dietary patterns derived from the 'Seven Countries Study', conducted in Finland, Holland, Italy, Greece, United States, Japan and Yugoslavia by the American scientist Ancel Keys, who decided to study the relationship between diet, lifestyle and cardiovascular disease between different populations over an extended period of time (34). This investigation proved that populations with high dietary intake of vegetables, herbs, olive oil and bread compared to a rather moderate use of meat presented a reduced or lower incidence of coronary heart disease (35). The Seven Country Studies was the pioneer in demonstrating correlation between heart diseases and traditional eating patterns including the Mediterranean diet (MD). This longitudinal study enrolled a total of 12,763 middle aged men (40-59 years old) divided in 16 cohorts from seven countries. Statistical analysis of the food records of the dietary surveys from the 1960s showed that dietary patterns in the Mediterranean basin were associated with lower incidence and mortality from coronary heart disease and lower all-cause mortality. In particular, low dietary saturated and trans

fatty acids and dietary cholesterol, typical of MD, were significant determinants of lower coronary heart disease death rates (36).

MD is one of the healthiest dietary patterns, originally followed by poor rural societies around the Mediterranean basin (37). Foods typically consumed in the Mediterranean area were first described in the 1950s by Keys, who defined MD as a diet rich in fresh vegetables and legumes, low in meat and sweets (38). To date, other details have been integrated to MD definition, in particular the high content of fats and proteins deriving from vegetable sources (such as extra virgin olive oil and nuts); dairy products, fish and poultry consumed in low to moderate amount and the low content of sweets (38–40). Traditional MD is therefore characterized by a reduced consumption of animal fats and cholesterol and a high intake of fresh foods rich in fiber, antioxidants and unsaturated fats, including the long-chain omega-3 polyunsaturated fatty acids from fish (41). Traditional MD was further described and delineated in 1995 by Willett and colleagues (40), who introduced the Mediterranean diet pyramid. This simplified representation graphically divided foods according to their recommended frequency of consumption. During the same year, Trichopoulos and colleagues introduced a score to evaluate MD adherence, thus facilitating the evaluation of epidemiological associations between MD consumption and healthy outcomes (42). Several large scale cohort observational studies demonstrated the association between daily adherence to MD and preventive effects on obesity, diabetes, CVD and cancer (34,39,43,44). Moreover, high Mediterranean Adequacy Index (MAI), a score developed in 2004 to assess how close a diet is to the Healthy Reference National Mediterranean Diet (HRNMD) was inversely correlated with 50-year coronary heart disease mortality rates (45). The Nurses' health study also contributed significantly to current healthy eating guidelines around the world. This prospective follow-up study was initially designed by Dr. Frank Speizer in 1976 to examine relations between contraception and breast cancer. 121,700 nurses aged 30 to 55 in 1976 were enrolled for the study and follow-up questionnaires about diseases and health-related topics were collected every two years (46). Since investigators recognized the key role of diet in determining chronic diseases' development, food-frequency questionnaires were also introduced in 1980 for all participants. From 1982, blood, urine and saliva samples were collected to further explore the relationship between diverse biological markers and disease risk. Nurses' Health Study II (NHS II) and NHS III were created respectively in 1989 and 2010, expanding data collection in terms of biological samples and questionnaires, thus generating a large volume of highly relevant and multidimensional data about lifestyle, nutrition and human health relationship. In particular, many correlations were observed

between diet and risk for certain diseases. Data from 76,690 women from NHS and 93,295 from NHS II showed that adherence to a plant-based diet may reduce the risk of breast cancer (47). Moreover, trans fatty acids intake was significantly associated with higher risks of coronary heart disease when analyzing dietary data from 85,095 women enrolled in the NHS (48).

Observational studies involving large cohorts constitute a powerful tool to examine the effects of dietary choices in the long-term. However, the strongest scientific support for the health effects of MD comes from dietary interventions designed to provide cause and effect evidence of long term intake of MD and reduced risk of chronic diseases.

The preventive effects of MD on diabetes and CVD risk were reported by the PREDIMED (Prevención con Dieta Mediterránea) multicenter trial (39). This dietary intervention explored the efficacy of two Mediterranean diets supplemented with nuts or extra virgin olive oil over a control diet, in a cohort of nondiabetic subjects with heart risk factors. Both MD significantly reduced the rates of death from stroke by 28% and the risk of type 2 diabetes by 52% (39), without any caloric restriction. The 18-month Dietary Intervention Randomized Controlled Trial Polyphenols Unprocessed (DIRECT PLUS) randomized clinical trial evaluated the effects of MD enriched in green polyphenols from Mankai (a *Wolffia globosa* aquatic plant strain), green tea and walnuts on non-alcoholic fatty liver disease (NAFLD) (49) and cardiometabolic risk (50). Investigators assigned 294 participants with abdominal obesity or dyslipidaemia into healthy dietary guidelines (HDG), MD and green-MD groups, all accompanied by physical activity. Within 6 months of intervention, the green-MD resulted in significant decrease of low-density lipoprotein cholesterol and diastolic blood pressure, thus reducing cardiovascular risk (50). After 18 months of dietary induction, NAFLD prevalence declined in all experimental groups and especially in the green-MD group. Moreover, both MD groups showed moderate weight-loss, with almost double intrahepatic fat (IHF) % loss in green-MD as compared with MD and HDG (49). IHF% reduction was also associated with beneficial changes in cardiometabolic and inflammatory parameters, thus supporting existing evidences on the positive association between MD and cardiometabolic health. Moreover, this study introduced new healthy outcomes associated with Mediterranean dietary pattern (and in particular MD further enriched with green polyphenols) when compared with other healthy nutritional strategies, thus suggesting MD as an effective nutritional tool for the treatment of NAFLD.

These results on the protective role of MD have been further explored by Li and collaborators (2020) (51), who combined metabolomics workflow and statistical modeling analysis. The authors pooled data from PREDIMED trial, US Nurses' Health Studies Land II and Health Professionals

Follow-up Study (NHS/HPFS) (presented at the end of this section) to investigate whether a distinctive metabolic signature exists for MD adherence and whether this signature could be associated with CVD risk. The authors identified a panel of 67 metabolites most significantly associated with MD adherence, according to Mediterranean Diet Adherence Score (MEDAS). This signature was primarily composed of metabolites involved in polyunsaturated fatty acid or lipid metabolic pathways, thus reflecting the high intake of unsaturated fats, typical of MD. All these findings emphasized the role of healthy unsaturated fats in determining the protective role of MD against inflammatory diseases, even partially.

In 2019, the EAT Lancet Commission defined the MD as an example of reference diet, based on health considerations (1). Due to the low intake of red meat, high intake of vegetables and healthy fats, MD should be considered as template for a universal healthy reference diet, able to ensure both human health and environmental sustainability.

Traditional MD is now progressively eroding because of a change in eating habits, which have become increasingly closer to a modern Western-style diet, which will be discussed in detail in section 2.2. For this reason, a new revised MD and food lifestyle pyramid have been proposed by scientific experts of the Mediterranean Diet Foundation's International Scientific Committee and from members that met in 2009 during the III CIISCAM Conference 'The Mediterranean Diet today, a model of sustainable diet' in Parma, Italy. The new revised MD was conceived to be adapted to contemporary lifestyles, also taking into account the environmental sustainability. Revised MD dietary choices not only include specific set of foods, but represent a cultural and socio-economic model focused on the whole food chain. Since MD is traditionally a plant-centered diet, founded on the reduction of animal products consumption, this implies a lower demand for environmental resources and a lower overall impact on the ecosystem when compared to current Western dietary patterns (52–54). Based on existing evidence supporting the MD contribution to human health and general well-being, together with environmental sustainability, the updated MD pyramid summarizes key dietary guidelines for a healthy diet and may allow a higher compliance among the population.

2.2 Modern Western style diet

Economic progress and history shaped our dietary habits over centuries. Cooking trends changed over the ages and shifts in dietary pattern are still moving quickly, being manipulated by industrialization and globalization. This shift, otherwise called 'nutrition transition' (55), has been characterized by changes in nutritional intake associated with economic development and

agricultural transformation in the 18th ,19th and above all, the 20th centuries. The 'nutrition transition' process refers to a decrease in fresh and plant-based food consumption towards ultra-processed, hypercaloric diets, high in sugar, saturated and modified fats, and red meat (56). The resultant modern Western style diet (MWD) is a model of diet (57) characterized by an overavailability of food, high sugar and saturated fats intakes, as well as high intakes of red meat, refined grains and salt, with minimal intake of fruit, vegetables, fish and legumes (58,59). The MWD is displacing dietary patterns based on meals prepared using unprocessed ingredients by those that are based on high- and ultra-processed food (60). Food processing was originally developed to make foods safe, storable and transportable through cooking, smoking or fermentation techniques (61). In the 20th century, food processing evolved, starting to include new operations and technologies aimed to increase palatability and production of products marketed to satisfy the consumer's desires (61). A global classification system known as NOVA has been created in Brazil by the Centre for Epidemiological Studies in Health and Nutrition at the School of Public Health, University of São Paulo in order to classify foods based on the degree of processing (62). Currently, foods and products are classified in four main groups, according to their nature and purpose of industrial food processing. Group 1 include unprocessed or minimally processed foods, such as dried fruits and legumes, frozen meats and seafood and mineral water. Group 2 is of processed culinary ingredients (i.e. plant oils, starches and flours, uncooked pastas and salt). Group 3 and 4 are of ready-to-consume products including respectively processed food and what NOVA terms ultra-processed products (UPFs) (i.e. chips, snacks, breakfast cereals and many other pre-prepared dishes) (62). Unlike minimal processed food, UPFs are designed to be ready-to-eat, and specifically for a consumer who may not have the time to devote to home-food preparation. Based on the description provided by Martínez Steele and colleagues (2016) (63), UPFs typically include hydrolyzed protein, modified starches, hydrogenated oils and additives, whose purpose is to improve the sensorial qualities of the final product. Processed foods consumption increased worldwide because of their low cost and the aggressive marketing by large food companies (64,65). In 2016, Martínez Steele and colleagues (63) analyzed dietary data (i.e. 24 h recalls interviews) from the 2009-2010 NHANES (National Health and Nutrition Examination Survey), a continuous, nationally representative, cross-sectional survey of the civilian US residents in order to study the contribution of UPFs to the national diet. Surveys from 9317 participants revealed that UPFs comprised 57.9% of energy intake and contributed 89.7% of the energy intake from added sugars in

the USA. Because of this sharp rise in consumption, their effects on human health must be urgently devised.

Research done on high- and ultra-processed food over the last few years has shown an alarming correlation between overconsumption in modern Western dietary pattern (WDP), metabolic diseases risk (66) and all-cause mortality (67,68). A recent human randomized study of Hall and collaborators (2019) (69) suggested the role of UPFs in determining obesity and related diseases. The authors selected 20 weight-stable adults to receive an unprocessed diet and an ultra-processed diet for 2 weeks each, in a random order. Despite the two diets being isocaloric, participants gained or lost weight during the ultra-processed or unprocessed diet, respectively. Similar conclusions were drawn by Rauber and collaborators (2020) (70) who analyzed data from the National Diet and Nutrition Survey Rolling Programme (NDSD), a 8-year continuous cross-sectional survey of dietary habits and nutrient intakes in the UK. The highest consumption of UPFs was associated with higher Body Mass Index (BMI) and waist circumference in both males and females participants. These results stress the importance of limiting or avoiding consumption of UPFs, whatever dietary habits are followed.

In addition to the effects of excessive UPFs consumption, many studies revealed the association between macronutrients imbalance typical of modern WDP and increased risk of chronic diseases. High consumption of refined sugar, and especially of fructose corn syrup, are key factors promoting insulin resistance and hyperinsulinemia. Feeding studies in rats showed that fructose supplementation to regular chow caused fatty liver and impaired insulin signaling in liver, white adipose tissue and skeletal muscle (71). Similar results were previously reported by Stanhope and colleagues (2009), who reported that consumption of 25% of daily energy requirement from fructose-sweetened (but not glucose-sweetened) beverages for 10 weeks impaired insulin metabolism and promoted dyslipidemia in 17 obese and overweight subjects (72). Moreover, evidence from a cohort study involving 188 symptomatic stable patients with coronary artery disease (CAD), demonstrated that WDP is positively associated with the severity of CAD lesions (73). These findings highlight the role of unhealthy dietary patterns and in particular of a modern WDP in determining chronic diseases both in animal models and in humans.

Harmful effects of modern Western style diet also spill over into environmental sustainability. Due to its massive consumption of high- and ultra-processed foods and animal products, WDP is usually associated with intensive land-use and livestock, as well as water and energy consumption and higher greenhouse gas (GHG) emissions when compared to the Mediterranean diet (53,74).

Sáez-Almendros and colleagues (2013) (53) analyzed the sustainability of WDP, exemplified using FAOSTAT database in 2008, compared to the Spanish dietary pattern and to the new MD, estimated from the FAO food balance sheets for 2007. A progressive shift of the Spanish population towards WDP would increase GHG emissions, agricultural land use, energy and water consumption of between 12% and 72% when compared to the MD. Unfortunately, due to speed at which ultra-processed foods have become mainstream in recent decades, there is still a lack of in-depth data on their environmental impact in the long term. Moreover, assessing their links with alteration of food system sustainability could be tricky, because of the variety and complexity of factors involved. However, these first evidences solicit the importance to move on from dietary choices which only consider nutrients and health to one taking into account environmental footprint.

3. Food chain microbiomes

Besides the clear link between gut microbiome and human health, microbiomes have a crucial role in maintaining life on Earth and are indispensable for several food production processes. Soil microbiome is essential to provide essential nutrients to plants or animals (75), marine microbiome has a critical role in oxygen production, nutrient cycling and organic matter degradation (76,77) and microbiomes are also essential for biogeochemical cycles (77).

Figure 1. A schematic representation of the food chain microbiome, connecting human, animals and environmental health with production and waste valorization.

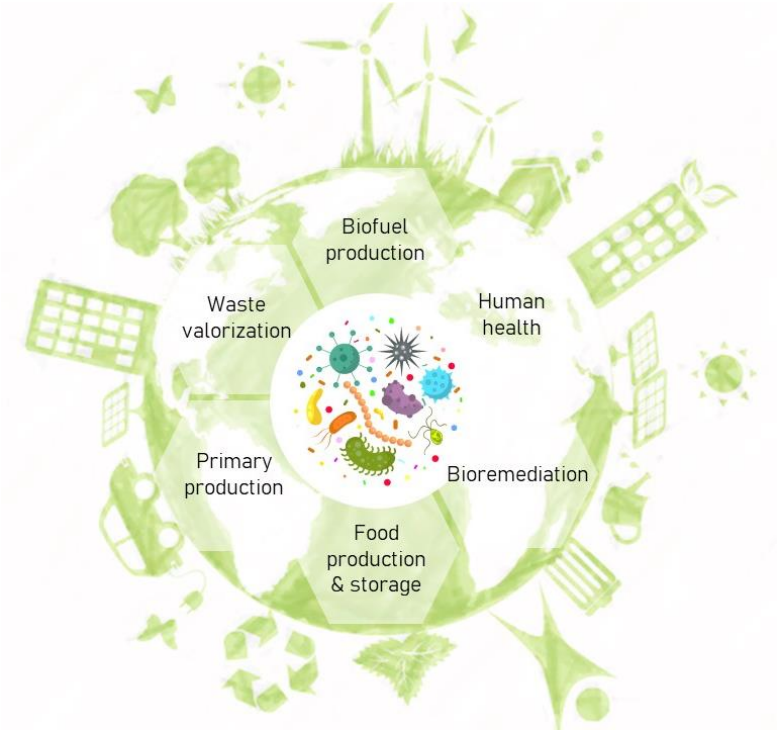

The interconnection between different microbiomes in the environment and in particular in the food system suggests the great potential of the microbiota to improve food production, nutrition security, health, waste management and overall sustainability of the agri-food production system (**Figure 1**).

Microbiomes can be exploited to valorize waste material, in order to produce biogas, biofuels (methane, CH_4) or useful chemicals (i.e. plastics, fatty acids, alcohols) starting from organic material or CO_2 (78–81). According to the last FAO report on food waste and losses, global food waste generates 4.4 gigatons CO_2/year, which is equivalent to approximately 8-10% of the total anthropogenic GHG emissions and cost about 1 trillion USD2012 per year (82). Hence, the application of innovative technologies able to exploit microbiome metabolism are essential to face this challenge. The analysis of the microbiota associated with food waste could teach us how to improve the functionality of the entire community, and in turn the efficiency of the bioprocess.

Microbial resilience and resistance are two critical aspects to evaluate microbiomes' response to pollutants or toxic compounds. Moreover, the study of microbes along the food chain could provide intervention strategies against foodborne infections, which represent a global public health and economic challenge. Centers for Disease Control and Prevention (CDC) estimates that each year 48 million people get sick from foodborne illness, with 31 major pathogen causing 9.4 million episodes in the United States (83). Improved knowledge of food chain microbiomes could protect us from foodborne pathogens. All these aspects are joined together through the "one health" concept, linking environment, food and animal and human health.

Two of the most important food chain microbiomes, capable of impacting on human health, nutrition and disease risk, are represented by fermented foods and by the gut microbiota in both humans and production animals. As it will be discussed in detail in the next paragraph, microbiomes associated with foods, including microbiomes present on raw ingredients and isolated strains of fermentative bacteria and yeast, are employed in the production and preservation of fermented foods and beverages (84), which consumption is related to beneficial effects for human health (85,86). Fermented foods are an example of how food chain microbiomes are employed traditionally to preserve raw foods, improving their organoleptic quality (i.e. by producing vitamins, amino acids, or by degrading recalcitrant plant macromolecules during the fermentation process) and improving their safety through the inhibition of putative food poisoning strains (30,85). Research on food microbes could also supply additional details about food microbial spoilage, which is one of the biggest threats to food production sector. Understanding which microbes are fully or partially

responsible for food deterioration would prevent food losses due to spoilage, reducing food production footprint. Animal and human gut microbiomes represent the last essential brick of food chain microbiomes. Because of the impact that the gut microbiomes have in modulating gut health, inflammation and immune system activity (87), there is much interesting in learning how gut microbiomes could be exploited to improve welfare of production animals, nutritional quality of our animal foods, and to reduce environmental footprint of animal derived food products.

4. The gut microbiota (GM)

The term "gut microbiota" comprises all microorganisms (Archaea, Bacteria, Eukarya and viruses) colonizing the gastrointestinal tract of humans and any animal with an organized intestine. This consortium of microbes co-evolved with the host, reaching a mutualistic relationship with a fundamental interaction with the host, both for metabolic homeostasis maintenance, and during disease state. The host provides a stable environment and nutrients through diet while GM provides microbial metabolites and protection against invading pathogens (87).

Bacterial load gradually increases along the human gastrointestinal (g.i.) tract, going from about 10^{2-4} bacteria/gram of content in the stomach to 10^{3-5} bacteria/gram in the duodenum and jejunum, 10^{8}/gram in the ileum and 10^{11-12}/gram in the colon (87–89). This density gradient is mainly influenced by pH, luminal oxygen concentration, immune and digestive secretions and the flow rate of digesta in the anatomical portion considered (89). Together with bacterial load, also the gut microbiota composition is shaped by microbial habitat (i.e. g.i. portion studied, pH and oxygen levels) (89). However, the diversity of the human gut microbiota, defined as 'the number and abundance distribution of distinct types of organisms within a given body habitat' (90) is unique to each individual (89,90). To evaluate gut microbiota diversity, two levels of diversity measurements are typically employed, first introduced by Whittaker in 1960 (91). These levels include α-diversity, which summarizes species richness and evenness within a given community (sample), and beta-diversity, which measures dissimilarities between communities. In this PhD thesis, three different indices were used to analyze changes in bacterial α-diversity, namely the observed number of OTUs, the Chao1 index and the Shannon entropy index. OTUs number is the simplest measure of α-diversity. It is based on sequencing data and represents the count of OTUs actually observed in samples, thus giving a measure of bacterial richness (92). Chao1 is a non-parametric, abundance-based index used to estimate richness, i.e. to estimate the number of expected OTUs given all the bacterial taxa identified in samples (93). Chao1 index assumes that rare species can provide the most

information regarding missing species and uses singletons and doubletons to estimate the number of missing species (93). Chao1 index is suitable for data sets skewed toward the low-abundance species (94). Compared to OTUs number and Chao1 index, Shannon's diversity index depends on both species richness and the evenness with which bacteria are distributed among different taxa (95). Since evenness represents a measure of the relative abundance of the different taxa in a community, Shannon index is frequently used to measure the diversity of a bacterial community (95). On the other hand, to evaluate bacterial β-diversity we employed three different measures, including Bray-Curtis dissimilarity index, weighted and unweighted UniFrac. Bray Curtis dissimilarity index measures the difference in OTUs diversity, thus quantifying the compositional dissimilarity between samples (96). UniFrac β-diversity measures incorporate phylogenetic information in the computation, thus accounting for the degree of divergence between sequences. UniFrac method measures the phylogenetic distance between taxa, as the fraction of the branch length of the phylogenetic tree that leads to descendants from only one of a pair of environments (97). Unweighted and weighted represent the qualitative and quantitative variants of UniFrac distance, respectively (98). Unweighted UniFrac only considers presence or absence of each taxon, while weighted UniFrac considers the relative taxon abundance, thus being particularly useful to reveal community differences that are caused by changes in the relative abundance of a particular taxon (97,98).

From near sterility at birth, GM taxonomic diversity increases with growth of the host, reaching a stable and complex community about 3 years of age (99). After that period, Bacteroides, Firmicutes, Actinobacteria, Proteobacteria and Verrucomicrobia can be identified as the five predominant phyla, with Fusobacteria, Tenericutes, Spirochaetes and TM7 in lower abundance (89,90,100). Anaerobic conditions strongly influence bacterial populations inhabiting the human colon. The dominant colonic microbiota comprises mainly strict anaerobes including *Bacteroides, Clostridium, Fusobacterium, Ruminococcus, Butryvibrio* and *Bifidobacterium* spp., all able to derive energy through fermentation processes and thus considered as beneficial bacteria related to health status (101,102).

Variations in the relative abundance of these main phyla composition take place continuously also in the same individual, due to age transition and to environmental factors such as diet and antibiotic use (103). The age-related GM remodeling was reported in a Japanese cross-sectional study conducted by Odamaki and colleagues (2016) (104). Fecal samples from 367 healthy subjects between the ages of 0 and 104 years were analyzed by 16S rRNA gene sequencing, highlighting differences in GM composition from infants to the elderly. Although existing differences among individuals, a

significant decrease in the relative abundance of Actinobacteria and especially in *Bifidobacterium* genus was observed during the aging process, together with an increase in Proteobacteria and *Clostridium* genus. The same shift has been recently observed in a cross-sectional European study performed on 230 healthy subjects (105). Participants were assigned to two groups based on their age: 20 to 50 years (n=85) and more than 60 years (n=145). Fresh fecal samples were collected and processed for fluorescence in situ hybridization coupled with flow cytometry. Beneficial bacteria *Bifidobacterium* and *Faecalibacterium prausnitzii* significantly decreased in elderly subjects, while an opposite trend was observed for facultative anaerobes *Streptococcus* and *Enterococcus*. These age-associated changes reflect the gut microbiota maturation during lifespan and might be partially related to malnutrition and rising need for anti-inflammatory drugs or antibiotics which accompany the aging process (106).

Diet plays a major role in shaping gut microbiota composition and also its metabolic output in terms of the metabolites it produces. Carbohydrate or saccharolytic fermentation is the predominant form of energy metabolism within the anaerobic colonic microbiota and carbohydrate in the colon comes from dietary fiber, resistant starch and other dietary components and also from mucin, the high molecular weight, heavily glycosylated proteins which comprise the mucus layer covering the alimentary tract from mouth to anus (107)**.** Dietary fiber fermentation leads to the formation of beneficial metabolites with *in vivo* activity, such as short-chain fatty acids (SCFA). SCFA are fatty acids with less than six carbon atoms, mainly represented by acetate, propionate and butyrate (108) with a molar ratio of 60:20:20 (109).

The primary source of endogenous SCFA is the indigested dietary fibre fermented by the colonic microbiota (110). Under anaerobic conditions, three different pathways are used by bacteria to ferment those complex carbohydrates, producing SCFA energy as ATP (**Figure 2**) (111,112). SCFA production through colonic GM fermentation is described by the following equation (113):

$59\ C_6H_{12}O_6 + 38\ H_2O \rightarrow 60$ acetate + 22 propionate + 18 butyrate + $96\ CO_2 + 256\ H^+$

Several *in vitro* and *in vivo* studies contributed to identify and characterize bacteria responsible for SCFA production. After 16S rRNA gene sequencing analysis on human feaces, *Faecalibacterium prausnitzii, Eubacterium rectale, Roseburia intestinalis* and *Ruminococcus bromii* appear to be the main taxa responsible for butyrate production (114–116). Propionate production is attributable to different *Bifidobacterium* and *Bacteroides* species (117–119). The intestinal mucus layer could also be used as a carbohydrate source for SCFA production. *Akkermansia muciniphila* and *Bifidobacterium bifidum* utilise mucin proteins as a growth substrate, thus producing both acetate and propionate (120–122).

Figure 2. Summary of indigested fibre fermentation by colonic microbiota. Three different pathways lead acetate, propionate and butyrate production starting from glycolysis end-product phosphoenolpyruvate (PEP). Reduced nicotinamide adenine dinucleotide (NADH) coenzyme, methane (CH_4), molecular hydrogen (H_2) carbon dioxide (CO_2) are also produced as by-products. Adapted from den Besten *et al.* (111).

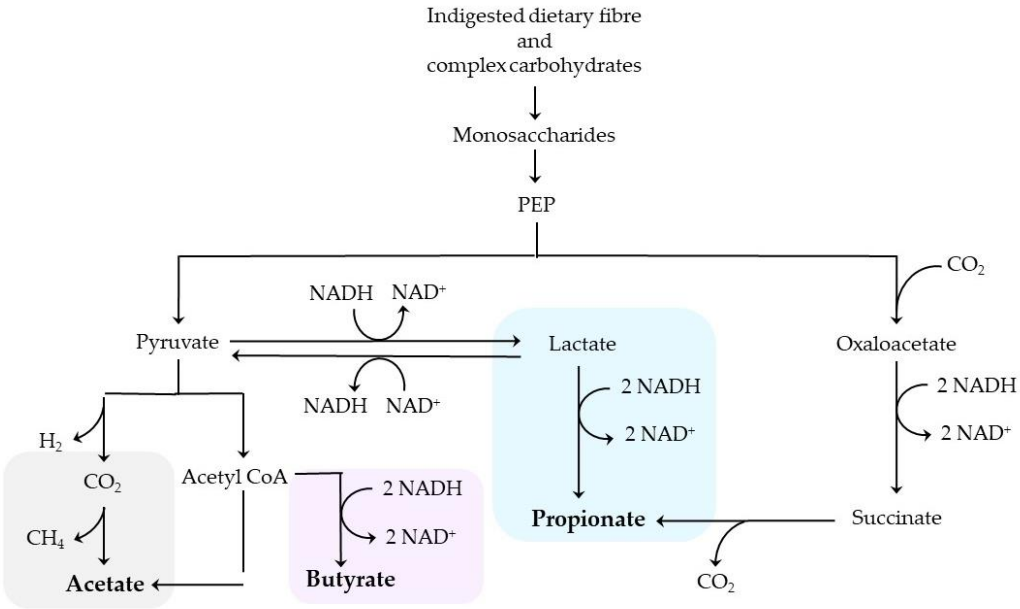

Once they are produced, acetate is primarily used for cholesterol synthesis and *de novo* lipogenesis (123), propionate is shunted to the liver where it is converted into glucose through gluconeogenesis, but can also inhibit cholesterol biosynthesis from acetate, and butyrate serves as a local fuel for enterocytes (124). Acetate is the only SCFA that can be found in considerable amounts in peripheral blood, since it's rapidly absorbed in the proximal colon and transported to the liver via the portal vein (125). Here, it becomes a substrate of acyl-CoA short-chain synthetase-2 (ACCS2) enzyme which expends ATP to generate acetyl coenzyme A (acetyl-CoA), the universal energy and carbon currency (123). Acetate also has a role in adipogenesis together with propionate. Hong *et al.* (2005) (126) demonstrated that acetate and propionate both stimulate fat accumulation through binding the free fatty acid receptor-2 (FFA2) on differentiated 3T3-L1 adipocytes. Recently, Jiao *et al.* (2021) (127) demonstrated the ability of all these three main SCFA in suppressing appetite and attenuating fat deposition in C57BL/6J mice under high-fat diet, via regulating glucagon-like peptide 1 (GLP-1), peptide YY (PYY) and leptin hormones. Despite its physiologic effects outside the intestine, butyrate is principally used in the gut where it is produced. This has been hypothesized after measuring its concentrations in intestinal content and portal blood obtained soon after death from sudden death victims: butyrate molar proportion of total SCFA fell from 21% in the gut lumen to 8% in the portal blood (109). Monocarboxylate transporters MCT1 and SMCT1 (Sodium-coupled monocarboxylate transporter 1) transfer butyrate from the gut lumen to colonocytes cytoplasm, where it could be

oxidized for energy production (128). Zhou and colleagues (2018) (129) confirmed the role of butyrate produced by *F. prausnitzii* in ameliorating colorectal colitis through T cell regulation in Sprague-Dawley rat model. Recently, alleviation of visceral hypersensitivity in irritable bowel syndrome (IBS) was observed in both HT-29 cells and mouse model after butyrate treatment (130).

Other than serve as metabolic substrates, these microbial metabolites have been shown to modulate host physiology through multiple pathways including the interaction with G-protein coupled receptors GPCRs (131), improving gut barrier function (132) and modulating the production of several hormones (133,134). SCFA can also influence a broad spectrum of inflammatory and immunitary responses. GPCRs are the largest family of transmembrane receptors in Eukaryotes, transducing extracellular signals across the plasma membrane and activating intracellular response through a number of secondary messangers such as cyclic AMP (cAMP) - dependent patwhays (131). Two of these receptors, FFAR2 and FFAR3 (previously designated as GPR43 and GPR41) are activated by SCFA (135). Research done on FFA2- and FFA3-mediated effects has elucidated the role of SCFA (and thus of the resident microbiota) in immune regulation with implications in metabolic conditions and inflammatory disorders such as type 2 diabetes mellitus (T2DM). Murine knockout models of FFAR2 have shown altered metabolic parameters including reduced SCFA-triggered GLP-1 secretion and impaired glucose tolerance, resembling what happens in diabetic subjects (136). GLP-1 is an anorexigenic gut hormone with a key role in maintaining glucose homeostasis through regulation of insulin and glucagon secretion (137). Suzuki and Aoe (2021) (138) further investigated the interaction of SCFA derived from barley beta-glucan fermentation and GLP-1 levels. An early study from Liu *et al.* (2021) (139) demonstrated the extensiveness of SCFA interactions, reporting the presence of SCFA receptors in both mice and human lung macrophages. These findings supported the hypothesis that gut-originating SCFA regulate inflammatory and injury responses not only in the gut, but also in other tissues and organs, thus connecting diet, gut and host health. SCFA are involved in the reduction of intestinal inflammation through the suppression of pro-inflammatory mediators and the induction of anti-inflammatory cytokines (140,141). In particular, different studies described the ability of butyrate in decreasing immune cells activation, proliferation and inflammatory cytokines production through the modulation of histone deacetylases (HDAC), thus ameliorating mucosal inflammation and reducing the risk of colon cancer (142–146). Taken together, these results confirm the fundamental role of SCFA in connecting diet, the gut microbiota and host metabolic and immune function, in both healthy physiological and pathological states.

4.1 The gut microbiota in obesity

In 2004, Bäckhed and colleagues observed that conventionalization of adult germ-free mice with a normal microbiota increased total body fat by 57% despite diminished food intake (147). This generated a substantial interest around the role of the gut microbiota in obesity. Afterwards, many studies compared gut microbial profiles of obese and lean mice, observing that the Firmicutes/Bacteroidetes (F/B) ratio significantly increased in obese animals and thus suggesting this ratio as an obesity-related physiological indicator (148,149). In particular, Ley and colleagues (2005) (148) suggested that increased F/B ratio in a mouse model of obesity may increase energy uptake and storage, thus promoting adiposity and affecting energy homeostasis. However, the reliability of this parameter has become increasingly questioned, since some other studies did not observe any modifications of F/B ratio in obesity or even reported opposite results (150–152). Nevertheless, obesity has been associated with decreased bacterial diversity and richness, thus suggesting the existence of other compositional modifications both in animal models and human subjects which might be more relevant than the F/B ratio alone (153). In particular, some specific bacteria appear to have causal relationship with obesity or at least have strong correlations with body weight. As an example, obesity is associated with lower abundance of *Akkermansia muciniphila* (Verrucomicrobia phylum) a mucin degrading bacterium typically correlated with a healthier metabolic status and with weight loss (154,155). Depommier and colleagues (2019) evaluated the effects of *A. muciniphila* supplementation in obese subjects during a randomized, double-blind, placebo-controlled study. Compared to placebo, *A. muciniphila* improved insulin sensitivity, while reduced insulinemia, plasma total cholesterol and relevant blood markers for liver dysfunction and inflammation (156). Together with *Akkermansia muciniphila,* also *Bifidobacterium* genus, *Faecalibacterium prausnitzii* and *Bacteroides thetaiotaomicon* were observed significantly reduced in obesity both in animal and human studies (157–159). These findings suggest the existance of an 'obesity-gut microbial phenotype' in which putative resident beneficial bacteria are significantly decreased.

Several microbial metabolites exert beneficial activities against obesity and associated conditions. Secondary and tertiary bile acids (BAs) are generated by gut bacteria through the enzymatic modification of primary BAs, formed in the liver from cholesterol and then released into the intestine to afford dietary lipids and vitamins absorption (160). Circulating BAs can regulate whole-body glucose and lipid metabolism through the stimulation of nuclear hormone receptor farnesoid X receptor (FXR), Vitamin D receptor, Pregnane-activated Receptor (PXR), as well as the membrane receptor G-protein-coupled bile acid receptor (TGR5) (161). Since gut bacteria have the potential to

regulate host metabolism and physiology through modifying the pool of circulating BAs, BAs represent one of the most important metabolic mediators between GM and obesity associated diseases (161). Vincent *et al.* (2013) reported higher circulating levels of BAs in obese patients with type 2 diabetes (162), whereas in another study impaired levels of 12α-hydroxylated secondary BA were associated with lower insulin sensitivity and higher plasma triglycerides (163), highlighting the role of BAs in several metabolic disorders. In a human controlled-feeding, randomized crossover study, 42 g/day of walnuts consumption for 2-3 weeks decreased fecal secondary BAs pool and lowered serum LDL cholesterol by modulating the gut microbiota composition, thus suggesting that GM may contribute to the beneficial health effects of walnut consumption, even through BA metabolism (164). Phenolic compounds deriving from GM metabolism of dietary polyphenols can also exert their beneficial effects protecting against obesity related diseases. As well as BAs, polyphenols are involved in the regulation of energy metabolism. Many different polyphenol extracts and plant foods, especially berries, have been shown to reduce obesity and markers of metabolic disease in animal models (165). Some studies have gone further, and demonstrated viable mechanisms of effect involving alterations in microbially produced bile acid profiles known to regulate host metabolis, through FXR for example, and inflammation via TGR5 regulated pathways (166,167). Dietary supplementation with the polyphenol rich berry camu camu (*Myrciaria dubia*) significantly modulated gut microbiota composition in high-fat/high-sucrose fed obese mice, increasing relative abundances of *A. muciniphila* (168). Moreover, camu camu extract upregulated the mRNA expression of genes involved in brown adipose tissue thermogenesis, thus preventing obesity associated conditions including weight gain, fat accumulation and metabolic inflammation. Similarly, supplementation of a polyphenol-rich rhubarb extract in mice prevented high-fat diet-induced obesity, diabetes, visceral adiposity and adipose tissue inflammation without any modification in food intake (169). *A. muciniphila* in particular, was positively associated with all these beneficial effect, supporting a reciprocal interaction between dietary polyphenols and microbial metabolism.

5. GM and immune system

5.1 The immune system: structure and function

The immune system (IS) is defined as the network of cells, tissues and molecules that recognizes a number of antigens and that defends the body against infections and other diseases. The IS includes white blood cells together with primary and secondary lymphoid organs, such as the

thymus, spleen, tonsils, lymph nodes, lymph vessels and the bone marrow (170). The IS defense mechanisms can be divided into innate (general) and adaptive (specialized) responses, which closely cooperate to provide adequate resistance against pathogens and diseases. The innate IS represents the first line of defense against foreign molecules, which it recognizes as pathogen associated molecular patterns (PAMPs). It includes physical or anatomical barriers (i.e. mucous membranes, skin and tight junctions), phagocytic cells like the macrophages, and the complement system, a cascade of more than 30 proteins acting in concert against pathogens (171). The innate immune response is not specific to a particular pathogen and responds in the same way to all microorganisms and alien substances, acting quickly and widely (171). In vertebrates, the epithelial surfaces, including those of the gastrointestinal tract, are the first anatomical barrier separating the outside from the inside of the body. In particular, the permeability of the gut epithelium is controlled by tight junctions (TJ), intercellular junctional complexes forming semi-permeable connections between neighboring cells and preventing entry by potential pathogens (171). TJ consist in the assembly of integral transmembrane proteins and peripheral membrane proteins, which interact with actin cytoskeleton to maintain intestinal barrier function (172). Actin and signalling proteins are connected to TJ proteins by peripheral membrane adaptor proteins known as zonula occludens (ZO) (172). TJ proteins are finely regulated by different signalling pathways, including mitogen-activated protein kinase (MAPK) signaling and phosphatidylinositol-3-kinase/protein kinase B (PI3K/Akt) pathway (173,174). These signal transduction pathways determine phosphorylation, distribution and expression levels of TJ proteins, thus dynamically regulating TJ integrity (172). Occludin and claudins represent the most abundant classes of integral transmembrane TJ proteins and animal studies indicated their importance in maintaining the integrity of TJ (172,175,176). As the other interior epithelial surfaces, the gut epithelium is also covered with a mucus layer, which protects cells against mechanical insults and dehydration, and prevents pathogen translocation into underlying tissues (177,178). Specialized goblet cells constitutively produce the mucus covering the intestinal epithelial surface, secreting up to 10 liters of mucus/day (179). The mucus is mainly composed by water (approximately 90–95%), electrolytes (1% w/v), lipids (1-2%) and proteins. Mucin glycoproteins represent the major functional components of mucus, and confer it elasticity and viscosity and act as substrates for specific gut bacteria (177,178). Bacterial fermentation products are key players in mucoprotection. In mono- and co-cultures of epithelial cells and myofibroblasts, all three main SCFA acetate, propionate and butyrate stimulated mucin-2 (MUC2) protein expression in intestinal epithelial cells (180). Burger-van Paassen and colleagues (2009) observed that

incubation of human goblet cell-like OLS174T cells with 1 mM butyrate or 1-15 mM propionate increased MUC2 expression, thereby influencing epithelial protection (181). Despite being influenced by gut bacteria metabolites, intestinal mucus requires the presence of GM to develop and to maintain its thickness and structure (182). Mucus–GM interaction will be discussed in detail in section 5.2.

The induction of the adaptive immune response begins when the innate immune response fails to eliminate the infectious organism. Any substance capable of stimulating the adaptive immune system is referred to as an antigen (171). The adaptive response is delivered by B and T lymphocytes, which provide humoral and cell-mediated immunity, respectively. In the humoral response, B cells secrete appropriate antibodies, blood glycoproteins able to neutralize the antigen (183). On the other hand, T-cell mediated immunity does not involve antibodies production, but rather involves the activation of phagocytes and specific cytotoxic T lymphocytes (183). Due to its destructive potential, the adaptive immunity is finely regulated by the innate immune cells according to the 'three-signal paradigm' (184). This model has been inspired by an intuition of Charles Janeway Jr., who proposed that innate cells should use specific pattern recognition receptors (PRRs) to recognize PAMPs (185). This binding triggers a signal cascade, where 1) the innate cells (i.e. dendritic cells) present the associated antigen to lymphocytes, along with 2) co-stimulation and 3) innate cytokines production to activate and differentiate naïve T lymphocytes. Adaptive immunity generates immunological memory, which ensure a faster and enhanced response when a specific pathogen is encountered a second time (185), thus providing the rationale for vaccines development (186).

5.2 How the host recognizes gut microbiota

The immune system has co-evolved with gut microbiota, developing tolerance mechanisms towards GM and common foods components thus permitting its colonization without triggering undue inflammation (187). How the host recognizes different microbial species, discriminating between commensal and pathogens, is still a matter of investigation. A primary detection level occurs through the mucus overlaying intestinal surface, which constitutes a physical barrier limiting bacterial access to the epithelium (188), but also provide an ideal habitat for the gut microbiota. The O-glycans of the MUC2 constitute attachment sites used by bacterial adhesins and serve as an energy source for the commensal bacteria, so-called 'mucolytic bacteria' (178). Mucolytic bacteria mainly include *Akkermansia muciniphila, Bifidobacterium bifidum, Bacteroides fragilis, Bacteroides thetaiotaomicron, Ruminococcus gravus* and *Ruminococcus torques* (178). In support of this hypothesis, supplementation of mucin-derived O-glycans to diet significantly improve gut microbiota recovery

after antibiotic treatment, increasing the relative abundance of the mucolytic *A. muciniphila* in mouse (189). Defects in mucus layer thickness and structure could also interrupt host:microbiota cross-talk and thus leading to microbial penetration across the intestinal barrier. In 2008, Johansson and colleagues (190) observed that mice deficient in glycoprotein MUC2 displayed alarming bacterial penetration in the colonic epithelium, and developed colitis. These results confirm that the mucus layer helps to maintain sequestration of the GM to the intestinal lumen, thus limiting the immune system from over-reacting to beneficial microbes.

The immune system is able to distinguish between self and non-self through pattern recognition receptors (PRRs). PRRs recognize bacterial components and are responsible for innate immune response in the host (141). They are expressed on all human innate immune cells, including macrophages, granulocytes, dendritic cells (DCs) and natural killer cells (191). Several classes of PRRs have been identified, depending on their structure, location and function. Among them, cell surface or intracellular Toll-like receptors (TLRs) and cytoplasmic NOD-like receptors (NLRs) are broadly expressed in human immune cells (**Table 3**), where they regulate the inflammatory response and immune homeostasis through gene expression of cytokines and other immune mediators (141). TLRs and NLRs are the two major classes of innate immune sensors, which provide a quick and generic response against a huge number of antigens (**Table 1, 2**). The capacity of a small number of TLRs or NLRs to detect a broad range of pathogens and other foreign substances depends on their ability to recognise molecules shared by different microorganism, such as components of microbial cell walls and membranes (192–194)**.** Nucleotide-binding oligomerization domain-containing protein 2 (NOD2) mutation has been linked to several inflammatory diseases including Crohn's disease (CD). This was first observed in 2001, when 2 independent groups identified the gene NOD2 as the first susceptibility gene for CD (195,196). A large cohort study recently provided new insights into the genetics of CD (197). Whole-exome sequencing on 1183 pediatric and early onset inflammatory bowel disease (IBD) patients (ages 0–18.5 years) demonstrated that recessive inheritance of one of three NOD2 loss-of-function alleles is responsible for loss of NOD2 protein function, thus representing a mechanistic driver of early onset IBD and accounting for 7-10% of CD cases. On the other hand, over activation of PRR can also lead to the disruption of immune homeostasis, increasing the risk for several inflammatory diseases. Overexpression of TLR2 has been observed in a rat model of colon cancer when compared with normal gut epithelial tissues (198). Moreover, Meng and colleagues (2020) (199) recently observed that the use of TLR2 agonists significantly enhances the proliferation and invasion capabilities of colon cancer cells in a colitis-

associated cancer (CAC) mouse model. These results point out the critical role of PRRs regulation and expression as determinants of host health and disease.

Table 1. List of common bacterial Toll-like receptors (TLRs), their localization in human cells, their bacterial ligands and activated pathways. Intracellular TLRs (also known as 'nucleic acid sensors') are localized to endoplasmic reticulum, endosomes and lysosomes (200). PG: peptidoglycan, LAM: lipoarabinomannan, LPS: lipopolysaccharide, LTA: lipoteichoic acid, MyD88: Myeloid differentiation primary response 88, TRIF: TIR-domain-containing adapter-inducing interferon-β, AP-1: Activator protein-1, NF-kB: Nuclear factor-kB, IRF: Interferon-regulatory factor, TNF-α: Tumor necrosis factor-α, IL: interleukin, IFN-I: Interferon-1.

TLR	Localization	Ligands	Signaling adaptor	Activated target	Released cytokines	References
TLR1	Cell surface	Triacyl lipopeptides	MyD88	AP-1 NF-kB	TNF-α IL-1 IL-6	(201–203)
TLR2	Cell surface	Lipoprotein PG LTA LAM	MyD88	AP-1 NF-kB	TNF-α IL-1 IL-6	(202–206)
TLR4	Cell surface	LPS	MyD88 TRIF	NF-Kb IRF-3	IFN-I	(202,203,207,208)
TLR5	Cell surface	Flagellin	MyD88	AP-1 NF-kB	TNF-α IL-1 IL-6	(202,203,209)
TLR6	Cell surface	LTA	MyD88	AP-1 NF-kB	TNF-α IL-1 IL-6	(202,203,210)
TLR9	Intracellular	CpG DNA	MyD88	AP-1 NF-kB IRF-7	TNF-α IL-1 IL-6 IFN-I	(202,203,211)

Table 2. List of common bacterial NOD-like receptors (NLRs), their localization in human cells, their bacterial ligands and activated pathways. PG: peptidoglycan, LPS: lipopolysaccharide, NF-kB: Nuclear factor-kB, MAPK: mitogen-activated protein kinase, TNF: Tumor necrosis factor, IL: interleukin.

NLR	Synonyms	Localization	Ligands	Activated target	Released cytokines	References
NOD1	CARD4 NLRC1	Cytosolic	PG motifs LPS	NF-kB MAPK	TNF IL-1β	(212–217)
NOD2	CARD15 NLRC2	Cytosolic	PG motifs LPS	NF-kB MAPK caspase 9	TNF IL-1β	(196,215–218)
IPAF	CARD12 NLRC4 CLAN	Cytosolic	Flagellin	Nf-kB caspase-1	TNF IL-1β	(219–221)

NLRP1	CARD7 CLR17.1 DEFCAP	Cytosolic	*Bacillus anthracis* toxin PG	caspase-1	IL-1β IL-8	(222–225)

Table 3. Common TLRs and NLRs expressed by immune cells.

Cells	TLRs	References	NLRs	References
Granulocytes	TLR 1, 2, 4, 5, 6, 9	(209)	NOD2, IPAF	(226,227)
Monocytes/macrophages	TLR 1, 2, 4, 5, 6	(192,228)	NOD1, NOD2, IPAF	(196,226,229)
Dendritic cells	TLR 1, 2, 4, 5, 6, 9	(228,230)	NOD1, NOD2	(196,227)
B lymphocytes	TLR 1, 6, 9	(231)	NOD1, NOD2	(193)
T lymphocytes	TLR 2, 5, 9	(232)	NOD1, NOD2, IPAF, NLRP1	(233,234)

However, these classes of PPRs are not exclusive to pathogenic or disease mechanisms and represent a key factor in GM recognition by the host (187). In fact, PRRs maintain the homeostatic and mutualistic relationship between our immune system and our microbes, allowing a controlled tolerance towards the presence of commensal or mutualistic gut microbes. This is achieved by differentially expressing multiple types of PRRs. In the human colon, TLR3 and TLR5 are constitutively expressed, whereas TLR2 and TLR4 can be induced by the time of need (235). This strategy avoid a constant over-activation of PRR signaling pathways and is essential for the gut barrier function. Price and colleagues (2018) (236) mapped the localization of distinct TLRs in mice intestinal epithelium, revealing a diversified pattern of expression depending on the region of the gastrointestinal tract. These results confirm the existence of a specific correspondence between autochthonous microbes and certain classes of receptors. Furthermore, the immune system controls and regulates the composition of commensal inhabitants, producing antimicrobial peptides (AMPs). Intestinal AMPs are mainly produced by Paneth cells and enterocytes, and represent a primitive and generic innate defense mechanism (237). Their critical role in the GM equilibrium maintenance is widely demonstrated, since impaired AMP responses can increase host susceptibility to gastrointestinal infections (238,239) and has been associated with IBD condition (240). PRRs stimulation induce a rapid response, including the release of AMPs and the activation of Myd88 and NF-κB mediated inflammatory signalling (241) (**Table 1,2**). Frantz and colleagues investigated the role of MyD88-dependent TLRs signalling in mice not expressing *MyD88* gene (242). Loss of epithelial MyD88 pathway was associated with a dramatic increase in mucus-associated bacteria and bacterial translocation, together with impaired gut barrier function. These results confirmed MyD88 and specifically PRRs response as key mediators of microbial-host cross-talk.

5.3 Diet and immune system

Diet deeply influence the immune system activity. Secondary metabolites deriving from colonic gut microbiota saccharolytic fermentation, together with polyphenols and other phytochemicals directly present in food can interact with immune cells, enhancing or disrupting their differentiation and activity. Microbial metabolites, especially SCFA and small phenolic compounds derived from plant polyphenols are often involved in the regulation of host defense mechanisms, protecting against pathogens or preventing inflammatory states. Pre-administration of certain *Bifidobacterium* strains prevents colonic epithelial cell death in gnotobiotic mice infected with enterohemorrhagic *Escherichia coli* O157:H7 (243). The protective effect of those selected Bifidobacteria have been addressed to their different metabolic activity and especially to acetate, which was detected at significantly higher concentration in the feces from mice colonized by the 'protective' strains compared with the 'non-protective' strains. Moreover, Furusawa and colleagues (2013) (244) demonstrated that butyrate stimulates the differentiation of colonic regulatory T-cells (Treg), which modulate the immune response, thereby maintain self-tolerance and avoid chronic inflammatory autoimmune diseases (245). Stimulation of splenic naïve $CD4^+$ T cells with butyrate *in vitro* significantly increased the frequency of $Foxp3^+$ Treg cells, which are normally generated to maintain immune tolerance and homeostasis of the immune system (246). To confirm these results, pathogen-free C57BL/6 mice were fed modified diets containing acetylated, propionylated or butyrylated high-amylose maize starches. Consistent with *in vitro* observations, the diet containing high level of butyrate significantly stimulated colonic Treg cells proliferation. SCFA can also mediate their effects through the activation of GPCRs which are expressed variously in several immune cells (135). Singh and colleagues (2014) (247) demonstrated that butyrate promoted Treg cells differentiation and anti-inflammatory pathways in macrophages and DCs cells in mice colon, through binding G-protein coupled receptor GPR109A. GPCR-deficient mice exhibited severe inflammation in models of colitis (248) and immunohistochemical analysis of intestinal biopsies from Crohn's disease patients revealed a reduction in the expression of FFAR2 when compared to healthy subjects **(249)**, suggesting that GPCRs stimulation by SCFA is necessary for the resolution of certain inflammatory responses. The interplay among microbial metabolites and the immune system is critically influenced by environmental factors, and especially diet. In 2016, Agus and colleagues (249) analyzed the effects of a high-fat high-sugar (HF/HS) diet on invasive *E.coli* infection and intestinal inflammation in C57BL/6 mice. When compared to mice fed a conventional chow, quantification of immune-histochemical staining and Western blot analysis showed a reduced FFAR2 expression in

HF/HS mice. As well as SCFA, small phenolic compounds derived from gut microbiota metabolism could also influence the immune system activity. Polyphenols are bioactive compounds with immunomodulatory activity (250). These micronutrients naturally occur in plants as secondary metabolites involved in plant defense mechanisms or in signaling pathways and other growth processes (251). Current evidence strongly suggests that dietary polyphenols interact with both the innate and adaptive immune systems, thus contributing to the prevention of several diseases. In particular, polyphenols act as anti-inflammatory mediators, regulating immune cell activities and decreasing pro-inflammatory cytokine production. A study on pomegranate peel polyphenols (PPPs) and their main components punicalagin (PC) and ellagic acid (EA) demonstrated their potent anti-inflammatory activity in RAW264.7 macrophages stimulated with LPS (252). The molecular mechanism of PPPs, PC and EA consists in the inhibition of mRNA and protein expression of TLR4, which is normally induced by LPS. The decreased expression of TLR4 could explain the inhibition of inflammatory signaling pathways, and therefore of related mediators and transcription factors, including NF-kB. It has also been shown that polyphenols can influence DCs differentiation and activity, thus modulating the immune activation. As an example, a polyphenols rich extract from blackberry suppressed the release of the pro-inflammatory cytokine IL-12 by bone marrow-derived DCs from mouse *in vitro* (253). Another study from Ahn and colleagues demonstrated the role of epigallocatechin gallate (EGCG) in decreasing LPS-induced maturation of mouse DCs *in vitro*, acting thorugh the inhibition of NF-kB inflammatory pathway (254). Moreover, polyphenols have been associated with the modulation of enzymatic signaling pathways related to T cell proliferation. A study on mice demonstrated that green tea EGCG supplementation increased the frequency of Treg cells in spleen and mesenteric lymph nodes, thus suppressing the activity of cytotoxic T cells and the production of pro-inflammatory interferon-γ (IFN-γ) **(255)**. These results confirm the protective role of dietary polyphenols in intestinal and systemic inflammation, acting both on the production of inflammatory mediators and on the activity of receptors involved in bacterial components sensing. **Figure 3** summarizes the main immune and inflammatory pathways regulated by polyphenols.

Figure 3. Effects of dietary polyphenols on immune cells activity and differentiation. Created with BioRender.com.

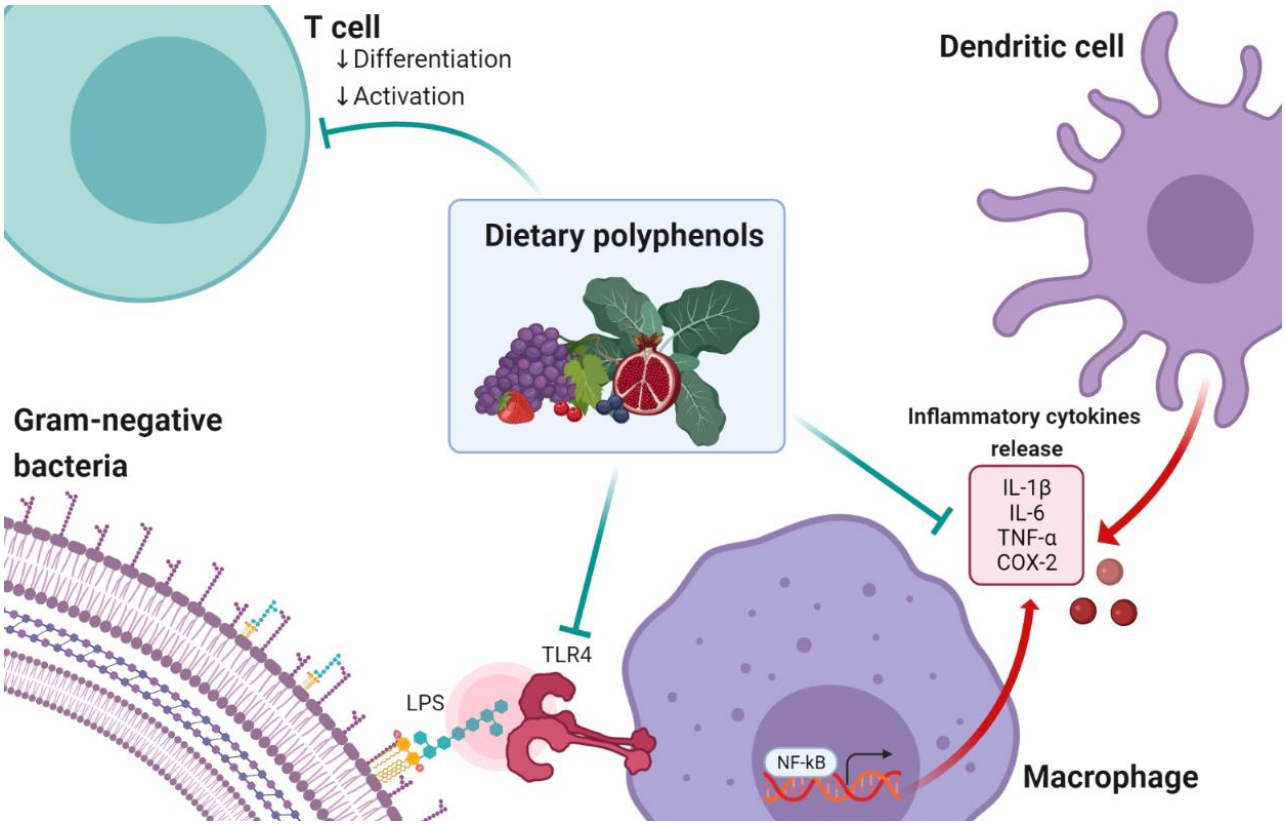

Both SCFA and phenolic acids are examples of metabolites normally produced by the gut microbiota when exposed to a healthy diet, rich in fruits and vegetables and thus in fermentable carbohydrates. However, certain compounds present at high concentration in unhealthy diets can also interact with the immune system promoting inflammatory pathways and thus leading to the pathogenesis of many degenerative diseases. Advanced glycation end-products (AGE), which structure and function will be described in Chapter 6, are adducts deriving from the glycation of proteins with reducing sugars, which typically occurs in highly-processed foods (256). Van der Lugt and colleagues (2018) (257) demonstrated the role of AGE in stimulating the innate immune response in human differentiated macrophages, inducing pro-inflammatory cytokine Tumor necrosis factor-α (TNF-α) secretion through binding to their receptors (RAGE) and activating NF-kB. Price and colleagues (2004) (258) studied the interaction of AGE with innate immune cells in vitro, isolating dendritic cells from human peripheral blood. Exposure of cells to different concentration of glycated products lead DCs to remain immature, thus failing in the maturation and migration processes and compromising their role as immune sentinels. This process has been suggested as a potential mechanism causing vascular complications in diabetes. Immature DCs accumulate in the vascular epithelium, thus predisposing to local inflammation and to vascular damage.

These findings illustrate how diet can influence the immune system establishing and maintaining immunological homeostasis in the gut and protecting the host against inflammation or on the other hand, inducing disease pathogenesis.

5.4 Leaky gut and inflammation

The intestinal epithelium allows the absorption of nutrients and water and constitute a physical barrier separating the gut lumen from the bloodstream, thus providing protection against pathogens (259,260). This barrier is considered as part of the immune system and comprises the mucus layer, the intestinal epithelium itself, and the mucosal immune system. The intestinal epithelium consists of a polarized monolayer of enterocytes joined together by TJ and alternated with various other cell types (261). Among them, mucus-producing goblet cells, enteroendocrine cells and only in the small intestine, Paneth cells, promote the physiological role of the gut barrier (262). Moreover, numerous immune cells proliferate underneath the epithelium, inside the *lamina propria* (262) (**Figure 4**).

Figure 4. Gut barrier organization. The intestinal epithelium is composed of a monolayer of enterocytes, covered by a mucus layer (which structure and function are described in sections 5.1 and 5.2) and alternated with several other cell types. Numerous immune cells inhabit the *lamina propria*, regulating the intestinal immune function and the microbial tolerance. The impact of different dietary habits is illustrated: compared to a healthy diet, modern Western diet leads to mucus narrowing, increased intestinal permeability and higher LPS translocation across the gut barrier.

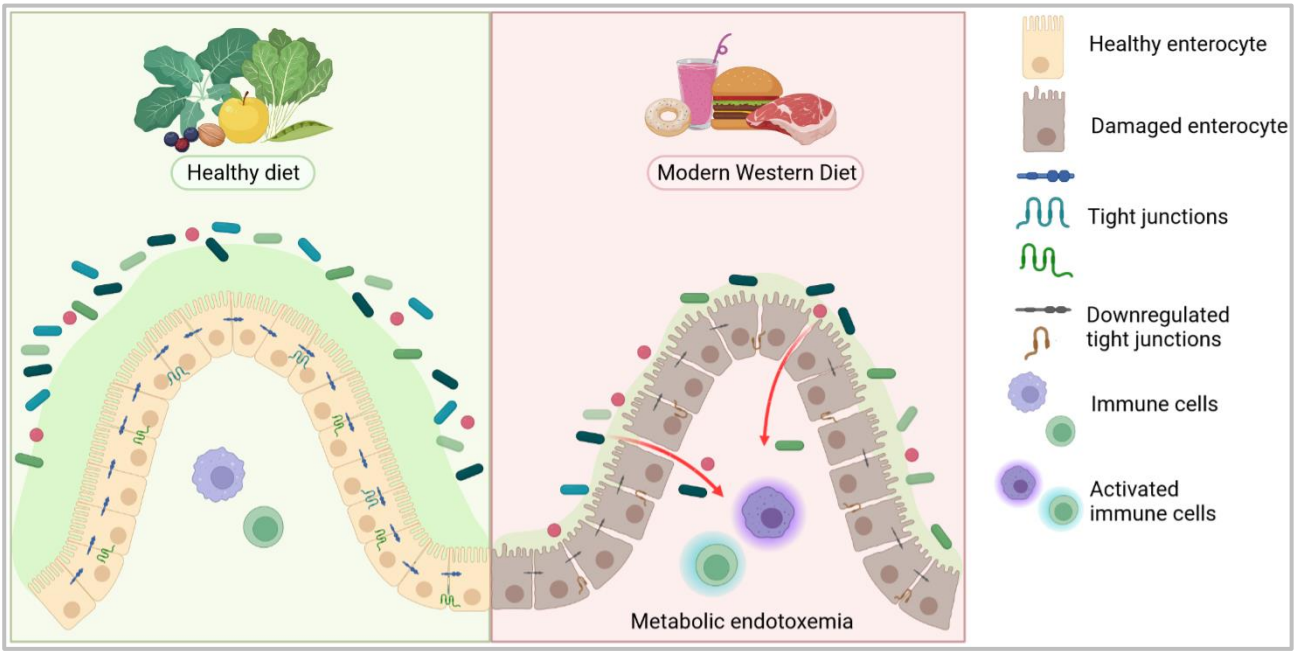

The cross talk between these main components, together with the ability of the single layer enterocytes to attach to one another ensures the proper functioning of the intestinal barrier. Alterations of this equilibrium or abnormalities in TJ's function lead to augmented gut permeability (i.e. 'leaky gut') with a concomitant absorption of bacterial lipopolysaccharide A (LPS) into the

bloodstream. LPS is a component of gram-negative bacteria outer membrane, known to promote local or systemic inflammatory response through the TLR4 activated pathway. Sustained, high plasma LPS concentrations causes inflammation as a consequence of pro-inflammatory cytokines release and this determines the so-called metabolic endotoxemia (262,263). The term 'metabolic endotoxemia' was first introduced in 2007 by Cani and colleagues (263), who demonstrated that mice under a high-fat diet resulted in adipose tissue inflammation, insulin resistance and non-alcoholic fatty liver disease (NAFLD) in response to increased plasma LPS upon loss of intestinal barrier function. This inflammatory status was proposed to be at the root of several chronic diseases, including obesity and diabetes.

Diet strongly influences gut barrier function and maintenance, being one of the major factors inducing (or protecting against) the leaky gut condition. Specifically, GM and metabolites deriving from microbial biotransformation of fibre, polyphenols and other phytochemicals provided by diet regulate intestinal permeability through the modulation of TJ proteins. As an example, urolithin A, one of the main colonic metabolites deriving from GM transformation of ellagitannins, has been shown to upregulate epithelial TJ proteins through activation of nuclear factor erythroid 2-related factor 2 (Nrf2) signaling pathway (264). The role of polyphenols in reducing metabolic endotoxemia through GM modulation has been recently demonstrated by Chen and colleagues (2020) (265), who showed that resveratrol administration in high fat diet-fed mice significantly ameliorated endotoxemia and intestinal barrier defects, with a concomitant increase in *Akkermansia* relative abundances. Also short-chain fatty acids could strengthen TJ, thus maintaining gut barrier function (266). GM contribution towards the pathophysiological regulation of metabolic endotoxemia has been further investigated through the use of a prebiotic oligofructose in high fat diet-fed mice (267). The authors demonstrated that oligofructose supplementation normalized endotoxemia to control levels and totally restored quantities of bifidobacteria, revealing a significant negative correlation between endotoxemia and *Bifidobacterium* spp. Plasma LPS levels have been investigated in association with some features typical of modern Western style diet. A high consumption of noncaloric sweeteners in presence or absence of a high-fat diet has been associated with both metabolic endotoxemia and gut microbiota dysregulation in mice (268). In particular, sucralose and steviol consumption significantly depleted commensal genera *Lactococcus* and *Bifidobacterium*, while increased the number of genes involved in LPS synthesis (268), thus supporting the idea that GM has a key role in preventing low-grade and chronic inflammation.

Circulating LPS levels have also been proposed as an inflammation stressor in human obesity. When considering 33 obese patients recruited pre-surgery, higher LPS blood concentrations were responsible for higher inflammatory genes expression in visceral and subcutaneous adipose tissue (269). Loss of intestinal barrier function in obesity has also been correlated to defective inner colonic mucus layer and dysregulated gut microbiota community in mice (177). Nevertheless, LPS-induced inflammation has been observed in type 2 diabetes (T2DM) (270). When compared to healthy control subjects, T2DM patients had circulating LPS levels 76% higher. This alarming result also correlated with increased inflammatory pathways activation and pro-inflammatory cytokines secretion. In summary, existing evidence suggests that diet influences gut microbial composition, thus modulating gut barrier function and, finally, the inflammatory state of the host.

6. AGE-enriched diets: an example of negative GM modulation

Advanced glycation end-products (AGE) represent a wide class of reactive molecules normally present at elevated concentration in highly processed food. AGE are formed in non-enzymatic reactions of reducing sugars with free amino acids groups through the Maillard reaction and some of the resultant molecules are toxic (271). High sugar concentration and high-temperature cooking, typical features of highly processed food are both responsible for higher AGE generation (256). AGE can enhance palatability and flavor of thermally processed foods. Excessive intake of dietary AGE has been recently linked to the development of obesity, diabetes related complications, CVD and cancer (256,272). A randomized crossover dietary intervention in healthy volunteers tested the effects of a habitual diet containing high-heat-treated foods, compared to a steamed diet low in Maillard reaction products. Although both diets had comparable nutritional composition, a 10% higher caloric intake was observed in volunteers following the thermally processed foods enriched diet, as a result of a higher overall food consumption and higher energy density (273). Interestingly, participants following the processed diet showed significantly higher levels of Nε-carboxymethyl lysine (CML) in urinary excretion and fasting plasma when compared to the control dietary group. CML is an advanced glycation end-product previously reported to activate both nuclear factor-kappa B (NF-κB) and MAP kinase inflammatory pathways by binding to receptor for AGE (RAGE) *in vitro* (274–276). It is plausible that the heterogeneous spectrum of dietary AGE related diseases reflects their capacity to bind a wide range of RAGE, thus triggering different inflammatory pathways (272). AGE-RAGE binding complex works as a positive feedback, leading to a prolonged period of expression and to a redundant downstream molecular activation, thus causing a prolonged

inflammation (277,278). This mechanism may explain why RAGE-dependent pathways are frequently involved in the pathogenesis of several inflammatory chronic diseases. AGE-RAGE axis is implicated in the growth and progression of human colon cancer cell lines in several *in vitro* studies. Kuniyasu *et al.* (2003) (279) first showed that RAGE was expressed in 4 colorectal carcinoma (CRC) cell lines, including Colo320, DLD1, WiDr and TCO and that its expression was positively correlated with cancer cell migration and invasion *in vitro*. In another study, Zill and colleagues (2001) observed RAGE expression in Caco-2 human colon carcinoma cell line, demonstrating that AGE treatment resulted in inflammatory p44/42 (ERK1/2) MAP kinases activation in a time- and dose-dependent manner (274). Furthermore, binding of AGE to RAGE has been suggested to have a role during early and late stages of colorectal carcinogenesis, since it seems to be directly associated with tumor grade (280).

Besides cancer, dietary AGE are involved in the pathogenesis of several other chronic diseases, where inflammation is a common pathological feature.. A human study detected the importance of reducing dietary AGE to improve insulin resistance in type 2 diabetic subjects (281). The investigator randomly assigned 18 type 2 diabetic patients and 18 healthy subjects to a standard diet (containing > AGE equivalents (eq)/day) or an isocaloric AGE-restricted diet (<10 AGE Eq/day) for 4 months. Plasma insulin, together with several inflammatory markers such as TNF-α and NF-κB significantly decreased in type 2 diabetic patients following the AGE-restricted diet, suggesting the critical role of AGE in contributing to insulin resistance and to inflammation state in clinical type 2 diabetes. Effects of reducing dietary intake of AGE on obesity-associated complications have also been investigated. In a randomized, crossover clinical trial, the effects of a low-AGE-containing diet were assessed in overweight and obese individuals (282). The dietary intervention consisted of 2 weeks each of low- and high-AGE diet separated by a 4 weeks wash-out period. Low-AGE diet significantly improved renal function, calculated using both urinary albumin/creatinine ratios and plasma cystatin C levels; and ameliorated inflammatory profile, reducing plasma chemoattractant protein-1 (MCP-1).

6.1 AGE and GM modulation

Since many dietary AGE have high molecular weight, they are not readily absorbed in the small intestine, and instead reach the colon, thus becoming available for gut microbiota metabolism (283,284). Here, AGE can impact both GM community composition, and their production of microbial metabolites. Alterations in colonic microbiota composition due to dietary glycated protein has been reported by Mills and colleagues (2008) who investigated the effect of native, heated and

glycated bovine serum albumin (BSA) on the ulcerative colitis (UC) and non-UC colonic microbiota *in vitro* (285). Compared to native BSA, glycated BSA significantly altered gut microbiota composition of UC patients *in vitro*, increasing sulphate-reducing bacteria clostridia and bacteroides and decreasing putatively beneficial lactobacilli, eubacteria and bifidobacteria. However, glycated BSA incubation in non-UC controls also increased the abundance of sulphate-reducing bacteria, but was not associated with changes in other bacterial groups, thus suggesting that microbial composition at baseline strongly influence the interaction of the whole community with glycated proteins. Fermentation of glycated fish protein using an *in vitro* batch culture model of human distal colon was associated with higher Firmicutes/Bacteroidetes (F/B) ratio, together with specific changes in some proteolytic and potentially harmful bacteria genera, including *Bacteroides, Dialister* and *Parabacteroides* (286). Several other *in vitro* studies analyzed the effects of glycated protein incubation with faecal samples from healthy volunteers, employing fluorescent *in situ* hybridization (FISH) with genus-specific 16S rRNA-targeted oligonucleotide probes, observing large inter-individual differences with regard to bifidobacteria and lactobacilli (287–289). Interestingly, some of these *in vitro* studies investigated the effects of AGE-s enriched diet on SCFA production, and showed variable results. Fermentation of faeces from UC-patients with glycated BSA did not affect SCFA production when compared to non-UC controls (285), whereas faecal batch cultures with glycated fish protein observed an increase in acetate concentrations (286).

In parallel with *in vitro* studies, several studies used animal models to assess the impact of AGE-enriched diet on caecal or faecal microbiome. Qu and colleagues (2017) (290) characterized the effect of dietary AGE on the alterations in the gut microbial ecology and on colon permeability of Sprague-Dawley rats fed a heat-treated AIN-93G diet high in AGE. AGE-enriched diet negatively affected diversity and richness of the microbiota when compared to a low-AGE diet, reducing saccharolytic SCFA-producing bacteria such as *Ruminococcaceae* and *Alloprevotella* and increasing some putatively harmful bacteria such as *Desulfovibrio* (the main SRB within the human gut microbiota) and *Bacteroides*. Moreover, this was associated with a decreased expression of TJ proteins in colon, thus suggesting the detrimental role of AGE in increasing gut permeability and dysregulating gut microbial community composition. Similarly to the *in vitro* findings, several animal studies showed that high-AGE diet were associated with higher F/B ratio in mice and catfishes (291,292).

To date, data coming from human *in vivo* studies focusing on AGE:GM interaction are scarce. In a pilot randomized open label controlled trial from Yacoub and colleagues (2017), the effects of dietary AGE on the GM of patients undergoing peritoneal dialysis (PD) was investigated. Twenty

PD subjects habitually consuming a high-AGE diet were recruited and randomly allocated into a group continuing the same diet (HAGE) or in a group with AGE restriction (LAGE) for one month. Dietary AGE restriction significantly altered GM composition, increasing relative abundances of different *Clostridium* spp. and *Ruminococcus gauvreauii* and decreasing *Prevotella copri* and *Bifidobacterium animalis.* In a previous crossover trial, the effects of AGE enriched diet was assessed on the gut microbiota of adolescent males following a high-AGE diet for two weeks (293). AGE intake was associated with a decrease in *Lactobacilli* together with an increase in Enterobacteria, while no significant changes were observed in *Bifidobacterium* or *Clostridium* spp. Given the inconsistent and insufficient evidence about the response of gut microbial populations to glycated products *in vivo*, further studies are required to assess the impact of different AGE on the composition and metabolism of the gut microbiota. A deeper understanding of AGE:GM interactions may also provide new insights regarding the AGE-related negative healthy outcomes, their role in inflammation, which are of great interest considering the dramatic abundance of these molecules in the modern Western processed diet.

7. Benefits of vegetable foods

Whole plant foods include fruits, vegetables, whole grains and legumes. Healthy benefits connected to whole plant food consumption are related to their high content in fibre and phytochemicals. Phytochemicals represent a powerful class of non-nutrient secondary metabolites normally present in plant-based foods, including polyphenols, isothiocyanates, alkaloids and vitamins (294). These compounds are produced as defense molecules, protecting the plant from herbivores, pests, pathogens, UV light and oxidative stress (295). They also contribute to organoleptic characteristics of foods, imparting them qualities such as aroma, flavor or color (294). Moreover, dietary phytochemicals have been widely investigated for their anti-inflammatory and anti-cancer properties, thanks to their ability to modulate and alter several antioxidant and signaling pathways (296,297). In this context the gut microbiota represents the major driver in whole plant foodstuff digestion, thanks to its capability to ferment fibre and metabolize polyphenols, which both arrive almost indigested in the colonic compartment and results in the production of a range of biologically active small molecules, including the SCFA and small phenolic acids (298).

7.1 Gut microbiota role in determining beneficial effects of vegetable foods

The application of the metabolomics approach allowed us to realize that several benefits attributed to phytochemical depend on their interaction with human gut microbiota. Because of their

chemical structure, phytochemicals are poorly absorbed by the human intestine and they are prone to be retained in the gut lumen. Here they can positively affect GM community composition, either supporting the growth and relative abundance of certain gut microbiota members (299,300) or having antimicrobial or bacteriostatic effects on others (299,301) . As an example, different polyphenols have been shown to inhibit the growth of different human intestinal microbiota representatives (301). *Enterococcus caccae, Bifidobacterium catenulatum, E. coli, Ruminococcus gauvreauii* and *Lactobacillus* sp. were grown in liquid medium to give a final concentration of 1.5 x 10^8 colony forming unit/ml and polyphenols were added to liquid medium at different final concentration of 20, 100 or 250 μg/ml in order to assess the minimal inhibitory concentration (MIC) for each polyphenolic compound. High concentration of naringenin and hesperetin (MIC ≥ 250) inhibited growth of almost all analyzed bacteria, thus acting as bacteriostats. Hidalgo and colleagues (2012) observed a positive modulation of intestinal bacterial modulation testing different anthocyanins in a pH-controlled, stirred, batch-culture *in vitro* fermentation reflecting the distal region of the human large

intestine (299). Malvidin-3-glucoside caused a significant increase in the growth of beneficial bacteria including *Bifidobacterium* spp. and *Lactobacillus* spp. when compared to the control. An *in vivo* animal study from Gu and colleagues (2019) (REF) defined the effects of black raspberry (BRB) anthocyanins on the mice colon microbiota by feeding mice 10% w/w freeze-dried BRB powder for 6 weeks. 16S rRNA gene sequencing revealed that BRB anthocyanins significantly altered luminal abundances of Firmicutes (*Clostridium* spp.) and Bacteroidetes (*Barnesiella* spp.).

A polyphenol-rich diet has been related to increased abundance of beneficial bacteria like *Bifidobacterium*, *Lactobacillus*, *Akkermansia muciniphila* and *Faecalibacterium prausnitzii* (302). *A. municiphila* is an obligate anaerobe bacterium with the capacity to restore mucus layer thickness and gut barrier function (303). A study in C57BL/6J mice fed a high-fat diet (HFD) supplemented with grape polyphenols, reported an intestinal bloom of *A. muciniphila*. This polyphenols-enriched diet also prevented HFD-induced metabolic dysfunctions, lowering systemic inflammation and improving gut barrier integrity (304). In 2016, Moreno-Indias (305) and colleagues investigate the effects of red wine polyphenols on the modulation of gut microbial populations and reduction of markers related to metabolic syndrome. The authors involved 10 patients with metabolic syndrome (MS) and 10 healthy volunteers in a randomized, crossover intervention study, with subjects consuming red or de-alcoholized red wine over a 30 day period. In MS-patients, red wine polyphenols enhance the growth of *Lactobacillus* and butyrate-producing bacterium *F. prausnitzii.*

Similarly, an increase in urinary concentrations of syringic-acid, *p*-coumaric acid, 4-hydroxybenzoic acid and homovanillic acid was observed alongside a significant increase of *Bifidobacterium*, after red wine or dealcoholized red wine consumption for 20 days (306). It was not established whether these compounds derived from gut microbial metabolism, but previous studies observed that syringic, *p*-coumaric and homovanillic acids may all come from malvidin and delphinidin degradation from different strains of *Bifidobacterium* and *Lactobacillus* genera. In a double-blind randomized controlled trial involving 66 men, a significant increase in *Anaerostipes* was observed after consumption of a polyphenol-rich extract from the fruit *Aronia melanocarpa*, thus suggesting the role of some flavonoids (mainly quercetin) in modulating the growth of this butyrate-producing bacterial genus (307). Interestingly, Most *et al*. (2017) (308) highlighted some differences between overweight men and women response to 12-week EGCG and resveratrol supplementation, thus suggesting the role of sex in modulating differences in gut microbiota composition. All these results stress the attention on the complex cross-talk involving both human and microbial metabolism, including some interactions with the host's endocrine function.

On the other hand, gut microbes are able to metabolize phytochemicals, influencing their bioavailability and thus generating several bioactive compounds with *in vivo* activity (309). For example, urolithin A, a microbial metabolite of ellagitannins, increased muscle function in both young and old C57BL/6 mice, assessed by a measurement of exercise capacity before and after treatment (310)**.** Microbial polyphenols metabolites may also exert their beneficial effects within the intestinal tract. Urolithin A has been reported to inhibit metastasis of in human sw620 colorectal cancer cell lines (311). Moreover, beneficial effects of polyphenol microbial metabolites were observed by incubating human adenoma cells LT97 with dihydroxyphenylacetic acid (ES) and 3-(3,4-dihydroxyphenyl)-propionic acid (PS), microbial metabolites of quercetin and chlorogenic acid, respectively (312). Polyphenol metabolites significantly upregulate glutathione S-transferase T2 (GSTT2) expression and decreased cyclooxygenase-2 (COX-2), thus confirming their anti-inflammatory and chemopreventive potential.

Plant polyphenols are reported to modulate several inflammation-associated cellular pathways. NF-κB is a group of transcription factors involved in immune function control, which mediates the expression of COX-2 and the synthesis of numerous pro-inflammatory cytokines (313). During chronic and low-grade systemic inflammation, typical of obese and diabetic subjects, immune cells produce excessive amount of reactive oxygen species (ROS), which can also reinforce the inflammatory response mediated by NF-κB (314,315). As well documented in several studies, many

polyphenols exert their anti-inflammatory effect by negative regulation of NF-κB. In an osteoarthritic mouse model, mesenchymal stem cells treated with curcumin mediated a therapeutic effects on animals, downregulating NF-κB in chondrocytes and slowing OA progression (316). Another study from Ghasemi *et al*. (2019) (317) reported an anti-proliferative effect of curcumin in Hella human cervical cancer monolayers cell cultures and spheroids models. Curcumin exerted its anti-cancer and anti-inflammatory effects through the impairment of NF-κB pathways, suggesting its potential role in cancer therapy. Modulation of NF-κB has also been documented in relation to EGCG. Its role in inhibition of NF-κB inflammatory responses has been demonstrated in human bronchial epithelial cells (318) and in colon cancer cells (319). EGCG likewise exhibited anti-hypertensive and anti-thrombogenic properties by suppressing NF-κB pathway. Reddy and colleagues (2020) (320) recently demonstrated EGCG's ability in regulating endothelial function, suppressing inflammatory responses in human coronary artery endothelial cells (HCAECs). This underpins several epidemiological and cohort studies that found associations between CVD and EGCG supplementation (321,322).

Among gut microbiota fermentation products, SCFA have been widely studied in association with host health and immune function. As discussed in Chapter 3, acetate, propionate and butyrate are the most abundant SCFA in human colon (109). Their production can be modulated by dietary phytochemicals. Parkar and colleagues (2013) (323) employed an *in vitro* batch fermentation model to analyze gut microbial interactions with polyphenols chlorogenic acid, caffeic acid, rutin and quercetin. Fresh human fecal slurry was mixed with a sterile broth and then incubated with each of the polyphenols or inulin as control, under anaerobiosis, with shaking for 72 h. An overall increase in bacterial relative abundances was observed in all fermenta generated from microbial breakdown of polyphenols, and this was accompanied by increased generation of SCFA. In particular, an increase in propionate was noted with the substrate rutin, thus confirming previous studies observing that the propionate-producers *Bacteroides* constitutively generate glucosidases enzymes required for rutin breakdown (324,325). Moreover, several studies observed that different bacteria from rats and human intestine, including *Eubacterium ramulus* and *Clostridium orbiscidens*, were associated with quercetin fermentation, leading to the formation of both acetate and butyrate (326,327).

7.2 Brassica vegetables and their health effects

Cruciferous or Brassica vegetables include a large number of edible varieties and they are widely distributed around the world. In recent years, a strong interest in *Brassicaceae* health promoting

properties has emerged, due to scientific evidence demonstrating their anti-inflammatory and anti-oxidant properties (328). Different case-control studies demonstrated that regular consumption of cruciferous vegetable is inversely associated with stomach (329), ovarian (330), bladder (331) cancer risk, thus motivating further studies on the underlying mechanisms of action and ultimately, randomized control trials t prove cause and effect between ingestion of *Brassicaceae* and reduction in biomarkers of disease risk.

The unique characteristic of this plant family is its content of glucosinolates, sulfur-containing metabolites serving as defense compounds in the plant (332). Most of beneficial properties related to Brassica consumption have been supposed to be due to glucosinolates and to their metabolites. Glucosinolates (GLS) can be hydrolyzed by myrosinase enzymes, generating isothiocyanates, thiocyanates and other molecules that exert an *in vivo* activity. Myrosinases are physically separated from glucosinolates in intact plant cells, but they can come into contact after chopping during food preparation (333). On the other hand, the cooking process completely inactivates myrosinase, thus inhibiting the formation of glucosinolate derivatives (334). Several studies considered the role of GLS and metabolites in preventing the risk associated with inflammatory diseases. Lohning and colleagues (2021) (335) recently employed an array of *in vivo* and *in vitro* techniques to investigate the role of 6-(methylsulfinyl)hexyl isothiocyanates in the alleviation of inflammatory bowel disease (IBD) in mice. The immune response in IBD results from the activation of several signaling pathways, including NF-κB (336). Since glycogen synthase kinase 3 beta (GSK-3β) is a potent driver of inflammation which regulates the nuclear factor-kappa B (337), the authors investigated a potential role for 6-MITC as a GSK-3β inhibitor for the alleviation of IBD. Combining results from a murine macrophage cell line and from a murine model of colitis, they demonstrated the role of 6-MITC in alleviating inflammation through competitive inhibition of GSK-3β/ NF-κB pathway. Another study from Zeng *et al.* (2021) (338) demonstrated that the isothiocyanate sulforaphane was able to exert its anti-inflammatory activity through the modulation of TLR pathway in monocyte-derived macrophages after stimulation with LPS.

Several of Brassica related benefits are mediated by human gut microbiota. Different bacteria isolated from the mammalian gut, including *Enterobacteriaceae* (339), *Bifidobacterium* spp. (340), *Bacteroides* spp. (341) and *Lactobacillus* spp. (342), appear to have myrosinase-like glycoside hydrolases able to cleave GLS. Hence, once GLS reach the colon, they undergo microbial myrosinase hydrolysis generating isothiocyanates (ITCs) and nitriles (343). Glucoraphanin (GRP) is the major GSL found in broccoli (344). Upon hydrolysis, GRP produces the bioactive ITC sulforaphane (SFN),

which has anti-inflammatory and chemopreventive properties. As an example, sulforaphane ameliorated the clinical picture in a mouse model of alcoholic liver fibrosis, by acting as a suppressor of LPS/TLR-4 inflammation pathway (163). In another study (164), sulforaphane was able to reverse LPS/IFN-γ-mediated inflammation *in vitro*. Another mechanism through which GLS metabolites exert their beneficial effects involves aryl hydrocarbon receptor (AhR). AhR constitutes one of the most studied pathway involved in anti-cancer properties of Cruciferous vegetables, inhibiting NF-κB-mediated inflammation and increasing Nrf2 signaling pathway (166–168). Microbial myrosinase present in the human intestine is able to convert GLS into AhR ligands (169). Taken together, these findings suggest that SFN, commonly found as a result of Brassica microbial fermentation, is able to counteract different inflammation, states including metabolic endotoxemia.

Several studies also reported changes in GM composition and metabolism driven by Brassica consumption. C57BL/6 mice fed a high-fat diet supplemented with kale (*B. oleracea* var *acephala*) resulted in lower F/B ratio and increased *Bacteroides thetaiotaomicron* abundances in faeces when compared to the control high-fat diet. Moreover, mice fed kale showed reduced inflammatory parameters in adipose tissue and enhanced GM metabolic functions, including glycan degradation and xenobiotic metabolism (345). In a human controlled feeding, randomized, crossover study, daily consumption of cooked broccoli prepared with raw daikon to provide a source of myrosinase, significantly modulated GM composition, lowering F/B ratio and increasing *Bacteroides* by 8% relative to a control diet containing no Brassica (346). Broccoli consumption also seemed to increase different endocrine and metabolic pathways as a result of a functional analysis performed using the predictive tool PICRUSt. These evidences support the hypothesis that Brassica strongly influence the gut microbiota composition, modulating the community structure and thus its metabolic function. The reciprocal interaction between gut microbes and Cruciferous vegetables underlies many of the beneficial effects of these plants.

8. Fermented foods

In 2017, Marco and colleagues defined food fermentation as 'a controlled microbial growth and enzymatic conversions of major and minor food components' (30). Fermentation has been used since ancient times to preserve a wide variety foods, whether of vegetable or animal origin and fermented foods and beverages still account for a major part of human diets. Traditional fermented foods principally include milk derivatives (e.g. chesse and yoghurt), cereal-based foods, fruits, vegetables, bier and wine. Food fermentation is a transformative process. Starting raw materials are

progressively modified (i.e. fermented) by starter cultures or spontaneous microorganisms (i.e. naturally present in the raw food or processing environment), thus acquiring new properties, including flavor and aroma, preservation or texture (30,347–350). Moreover, as the fermentative process can result in reduction in anti-nutrients and toxic compound removal, fermentation can contribute to extend food shelf-life and food safety (85).

Depending on which food category is considered, several taxa of fermenting microorganisms could be spontaneously involved or selectively employed to produce fermented foods. Lactic acid bacteria (LAB) belonging to *Lactobacillus*, *Lactococcus*, *Leuconostoc*, *Pediococcus* and *Streptococcus* genera have been identified as the most important bacteria involved in food fermentations and some strains wihtin these genera have potential probiotic properties (30,349,351). Probiotics are defined by FAO/WHO as 'live microorganisms which when administered in adequate amounts confer a health benefit on the host'(352). Each LAB strain has unique genetic traits that may lead to the expression of different phenotypes and, to date, the genetic basis for the probiotic properties is still not well defined. As an example, *Escherichia coli* species comprehends significant pathogenic strains, including enterohaemorragic *E. coli* O157:H7 and uropathogenic *E.coli,* but also the probiotic strain Nissle 1917, which probiotic activity involved competition with pathogens (353), protection of mucosal integrity and modulation of gut barrier function (354,355). Nissle is phylogenetically closely-related to enterohaemorragic and uropatogenic *E. coli* (356). However, slight (and still incompletely characterized) differences in its macromolecular structures may drive its distinct and beneficial interactions with host tissues, thus highlighting the unicity of strain-related probiotic traits (357,358).

For this reason, not all LAB belonging to the same genera or to the same species could drive the same beneficial effect when ingested in fermented foods or in probiotics. These differences have been clearly demonstrated by Berger and colleagues in 2007, who analyzed a set of *Lactobacillus acidophilus* by multilocus sequence analysis, DNA typing, microarray analysis and *in silico* whole-genome alignments. This polyphasic analysis demonstrated a stepwise decrease in similarity between members of the *L. acidophilus* group, thus suggesting a vertical evolution of bacteria belonging to this species (359). In a previous study, whole-genome transcriptional profiling of *L. acidophilus* revealed the key role of environmental and growing conditions (pH, nutrients concentrations) in impacting the expression of genes involved in the probiotic or beneficial activity (360).

LAB contained in fermented foods have been widely investigated, since they are supposed to exert beneficial effects in human health and disease. Some of the microorganisms present in fermented foods survive transit through the gastrointestinal tract and reach the colon, even though their presence appears to be transient. Milani *et al.* (2019) reported the transient colonization of human gut by Parmesan cheese bacteria during a pilot study involving 20 healthy individuals (361). Enrolled subjects were requested to eat 45 g/day of fresh Parmesan cheese for 14 days. Among them, and a subgroup of 10 individuals drank 200 ml of pasteurized cow's milk containing *Bifidobacterium mongoliense* BMONG18, each day during and after the seven days of Parmesan cheese consumption (Milk group). Data from 16S rRNA gene microbial profiling from feces revealed that BMONG18 successfully colonized gut in individuals of the Milk group, even if a decrease in its abundance was observed 1 week after removal of Parmesan cheese from the daily diet. Zhang and colleagues (2016) investigated the permissivity (i.e. colonization resistance) of resident gut microbiota for transient foodborne bacteria (362). Following fermented milk product containing five different LAB strains to both conventional and gnotobiotic (i.e. with a defined gut microbiota) rats, 16S rRNA analysis revealed inter-individual variability in resistance and resilience mechanism in response to foodborne bacteria. Different probiotic strains belonging to the same species can mediate different physiological effects in the gut. Mujagic and colleagues (2017) (363) investigated the effects on three *Lactobacillus plantarum* strains on small intestinal barrier function and gut mucosal gene transcription in a randomized controlled trial. Ten healthy subjects partecipated in four intervention periods, each consisting of 7-day oral intake of either *L. plantarum* WCFS1, CIP104448, TIFN101 or placebo, followed by a 4 weeks wash-out. At the end of the intervention, TIFN101 strains showed the most pronounced probiotic activity with specific gut barrier protection effect, while these effect was less pronunced in the other strains, thus confirming that the probiotic activity is highly strain dependent and could considerably differ within the same species. Nonetheless, foodborne microorganisms may still exert beneficial effects during their period of stay in the gut, through competition with pathogenic bacteria or by producing fermentation-derived metabolites with health benefits (351,364). A recent study from Kaur and colleagues (2021) (365) reported potential protective effects of *Lactobacillus rhamnosus* MTCC-5897 on gut health in a murine ulcerative colitis model. Consumption of whey fermented with probiotic *L. rhamnosus* MTCC-5897 significantly improved intestinal barrier integrity and immune homeostasis in mice.

As already mentioned above, some fermented foods could be considered as probiotics because of their content of certain *Lactobacillus* strains and other fermentative bacteria, which directly pass from

food to gut. Consumption of black barley fermented with *Lactobacillus plantarum* JCM15041 partially restored diet-induced fatty liver in rats under high fat diet (366). Twenty-eight SPF Sprague Dawley rats were randomly divided into a normal control group receiving standard diet (NC), a high fat diet (HF), a group receiving high fat diet and *L. plantarum* (HL) and one receiving the high fat diet supplemented with fermented black barley (HB). After 12 weeks rats fed HB diet showed significant inhibition in body weight increase and decreased fat accumulation in liver and abdominal adipose tissue when compared with the other groups, without differences in feed intake. Moreover, common indicators of liver function (i.e. serum levels of alanine aminotransferase and aspartate aminotransferase) where significantly restored in HB group. These findings suggest the role of fermented foods in preventing chronic diseases associated with modern Western style diets. Also, several studies described health benefits of fermented black tea (Kombucha) in mice (367,368), which antidiabetic and antioxidant effects were found to be more effective than non-fermented black tea. Alleviation in diabetic symptoms and comorbidities were observed in association with consumption of kefir, 'a natural complex fermented milk product containing more than 50 species of probiotic bacteria and yeast' (369). Bourrie *et al.* (2018) (370) observed an improvement in plasma and liver lipid profile in mice fed high-fat diet supplemented with kefir, suggesting that kefir is able to counter high-fat diet metabolic unbalances. A correlation between kefir healthy properties and gut microbiota modulation was recently reported from Gao and colleagues, who investigated the role of kefir milk (KM) consumption in human microbiota-associated rats under high-fat diet conditions. The association between adiposity gene expression and regulation of intestinal bacteria populations raised the idea of using fermented foods as a potential functional foods to reduce fat deposition. All of these findings further support the role of fermented foods and their microbiota in modulating host health.

8.1 Brassica as an example of traditional fermented food

Fermented *Brassicaceae* vegetables represent an example of ubiquitous and traditionally fermented foods. Some of the most famous examples include 'Kimchi', a Korean food prepared seasoning Chinese cabbage (*Brassica rapa*) with a mixture of spices, and Sauerkraut (349). Sauerkraut is the most important European fermented vegetable, deriving from spontaneous malolactic fermentation of fresh white cabbage (*Brassica oleracea* L. var. *capitata*) salted with 2-3% (w/w) sodium chloride (371,372). Among microorganisms driving the Sauerkraut production, *Lactobacillus brevis, L. plantarum, Leuconostoc mesenteroides*, *Pediococcus* spp. and *Weissella* spp. are of special importance (372). Recently, Tanaka and colleagues (2021) (373) evaluated the effects of dietary supplementation

of Nozawana, a fermented Japanese *Brassica rapa* on gut microbiota composition and concurrent health-promoting effects. The authors coupled a pilot intervention study in healthy human volunteers to an *in vivo* animal study. Both in humans and mice, fermented *B. rapa* ingestion improved bowel function as assessed using defecation frequency scores. Interestingly, feeding mice with this fermented vegetable significantly increased interferon-γ (INF-γ) and Tumor necrosis factor-α (TNF-α) production in spleen cells under LPS stimulation, suggesting an improved immune response. In another study, the utilization of *L. mesenteroides* as starter culture for sauerkraut production significantly improved cabbage antioxidant activity in LPS-induced macrophages (374). A detailed study was recently performed to evaluate therapeutic potential of exopolysaccharides by *L. paracaserei* isolated from sauerkraut, whose antioxidant properties have been assessed (375). Similarly, the supplementation of *L. plantarum* Shinshu N-07 isolated from fermented *Brassica rapa* to diet-induced obese mice, significantly decreased epididymal adipose tissue weight and adipocyte size when compared with those fed the unsupplemented high-fat diet (376).

Nielsen and colleagues (2018) investigated the effect of daily sauerkraut supplementation in irritable bowel syndrome (IBS) patients through a randomized double-blinded intervention study (377). Thirty-four Norwegian patients with IBS diagnosed using Rome III criteria, were consuming either pasteurized (control; PS) or unpasteurized sauerkraut (intervention; UPS) as a supplement to their daily diet for 6 weeks and IBS symptoms were assessed using the questionnaire IBS-Symptom Severity Score (IBS-SSS). In both group, a significant reduction on IBS-SSS score was observed between the baseline and end of trial, thus suggesting that the factors responsible for sauerkraut health benefits go beyond the sole presence of viable LAB. However, a limitation of this study was the absence of a control group consuming raw cabbage, thus making it impossible to determine whether the amelioration in IBS-SSS score was related to fermentation metabolites or to the cabbage itself. Besides their content in probiotic strains, fermented *Brassicaceae* are differentiated from all other fermented foods because of their content in phytochemicals. During the fermentation process, bacterial metabolism convert certain compounds to biologically active metabolites (378,379). For example, during Sauerkraut production, glucosinolates undergo complete hydrolysis forming several secondary metabolites such as ascorbigen, indol-3-carbinol (I3C), sulforaphane and allyl isothiocyanate (374,380), all bioactive metabolites which could contribute to the beneficial health effects of sauerkraut (381).

Understanding the importance of Brassica fermented foods could help in discovery of novel therapies for gut inflammation and related diseases. Moreover, including fermented foods in our

diets would improve overall health, acting as a protective factor against low-grade inflammation typical of modern Western lifestyle (30).

9. The potential of food chain microbiomes to improve sustainability, productivity and food quality

Population growth, dramatic changes in demography, increased food demand and environmental vulnerability all represent current and pressing societal challenges for the near future. The world's population is expected to increase from 7.7 billion currently to 9.7 billion in 2050, according to the World Population Prospects from United Nations (382). As the population grows, so do its demands for food, water sources and health care. The global food production represents one of the largest footprint caused by humans on the whole planet and constitutes the factor on which we can operate most immediately to reverse the trend (1,2). The adoption of healthy and sustainable dietary habits and food systems has been recognised as a key strategy to prevent all forms of malnutrition and environmental damage from food production and consumption practices (383). As an example, the choice of vegetable proteins cause fewer adverse environmental effects than does animal source proteins and this is true across different environmental indicators such as land and water use, greenhouse emission and eutrophication potential (1). In 2018, Hilborn and colleagues (384) examinated the environmental impact of different sources of animal protein production, including livestock, aquaculture and capture fisheries. Compared to terrestrial animal production, fish and seafood are considered to have a lower environmental impact, although with many differences between specific products or depending on the production/capture method being used. The EAT Lancet Commission on Healthy Diets from Sustainable Food Systems recommended fish consumption into the healthy reference diet (1). Fish (used in the broadest meaning to include all aquatic animals) has a wide range of nutritional benefits. It is rich in omega-3 fatty acids, which regular consumption is associated to reduced risk of cardiovascular disease (385,386) and is considered to be essential in supporting child neurodevelopment during pregnancy (387,388). Fish also provides highly bioavailable micronutrients, including vitamins A and D, calcium, iron, iodine and zinc (389).

Global food fish consumption increased by 122% from 1990 to 2018 and fish production is growing at a constant average annual rate of 3.2% (2). However, this is largely due to an increase in aquaculture production rates, while supply from capture fisheries is relatively stable since 90s (2).

This trends are mainly attributable to several environmental issues hindering fishing practices, primarily the excessive exploitation and potential collapse of wild fish stocks, overfishing and bycatch (2). In this scenario, future supply of seafood should be provided by aquaculture, which currently confirmed its record as the fastest growing food production sector in terms of global annual production (2). The total European production of fish by aquaculture was 2,570,242 tons in 2019, with salmon, trout, seabream, seabass and carp species representing 95% of the total European production (390). However, feeds for aquacultured species have historically relied on the use of fish meal and fish oil derived from wild fisheries, as main protein and fat sources. Inclusion of wild derived fish products in aquafeeds is no longer tenable due to cost and impact on wild fish stocks (391). For this reason, more cost effective and innovative ingredients are now being studied as sustainable alternatives. Vegetable protein-rich feeds (VM) have been proposed as replacements for fishmeal in aquafeeds because of their cost-effectivenness (392,393). However, when compared to fishmeal or to other alternative ingredients, such as animal by-products, VM showed higher environmental impact in terms of carbon footprint (394). Moreover, VM contain anti-nutritional factors and complex indigestible carbohydrates, are poor in essential amino acids and omega-3 (395) and their use in feeds for carnivorous species often lead to adverse effects on fish health, including intestinal enteritis, and thus on fish growth performance (395). For these reasons, new feed ingredients, including insect meals and animal-by product meals are being investigated as innovative protein sources for aquafeeds. Both these alternatives have a nutritional composition comparable to feeds containing FM, but with a lower carbon footprint (394). The analysis of these novel ingredients is now focused on their effects on animals' health, which determine growth rates.

Animal wellbeing is strongly influenced by gut health. As in the case of humans, fish gut health is essential for nutrient absorption, for immune system activity and to prevent inflammation (396,397). The gut microbiota and its metabolites play a key role in maintaining gut health, protecting intestinal integrity and thus supporting fish growth performances (398,399). It is crucial to evaluate GM:fish health relationship in the search for more sustainable and efficient feeds, since the GM composition is strictly influenced by aquafeeds ingredients (400). As an example, insect meal inclusion in rainbow trout feed has been shown to promote the growth of putative beneficial genera *Mycoplasma, Actinomyces, Corynebacterium* and *Lactobacillus* (401). Moreover, a stable microbial community is essential to protect towards pathogens invasion. Irianto and Austin (2002) demonstrated that feeding rainbow trout with probiotics containing *Aeromonas hydrophila, Vibrio fluvialis, Carnobacterium* sp. and *Micrococcus luteus* for 2 weeks, significantly stimulated humoral and

cellular immunity, thus enhancing fish immune function (402). Similar results were obtained by Panigrahi (2004) and Balcázar (2007) who observed enhanced innate immune response in trout after administration of probiotic *Lactobacillus, Lactococcus* or *Leuconostoc* strains (403,404). For this reason, supporting the growth of beneficial microbial communities in fish gut through innovative feed ingredients may be the future strategy to improve fish health and aquaculture productivity.

A deeper analysis of food chain microbiomes would be useful in finding new sustainable ingredients for aquafeeds. In recent years, some studies begun to suggest the use of microorganisms, particularly fungi, to to convert agro-industrial wastes to obtain products with high nutritive value and increased digestibility. Utilization of human food waste as non conventional resource for animal feed is achieved by a solid-state fermentation (SSF) (405). During this process, waste material is progressively fermented by microorganism, thus producing biomass with high protein, fat, vitamins and amino acids profile (406). Rajesh and colleagues investigated the application of fungi *Aspergillus niger* to enhance vegetable waste through SSF. After approximately 1 week of fermentation, the nutritional value of the vegetable waste was significantly improved, therefore becoming an ideal candidate for use in aquafeed industry (407). Interestingly, also aquafeed-associated microbiome could play a key role in determining fish health, being transferred from feed ingredients to the host and thus fortifying the fish immune function. Hamid *et al.* (2021) (408) recently evaluated the effects of probiotic *Enterococcus hirae* isolated from vegetable waste on hybrid catfish (*Clarias gariepinus* × *Clarias macrocephalus*) immune response, growth and disease resistance. Both short- and long-term supplementation of *E. hirae* in feeds significantly improved fish growth performances, gut health and immune protection against the *Aeromonas hydrophyla* infection. Food chain microbiomes and in particular microbiomes associated with fish gastrointestinal tract and with the aquafeeds production therefore pose considerable thus far untapped potential to improve cost effectiveness, production yields, animal welfare and nutritional quality of farmed fish.

10. Conclusive remarks

Several aspects should be taken into account when talking about healthy dietary patterns. Due to constant population growth, to the spreading of under- and over-nutrition and to pressing environmental challenges, a universal healthy reference diet should be designed in order to be nutricious, sustainable and health-promoting (1). Scientific knowledge provide a basis to design the reference healthy diet, which should be rich in fruits and vegetables, whole grains, nuts and unsaturated oils, while low in red meat, processed foods and simple sugars (1). Data from several

large scale cohort observational studies offered robust evidence regarding the correlation between different dietary patterns and healthy outcomes (34,39,44,49). Together with a reduction in red meat intake, healthy reference diet should be based on an increased fish consumption, about two servings per week according to the EAT-Lancet Commission (1). Regular fish intake has been associated with reduced risk of cardiovascular, hepatic, neurodegenerative and inflammatory diseases (386,409,410). Fish is rich in omega-3 fatty acids, which are well-known regulators of various inflammatory pathways, including those mediated by NF-kB and TLR (411,412). These observations pose fish as one of the most important component of healthy eating patterns. Fermented foods, especially fermented plant foods should also be introduced into our modern healthy diets. Fermented vegetables have a unique fiber and polyphenols profile associated with their health potential (378,379). Different studies reported anti-inflammatory and gut health protective properties of vegetable fermented foods, thus justifying their introduction in our diets (373,377,381). The Mediterranean diet constitute an example of healthy diet. Its consumption has been associated with decrease risk of obesity, diabetes, cardiovascular disease and cancer (1,35,49,413), together with lower environmental impact when compared to our modern Western dietary pattern (WDP) (52–54). The Industrial and green Revolutions, together with modern mas production of cheap ultraprocessed foods, has brought with it a drastic change in our eating habits, which today are characterized by high simple sugar and saturated fats intakes, as well as high intakes of red meat (58,59). The macronutrient imbalance, together with high levels of glycated metabolites (i.e. AGE) coming from excessive consumption of ultraprocessed foods, correlate modern WDP to chronic low-grade inflammation, thus linking to obesity, metabolic syndrome, insulin resistance, dyslipidemia and all cause mortality (67,68).

Together with the definition of a reference healthy diet, a transformation of the global food system is urgently needed. The modulation of environmental microbiomes along the food chain could represent a concrete and innovative approach to reach agri-food sustainability. Microbes are involved in many and disparate processes, from biogeochemical cycles, organic matter degradation, animal and humans health to food processing. A complete understanding of their metabolic potential along the food chain is essential to reach overall health and sustainability. By understanding which bacteria are responsible for food spoilage we could reduce food waste and losses while increasing food safety and valorizing food wastes into new innovative ingredients, including feeds for aquaculture (414).

A microbial interaction of great interest is the one connecting diet, the human gut microbiota and health. Diet strongly influences the gut microbiota composition and its metabolic activity (103,249). Several dietary components interact with the intestinal bacteria community, which is known to impact metabolic functions as well as immune responses in the host (141,187). GM is essential to assimilate complex dietary nutrients, as well as maintaining gut barrier function and immune system homeostasis (178). The beneficial activity of the GM starts from the fermentation of complex carbohydrates and other dietary components, which leads to the production of several microbial metabolites including SCFA, phenolic derivatives and many other bioactive compounds (109,309). All these molecules interact with different host cell signaling receptors, acting as anti-inflammatory, antioxidant, anti-cancer mediators and regulators of host energy metabolism and storage (111,252,415). For this reason, dysregulation of GM composition related to pathologic conditions (including diabetes, obesity and other chronic inflammatory diseases), or caused by a Western style diet affects not only gastrointestinal tract, but also influence overall health of the host.

Aquaculture is one of the most important food production sectors, but more sustainable feeds replacing fish meals and fish oils are required in order to preserve the marine environment and to reduce costs (2). In the search of innovative feed, the impact of alternative ingredients on fish GM composition should be taken into account. In fact, alterations in gut microbial communities have been associated with adverse effects on fish health, including impaired immune system activity, reduced nutrients absorption and reduced growth performances (395,396).

Although the role of microbiomes in health and sustainability has been widely studied and investigated, we still know very little about microbial communities and their flux along the food chain. More studies are needed to fully characterize food chain microbiomes, to link diet:microbes interaction in the gut with the host health. Recognizing the role of gut microbiomes in supporting sustainable, nutricious and health-promoting diet is essential to move towards a positive, sustainable and healthy future. A better manipulation of these interactions could improve both nutritional and environmental sustainability of the food chain connecting humans, animals and environment into the 'One health' concept.

Aim of this PhD thesis

The overall aim of my PhD thesis is to investigate how sustainable, health-promoting and nutritious diets could be achieved by exploiting and modulating the food chain microbiomes with a particular focus on diet:microbe interactions in the gut. This was achieved through the following objectives:

- To investigate the impact of the modern Western-style diet on the mammalian gut microbiota and specifically investigate whether dietary advanced glycation end products (AGE) common in ultra-processed foods, could induce changes in the gut microbiome similar to those reported for metabolic disease and investigate whether these microbiota changes might be linked to the observed detrimental impact of AGE on host systemic inflammation.
- To investigate whether whole plant foods, in this case two species important for the local food production system, can mediate a beneficial modulation of the gut microbiota, increasing abundance of health promoting bacteria, production of biologically active beneficial metabolites and improving markers of gut health using an *in vitro* fermentation system and models of intestinal mucosal integrity and immune function.
- To characterize the successional development of a locally produced fermented food, create a biobank of lactic acid bacteria of putative biotechnological and health (probiotic) importance, and investigate whether sauerkraut water can impact on markers of gut health using preclinical *in vitro* models of intestinal integrity and immune function.
- To investigate how novel, sustainable and environmentally friendly animal feeds impact on the composition and immune effects of the intestinal microbiota of farmed trout and evaluate the potential of the fish intestinal microbiome as a modifiable target to improve trout health and production yields.

The thesis is organized into 6 chapters. The first chapter is a descriptive literature review discussing the evolution of healthy human dietary habits, the composition and health effect of the human gut microbiota, how the foods known to make up healthy dietary patterns appear to work through the gut microbiota, and how food chain microbiomes and in particular, gut associated microbiomes, might be harnessed to improve dietary sustainability and nutritional quality. Chapter 2 describes how the gut microbiota (GM) could mediate some of the harmful metabolic effects of

AGE-enriched diets in mice, identifying the GM as a possible modifiable risk factor in metabolic and inflammatory diseases associated with the modern Western-style diet (MWD). Chapter 3 and 4 report respectively *in vitro* experiments investigating whether two locally important brassica crops, Broccolo of Torbole and *Moringa oleifera*, through their glucosinolates and polyphenols compositions and their interactions with the GM, might improve markers of gut health. Chapter 5 reports a multi-disciplinary characterization of organic, locally produced sauerkraut, in which culture based microbiology, metagenomics, NMR based metabolomics and *in vitro* intestinal epithelium models were employed to characterize both the associated food chain microbiome and investigate whether sauerkraut water could improve markers of gut health. Finally, Chapter 6 investigates how the intestinal microbiome of farmed trout may be modulated by novel, environmentally friendly and sustainable diets, to improve the gut health, immune function and production of farmed trout, an important source of nutritious fats and non-red meat derived protein for a sustainable and healthy human diet.

References

1. Willett W, Rockström J, Loken B, Springmann M, Lang T, Vermeulen S, et al. Food in the Anthropocene: the EAT–Lancet Commission on healthy diets from sustainable food systems. The Lancet. 2019 Feb;393(10170):447–92.

2. FAO. The State of World Fisheries and Aquaculture 2020 [Internet]. 2020 [cited 2021 May 20]. Available from: http://www.fao.org/documents/card/en/c/ca9229en

3. WHO. Obesity and overweight. Updated February 2018. [Internet]. 2018. Available from: https://www.who.int/en/news-room/fact-sheets/detail/obesity-and-overweight

4. Koohafkan P, FAO, editors. The state of the world's land and water resources for food and agriculture: managing systems at risk. Abingdon: Earthscan [u.a.]; 2011. 285 p.

5. Poore J, Nemecek T. Reducing food's environmental impacts through producers and consumers. Science. 2018 Jun 1;360(6392):987–92.

6. The Lancet. A future direction for tackling malnutrition. The Lancet. 2020 Jan;395(10217):2.

7. Tam BT, Morais JA, Santosa S. Obesity and ageing: Two sides of the same coin. Obesity Reviews [Internet]. 2020 Apr [cited 2021 May 24];21(4). Available from: https://onlinelibrary.wiley.com/doi/abs/10.1111/obr.12991

8. Kenchaiah S, Evans JC, Levy D, Wilson PWF, Benjamin EJ, Larson MG, et al. Obesity and the Risk of Heart Failure. N Engl J Med. 2002 Aug;347(5):305–13.

9. Ballak DB, Stienstra R, Tack CJ, Dinarello CA, van Diepen JA. IL-1 family members in the pathogenesis and treatment of metabolic disease: Focus on adipose tissue inflammation and insulin resistance. Cytokine. 2015 Oct;75(2):280–90.

10. Boden G, Homko C, Barrero CA, Stein TP, Chen X, Cheung P, et al. Excessive caloric intake acutely causes oxidative stress, GLUT4 carbonylation, and insulin resistance in healthy men. Sci Transl Med. 2015 Sep 9;7(304):304re7-304re7.

11. Sjöström L, Larsson B, Backman L, Bengtsson C, Bouchard C, Dahlgren S, et al. Swedish obese subjects (SOS). Recruitment for an intervention study and a selected description of the obese state. Int J Obes Relat Metab Disord. 1992 Jun;16(6):465–79.

12. Sjöström L, Narbro K, Sjöström CD, Karason K, Larsson B, Wedel H, et al. Effects of Bariatric Surgery on Mortality in Swedish Obese Subjects. N Engl J Med. 2007 Aug 23;357(8):741–52.

13. Sjöström L, Lindroos A-K, Peltonen M, Torgerson J, Bouchard C, Carlsson B, et al. Lifestyle, Diabetes, and Cardiovascular Risk Factors 10 Years after Bariatric Surgery. N Engl J Med. 2004 Dec 23;351(26):2683–93.

14. Sjöström L, Gummesson A, Sjöström CD, Narbro K, Peltonen M, Wedel H, et al. Effects of bariatric surgery on cancer incidence in obese patients in Sweden (Swedish Obese Subjects Study): a prospective, controlled intervention trial. The Lancet Oncology. 2009 Jul;10(7):653–62.

15. Carlsson LMS, Peltonen M, Ahlin S, Anveden Å, Bouchard C, Carlsson B, et al. Bariatric Surgery and Prevention of Type 2 Diabetes in Swedish Obese Subjects. N Engl J Med. 2012 Aug 23;367(8):695–704.

16. Gregor MF, Hotamisligil GS. Inflammatory Mechanisms in Obesity. Annu Rev Immunol. 2011 Apr 23;29(1):415–45.

17. Hiilamo A, Lallukka T, Mänty M, Kouvonen A. Obesity and socioeconomic disadvantage in midlife female public sector employees: a cohort study. BMC Public Health. 2017 Dec;17(1):842.

18. Dick K, Schneider JE, Briggs A, Lecomte P, Regnier SA, Lean M. Mendelian randomization: estimation of inpatient hospital costs attributable to obesity. Health Econ Rev. 2021 Dec;11(1):16.

19. Ramasamy A, Laliberté F, Aktavoukian SA, Lejeune D, DerSarkissian M, Cavanaugh C, et al. Direct and Indirect Cost of Obesity Among the Privately Insured in the United States: A Focus on the Impact by Type of Industry. Journal of Occupational & Environmental Medicine. 2019 Nov;61(11):877–86.

20. Finkelstein EA, Fiebelkorn IC, Wang G. State-Level Estimates of Annual Medical Expenditures Attributable to Obesity*. Obesity Research. 2004 Jan;12(1):18–24.

21. Czernichow S, Bain SC, Capehorn M, Bøgelund M, Madsen ME, Yssing C, et al. Costs of the COVID -19 pandemic associated with obesity in Europe: A health-care cost model. Clin Obes [Internet]. 2021 Apr [cited 2021 May 25];11(2). Available from: https://onlinelibrary.wiley.com/doi/10.1111/cob.12442

22. Flegal KM, Kruszon-Moran D, Carroll MD, Fryar CD, Ogden CL. Trends in Obesity Among Adults in the United States, 2005 to 2014. JAMA. 2016 Jun 7;315(21):2284.

23. Peralta M, Ramos M, Lipert A, Martins J, Marques A. Prevalence and trends of overweight and obesity in older adults from 10 European countries from 2005 to 2013. Scand J Public Health. 2018 Jul;46(5):522–9.

24. Masters RK, Powers DA, Link BG. Obesity and US Mortality Risk Over the Adult Life Course. American Journal of Epidemiology. 2013 Mar 1;177(5):431–42.

25. Salvestrini V, Sell C, Lorenzini A. Obesity May Accelerate the Aging Process. Front Endocrinol. 2019 May 3;10:266.

26. Horvath S, Erhart W, Brosch M, Ammerpohl O, von Schonfels W, Ahrens M, et al. Obesity accelerates epigenetic aging of human liver. Proceedings of the National Academy of Sciences. 2014 Oct 28;111(43):15538–43.

27. Lee M, Martin H, Firpo MA, Demerath EW. Inverse association between adiposity and telomere length: The fels longitudinal study. Am J Hum Biol. 2011 Jan;23(1):100–6.

28. WHO, editor. World report on ageing and health. Geneva: WHO; 2015. 246 p.

29. Marchesi JR, Ravel J. The vocabulary of microbiome research: a proposal. Microbiome. 2015 Dec;3(1):31, s40168-015-0094–5.

30. Marco ML, Heeney D, Binda S, Cifelli CJ, Cotter PD, Foligné B, et al. Health benefits of fermented foods: microbiota and beyond. Current Opinion in Biotechnology. 2017 Apr;44:94–102.

31. Roberta AM, Alejandra PG. Quorum Sensing as a Mechanism of Microbial Control and Food Safety. In: Microbial Contamination and Food Degradation [Internet]. Elsevier; 2018 [cited 2021 Aug 20]. p. 85–107. Available from: https://linkinghub.elsevier.com/retrieve/pii/B9780128115152000044

32. Schluter J, Foster KR. The Evolution of Mutualism in Gut Microbiota Via Host Epithelial Selection. Ellner SP, editor. PLoS Biol. 2012 Nov 20;10(11):e1001424.

33. CREA. Linee guida per una sana alimentazione. Ministero della Salute; 2018.

34. Keys A, Aravanis C, Blackburn H, Buzina R, Djordjevic BS, Dontas AS, et al. Seven Countries: A Multivariate Analysis of Death and Coronary Heart Disease [Internet]. 2014 [cited 2021 Aug 24]. Available from: https://0-doi-org.pugwash.lib.warwick.ac.uk/10.4159/harvard.9780674497887

35. Menotti A, Keys A, Blackburn H, Kromhout D, Karvonen M, Nissinen A, et al. Comparison of multivariate predictive power of major risk factors for coronary heart diseases in different countries: results from eight nations of the Seven Countries Study, 25-year follow-up. J Cardiovasc Risk. 1996 Feb;3(1):69–75.

36. Kromhout D, Menotti A, Bloemberg B, Aravanis C, Blackburn H, Buzina R, et al. Dietary Saturated and transFatty Acids and Cholesterol and 25-Year Mortality from Coronary Heart Disease: The Seven Countries Study. Preventive Medicine. 1995 May;24(3):308–15.

37. Trichopoulou A. Traditional Mediterranean diet and longevity in the elderly: a review. Public Health Nutr. 2004 Oct;7(7):943–7.

38. Keys AB, Keys M. How to eat well and stay well the Mediterranean way. 1st ed. Garden City, N.Y: Doubleday; 1975. 488 p.

39. Estruch R, Ros E, Salas-Salvadó J, Covas M-I, Corella D, Arós F, et al. Primary Prevention of Cardiovascular Disease with a Mediterranean Diet Supplemented with Extra-Virgin Olive Oil or Nuts. N Engl J Med. 2018 Jun 21;378(25):e34.

40. Willett WC, Sacks F, Trichopoulou A, Drescher G, Ferro-Luzzi A, Helsing E, et al. Mediterranean diet pyramid: a cultural model for healthy eating. The American Journal of Clinical Nutrition. 1995 Jun 1;61(6):1402S-1406S.

41. Huhn S, Kharabian Masouleh S, Stumvoll M, Villringer A, Witte AV. Components of a Mediterranean diet and their impact on cognitive functions in aging. Front Aging Neurosci [Internet]. 2015 Jul 8 [cited 2021 Oct 12];7. Available from: http://journal.frontiersin.org/Article/10.3389/fnagi.2015.00132/abstract

42. Trichopoulou A, Kouris-Blazos A, Wahlqvist ML, Gnardellis C, Lagiou P, Polychronopoulos E, et al. Diet and overall survival in elderly people. BMJ. 1995 Dec 2;311(7018):1457–60.

43. Salas-Salvadó J, Bulló M, Estruch R, Ros E, Covas M-I, Ibarrola-Jurado N, et al. Prevention of Diabetes With Mediterranean Diets: A Subgroup Analysis of a Randomized Trial. Ann Intern Med. 2014 Jan 7;160(1):1–10.

44. Colditz GA, Manson JE, Hankinson SE. The Nurses' Health Study: 20-Year Contribution to the Understanding of Health Among Women. Journal of Women's Health. 1997 Feb;6(1):49–62.

45. Kromhout D, Menotti A, Alberti-Fidanza A, Puddu PE, Hollman P, Kafatos A, et al. Comparative ecologic relationships of saturated fat, sucrose, food groups, and a Mediterranean food pattern score to 50-year coronary heart disease mortality rates among 16 cohorts of the Seven Countries Study. Eur J Clin Nutr. 2018 Aug;72(8):1103–10.

46. Bao Y, Bertoia ML, Lenart EB, Stampfer MJ, Willett WC, Speizer FE, et al. Origin, Methods, and Evolution of the Three Nurses' Health Studies. Am J Public Health. 2016 Sep;106(9):1573–81.

47. Romanos-Nanclares A, Willett WC, Rosner BA, Collins LC, Hu FB, Toledo E, et al. Healthful and unhealthful plant-based diets and risk of breast cancer in U.S. women: results from the Nurses' Health Studies. Cancer Epidemiol Biomarkers Prev. 2021 Jul 21;cebp.EPI-21-0352-E.2021.

48. Willett W. Intake of trans fatty acids and risk of coronary heart disease among women. The Lancet. 1993 Mar;341(8845):581–5.

49. Yaskolka Meir A, Rinott E, Tsaban G, Zelicha H, Kaplan A, Rosen P, et al. Effect of green-Mediterranean diet on intrahepatic fat: the DIRECT PLUS randomised controlled trial. Gut. 2021 Jan 18;gutjnl-2020-323106.

50. Tsaban G, Yaskolka Meir A, Rinott E, Zelicha H, Kaplan A, Shalev A, et al. The effect of green Mediterranean diet on cardiometabolic risk; a randomised controlled trial. Heart. 2021 Jul;107(13):1054–61.

51. Li J, Guasch-Ferré M, Chung W, Ruiz-Canela M, Toledo E, Corella D, et al. The Mediterranean diet, plasma metabolome, and cardiovascular disease risk. Eur Heart J. 2020 Jul 21;41(28):2645–56.

52. Gussow JD. Mediterranean diets: are they environmentally responsible? The American Journal of Clinical Nutrition. 1995 Jun 1;61(6):1383S-1389S.

53. Sáez-Almendros S, Obrador B, Bach-Faig A, Serra-Majem L. Environmental footprints of Mediterranean versus Western dietary patterns: beyond the health benefits of the Mediterranean diet. Environ Health. 2013 Dec;12(1):118.

54. Pairotti MB, Cerutti AK, Martini F, Vesce E, Padovan D, Beltramo R. Energy consumption and GHG emission of the Mediterranean diet: a systemic assessment using a hybrid LCA-IO method. Journal of Cleaner Production. 2015 Sep;103:507–16.

55. Popkin BM. Nutritional Patterns and Transitions. Population and Development Review. 1993 Mar;19(1):138.

56. Bodirsky BL, Dietrich JP, Martinelli E, Stenstad A, Pradhan P, Gabrysch S, et al. The ongoing nutrition transition thwarts long-term targets for food security, public health and environmental protection. Sci Rep. 2020 Dec;10(1):19778.

57. Cordain L, Eaton SB, Sebastian A, Mann N, Lindeberg S, Watkins BA, et al. Origins and evolution of the Western diet: health implications for the 21st century. The American Journal of Clinical Nutrition. 2005 Feb 1;81(2):341–54.

58. Hu FB. Dietary pattern analysis: a new direction in nutritional epidemiology: Current Opinion in Lipidology. 2002 Feb;13(1):3–9.

59. Odermatt A. The Western-style diet: a major risk factor for impaired kidney function and chronic kidney disease. American Journal of Physiology-Renal Physiology. 2011 Nov;301(5):F919–31.

60. Monteiro CA. Nutrition and health. The issue is not food, nor nutrients, so much as processing. Public Health Nutr. 2009 May;12(5):729–31.

61. Knorr D, Watzke H. Food Processing at a Crossroad. Front Nutr. 2019 Jun 25;6:85.

62. Monteiro CA, Cannon G, Levy RB, Claro R, Moubarac J-C. The Food System. Ultra-processing. The big issue for nutrition, disease, health, well - being. [Commentary]. World Nutrition. 2012 Dec;3(12):527–69.

63. Martínez Steele E, Baraldi LG, Louzada ML da C, Moubarac J-C, Mozaffarian D, Monteiro CA. Ultra-processed foods and added sugars in the US diet: evidence from a nationally representative cross-sectional study. BMJ Open. 2016 Jan;6(3):e009892.

64. Gupta S, Hawk T, Aggarwal A, Drewnowski A. Characterizing Ultra-Processed Foods by Energy Density, Nutrient Density, and Cost. Front Nutr. 2019 May 28;6:70.

65. Ayton A, Ibrahim A. The dramatic rise of ultra-processed foods. BMJ. 2019 Aug 5;l4970.

66. Martínez Steele E, Juul F, Neri D, Rauber F, Monteiro CA. Dietary share of ultra-processed foods and metabolic syndrome in the US adult population. Preventive Medicine. 2019 Aug;125:40–8.

67. Schnabel L, Kesse-Guyot E, Allès B, Touvier M, Srour B, Hercberg S, et al. Association Between Ultraprocessed Food Consumption and Risk of Mortality Among Middle-aged Adults in France. JAMA Intern Med. 2019 Apr 1;179(4):490.

68. Rico-Campà A, Martínez-González MA, Alvarez-Alvarez I, Mendonça R de D, de la Fuente-Arrillaga C, Gómez-Donoso C, et al. Association between consumption of ultra-processed foods and all cause mortality: SUN prospective cohort study. BMJ. 2019 May 29;l1949.

69. Hall KD, Ayuketah A, Brychta R, Cai H, Cassimatis T, Chen KY, et al. Ultra-Processed Diets Cause Excess Calorie Intake and Weight Gain: An Inpatient Randomized Controlled Trial of Ad Libitum Food Intake. Cell Metabolism. 2019 Jul;30(1):67-77.e3.

70. Rauber F, Steele EM, Louzada ML da C, Millett C, Monteiro CA, Levy RB. Ultra-processed food consumption and indicators of obesity in the United Kingdom population (2008-2016). Meyre D, editor. PLoS ONE. 2020 May 1;15(5):e0232676.

71. Baena M, Sangüesa G, Dávalos A, Latasa M-J, Sala-Vila A, Sánchez RM, et al. Fructose, but not glucose, impairs insulin signaling in the three major insulin-sensitive tissues. Sci Rep. 2016 Sep;6(1):26149.

72. Stanhope KL, Schwarz JM, Keim NL, Griffen SC, Bremer AA, Graham JL, et al. Consuming fructose-sweetened, not glucose-sweetened, beverages increases visceral adiposity and lipids and decreases insulin sensitivity in overweight/obese humans. J Clin Invest. 2009 May 1;119(5):1322–34.

73. Oikonomou E, Psaltopoulou T, Georgiopoulos G, Siasos G, Kokkou E, Antonopoulos A, et al. Western Dietary Pattern Is Associated With Severe Coronary Artery Disease. Angiology. 2018 Apr;69(4):339–46.

74. Fardet A, Rock E. Ultra-Processed Foods and Food System Sustainability: What Are the Links? Sustainability. 2020 Aug 4;12(15):6280.

75. Bar-On YM, Phillips R, Milo R. The biomass distribution on Earth. Proc Natl Acad Sci USA. 2018 Jun 19;115(25):6506–11.

76. Arrigo KR. Marine microorganisms and global nutrient cycles. Nature. 2005 Sep 15;437(7057):349–55.

77. Falkowski PG, Fenchel T, Delong EF. The Microbial Engines That Drive Earth's Biogeochemical Cycles. Science. 2008 May 23;320(5879):1034–9.

78. Agler MT, Spirito CM, Usack JG, Werner JJ, Angenent LT. Chain elongation with reactor microbiomes: upgrading dilute ethanol to medium-chain carboxylates. Energy Environ Sci. 2012;5(8):8189.

79. Marshall CW, Ross DE, Fichot EB, Norman RS, May HD. Electrosynthesis of Commodity Chemicals by an Autotrophic Microbial Community. Appl Environ Microbiol. 2012 Dec;78(23):8412–20.

80. Ito T, Yoshiguchi K, Ariesyady HD, Okabe S. Identification and quantification of key microbial trophic groups of methanogenic glucose degradation in an anaerobic digester sludge. Bioresource Technology. 2012 Nov;123:599–607.

81. Bizukojc M, Dietz D, Sun J, Zeng A-P. Metabolic modelling of syntrophic-like growth of a 1,3-propanediol producer, Clostridium butyricum, and a methanogenic archeon, Methanosarcina mazei, under anaerobic conditions. Bioprocess Biosyst Eng. 2010 May;33(4):507–23.

82. Mbow C, Rosenzweig C, Barioni LG, Benton TG, Herrero M, Krishnapillai M, et al. Food Security. In: Climate Change and Land: an IPCC special report on climate change, desertification, land degradation, sustainable land management, food security, and greenhouse gas fluxes in terrestrial ecosystems. 2019.

83. Scallan E, Hoekstra RM, Angulo FJ, Tauxe RV, Widdowson M-A, Roy SL, et al. Foodborne Illness Acquired in the United States—Major Pathogens. Emerg Infect Dis. 2011 Jan;17(1):7–15.

84. Tamang JP, Cotter PD, Endo A, Han NS, Kort R, Liu SQ, et al. Fermented foods in a global age: East meets West. Comprehensive Reviews in Food Science and Food Safety. 2020 Jan;19(1):184–217.

85. Battcock M, Azam-Ali S. Fermented fruits and vegetables: a global perspective. Rome: Food and Agriculture Organization of the United Nations; 1998. 96 p. (FAO agricultural services bulletin).

86. Marco ML, Sanders ME, Gänzle M, Arrieta MC, Cotter PD, De Vuyst L, et al. The International Scientific Association for Probiotics and Prebiotics (ISAPP) consensus statement on fermented foods. Nat Rev Gastroenterol Hepatol. 2021 Mar;18(3):196–208.

87. Fava F, Rizzetto L, Tuohy KM. Gut microbiota and health: connecting actors across the metabolic system. Proc Nutr Soc. 2019 May;78(02):177–88.

88. Avelar Rodriguez D, Ryan PM, Toro Monjaraz EM, Ramirez Mayans JA, Quigley EM. Small Intestinal Bacterial Overgrowth in Children: A State-Of-The-Art Review. Front Pediatr. 2019 Sep 4;7:363.

89. Hillman ET, Lu H, Yao T, Nakatsu CH. Microbial Ecology along the Gastrointestinal Tract. Microbes and environments. 2017;32(4):300–13.

90. The Human Microbiome Project Consortium. Structure, function and diversity of the healthy human microbiome. Nature. 2012 Jun;486(7402):207–14.

91. Whittaker RH. Vegetation of the Siskiyou Mountains, Oregon and California. Ecological Monographs. 1960 Jul;30(3):279–338.

92. Kim B-R, Shin J, Guevarra RB, Lee JH, Kim DW, Seol K-H, et al. Deciphering Diversity Indices for a Better Understanding of Microbial Communities. Journal of Microbiology and Biotechnology. 2017 Dec 28;27(12):2089–93.

93. Chao A. Nonparametric estimation of the number of classes in a population. Scand J Statist. 1984;11(4):265–70.

94. Hughes JB, Hellmann JJ, Ricketts TH, Bohannan BJM. Counting the Uncountable: Statistical Approaches to Estimating Microbial Diversity. Appl Environ Microbiol. 2001 Oct;67(10):4399–406.

95. Schloss PD, Westcott SL, Ryabin T, Hall JR, Hartmann M, Hollister EB, et al. Introducing mothur: Open-Source, Platform-Independent, Community-Supported Software for Describing and Comparing Microbial Communities. Appl Environ Microbiol. 2009 Dec;75(23):7537–41.

96. Qian X-B, Chen T, Xu Y-P, Chen L, Sun F-X, Lu M-P, et al. A guide to human microbiome research: study design, sample collection, and bioinformatics analysis. Chinese Medical Journal. 2020 Aug 5;133(15):1844–55.

97. Lozupone C, Knight R. UniFrac: a New Phylogenetic Method for Comparing Microbial Communities. Appl Environ Microbiol. 2005 Dec;71(12):8228–35.

98. Lozupone CA, Hamady M, Kelley ST, Knight R. Quantitative and Qualitative β Diversity Measures Lead to Different Insights into Factors That Structure Microbial Communities. Appl Environ Microbiol. 2007 Mar;73(5):1576–85.

99. Derrien M, Alvarez A-S, de Vos WM. The Gut Microbiota in the First Decade of Life. Trends in Microbiology. 2019 Dec;27(12):997–1010.

100. Belizário JE, Napolitano M. Human microbiomes and their roles in dysbiosis, common diseases, and novel therapeutic approaches. Front Microbiol [Internet]. 2015 Oct 6 [cited 2021 Jul 29];6. Available from: http://journal.frontiersin.org/Article/10.3389/fmicb.2015.01050/abstract

101. Blaut M.*, Collins MD, Welling GW, Doré J, van Loo J, de Vos W. Molecular biological methods for studying the gut microbiota: the EU human gut flora project. British Journal of Nutrition. 2002 May 1;87(6):203–11.

102. Fava F. Intestinal microbiota in inflammatory bowel disease: Friend of foe? WJG. 2011;17(5):557.

103. Rinninella E, Raoul P, Cintoni M, Franceschi F, Miggiano G, Gasbarrini A, et al. What is the Healthy Gut Microbiota Composition? A Changing Ecosystem across Age, Environment, Diet, and Diseases. Microorganisms. 2019 Jan 10;7(1):14.

104. Odamaki T, Kato K, Sugahara H, Hashikura N, Takahashi S, Xiao J, et al. Age-related changes in gut microbiota composition from newborn to centenarian: a cross-sectional study. BMC Microbiol. 2016 Dec;16(1):90.

105. Mueller S, Saunier K, Hanisch C, Norin E, Alm L, Midtvedt T, et al. Differences in Fecal Microbiota in Different European Study Populations in Relation to Age, Gender, and Country: a Cross-Sectional Study. Appl Environ Microbiol. 2006 Feb;72(2):1027–33.

106. Vaiserman AM, Koliada AK, Marotta F. Gut microbiota: A player in aging and a target for anti-aging intervention. Ageing Research Reviews. 2017 May;35:36–45.

107. Brownlee IA. The physiological roles of dietary fibre. Food Hydrocolloids. 2011 Mar;25(2):238–50.

108. Miller TL, Wolin MJ. Pathways of acetate, propionate, and butyrate formation by the human fecal microbial flora. Appl Environ Microbiol. 1996 May;62(5):1589–92.

109. Cummings JH, Pomare EW, Branch WJ, Naylor CP, Macfarlane GT. Short chain fatty acids in human large intestine, portal, hepatic and venous blood. Gut. 1987 Oct 1;28(10):1221–7.

110. van de Wouw M, Boehme M, Lyte JM, Wiley N, Strain C, O'Sullivan O, et al. Short-chain fatty acids: microbial metabolites that alleviate stress-induced brain-gut axis alterations. J Physiol. 2018 Oct;596(20):4923–44.

111. den Besten G, van Eunen K, Groen AK, Venema K, Reijngoud D-J, Bakker BM. The role of short-chain fatty acids in the interplay between diet, gut microbiota, and host energy metabolism. Journal of Lipid Research. 2013 Sep;54(9):2325–40.

112. Blaak EE, Canfora EE, Theis S, Frost G, Groen AK, Mithieux G, et al. Short chain fatty acids in human gut and metabolic health. Beneficial Microbes. 2020 Sep 1;11(5):411–55.

113. Gibson GR, Macfarlane GT, editors. Human colonic bacteria: role in nutrition, physiology, and pathology. Boca Raton: CRC Press; 1995. 292 p.

114. Louis P, Young P, Holtrop G, Flint HJ. Diversity of human colonic butyrate-producing bacteria revealed by analysis of the butyryl-CoA:acetate CoA-transferase gene. Environmental Microbiology. 2010 Feb;12(2):304–14.

115. Barcenilla A, Pryde SE, Martin JC, Duncan SH, Stewart CS, Henderson C, et al. Phylogenetic Relationships of Butyrate-Producing Bacteria from the Human Gut. Appl Environ Microbiol. 2000 Apr;66(4):1654–61.

116. Duncan SH, Hold GL, Barcenilla A, Stewart CS, Flint HJ. Roseburia intestinalis sp. nov., a novel saccharolytic, butyrate-producing bacterium from human faeces. International Journal of Systematic and Evolutionary Microbiology. 2002 Sep 1;52(5):1615–20.

117. LeBlanc JG, Chain F, Martín R, Bermúdez-Humarán LG, Courau S, Langella P. Beneficial effects on host energy metabolism of short-chain fatty acids and vitamins produced by commensal and probiotic bacteria. Microb Cell Fact. 2017 Dec;16(1):79.

118. Shimizu J, Kubota T, Takada E, Takai K, Fujiwara N, Arimitsu N, et al. Propionate-producing bacteria in the intestine may associate with skewed responses of IL10-producing regulatory T cells in patients with relapsing polychondritis. Wilson BA, editor. PLoS ONE. 2018 Sep 20;13(9):e0203657.

119. Reichardt N, Duncan SH, Young P, Belenguer A, McWilliam Leitch C, Scott KP, et al. Phylogenetic distribution of three pathways for propionate production within the human gut microbiota. ISME J. 2014 Jun;8(6):1323–35.

120. Pessione E. Lactic acid bacteria contribution to gut microbiota complexity: lights and shadows. Front Cell Inf Microbio [Internet]. 2012 [cited 2021 Aug 2];2. Available from: http://journal.frontiersin.org/article/10.3389/fcimb.2012.00086/abstract

121. Belzer C, Chia LW, Aalvink S, Chamlagain B, Piironen V, Knol J, et al. Microbial Metabolic Networks at the Mucus Layer Lead to Diet-Independent Butyrate and Vitamin B 12 Production by Intestinal Symbionts. Dubilier N, editor. mBio [Internet]. 2017 Nov 8 [cited 2021 Aug 2];8(5). Available from: https://journals.asm.org/doi/10.1128/mBio.00770-17

122. Louis P, Flint HJ. Formation of propionate and butyrate by the human colonic microbiota. Environ Microbiol. 2017 Jan;19(1):29–41.

123. Moffett JR, Puthillathu N, Vengilote R, Jaworski DM, Namboodiri AM. Acetate Revisited: A Key Biomolecule at the Nexus of Metabolism, Epigenetics and Oncogenesis-Part 1: Acetyl-CoA, Acetogenesis and Acyl-CoA Short-Chain Synthetases. Front Physiol. 2020;11:580167.

124. Parada Venegas D, De la Fuente MK, Landskron G, González MJ, Quera R, Dijkstra G, et al. Short Chain Fatty Acids (SCFAs)-Mediated Gut Epithelial and Immune Regulation and Its Relevance for Inflammatory Bowel Diseases. Front Immunol. 2019 Mar 11;10:277.

125. Boets E, Gomand SV, Deroover L, Preston T, Vermeulen K, De Preter V, et al. Systemic availability and metabolism of colonic-derived short-chain fatty acids in healthy subjects: a stable isotope study: Short-chain fatty acid systemic availability and metabolism in humans. J Physiol. 2017 Jan 15;595(2):541–55.

126. Hong Y-H, Nishimura Y, Hishikawa D, Tsuzuki H, Miyahara H, Gotoh C, et al. Acetate and Propionate Short Chain Fatty Acids Stimulate Adipogenesis via GPCR43. Endocrinology. 2005 Dec 1;146(12):5092–9.

127. Jiao A, Yu B, He J, Yu J, Zheng P, Luo Y, et al. Sodium acetate, propionate, and butyrate reduce fat accumulation in mice via modulating appetite and relevant genes. Nutrition. 2021 Jul;87–88:111198.

128. Salvi PS, Cowles RA. Butyrate and the Intestinal Epithelium: Modulation of Proliferation and Inflammation in Homeostasis and Disease. Cells. 2021 Jul 14;10(7):1775.

129. Zhou L, Zhang M, Wang Y, Dorfman RG, Liu H, Yu T, et al. Faecalibacterium prausnitzii Produces Butyrate to Maintain Th17/Treg Balance and to Ameliorate Colorectal Colitis by Inhibiting Histone Deacetylase 1. Inflammatory Bowel Diseases. 2018 Aug 16;24(9):1926–40.

130. He Y, Tan Y, Zhu J, Wu X, Huang Z, Chen H, et al. Effect of sodium butyrate regulating IRAK1 (interleukin-1 receptor-associated kinase 1) on visceral hypersensitivity in irritable bowel syndrome and its mechanism. Bioengineered. 2021 Jan 1;12(1):1436–44.

131. Milligan G, Shimpukade B, Ulven T, Hudson BD. Complex Pharmacology of Free Fatty Acid Receptors. Chem Rev. 2017 Jan 11;117(1):67–110.

132. Sencio V, Barthelemy A, Tavares LP, Machado MG, Soulard D, Cuinat C, et al. Gut Dysbiosis during Influenza Contributes to Pulmonary Pneumococcal Superinfection through Altered Short-Chain Fatty Acid Production. Cell Reports. 2020 Mar;30(9):2934-2947.e6.

133. Nishida A, Miyamoto J, Shimizu H, Kimura I. Gut microbial short-chain fatty acids-mediated olfactory receptor 78 stimulation promotes anorexigenic gut hormone peptide YY secretion in mice. Biochemical and Biophysical Research Communications. 2021 Jun;557:48–54.

134. Kumar V, Khare P, Devi K, Kaur J, Kumar V, Kiran Kondepudi K, et al. Short-chain fatty acids increase intracellular calcium levels and enhance gut hormone release from STC-1 cells *via* transient receptor potential Ankyrin1. Fundam Clin Pharmacol. 2021 Mar 17;fcp.12663.

135. Brown AJ, Goldsworthy SM, Barnes AA, Eilert MM, Tcheang L, Daniels D, et al. The Orphan G protein-coupled receptors GPR41 and GPR43 are activated by propionate and other short chain carboxylic acids. J Biol Chem. 2003 Mar 28;278(13):11312–9.

136. Tolhurst G, Heffron H, Lam YS, Parker HE, Habib AM, Diakogiannaki E, et al. Short-Chain Fatty Acids Stimulate Glucagon-Like Peptide-1 Secretion via the G-Protein-Coupled Receptor FFAR2. Diabetes. 2012 Feb 1;61(2):364–71.

137. Hunt JE, Holst JJ, Jeppesen PB, Kissow H. GLP-1 and Intestinal Diseases. Biomedicines. 2021 Apr 5;9(4).

138. Suzuki S, Aoe S. High β-Glucan Barley Supplementation Improves Glucose Tolerance by Increasing GLP-1 Secretion in Diet-Induced Obesity Mice. Nutrients. 2021 Feb 6;13(2):527.

139. Liu Q, Tian X, Maruyama D, Arjomandi M, Prakash A. Lung Immune Tone via Gut-Lung Axis: Gut-derived LPS and Short-chain Fatty Acids' immunometabolic regulation of Lung IL-1β, FFAR2 and FFAR3 Expression. American Journal of Physiology-Lung Cellular and Molecular Physiology. 2021 Apr 14;ajplung.00421.2020.

140. van der Hee B, Wells JM. Microbial Regulation of Host Physiology by Short-chain Fatty Acids. Trends in Microbiology. 2021 Mar;S0966842X21000354.

141. Yoo J, Groer M, Dutra S, Sarkar A, McSkimming D. Gut Microbiota and Immune System Interactions. Microorganisms. 2020 Oct 15;8(10):1587.

142. Li G, Lin J, Zhang C, Gao H, Lu H, Gao X, et al. Microbiota metabolite butyrate constrains neutrophil functions and ameliorates mucosal inflammation in inflammatory bowel disease. Gut Microbes. 2021 Jan 1;13(1):1968257.

143. Kibbie JJ, Dillon SM, Thompson TA, Purba CM, McCarter MD, Wilson CC. Butyrate directly decreases human gut lamina propria CD4 T cell function through histone deacetylase (HDAC) inhibition and GPR43 signaling. Immunobiology. 2021 Sep;226(5):152126.

144. Chen J, Zhao K-N, Vitetta L. Effects of Intestinal Microbial–Elaborated Butyrate on Oncogenic Signaling Pathways. Nutrients. 2019 May 7;11(5):1026.

145. Mirzaei R, Afaghi A, Babakhani S, Sohrabi MR, Hosseini-Fard SR, Babolhavaeji K, et al. Role of microbiota-derived short-chain fatty acids in cancer development and prevention. Biomedicine & Pharmacotherapy. 2021 Jul;139:111619.

146. Bultman SJ. Interplay between diet, gut microbiota, epigenetic events, and colorectal cancer. Mol Nutr Food Res. 2017 Jan;61(1):1500902.

147. Backhed F, Ding H, Wang T, Hooper LV, Koh GY, Nagy A, et al. The gut microbiota as an environmental factor that regulates fat storage. Proceedings of the National Academy of Sciences. 2004 Nov 2;101(44):15718–23.

148. Ley RE, Backhed F, Turnbaugh P, Lozupone CA, Knight RD, Gordon JI. Obesity alters gut microbial ecology. Proceedings of the National Academy of Sciences. 2005 Aug 2;102(31):11070–5.

149. Turnbaugh PJ, Ley RE, Mahowald MA, Magrini V, Mardis ER, Gordon JI. An obesity-associated gut microbiome with increased capacity for energy harvest. Nature. 2006 Dec;444(7122):1027–31.

150. Zhang H, DiBaise JK, Zuccolo A, Kudrna D, Braidotti M, Yu Y, et al. Human gut microbiota in obesity and after gastric bypass. Proceedings of the National Academy of Sciences. 2009 Feb 17;106(7):2365–70.

151. Jumpertz R, Le DS, Turnbaugh PJ, Trinidad C, Bogardus C, Gordon JI, et al. Energy-balance studies reveal associations between gut microbes, caloric load, and nutrient absorption in humans. The American Journal of Clinical Nutrition. 2011 Jul 1;94(1):58–65.

152. Patil DP, Dhotre DP, Chavan SG, Sultan A, Jain DS, Lanjekar VB, et al. Molecular analysis of gut microbiota in obesity among Indian individuals. J Biosci. 2012 Sep;37(4):647–57.

153. MetaHIT consortium, Le Chatelier E, Nielsen T, Qin J, Prifti E, Hildebrand F, et al. Richness of human gut microbiome correlates with metabolic markers. Nature. 2013 Aug 29;500(7464):541–6.

154. Dao MC, Everard A, Aron-Wisnewsky J, Sokolovska N, Prifti E, Verger EO, et al. *Akkermansia muciniphila* and improved metabolic health during a dietary intervention in obesity: relationship with gut microbiome richness and ecology. Gut. 2016 Mar;65(3):426–36.

155. Everard A, Belzer C, Geurts L, Ouwerkerk JP, Druart C, Bindels LB, et al. Cross-talk between Akkermansia muciniphila and intestinal epithelium controls diet-induced obesity. Proceedings of the National Academy of Sciences. 2013 May 28;110(22):9066–71.

156. Depommier C, Everard A, Druart C, Plovier H, Van Hul M, Vieira-Silva S, et al. Supplementation with Akkermansia muciniphila in overweight and obese human volunteers: a proof-of-concept exploratory study. Nat Med. 2019 Jul;25(7):1096–103.

157. Sroka-Oleksiak A, Młodzińska A, Bulanda M, Salamon D, Major P, Stanek M, et al. Metagenomic Analysis of Duodenal Microbiota Reveals a Potential Biomarker of Dysbiosis in the Course of Obesity and Type 2 Diabetes: A Pilot Study. JCM. 2020 Jan 29;9(2):369.

158. Remely M, Hippe B, Zanner J, Aumueller E, Brath H, G. Haslberger A. Gut Microbiota of Obese, Type 2 Diabetic Individuals is Enriched in Faecalibacterium prausnitzii, Akkermansia muciniphila and Peptostreptococcus anaerobius after Weight Loss. EMIDDT. 2016 Sep 22;16(2):99–106.

159. Liu R, Hong J, Xu X, Feng Q, Zhang D, Gu Y, et al. Gut microbiome and serum metabolome alterations in obesity and after weight-loss intervention. Nat Med. 2017 Jul;23(7):859–68.

160. Chiang JYL. Bile acids: regulation of synthesis. Journal of Lipid Research. 2009 Oct;50(10):1955–66.

161. Ridlon JM, Harris SC, Bhowmik S, Kang D-J, Hylemon PB. Consequences of bile salt biotransformations by intestinal bacteria. Gut Microbes. 2016 Jan 2;7(1):22–39.

162. Vincent RP, Omar S, Ghozlan S, Taylor DR, Cross G, Sherwood RA, et al. Higher circulating bile acid concentrations in obese patients with type 2 diabetes. Ann Clin Biochem. 2013 Jul;50(4):360–4.

163. Haeusler RA, Astiarraga B, Camastra S, Accili D, Ferrannini E. Human Insulin Resistance Is Associated With Increased Plasma Levels of 12 -Hydroxylated Bile Acids. Diabetes. 2013 Dec 1;62(12):4184–91.

164. Holscher HD, Guetterman HM, Swanson KS, An R, Matthan NR, Lichtenstein AH, et al. Walnut Consumption Alters the Gastrointestinal Microbiota, Microbially Derived Secondary Bile Acids, and Health Markers in Healthy Adults: A Randomized Controlled Trial. The Journal of Nutrition. 2018 Jun 1;148(6):861–7.

165. Diotallevi C, Fava F, Gobbetti M, Tuohy K. Healthy dietary patterns to reduce obesity-related metabolic disease: polyphenol-microbiome interactions unifying health effects across geography. Current Opinion in Clinical Nutrition & Metabolic Care. 2020 Nov;23(6):437–44.

166. Han X, Guo J, Yin M, Liu Y, You Y, Zhan J, et al. Grape Extract Activates Brown Adipose Tissue Through Pathway Involving the Regulation of Gut Microbiota and Bile Acid. Mol Nutr Food Res. 2020 May;64(10):2000149.

167. Guo J, Han X, Tan H, Huang W, You Y, Zhan J. Blueberry Extract Improves Obesity through Regulation of the Gut Microbiota and Bile Acids via Pathways Involving FXR and TGR5. iScience. 2019 Sep;19:676–90.

168. Anhê FF, Nachbar RT, Varin TV, Trottier J, Dudonné S, Le Barz M, et al. Treatment with camu camu (*Myrciaria dubia*) prevents obesity by altering the gut microbiota and increasing energy expenditure in diet-induced obese mice. Gut. 2019 Mar;68(3):453–64.

169. Régnier M, Rastelli M, Morissette A, Suriano F, Le Roy T, Pilon G, et al. Rhubarb Supplementation Prevents Diet-Induced Obesity and Diabetes in Association with Increased Akkermansia muciniphila in Mice. Nutrients. 2020 Sep 24;12(10):2932.

170. National Cancer Institute. NCI Dictionary of Cancer Terms. In: 20.09d. 2020.

171. Alberts B, editor. Molecular biology of the cell. 4th ed. New York: Garland Science; 2002. 1548 p.

172. Lee B, Moon KM, Kim CY. Tight Junction in the Intestinal Epithelium: Its Association with Diseases and Regulation by Phytochemicals. Journal of Immunology Research. 2018 Dec 16;2018:1–11.

173. Harhaj NS, Antonetti DA. Regulation of tight junctions and loss of barrier function in pathophysiology. The International Journal of Biochemistry & Cell Biology. 2004 Jul;36(7):1206–37.

174. González-Mariscal L, Tapia R, Chamorro D. Crosstalk of tight junction components with signaling pathways. Biochimica et Biophysica Acta (BBA) - Biomembranes. 2008 Mar;1778(3):729–56.

175. Furuse M, Hata M, Furuse K, Yoshida Y, Haratake A, Sugitani Y, et al. Claudin-based tight junctions are crucial for the mammalian epidermal barrier. Journal of Cell Biology. 2002 Mar 18;156(6):1099–111.

176. Saitou M, Furuse M, Sasaki H, Schulzke J-D, Fromm M, Takano H, et al. Complex Phenotype of Mice Lacking Occludin, a Component of Tight Junction Strands. Nelson WJ, editor. MBoC. 2000 Dec;11(12):4131–42.

177. Schroeder BO, Birchenough GMH, Pradhan M, Nyström EEL, Henricsson M, Hansson GC, et al. Obesity-associated microbiota contributes to mucus layer defects in genetically obese mice. Journal of Biological Chemistry. 2020 Nov;295(46):15712–26.

178. Paone P, Cani PD. Mucus barrier, mucins and gut microbiota: the expected slimy partners? Gut. 2020 Dec;69(12):2232–43.

179. Cone RA. Mucus. In: Mucosal Immunology [Internet]. Elsevier; 2005 [cited 2021 Aug 4]. p. 49–72. Available from: https://linkinghub.elsevier.com/retrieve/pii/B9780124915435500085

180. Willemsen LEM. Short chain fatty acids stimulate epithelial mucin 2 expression through differential effects on prostaglandin E1 and E2 production by intestinal myofibroblasts. Gut. 2003 Oct 1;52(10):1442–7.

181. Burger-van Paassen N, Vincent A, Puiman PJ, van der Sluis M, Bouma J, Boehm G, et al. The regulation of intestinal mucin MUC2 expression by short-chain fatty acids: implications for epithelial protection. Biochemical Journal. 2009 Jun 1;420(2):211–9.

182. Szentkuti L, Riedesel H, Enss M-L, Gaertner K, von Engelhardt W. Pre-epithelial mucus layer in the colon of conventional and germ-free rats. Histochem J. 1990 Sep;22(9):491–7.

183. Janeway C, editor. Immunobiology: the immune system in health and disease ; [animated CD-ROM inside]. 5. ed. New York, NY: Garland Publ. [u.a.]; 2001. 732 p.

184. Curtsinger JM, Schmidt CS, Mondino A, Lins DC, Kedl RM, Jenkins MK, et al. Inflammatory cytokines provide a third signal for activation of naive CD4+ and CD8+ T cells. J Immunol. 1999 Mar 15;162(6):3256–62.

185. Janeway CA. Approaching the Asymptote? Evolution and Revolution in Immunology. Cold Spring Harbor Symposia on Quantitative Biology. 1989 Jan 1;54(0):1–13.

186. Moticka E. A history perspective on evidence-based immunology. Boston, MA: Elsevier; 2015.

187. Chu H, Mazmanian SK. Innate immune recognition of the microbiota promotes host-microbial symbiosis. Nat Immunol. 2013 Jul;14(7):668–75.

188. Srinivasan N. Telling apart friend from foe: discriminating between commensals and pathogens at mucosal sites. Innate Immun. 2010 Dec;16(6):391–404.

189. Pruss KM, Marcobal A, Southwick AM, Dahan D, Smits SA, Ferreyra JA, et al. Mucin-derived O-glycans supplemented to diet mitigate diverse microbiota perturbations. ISME J. 2021 Feb;15(2):577–91.

190. Johansson MEV, Phillipson M, Petersson J, Velcich A, Holm L, Hansson GC. The inner of the two Muc2 mucin-dependent mucus layers in colon is devoid of bacteria. Proceedings of the National Academy of Sciences. 2008 Sep 30;105(39):15064–9.

191. Delneste Y, Beauvillain C, Jeannin P. Immunité naturelle: Structure et fonction des *Toll-like receptors*. Med Sci (Paris). 2007 Jan;23(1):67–74.

192. Iwasaki A, Medzhitov R. Toll-like receptor control of the adaptive immune responses. Nat Immunol. 2004 Oct;5(10):987–95.

193.Petterson T, Jendholm J, Månsson A, Bjartell A, Riesbeck K, Cardell L-O. Effects of NOD-like receptors in human B lymphocytes and crosstalk between NOD1/NOD2 and Toll-like receptors. Journal of Leukocyte Biology. 2011 Feb;89(2):177–87.

194. Uchimura T, Oyama Y, Deng M, Guo H, Wilson JE, Rampanelli E, et al. The Innate Immune Sensor NLRC3 Acts as a Rheostat that Fine-Tunes T Cell Responses in Infection and Autoimmunity. Immunity. 2018 Dec;49(6):1049-1061.e6.

195. Hugot J-P, Chamaillard M, Zouali H, Lesage S, Cézard J-P, Belaiche J, et al. Association of NOD2 leucine-rich repeat variants with susceptibility to Crohn's disease. Nature. 2001 May;411(6837):599–603.

196. Ogura Y, Inohara N, Benito A, Chen FF, Yamaoka S, Núñez G. Nod2, a Nod1/Apaf-1 Family Member That Is Restricted to Monocytes and Activates NF-κB. Journal of Biological Chemistry. 2001 Feb;276(7):4812–8.

197. Horowitz JE, Warner N, Staples J, Crowley E, Gosalia N, Murchie R, et al. Mutation spectrum of NOD2 reveals recessive inheritance as a main driver of Early Onset Crohn's Disease. Sci Rep. 2021 Dec;11(1):5595.

198. Kuugbee ED, Shang X, Gamallat Y, Bamba D, Awadasseid A, Suliman MA, et al. Structural Change in Microbiota by a Probiotic Cocktail Enhances the Gut Barrier and Reduces Cancer via TLR2 Signaling in a Rat Model of Colon Cancer. Dig Dis Sci. 2016 Oct;61(10):2908–20.

199. Meng S, Li Y, Zang X, Jiang Z, Ning H, Li J. Effect of TLR2 on the proliferation of inflammation-related colorectal cancer and sporadic colorectal cancer. Cancer Cell Int. 2020 Dec;20(1):95.

200. Sellge G, Kufer TA. PRR-signaling pathways: Learning from microbial tactics. Seminars in Immunology. 2015 Mar;27(2):75–84.

201. Takeuchi O, Sato S, Horiuchi T, Hoshino K, Takeda K, Dong Z, et al. Cutting Edge: Role of Toll-Like Receptor 1 in Mediating Immune Response to Microbial Lipoproteins. J Immunol. 2002 Jul 1;169(1):10–4.

202. Shah M, Shah K, Ganna P, Patel A. Toll-like receptors: A double edge sword. J Interdiscip Dentistry. 2013;3(2):57.

203. El-Zayat SR, Sibaii H, Mannaa FA. Toll-like receptors activation, signaling, and targeting: an overview. Bull Natl Res Cent. 2019 Dec;43(1):187.

204. Aliprantis AO. Cell Activation and Apoptosis by Bacterial Lipoproteins Through Toll-like Receptor-2. Science. 1999 Jul 30;285(5428):736–9.

205. Lien E, Sellati TJ, Yoshimura A, Flo TH, Rawadi G, Finberg RW, et al. Toll-like Receptor 2 Functions as a Pattern Recognition Receptor for Diverse Bacterial Products. Journal of Biological Chemistry. 1999 Nov;274(47):33419–25.

206. Echchannaoui H, Frei K, Schnell C, Leib SL, Zimmerli W, Landmann R. Toll-Like Receptor 2–Deficient Mice Are Highly Susceptible to *Streptococcus pneumoniae* Meningitis because of Reduced Bacterial Clearing and Enhanced Inflammation. J INFECT DIS. 2002 Sep 15;186(6):798–806.

207. Shimazu R, Akashi S, Ogata H, Nagai Y, Fukudome K, Miyake K, et al. MD-2, a Molecule that Confers Lipopolysaccharide Responsiveness on Toll-like Receptor 4. Journal of Experimental Medicine. 1999 Jun 7;189(11):1777–82.

208. Poltorak A. Defective LPS Signaling in C3H/HeJ and C57BL/10ScCr Mice: Mutations in Tlr4 Gene. Science. 1998 Dec 11;282(5396):2085–8.

209. Hayashi F, Smith KD, Ozinsky A, Hawn TR, Yi EC, Goodlett DR, et al. The innate immune response to bacterial flagellin is mediated by Toll-like receptor 5. Nature. 2001 Apr;410(6832):1099–103.

210. Takeuchi O, Kawai T, Mühlradt PF, Morr M, Radolf JD, Zychlinsky A, et al. Discrimination of bacterial lipoproteins by Toll-like receptor 6. International Immunology. 2001 Jul;13(7):933–40.

211. Hemmi H, Takeuchi O, Kawai T, Kaisho T, Sato S, Sanjo H, et al. A Toll-like receptor recognizes bacterial DNA. Nature. 2000 Dec 7;408(6813):740–5.

212. Chamaillard M, Hashimoto M, Horie Y, Masumoto J, Qiu S, Saab L, et al. An essential role for NOD1 in host recognition of bacterial peptidoglycan containing diaminopimelic acid. Nat Immunol. 2003 Jul;4(7):702–7.

213. Girardin SE. Nod1 Detects a Unique Muropeptide from Gram-Negative Bacterial Peptidoglycan. Science. 2003 Jun 6;300(5625):1584–7.

214. Uehara A, Fujimoto Y, Kawasaki A, Kusumoto S, Fukase K, Takada H. *Meso* -Diaminopimelic Acid and *Meso* -Lanthionine, Amino Acids Specific to Bacterial Peptidoglycans, Activate Human Epithelial Cells through NOD1. J Immunol. 2006 Aug 1;177(3):1796–804.

215. Girardin SE, Travassos LH, Hervé M, Blanot D, Boneca IG, Philpott DJ, et al. Peptidoglycan Molecular Requirements Allowing Detection by Nod1 and Nod2. Journal of Biological Chemistry. 2003 Oct;278(43):41702–8.

216. Inohara N, Ogura Y, Chen FF, Muto A, Nuñez G. Human Nod1 Confers Responsiveness to Bacterial Lipopolysaccharides. Journal of Biological Chemistry. 2001 Jan;276(4):2551–4.

217. Strober W, Murray PJ, Kitani A, Watanabe T. Signalling pathways and molecular interactions of NOD1 and NOD2. Nat Rev Immunol. 2006 Jan;6(1):9–20.

218. Girardin SE, Boneca IG, Viala J, Chamaillard M, Labigne A, Thomas G, et al. Nod2 Is a General Sensor of Peptidoglycan through Muramyl Dipeptide (MDP) Detection. Journal of Biological Chemistry. 2003 Mar;278(11):8869–72.

219. Franchi L, Amer A, Body-Malapel M, Kanneganti T-D, Özören N, Jagirdar R, et al. Cytosolic flagellin requires Ipaf for activation of caspase-1 and interleukin 1β in salmonella-infected macrophages. Nat Immunol. 2006 Jun;7(6):576–82.

220. Miao EA, Alpuche-Aranda CM, Dors M, Clark AE, Bader MW, Miller SI, et al. Cytoplasmic flagellin activates caspase-1 and secretion of interleukin 1β via Ipaf. Nat Immunol. 2006 Jun;7(6):569–75.

221. Geddes BJ, Wang L, Huang W-J, Lavellee M, Manji GA, Brown M, et al. Human CARD12 Is a Novel CED4/Apaf-1 Family Member That Induces Apoptosis. Biochemical and Biophysical Research Communications. 2001 Jun;284(1):77–82.

222. Levinsohn JL, Newman ZL, Hellmich KA, Fattah R, Getz MA, Liu S, et al. Anthrax Lethal Factor Cleavage of Nlrp1 Is Required for Activation of the Inflammasome. Young JAT, editor. PLoS Pathog. 2012 Mar 29;8(3):e1002638.

223. Hellmich KA, Levinsohn JL, Fattah R, Newman ZL, Maier N, Sastalla I, et al. Anthrax Lethal Factor Cleaves Mouse Nlrp1b in Both Toxin-Sensitive and Toxin-Resistant Macrophages. Mantis NJ, editor. PLoS ONE. 2012 Nov 12;7(11):e49741.

224. Faustin B, Lartigue L, Bruey J-M, Luciano F, Sergienko E, Bailly-Maitre B, et al. Reconstituted NALP1 Inflammasome Reveals Two-Step Mechanism of Caspase-1 Activation. Molecular Cell. 2007 Mar;25(5):713–24.

225. Finger JN, Lich JD, Dare LC, Cook MN, Brown KK, Duraiswami C, et al. Autolytic Proteolysis within the Function to Find Domain (FIIND) Is Required for NLRP1 Inflammasome Activity. Journal of Biological Chemistry. 2012 Jul;287(30):25030–7.

226. Damiano JS, Stehlik C, Pio F, Godzik A, Reed JC. CLAN, a Novel Human CED-4-like Gene. Genomics. 2001 Jul;75(1–3):77–83.

227. Gutierrez O, Pipaon C, Inohara N, Fontalba A, Ogura Y, Prosper F, et al. Induction of Nod2 in Myelomonocytic and Intestinal Epithelial Cells via Nuclear Factor-κB Activation. Journal of Biological Chemistry. 2002 Nov;277(44):41701–5.

228. Krutzik SR, Tan B, Li H, Ochoa MT, Liu PT, Sharfstein SE, et al. TLR activation triggers the rapid differentiation of monocytes into macrophages and dendritic cells. Nat Med. 2005 Jun;11(6):653–60.

229. Miao EA, Ernst RK, Dors M, Mao DP, Aderem A. Pseudomonas aeruginosa activates caspase 1 through Ipaf. Proceedings of the National Academy of Sciences. 2008 Feb 19;105(7):2562–7.

230. Hornung V, Rothenfusser S, Britsch S, Krug A, Jahrsdörfer B, Giese T, et al. Quantitative Expression of Toll-Like Receptor 1–10 mRNA in Cellular Subsets of Human Peripheral Blood Mononuclear Cells and Sensitivity to CpG Oligodeoxynucleotides. J Immunol. 2002 May 1;168(9):4531–7.

231. Hua Z, Hou B. TLR signaling in B-cell development and activation. Cell Mol Immunol. 2013 Mar;10(2):103–6.

232. Agrawal S, Agrawal A, Doughty B, Gerwitz A, Blenis J, Van Dyke T, et al. Cutting Edge: Different Toll-Like Receptor Agonists Instruct Dendritic Cells to Induce Distinct Th Responses via Differential Modulation of Extracellular Signal-Regulated Kinase-Mitogen-Activated Protein Kinase and c-Fos. J Immunol. 2003 Nov 15;171(10):4984–9.

233. Costa FRC, Leite JA, Rassi DM, da Silva JF, Elias-Oliveira J, Guimarães JB, et al. NLRP1 acts as a negative regulator of Th17 cell programming in mice and humans with autoimmune diabetes. Cell Reports. 2021 May;35(8):109176.

234. Gupta S, Butcher E, Paul W. Lymphocyte Activation and Immune Regulation IX: Homeostasis and Lymphocyte Traffic [Internet]. Boston, MA: Springer US : Imprint : Springer; 2002 [cited 2021 Aug 30]. Available from: http://public.ebookcentral.proquest.com/choice/publicfullrecord.aspx?p=3068818

235. Hausmann M, Kiessling S, Mestermann S, Webb G, Spöttl T, Andus T, et al. Toll-like receptors 2 and 4 are up-regulated during intestinal inflammation. Gastroenterology. 2002 Jun;122(7):1987–2000.

236. Price AE, Shamardani K, Lugo KA, Deguine J, Roberts AW, Lee BL, et al. A Map of Toll-like Receptor Expression in the Intestinal Epithelium Reveals Distinct Spatial, Cell Type-Specific, and Temporal Patterns. Immunity. 2018 Sep;49(3):560-575.e6.

237. Huan Y, Kong Q, Mou H, Yi H. Antimicrobial Peptides: Classification, Design, Application and Research Progress in Multiple Fields. Front Microbiol. 2020 Oct 16;11:582779.

238. Muniz LR, Knosp C, Yeretssian G. Intestinal antimicrobial peptides during homeostasis, infection, and disease. Front Immun [Internet]. 2012 [cited 2021 Sep 6];3. Available from: http://journal.frontiersin.org/article/10.3389/fimmu.2012.00310/abstract

239. Mwangi J, Yin Y, Wang G, Yang M, Li Y, Zhang Z, et al. The antimicrobial peptide ZY4 combats multidrug-resistant *Pseudomonas aeruginosa* and *Acinetobacter baumannii* infection. Proc Natl Acad Sci USA. 2019 Dec 26;116(52):26516–22.

240. Yao X, Zhang C, Xing Y, Xue G, Zhang Q, Pan F, et al. Remodelling of the gut microbiota by hyperactive NLRP3 induces regulatory T cells to maintain homeostasis. Nat Commun. 2017 Dec;8(1):1896.

241. Liévin-Le Moal V, Servin AL. The Front Line of Enteric Host Defense against Unwelcome Intrusion of Harmful Microorganisms: Mucins, Antimicrobial Peptides, and Microbiota. Clin Microbiol Rev. 2006 Apr;19(2):315–37.

242. Frantz AL, Rogier EW, Weber CR, Shen L, Cohen DA, Fenton LA, et al. Targeted deletion of MyD88 in intestinal epithelial cells results in compromised antibacterial immunity associated with downregulation of polymeric immunoglobulin receptor, mucin-2, and antibacterial peptides. Mucosal Immunol. 2012 Sep;5(5):501–12.

243. Fukuda S, Toh H, Taylor TD, Ohno H, Hattori M. Acetate-producing bifidobacteria protect the host from enteropathogenic infection via carbohydrate transporters. Gut Microbes. 2012 Sep 20;3(5):449–54.

244. Furusawa Y, Obata Y, Fukuda S, Endo TA, Nakato G, Takahashi D, et al. Commensal microbe-derived butyrate induces the differentiation of colonic regulatory T cells. Nature. 2013 Dec 19;504(7480):446–50.

245. Vignali DAA, Collison LW, Workman CJ. How regulatory T cells work. Nat Rev Immunol. 2008 Jul;8(7):523–32.

246. Li Z, Li D, Tsun A, Li B. FOXP3+ regulatory T cells and their functional regulation. Cell Mol Immunol. 2015 Sep;12(5):558–65.

247. Singh N, Gurav A, Sivaprakasam S, Brady E, Padia R, Shi H, et al. Activation of Gpr109a, Receptor for Niacin and the Commensal Metabolite Butyrate, Suppresses Colonic Inflammation and Carcinogenesis. Immunity. 2014 Jan;40(1):128–39.

248. Maslowski KM, Vieira AT, Ng A, Kranich J, Sierro F, Di Yu, et al. Regulation of inflammatory responses by gut microbiota and chemoattractant receptor GPR43. Nature. 2009 Oct;461(7268):1282–6.

249. Agus A, Denizot J, Thévenot J, Martinez-Medina M, Massier S, Sauvanet P, et al. Western diet induces a shift in microbiota composition enhancing susceptibility to Adherent-Invasive E. coli infection and intestinal inflammation. Sci Rep. 2016 May;6(1):19032.

250. Szliszka E, Krol W. The role of dietary polyphenols in tumor necrosis factor-related apoptosis inducing ligand (TRAIL)-induced apoptosis for cancer chemoprevention. European Journal of Cancer Prevention. 2011 Jan;20(1):63–9.

251. Beckman CH. Phenolic-storing cells: keys to programmed cell death and periderm formation in wilt disease resistance and in general defence responses in plants? Physiological and Molecular Plant Pathology. 2000 Sep;57(3):101–10.

252. Du L, Li J, Zhang X, Wang L, Zhang W, Yang M, et al. Pomegranate peel polyphenols inhibits inflammation in LPS-induced RAW264.7 macrophages via the suppression of TLR4/NF-κB pathway activation. Food & Nutrition Research [Internet]. 2019 Apr 23 [cited 2021 Aug 18];63(0). Available from: http://www.foodandnutritionresearch.net/index.php/fnr/article/view/3392

253. Dai J, Patel JD, Mumper RJ. Characterization of Blackberry Extract and Its Antiproliferative and Anti-Inflammatory Properties. Journal of Medicinal Food. 2007 Jun;10(2):258–65.

254. Ahn S-C, Kim G-Y, Kim J-H, Baik S-W, Han M-K, Lee H-J, et al. Epigallocatechin-3-gallate, constituent of green tea, suppresses the LPS-induced phenotypic and functional maturation of murine dendritic cells through inhibition of mitogen-activated protein kinases and NF-κB. Biochemical and Biophysical Research Communications. 2004 Jan;313(1):148–55.

255. Wong CP, Nguyen LP, Noh SK, Bray TM, Bruno RS, Ho E. Induction of regulatory T cells by green tea polyphenol EGCG. Immunology Letters. 2011 Sep;139(1–2):7–13.

256. Sergi D, Boulestin H, Campbell FM, Williams LM. The Role of Dietary Advanced Glycation End Products in Metabolic Dysfunction. Mol Nutr Food Res. 2021 Jan;65(1):1900934.

257. van der Lugt T, Weseler A, Gebbink W, Vrolijk M, Opperhuizen A, Bast A. Dietary Advanced Glycation Endproducts Induce an Inflammatory Response in Human Macrophages in Vitro. Nutrients. 2018 Dec 2;10(12):1868.

258. Price CL, Sharp PS, North ME, Rainbow SJ, Knight SC. Advanced Glycation End Products Modulate the Maturation and Function of Peripheral Blood Dendritic Cells. Diabetes. 2004 Jun 1;53(6):1452–8.

259. Ghosh SS, Wang J, Yannie PJ, Ghosh S. Intestinal Barrier Dysfunction, LPS Translocation, and Disease Development. Journal of the Endocrine Society. 2020 Feb 1;4(2):bvz039.

260. Ghosh S, Whitley CS, Haribabu B, Jala VR. Regulation of Intestinal Barrier Function by Microbial Metabolites. Cellular and Molecular Gastroenterology and Hepatology. 2021;11(5):1463–82.

261. Madsen K, Park H. Immunologic Response in the Host. In: The Microbiota in Gastrointestinal Pathophysiology [Internet]. Elsevier; 2017 [cited 2021 Aug 4]. p. 233–41. Available from: https://linkinghub.elsevier.com/retrieve/pii/B9780128040249000264

262. Mohammad S, Thiemermann C. Role of Metabolic Endotoxemia in Systemic Inflammation and Potential Interventions. Front Immunol. 2021 Jan 11;11:594150.

263. Cani PD, Amar J, Iglesias MA, Poggi M, Knauf C, Bastelica D, et al. Metabolic Endotoxemia Initiates Obesity and Insulin Resistance. Diabetes. 2007 Jul 1;56(7):1761–72.

264. Singh R, Chandrashekharappa S, Bodduluri SR, Baby BV, Hegde B, Kotla NG, et al. Enhancement of the gut barrier integrity by a microbial metabolite through the Nrf2 pathway. Nat Commun. 2019 Dec;10(1):89.

265. Chen K, Zhao H, Shu L, Xing H, Wang C, Lu C, et al. Effect of resveratrol on intestinal tight junction proteins and the gut microbiome in high-fat diet-fed insulin resistant mice. International Journal of Food Sciences and Nutrition. 2020 Nov 16;71(8):965–78.

266. Hsieh C-Y, Osaka T, Moriyama E, Date Y, Kikuchi J, Tsuneda S. Strengthening of the intestinal epithelial tight junction by *Bifidobacterium bifidum*. Physiol Rep. 2015 Mar;3(3):e12327.

267. Cani PD, Neyrinck AM, Fava F, Knauf C, Burcelin RG, Tuohy KM, et al. Selective increases of bifidobacteria in gut microflora improve high-fat-diet-induced diabetes in mice through a mechanism associated with endotoxaemia. Diabetologia. 2007 Oct 1;50(11):2374–83.

268. Sánchez-Tapia M, Miller AW, Granados-Portillo O, Tovar AR, Torres N. The development of metabolic endotoxemia is dependent on the type of sweetener and the presence of saturated fat in the diet. Gut Microbes. 2020 Nov 9;12(1):1801301.

269. Clemente-Postigo M, Oliva-Olivera W, Coin-Aragüez L, Ramos-Molina B, Giraldez-Perez RM, Lhamyani S, et al. Metabolic endotoxemia promotes adipose dysfunction and inflammation in

human obesity. American Journal of Physiology-Endocrinology and Metabolism. 2019 Feb 1;316(2):E319–32.

270. Creely SJ, McTernan PG, Kusminski CM, Fisher ff. M, Da Silva NF, Khanolkar M, et al. Lipopolysaccharide activates an innate immune system response in human adipose tissue in obesity and type 2 diabetes. American Journal of Physiology-Endocrinology and Metabolism. 2007 Mar;292(3):E740–7.

271. Gillery P, Jaisson S. Post-translational modification derived products (PTMDPs): toxins in chronic diseases? Clinical Chemistry and Laboratory Medicine [Internet]. 2014 Jan 1 [cited 2021 May 21];52(1). Available from: https://www.degruyter.com/document/doi/10.1515/cclm-2012-0880/html

272. Egaña-Gorroño L, López-Díez R, Yepuri G, Ramirez LS, Reverdatto S, Gugger PF, et al. Receptor for Advanced Glycation End Products (RAGE) and Mechanisms and Therapeutic Opportunities in Diabetes and Cardiovascular Disease: Insights From Human Subjects and Animal Models. Front Cardiovasc Med. 2020 Mar 10;7:37.

273. Birlouez-Aragon I, Saavedra G, Tessier FJ, Galinier A, Ait-Ameur L, Lacoste F, et al. A diet based on high-heat-treated foods promotes risk factors for diabetes mellitus and cardiovascular diseases. The American Journal of Clinical Nutrition. 2010 May 1;91(5):1220–6.

274. Zill H, Günther R, Erbersdobler HF, Fölsch UR, Faist V. RAGE Expression and AGE-Induced MAP Kinase Activation in Caco-2 Cells. Biochemical and Biophysical Research Communications. 2001 Nov;288(5):1108–11.

275. Zill H, Bek S, Hofmann T, Huber J, Frank O, Lindenmeier M, et al. RAGE-mediated MAPK activation by food-derived AGE and non-AGE products. Biochemical and Biophysical Research Communications. 2003 Jan;300(2):311–5.

276. Kislinger T, Fu C, Huber B, Qu W, Taguchi A, Du Yan S, et al. N ε-(Carboxymethyl)Lysine Adducts of Proteins Are Ligands for Receptor for Advanced Glycation End Products That Activate Cell Signaling Pathways and Modulate Gene Expression. Journal of Biological Chemistry. 1999 Oct;274(44):31740–9.

277. Amadori M, editor. The innate immune response to noninfectious stressors: human and animal models. Amsterdam ; Boston: Elsevier/AP, Academic Press is an imprint of Elsevier; 2016. 247 p.

278. Mollace A, Coluccio ML, Donato G, Mollace V, Malara N. Cross-talks in colon cancer between RAGE/AGEs axis and inflammation/immunotherapy. Oncotarget. 2021 Jun 22;12(13):1281–95.

279. Kuniyasu H, Chihara Y, Kondo H. Differential effects between amphoterin and advanced glycation end products on colon cancer cells. Int J Cancer. 2003 May 10;104(6):722–7.

280. Sakellariou S, Fragkou P, Levidou G, Gargalionis AN, Piperi C, Dalagiorgou G, et al. Clinical significance of AGE-RAGE axis in colorectal cancer: associations with glyoxalase-I, adiponectin receptor expression and prognosis. BMC Cancer. 2016 Dec;16(1):174.

281. Uribarri J, Cai W, Ramdas M, Goodman S, Pyzik R, Chen X, et al. Restriction of Advanced Glycation End Products Improves Insulin Resistance in Human Type 2 Diabetes: Potential role of AGER1 and SIRT1. Diabetes Care. 2011 Jul 1;34(7):1610–6.

282. Harcourt BE, Sourris KC, Coughlan MT, Walker KZ, Dougherty SL, Andrikopoulos S, et al. Targeted reduction of advanced glycation improves renal function in obesity. Kidney International. 2011 Jul;80(2):190–8.

283. Delgado-Andrade C. Carboxymethyl-lysine: thirty years of investigation in the field of AGE formation. Food Funct. 2016;7(1):46–57.

284. Faist V, Erbersdobler HF. Metabolic Transit and in vivo Effects of Melanoidins and Precursor Compounds Deriving from the Maillard Reaction. Ann Nutr Metab. 2001;45(1):1–12.

285. Mills DJS, Tuohy KM, Booth J, Buck M, Crabbe MJC, Gibson GR, et al. Dietary glycated protein modulates the colonic microbiota towards a more detrimental composition in ulcerative colitis patients and non-ulcerative colitis subjects. Journal of Applied Microbiology. 2008 Sep;105(3):706–14.

286. Yang Y, Wu H, Dong S, Jin W, Han K, Ren Y, et al. Glycation of fish protein impacts its fermentation metabolites and gut microbiota during in vitro human colonic fermentation. Food Research International. 2018 Nov;113:189–96.

287. Świątecka D, Dominika Ś, Narbad A, Arjan N, Ridgway KP, Karyn RP, et al. The study on the impact of glycated pea proteins on human intestinal bacteria. Int J Food Microbiol. 2011 Jan 31;145(1):267–72.

288. Dell'Aquila C, Ames JM, Gibson GR, Wynne AG. Fermentation of heated gluten systems by gut microflora. European Food Research and Technology. 2003 Nov 1;217(5):382–6.

289. Helou C, Denis S, Spatz M, Marier D, Rame V, Alric M, et al. Insights into bread melanoidins: fate in the upper digestive tract and impact on the gut microbiota using in vitro systems. Food Funct. 2015;6(12):3737–45.

290. Qu W, Yuan X, Zhao J, Zhang Y, Hu J, Wang J, et al. Dietary advanced glycation end products modify gut microbial composition and partially increase colon permeability in rats. Mol Nutr Food Res. 2017 Oct;61(10):1700118.

291. Marungruang N, Fåk F, Tareke E. Heat-treated high-fat diet modifies gut microbiota and metabolic markers in apoe−/− mice. Nutr Metab (Lond). 2016 Dec;13(1):22.

292. Zhang Z, Li D. Thermal processing of food reduces gut microbiota diversity of the host and triggers adaptation of the microbiota: evidence from two vertebrates. Microbiome. 2018 Dec;6(1):99.

293. Seiquer I, Rubio LA, Peinado MJ, Delgado-Andrade C, Navarro MP. Maillard reaction products modulate gut microbiota composition in adolescents. Mol Nutr Food Res. 2014 Jul;58(7):1552–60.

294. Forni C, Facchiano F, Bartoli M, Pieretti S, Facchiano A, D'Arcangelo D, et al. Beneficial Role of Phytochemicals on Oxidative Stress and Age-Related Diseases. BioMed Research International. 2019 Apr 7;2019:1–16.

295. Bennett RN, Wallsgrove RM. Secondary metabolites in plant defence mechanisms. New Phytologist. 1994 Aug;127(4):617–33.

296. Zhang Y-J, Gan R-Y, Li S, Zhou Y, Li A-N, Xu D-P, et al. Antioxidant Phytochemicals for the Prevention and Treatment of Chronic Diseases. Molecules. 2015 Nov 27;20(12):21138–56.

297. Liskova A, Stefanicka P, Samec M, Smejkal K, Zubor P, Bielik T, et al. Dietary phytochemicals as the potential protectors against carcinogenesis and their role in cancer chemoprevention. Clin Exp Med. 2020 May;20(2):173–90.

298. Martel J, Ojcius DM, Ko Y-F, Young JD. Phytochemicals as Prebiotics and Biological Stress Inducers. Trends in Biochemical Sciences. 2020 Jun;45(6):462–71.

299. Hidalgo M, Oruna-Concha MJ, Kolida S, Walton GE, Kallithraka S, Spencer JPE, et al. Metabolism of Anthocyanins by Human Gut Microflora and Their Influence on Gut Bacterial Growth. J Agric Food Chem. 2012 Apr 18;60(15):3882–90.

300. Zhu Y, Sun H, He S, Lou Q, Yu M, Tang M, et al. Metabolism and prebiotics activity of anthocyanins from black rice (Oryza sativa L.) in vitro. Lightfoot DA, editor. PLoS ONE. 2018 Apr 9;13(4):e0195754.

301. Duda-Chodak A. The inhibitory effect of polyphenols on human gut microbiota. J Physiol Pharmacol. 2012 Oct;63(5):497–503.

302. Corrêa TAF, Rogero MM, Hassimotto NMA, Lajolo FM. The Two-Way Polyphenols-Microbiota Interactions and Their Effects on Obesity and Related Metabolic Diseases. Front Nutr. 2019 Dec 20;6:188.

303. Cheng D, Xie MZ. A review of a potential and promising probiotic candidate-Akkermansia muciniphila. J Appl Microbiol. 2021 Jun;130(6):1813–22.

304. Roopchand DE, Carmody RN, Kuhn P, Moskal K, Rojas-Silva P, Turnbaugh PJ, et al. Dietary Polyphenols Promote Growth of the Gut Bacterium Akkermansia muciniphila and Attenuate High-Fat Diet-Induced Metabolic Syndrome. Diabetes. 2015 Aug;64(8):2847–58.

305. Moreno-Indias I, Sánchez-Alcoholado L, Pérez-Martínez P, Andrés-Lacueva C, Cardona F, Tinahones F, et al. Red wine polyphenols modulate fecal microbiota and reduce markers of the metabolic syndrome in obese patients. Food Funct. 2016;7(4):1775–87.

306. Boto-Ordóñez M, Urpi-Sarda M, Queipo-Ortuño MI, Tulipani S, Tinahones FJ, Andres-Lacueva C. High levels of Bifidobacteria are associated with increased levels of anthocyanin microbial metabolites: a randomized clinical trial. Food Funct. 2014;5(8):1932–8.

307. Istas G, Wood E, Le Sayec M, Rawlings C, Yoon J, Dandavate V, et al. Effects of aronia berry (poly)phenols on vascular function and gut microbiota: a double-blind randomized controlled trial in adult men. The American Journal of Clinical Nutrition. 2019 Aug 1;110(2):316–29.

308. Most J, Penders J, Lucchesi M, Goossens GH, Blaak EE. Gut microbiota composition in relation to the metabolic response to 12-week combined polyphenol supplementation in overweight men and women. Eur J Clin Nutr. 2017 Sep;71(9):1040–5.

309. Kawabata K, Yoshioka Y, Terao J. Role of Intestinal Microbiota in the Bioavailability and Physiological Functions of Dietary Polyphenols. Molecules. 2019 Jan 21;24(2):370.

310. Ryu D, Mouchiroud L, Andreux PA, Katsyuba E, Moullan N, Nicolet-dit-Félix AA, et al. Urolithin A induces mitophagy and prolongs lifespan in C. elegans and increases muscle function in rodents. Nat Med. 2016 Aug;22(8):879–88.

311. Zhao W, Shi F, Guo Z, Zhao J, Song X, Yang H. Metabolite of ellagitannins, urolithin A induces autophagy and inhibits metastasis in human sw620 colorectal cancer cells. Mol Carcinog. 2018 Feb;57(2):193–200.

312. Miene C, Weise A, Glei M. Impact of Polyphenol Metabolites Produced by Colonic Microbiota on Expression of COX-2 and GSTT2 in Human Colon Cells (LT97). Nutrition and Cancer. 2011 May;63(4):653–62.

313. Moynagh PN. The NF-κB pathway. Journal of Cell Science. 2005 Oct 15;118(20):4589–92.

314. Grivennikov SI, Greten FR, Karin M. Immunity, Inflammation, and Cancer. Cell. 2010 Mar;140(6):883–99.

315. Morgan MJ, Liu Z. Crosstalk of reactive oxygen species and NF-κB signaling. Cell Res. 2011 Jan;21(1):103–15.

316. Qiu B, Xu X, Yi P, Hao Y. Curcumin reinforces MSC-derived exosomes in attenuating osteoarthritis via modulating the miR-124/NF-kB and miR-143/ROCK1/TLR9 signalling pathways. J Cell Mol Med. 2020 Sep;24(18):10855–65.

317. Ghasemi F, Shafiee M, Banikazemi Z, Pourhanifeh MH, Khanbabaei H, Shamshirian A, et al. Curcumin inhibits NF-kB and Wnt/β-catenin pathways in cervical cancer cells. Pathology - Research and Practice. 2019 Oct;215(10):152556.

318. Lakshmi SP, Reddy AT, Kodidhela LD, Varadacharyulu NC. The tea catechin epigallocatechin gallate inhibits NF-κB-mediated transcriptional activation by covalent modification. Arch Biochem Biophys. 2020 Nov 30;695:108620.

319. Peng G, Dixon DA, Muga SJ, Smith TJ, Wargovich MJ. Green tea polyphenol (−)-epigallocatechin-3-gallate inhibits cyclooxygenase-2 expression in colon carcinogenesis. Mol Carcinog. 2006 May;45(5):309–19.

320. Reddy AT, Lakshmi SP, Maruthi Prasad E, Varadacharyulu NCh, Kodidhela LD. Epigallocatechin gallate suppresses inflammation in human coronary artery endothelial cells by inhibiting NF-κB. Life Sciences. 2020 Oct;258:118136.

321. Chatree S, Sitticharoon C, Maikaew P, Pongwattanapakin K, Keadkraichaiwat I, Churintaraphan M, et al. Epigallocatechin gallate decreases plasma triglyceride, blood pressure, and serum kisspeptin in obese human subjects. Exp Biol Med (Maywood). 2021 Jan;246(2):163–76.

322. Samavat H, Newman AR, Wang R, Yuan J-M, Wu AH, Kurzer MS. Effects of green tea catechin extract on serum lipids in postmenopausal women: a randomized, placebo-controlled clinical trial. Am J Clin Nutr. 2016 Dec;104(6):1671–82.

323. Parkar SG, Trower TM, Stevenson DE. Fecal microbial metabolism of polyphenols and its effects on human gut microbiota. Anaerobe. 2013 Oct;23:12–9.

324. Bokkenheuser VD, Shackleton CH, Winter J. Hydrolysis of dietary flavonoid glycosides by strains of intestinal Bacteroides from humans. Biochemical Journal. 1987 Dec 15;248(3):953–6.

325. Louis P, Scott KP, Duncan SH, Flint HJ. Understanding the effects of diet on bacterial metabolism in the large intestine. J Appl Microbiol. 2007 May;102(5):1197–208.

326. Braune A, Gütschow M, Engst W, Blaut M. Degradation of Quercetin and Luteolin by *Eubacterium ramulus*. Appl Environ Microbiol. 2001 Dec;67(12):5558–67.

327. Schoefer L, Mohan R, Schwiertz A, Braune A, Blaut M. Anaerobic Degradation of Flavonoids by *Clostridium orbiscindens*. Appl Environ Microbiol. 2003 Oct;69(10):5849–54.

328. Favela-González KM, Hernández-Almanza AY, De la Fuente-Salcido NM. The value of bioactive compounds of cruciferous vegetables (*Brassica*) as antimicrobials and antioxidants: A review. J Food Biochem [Internet]. 2020 Oct [cited 2021 May 21];44(10). Available from: https://onlinelibrary.wiley.com/doi/10.1111/jfbc.13414

329. Morrison MEW, Joseph JM, McCann SE, Tang L, Almohanna HM, Moysich KB. Cruciferous Vegetable Consumption and Stomach Cancer: A Case-Control Study. Nutrition and Cancer. 2020 Jan 2;72(1):52–61.

330. McManus H, Moysich KB, Tang L, Joseph J, McCann SE. Usual Cruciferous Vegetable Consumption and Ovarian Cancer: A Case-Control Study. Nutrition and Cancer. 2018 May 19;70(4):678–83.

331. Tang L, Zirpoli GR, Guru K, Moysich KB, Zhang Y, Ambrosone CB, et al. Consumption of Raw Cruciferous Vegetables is Inversely Associated with Bladder Cancer Risk. Cancer Epidemiol Biomarkers Prev. 2008 Apr;17(4):938–44.

332. Mahn A, Castillo A. Potential of Sulforaphane as a Natural Immune System Enhancer: A Review. Molecules. 2021 Feb 1;26(3):752.

333. Verhoeven DTH, Verhagen H, Goldbohm RA, van den Brandt PA, van Poppel G. A review of mechanisms underlying anticarcinogenicity by brassica vegetables. Chemico-Biological Interactions. 1997 Feb;103(2):79–129.

334. Koper JEB, Kortekaas M, Loonen LMP, Huang Z, Wells JM, Gill CIR, et al. Aryl hydrocarbon Receptor activation during *in vitro* and *in vivo* digestion of raw and cooked broccoli (*brassica oleracea* var. *Italica*). Food Funct. 2020;11(5):4026–37.

335. Lohning A, Kidachi Y, Kamiie K, Sasaki K, Ryoyama K, Yamaguchi H. 6-(methylsulfinyl)hexyl isothiocyanate (6-MITC) from Wasabia japonica alleviates inflammatory bowel disease (IBD) by potential inhibition of glycogen synthase kinase 3 beta (GSK-3β). European Journal of Medicinal Chemistry. 2021 Apr;216:113250.

336. Liu T, Zhang L, Joo D, Sun S-C. NF-κB signaling in inflammation. Sig Transduct Target Ther. 2017 Dec;2(1):17023.

337. Hoffmeister L, Diekmann M, Brand K, Huber R. GSK3: A Kinase Balancing Promotion and Resolution of Inflammation. Cells. 2020 Mar 28;9(4):820.

338. Zeng X, Liu X, Bao H. Sulforaphane suppresses lipopolysaccharide- and Pam3CysSerLys4-mediated inflammation in chronic obstructive pulmonary disease via toll-like receptors. Viguera AC, editor. FEBS Open Bio. 2021 May;11(5):1313–21.

339. Mullaney JA, Kelly WJ, McGhie TK, Ansell J, Heyes JA. Lactic Acid Bacteria Convert Glucosinolates to Nitriles Efficiently Yet Differently from Enterobacteriaceae. J Agric Food Chem. 2013 Mar 27;61(12):3039–46.

340. Cheng D-L, Hashimoto K, Uda Y. In vitro digestion of sinigrin and glucotropaeolin by single strains of Bifidobacterium and identification of the digestive products. Food and Chemical Toxicology. 2004 Mar;42(3):351–7.

341. Elfoul L, Rabot S, Khelifa N, Quinsac A, Duguay A, Rimbault A. Formation of allyl isothiocyanate from sinigrin in the digestive tract of rats monoassociated with a human colonic strain of Bacteroides thetaiotaomicron. FEMS Microbiology Letters. 2001 Apr;197(1):99–103.

342. Palop MLl, Smiths JP, ten Brink B. Degradation of sinigrin by Lactobacillus agilis strain R16. International Journal of Food Microbiology. 1995 Jul;26(2):219–29.

343. Narbad A, Rossiter JT. Gut Glucosinolate Metabolism and Isothiocyanate Production. Mol Nutr Food Res. 2018 Sep;62(18):1700991.

344. Gupta RC, Lall R, Srivastava A. Nutraceuticals efficacy, safety and toxicity [Internet]. 2021 [cited 2021 Sep 2]. Available from: http://www.vlebooks.com/vleweb/product/openreader?id=none&isbn=9780128212462

345. Shahinozzaman M, Raychaudhuri S, Fan S, Obanda DN. Kale Attenuates Inflammation and Modulates Gut Microbial Composition and Function in C57BL/6J Mice with Diet-Induced Obesity. Microorganisms. 2021 Jan 24;9(2):238.

346. Kaczmarek JL, Liu X, Charron CS, Novotny JA, Jeffery EH, Seifried HE, et al. Broccoli consumption affects the human gastrointestinal microbiota. The Journal of Nutritional Biochemistry. 2019 Jan;63:27–34.

347. Penland M, Falentin H, Parayre S, Pawtowski A, Maillard M-B, Thierry A, et al. Linking Pélardon artisanal goat cheese microbial communities to aroma compounds during cheese-making and ripening. International Journal of Food Microbiology. 2021 May;345:109130.

348.Moon S-H, Chang H-C. Rice Bran Fermentation Using Lactiplantibacillus plantarum EM as a Starter and the Potential of the Fermented Rice Bran as a Functional Food. Foods. 2021 Apr 29;10(5):978.

349. Shahbazi R, Sharifzad F, Bagheri R, Alsadi N, Yasavoli-Sharahi H, Matar C. Anti-Inflammatory and Immunomodulatory Properties of Fermented Plant Foods. Nutrients. 2021 Apr 30;13(5):1516.

350. García-Díez J, Saraiva C. Use of Starter Cultures in Foods from Animal Origin to Improve Their Safety. IJERPH. 2021 Mar 4;18(5):2544.

351. Dimidi E, Cox S, Rossi M, Whelan K. Fermented Foods: Definitions and Characteristics, Impact on the Gut Microbiota and Effects on Gastrointestinal Health and Disease. Nutrients. 2019 Aug 5;11(8):1806.

352. Food and Agriculture Organization of the United Nations, World Health Organization, editors. Probiotics in food: health and nutritional properties and guidelines for evaluation. Rome: Food and Agriculture Organization of the United Nations : World Health Organization; 2006. 50 p. (FAO food and nutrition paper).

353. Sassone-Corsi M, Nuccio S-P, Liu H, Hernandez D, Vu CT, Takahashi AA, et al. Microcins mediate competition among Enterobacteriaceae in the inflamed gut. Nature. 2016 Dec;540(7632):280–3.

354. Wang H, Bastian SE, Cheah KY, Lawrence A, Howarth GS. *Escherichia coli* Nissle 1917-derived factors reduce cell death and late apoptosis and increase transepithelial electrical resistance in a model of 5-fluorouracil-induced intestinal epithelial cell damage. Cancer Biology & Therapy. 2014 May;15(5):560–9.

355. Hering NA, Richter JF, Fromm A, Wieser A, Hartmann S, Günzel D, et al. TcpC protein from E. coli Nissle improves epithelial barrier function involving PKCζ and ERK1/2 signaling in HT-29/B6 cells. Mucosal Immunol. 2014 Mar;7(2):369–78.

356. Hancock V, Vejborg RM, Klemm P. Functional genomics of probiotic Escherichia coli Nissle 1917 and 83972, and UPEC strain CFT073: comparison of transcriptomes, growth and biofilm formation. Mol Genet Genomics. 2010 Dec;284(6):437–54.

357. van der Hooft JJJ, Goldstone RJ, Harris S, Burgess KEV, Smith DGE. Substantial Extracellular Metabolic Differences Found Between Phylogenetically Closely Related Probiotic and Pathogenic Strains of Escherichia coli. Front Microbiol. 2019 Feb 19;10:252.

358. Becker HM, Apladas A, Scharl M, Fried M, Rogler G. Probiotic ***Escherichia coli*** Nissle 1917 and Commensal ***E. coli*** K12 Differentially Affect the Inflammasome in Intestinal Epithelial Cells. Digestion. 2014;89(2):110–8.

359. Berger B, Pridmore RD, Barretto C, Delmas-Julien F, Schreiber K, Arigoni F, et al. Similarity and Differences in the *Lactobacillus acidophilus* Group Identified by Polyphasic Analysis and Comparative Genomics. J Bacteriol. 2007 Feb 15;189(4):1311–21.

360. Barrangou R, Azcarate-Peril MA, Duong T, Conners SB, Kelly RM, Klaenhammer TR. Global analysis of carbohydrate utilization by Lactobacillus acidophilus using cDNA microarrays. Proceedings of the National Academy of Sciences. 2006 Mar 7;103(10):3816–21.

361. Milani C, Duranti S, Napoli S, Alessandri G, Mancabelli L, Anzalone R, et al. Colonization of the human gut by bovine bacteria present in Parmesan cheese. Nat Commun. 2019 Dec;10(1):1286.

362. Zhang C, Derrien M, Levenez F, Brazeilles R, Ballal SA, Kim J, et al. Ecological robustness of the gut microbiota in response to ingestion of transient food-borne microbes. ISME J. 2016 Sep;10(9):2235–45.

363. Mujagic Z, de Vos P, Boekschoten MV, Govers C, Pieters H-JHM, de Wit NJW, et al. The effects of Lactobacillus plantarum on small intestinal barrier function and mucosal gene transcription; a randomized double-blind placebo controlled trial. Sci Rep. 2017 Mar;7(1):40128.

364. Kodali VP, Sen R. Antioxidant and free radical scavenging activities of an exopolysaccharide from a probiotic bacterium. Biotechnol J. 2008 Feb;3(2):245–51.

365. Kaur H, Gupta T, Kapila S, Kapila R. Protective effects of potential probiotic *Lactobacillus rhamnosus* (MTCC-5897) fermented whey on reinforcement of intestinal epithelial barrier function in a colitis-induced murine model. Food Funct. 2021;10.1039.D0FO02641G.

366. Guan Q, Ding X-W, Zhong L-Y, Zhu C, Nie P, Song L-H. Beneficial effects of *Lactobacillus* -fermented black barley on high fat diet-induced fatty liver in rats. Food Funct. 2021;10.1039.D1FO00290B.

367. Bhattacharya S, Gachhui R, Sil PC. Effect of Kombucha, a fermented black tea in attenuating oxidative stress mediated tissue damage in alloxan induced diabetic rats. Food and Chemical Toxicology. 2013 Oct;60:328–40.

368. Zubaidah E, Afgani CA, Kalsum U, Srianta I, Blanc PJ. Comparison of in vivo antidiabetes activity of snake fruit Kombucha, black tea Kombucha and metformin. Biocatalysis and Agricultural Biotechnology. 2019 Jan;17:465–9.

369. Kim D-H, Jeong D, Kim H, Seo K-H. Modern perspectives on the health benefits of kefir in next generation sequencing era: Improvement of the host gut microbiota. Critical Reviews in Food Science and Nutrition. 2019 Jun 17;59(11):1782–93.

370. Bourrie BCT, Cotter PD, Willing BP. Traditional kefir reduces weight gain and improves plasma and liver lipid profiles more successfully than a commercial equivalent in a mouse model of obesity. Journal of Functional Foods. 2018 Jul;46:29–37.

371. Satora P, Skotniczny M, Strnad S, Ženišová K. Yeast Microbiota during Sauerkraut Fermentation and Its Characteristics. IJMS. 2020 Dec 18;21(24):9699.

372. Di Cagno R, Filannino P, Gobbetti M. Fermented Foods: Fermented Vegetables and Other Products. In: Encyclopedia of Food and Health [Internet]. Elsevier; 2016 [cited 2021 May 26]. p. 668–74. Available from: https://linkinghub.elsevier.com/retrieve/pii/B9780123849472002841

373. Tanaka S, Yamamoto K, Hamajima C, Takahashi F, Endo K, Uyeno Y. Dietary Supplementation with Fermented Brassica rapa L. Stimulates Defecation Accompanying Change in Colonic Bacterial Community Structure. Nutrients. 2021 May 28;13(6):1847.

374. Martinez-Villaluenga C, Peñas E, Sidro B, Ullate M, Frias J, Vidal-Valverde C. White cabbage fermentation improves ascorbigen content, antioxidant and nitric oxide production inhibitory activity in LPS-induced macrophages. LWT - Food Science and Technology. 2012 Apr;46(1):77–83.

375. Shankar T, Palpperumal S, Kathiresan D, Sankaralingam S, Balachandran C, Baskar K, et al. Biomedical and therapeutic potential of exopolysaccharides by Lactobacillus paracasei isolated from sauerkraut: Screening and characterization. Saudi Journal of Biological Sciences. 2021 May;28(5):2943–50.

376. Yin T, Bayanjargal S, Fang B, Inaba C, Mutoh M, Kawahara T, et al. *Lactobacillus plantarum* Shinshu N-07 isolated from fermented *Brassica rapa* L. attenuates visceral fat accumulation induced by high-fat diet in mice. Beneficial Microbes. 2020 Nov 15;11(7):655–67.

377. Nielsen ES, Garnås E, Jensen KJ, Hansen LH, Olsen PS, Ritz C, et al. Lacto-fermented sauerkraut improves symptoms in IBS patients independent of product pasteurisation – a pilot study. Food Funct. 2018;9(10):5323–35.

378. Şanlier N, Gökcen BB, Sezgin AC. Health benefits of fermented foods. Critical Reviews in Food Science and Nutrition. 2019 Feb 4;59(3):506–27.

379. Septembre-Malaterre A, Remize F, Poucheret P. Fruits and vegetables, as a source of nutritional compounds and phytochemicals: Changes in bioactive compounds during lactic fermentation. Food Research International. 2018 Feb;104:86–99.

380. Ciska E, Pathak DR. Glucosinolate derivatives in stored fermented cabbage. J Agric Food Chem. 2004 Dec 29;52(26):7938–43.

381. Frias J, Martinez-Villaluenga C, Peñas E, editors. Fermented foods in health and disease prevention. Amsterdam ; San Diego, CA: Academic Press; 2017. 760 p.

382. United Nations, Department of Economic and Social Affairs, Population Division. World population prospects Highlights, 2019 revision Highlights, 2019 revision. 2019.

383. HLPE. Nutrition and food systems. A report by the High Level Panel of Experts on Food Security and Nutrition of the Committee on World Food Securit. Rome; 2017.

384. Hilborn R, Banobi J, Hall SJ, Pucylowski T, Walsworth TE. The environmental cost of animal source foods. Front Ecol Environ. 2018 Aug;16(6):329–35.

385. Khan SU, Lone AN, Khan MS, Virani SS, Blumenthal RS, Nasir K, et al. Effect of omega-3 fatty acids on cardiovascular outcomes: A systematic review and meta-analysis. EClinicalMedicine. 2021 Aug;38:100997.

386. Mozaffarian D, Rimm EB. Fish Intake, Contaminants, and Human Health: Evaluating the Risks and the Benefits. JAMA. 2006 Oct 18;296(15):1885.

387. Cardoso C, Afonso C, Bandarra NM. Dietary DHA, bioaccessibility, and neurobehavioral development in children. Critical Reviews in Food Science and Nutrition. 2018 Oct 13;58(15):2617–31.

388. Oken E, Radesky JS, Wright RO, Bellinger DC, Amarasiriwardena CJ, Kleinman KP, et al. Maternal Fish Intake during Pregnancy, Blood Mercury Levels, and Child Cognition at Age 3 Years in a US Cohort. American Journal of Epidemiology. 2008 Mar 14;167(10):1171–81.

389. HLPE. Sustainable fisheries and aquaculture for food security and nutrition. A report by the High Level Panel of Experts on Food Security and Nutrition of the Committee on World Food Security. Rome; 2014.

390. The Federation of European Aquaculture Producers (FEAP). FEAP European Aquaculture Production Report 2014-2019. 2020.

391. Tacon AGJ, Metian M. Feed Matters: Satisfying the Feed Demand of Aquaculture. Reviews in Fisheries Science & Aquaculture. 2015 Jan 2;23(1):1–10.

392. Kaushik SJ, Hemre G-I. Plant proteins as alternative sources for fish feed and farmed fish quality. In: Improving Farmed Fish Quality and Safety [Internet]. Elsevier; 2008 [cited 2021 Sep 4]. p. 300–27. Available from: https://linkinghub.elsevier.com/retrieve/pii/B9781845692995500123

393. den Hartog LA, Sijtsma SR. Sustainable feed ingredients. In Victoria, Australia; 2013.

394. Maiolo S, Parisi G, Biondi N, Lunelli F, Tibaldi E, Pastres R. Fishmeal partial substitution within aquafeed formulations: life cycle assessment of four alternative protein sources. Int J Life Cycle Assess. 2020 Aug;25(8):1455–71.

395. Montero D, Izquierdo M. Welfare and Health of Fish Fed Vegetable Oils as Alternative Lipid Sources to Fish Oil. In: Turchini G, Ng W-K, Tocher D, editors. Fish Oil Replacement and Alternative Lipid Sources in Aquaculture Feeds [Internet]. CRC Press; 2010 [cited 2021 May 20]. p. 439–85. Available from: http://www.crcnetbase.com/doi/10.1201/9781439808634-c14

396. Cebra JJ. Influences of microbiota on intestinal immune system development. Am J Clin Nutr. 1999;69:1046S-1051S.

397. Pérez T, Balcázar JL, Ruiz-Zarzuela I, Halaihel N, Vendrell D, de Blas I, et al. Host–microbiota interactions within the fish intestinal ecosystem. Mucosal Immunol. 2010 Jul;3(4):355–60.

398. Bruni L, Pastorelli R, Viti C, Gasco L, Parisi G. Characterisation of the intestinal microbial communities of rainbow trout (Oncorhynchus mykiss) fed with Hermetia illucens (black soldier fly) partially defatted larva meal as partial dietary protein source. Aquaculture. 2018 Feb;487:56–63.

399. Rimoldi S, Antonini M, Gasco L, Moroni F, Terova G. Intestinal microbial communities of rainbow trout (Oncorhynchus mykiss) may be improved by feeding a Hermetia illucens meal/low-fishmeal diet. Fish Physiol Biochem. 2021 Apr;47(2):365–80.

400.Wu S, Wang G, Angert ER, Wang W, Li W, Zou H. Composition, Diversity, and Origin of the Bacterial Community in Grass Carp Intestine. Bereswill S, editor. PLoS ONE. 2012 Feb 20;7(2):e30440.

401. Terova G, Rimoldi S, Ascione C, Gini E, Ceccotti C, Gasco L. Rainbow trout (Oncorhynchus mykiss) gut microbiota is modulated by insect meal from Hermetia illucens prepupae in the diet. Rev Fish Biol Fisheries. 2019 Jun;29(2):465–86.

402.Irianto A, Austin B. Use of probiotics to control furunculosis in rainbow trout, Oncorhynchus mykiss (Walbaum). J Fish Diseases. 2002 Jun;25(6):333–42.

403. Panigrahi A, Kiron V, Kobayashi T, Puangkaew J, Satoh S, Sugita H. Immune responses in rainbow trout Oncorhynchus mykiss induced by a potential probiotic bacteria Lactobacillus rhamnosus JCM 1136. Veterinary Immunology and Immunopathology. 2004 Dec;102(4):379–88.

404. Balcázar JL, de Blas I, Ruiz-Zarzuela I, Vendrell D, Calvo AC, Márquez I, et al. Changes in intestinal microbiota and humoral immune response following probiotic administration in brown trout (*Salmo trutta*). Br J Nutr. 2007 Mar;97(3):522–7.

405. Pandey A, Soccol CR, Mitchell D. New developments in solid state fermentation: I-bioprocesses and products. Process Biochemistry. 2000 Jul;35(10):1153–69.

406. Stabnikova O. Biotransformation of vegetable and fruit processing wastes into yeast biomass enriched with selenium. Bioresource Technology. 2005 Apr;96(6):747–51.

407. Rajesh N, Imelda-Joseph, Paul Raj R. Value addition of vegetable wastes by solid-state fermentation using Aspergillus niger for use in aquafeed industry. Waste Management. 2010 Nov;30(11):2223–7.

408. Hamid NH, Daud HM, Kayansamruaj P, Hassim HA, Mohd Yusoff MS, Abu Bakar SN, et al. Short- and long-term probiotic effects of Enterococcus hirae isolated from fermented vegetable wastes on the growth, immune responses, and disease resistance of hybrid catfish (Clarias gariepinus × Clarias macrocephalus). Fish & Shellfish Immunology. 2021 Jul;114:1–19.

409. Jiang L, Wang J, Xiong K, Xu L, Zhang B, Ma A. Intake of Fish and Marine n-3 Polyunsaturated Fatty Acids and Risk of Cardiovascular Disease Mortality: A Meta-Analysis of Prospective Cohort Studies. Nutrients. 2021 Jul 9;13(7):2342.

410. Zheng J, Huang T, Yu Y, Hu X, Yang B, Li D. Fish consumption and CHD mortality: an updated meta-analysis of seventeen cohort studies. Public Health Nutr. 2012 Apr;15(4):725–37.

411. Calder PC. Omega-3 fatty acids and inflammatory processes: from molecules to man. Biochemical Society Transactions. 2017 Oct 15;45(5):1105–15.

412. Chen J, Jayachandran M, Bai W, Xu B. A critical review on the health benefits of fish consumption and its bioactive constituents. Food Chemistry. 2022 Feb;369:130874.

413. Perez-Araluce R, Martinez-Gonzalez MA, Fernández-Lázaro CI, Bes-Rastrollo M, Gea A, Carlos S. Mediterranean diet and the risk of COVID-19 in the 'Seguimiento Universidad de Navarra' cohort. Clinical Nutrition. 2021 Apr;S0261561421001904.

414. Gram L, Ravn L, Rasch M, Bruhn JB, Christensen AB, Givskov M. Food spoilage—interactions between food spoilage bacteria. International Journal of Food Microbiology. 2002 Sep;78(1–2):79–97.

415. Li Y, Rahman SU, Huang Y, Zhang Y, Ming P, Zhu L, et al. Green tea polyphenols decrease weight gain, ameliorate alteration of gut microbiota, and mitigate intestinal inflammation in canines with high-fat-diet-induced obesity. The Journal of Nutritional Biochemistry. 2020 Apr;78:108324.

Chapter 2: Effects of exogenous dietary advanced glycation end products on the cross-talk mechanisms linking microbiota to metabolic inflammation

Giulia Gaudioso[1,2]

Collaborators: Raffaella Mastrocola[3], Debora Collotta[4], Marie Le Berre[5], Alessia Sofia Cento[3], Gustavo Ferreira Alves[4], Fausto Chiazza[4], Roberta Verta[4], Ilaria Bertocchi[6], Friederike Manig[7], Michael Hellwig[7], Francesca Fava[1], Carlo Cifani[8], Manuela Aragno[3], Thomas Henle[7], Lokesh Joshi[5], Kieran Michael Tuohy[1] and Massimo Collino[4].

[1] Nutrition and Nutrigenomics Unit, Department of Food Quality and Nutrition, Research and Innovation Center, Fondazione Edmund Mach, 38098 Trento, Italy

[2] CIBIO – Department of Cellular, Computational and Integrative Biology, University of Trento, 38123 Trento, Italy

[3] Department of Clinical and Biological Sciences, University of Turin, 10125 Turin, Italy

[4] Department of Drug Science and Technology, University of Turin, 10125 Turin, Italy

[5] Biomedical Sciences, National University of Ireland, H91 TK33 Galway, Ireland

[6] Department of Neuroscience, University of Turin, 10124 Turin, Italy

[7] Chair of Food Chemistry, Technische Universität Dresden, 01062 Dresden, Germany

[8] Pharmacology Unit, School of Pharmacy, University of Camerino, 62032 Camerino, Italy

This chapter has been adapted from:

Mastrocola, R.; Collotta, D.; Gaudioso, G.; Le Berre, M.; Cento, A.S.; Ferreira Alves, G.; Chiazza, F.; Verta, R.; Bertocchi, I.; Manig, F.; Hellwig, M.; Fava, F.; Cifani, C.; Aragno, M.; Henle, T.; Joshi, L.; Tuohy, K.; Collino, M. Effects of Exogenous Dietary Advanced Glycation End Products on the Cross-Talk Mechanisms Linking Microbiota to Metabolic Inflammation. *Nutrients* **2020**, 12, 2497. https://doi.org/10.3390/nu12092497.

1. Introduction

The ageing of world population and the rapid changes in lifestyle which have occurred in recent decades have contributed to a growing epidemic of chronic metabolic and inflammatory diseases (1). In particular, nutrition is now considered one of the main modifiable risk factors for metabolic inflammation (known as "metaflammation"), which is a pathological feature characterizing many chronic diseases. Our modern Western-style diet (MWD) is characterized by high intake of sugar and saturated fats, and a concomitant low intake of fresh plant-based food (2). Moreover, MWD accounts for overconsumption of ultra-processed foods which contain high levels of advanced glycation end-products (AGEs) (3). These highly reactive compounds are derived from a first reaction between a reducing sugar and the amino group of proteins and give rise, through a sequence of dehydration, cyclization, fragmentation, and oxidation reactions, to final AGE-modified proteins, which are non-degradable by human digestive enzymes and are functionally compromised (4). A growing body of evidence is demonstrating the pivotal role of AGEs play in several pathogenic mechanisms underpinning oxidative stress, unresolved inflammation and endothelial dysfunction, all of which contribute to onset chronic diseases such as type 2 diabetes, atherosclerosis, cardiovascular diseases, and renal dysfunction (5). AGEs can be endogenously formed in conditions of hyperglycemia and dyslipidemia (6). However, AGEs can also be formed in foods during cooking or food processing. Indeed, particular conditions of cooking (high temperatures for long time, low level of hydration and high pH) generate large amounts of different classes of AGEs (7). Several databases reporting AGEs content of common ingredients and foods have been published, however, data are often contradictory and chemical characterization of AGEs is limited (8,9). Very recently, the Senate Commission on Food Safety of the German Research Foundation has published quality criteria for studies dealing with dietary glycation compounds and human health (10). Accordingly, the best methods available for quantification of AGEs rely on chromatographic analyses, and by using these methods, a daily intake of AGEs between 25 and 75 mg has been estimated (9). Even though dietary interventions which reduce AGEs intake have been demonstrated to be effective in reducing markers of oxidative stress, inflammation, and endothelial dysfunction in patients with diabetes or cardiometabolic diseases (11), many questions remain unanswered. We still do not know to what extent dietary AGEs contribute to the physiological pool of AGEs. Similarly, we still do not fully understand how AGEs can modify systemic and tissue proteins, including their post-translational modification such as glycosylation, and affect overall metabolism even in the absence

of pre-existing cardiometabolic disorders. It has been estimated that a fraction of ingested AGEs, that are not absorbed and not defecated, may be metabolized intraluminally by the mammalian gut microbiota (GM) (12). It has been recently shown that AGEs such as N-"-carboxymethyllysine (CML) can be metabolized by the human microbiota (13) and that *E. coli* is able to convert CML to mainly one metabolite, the biogenic amine N-carboxymethylcadaverine (14). Moreover, Mills and colleagues (2008) investigated the effect of glycated bovine serum albumin on the GM of ulcerative colitis (UC) subjects, highlighting the role of dietary glycated protein in driving dramatic alterations in colonic microbiota composition *in vitro* (15). More recently, Qu and collaborators (2017) demonstrated that dietary AGEs significantly impacted on gut microbial ecology of Sprague-Dawley rats, by negatively affecting diversity and richness, reducing saccharolytic SCFA-producing bacteria and increasing harmful bacteria such as *Desulfovibrio* (16). Hence, the present study, aimed to investigate the effects of an AGE-enriched diet (AGE-D) on gut microbiota composition and function, as well as on the development of metabolic inflammation, focusing on the molecular pathways activated by AGEs chronic exposure at organ and tissue levels. My personal contribution to this work, which is part of a larger collaboration with the University of Torino, measuring the impact of AGEs on the GM and to assess whether a diet enriched in AGEs may mediate its putative pro-inflammatory role at least in part, by reshaping the gut community structure. I performed the DNA extraction from murine faecal samples and 16S rRNA microbiota analysis by Illumina MiSeq high-throughput sequencing, followed by microbial community analysis using QIIME2.0 pipeline. Moreover, I made use of different statistical tests in R studio to analyze 16S rRNA sequencing results and to perform correlation analysis between GM composition, systemic metabolites and inflammatory markers. Finally, I contributed to the overall preparation of the manuscript, which is presented here as supplementary material.

2. Materials and methods

2.1 Animals, experimental design and feces collection

The *in vivo* experimental procedures here described were performed at the University of Torino. All experimental procedures were approved by the local Animal Use and Care Committee and the Ministry of Health (approval n° 42/2017-PR) and are in keeping with the European Directive 2010/63/EU on the protection of animals used for scientific purposes as well as the Guide for the Care and Use of Laboratory Animals. This study was carried out using 4-weeks old C57BL/6 male mice, housed in a controlled environment at 25 ± 2°C. Mice were randomly allocated to two experimental groups (n = 15 per group): mice fed with a control not-irradiated standard isocaloric diet (CD) and mice fed with an AGE-enriched diet (AGE-D) for 22 weeks. AGE-D was prepared replacing casein in the CD (200 g/kg of diet) by an equal amount of modified casein where 80.5% of arginine and 41.5% of lysine were modified. The diet contained 15 μmol of MG-H1 (methylglyoxal-derived 5-hydro-5-methylimidazolone) per g of diet. All groups received water and food *ad libitum*. Body weight and food/water intake were recorded weekly, whereas fasting glucose was recorded monthly. After 22 weeks of dietary manipulation, one day before the end of the experiment, feces were collected using metabolic cages (18 h starving) from CD (n = 8) and AGE-D (n = 10) mice.

2.2 Fecal Microbiota Analysis

Total genomic DNA extraction from frozen feces was carried out using QIAamp® PowerFecal® DNA Isolation kit (MoBio Laboratories, Inc., Carlsbad, CA, USA) and then subjected to PCR amplification by targeting 16S rRNA V3-V4 variable regions with specific bacterial primer set 341F (5′ CCTACGGGNGGCWGCAG 3′) and 806R (5′ GACTACNVGGGTWTCTAATCC 3′), as previously reported (17). PCR products were checked by gel electrophoresis and cleaned using Agencourt AMPure XP system (Beckman Coulter, Brea, CA, USA), following manufacturer's instructions. After 7 PCR cycles, (16S Metagenomic Sequencing Library Preparation, Illumina), Illumina adaptors were attached (Illumina Nextera XT Index Primer). Libraries were purified using Agencourt AMPure XP (Beckman) and then sequenced on an Illumina® MiSeq (PE300) platform (MiSeq Control Software 2.0.5 and Real-Time Analysis software 1.16.18). Sequences obtained from Illumina sequencing were analyzed using Quantitative Insights Into Microbial Ecology (QIIME) 2.0 pipeline (18). Percentage relative abundance of taxa from different dietary groups were compared using non parametric Wilcoxon statistical test. α and β-diversity estimates were determined using phyloseq R Package (19). Correlation between bacterial genera and systemic parameters in CD and

AGE-D groups was performed by Spearman correlation analysis. Unidentified genera include those whose percentage sequence homology with Greengenes database was below 95% (http://greengenes.lbl.gov) (20).

2.3 Statistical Analysis

All statistical analysis was performed using R studio version 3.6.2. Normal distribution of data was assessed by Shapiro–Wilk's test. Percentage relative abundance of taxa from different dietary groups was compared using nonparametric Wilcoxon test. Pairwise comparison among groups in terms of α-diversity was performed by Kruskal–Wallis test. Differences in the β-diversity were checked using the non-parametric Permutational Multivariate Analysis of Variance (PERMANOVA) and adonis tests with 999 permutations, via the vegan R Package (21). Correlation between bacterial taxa and immune and inflammatory measurements was performed by Spearman's correlation analysis. All p-values were adjusted using Benjamini-Hochberg false discovery rate (FDR) correction. After FDR correction, a p value < 0.05 was considered statistically significant. All data are expressed as the mean ± standard deviation, SD.

3. Results

3.1 Chronic AGEs Exposure Altered Microbial Community Profile

Illumina® MiSeq (PE300) sequencing of gut microbial 16S rRNA gene amplicons produced a total of 6,196,215 reads, with 126,453.37 ± 29,464.55 raw reads per sample. After QIIME 2.0 analysis, we removed chimeras, low quality sequences, and sequences that were identified as Cyanobacteria, and the total number of reads was 4,408,552, with 89,970.45 ± 21,973.12 raw reads per sample. Three different indices were used to analyzed changes in bacterial α-diversity, namely the observed number of OTUs, the Chao1 index and the Shannon entropy index (**Figure 1**). No differences were observed in gut microbial α-diversity at T0 (baseline) among the two groups. Compared to CD and to baseline, AGE enriched diet did not significantly affect bacterial α-diversity after 22 weeks of dietary treatment (**Figure 1**). In order to highlight differences in bacterial composition, we plotted β-diversity using Bray-Curtis dissimilarity index, weighted and unweighted UniFrac distances (**Figure 2**A, B, C). All the three β-diversity indices showed a clear separation of AGE-D mice from CD in fecal microbial composition at T22 weeks ($p < 0.001$) (**Figure 2**).

Figure 1. Bacterial α-diversity using observed OTUs, Chao1 and Shannon index, at baseline (T0) and after 22 weeks of dietary treatments: control diet (CD) or AGE-enriched diet (AGE-D). Different colors indicate different dietary treatments. Line inside the box represents the median (CD, n=8; AGE-D, n=10), whiskers from either side of the box represent the first and the third quartiles, respectively.

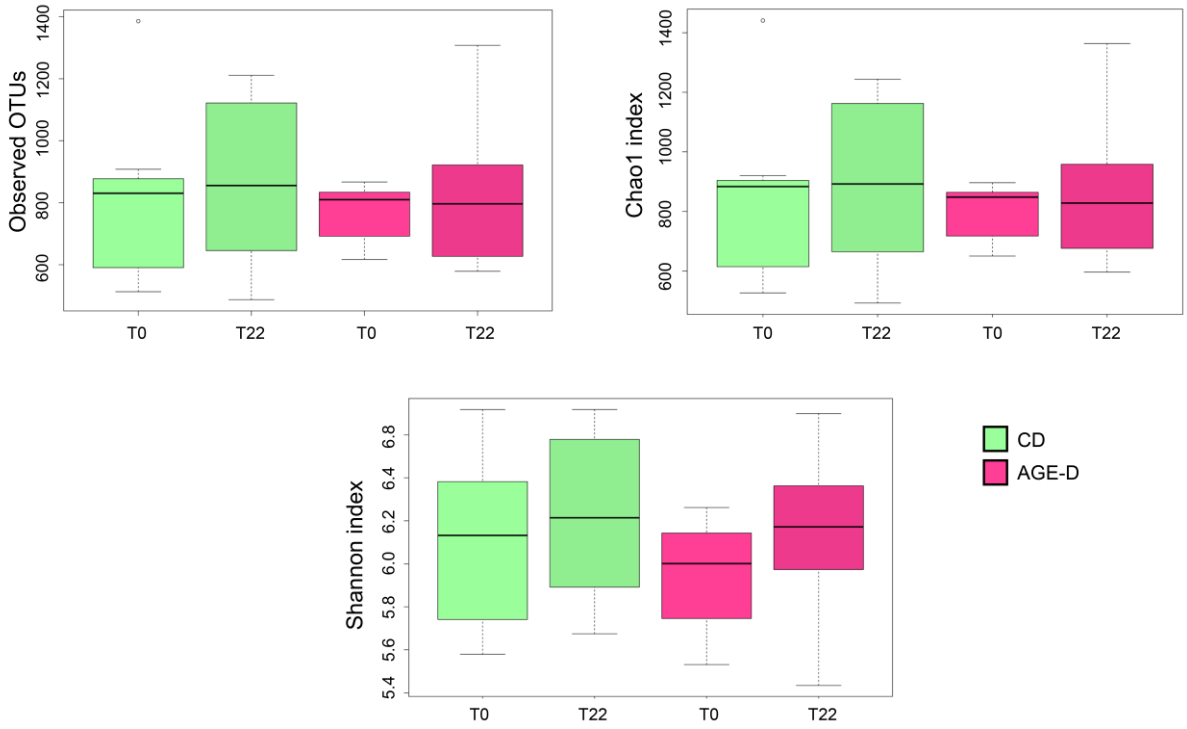

Figure 2. Principal Component Analysis (PCoA) representing the bacterial β-diversity according to Bray-Curtis dissimilarity index (**A**), unweighted (**B**) and weighted UniFrac analysis (**C**). Different colors indicate different dietary treatments (CD, control diet; AGE-D, AGE enriched diet) and different shapes indicate different timepoints, as shown in the legend.

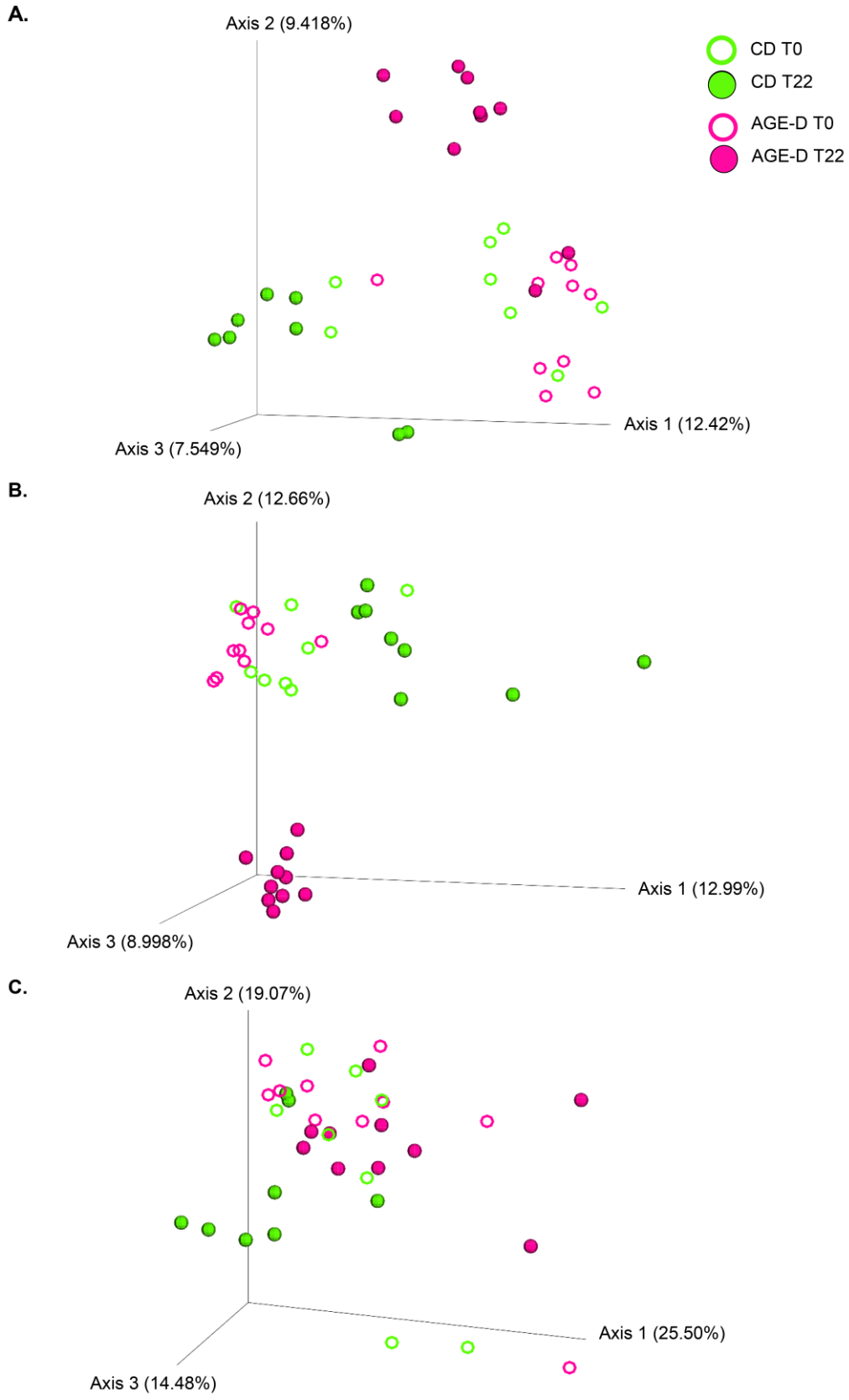

The statistically significant results of GM analysis in relative abundance of taxa are illustrated in **Figure 3**. At T0 there were no significant differences between the treatments in bacterial taxa abundance at every taxonomic level, from phylum to genus. After 22 weeks of dietary treatment, at family level, AGE-D mice had significantly lower S24-7 bacteria (Muribaculaceae, within the Bacteroidetes phylum, $p < 0.05$) and double the abundance of Lachnospiraceae ($p < 0.01$), in comparison to CD mice; while at the genus level, AGE-D mice had lower *Lactobacillus* ($p < 0.001$), *Prevotella* ($p < 0.01$), *Anaerostipes* ($p < 0.01$), and *Candidatus Arthromitus* ($p < 0.01$) and higher *Parabacteroides* ($p < 0.001$), *Ruminococcus* (Lachnospiraceae family, $p < 0.001$) and *Lawsonia* ($p = 0.01$) (**Figure 3**). There was a trend towards a decrease in Bacteroides/Firmicutes (F/B) ratio in the AGE-D group at T22, compared to CD, although not statistically significant ($p > 0.05$).

Figure 3. Boxplots of percentage relative abundance of fecal microbial genera in CD (n = 8) and AGE-D (n = 10) mice at 22 weeks (T22) of dietary intervention after 16SrRNA sequencing using V3-V4 targeted primers. "Unidentified genus 1": a genus within the Family S 24-7 which could not be assigned at a percentage sequence homology of at least 95% to any existing genera within the reference database (http://greengenes.lbl.gov).

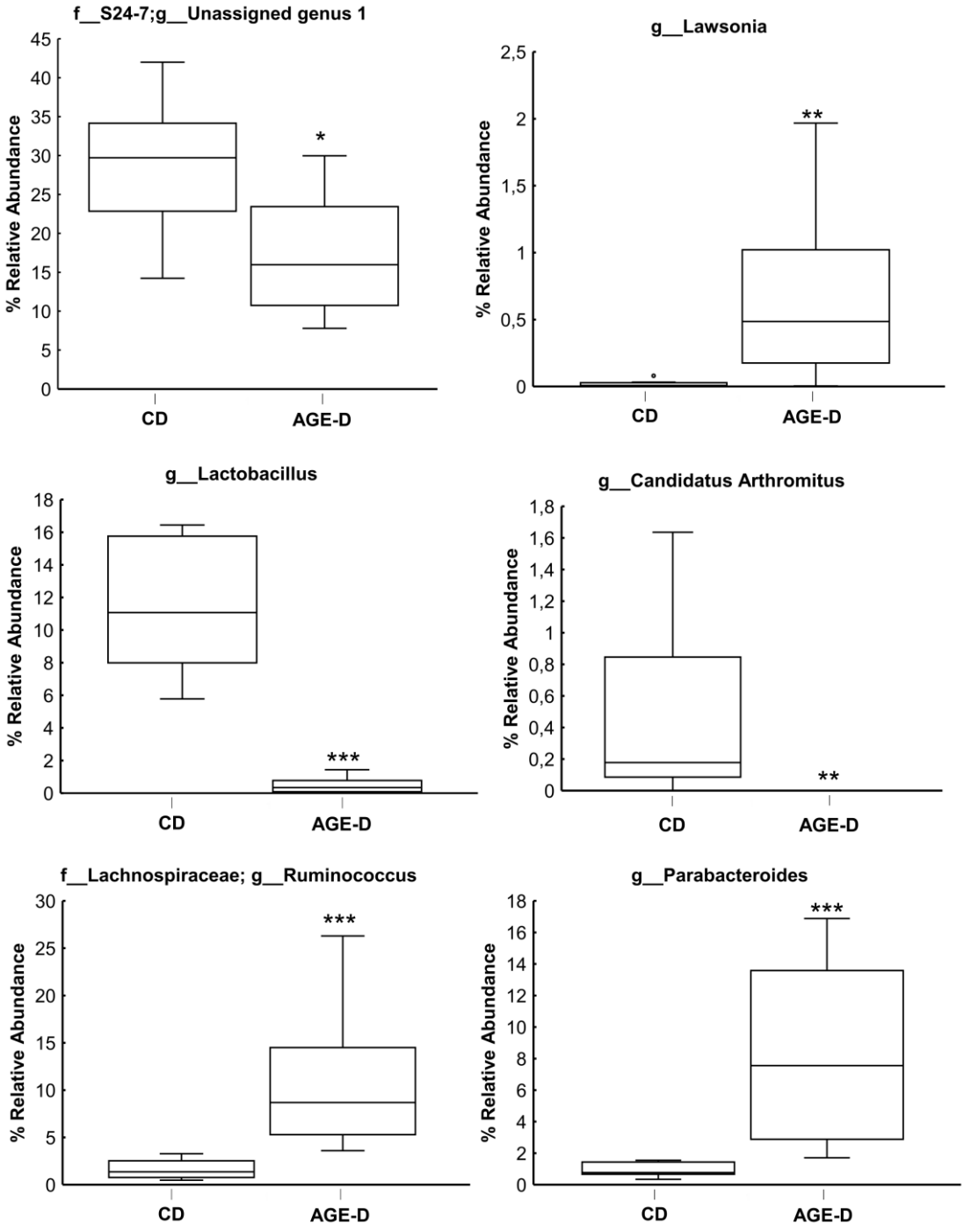

Figure 1. Continues from previous page.

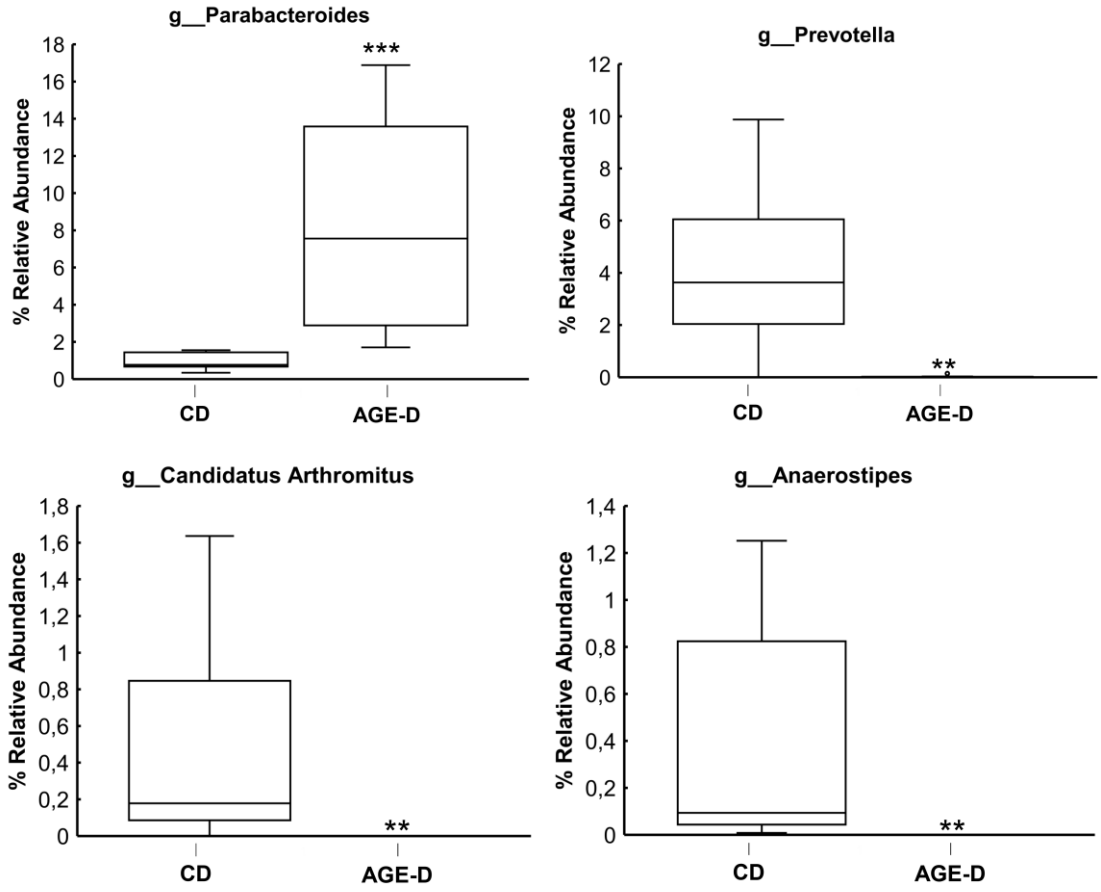

3.2 Correlation analysis between microbial genera and inflammatory and immune measurements

The heatmap of Spearman's rank correlation coefficients in **Figure 4** indicate significant correlation between relative abundance of bacterial families/genera and systemic inflammatory profiles and lipid/glucose related parameters which were measured by our collaborators at the University of Torino (**Table 1**). Indeed, the overall results obtained in CD and AGE-D groups showed that Lachnospiraceae, *Parabacteroides*, *Lawsonia* and *Ruminococcus* (Lachnospiraceae family) are all positively correlated to PAI-1, IL-1β, and IL-17 levels and negatively correlated to GIP and GLP-1. Furthermore, *Prevotella*, *Lactobacillus*, *Anaerostipes*, and *Candidatus Arthromitus* have a significant positive correlation with GIP and GLP-1, and a negative correlation with systemic inflammatory blood parameters PAI-1, IL-1β, and IL-17.

Table 1. Systemic inflammatory and lipid/glucose profile parameters at 22 weeks of the AGE-enriched diet (AGE-D) in comparison to the control diet (CD), measured by our collaborators at the University of Torino. GIP, gastric inhibitory peptide; GLP-1, glucagon-like peptide 1; PAI-1, plasminogen activator inhibitor-1; IL, interleukin. Data are expressed as mean ± SD. Statistical significance: * $p < 0.05$, ** $p < 0.01$ vs CD.

	CD	**AGE-D**
Blood glucose (mg/dL)	85,38 ± 6,19	92,70 ± 14,06
Insulin (pg/mL)	2.579,23 ± 691,16	3.883,65 ± 1.333,54*
GIP (pg/mL)	628,49 ± 73,84	462,62 ± 72,62*
GLP-1 (pg/mL)	642,45 ± 82,83	472,62 ± 79,31*
PAI-1 (pg/mL)	1.188,70 ± 373,13	2.320,14 ± 276,82**
IL-1β (pg/mL)	1,32 ± 1,02	8,79 ± 5,90**
IL-17 (pg/mL)	7,07 ± 3,53	18,57 ± 2,29*
Serum creatinine (mg/dL)	0,22 ± 0,03	0,32 ± 0,09

Figure 4. Heatmap of Spearman's correlation between the fecal bacteria genera and systemic measurements in CD and AGE-D groups. Dark red indicates positive correlation, while dark blue represents negative correlation. Stars indicate statistical significance after FDR correction (* $p < 0.05$, ** $p < 0.01$, *** $p < 0.001$). Genera and families were reported as "Unidentified" when they could not be assigned to any genera/family within a given family/order at a percentage sequence homology of 95% and 90%, respectively, to existing genera and families in the reference database (https://www.arb-silva.de/download/archive/, accessed on 13 July 2020).

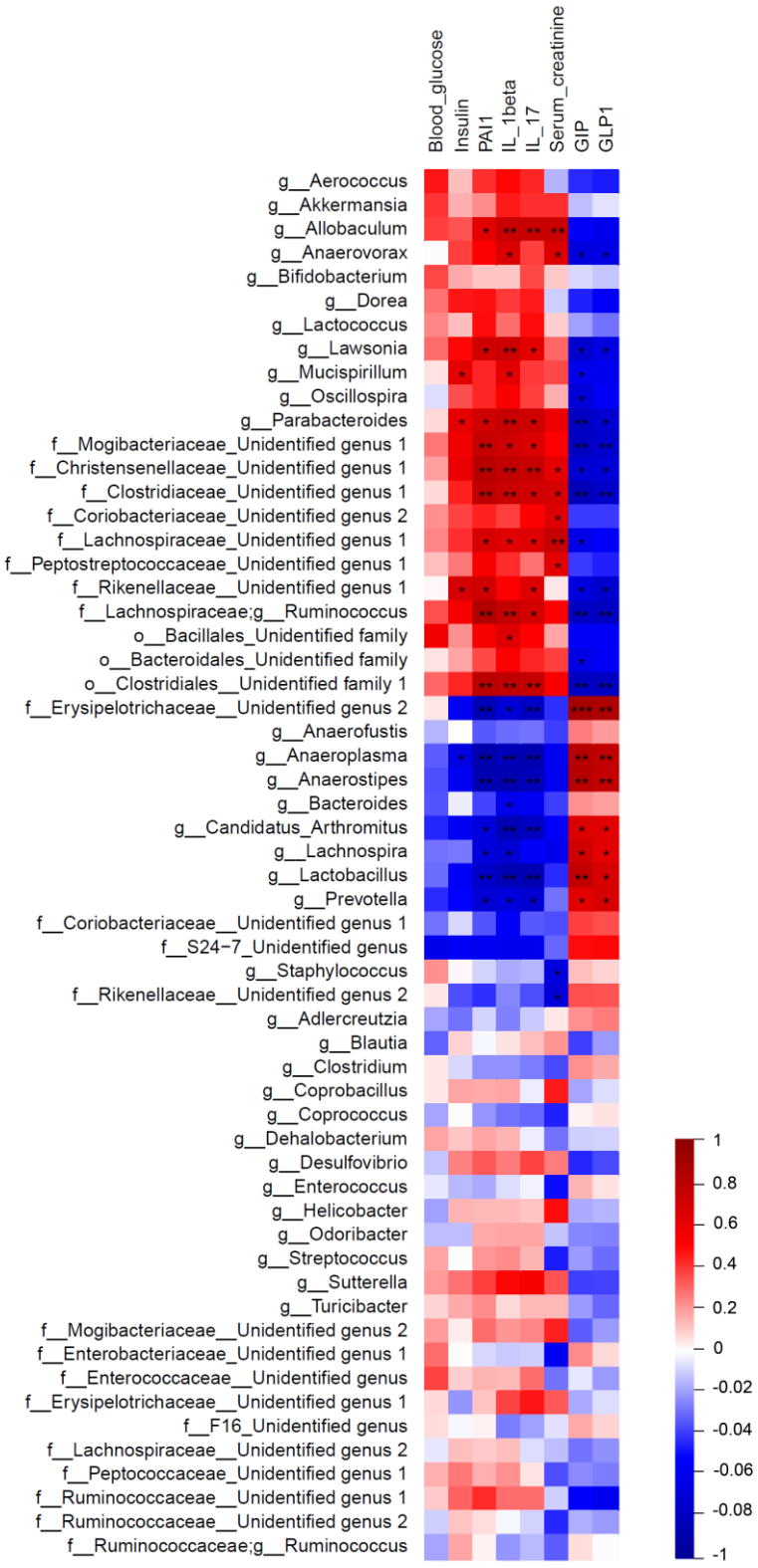

4. Discussion

Dietary AGEs represent an example of pro-inflammatory compounds present at significant concentrations in our modern Western style diet and have been implicated in the development of metabolic inflammation (2). In the present study we reported for the first time that the enrichment of a standard diet with MG-H1, a common dietary AGE found in highly processed foods (22), is sufficient to evoke alterations in microbiota homeostasis. A non-irradiated standard diet enriched in only MG-H1 was used to investigate the effective causal contribution of a well-characterized AGE in metabolic derangements, excluding the effect of other factors such as food processing products or alternative sources of AGEs. Maillard reaction, commonly known as protein glycation, normally occurs *in vivo* but it also occurs during the preparation of foods at high temperatures. Here, the AGEs diet was enriched in MG-H1, which is one of the most important Maillard reaction products identified and quantified in food and biological matrices (22), and the most abundant in body fluids of diabetes patients (23,24). The AGE-D differed from the control diet only for the presence of MG-H1 instead of a part of the arginine residues in the casein; thus, indicating that all the systemic and tissue alterations recorded in this investigation have to be related to this dietary modification.

Several cross-sectional and intervention studies have shown positive correlations between AGEs intake and their circulating levels, as measured by food databases (4,8,25). Isocaloric restrictions of dietary AGEs have been shown to decrease circulating AGEs levels and inflammatory biomarkers, and to improve endothelial dysfunction (26). However, the mechanisms linking dietary AGEs exposure to their absorption and their effective bioavailability, are still largely unknown. Interestingly, it has been recently suggested that some of the ingested AGEs are neither absorbed nor defecated and could be metabolized intraluminally by the GM (27). The intestinal AGEs processing is due to specific microorganisms and local AGEs accumulation may affect gut microbiota through negative selection for direct toxic effects, or positive selection favoring bacterial species that use AGEs as source of energy (28). AGEs have been previously shown to alter colonic microbiota composition *in vitro*, promoting the growth of sulphate-reducing bacteria, clostridia and Bacteroidetes and decreasing putatively beneficial lactobacilli and bifidobacteria (15). Here, for the first time, we demonstrated that a diet enrichment with a single AGE is sufficient to induce significant changes in the microbiota composition. Notably, the MG-H1 enriched diet used here was neither heated nor irradiated; thus, offering an appropriate experimental tool to detect the impact of AGEs on gut microbiota. Indeed, many contradictory data have been reported on the effect of

heated foods on microbiota due to the heterogeneity of compounds that are formed during thermal treatment (29–31). Our results showed marked differences in gut microbiota population of AGE-D mice, characterized by a depletion of commensal bacteria such as S24-7, *Candidatus Arthromitus* and *Anaerostipes*. Among them, *Candidatus Arthromitus* plays a key role in mouse intestinal immune function control and its downregulation may be associated with intestinal inflammatory imbalance (32). In addition, AGE-D mice showed a decrease of a butyrate-producing bacterial genus, *Anaerostipes*, that is inversely related to inflammation and insulin resistance, since butyrate is reported as one of the most important short-chain fatty acids (SCFAs) in the maintenance of colonic health (33). Moreover, we also found an increase of *Parabacteroides*, *Ruminococcus* (Lachnospiraceae family) and *Lawsonia* in the AGE-D group. An abnormal increase in Lachnospiraceae has been recently proposed as one of the factors involved in metabolic diseases such as diabetes and obesity (33), but the mechanism through which these bacteria affect these conditions is still unclear. It has been proposed that members of Lachnospiraceae may be involved in intestinal lipopolysaccharide translocation in blood, thus becoming one of the causes of the inflammatory processes which characterize these metabolic diseases (34). Our results support previous studies where *Lactobacillus* spp. ameliorate Type 2 diabetes by acting on GLP-1 incretin mechanism (35). *Prevotella* is a dietary fiber fermenter bacterium, known to increase after a high fiber intake (36) and to produce SCFAs (37), which affect satiety regulation and glucose metabolism by increasing GLP-1 and other gut hormones production (38). This mechanism may provide a link between *Prevotella* reduction in AGE-D mice and incretin production. Diet induced shifts in gut microbial population by modulating SCFAs production: we can speculate that AGE-enriched diet may affect incretin production by a microbiota-driven mechanism, in which *Prevotella* and other fiber-fermenting and SCFAs-producing bacteria are decreased. The rise of *Lawsonia* abundance was previously observed in diabetic mice fed with high-fat chow and was seen to decrease after metformin treatment, which normally acts by increasing GLP-1 production and glucose utilization (39–41). Furthermore, since results from our collaborators highlighted the role of AGEs in reducing GLP-1 levels, we speculated that the *Lawsonia* increase in AGE-D mice may be caused by incretins imbalance and systemic changes induced by MG-H1. Many of the microbial alterations observed in AGE-D group were significantly related to incretins and inflammatory markers levels and have been associated in previous studies with obesogenic and/or diabetogenic environments. In this study, we demonstrated that GM profile of AGE-D mice correlated with impaired systemic measures of metabolic disease markers, including plasma IL-1β, IL-17 and PAI-1 levels and negatively correlated to circulating incretins GIP and GLP-

1. In AGE-D mice, the increase in blood concentrations of pro-inflammatory cytokines IL-1β and IL-17, and of PAI-1, a key regulator of vascular remodeling involved in various thrombotic diseases (42), highlighted the role of dietary AGEs in inducing inflammation and vascular integrity impairment. Moreover, the reduction in incretins levels following AGE-D linked dietary AGEs with the development of metabolic disorders, since both GIP and GLP-1 are the two primary gut hormones involved in the modulation of glucose metabolism and have a protective role against metabolic disease in laboratory animals and in humans (43). Here, we performed a Spearman's correlation analysis to understand which bacteria could have a role in mediating AGE-D metabolic and inflammatory impairments. In particular, we found that Lachnospiraceae, *Parabacteroides*, *Lawsonia* and *Ruminococcus* (Lachnospiraceae family) showed a strong positive correlation with PAI-1, IL-1β, and IL-17 levels, while they showed a strong negative correlation with GIP and GLP-1. Furthermore, *Prevotella*, *Lactobacillus*, *Anaerostipes*, and *Candidatus Arthromitus* had a significant positive correlation with GIP and GLP-1, and a negative correlation with systemic inflammatory blood parameters PAI-1, IL-1β, and IL-17. These results suggest that a modern AGE-enriched diet, even if isocaloric, could induce detrimental changes in the host inflammatory state and metabolism. Interestingly, compared to CD, the AGE-D was not characterized by a higher body fat content, and mice fed with AGE-D did not show an increase in body weight gain and feeding behavior. This suggests that the simple enrichment of MG-H1 in the diet caused a reshaping of the microbiota towards a profile normally observed in high-fat diets or in the presence of inflammatory conditions such as diabetes. Our results showed that systemic imbalance caused by AGEs enrichment in diet, mainly in the pro-inflammatory profile, incretins axis, and glucose control, induced significant changes in gut microbial populations. Furthermore, these shifts resemble what has previously been seen in obesity, diabetes, and metabolic disorders (17).

Our findings support recent evidence describing the deleterious effects of high- and ultra-processed food consumption on the risk of chronic metabolic and inflammatory diseases in both animal and human studies (44–46), thus highlighting the importance of limiting their consumption whatever dietary habits are followed. Moreover, we provide new findings linking diet, inflammation and gut microbiota, demonstrating that some of the physiological effects of dietary AGE chronic exposure can be mediated by through the GM.

Our study has several limitations. First, the dietary content of MG-H1, which is far more than the amount that may normally be ingested. In addition, no significant changes in systemic lipid and glucose profile were recorded, despite the significant changes in the blood levels of key master

hormonal regulators of metabolism; thus, suggesting that longer kinetics of dietary manipulation and/or more severe dietary insult are required to obtain clinically relevant metabolic derangements. However, our findings help to elucidate the pivotal role of AGEs as a link between modern diet and health or disease risk, moving from correlation toward causation. Further experimental and clinical studies are needed to highlight the importance of specific AGEs in human metabolism and disease and to investigate how different AGEs impact on microbiota composition or are modified themselves by the gut microbiota. Further studies should also determine how AGEs can elicit specific signaling functions in the perspective of preventing the progression of diet-related metabolic derangements.

References

1. Singh R, Barden A, Mori T, Beilin L. Advanced glycation end-products: a review. Diabetologia. 2001 Feb 5;44(2):129–46.

2. Hu FB. Dietary pattern analysis: a new direction in nutritional epidemiology: Current Opinion in Lipidology. 2002 Feb;13(1):3–9.

3. Gillery P, Jaisson S. Post-translational modification derived products (PTMDPs): toxins in chronic diseases? Clinical Chemistry and Laboratory Medicine [Internet]. 2014 Jan 1 [cited 2021 May 21];52(1). Available from: https://www.degruyter.com/document/doi/10.1515/cclm-2012-0880/html

4. Poulsen MW, Hedegaard RV, Andersen JM, de Courten B, Bügel S, Nielsen J, et al. Advanced glycation endproducts in food and their effects on health. Food and Chemical Toxicology. 2013 Oct;60:10–37.

5. Cepas V, Collino M, Mayo JC, Sainz RM. Redox Signaling and Advanced Glycation Endproducts (AGEs) in Diet-Related Diseases. Antioxidants. 2020 Feb 6;9(2):142.

6. Vistoli G, De Maddis D, Cipak A, Zarkovic N, Carini M, Aldini G. Advanced glycoxidation and lipoxidation end products (AGEs and ALEs): an overview of their mechanisms of formation. Free Radical Research. 2013 Aug;47(sup1):3–27.

7. Luévano-Contreras C, Gómez-Ojeda A, Macías-Cervantes MH, Garay-Sevilla MaE. Dietary Advanced Glycation End Products and Cardiometabolic Risk. Curr Diab Rep. 2017 Aug;17(8):63.

8. Scheijen JLJM, Clevers E, Engelen L, Dagnelie PC, Brouns F, Stehouwer CDA, et al. Analysis of advanced glycation endproducts in selected food items by ultra-performance liquid chromatography tandem mass spectrometry: Presentation of a dietary AGE database. Food Chemistry. 2016 Jan;190:1145–50.

9. Henle T. AGEs in foods: Do they play a role in uremia? Kidney International. 2003 May;63:S145–7.

10. Hellwig M, Humpf H-U, Hengstler J, Mally A, Vieths S, Henle T. Quality Criteria for Studies on Dietary Glycation Compounds and Human Health: Opinion of the Senate Commission on Food Safety (SKLM) of the German Research Foundation (DFG). J Agric Food Chem. 2019 Oct 16;67(41):11307–11.

11. Kellow NJ, Savige GS. Dietary advanced glycation end-product restriction for the attenuation of insulin resistance, oxidative stress and endothelial dysfunction: a systematic review. Eur J Clin Nutr. 2013 Mar;67(3):239–48.

12. Qu W, Nie C, Zhao J, Ou X, Zhang Y, Yang S, et al. Microbiome–Metabolomics Analysis of the Impacts of Long-Term Dietary Advanced-Glycation-End-Product Consumption on C57BL/6 Mouse Fecal Microbiota and Metabolites. J Agric Food Chem. 2018 Aug 22;66(33):8864–75.

13. Hellwig M, Bunzel D, Huch M, Franz CMAP, Kulling SE, Henle T. Stability of Individual Maillard Reaction Products in the Presence of the Human Colonic Microbiota. J Agric Food Chem. 2015 Aug 5;63(30):6723–30.

14. Hellwig M, Auerbach C, Müller N, Samuel P, Kammann S, Beer F, et al. Metabolization of the Advanced Glycation End Product *N* -ε-Carboxymethyllysine (CML) by Different Probiotic *E. coli* Strains. J Agric Food Chem. 2019 Feb 20;67(7):1963–72.

15. Mills DJS, Tuohy KM, Booth J, Buck M, Crabbe MJC, Gibson GR, et al. Dietary glycated protein modulates the colonic microbiota towards a more detrimental composition in ulcerative colitis patients and non-ulcerative colitis subjects. Journal of Applied Microbiology. 2008 Sep;105(3):706–14.

16. Qu W, Yuan X, Zhao J, Zhang Y, Hu J, Wang J, et al. Dietary advanced glycation end products modify gut microbial composition and partially increase colon permeability in rats. Mol Nutr Food Res. 2017 Oct;61(10):1700118.

17. Basso N, Soricelli E, Castagneto-Gissey L, Casella G, Albanese D, Fava F, et al. Insulin Resistance, Microbiota, and Fat Distribution Changes by a New Model of Vertical Sleeve Gastrectomy in Obese Rats. Diabetes. 2016 Oct;65(10):2990–3001.

18. Bolyen E, Rideout JR, Dillon MR, Bokulich NA, Abnet CC, Al-Ghalith GA, et al. Reproducible, interactive, scalable and extensible microbiome data science using QIIME 2. Nat Biotechnol. 2019 Aug;37(8):852–7.

19. McMurdie PJ, Holmes S. phyloseq: An R Package for Reproducible Interactive Analysis and Graphics of Microbiome Census Data. Watson M, editor. PLoS ONE. 2013 Apr 22;8(4):e61217.

20. DeSantis TZ, Hugenholtz P, Larsen N, Rojas M, Brodie EL, Keller K, et al. Greengenes, a Chimera-Checked 16S rRNA Gene Database and Workbench Compatible with ARB. AEM. 2006 Jul;72(7):5069–72.

21. Oksanen J, Blanchet G, Kindt R, Legendre P, Minchin P, O'Hara B, et al. Vegan: Community Ecology Package. R Package Version 22-1. 2015;2:1–2.

22. Ahmed N, Mirshekar-Syahkal B, Kennish L, Karachalias N, Babaei-Jadidi R, Thornalley PJ. Assay of advanced glycation endproducts in selected beverages and food by liquid chromatography with tandem mass spectrometric detection. Mol Nutr Food Res. 2005 Jul;49(7):691–9.

23. van Eupen MG, Schram MT, Colhoun HM, Scheijen JL, Stehouwer CD, Schalkwijk CG. Plasma levels of advanced glycation endproducts are associated with type 1 diabetes and coronary artery calcification. Cardiovasc Diabetol. 2013 Dec;12(1):149.

24. Ahmed N, Babaei-Jadidi R, Howell SK, Beisswenger PJ, Thornalley PJ. Degradation products of proteins damaged by glycation, oxidation and nitration in clinical type 1 diabetes. Diabetologia. 2005 Aug;48(8):1590–603.

25. Uribarri J, Woodruff S, Goodman S, Cai W, Chen X, Pyzik R, et al. Advanced Glycation End Products in Foods and a Practical Guide to Their Reduction in the Diet. Journal of the American Dietetic Association. 2010 Jun;110(6):911-916.e12.

26. Uribarri J, Cai W, Ramdas M, Goodman S, Pyzik R, Chen X, et al. Restriction of Advanced Glycation End Products Improves Insulin Resistance in Human Type 2 Diabetes: Potential role of AGER1 and SIRT1. Diabetes Care. 2011 Jul 1;34(7):1610–6.

27. Delgado-Andrade C, Tessier FJ, Niquet-Leridon C, Seiquer I, Pilar Navarro M. Study of the urinary and faecal excretion of N ε-carboxymethyllysine in young human volunteers. Amino Acids. 2012 Aug;43(2):595–602.

28. Ames JM, Wynne A, Hofmann A, Plos S, Gibson GR. The effect of a model melanoidin mixture on faecal bacterial populations *in vitro*. Br J Nutr. 1999 Dec;82(6):489–95.

29. Zinöcker M, Lindseth I. The Western Diet–Microbiome-Host Interaction and Its Role in Metabolic Disease. Nutrients. 2018 Mar 17;10(3):365.

30. Delgado-Andrade C, Pastoriza de la Cueva S, Peinado MJ, Rufián-Henares JÁ, Navarro MP, Rubio LA. Modifications in bacterial groups and short chain fatty acid production in the gut of healthy adult rats after long-term consumption of dietary Maillard reaction products. Food Research International. 2017 Oct;100:134–42.

31. Helou C, Anton PM, Niquet-Léridon C, Spatz M, Tessier FJ, Gadonna-Widehem P. Fecal excretion of Maillard reaction products and the gut microbiota composition of rats fed with bread crust or bread crumb. Food Funct. 2017;8(8):2722–30.

32. Bolotin A, de Wouters T, Schnupf P, Bouchier C, Loux V, Rhimi M, et al. Genome Sequence of " *Candidatus* Arthromitus" sp. Strain SFB-Mouse-NL, a Commensal Bacterium with a Key Role in Postnatal Maturation of Gut Immune Functions. Genome Announc [Internet]. 2014 Aug 28 [cited 2021 Dec 1];2(4). Available from: https://journals.asm.org/doi/10.1128/genomeA.00705-14

33. Ma Q, Li Y, Wang J, Li P, Duan Y, Dai H, et al. Investigation of gut microbiome changes in type 1 diabetic mellitus rats based on high-throughput sequencing. Biomedicine & Pharmacotherapy. 2020 Apr;124:109873.

34. Kameyama K, Itoh K. Intestinal Colonization by a *Lachnospiraceae* Bacterium Contributes to the Development of Diabetes in Obese Mice. Microb Environ. 2014;29(4):427–30.

35. Wang Z, Saha S, Van Horn S, Thomas E, Traini C, Sathe G, et al. Gut microbiome differences between metformin- and liraglutide-treated T2DM subjects. Endocrinol Diab Metab. 2018 Jan;1(1):e00009.

36. De Filippo C, Cavalieri D, Di Paola M, Ramazzotti M, Poullet JB, Massart S, et al. Impact of diet in shaping gut microbiota revealed by a comparative study in children from Europe and rural Africa. Proceedings of the National Academy of Sciences. 2010 Aug 17;107(33):14691–6.

37. Chen T, Long W, Zhang C, Liu S, Zhao L, Hamaker BR. Fiber-utilizing capacity varies in Prevotella- versus Bacteroides-dominated gut microbiota. Sci Rep. 2017 Dec;7(1):2594.

38. Cani PD, Van Hul M, Lefort C, Depommier C, Rastelli M, Everard A. Microbial regulation of organismal energy homeostasis. Nat Metab. 2019 Jan;1(1):34–46.

39. Zhang C, Zhang M, Pang X, Zhao Y, Wang L, Zhao L. Structural resilience of the gut microbiota in adult mice under high-fat dietary perturbations. ISME J. 2012 Oct;6(10):1848–57.

40. Shin N-R, Lee J-C, Lee H-Y, Kim M-S, Whon TW, Lee M-S, et al. An increase in the *Akkermansia* spp. population induced by metformin treatment improves glucose homeostasis in diet-induced obese mice. Gut. 2014 May;63(5):727–35.

41. Whang A, Nagpal R, Yadav H. Bi-directional drug-microbiome interactions of anti-diabetics. EBioMedicine. 2019 Jan;39:591–602.

42. Tjärnlund-Wolf A, Brogren H, Lo EH, Wang X. Plasminogen Activator Inhibitor-1 and Thrombotic Cerebrovascular Diseases. Stroke. 2012 Oct;43(10):2833–9.

43. Kim W, Egan JM. The Role of Incretins in Glucose Homeostasis and Diabetes Treatment. Pharmacol Rev. 2008 Dec;60(4):470–512.

44. Stanhope KL, Schwarz JM, Keim NL, Griffen SC, Bremer AA, Graham JL, et al. Consuming fructose-sweetened, not glucose-sweetened, beverages increases visceral adiposity and lipids and decreases insulin sensitivity in overweight/obese humans. J Clin Invest. 2009 May 1;119(5):1322–34.

45. Oikonomou E, Psaltopoulou T, Georgiopoulos G, Siasos G, Kokkou E, Antonopoulos A, et al. Western Dietary Pattern Is Associated With Severe Coronary Artery Disease. Angiology. 2018 Apr;69(4):339–46.

46. Rauber F, Steele EM, Louzada ML da C, Millett C, Monteiro CA, Levy RB. Ultra-processed food consumption and indicators of obesity in the United Kingdom population (2008-2016). Meyre D, editor. PLoS ONE. 2020 May 1;15(5):e0232676.

Chapter 3: Measuring the potential of a regional variety of broccoli (*Brassica oleracea* var. *botrytis*) in modulating the human intestinal microbiota and gut permeability using *in vitro* fecal fermentations and Caco-2 cell models.

Giulia Gaudioso[1,2], Camilla Diotallevi[1,3], Daniele Perenzoni[4], Urska Vhrovsek[4], Fulvio Mattivi[2,4], Kieran Michael Tuohy[1] and Francesca Fava[1].

[1] Nutrition and Nutrigenomics Unit, Department of Food Quality and Nutrition, Research and Innovation Center, Fondazione Edmund Mach, 38098 Trento, Italy

[2] CIBIO – Department of Cellular, Computational and Integrative Biology, University of Trento, 38123 Trento, Italy

[3] Faculty of Science and Technology, Freie Universität Bozen-Libera Università di Bolzano, Bolzano

[4] Metabolomics Unit, Department of Food Quality and Nutrition, Research and Innovation Center, Fondazione Edmund Mach, 38098 Trento, Italy.

Abstract:

Brassica vegetables constitute a rich source of polyphenols, glucosinolates and fiber. A major proportion of these compounds escape absorption in the small intestine, and instead reach the colon, becoming available for gut microbiota (GM) metabolism. Here, fiber and phytochemicals are supposed to modulate GM composition and activity, thus producing bioactive compounds considered to be responsible for anti-inflammatory and anti-cancer properties of *Brassica*. Here, a local variety of broccoli (*Brassica oleracea* var. *botrytis*, BR) was digested and fermented *in vitro* using a pH-controlled anaerobic fecal fermentation model. The effects on GM composition were measured by 16S rRNA gene Illumina MiSeq sequencing (V3-V4 region) and QIIME2 pipeline analysis. Variation in polyphenols and glucosinolates during fermentations was assessed through Liquid Chromatography Triple Quadrupole Mass Spectrometry (LC-MS/MS), while short chain fatty acids (SCFA) were determined through gas chromatography-mass spectrometry (GC-MS/MS) analysis. To assess the role of BR microbial metabolites in modulating gut permeability, we employed an *in vitro* model of intestinal epithelium formed by human colorectal adenocarcinoma cells (Caco-2). BR significantly reduced bacterial α-diversity, decreasing *Alistipes* and *Ruminococcus 1* relative abundances and increasing *Escherichia-Shigella*. In terms of metabolic outputs, quercetin 3,4'-diglucoside, caffeic acid, ferulic acid and sinapic acid significantly decreased after 24 h of BR fermentation, thus confirming the role of GM in driving the metabolism of *Brassica* phytochemicals. 24 h incubation of BR faecal supernatants on Caco-2 monolayers did not improve nor decrease trans epithelial electric resistance (TEER), thus suggesting mechanisms other than barrier strengthening may account for the anti-inflammatory effects of broccoli.

1. Introduction

The EAT-Lancet Commission recently summarized the evidence describing healthy dietary patterns, confirming that 5-portions daily consumption of fruit and vegetables is essential to reduce risk of major chronic diseases, including cardiovascular disease, cancer and diabetes, and to promote overall wellbeing (1). *Brassicaceae* represent a family of vegetables broadly recognized for their potential health benefits. Their regular consumption has been associated with a decreased risk in developing various type of cancers via the induction of anti-inflammatory and antioxidant enzymes (2). *Brassica*-related benefits have been addressed to their unique phytochemical composition (3). In fact, besides being high in micronutrients and soluble fiber, *Brassica* vegetables constitute a rich source of polyphenols and glucosinolates, secondary metabolites produced by the plant as part of the defense system or acting as attractans for pollination and seed dispersion (4–7). Some of these molecules have been investigated during *in vitro* and animal *in vivo* studies for their potential beneficial effects on human health, including protection against obesity related diseases and weight gain (8,9), prevention of inflammatory states (10) and antioxidant capacity (11–13). The human gut microbiota (GM) may play a crucial role in mediating several of *Brassica* health effects, since it influences the bioavailability and the absorption of both glucosinolates and polyphenols (14–16). Colonic microbial metabolism of *Brassica* phytochemicals generates a broad spectrum of bioactive breakdown compounds, such as isothiocyanates and small phenolics (17–19). On the other hand, fiber and phytochemicals interact with human GM by regulating its composition and metabolism. A diet rich in polyphenols has been related to increased abundance of beneficial bacteria such as *Lactobacillus, Bifidobacterium* and *Akkermansia muciniphila* (20). Similarly, dietary fiber constitutes an important source of carbohydrate substrates for microbial fermentation, providing the energy and carbon source to support the gut microbiota. Fermentation of dietary fibers depends on their chemical composition and structure, with individual fibers favoring those bacteria which possess the necessary enzymes to degrade particular carbohydrates. Dominant and prevalent microorganisms involved in fiber fermentation include *Faecalibacterium*, *Roseburia*, *Bacteroides*, *Ruminococcus*, *Bifidobacterium* and *Prevotella* (21,22). The intestinal epithelium plays a crucial role in the absorption of nutrients and bioactive compounds deriving from microbial metabolism. The intestinal epithelial cells, together with the surrounding mucus layer and the mucosal immune system, constitute a physical barrier which protects against uncontrolled bacterial translocation through the epithelial mucosa to blood stream (23). Alterations of the gut barrier integrity lead to

augmented gut permeability (i.e. 'leaky gut') with a concomitant absorption of bacterial lipopolysaccharide A (LPS), a component of outer membrane in gram-negative bacteria known to promote local or systemic inflammation (24,25). Trans epithelial electric resistance (TEER) measurement is a reference technique used to measure gut barrier integrity in cell culture models of epithelial monolayers, thus representing a useful tool to understand how different compounds could influence the intestinal barrier function (26). There is evidence that daily consumption of a diet containing 10% to 15% (w/w) broccoli for 2 or 3 weeks can inhibit barrier dysfunction in chemically induced colitis mice model, thus reducing gut permeability and preventing undue inflammation (27,28).

The aim of this study was to investigate changes in gut microbiota composition and metabolism after *in vitro* anaerobic pH-controlled fecal fermentation of steam cooked Broccolo of Torbole (*Brassica oleracea* var. *botrytis*), a winter crop of broccoli ecotype selected because of its frequency of consumption in Trentino region. For this ecotype, both the florets and the broad outer leaves that surround a head of broccoli are normally consumed, while for other broccoli the main edible parts are the florets (and eventually the stalk). We investigated microbial metabolites production performing Liquid Chromatography Triple Quadrupole Mass Spectrometry (LC-MS/MS) analysis and we measured short chain fatty acids (SCFA) production over the fermentation process through gas chromatography-mass spectrometry (GC-MS/MS). Moreover, an *in vitro* model of intestinal epithelium formed by human colorectal adenocarcinoma cells (Caco-2) was employed to investigate a potential protective role of Broccolo of Torbole consumption on gut barrier integrity. Since intestinal permeability may trigger inflammatory cascades in other district of the organism *in vivo*, the *in vitro* intestinal model used in our study may elucidate the role of GM and its *Brassica* metabolites in maintaining gut barrier function.

2. Materials and methods

2.1 Broccoli collection and cooking

Broccolo of Torbole (*Brassica oleracea* var. *botrytis*) was obtained from a local farm in Linfano di Arco, Italy, in January 2020 and washed with tap water. Broccoli florets and leaves were cut into pieces of approximately 5 x 5 x 5 cm and then steamed for 30 minutes in a steam oven. Steamed broccoli were drained of water, portioned (leaves and florets in equal proportions), vacuum-packed and stored at –80 °C until further analysis were performed.

2.2 *In vitro* digestion

To simulate human digestion in the stomach and small intestine, the *in vitro* digestion protocol of Minekus *et al.* (2014) was used with some modifications (29). The same protocol was used to digest Broccolo of Torbole leaves and florets (BR), and the control substrates cellulose (CL) as a poorly fermented fiber, or as a readily fermented fiber inulin (IN). 30 g of sample was added to 30 mL of simulated salivary fluid (21 mL saline solution, 5.85 mL milliQ H_2O, 150 μL 0.3 M $CaCl_2(H_2O)_2$, 3 mL 1500 U mL^{-1} α-amylase, Sigma-Aldrich) and incubated for 2 min at 37°C while rotating at 150 rpm. Subsequently, the oral bolus was mixed to 100 mL of simulated gastric fluid (45 mL saline solution containing 10mg/mL lipid vescicles, Sigma Aldrich, 4.17 mL milliQ H_2O, 30 μL 0.3 M $CaCl_2(H_2O)_2$ and 9.6 mL 25000 U mL^{-1} pepsin, Sigma Aldrich) to simulate the gastric phase and pH was decreased to pH 3 with 5 M HCl. This mixture was incubated for 2 hours at 37 °C while rotating at 150 rpm. Finally, the food bolus passed to the intestinal phase, where it was mixed with 200 mL of simulated intestinal fluid (66 mL saline solution, 7.86 mL milliQ H_2O, 240 μL 0.3 M $CaCl_2(H_2O)_2$, 4.8 g porcine bile extract and 30 mL 800 U mL^{-1} pancreatin) and where the pH was increased to pH 7 using 5 M NaOH. This mixture was incubated for 2 hours at 37 °C while rotating at 150 rpm. To simulate passive intestinal absorption of water and hydrolytic products from digestion in the small intestine, *in vitro* dialysis was performed using Spectra/Por® Dialysis Membrane MWCO 1000 KDa (Repligen, Waltham, MA, USA). Samples were collected inside dialysis membranes and sealed at both ends. They were incubated overnight at 4 °C while rotating, inside tanks with a volume 100 times higher than the sample volume and filled with a 10 mM NaCl solution. After incubation, samples were frozen at – 80°C overnight and, subsequently, freeze-dried. Freeze-dried samples were milled using a sterile pestle, divided into portions of 2 g/each and then stored at –80 °C until further analysis.

2.3 Faecal batch cultures

Glass water-jacketed vessels (300 mL) were sterilized and filled aseptically with 180 mL of pre-sterilized basal nutrient medium according to Sanchez-Patan *et al.* 2012 (30). Fecal samples were collected from three healthy volunteers in total (age between 20 and 50 years, no antibiotic treatment in the 3 months preceding the experiment). 10% (wt/vol) faecal slurry was prepared by diluting freshly collected feces with anaerobic 1X PBS (pH 7.2). For each volunteer, four batch fermenters were run in parallel (corresponding to four different fermentation substrates, as described below), filled with sterile medium and inoculated with 20 mL of 10% (wt/vol) faecal slurry up to a total volume of 200 mL. Fermenters were assembled and autoclaved the day before the experiment. 180

mL of sterile boiling anaerobic medium were added and anaerobic conditions were maintained by O_2-free N_2 (15 mL/min) flow until the end of the experiment. Temperature was held at 37 °C using a circulating water bath (Thermo Fisher Scientific, Waltham, MA, USA), and pH was controlled between 5.5 and 5.9 using an automated pH FerMac 260 controller (Gloucester, England-GL208JH, UK) which added 0.5 M HCl or 0.5 M NaOH as required. An image of fementation vessels is shown in **Figure 1**.

Figure 1. Schematic representation of the faecal batch culture experiment.

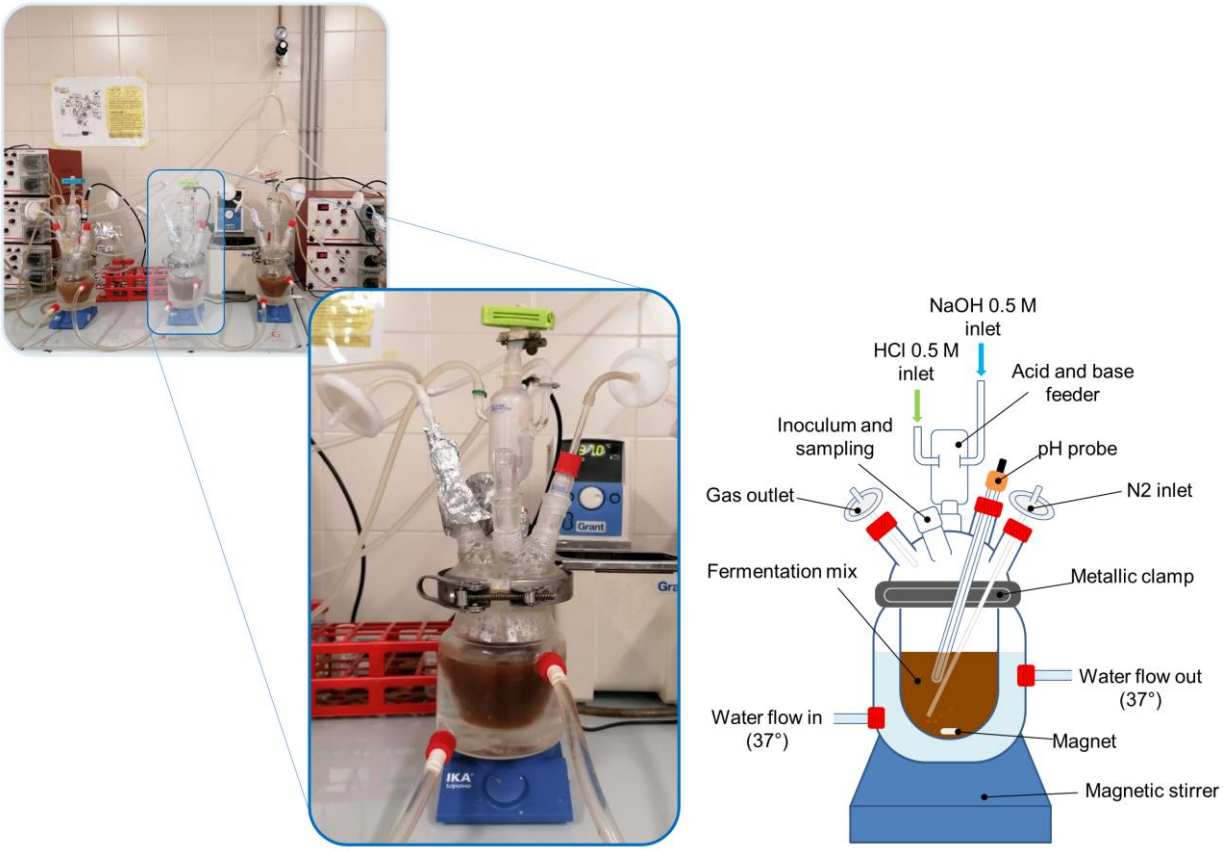

On the day of the experiment, fresh fecal sample was collected and slurries were prepared by homogenizing faeces in anoxic 1X PBS (pH 7.2) in Stomacher® 400 Circulator (Seward Ltd., UK). After inoculation with faecal slurry, 2 g of freeze-dried *in vitro* digested substrate were added in each fermenter. This amount of substrate was estimated in order to reflect colonic proportion of digested food and faecal slurry. Also, this considers that a total amount of approximately 200 g of material (including food particles, water, bacteria and mucus) could be measured at any given time in the large intestine (31). The experimental conditions were as follows: vessel 1, contained only faecal inoculum and no substrate (blank, BK); vessel 2, 1% (w/v) digested desugared inulin (IN, positive control), vessel 3, 1% (w/v) digested methylcellulose (CL, negative control) and vessel 4, 1% (w/v) steamed-cooked digested Broccolo of Torbole (BR). Batch cultures were carried out over 24 hours

and samples were obtained from each vessel at time 0 (baseline, after faecal inoculum), 5, 10, 24 hours. The chosen sampling time points were selected in order to comprise the lag (0 h), exponential (5 h), stationary (10 h) and death (24 h) phases of bacterial growth, thus having a comprehensive overview of the batch culture process. Samples were immediately centrifuged at 13000 *g* for 5 min. Pellets and supernatants were stored at –80 °C for microbiota and metabolite analysis respectively.

2.4 Gut microbiota analysis

Total DNA extraction from frozen pellets (10-20 mg) was performed using MP Biomedicals™ FastDNA™ SPIN DNA Isolation Kit for Feces (Thermo Fisher Scientific, Waltham, MA, USA), following manufacturer's instructions. DNA quality and concentration were measured using a NanoDrop® 8000 spectrophotometer (Thermo Fisher Scientific, Waltham, MA, USA). PCR amplification was performed by targeting 16S rRNA gene V3-V4 variable regions with the bacterial primer set 341F (5′-CCTACGGGNGGCWGCAG-3′) and 806R (5′-GACTACNVGGGTWTCTAATCC-3′), as previously reported (32). PCR amplification of each samples was carried out using 25 μL reactions, with 12.5 μL of 2X KAPA Hifi HotStart Ready Mix (Kapa Biosystems Ltd., UK), 0.5 μL of each primer, 2.5 μL DNA (5 ng/μL) and 9 μL. All PCR reactions were carried out using the Verity™ 96-well Thermal Cycler (Thermo Fisher Scientific, Waltham, MA, USA), according to the following protocol: 5 min at 95 °C, 30 cycles of 30 s at 95 °C, 30 s at 55 °C, and 30 s at 72 °C, followed by a final extension of 5 min at 72 °C. PCR products were checked by gel electrophoresis and cleaned using an Agencourt AMPure XP system (Beckman Coulter, Brea, CA, USA), following the manufacturer's instructions. After seven PCR cycles (16S Metagenomic Sequencing Library Preparation, Illumina), Illumina adaptors were attached (Illumina Nextera XT Index Primer). Libraries were purified using Agencourt AMPure XP (Beckman) and then sequenced on an Illumina® MiSeq (PE300) platform (MiSeq Control Software 2.0.5 and Real-Time Analysis software 1.16.18, Illumina, San Diego, CA, USA). Sequences obtained from Illumina sequencing were analyzed using the Quantitative Insights Into Microbial Ecology (QIIME) 2.0 pipeline (33). Unidentified taxa include those whose percentage sequence homology with Silva database was less than 95% (34). α- (within-sample richness) and β-diversity (between-sample dissimilarity) estimates were determined using the phyloseq R Package (35).

2.5 Metabolomic analysis

2.5.1 Supernatant preparation

Supernatants were thawed on ice and sterile-filtered using sterile Sartorius 0.22 μm filters (Thermo Fisher Scientific, Waltham, MA, USA). Filtered supernatant were used for metabolomics analysis of polyphenols, glucosinolates, isothiocyanates and indoles, performed through Liquid Chromatography Triple Quadrupole Mass Spectrometry (LC-MS/MS), while for short chain fatty acids (SCFA) analysis, performed through gas chromatography-mass spectrometry (GC-MS/MS).

2.5.2 LC-MS/MS

Analysis on glucosinolates and polyphenols were performed on a Sciex Triple Quad 6500+ (Sciex, USA) LC-MS/MS system. A protocol was developed to separate 45 compounds divided between polyphenols, glucosinolates, isothiocyanates and indoles through a single chromatographic run of 17 minutes. A complete list of the quantified compounds is provided in the *Results* section (**Table 3**), together with the range of concentration used for the calibration curve. Each compound was identified and quantified in multiple reaction monitoring (MRM) and dosed with its own calibration curve. Concentrations in BR supernatants quantified by LC-MS/MS were normalized according to the fermentation volume. Glucosinolates concentration were given as μmol/100g (**Table S3**), while polyphenol and indole-3-carbinol concentrations were reported as mg/kg (**Table S4**).

2.5.3 GC-MS/MS analysis of short chain fatty acids (SCFA)

Analysis of SCFAs was performed by the Metabolomics Unit at FEM-CRI, as previously described by Lotti *et al.* (2017) (36). Briefly, 10 μL of acidified water (15 % phosphoric acid), 20 μL of internal standard (IS) (acetic d4 45 mM; propionic d6 and butyric d7 10 mM; 2-ethyl butyric and decanoic acid-d19 2 mM) and 100 μL of fecal suspension, previously filtered, were mixed in a 2 mL tubes. A liquid–liquid extraction (LLE) was then performed using 980 μL of metil-t-butil ether (MTBE). The extraction was assisted by an orbital shaker (Multi RS-60; BioSan, Latvia) for 5 min with the following cycle program: 90 rpm of orbital rotation for 5 s followed by reciprocal motion at 20◦ (from the vertical plane) for 15 s. At this point, tubes were centrifuged at 25,314g at 5 °C for 5 min. Finally, the organic phase aliquot was transferred into 2 mL glass vial and subjected to GC–MS analysis in a split ratio 10:1 (total run-time of 6,5min). SCFA concentrations in faecal batch cultures were given as mmol/L (**Table 4**).

2.6 *In vitro* model of intestinal epithelium

2.6.1 Cell culture

Human epithelial colorectal adenocarcinoma Caco-2 cell line (ATCC® HTB-37™, number of passage between 50 and 60) were grown in Dulbecco's Modified Eagle's Medium (DMEM) with high glucose (4.5g/L) (Lonza, Switzerland) supplemented with 20% decomplemented (56°C, 60 minutes) fetal bovine serum (Lonza, Switzerland), 100 units/ml penicillin (Biological Industries, Israel), 100 µg/ml streptomycin (Biological Industries, Israel), 1% non-essential amino acids (Euroclone, Milan), 2 mM glutamine and 0,25 ug/ml Amphotericin B (Biological Industries, Israel). Before and during treatments, cell cultures were maintained in humidified atmosphere of 5% CO_2 in air at 37 °C. Before the experiment, Caco-2 cells were maintained in T-75 cm^2 flasks (Sarstedt, Nümbrecht, Germany) and passaged when they reached 70% confluence using 0.05% trypsin–0.5 mM EDTA (Lonza, Switzerland). Medium was refreshed every second day. Prior to seeding, transwell inserts were coated with rat tail collagen Type I (Sigma Aldrich), according to the manufacturer's instruction. For the experiment, Caco-2 cells were harvested to obtain a cell suspension of 1 X 10^5 cells/cm^2. 2.5 mL of cell suspension were added in transwell inserts with membrane filters (0.1 µm pore size; Falcon, Sacco s.r.l, Cadorago, Como, Italy) and grown for 13 days until a tight monolayer was formed (TEER measurements stable for two consecutive days). 1.5 mL of medium was added to the basolateral chamber. BR supernatants collected after 24 hours of faecal fermentation were thawed on ice and filter-sterilized using Sartorius 0.22 µm filters (Thermo Fisher Scientific, Waltham, MA, USA). Sterile supernatants from different donors were pooled and used as a single treatment for cell culture experiments. All control and test treatments were prepared on the day of the assay. 10 mM propionic acid and 7% ethanol were used as positive and negative controls, respectively. All treatments were diluted in culture medium and added at 10% of the total apical volume (2.5 mL).

2.6.2 Trans epithelial electrical resistance (TEER) measurement

TEER was measured using an epithelial volt-ohm-meter (EVOM, World Precision Instruments Inc., Sarasota, FL, USA). Plates were left at room temperature for exactly 25 minutes prior to TEER measurements. The integrity of cell monolayers was assessed just before the addition of testing substrates ($resistance_{T0}$). The media was then removed from basolateral and apical chambers and the control or test treatments added to the apical layer. Resistance was measured after 24 h ($resistance_{T24}$). The TEER was calculated using the following equation, as described in previous works (26,37,38):

$$TEER(\Omega\ cm^2) = resistance(\Omega) \times membrane\ area(cm^2)$$

Where area of the semipermeable membrane was 9.6 cm^2. The change in TEER for each insert was calculated using the following formula:

$$Change\ in\ TEER\ (\%) = TEER_{T24}\ (\Omega\ cm^2) / TEER_{T0}\ (\Omega\ cm^2) \times 100\%$$

Where $TEER_{T24}$ and $TEER_{T0}$ represent TEER after 24 hours treatment and TEER at baseline, respectively. This experiment was repeated three times.

2.7 Statistical analysis

All statistical analysis was performed using R studio version 3.6.2. Normal distribution of data was assessed by Shapiro–Wilk's test. Percentage relative abundance of taxa from different dietary groups was compared using nonparametric Wilcoxon test. Pairwise comparison among groups in terms of α-diversity was performed by Kruskal–Wallis test. Differences in the β-diversity were checked using the non-parametric Permutational Multivariate Analysis of Variance (PERMANOVA) and adonis tests with 999 permutations, via the vegan R Package (39). Correlation between bacterial taxa and microbial metabolites was performed by Spearman's correlation analysis. All p-values were adjusted using Benjamini-Hochberg false discovery rate (FDR) correction. After FDR correction, a p value < 0.05 was considered statistically significant. Statistical significance between TEER results was performed by unpaired t-test. All data are expressed as the mean ± standard deviation, SD.

3. Results

3.1 Gut microbial ecology

Illumina® MiSeq (PE300) sequencing of gut microbial 16S rRNA gene amplicons produced a total of 6,354,870 reads, with 119,903 ± 31,135.2 raw reads per sample. After QIIME 2.0 analysis, we removed chimeras, low quality sequences, and sequences that were identified as Cyanobacteria, and the total number of reads was 5,049,738, with 97,110.35 ± 23,062.02 raw reads per sample.

Three different indices were used to analyze changes in bacterial α-diversity, namely the observed number of OTUs, the Chao1 index and the Shannon entropy index (**Figure 2**). Tested substrates (Cellulose, CL; Inulin, IN; Broccolo of Torbole, BR) had different impacts on bacterial α-diversity, when compared to control (Blank, BK) at baseline (T0) and after 24 hours of anaerobic fermentation (T24). No significant differences were observed between the different treatments at time of inoculation (T0). After 24 hours of fermentation bacterial richness decreased for all substrates, except blank (**Figure 2** and **Table 1**). At T24 α-diversity of both IN and BR was lower

than BK, although for BR these differences were stronger were considering the Shannon index, while they did not quite reach statistical significance for OTUs and Chao1 (**Table 1**). In order to highlight differences in bacterial composition following fermentation of different substrates, we plotted β-diversity using Bray-Curtis dissimilarity matrix, weighted and unweighted UniFrac distances (**Figure 3**, **4** and **5**). Bray-Curtis and also weighted UniFrac PCoA plots show a clear separation of Donor3 from the other two donors, which was less evident when using unweighted UniFrac, thus highlighting a correspondence in results from these two quantitative measures, which both take into account sequence abundance, compared to the qualitative measure unweighted UniFrac, as previously suggested (40). Clustering of samples accorind to time was also observed and a good separation between substrates can be appreciated, especially whan using Bray-Curtis dissimilarity PCoA plot. Statistically significant comparisons among different treatments or different timepoints within the same treatment are reported in **Table 2**.

Figure 2. Bacterial α-diversity using observed OTUs, Chao1 and Shannon index, at baseline (T0) and after 24 hours of fermentation (T24) of four fermentation substrates: Blank (BK), Broccolo of Torbole (BR), Inulin (IN) or Cellulose (CL). Different colors indicate different substrates. Line inside the box represents the median (n=3), whiskers from either side of the box represent the first and the third quartiles, respectively. *=significantly different from BK; ••=significantly different from T0 within the same substrate.

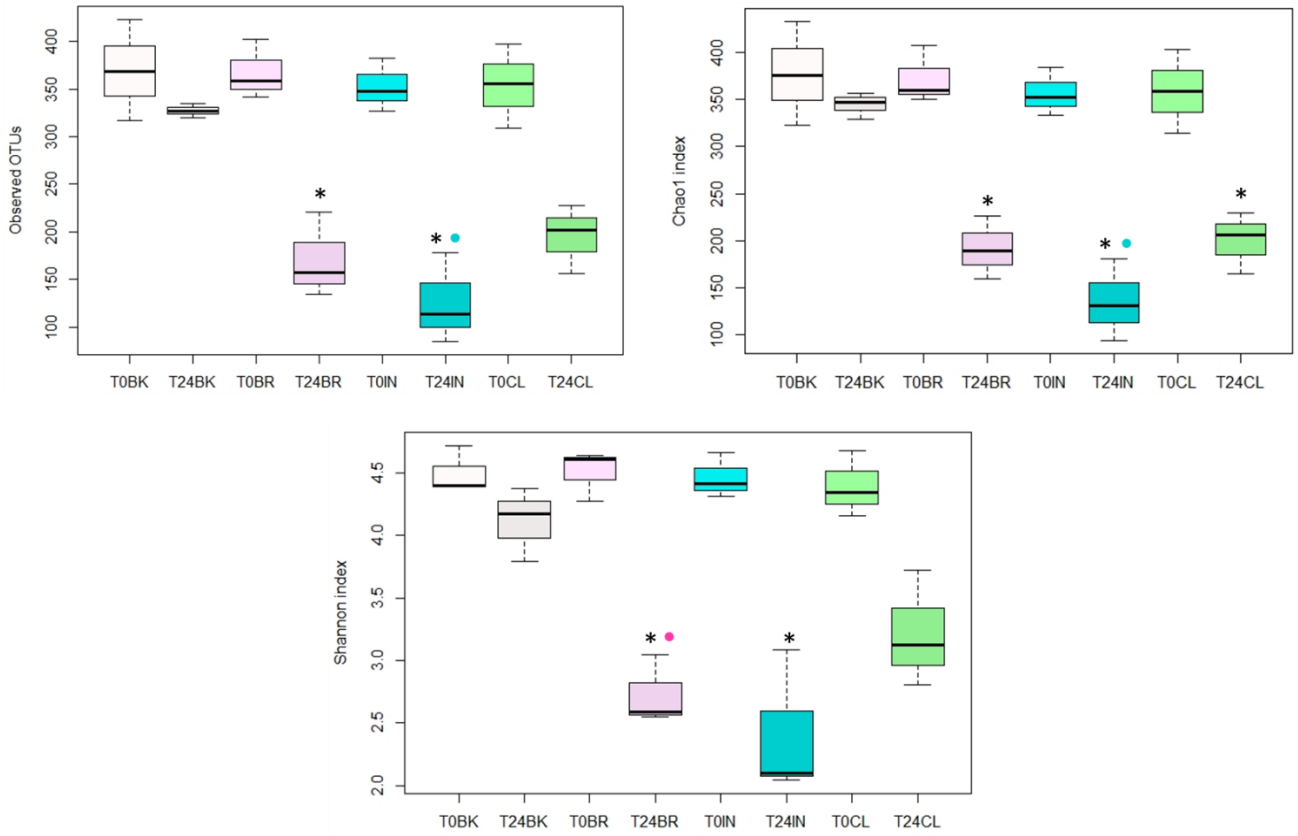

Table 1. Measure of bacterial diversity. α-diversity calculated on the number of observed OTUs, the Chao1 index and the Shannon entropy index at four different time points: at time of inoculation (T0) and after 5 (T5), 10 (T10) and 24 hours (T24) (**A**). p value calculated after comparing α-diversity indices between fermentation substrates at T24 (**B**) or after comparing T0 to 24 values within the same substrate (**C**) calculated using Kruskal-Wallis post-hoc Dunn's test and FDR correction (**B**). BK, blank; BR, Broccolo; IN, inulin; CL, cellulose.

A.		**Observed OTUs**		**Chao1**		**Shannon**	
Treatment	**Timepoint**	**mean ± SD**		**mean ± SD**		**mean ± SD**	
BK	T0	369.3	53.0	376.7	55.0	4.5	0.2
BR	T0	367.3	31.1	372.3	30.4	4.5	0.2
IN	T0	352.3	27.8	356.5	25.8	4.5	0.2
CL	T0	353.7	44.0	358.8	44.3	4.4	0.3
BK	T24	327.3	7.5	344.2	14.0	4.1	0.3
BR	T24	170.7	45.1	191.9	33.3	2.7	0.3
IN	T24	125.7	47.6	135.2	43.4	2.4	0.6
CL	T24	195.3	36.5	199.9	32.6	3.2	0.5

B.	**p value**		
Comparison at T24	**Observed**	**Chao1**	**Shannon**
BK vs BR	0.076	0.076	0.034
BK vs IN	0.040	0.028	0.055
BK vs CL	0.110	0.110	0.320
BR vs IN	0.514	0.370	0.734
BR vs CL	0.651	0.734	0.370
CL vs IN	0.319	0.261	0.348

C.	**p value**		
Comparison	**Observed**	**Chao1**	**Shannon**
T0BK vs T24BK	1	0.976	0.420
T0BRvs T24BR	0.032	0.038	0.028
T0IN vs T24IN	0.028	0.013	0.028
T0CL vs T24CL	0.028	0.019	0.104

Figure 3. Principal Component Analysis (PCoA) representing the bacterial β-diversity according to Bray-Curtis dissimilarity index (n = 3 for each fermentation substrate at each time point). Different colors indicate different fecal donors (D1, D2, D3) and different shapes indicate T0 and T24 time points (**A**). Different colors highlight different time points (**B**). Different colors indicate different substrates and different shapes highlight T0 and T24 time points (**C**).

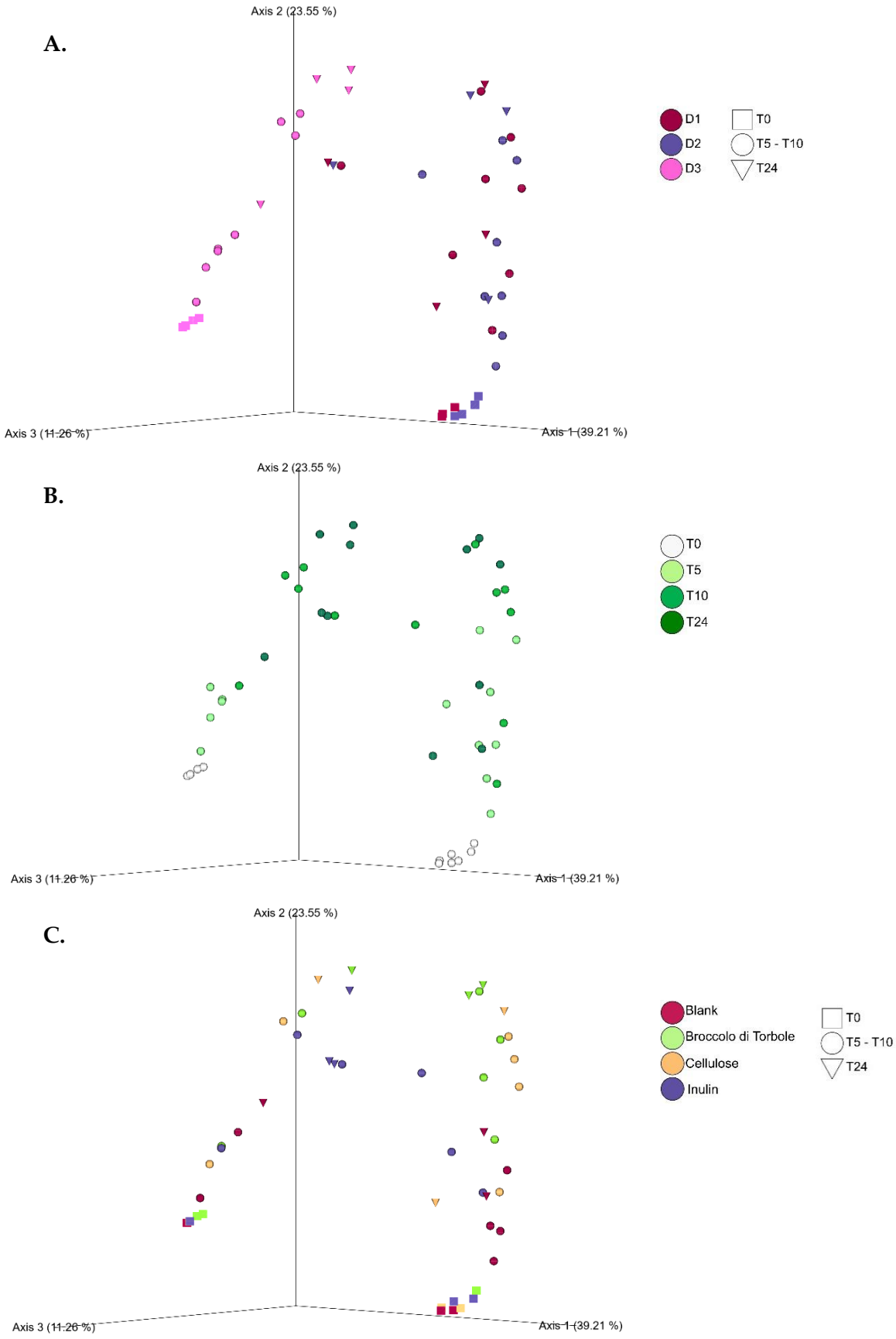

Figure 4. Principal Component Analysis (PCoA) representing the bacterial β-diversity according to unweighted UniFrac distance (n = 3 for each fermentation substrate at each time point). Different colors indicate different fecal donors (D1,2,3) and different shapes highlight T0 and T24 time points (**A**). Different colors highlight different time points (**B**). Different colors indicate different substrates and different shapes highlight T0 and T24 time points (**C**).

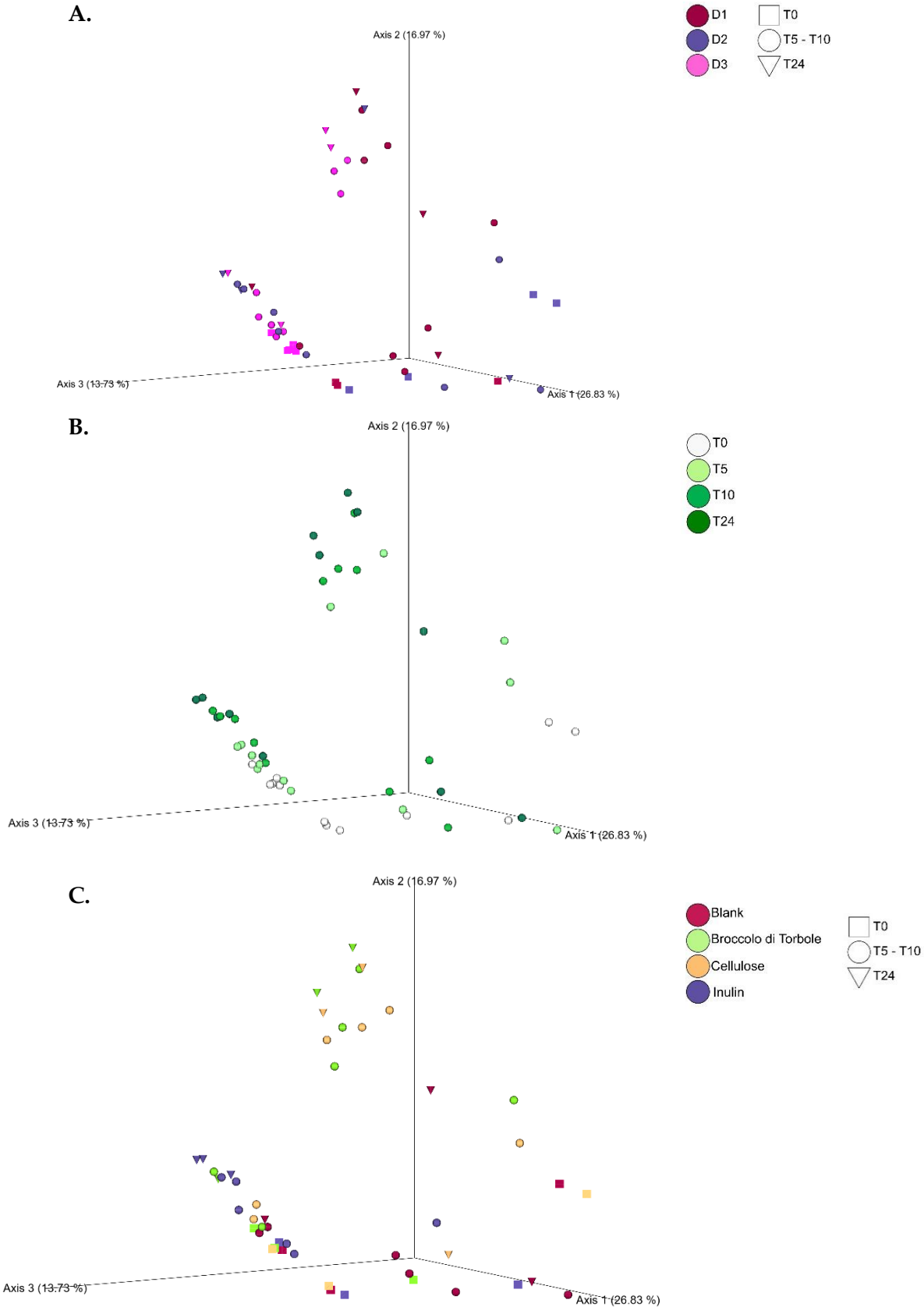

Figure 5. Principal Component Analysis (PCoA) representing the bacterial β-diversity according to weighted UniFrac distance (n = 3 for each fermentation substrate at each time point). Different colors indicate different fecal donors (D1,2,3) and different shapes highlight T0 and T24 time points (**A**). Different colors highlight different time points (**B**). Different colors indicate different substrates and different shapes highlight T0 and T24 time points (**C**).

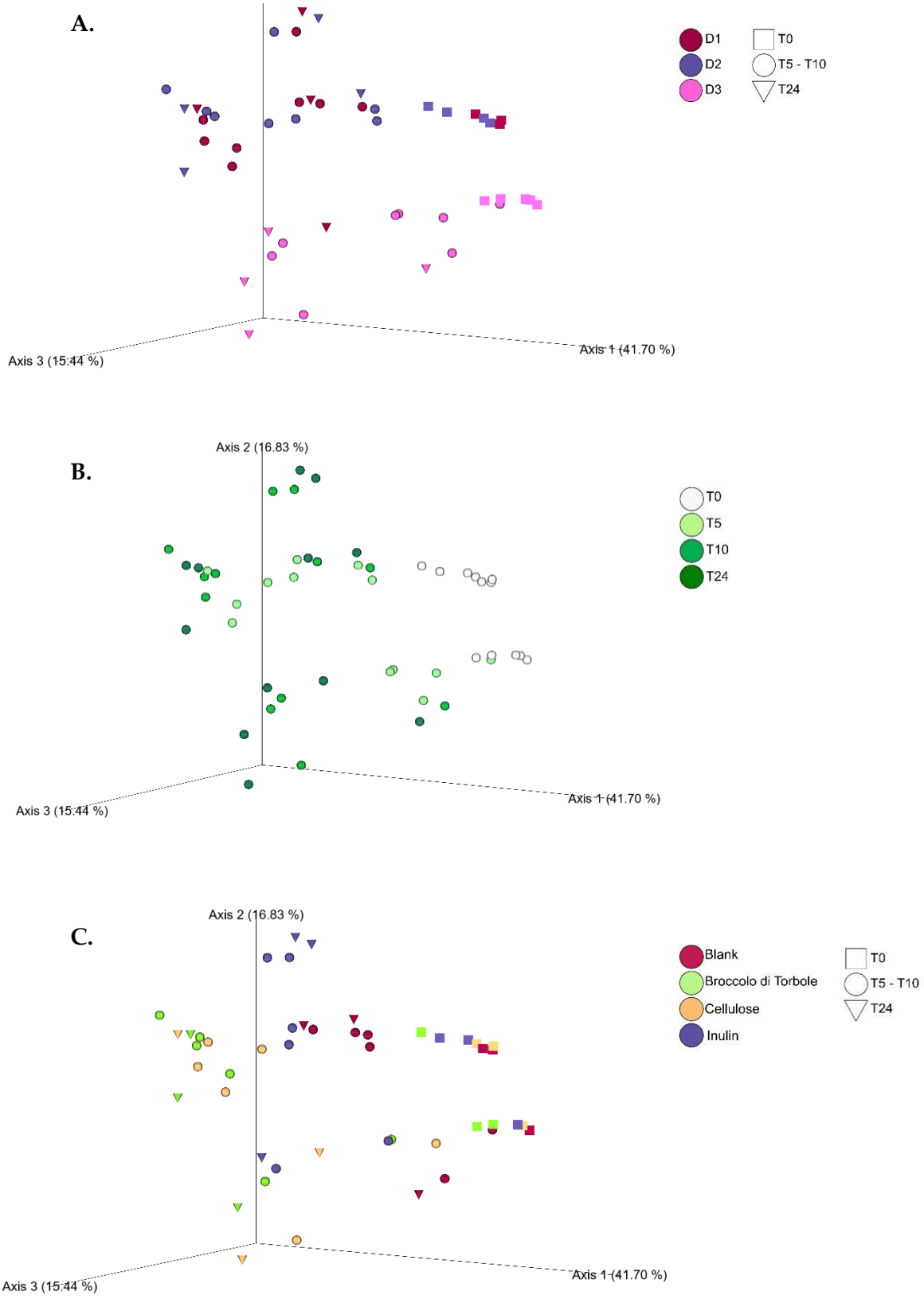

Table 2. p values of statistically significant differences after pairwise comparisons of bacterial β-diversity indices(permanova with 999 permutations) at specific fermentation timepoints. n.s., not significant.

		p value	
Comparison	**Bray-Curtis**	**weighted UniFrac**	**unweighted UniFrac**
T0 BR vs T10 BR	0.046	0.029	n.s.
T0 BR vs T24 BR	0.031	0.028	n.s.
T5 BR vs T24 BR	0.049	n.s.	n.s.
T24 BR vs T24 BK	n.s.	0.025	n.s.

The results of gut microbiota analysis in relative abundance of taxa are illustrated in **Figure 6** and in supplementary material (**Table S1** and **S2**). Firmicutes, Bacteroidetes, Actinobacteria and Proteobacteria were the most represented phyla in all samples, regardless of fermentation substrate, timepoint and donor, covering between 96% and 99% of all identified phyla (**Figure 6**A, **Table S1**). At T0 there were no significant differences between the treatments in bacterial taxa abundance at every taxonomic level, from phylum to genus. Relative abundance of *Escherichia-Shigella* were significantly higher ($p = 0.0403$) after 24 hours of BR fermentation when compared to T0, while *Alistipes* ($p = 0.0489$) and *Ruminococcus 1* ($p = 0.0379$) genera decreased over time after BR administration. A significant decrease between baseline (T0) and the end of fermentation (T24) was also observed in the relative abundance of *Coprococcus* ($p = 0.0448$), and *Ruminiclostridium 9* ($p = 0392$) genera when IN was used as fermentation substrate. The relative abundance of *Lachnospiraceae UCG004* was significantly higher ($p = 0.0397$) after 24 hours of BR fermentation compared to IN. There was a trend towards an increase in Actinobacteria in IN samples over time, and an increase in Bacteroides/Firmicutes (F/B) ratio in BR at T24, although not statistically significant ($p > 0.05$). Significant changes in the relative abundance of specific taxa after 24 hours of fermentation and compared to baseline samples from the same substrate were observed, however, these were not significant after FDR correction.

Figure 6. Percentage bacterial relative abundance of phyla (**A**) and genera (**B**) at time of feces inoculation (T0) and after 5 (T5), 10 (T10) and 24 (T24) hours of *in vitro* batch culture fermentation (n=3 healthy donors). Fermenters were administrated with IN, CL, BR as the substrates (treatments). Values are mean percentage relative abundance, n=3. Less abundant phyla include bacteria with a relative abundance less than 0.01% in fewer than 25% of samples; less abundant genera include bacteria with a relative abundance less than 0.1% in fewer than 25% of samples.

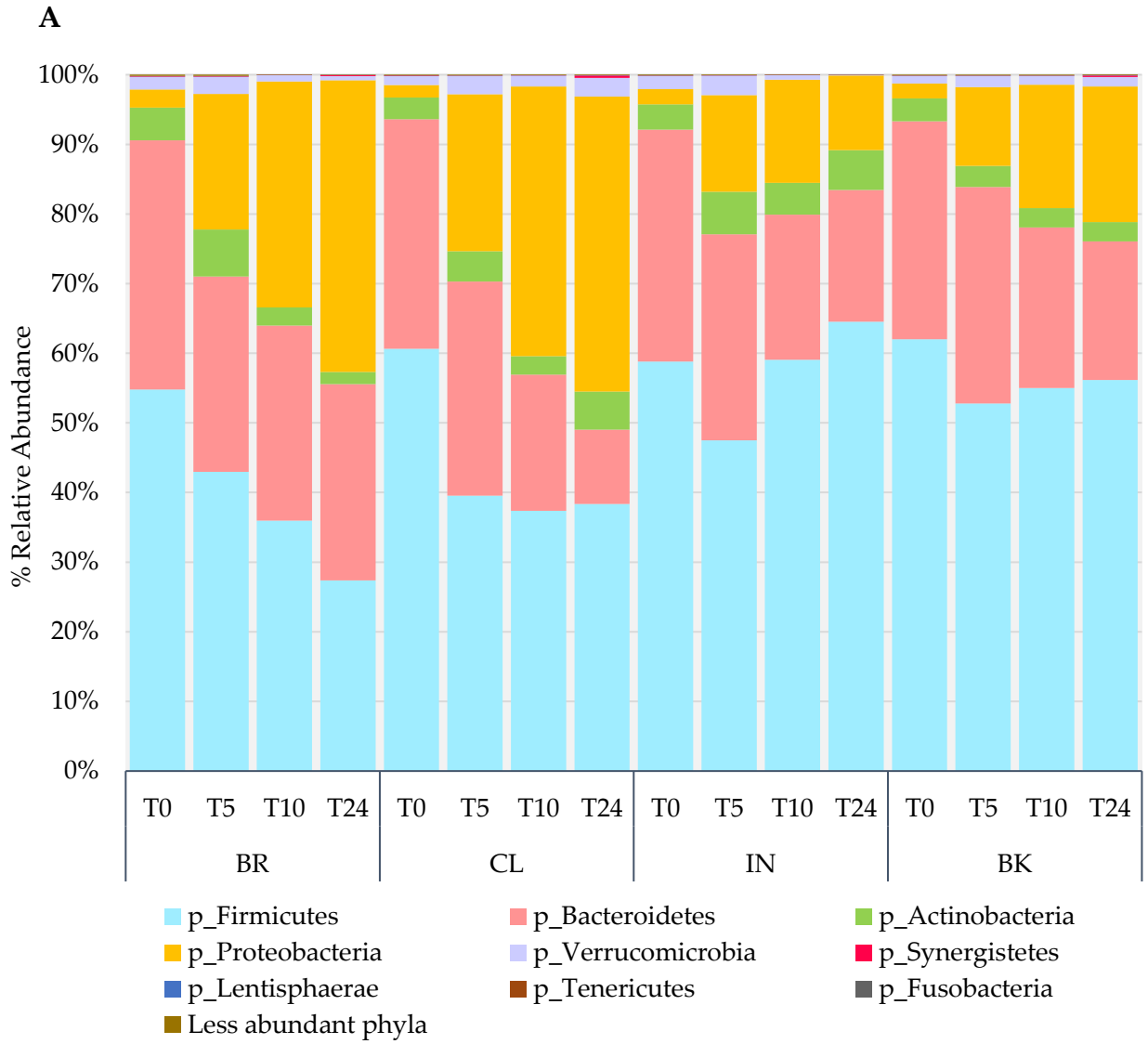

B.

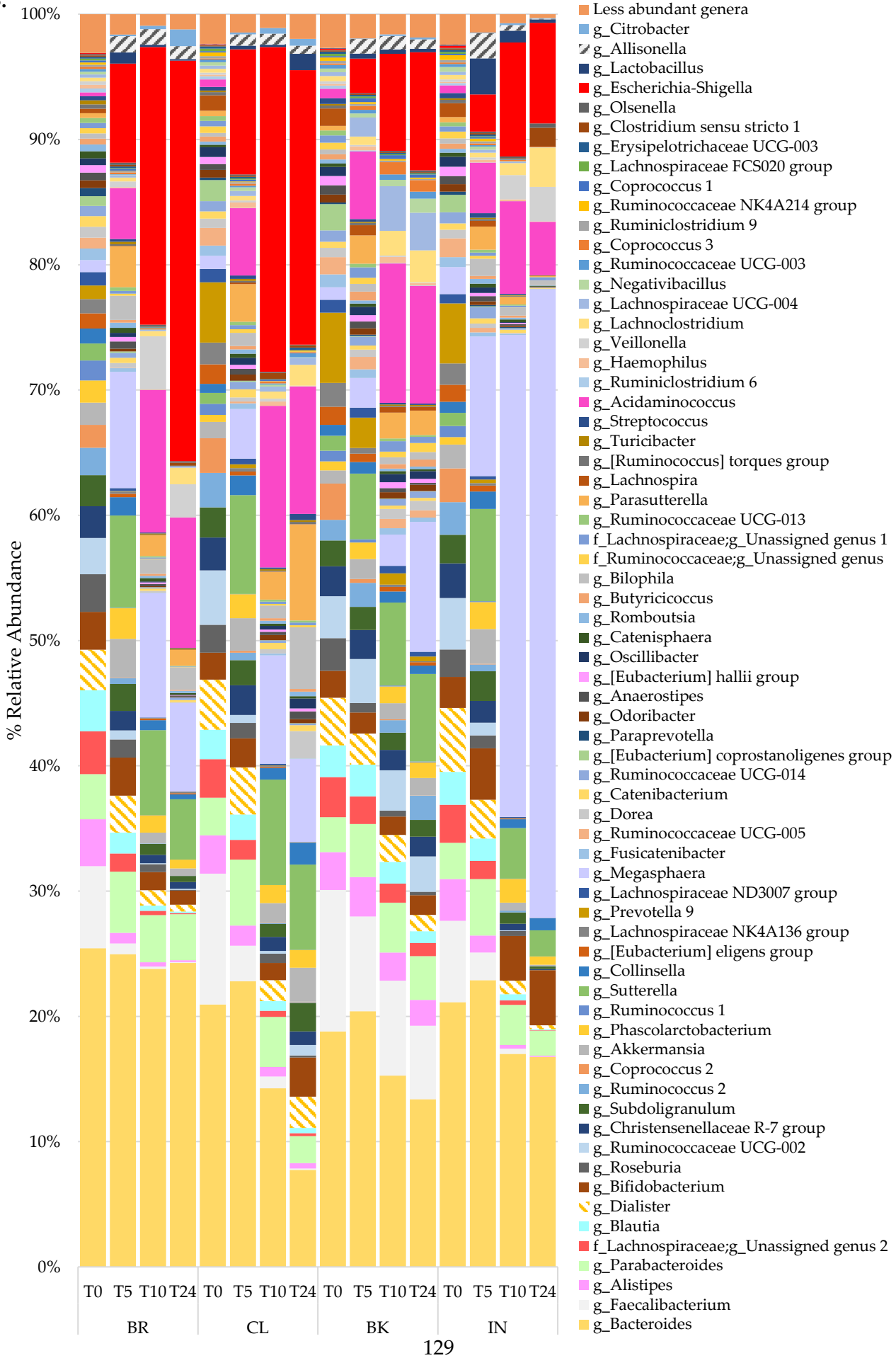
100%
90%
80%
70%
60%
50%
40%
30%
20%
10%
0%
% Relative Abundance
T0 T5 T10 T24 T0 T5 T10 T24 T0 T5 T10 T24 T0 T5 T10 T24
BR
CL
BK
IN
Less abundant genera
g_Citrobacter
g_Allisonella
g_Lactobacillus
g_Escherichia-Shigella
g_Olsenella
g_Clostridium sensu stricto 1
g_Erysipelotrichaceae UCG-003
g_Lachnospiraceae FCS020 group
g_Coprococcus 1
g_Ruminococcaceae NK4A214 group
g_Ruminiclostridium 9
g_Coprococcus 3
g_Ruminococcaceae UCG-003
g_Negativibacillus
g_Lachnospiraceae UCG-004
g_Lachnoclostridium
g_Veillonella
g_Haemophilus
g_Ruminiclostridium 6
g_Acidaminococcus
g_Streptococcus
g_Turicibacter
g_[Ruminococcus] torques group
g_Lachnospira
g_Parasutterella
g_Ruminococcaceae UCG-013
f_Lachnospiraceae;g_Unassigned genus 1
f_Ruminococcaceae;g_Unassigned genus
g_Bilophila
g_Butyricicoccus
g_Romboutsia
g_Catenisphaera
g_Oscillibacter
g_[Eubacterium] hallii group
g_Anaerostipes
g_Odoribacter
g_Paraprevotella
g_[Eubacterium] coprostanoligenes group
g_Ruminococcaceae UCG-014
g_Catenibacterium
g_Dorea
g_Ruminococcaceae UCG-005
g_Fusicatenibacter
g_Megasphaera
g_Lachnospiraceae ND3007 group
g_Prevotella 9
g_Lachnospiraceae NK4A136 group
g_[Eubacterium] eligens group
g_Collinsella
g_Sutterella
g_Ruminococcus 1
g_Phascolarctobacterium
g_Akkermansia
g_Coprococcus 2
g_Ruminococcus 2
g_Subdoligranulum
g_Christensenellaceae R-7 group
g_Ruminococcaceae UCG-002
g_Roseburia
g_Bifidobacterium
g_Dialister
g_Blautia
f_Lachnospiraceae;g_Unassigned genus 2
g_Parabacteroides
g_Alistipes
g_Faecalibacterium
g_Bacteroides

3.2 Microbial metabolite analysis through LC-MS/MS

Targeted LC-MS/MS was performed by the Metabolomics Unit at Fondazione Edmund Mach to quantify a set of polyphenols and glucosinolates and their derivatives (summarized in **Table 3**) in BR supernatants.

Table 3. List of polyphenols, glucosinolates and their derivatives analyzed in BR supernatant through LC-MS/MS. For each compound it has been specified if it was present in the plant or if it derived from microbial breakdown (▪) (41–46).

Glucosinolates	**Origin**
4- methoxyglucobrassicin	Plant
4-Hydroxyglucobrassicin	Plant
Glucoalyssin	Plant
Glucobrassicanapin	Plant
Glucobrassicin	Plant
Glucocheirolin	Plant
Glucoerucin	Plant
Glucoiberin	Plant
Glucoiberverin	Plant
Gluconapin	Plant
Gluconasturtin	Plant
Glucoraphanin	Plant
Glucotropaeolin	Plant
Glucomoringin	Plant
Neoglucobrassicin	Plant
Progoitrin	Plant
Sinalbin	Plant
Sinigrin	Plant
Moringin▪	Microbial derivative of glucomoringin
Sulforaphane▪	Microbial derivative of glucoraphanin
Polyphenols and indoles	
4-aminobenzoic acid	Plant
Caffeic acid	Plant
Catechin	Plant
Cinnamic acid	Plant
p-coumaric acid	Plant
Ferulic acid	Plant
Isorhamnetin-3-glucoside	Plant
Quercetin-3-glucoside	Plant
Quercetin-3,4-diglucoside	Plant
Sinapic acid	Plant
Synapyl alcohol	Plant
Syringaldehyde	Plant
Syringic acid	Plant
Chlorogenic acid	Plant
Neochlorogenic acid	Plant
Cryptochlorogenic acid	Plant
Indole-3-acetonitrile▪	Microbial derivative of glucobrassicin

The results of metabolite quantification are shown in **Figure 7** and **8**. Metabolites that were below the detection limit in ≥ 70% of total samples were excluded from further analysis. Statistical analysis showed that a number of polyphenol metabolites were significantly lower after 24 hours of faecal fermentation of BR, when compared to baseline (T0). In particular, caffeic acid (T0: 35.42 ± 13.61 mg/L; T24: 0.00 ± 0.00 mg/L, mean ± SD, p = 0.0481), ferulic acid (T0: 30.96 ± 7.52 mg/L; T24: 5.51 ± 2.49 mg/L, mean ± SD, p = 0.0395), quercetin 3,4'-diglucoside (T0: 167.55 ± 45.17 mg/L; T24: 9.85 ± 3.83 mg/L, mean ± SD, p = 0.0134) and sinapic acid (T0: 300.40 ± 81.29 mg/L; T24: 36.34 ± 37.63 mg/L, mean ± SD, p = 0.0279), as reported in **Figure 8**A. Changes in glucosinolate profiles were observed during BR fermentation, although these observations did not reach statistical significance. Glucosinolates and polyphenols concentrations are reported in **Table S3** and **S4**.

Figure 7. Individual line plots of glucosinolates identified by LC-MS/MS during BR fermentation. The plots show the changes in concentration (µmol/100g) between experimental timepoints, starting from T0 (inoculation time) and after 5 (T5), 10 (T10) and 24 (T24) hours of fecal fermentation, with compounds splitted represented in different panels according to their concentrations. The error bars correspond to the positive standard deviation (n=3 donors). No significant differences were observed. Catechin, cinnamic acid, p-coumaric acid, isorhamnetin-3-glucoside and cryptochlorogenic acid are not shown, since the levels fell below the limit of quantification. Sinigrin, gluconapin, glucocheirolin, protogoitrin, sinalbin, gluconasturtin, glucoalyssin and glucomoringin are not shown, since the levels fell below the limit of quantification.

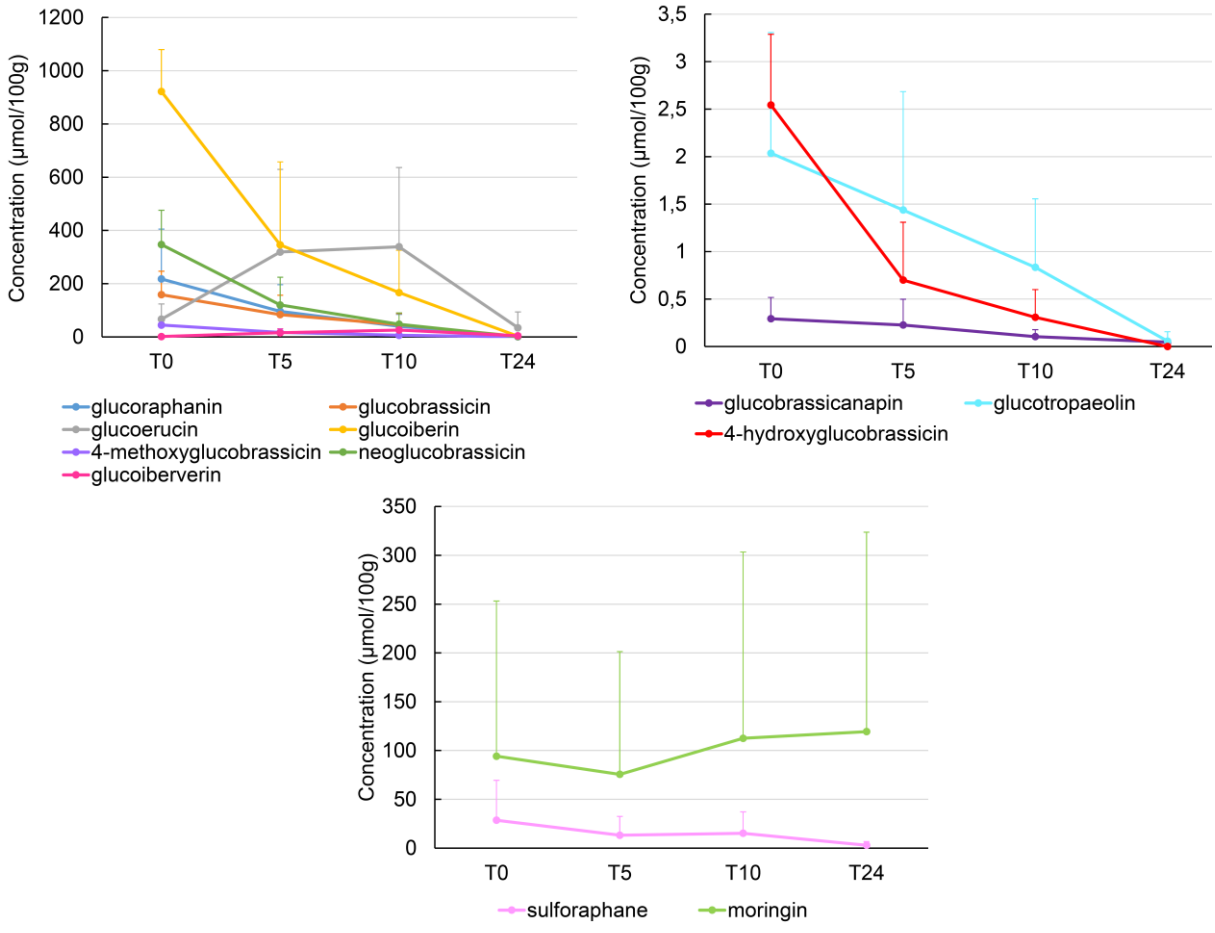

Figure 8. Individual line plots of polyphenols identified by LC-MS/MS during BR fermentation. The plots compare the concentration (mg/kg) changes between all experimental timepoints, starting from T0 (inoculation time) and after 5 (T5), 10 (T10) and 24 (T24) hours of fecal fermentation. The error bars correspond to the positive standard deviation (n=3 donors). Stars (*) indicate statistical significance between T0 and T24 after Kruskal–Wallis test, followed by the post-hoc Dunn's test with FDR p value correction, within the same compound (* colors correspond to the color of the relative compound) (p values are described in the text). Catechin, cinnamic acid, p-coumaric acid, isorhamnetin-3-glucoside and cryptochlorogenic acid are not shown, since they were not detected in > 70% of the samples.

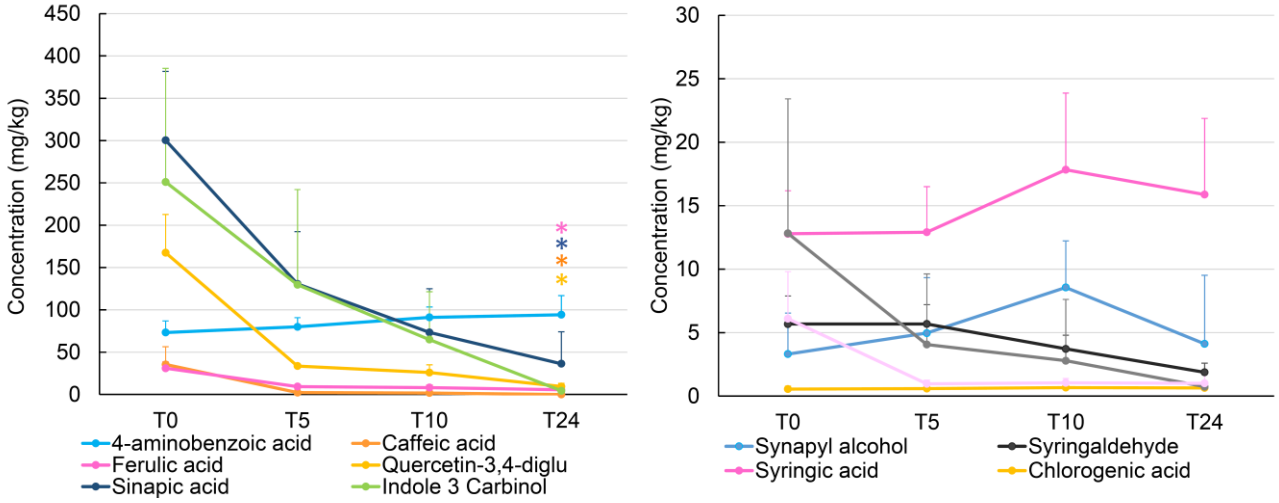

3.3 Correlation analysis between microbial genera and metabolites

Spearman's correlation analysis was performed to correlate microbial relative abundances with polyphenols and glucosinolates concentrations in fermentation supernatants. Statistically significant correlations were observed between relative abundance of GM genera and concentration of the quantified compounds (**Figure 9** and **10**).

Figure 9. Spearman's correlation between the relative abundance of gut microbial genera and target glucosinolates identified by LC-MS/MS in BR supernatants. A positive correlation is indicated by dark red, a negative correlation by dark blue. Stars indicate statistical significance after FDR correction (* $p < 0.05$, ** $p < 0.01$, *** $p < 0.001$). Genera were reported as "Uncultured" when they could not be assigned to any genus (g) within the reference database (https://www.arb-silva.de/download/archive/, accessed on 13 July 2020), at a percentage sequence homology of 95% for genus.

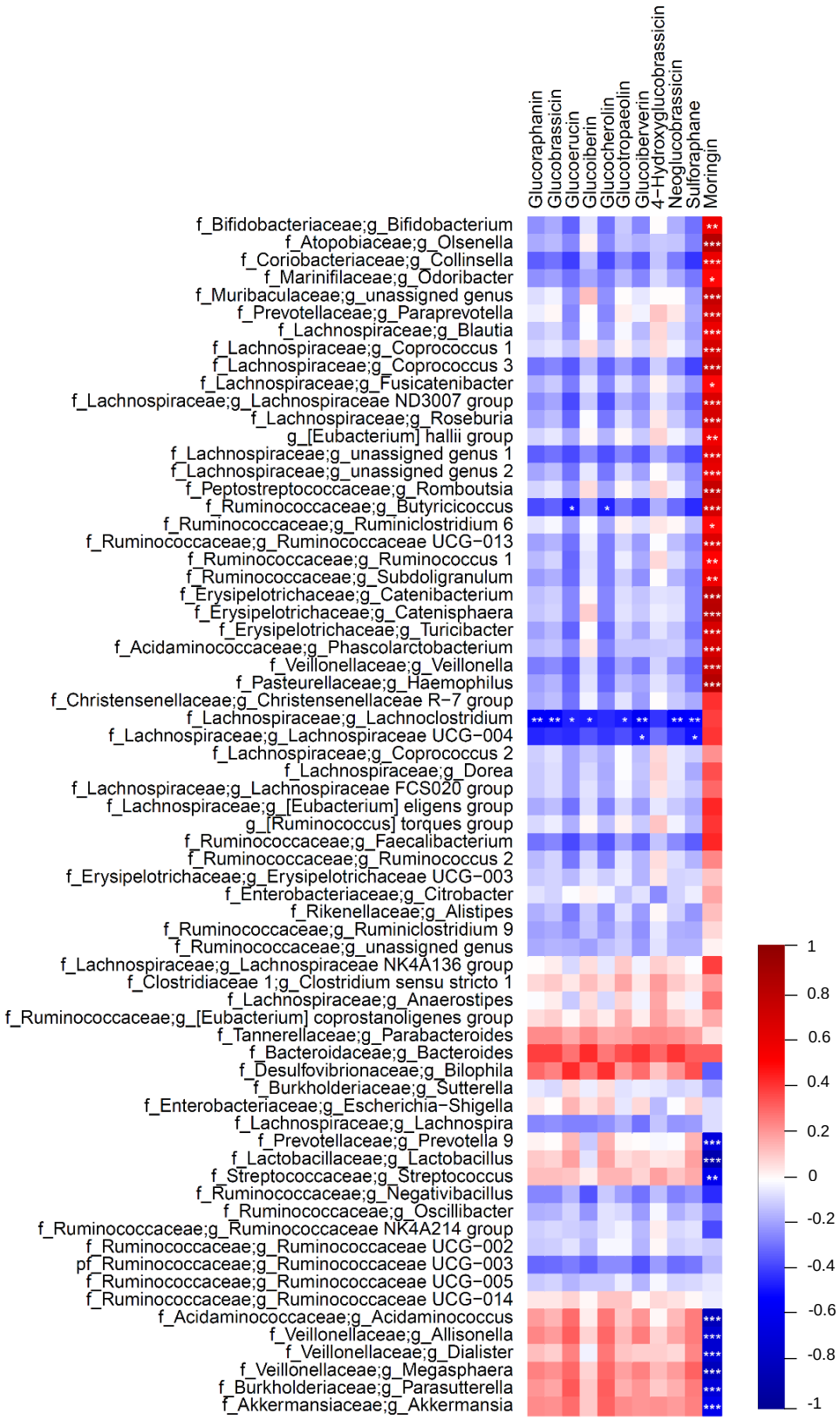

Figure 10. Spearman's correlation between the relative abundance of gut microbial genera and target polyphenols identified by LC-MS/MS in BR supernatants. A positive correlation is indicated by dark red, a negative correlation by dark blue. Stars indicate statistical significance after FDR correction (* $p < 0.05$, ** $p < 0.01$, *** $p < 0.001$). Genera were reported as "Uncultured" when they could not be assigned to any genus (g) within the reference database (https://www.arb-silva.de/download/archive/, accessed on 13 July 2020), at a percentage sequence homology of 95% for genus.

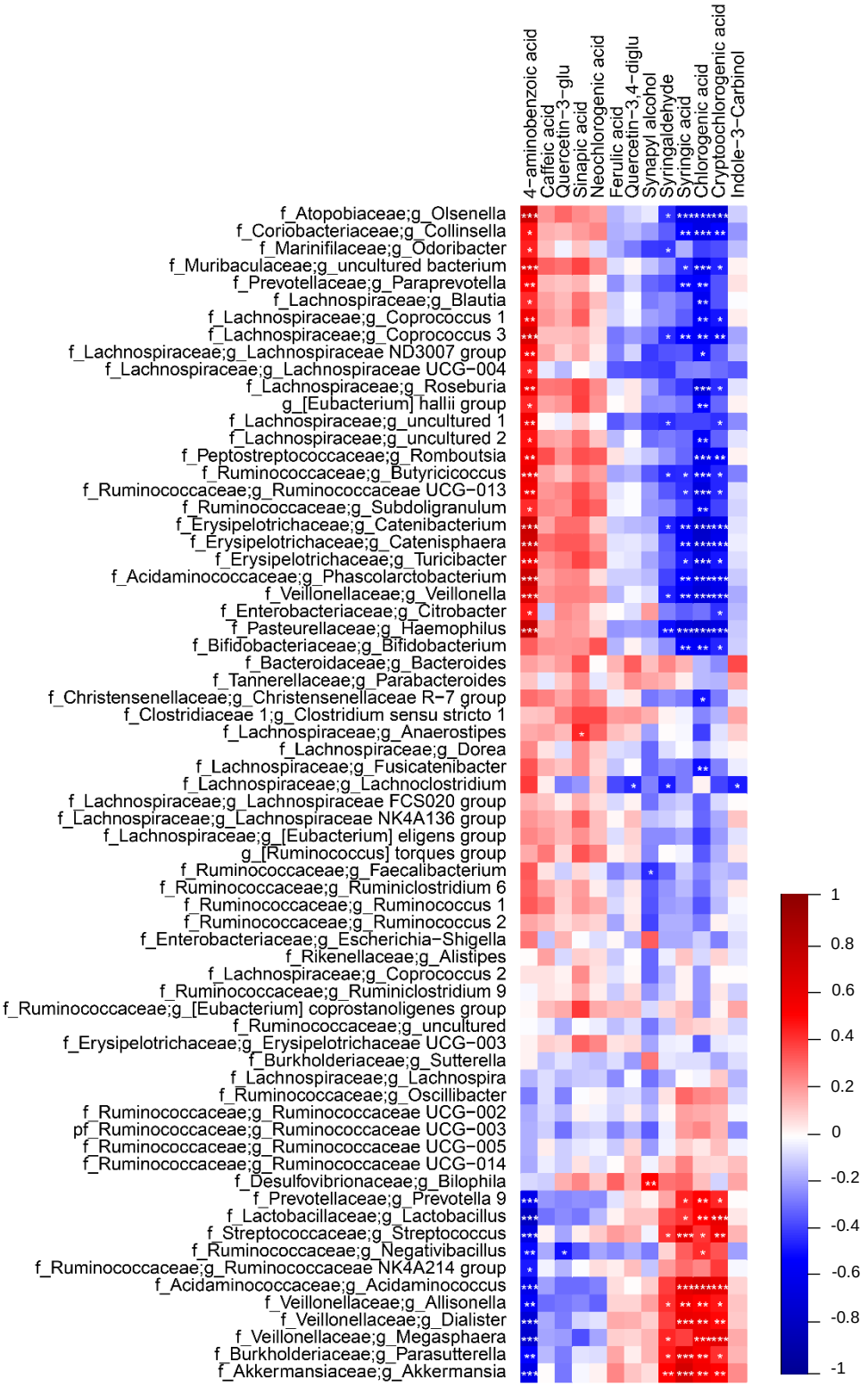

3.4 SCFA production

Changes in SCFA concentrations at the baseline and after 24-hours batch culture fermentation with the different treatments are shown in **Table 4**. Acetic, propionic and butyric acids, the main SCFAs produced by gut microbiota fermentation, all showed a marked increase between T0 and T24, although these results did not reach statistical significance. Fermentation of IN gave the highest production of butyric acid ($p > 0.05$), followed by BR, BK and CL. BR resulted in the highest production of propionate, although this was not statistically significant compared to the other treatments.

Table 4. SCFA concentrations (mmol/L) in fecal batch cultures at T24 with respect to the baseline (T0) of BK, BR, IN and CL. Values are mean ± SD. No significant differences where observed.

	BK		BR		IN		CL	
	T0	T24	T0	T24	T0	T24	T0	T24
acetic acid	1,88 ± 1,00	10,79 ± 2,73	1,26 ± 0,37	10,42 ± 0,15	1,26 ± 0,14	10,06 ± 2,32	1,01 ± 0,03	8,10 ± 2,03
propionic acid	0,39 ± 0,09	2,20 ± 0,58	0,32 ± 0,07	3,81 ± 1,08	0,30 ± 0,02	0,84 ± 0,69	0,28 ± 0,01	1,67 ± 0,07
isobutyric acid	0,03 ± 0,00	1,06 ± 0,01	0,04 ± 0,01	1,19 ± 0,14	0,03 ± 0,00	0,40 ± 0,03	0,03 ± 0,00	1,00 ± 0,09
butyric acid	0,38 ± 0,29	5,81 ± 0,13	0,29 ± 0,09	6,25 ± 1,23	0,23 ± 0,03	25,06 ± 2,40	0,28 ± 0,04	3,95 ± 1,25
isovaleric acid	0,03 ± 0,01	1,16 ± 0,04	0,03 ± 0,01	1,00 ± 0,18	0,02 ± 0,00	0,42 ± 0,02	0,02 ± 0,00	0,85 ± 0,14
2-methylbutyric acid	0,02 ± 0,00	0,72 ± 0,00	0,02 ± 0,00	0,84 ± 0,11	0,02 ± 0,00	0,21 ± 0,01	0,02 ± 0,00	0,73 ± 0,07
valeric acid	0,06 ± 0,01	2,72 ± 0,66	0,07 ± 0,02	3,69 ± 0,42	0,05 ± 0,01	4,94 ± 1,96	0,04 ± 0,00	1,72 ± 0,63
hexanoic acid	0,05 ± 0,01	0,56 ± 0,02	0,04 ± 0,01	0,74 ± 0,33	0,04 ± 0,02	8,19 ± 1,68	0,04 ± 0,00	0,26 ± 0,19

3.5 Effects of Broccolo supernatants on TEER measurements

TEER (Ωcm^2) was calculated as described in Section 2.6.2. **Figure 11** reports changes in TEER expressed as % of increase or decrease after 24 hours incubation with test substrates, compared to baseline TEER. Compared to control medium , the results obtained showed a clear-cut reduction of TEER after 24 hours exposure to ethanol (medium: 114.11 ± 168.71, EtOH: -1176.54 ± 147.65; $p = 0.0002$), as well as a clear TEER improvement after 24 hours exposure to propionic acid (propionic acid: 637.86 ± 252.88; $p < 0.0001$). However, exposure to 10% BR fermentation supernatants did not improve nor decreased epithelial barrier function.

Figure 11. Changes in trans-epithelial electrical resistance (TEER) across differentiated Caco-2 monolayers in presence/absence of test substrates. The change in TEER is the percentage (%) change compared to the initial TEER for each monolayer. The values plotted are the means for three experimental replicates ± the error bars show the standard deviation (SD). Stars indicate statistical significance when compared to control medium. BR, Broccolo of Torbole; EtOH; ethanol.

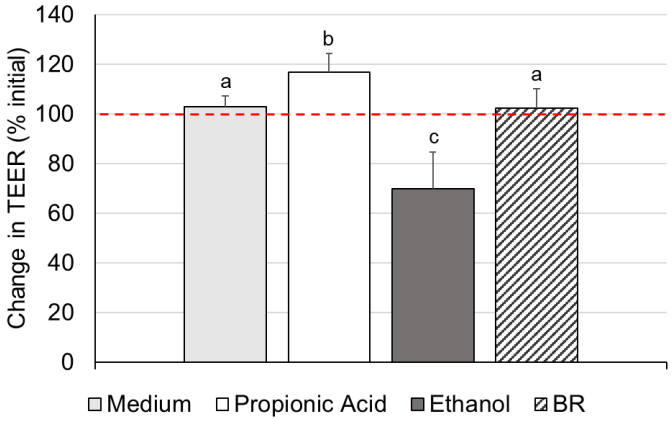

4. Discussion

In this study we evaluated the modulatory effect of a local variety of broccoli (*Brassica oleracea* var. *botrytis*) on the human gut microbiota composition and metabolic activity, combining anaerobic pH controlled *in vitro* batch cultures of faecal microbiota from healthy donors, 16S rRNA sequencing, and hyphenated tandem mass spectroscopy (LC-MS/MS and GC-MS/MS). We used an *in vitro* model of intestinal epithelium consisting of Caco-2 cell line to investigate if faecal supernatants of Broccolo of Torbole were able to improve gut barrier function. *Brassica* vegetables are a good source of dietary fiber and phytonutrients, both considered to be responsible for most of beneficial properties related to *Brassica* consumption (3). It has been proposed that some of *Brassica* related health benefits could be mediated by GM, since different bacteria isolated from the mammalian gut, including *Enterobacteriaceae*, *Bifidobacterium* spp., *Bacteroides* spp. and *Lactobacillus* spp. have myrosinase-like glycoside enzymes able to hydrolyze glucosinolates, producing bioactive isothiocyanates (14,15,47). On the other hand, *Brassica* consumption has been reported to modulate GM composition and metabolism. However, the majority of studies focused on the role of individual phytochemicals in affecting GM, while there is far less knowledge on the impact of whole *Brassica* consumption on the human gastrointestinal microbiota. In our study, the β-diversity analysis unveiled a significant shift in GM composition over 24 hours of BR fermentation and showed a partitioning by different donors, thus confirming the existence of inter-individual variation in the intestinal microbiota (48,49). Interestingly, bacterial α-diversity after 24 hours fermentation was significantly lower in IN and BR

when compared to BK, both for Chao1 and Shannon indices. The presence of a single source of fermentable material in BR and IN fermenters may have selected for specific taxa capable of using available nutrients as growth substrates, thus prevailing over those species that were unable to use BR or IN as energy or carbon sources. In one human placebo-controlled randomized, crossover feeding study in healthy adults, consisting of two 18-day treatment periods separated by a 24-day washout, daily consumption of 200 g of cooked broccoli prepared with 20 g of raw daikon radish in order to provide a source of myrosinase, significantly increased Bacteroidetes/Firmicutes (B/F) ratio when compared to a control diet with no *Brassica* (50). In the same study, no changes were observed in bacterial α-diversity as a results of broccoli consumption, while, similarly to our results, β-diversity significantly changed over time, being primarily related to the increase in B/F ratio. Here, we also observed an increase in B/F over 24 h of BR fermentation, although this result did not reach statistical significance after FDR correction. Another randomized, crossover study by Kellingray and colleagues in 2017 (51) demonstrated that a diet rich in *Brassica* vegetable was associated with an increase in lactobacilli and with a decrease in sulphate-reducing bacteria relative abundances, identified through 16S rRNA next generation sequencing techniques. These results support the hypothesis that *Brassica* consumption may modulate the composition of human GM, thus promoting certain bacterial species capable of utilizing phytochemicals and fibers contained in broccoli and thus driving some of the beneficial effects related to their consumption. When looking at percentage relative abundances after 24 hours of BR fermentation, we observed a decrease in *Alistipes* genus relative abundance, within Bacteroidetes phylum. *Alistipes* is a genus typically isolated from patients suffering from appendicitis and rectal abscess (52). Several studies reported an increase in *Alistipes* abundance related to high-fat diet consumption. *Alistipes* spp. were previously identified as 'lipophilic' microbes by Agans and colleagues (2018) (53), due to their ability to utilize fats for *in vitro* growth, also matching the majority of the findings from previous high-fat intervention animal studies (22,54,55). Notably, *Alistipes* has also been associated with adherence to the Western style diet, since its abundance typically increased in animal-based diets and decreased when consuming a fiber-rich diet (21,56). In line with these observations, our results suggested that the presence of complex carbohydrates and fiber in BR fermentation decreased *Alistipes* over time. Within the Firmicutes phylum, *Ruminococcus 1* relative abundances significantly decreased throughout 24 hours of BR fermentation. In support to our results, *Ruminococcus* abundance was previously shown to decrease after dietary administration of epigallocatechin-3-gallate (EGCG) or black raspberry phenolic extract to mice under a high-fat diet (57,58), suggesting a putative role of BR polyphenols

in lowering *Ruminococcus 1* relative abundance during fecal fermentation. However, to our knowledge no previous study investigated the role of *Ruminococcus 1* in determining beneficial or detrimental effects for human health. A significant increase of the enterobacteria *Escherichia-Shigella* (Proteobacteria phylum) relative abundances was also observed after 24 hours of BR fermentation. This resembles CL fermentation, where also a strong increase in *Escherichia-Shigella* was observed at T24, although it was not statistically significant. The dosage of dietary cellulose and fiber appears to strongly promote *Escherichia-Shigella* abundance, since previous studies reported a boost in *Escherichia-Shigella* abundances when feeding rabbits with high fiber diet (59) or when using carboxymethilcellulose as fiber substrate during *in vitro* fecal fermentation (60). Since different strains belonging to *Escherichia-Shigella* genus also showed the ability of degrading glucosinolates from broccoli (61), we speculate that high complex-fiber and high-glucosinolates content in BR supernatant may have created a more favorable environment for *Escherichia-Shigella* colonization, as previously suggested (61,62). GM composition variations observed by fermenting the other substrates are also in agreement with previous findings. In our study, *Ruminiclostridium 9* relative abundances significantly decreased after 24 hours of IN fermentation, resembling what recently observed *in vivo* by Ferrario and colleagues (2017) (63) after supplementing with inulin the normal chow diet to adult male rats. IN fermentation was also associated with a decrease in *Coprococcus 2* relative abundance. This is consistent with previous studies where inulin supplementation caused a reduction in *Coprococcus* relative abundances during a randomized, cross-over, human intervention study (64) and during an animal dietary intervention study (65). Since both *Ruminiclostridium 9* and *Coprococcus 2* are reported as typical human gut commensal (66,67), we speculate that their decrease during IN fermentation should be addressed to their inability in our *in vitro* system to compete with bacteria that are better adapted in using IN as unique food source, such as *Megasphaera.* We observed a dramatic increase in *Megasphaera* relative abundance after 24 hours of IN fermentation, although this result did not reach statistically significance, probably due to the high interindividual variability between donors. Previous studies reported *Megasphaera* as an efficient butyrate and hexanoic acid producer (68,69), which is consistent with our results on SCFA using GC-MS/MS, thus suggesting that both butyrate and hexanoic acid might have been produced by Megasphaera during IN fermentation. These data suggest the role of inulin in shaping gut microbial populations by promoting the growth of specific taxa and therefore exerting a selective pressure on certain taxonomic groups, thus significantly affecting α-diversity, as we observed after 24 hours of inulin fermentation.

In terms of metabolic output, LC-MS/MS targeted metabolomics on BR supernatants confirmed that bacterial fermentation plays an important role in the metabolism of polyphenols, as previously suggested (20,70). Understanding how polyphenols and glucosinolates are absorbed and metabolized in the human intestine is matter of great interest. During *in vivo* gastrointestinal digestion, several factors including pH, enzymes and microbiota composition strongly influence the fate of plant-derived compounds (71). In this work, we employed an *in vitro* model of digestion, selected and modified from Minekus *et al.* (2014) (29). To date, numerous digestion models exist that can be used to mimic *in vivo* situation, characterized by small variations in acidity, mineral composition and enzymes origin. Certainly, all these factors may be responsible for slight changes in polyphenols and GLS absorption, thus affecting their bioavailability. However, we adapted our protocol to be as far as possible similar to the conditions that might have occurred *in vivo*. This allowed us to reach a compromise between accuracy, feasibility and reproducibility.In this study, a total of twelve glucosinolates and twelve polyphenols were identified. Caffeic acid, ferulic acid, sinapic acid and quercetin 3-4'-diglucoside significantly decreased over time during BR fermentation. These polyphenolic compounds are commonly found in *Brassica* crops, being involved in processes like UV protection, defense mechanisms and pigmentation (72,73). Boiling process significantly decreases their amounts, however they are still identifiable after cooking (73). In our study, the BR were steamed, since this is the way of cooking which better preserve these hydrophilic compounds. Since previous studies confirmed the role of GM in bio-transforming caffeic, ferulic, sinapic acid and quercetin 3-4'-diglucoside in their metabolites (74–77) it was not surprising to observe their progressive decrease over 24 hours of fecal fermentation. Few studies reported correlation analysis between bacterial taxa and broccoli polyphenols metabolism. Here, we performed a Spearman's correlation analysis to understand which bacteria could have a role in Broccolo of Torbole phytochemicals biotransformation. In particular, we found that certain compounds increased together with the increase of certain microbes and vice versa. As an example, syringaldehyde, syringic acid, chlorogenic acid and cryptochlorogenic acid showed a strong positive correlation with *Prevotella*, *Lactobacillus*, *Streptococcus*, *Negativibacillus*, *Acidaminococcus*, *Dialister*, *Allisonella*, *Megasphaera*, *Parasutterella* and *Akkermansia*, while 4-aminobenzoic acid showed a strong negative correlation with the same genera. On the other hand, *Roseburia, Veillonella, Turicibacter, Olsenella,* different genera belonging to Lachnospiraceae, Ruminococcaceae and Erysipelotrichaceae were positively correlated with 4-aminobenzoic acid while showed a strong negative correlation with syringaldehyde, syringic acid, chlorogenic acid and cryptochlorogenic acid. However, since

small significant changes were shown both in the gut microbiota composition and in target glucosinolates or polyphenols concentrations over time, it is difficult to delineate clear metabolic pathways between specific bacterial taxa and target compounds.

Results from GC-MS/MS analysis showed that SCFA concentrations increased after 24 h of fermentation, regardless of the fermentation substrate, although no statistical significance was observed. BR and IN showed a higher amount of total SCFA production when compared to CL and BK fermentation, suggesting a high fermentable fiber content in both BR and IN substrates. Since soluble fibers like inulin are preferentially used as fermentation substrate by human GM to produce SCFA, it was not surprising to observe that IN fermentation produced more SCFA than BR. Endogenous SCFA primarily derive from indigested fiber fermentation by the colonic microbiota (78). Besides serving as energy fuel for colonocytes (79), SCFA, and in particular butyrate, improve the gut health by strengthening the gut barrier function and thus preventing or decreasing gut permeability (79). Lewis and colleagues demonstrated the role of butyrate in reducing bacterial translocation across T84 cell monolayers *in vitro*, thus reducing NF-kB and related inflammatory pathway activation (80). Previous studies also considered the role of glucosinolates and polyphenols in preventing inflammatory diseases by maintaining epithelial barrier integrity. As an example, sulforaphane repaired physiological destruction of the gut barrier induced by bladder cancer in C57BL/6 mice, inducing the upregulation of tight junction proteins (81). Another study from Riemschneider *et al.* (2021) (82) demonstrated that quercetin and indol-3-carbinol gavage administration significantly restored epithelial integrity by induction of tight junction proteins in a mouse model of chronic colitis. Since glucosinolates, polyphenols and SCFA are typically found in cruciferous vegetables or as end-products of bacterial fermentation, as well as in our BR supernatants as demonstrated by LC-MS/MS and GC-MS/MS; and since animal feeding studies highlighted that dietary broccoli can inhibit barrier dysfunction in chemically induced colitis mice model (27,28), we decided to investigate whether BR fecal supernatants could improve gut barrier function, thus being responsible for *Brassica* anti-inflammatory properties. To this end, an *in vitro* model of human intestinal epithelium was used, testing filtered BR supernatants on Caco-2 cell line monolayers. However, TEER measurements showed no big effect when compared to control medium. We observed that sulforaphane, as well as quercetin and indol-3-carbinol, previously proven to be highly effective in improving gut barrier function (81,82), slowly decreased over the fermentation process, reaching their lowest concentration at T24. It is a question of future research to investigate whether metabolites produced at earlier time than T24 may mediate significant

physiological effect on the intestinal barrier integrity. On the other hand, the failure of BR supernatant to improve gut barrier function may be due to the fact that the anti-inflammatory and gut-health promoting effects of *Brassica* consumption are not tied to strengthening of the barrier integrity, but to some other modulatory effects on inflammation pathways, which were not matter of investigation in this thesis.

In conclusion, we demonstrated that *in vitro* anaerobic faecal fermentation of Broccolo of Torbole ecotype caused significant changes in human gut microbiota composition, not all of which are considered as health promoting. Moreover, we observed changes in some polyphenols, thus confirming the role of bacteria in driving the metabolism of different *Brassica* phytochemicals. Finally, we highlight several putative correlations between specific taxa and metabolites. We suggested that the lack of statistical significance may be related to the low number of experimental replicates and to intestinal microbiota variation among volunteers. For this reason, further *in vitro* and *in vivo* analysis are required to explore the network existing between GM, their metabolites and *Brassica*-related benefits.

Supplementary material

Table S1. Mean relative abundance (%) ± standard deviations (SD) of bacterial OTUs at phylum level upon no substrate (BK, **A**), Broccolo of Torbole (BR, **B**), inulin (IN, **C**) and cellulose (CL, **D**) treatment. Data are reported at time of inoculum (T0) and after 5 (T5), 10 (T10) and 24 (T24) hours of fecal fermentation.

A. BK	**T0**		**T5**		**T10**		**T24**	
	mean ± sd		**mean ± sd**		**mean ± sd**		**mean ± sd**	
p_Euryarchaeota	0.07	0.11	0.07	0.11	0.07	0.12	0.06	0.10
p_Actinobacteria	3.28	1.66	3.04	2.06	2.80	1.95	2.75	1.96
p_Bacteroidetes	31.30	5.55	31.09	3.91	23.04	4.37	19.93	2.16
p_Epsilonbacteraeota	0.00	0.00	0.00	0.00	0.00	0.00	0.00	0.00
p_Firmicutes	62.01	4.36	52.79	6.24	55.01	0.80	56.14	4.97
p_Fusobacteria	0.00	0.00	0.00	0.00	0.00	0.00	0.00	0.00
p_Lentisphaerae	0.03	0.04	0.02	0.01	0.01	0.01	0.03	0.01
p_Patescibacteria	0.00	0.01	0.00	0.00	0.00	0.00	0.00	0.00
p_Proteobacteria	2.16	0.13	11.31	3.95	17.71	3.06	19.47	5.85
p_Synergistetes	0.05	0.09	0.05	0.08	0.05	0.08	0.20	0.34
p_Tenericutes	0.05	0.05	0.02	0.04	0.02	0.04	0.02	0.03
p_Verrucomicrobia	1.04	1.20	1.61	1.70	1.29	1.12	1.39	1.41
B. BR	**T0**		**T5**		**T10**		**T24**	
	mean ± sd		**mean ± sd**		**mean ± sd**		**mean ± sd**	
p_Euryarchaeota	0.14	0.14	0.10	0.18	0.03	0.04	0.03	0.03
p_Actinobacteria	4.69	1.68	5.18	3.85	2.61	2.99	1.75	2.06
p_Bacteroidetes	35.79	1.44	31.23	10.92	28.05	11.20	28.21	6.08
p_Epsilonbacteraeota	0.00	0.00	0.00	0.00	0.00	0.00	0.00	0.00
p_Firmicutes	54.78	2.32	39.47	7.57	35.94	5.94	27.37	9.08
p_Fusobacteria	0.00	0.00	0.00	0.00	0.00	0.00	0.00	0.00
p_Lentisphaerae	0.06	0.02	0.04	0.03	0.02	0.01	0.03	0.01
p_Patescibacteria	0.00	0.00	0.00	0.00	0.00	0.00	0.00	0.00
p_Proteobacteria	2.63	0.32	20.81	10.45	32.44	7.18	41.89	11.86
p_Synergistetes	0.08	0.07	0.05	0.09	0.03	0.05	0.12	0.13
p_Tenericutes	0.04	0.04	0.01	0.02	0.01	0.01	0.01	0.01
p_Verrucomicrobia	1.79	2.72	3.10	3.16	0.87	0.76	0.59	0.55
C. IN	**T0**		**T5**		**T10**		**T24**	
	mean ± sd		**mean ± sd**		**mean ± sd**		**mean ± sd**	
p_Euryarchaeota	0.06	0.11	0.06	0.10	0.02	0.04	0.00	0.01
p_Actinobacteria	3.63	1.49	6.10	2.71	4.58	4.72	5.73	7.72
p_Bacteroidetes	33.31	3.63	29.61	9.43	20.83	14.58	18.89	16.19
p_Epsilonbacteraeota	0.00	0.00	0.00	0.00	0.00	0.00	0.00	0.00
p_Firmicutes	58.82	4.17	47.48	7.86	59.07	28.19	64.54	32.93
p_Fusobacteria	0.00	0.00	0.00	0.00	0.00	0.00	0.00	0.00
p_Lentisphaerae	0.03	0.03	0.04	0.02	0.01	0.00	0.00	0.00
p_Patescibacteria	0.00	0.00	0.01	0.01	0.00	0.00	0.00	0.00
p_Proteobacteria	2.18	0.34	13.89	4.07	14.81	9.43	10.70	10.10
p_Synergistetes	0.05	0.08	0.04	0.08	0.02	0.04	0.02	0.03

p_Tenericutes	0.02	0.04	0.01	0.02	0.00	0.01	0.00	0.00
p_Verrucomicrobia	1.90	2.02	2.76	3.19	0.63	0.70	0.10	0.04
D. CL	**T0**		**T5**		**T10**		**T24**	
	mean ± sd		**mean ± sd**		**mean ± sd**		**mean ± sd**	
p_Euryarchaeota	0.07	0.12	0.08	0.14	0.06	0.11	0.06	0.11
p_Actinobacteria	3.11	1.77	4.35	2.95	2.65	1.96	5.43	5.11
p_Bacteroidetes	32.96	5.43	30.75	5.37	19.53	3.08	10.67	3.48
p_Epsilonbacteraeota	0.00	0.00	0.00	0.00	0.00	0.00	0.00	0.00
p_Firmicutes	60.64	3.46	39.54	10.62	37.39	7.92	38.37	17.83
p_Fusobacteria	0.00	0.00	0.00	0.00	0.00	0.00	0.00	0.00
p_Lentisphaerae	0.03	0.03	0.02	0.00	0.02	0.01	0.04	0.04
p_Patescibacteria	0.00	0.00	0.00	0.00	0.00	0.00	0.01	0.01
p_Proteobacteria	1.80	0.55	22.57	13.57	38.71	9.34	42.38	17.62
p_Synergistetes	0.06	0.10	0.05	0.08	0.04	0.07	0.32	0.56
p_Tenericutes	0.03	0.05	0.02	0.03	0.01	0.02	0.00	0.01
p_Verrucomicrobia	1.29	1.81	2.62	2.70	1.58	1.39	2.71	2.49

Table S2. Mean relative abundance (%) ± standard deviations (SD) of bacterial OTUs at genus level upon no substrate (BK, **A**), Broccolo of Torbole (BR, **B**), inulin (IN, **C**) and cellulose (CL, **D**) treatment. Data are reported at time of inoculum (T0) and after 5 (T5), 10 (T10) and 24 (T24) hours of fecal fermentation.

A. BK	**T0**		**T5**		**T10**		**T24**	
	mean ± sd		**mean ± sd**		**mean ± sd**		**mean ± sd**	
g_[Eubacterium] coprostanoligenes group	2.10	1.04	0.07	0.03	0.02	0.00	0.02	0.01
g_[Eubacterium] eligens group	1.46	0.09	0.67	0.30	0.37	0.29	0.27	0.31
g_[Eubacterium] hallii group	0.75	0.54	0.52	0.43	0.47	0.50	0.33	0.30
g_[Ruminococcus] torques group	0.23	0.11	0.17	0.13	0.09	0.06	0.06	0.02
g_Acidaminococcus	0.76	0.68	5.38	5.05	11.12	10.53	9.40	8.88
g_Akkermansia	1.04	1.21	1.61	1.70	1.29	1.12	1.39	1.41
g_Alistipes	3.01	1.71	3.14	0.54	2.24	0.88	2.06	0.89
g_Allisonella	0.02	0.01	1.18	1.08	1.08	0.94	0.75	0.66
g_Anaerostipes	0.73	0.26	0.53	0.12	0.33	0.04	0.14	0.04
g_Bacteroides	18.81	2.32	20.41	3.25	15.27	3.54	13.39	1.91
g_Bifidobacterium	2.15	0.77	1.68	0.69	1.46	0.54	1.59	0.90
g_Bilophila	0.37	0.18	0.62	0.32	0.54	0.22	0.59	0.26
g_Blautia	2.54	1.93	2.53	2.58	1.74	1.97	0.95	0.71
g_Butyricicoccus	0.43	0.35	0.71	0.90	0.37	0.42	0.56	0.82
g_Catenibacterium	0.49	0.85	0.32	0.56	0.28	0.48	0.25	0.43
g_Catenisphaera	0.27	0.46	0.25	0.43	0.23	0.41	0.15	0.25
g_Christensenellaceae R-7 group	2.39	0.27	2.32	0.59	1.64	0.52	1.58	0.84
g_Citrobacter	0.00	0.00	0.03	0.05	0.13	0.20	0.16	0.25
g_Clostridium sensu stricto 1	0.10	0.01	0.06	0.01	0.06	0.02	0.04	0.02
g_Collinsella	0.86	0.67	0.91	0.78	0.88	0.78	0.68	0.42
g_Coprococcus 1	0.12	0.09	0.30	0.43	0.31	0.47	0.24	0.35
g_Coprococcus 2	2.90	1.59	0.31	0.20	0.07	0.05	0.02	0.01
g_Coprococcus 3	0.14	0.17	0.29	0.44	0.98	1.56	0.92	1.23
g_Dialister	3.79	3.32	2.48	2.17	2.14	1.86	1.29	1.19
g_Dorea	0.75	0.48	0.58	0.31	0.80	0.46	0.76	0.39
g_Erysipelotrichaceae UCG-003	0.18	0.03	0.13	0.05	0.10	0.04	0.06	0.01
g_Escherichia-Shigella	0.10	0.07	2.77	2.13	7.74	5.22	9.44	6.60
g_Faecalibacterium	11.29	1.74	7.57	2.72	7.59	2.90	5.86	3.14
g_Fusicatenibacter	1.03	0.87	0.70	0.76	0.50	0.56	0.35	0.24
g_Haemophilus	0.13	0.22	0.32	0.55	0.48	0.84	0.21	0.36
g_Lachnoclostridium	0.42	0.09	0.66	0.35	1.97	1.18	2.55	0.96
g_Lachnospira	1.39	1.12	0.82	0.62	0.45	0.25	0.29	0.19
g_Lachnospiraceae FCS020 group	0.17	0.07	0.14	0.08	0.08	0.05	0.08	0.00
g_Lachnospiraceae ND3007 group	1.03	1.11	0.79	0.89	0.60	0.80	0.38	0.55
g_Lachnospiraceae NK4A136 group	1.90	0.74	0.45	0.15	0.18	0.11	0.07	0.04
g_Lachnospiraceae UCG-004	0.32	0.29	1.52	0.95	3.55	3.14	3.01	3.43
g_Lactobacillus	0.05	0.06	0.40	0.55	0.34	0.45	0.26	0.34
g_Megasphaera	1.00	0.94	2.37	2.89	2.50	2.56	10.37	9.09
g_Negativibacillus	0.29	0.24	0.33	0.32	0.51	0.66	1.12	1.37
g_Odoribacter	0.64	0.11	0.52	0.07	0.50	0.26	0.50	0.34
g_Olsenella	0.04	0.07	0.08	0.14	0.10	0.18	0.14	0.24
g_Oscillibacter	0.73	0.41	0.67	0.30	0.64	0.41	0.62	0.33
g_Parabacteroides	2.79	0.72	4.23	0.96	3.99	0.24	3.49	0.63
g_Paraprevotella	0.14	0.24	0.10	0.17	0.01	0.02	0.02	0.03

g_Parasutterella	0.37	0.29	2.27	1.92	2.08	1.73	1.95	1.65
g_Phascolarctobacterium	0.73	1.26	1.31	2.28	1.35	2.33	1.25	2.16
g_Prevotella 9	5.61	6.77	2.43	2.66	0.90	0.81	0.37	0.36
g_Romboutsia	0.31	0.27	0.25	0.25	0.20	0.18	0.21	0.22
g_Roseburia	2.61	2.66	0.76	0.82	0.48	0.60	0.26	0.22
g_Ruminiclostridium 6	0.26	0.14	0.10	0.10	0.05	0.06	0.03	0.03
g_Ruminiclostridium 9	0.20	0.01	0.17	0.04	0.13	0.06	0.09	0.05
g_Ruminococcaceae NK4A214 group	0.26	0.25	0.15	0.16	0.12	0.12	0.11	0.12
g_Ruminococcaceae UCG-002	3.34	2.29	3.51	2.33	3.21	2.40	2.82	1.42
g_Ruminococcaceae UCG-003	0.28	0.15	0.29	0.05	0.43	0.23	0.56	0.35
g_Ruminococcaceae UCG-005	1.37	0.95	0.99	0.60	0.73	0.47	0.58	0.38
g_Ruminococcaceae UCG-013	0.40	0.23	0.30	0.30	0.21	0.21	0.15	0.14
g_Ruminococcaceae UCG-014	0.90	0.96	0.70	0.53	0.53	0.38	0.51	0.40
g_Ruminococcus 1	0.85	0.35	0.25	0.27	0.07	0.05	0.07	0.06
g_Ruminococcus 2	1.65	0.41	1.91	0.82	0.99	0.42	1.94	0.21
g_Streptococcus	0.45	0.31	0.22	0.16	0.14	0.10	0.11	0.08
g_Subdoligranulum	2.06	0.59	1.84	1.03	1.37	0.94	1.34	1.02
g_Sutterella	1.19	0.34	5.25	2.96	6.63	1.55	6.98	0.51
g_Turicibacter	0.14	0.21	0.10	0.15	0.09	0.14	0.09	0.14
g_uncultured bacterium	0.21	0.37	0.19	0.32	0.08	0.13	0.04	0.08
g_Veillonella	0.21	0.24	0.11	0.17	0.12	0.19	0.05	0.07
f_Lachnospiraceae;g_uncultured genus 1	0.56	0.23	0.83	0.91	0.82	0.66	0.49	0.29
f_Lachnospiraceae;g_uncultured genus 2	3.21	3.11	2.22	2.11	1.52	1.46	1.05	0.61
f_Ruminococcaceae;g_uncultured	0.56	0.20	0.48	0.05	0.45	0.11	0.73	0.31

B. BR	**T0**		**T5**		**T10**		**T24**	
	mean ± sd		**mean ± sd**		**mean ± sd**		**mean ± sd**	
g_[Eubacterium] coprostanoligenes group	0.77	0.07	0.11	0.06	0.01	0.01	0.01	0.02
g_[Eubacterium] eligens group	1.21	0.10	0.29	0.49	0.11	0.20	0.09	0.13
g_[Eubacterium] hallii group	0.60	0.15	0.36	0.18	0.11	0.14	0.05	0.04
g_[Ruminococcus] torques group	0.34	0.12	0.12	0.06	0.05	0.05	0.01	0.00
g_Acidaminococcus	0.31	0.54	4.06	3.55	11.39	9.87	10.41	9.15
g_Akkermansia	1.78	2.73	3.10	3.16	0.87	0.76	0.59	0.55
g_Alistipes	3.75	1.53	0.83	0.65	0.34	0.39	0.16	0.04
g_Allisonella	0.00	0.00	1.30	1.37	1.25	1.09	1.03	1.12
g_Anaerostipes	0.61	0.15	0.57	0.15	0.18	0.09	0.09	0.01
g_Bacteroides	25.44	2.10	24.97	10.12	23.79	10.93	24.26	6.81
g_Bifidobacterium	3.02	0.73	3.04	1.86	1.45	1.56	1.12	1.32
g_Bilophila	0.42	0.38	1.94	0.88	1.18	0.17	1.79	0.54
g_Blautia	3.29	1.73	1.66	1.50	0.41	0.43	0.12	0.03
g_Butyricicoccus	0.48	0.31	0.22	0.37	0.17	0.29	0.08	0.14
g_Catenibacterium	0.86	0.75	0.41	0.71	0.19	0.32	0.17	0.26
g_Catenisphaera	0.55	0.51	0.39	0.67	0.27	0.47	0.14	0.24
g_Christensenellaceae R-7 group	2.54	0.14	1.56	1.55	0.67	1.00	0.53	0.45
g_Citrobacter	0.00	0.00	0.14	0.18	0.26	0.37	1.33	1.34
g_Clostridium sensu stricto 1	0.12	0.01	0.13	0.02	0.05	0.03	0.22	0.30
g_Collinsella	1.21	0.71	1.45	1.61	0.80	1.12	0.41	0.48
g_Coprococcus 1	0.17	0.09	0.15	0.17	0.04	0.05	0.01	0.02
g_Coprococcus 2	1.82	0.12	0.03	0.02	0.00	0.00	0.00	0.00

g_Coprococcus 3	0.18	0.10	0.14	0.21	0.08	0.13	0.02	0.04
g_Dialister	3.24	5.61	2.94	2.56	1.23	1.08	0.54	0.49
g_Dorea	0.86	0.31	0.39	0.03	0.09	0.04	0.05	0.02
g_Erysipelotrichaceae UCG-003	0.13	0.03	0.14	0.06	0.05	0.02	0.03	0.01
g_Escherichia-Shigella	0.06	0.03	7.91	8.47	22.18	7.40	31.96	9.78
g_Faecalibacterium	6.55	3.62	0.86	1.31	0.18	0.28	0.07	0.08
g_Fusicatenibacter	0.92	0.40	0.28	0.30	0.07	0.10	0.01	0.01
g_Haemophilus	0.30	0.27	0.06	0.11	0.02	0.04	0.01	0.01
g_Lachnoclostridium	0.28	0.06	0.30	0.22	0.42	0.69	1.34	2.27
g_Lachnospira	0.37	0.30	0.04	0.03	0.00	0.00	0.00	0.01
g_Lachnospiraceae FCS020 group	0.15	0.01	0.06	0.03	0.01	0.01	0.00	0.00
g_Lachnospiraceae ND3007 group	1.06	0.91	0.24	0.41	0.05	0.08	0.00	0.00
g_Lachnospiraceae NK4A136 group	1.14	0.16	0.18	0.12	0.03	0.06	0.11	0.18
g_Lachnospiraceae UCG-004	0.25	0.10	0.22	0.29	0.11	0.18	0.09	0.13
g_Lactobacillus	0.02	0.03	0.89	1.08	0.17	0.20	0.14	0.20
g_Megasphaera	0.96	1.62	9.29	8.97	9.94	10.00	7.07	7.80
g_Negativibacillus	0.22	0.36	0.02	0.02	0.00	0.00	0.00	0.00
g_Odoribacter	0.63	0.10	0.22	0.25	0.08	0.05	0.05	0.03
g_Olsenella	0.11	0.09	0.18	0.30	0.12	0.20	0.14	0.24
g_Oscillibacter	0.56	0.65	0.34	0.13	0.08	0.01	0.01	0.00
g_Parabacteroides	3.59	0.21	4.90	0.96	3.76	0.46	3.67	1.39
g_Paraprevotella	0.64	0.56	0.00	0.00	0.00	0.00	0.00	0.00
g_Parasutterella	0.38	0.46	3.28	2.61	1.67	1.27	1.29	1.12
g_Phascolarctobacterium	1.77	1.54	2.45	4.24	1.38	2.39	0.71	0.61
g_Prevotella 9	1.10	1.90	0.02	0.03	0.01	0.01	0.01	0.01
g_Romboutsia	0.54	0.20	0.42	0.37	0.18	0.20	0.18	0.22
g_Roseburia	2.99	2.08	1.46	2.27	0.63	1.06	0.08	0.13
g_Ruminiclostridium 6	0.30	0.20	0.01	0.02	0.00	0.00	0.01	0.01
g_Ruminiclostridium 9	0.17	0.00	0.10	0.08	0.03	0.05	0.01	0.01
g_Ruminococcaceae NK4A214 group	0.17	0.27	0.03	0.03	0.00	0.00	0.00	0.00
g_Ruminococcaceae UCG-002	2.90	3.87	0.72	0.37	0.06	0.03	0.08	0.12
g_Ruminococcaceae UCG-003	0.21	0.26	0.04	0.05	0.01	0.01	0.00	0.01
g_Ruminococcaceae UCG-005	0.87	1.06	0.04	0.01	0.01	0.01	0.01	0.02
g_Ruminococcaceae UCG-013	0.40	0.21	0.28	0.29	0.11	0.16	0.06	0.08
g_Ruminococcaceae UCG-014	0.81	0.90	0.40	0.19	0.10	0.06	0.20	0.29
g_Ruminococcus 1	1.58	0.76	0.03	0.05	0.00	0.01	0.00	0.00
g_Ruminococcus 2	2.20	0.90	0.46	0.49	0.04	0.02	0.01	0.02
g_Streptococcus	0.31	0.31	0.22	0.15	0.07	0.05	0.04	0.04
g_Subdoligranulum	2.47	0.45	2.15	2.03	0.88	1.13	0.49	0.61
g_Sutterella	1.35	0.42	7.37	1.51	6.79	1.06	4.81	3.05
g_Turicibacter	0.33	0.28	0.20	0.32	0.09	0.15	0.08	0.11
g_uncultured bacterium	0.45	0.39	0.28	0.48	0.06	0.11	0.06	0.08
g_Veillonella	0.28	0.20	0.45	0.76	4.26	7.37	2.63	4.56
f_Lachnospiraceae;g_uncultured genus 1	0.41	0.10	0.23	0.26	0.09	0.15	0.04	0.04
f_Lachnospiraceae;g_uncultured genus 2	3.42	2.29	1.44	1.78	0.36	0.51	0.10	0.08
f_Ruminococcaceae;g_uncultured	0.42	0.19	0.16	0.01	0.03	0.01	0.02	0.03

C. IN	**T0**	**T5**	**T10**	**T24**

	mean ± sd		mean ± sd		mean ± sd		mean ± sd	
g_[Eubacterium] coprostanoligenes group	1.39	0.46	0.08	0.03	0.00	0.00	0.00	0.00
g_[Eubacterium] eligens group	1.37	0.34	0.47	0.22	0.05	0.08	0.00	0.00
g_[Eubacterium] hallii group	0.73	0.38	0.25	0.16	0.09	0.14	0.03	0.05
g_[Ruminococcus] torques group	0.27	0.13	0.14	0.07	0.06	0.07	0.01	0.01
g_Acidaminococcus	0.63	0.54	4.02	3.50	7.41	7.90	4.26	3.77
g_Akkermansia	1.90	2.03	2.76	3.19	0.63	0.70	0.10	0.05
g_Alistipes	3.33	1.57	1.36	0.44	0.29	0.14	0.08	0.04
g_Allisonella	0.01	0.02	2.00	2.20	0.47	0.56	0.06	0.06
g_Anaerostipes	0.66	0.26	0.41	0.12	0.12	0.11	0.02	0.01
g_Bacteroides	21.13	2.04	22.88	8.96	17.01	12.04	16.76	15.05
g_Bifidobacterium	2.47	0.63	4.11	1.53	3.56	3.69	4.38	5.64
g_Bilophila	0.42	0.26	1.37	0.84	0.63	0.31	0.36	0.09
g_Blautia	2.64	2.40	1.80	1.33	0.48	0.58	0.08	0.09
g_Butyricicoccus	0.42	0.46	0.24	0.33	0.15	0.26	0.02	0.03
g_Catenibacterium	0.51	0.89	0.42	0.72	0.25	0.44	0.06	0.11
g_Catenisphaera	0.32	0.56	0.30	0.52	0.22	0.39	0.06	0.11
g_Christensenellaceae R-7 group	2.75	0.77	1.72	0.34	0.52	0.50	0.07	0.07
g_Citrobacter	0.00	0.00	0.05	0.08	0.14	0.23	0.06	0.11
g_Clostridium sensu stricto 1	0.10	0.04	0.11	0.06	0.04	0.03	1.50	2.58
g_Collinsella	0.88	0.66	1.40	0.95	0.70	0.71	0.97	1.43
g_Coprococcus 1	0.12	0.11	0.11	0.12	0.03	0.05	0.00	0.00
g_Coprococcus 2	2.71	0.69	0.06	0.04	0.00	0.00	0.00	0.00
g_Coprococcus 3	0.13	0.17	0.15	0.21	0.10	0.18	0.05	0.09
g_Dialister	5.09	4.44	3.09	2.81	1.09	1.17	0.33	0.30
g_Dorea	0.68	0.38	0.34	0.21	0.07	0.08	0.04	0.06
g_Erysipelotrichaceae UCG-003	0.17	0.04	0.15	0.02	0.04	0.03	0.01	0.01
g_Escherichia-Shigella	0.18	0.22	2.98	2.08	9.11	8.92	8.03	10.05
g_Faecalibacterium	6.50	2.54	2.22	2.84	0.41	0.60	0.02	0.01
g_Fusicatenibacter	0.80	0.55	0.32	0.13	0.08	0.08	0.00	0.00
g_Haemophilus	0.09	0.16	0.23	0.40	0.15	0.25	0.03	0.05
g_Lachnoclostridium	0.35	0.12	0.37	0.21	0.97	1.61	3.14	5.38
g_Lachnospira	1.11	0.96	0.45	0.51	0.03	0.02	0.00	0.00
g_Lachnospiraceae FCS020 group	0.16	0.03	0.07	0.04	0.01	0.01	0.00	0.00
g_Lachnospiraceae ND3007 group	0.75	1.03	0.28	0.48	0.08	0.14	0.00	0.00
g_Lachnospiraceae NK4A136 group	1.70	0.63	0.19	0.14	0.02	0.04	0.01	0.01
g_Lachnospiraceae UCG-004	0.26	0.18	0.24	0.21	0.10	0.15	0.02	0.03
g_Lactobacillus	0.06	0.06	2.88	3.30	0.93	0.91	0.27	0.37
g_Megasphaera	2.16	2.06	11.15	12.84	38.49	36.96	50.21	43.77
g_Negativibacillus	0.39	0.33	0.25	0.27	0.03	0.03	0.00	0.00
g_Odoribacter	0.60	0.17	0.28	0.17	0.10	0.13	0.03	0.03
g_Olsenella	0.05	0.08	0.12	0.20	0.13	0.22	0.34	0.59
g_Oscillibacter	0.81	0.54	0.44	0.28	0.05	0.04	0.00	0.01
g_Parabacteroides	2.91	0.49	4.50	0.72	3.20	2.06	2.00	1.11
g_Paraprevotella	0.25	0.44	0.11	0.20	0.11	0.18	0.01	0.01
g_Parasutterella	0.42	0.35	1.84	1.61	0.62	0.66	0.08	0.05
g_Phascolarctobacterium	0.60	1.04	2.16	3.74	1.89	3.28	0.68	1.17
g_Prevotella 9	4.79	5.44	0.29	0.47	0.02	0.02	0.01	0.01
g_Romboutsia	0.30	0.22	0.39	0.26	0.14	0.12	0.06	0.07

g_Roseburia	2.20	2.59	1.02	1.44	0.41	0.68	0.02	0.03
g_Ruminiclostridium 6	0.18	0.25	0.02	0.03	0.00	0.00	0.00	0.00
g_Ruminiclostridium 9	0.21	0.02	0.16	0.09	0.02	0.02	0.00	0.00
g_Ruminococcaceae NK4A214 group	0.36	0.33	0.22	0.24	0.00	0.00	0.00	0.00
g_Ruminococcaceae UCG-002	4.11	3.07	1.03	0.65	0.06	0.03	0.00	0.00
g_Ruminococcaceae UCG-003	0.22	0.13	0.12	0.02	0.02	0.02	0.00	0.00
g_Ruminococcaceae UCG-005	1.50	1.10	0.36	0.33	0.01	0.01	0.00	0.00
g_Ruminococcaceae UCG-013	0.32	0.20	0.24	0.19	0.09	0.12	0.02	0.04
g_Ruminococcaceae UCG-014	0.89	1.00	0.89	0.89	0.12	0.07	0.01	0.00
g_Ruminococcus 1	0.89	0.77	0.07	0.11	0.02	0.03	0.00	0.00
g_Ruminococcus 2	2.60	1.13	0.54	0.41	0.15	0.19	0.02	0.01
g_Streptococcus	0.42	0.30	0.37	0.32	0.08	0.07	0.02	0.02
g_Subdoligranulum	2.29	0.61	2.38	1.75	0.90	1.17	0.23	0.26
g_Sutterella	1.04	0.15	7.36	2.70	4.04	0.70	2.08	1.02
g_Turicibacter	0.12	0.18	0.11	0.16	0.06	0.11	0.03	0.05
g_uncultured bacterium	0.20	0.34	0.15	0.26	0.09	0.15	0.01	0.02
g_Veillonella	0.20	0.20	0.18	0.26	1.92	3.33	2.76	4.77
f_Lachnospiraceae;g_uncultured genus 1	0.41	0.17	0.24	0.31	0.14	0.22	0.24	0.42
f_Lachnospiraceae;g_uncultured genus 2	3.02	3.46	1.43	1.60	0.37	0.58	0.03	0.06
f_Ruminococcaceae;g_uncultured	0.54	0.21	0.23	0.09	0.03	0.02	0.00	0.00

D. CL	**T0**		**T5**		**T10**		**T24**	
	mean ± sd		**mean ± sd**		**mean ± sd**		**mean ± sd**	
g_[Eubacterium] coprostanoligenes group	1.69	0.73	0.10	0.12	0.03	0.02	0.04	0.05
g_[Eubacterium] eligens group	1.56	0.23	0.32	0.43	0.09	0.15	0.01	0.02
g_[Eubacterium] hallii group	0.55	0.60	0.33	0.26	0.17	0.20	0.24	0.25
g_[Ruminococcus] torques group	0.24	0.13	0.12	0.06	0.08	0.06	0.18	0.26
g_Acidaminococcus	0.61	0.56	5.37	4.68	12.90	11.17	10.18	17.41
g_Akkermansia	1.29	1.82	2.62	2.70	1.58	1.39	2.71	2.49
g_Alistipes	3.06	1.20	1.61	0.15	0.76	0.16	0.43	0.21
g_Allisonella	0.01	0.01	0.91	0.93	0.89	0.80	0.64	0.58
g_Anaerostipes	0.48	0.37	0.45	0.17	0.26	0.17	0.60	0.67
g_Bacteroides	20.95	0.42	22.80	4.61	14.26	2.23	7.74	3.36
g_Bifidobacterium	2.15	0.93	2.32	1.08	1.37	0.73	3.13	2.97
g_Bilophila	0.29	0.21	1.04	0.45	1.02	0.32	4.93	6.28
g_Blautia	2.36	1.46	2.04	2.15	0.79	0.91	0.41	0.33
g_Butyricicoccus	0.40	0.40	0.28	0.34	0.20	0.26	0.21	0.18
g_Catenibacterium	0.57	0.98	0.65	1.13	0.49	0.86	0.48	0.82
g_Catenisphaera	0.21	0.36	0.32	0.55	0.17	0.30	0.19	0.32
g_Christensenellaceae R-7 group	2.62	0.63	2.38	0.84	1.13	0.92	1.07	0.93
g_Citrobacter	0.00	0.00	0.13	0.18	0.45	0.72	0.55	0.57
g_Clostridium sensu stricto 1	0.07	0.06	0.09	0.04	0.49	0.79	0.18	0.21
g_Collinsella	0.71	0.65	1.57	1.50	0.95	0.93	1.76	1.72
g_Coprococcus 1	0.12	0.11	0.14	0.20	0.06	0.09	0.03	0.03
g_Coprococcus 2	2.77	0.47	0.14	0.17	0.03	0.05	0.03	0.06
g_Coprococcus 3	0.11	0.15	0.17	0.26	0.15	0.25	0.09	0.11
g_Dialister	4.00	3.46	3.76	3.29	1.66	1.53	2.50	2.89
g_Dorea	0.74	0.38	0.32	0.18	0.32	0.22	2.19	3.61
g_Erysipelotrichaceae UCG-003	0.18	0.03	0.13	0.05	0.07	0.02	0.19	0.25
g_Escherichia-Shigella	0.06	0.02	9.98	10.67	25.94	9.54	21.91	22.72

g_Faecalibacterium	10.45	0.77	2.84	3.48	0.95	0.88	0.12	0.06
g_Fusicatenibacter	0.82	0.84	0.45	0.51	0.16	0.23	0.04	0.05
g_Haemophilus	0.12	0.21	0.44	0.76	0.36	0.62	0.03	0.05
g_Lachnoclostridium	0.29	0.09	0.37	0.15	0.56	0.34	1.65	0.69
g_Lachnospira	1.25	0.82	0.14	0.09	0.02	0.02	0.01	0.01
g_Lachnospiraceae FCS020 group	0.19	0.04	0.09	0.07	0.01	0.01	0.01	0.01
g_Lachnospiraceae ND3007 group	1.07	0.85	0.45	0.77	0.15	0.26	0.00	0.00
g_Lachnospiraceae NK4A136 group	1.73	0.57	0.26	0.27	0.05	0.05	0.02	0.03
g_Lachnospiraceae UCG-004	0.25	0.24	0.39	0.39	0.41	0.31	0.56	0.47
g_Lactobacillus	0.02	0.02	0.30	0.33	0.17	0.20	1.31	2.12
g_Megasphaera	1.04	0.93	3.97	3.49	8.65	7.51	6.63	8.51
g_Negativibacillus	0.28	0.30	0.29	0.35	0.15	0.13	0.05	0.07
g_Odoribacter	0.61	0.19	0.49	0.31	0.41	0.35	0.33	0.39
g_Olsenella	0.04	0.07	0.10	0.18	0.08	0.14	0.05	0.09
g_Oscillibacter	0.78	0.48	0.56	0.38	0.30	0.15	0.79	1.15
g_Parabacteroides	3.00	0.42	5.26	1.91	4.00	1.39	2.16	0.19
g_Paraprevotella	0.21	0.36	0.00	0.00	0.00	0.00	0.00	0.00
g_Parasutterella	0.43	0.32	2.99	2.23	2.22	1.66	7.68	10.46
g_Phascolarctobacterium	0.57	0.99	1.90	3.30	1.44	2.49	1.43	2.48
g_Prevotella 9	4.81	5.49	0.31	0.33	0.03	0.03	0.00	0.01
g_Romboutsia	0.25	0.24	0.34	0.31	0.24	0.26	0.36	0.26
g_Roseburia	2.22	2.56	1.23	1.89	0.74	1.22	0.16	0.21
g_Ruminiclostridium 6	0.25	0.18	0.02	0.04	0.00	0.00	0.00	0.00
g_Ruminiclostridium 9	0.17	0.06	0.12	0.07	0.05	0.04	0.03	0.05
g_Ruminococcaceae NK4A214 group	0.29	0.27	0.06	0.06	0.01	0.01	0.10	0.17
g_Ruminococcaceae UCG-002	4.34	3.08	0.62	0.40	0.22	0.12	0.84	1.39
g_Ruminococcaceae UCG-003	0.20	0.10	0.13	0.03	0.09	0.10	0.32	0.56
g_Ruminococcaceae UCG-005	1.41	1.06	0.15	0.19	0.01	0.01	0.00	0.00
g_Ruminococcaceae UCG-013	0.38	0.28	0.28	0.38	0.16	0.24	0.16	0.15
g_Ruminococcaceae UCG-014	0.82	0.86	0.59	0.70	0.20	0.15	0.12	0.10
g_Ruminococcus 1	0.88	0.72	0.03	0.04	0.01	0.01	0.01	0.01
g_Ruminococcus 2	2.75	1.22	0.59	0.76	0.07	0.05	0.07	0.08
g_Streptococcus	0.29	0.29	0.28	0.19	0.12	0.09	0.48	0.67
g_Subdoligranulum	2.42	0.72	2.01	1.47	1.02	0.91	2.28	2.18
g_Sutterella	0.88	0.50	7.87	3.59	8.41	0.87	6.79	6.47
g_Turicibacter	0.13	0.21	0.16	0.25	0.11	0.18	0.15	0.18
g_uncultured bacterium	0.22	0.38	0.20	0.35	0.05	0.08	0.00	0.00
g_Veillonella	0.17	0.21	0.16	0.27	0.23	0.39	0.04	0.08
f_Lachnospiraceae;g_uncultured genus 1	0.42	0.23	0.33	0.43	0.19	0.21	0.21	0.25
f_Lachnospiraceae;g_uncultured genus 2	3.07	3.31	1.57	1.90	0.48	0.63	0.23	0.19
f_Ruminococcaceae;g_uncultured	0.53	0.23	0.29	0.16	0.12	0.02	0.16	0.19

Table S3. Glucosinolates concentration (μmol/100g) in BR supernatant quantified by LC-MS/MS and normalized according to fermentation volume. Data represent the mean and standard deviation (SD) at time of inoculation (T0) and after 5 (T5), 10 (T10) and 24 hours (T24) of Broccolo fecal fermentation (n=3 donors). Sinigrin, gluconapin, glucocheirolin, protogoitrin, sinalbin, gluconasturtin, glucoalyssin and glucomoringin are not shown, since the levels fell below the limit of quantification.

	BR			
	T0	T5	T10	T24
Glucoraphanin				
Mean	217.46	95.88	39.86	2.75
SD	187.69	100.31	44.19	2.83
Glucobrassicin				
Mean	158.70	83.72	46.01	2.24
SD	88.14	72.73	41.98	1.94
Glucoerucin				
Mean	66.41	318.87	338.58	34.23
SD	57.72	310.56	297.95	59.28
Glucoiberin				
Mean	921.85	345.59	166.48	2.73
SD	158.02	312.28	158.84	2.84
Glucotropaeolin				
Mean	2.04	1.44	0.83	0.06
SD	1.27	1.25	0.72	0.10
Glucobrassicanapin				
Mean	0.29	0.23	0.10	0.04
SD	0.22	0.27	0.07	0.01
Glucoiberverin				
Mean	1.28	15.50	25.79	4.28
SD	0.70	14.82	23.74	7.15
4-Hydroxyglucobrassicin				
Mean	2.54	0.70	0.31	0.00
SD	0.74	0.61	0.29	0.00
4-Methoxyglucobrassicin				
Mean	44.22	16.91	5.95	0.20
SD	8.18	5.49	4.18	0.34
Neoglucobrassicin				
Mean	346.91	119.94	47.43	0.92
SD	128.79	104.07	42.89	0.87
Sulforaphane				
Mean	28.58	13.21	15.21	2.96
SD	40.83	19.20	21.87	3.81
Moringin				
Mean	94.16	75.57	112.49	119.31
SD	158.93	125.80	190.84	204.31

Table S4. Polyphenol and indole-3-carbinol concentrations (mg/kg) in BR supernatant quantified by LC-MS/MS and normalized according to fermentation volume. Data represent the mean and standard deviation (SD) at time of inoculation (T0) and after 5 (T5), 10 (T10) and 24 hours (T24) of Broccolo fecal fermentation (n=3 donors). Catechin, cinnamic acid, p-coumaric acid, isorhamnetin-3-glucoside and cryptochlorogenic acid are not shown, since the levels fell below the limit of quantification.

	BR			
	T0	T5	T10	T24
4-Aminobenzoic acid				
Mean	73.22	79.90	91.05	94.16
SD	13.62	10.78	12.39	22.57
Caffeic acid				
Mean	35.42	2.21	1.74	0.00
SD	21.00	3.83	3.02	0.00
Ferulic acid				
Mean	30.96	9.31	8.13	5.51
SD	7.52	2.28	2.90	2.49
Quercetin-3-glucoside				
Mean	6.10	0.98	1.05	1.01
SD	3.71	0.29	0.35	0.70
Quercetin 3,4'-diglucoside				
Mean	167.55	33.57	25.95	9.35
SD	45.17	2.10	9.12	3.83
Sinapic acid				
Mean	300.41	130.60	73.36	36.34
SD	81.29	61.81	51.49	37.63
Synapyl alcohol				
Mean	3.32	4.97	8.56	4.12
SD	3.23	4.37	3.67	5.40
Syringaldehyde				
Mean	5.68	5.69	3.72	1.88
SD	2.22	1.52	1.08	0.72
Syringic acid				
Mean	12.79	12.92	17.84	15.88
SD	3.38	3.59	6.04	6.01
Chlorogenic acid				
Mean	0.56	0.60	0.68	0.65
SD	0.23	0.04	0.17	0.14
Neochlorogenic acid				
Mean	12.82	4.07	2.79	0.74
SD	10.60	5.56	4.83	1.29
Indole-3-carbinol				
Mean	251.06	129.70	64.85	4.35
SD	134.14	112.41	56.55	7.53

References

1. Willett W, Rockström J, Loken B, Springmann M, Lang T, Vermeulen S, et al. Food in the Anthropocene: the EAT–Lancet Commission on healthy diets from sustainable food systems. The Lancet. 2019 Feb;393(10170):447–92.

2. Fuentes F, Paredes-Gonzalez X, Kong A-NT. Dietary Glucosinolates Sulforaphane, Phenethyl Isothiocyanate, Indole-3-Carbinol/3,3′-Diindolylmethane: Antioxidative Stress/Inflammation, Nrf2, Epigenetics/Epigenomics and In Vivo Cancer Chemopreventive Efficacy. Curr Pharmacol Rep. 2015 Jun;1(3):179–96.

3. Favela-González KM, Hernández-Almanza AY, De la Fuente-Salcido NM. The value of bioactive compounds of cruciferous vegetables (*Brassica*) as antimicrobials and antioxidants: A review. J Food Biochem [Internet]. 2020 Oct [cited 2021 May 21];44(10). Available from: https://onlinelibrary.wiley.com/doi/10.1111/jfbc.13414

4. Jahangir M, Kim HK, Choi YH, Verpoorte R. Health-Affecting Compounds in *Brassicaceae*. Comprehensive Reviews in Food Science and Food Safety. 2009 Apr;8(2):31–43.

5. Beckman CH. Phenolic-storing cells: keys to programmed cell death and periderm formation in wilt disease resistance and in general defence responses in plants? Physiological and Molecular Plant Pathology. 2000 Sep;57(3):101–10.

6. Bennett RN, Wallsgrove RM. Secondary metabolites in plant defence mechanisms. New Phytologist. 1994 Aug;127(4):617–33.

7. Mahn A, Castillo A. Potential of Sulforaphane as a Natural Immune System Enhancer: A Review. Molecules. 2021 Feb 1;26(3):752.

8. Anhê FF, Nachbar RT, Varin TV, Trottier J, Dudonné S, Le Barz M, et al. Treatment with camu camu (*Myrciaria dubia*) prevents obesity by altering the gut microbiota and increasing energy expenditure in diet-induced obese mice. Gut. 2019 Mar;68(3):453–64.

9. Régnier M, Rastelli M, Morissette A, Suriano F, Le Roy T, Pilon G, et al. Rhubarb Supplementation Prevents Diet-Induced Obesity and Diabetes in Association with Increased Akkermansia muciniphila in Mice. Nutrients. 2020 Sep 24;12(10):2932.

10. Du L, Li J, Zhang X, Wang L, Zhang W, Yang M, et al. Pomegranate peel polyphenols inhibits inflammation in LPS-induced RAW264.7 macrophages via the suppression of TLR4/NF-κB pathway activation. Food & Nutrition Research [Internet]. 2019 Apr 23 [cited 2021 Aug 18];63(0). Available from: http://www.foodandnutritionresearch.net/index.php/fnr/article/view/3392

11. Vicas SI, Teusdea AC, Carbunar M, Socaci SA, Socaciu C. Glucosinolates Profile and Antioxidant Capacity of Romanian Brassica Vegetables Obtained by Organic and Conventional Agricultural Practices. Plant Foods Hum Nutr. 2013 Sep;68(3):313–21.

12. Barillari J, Canistro D, Paolini M, Ferroni F, Pedulli GF, Iori R, et al. Direct Antioxidant Activity of Purified Glucoerucin, the Dietary Secondary Metabolite Contained in Rocket (*Eruca sativa* Mill.) Seeds and Sprouts. J Agric Food Chem. 2005 Apr 1;53(7):2475–82.

13. Barillari J, Iori R, Papi A, Orlandi M, Bartolini G, Gabbanini S, et al. Kaiware Daikon (Raphanus sativus L.) Extract: A Naturally Multipotent Chemopreventive Agent. J Agric Food Chem. 2008 Sep 10;56(17):7823–30.

14. Elfoul L, Rabot S, Khelifa N, Quinsac A, Duguay A, Rimbault A. Formation of allyl isothiocyanate from sinigrin in the digestive tract of rats monoassociated with a human colonic strain of Bacteroides thetaiotaomicron. FEMS Microbiology Letters. 2001 Apr;197(1):99–103.

15. Palop MLl, Smiths JP, ten Brink B. Degradation of sinigrin by Lactobacillus agilis strain R16. International Journal of Food Microbiology. 1995 Jul;26(2):219–29.

16. Martel J, Ojcius DM, Ko Y-F, Young JD. Phytochemicals as Prebiotics and Biological Stress Inducers. Trends in Biochemical Sciences. 2020 Jun;45(6):462–71.

17. Lohning A, Kidachi Y, Kamiie K, Sasaki K, Ryoyama K, Yamaguchi H. 6-(methylsulfinyl)hexyl isothiocyanate (6-MITC) from Wasabia japonica alleviates inflammatory bowel disease (IBD) by potential inhibition of glycogen synthase kinase 3 beta (GSK-3β). European Journal of Medicinal Chemistry. 2021 Apr;216:113250.

18. Narbad A, Rossiter JT. Gut Glucosinolate Metabolism and Isothiocyanate Production. Mol Nutr Food Res. 2018 Sep;62(18):1700991.

19. Kawabata K, Yoshioka Y, Terao J. Role of Intestinal Microbiota in the Bioavailability and Physiological Functions of Dietary Polyphenols. Molecules. 2019 Jan 21;24(2):370.

20. Roopchand DE, Carmody RN, Kuhn P, Moskal K, Rojas-Silva P, Turnbaugh PJ, et al. Dietary Polyphenols Promote Growth of the Gut Bacterium Akkermansia muciniphila and Attenuate High-Fat Diet-Induced Metabolic Syndrome. Diabetes. 2015 Aug;64(8):2847–58.

21. Wu GD, Chen J, Hoffmann C, Bittinger K, Chen Y-Y, Keilbaugh SA, et al. Linking Long-Term Dietary Patterns with Gut Microbial Enterotypes. Science. 2011 Oct 7;334(6052):105–8.

22. David LA, Maurice CF, Carmody RN, Gootenberg DB, Button JE, Wolfe BE, et al. Diet rapidly and reproducibly alters the human gut microbiome. Nature. 2014 Jan;505(7484):559–63.

23. Madsen K, Park H. Immunologic Response in the Host. In: The Microbiota in Gastrointestinal Pathophysiology [Internet]. Elsevier; 2017 [cited 2021 Aug 4]. p. 233–41. Available from: https://linkinghub.elsevier.com/retrieve/pii/B9780128040249000264

24. Mohammad S, Thiemermann C. Role of Metabolic Endotoxemia in Systemic Inflammation and Potential Interventions. Front Immunol. 2021 Jan 11;11:594150.

25. Cani PD, Amar J, Iglesias MA, Poggi M, Knauf C, Bastelica D, et al. Metabolic Endotoxemia Initiates Obesity and Insulin Resistance. Diabetes. 2007 Jul 1;56(7):1761–72.

26. Srinivasan B, Kolli AR, Esch MB, Abaci HE, Shuler ML, Hickman JJ. TEER Measurement Techniques for In Vitro Barrier Model Systems. J Lab Autom. 2015 Apr;20(2):107–26.

27. Wang Y, Jeffery E, Miller M, Wallig M, Wu Y. Lightly Cooked Broccoli Is as Effective as Raw Broccoli in Mitigating Dextran Sulfate Sodium-Induced Colitis in Mice. Nutrients. 2018 Jun 8;10(6):748.

28. Hubbard TD, Murray IA, Nichols RG, Cassel K, Podolsky M, Kuzu G, et al. Dietary broccoli impacts microbial community structure and attenuates chemically induced colitis in mice in an Ah receptor dependent manner. Journal of Functional Foods. 2017 Oct;37:685–98.

29. Minekus M, Alminger M, Alvito P, Ballance S, Bohn T, Bourlieu C, et al. A standardised static *in vitro* digestion method suitable for food – an international consensus. Food Funct. 2014;5(6):1113–24.

30. Sánchez-Patán F, Cueva C, Monagas M, Walton GE, Gibson GRM, Quintanilla-López JE, et al. In vitro fermentation of a red wine extract by human gut microbiota: changes in microbial groups and formation of phenolic metabolites. J Agric Food Chem. 2012 Mar 7;60(9):2136–47.

31. Frayn KN. Metabolic Regulation: a Human Perspective. [Internet]. Somerset: Wiley; 2013 [cited 2022 Feb 3]. Available from: http://public.ebookcentral.proquest.com/choice/publicfullrecord.aspx?p=4037568

32. Klindworth A, Pruesse E, Schweer T, Peplies J, Quast C, Horn M, et al. Evaluation of general 16S ribosomal RNA gene PCR primers for classical and next-generation sequencing-based diversity studies. Nucleic Acids Research. 2013 Jan 1;41(1):e1–e1.

33. Bolyen E, Rideout JR, Dillon MR, Bokulich NA, Abnet CC, Al-Ghalith GA, et al. Reproducible, interactive, scalable and extensible microbiome data science using QIIME 2. Nat Biotechnol. 2019 Aug;37(8):852–7.

34. Quast C, Pruesse E, Yilmaz P, Gerken J, Schweer T, Yarza P, et al. The SILVA ribosomal RNA gene database project: improved data processing and web-based tools. Nucleic Acids Research. 2012 Nov 27;41(D1):D590–6.

35. McMurdie PJ, Holmes S. phyloseq: An R Package for Reproducible Interactive Analysis and Graphics of Microbiome Census Data. Watson M, editor. PLoS ONE. 2013 Apr 22;8(4):e61217.

36. Lotti C, Rubert J, Fava F, Tuohy K, Mattivi F, Vrhovsek U. Development of a fast and cost-effective gas chromatography–mass spectrometry method for the quantification of short-chain and medium-chain fatty acids in human biofluids. Anal Bioanal Chem. 2017 Sep;409(23):5555–67.

37. Anderson RC, Cookson AL, McNabb WC, Park Z, McCann MJ, Kelly WJ, et al. Lactobacillus plantarum MB452 enhances the function of the intestinal barrier by increasing the expression levels of genes involved in tight junction formation. BMC Microbiol. 2010;10(1):316.

38. Coates EM, Popa G, Gill CI, McCann MJ, McDougall GJ, Stewart D, et al. Colon-available raspberry polyphenols exhibit anti-cancer effects on in vitro models of colon cancer. J Carcinog. 2007;6(1):4.

39. Oksanen J, Blanchet G, Kindt R, Legendre P, Minchin P, O'Hara B, et al. Vegan: Community Ecology Package. R Package Version 22-1. 2015;2:1–2.

40. Parks DH, Beiko RG. Measures of phylogenetic differentiation provide robust and complementary insights into microbial communities. ISME J. 2013 Jan;7(1):173–83.

41. Di Gioia F, Pinela J, de Haro Bailón A, Fereira ICFR, Petropoulos SA. The dilemma of "good" and "bad" glucosinolates and the potential to regulate their content. In: Glucosinolates: Properties, Recovery, and Applications [Internet]. Elsevier; 2020 [cited 2021 Oct 18]. p. 1–45. Available from: https://linkinghub.elsevier.com/retrieve/pii/B9780128164938000019

42. Szmigielska AM, Schoenau JJ. Use of Anion-Exchange Membrane Extraction for the High-Performance Liquid Chromatographic Analysis of Mustard Seed Glucosinolates. J Agric Food Chem. 2000 Nov 1;48(11):5190–4.

43. Kim HW, Ko HC, Baek HJ, Cho SM, Jang HH, Lee YM, et al. Identification and quantification of glucosinolates in Korean leaf mustard germplasm (Brassica juncea var. integrifolia) by liquid chromatography–electrospray ionization/tandem mass spectrometry. Eur Food Res Technol. 2016 Sep;242(9):1479–84.

44. Bellostas N, Kachlicki P, Sørensen JC, Sørensen H. Glucosinolate profiling of seeds and sprouts of B. oleracea varieties used for food. Scientia Horticulturae. 2007 Nov;114(4):234–42.

45. Heaney RK, Fenwick GR. The analysis of glucosinolates inBrassica species using gas chromatography. Direct determination of the thiocyanate ion precursors, glucobrassicin and neoglucobrassicin. J Sci Food Agric. 1980 Jun;31(6):593–9.

46. McDanell R, McLean AEM, Hanley AB, Heaney RK, Fenwick GR. Chemical and biological properties of indole glucosinolates (glucobrassicins): A review. Food and Chemical Toxicology. 1988 Jan;26(1):59–70.

47. Mullaney JA, Kelly WJ, McGhie TK, Ansell J, Heyes JA. Lactic Acid Bacteria Convert Glucosinolates to Nitriles Efficiently Yet Differently from Enterobacteriaceae. J Agric Food Chem. 2013 Mar 27;61(12):3039–46.

48. Walker AW, Ince J, Duncan SH, Webster LM, Holtrop G, Ze X, et al. Dominant and diet-responsive groups of bacteria within the human colonic microbiota. ISME J. 2011 Feb;5(2):220–30.

49. Salonen A, Lahti L, Salojärvi J, Holtrop G, Korpela K, Duncan SH, et al. Impact of diet and individual variation on intestinal microbiota composition and fermentation products in obese men. ISME J. 2014 Nov;8(11):2218–30.

50. Kaczmarek JL, Liu X, Charron CS, Novotny JA, Jeffery EH, Seifried HE, et al. Broccoli consumption affects the human gastrointestinal microbiota. The Journal of Nutritional Biochemistry. 2019 Jan;63:27–34.

51. Kellingray L, Tapp HS, Saha S, Doleman JF, Narbad A, Mithen RF. Consumption of a diet rich in *Brassica* vegetables is associated with a reduced abundance of sulphate-reducing bacteria: A randomised crossover study. Mol Nutr Food Res. 2017 Sep;61(9):1600992.

52. Rautio M, Eerola E, Väisänen-Tunkelrott M-L, Molitoris D, Lawson P, Collins MD, et al. Reclassification of Bacteroides putredinis (Weinberg et al., 1937) in a New Genus Alistipes gen. nov., as Alistipes putredinis comb. nov., and Description of Alistipes finegoldii sp. nov., from Human Sources. Systematic and Applied Microbiology. 2003 Jan;26(2):182–8.

53. Agans R, Gordon A, Kramer DL, Perez-Burillo S, Rufián-Henares JA, Paliy O. Dietary Fatty Acids Sustain the Growth of the Human Gut Microbiota. Dudley EG, editor. Appl Environ Microbiol [Internet]. 2018 Nov [cited 2021 Sep 30];84(21). Available from: https://journals.asm.org/doi/10.1128/AEM.01525-18

54. Daniel H, Gholami AM, Berry D, Desmarchelier C, Hahne H, Loh G, et al. High-fat diet alters gut microbiota physiology in mice. ISME J. 2014 Feb;8(2):295–308.

55. Zhang C, Zhang M, Pang X, Zhao Y, Wang L, Zhao L. Structural resilience of the gut microbiota in adult mice under high-fat dietary perturbations. ISME J. 2012 Oct;6(10):1848–57.

56. Yatsunenko T, Rey FE, Manary MJ, Trehan I, Dominguez-Bello MG, Contreras M, et al. Human gut microbiome viewed across age and geography. Nature. 2012 Jun;486(7402):222–7.

57. Tu P, Bian X, Chi L, Gao B, Ru H, Knobloch TJ, et al. Characterization of the Functional Changes in Mouse Gut Microbiome Associated with Increased *Akkermansia muciniphila* Population Modulated by Dietary Black Raspberries. ACS Omega. 2018 Sep 30;3(9):10927–37.

58. Ushiroda C, Naito Y, Takagi T, Uchiyama K, Mizushima K, Higashimura Y, et al. Green tea polyphenol (epigallocatechin-3-gallate) improves gut dysbiosis and serum bile acids dysregulation in high-fat diet-fed mice. J Clin Biochem Nutr. 2019;65(1):34–46.

59. Zhu Y, Wang C, Li F. Impact of dietary fiber/starch ratio in shaping caecal microbiota in rabbits. Can J Microbiol. 2015 Oct;61(10):771–84.

60. Chen M, Fan B, Liu S, Imam KMSU, Xie Y, Wen B, et al. The in vitro Effect of Fibers With Different Degrees of Polymerization on Human Gut Bacteria. Front Microbiol. 2020 May 15;11:819.

61. Kellingray L, Le Gall G, Doleman JF, Narbad A, Mithen RF. Effects of in vitro metabolism of a broccoli leachate, glucosinolates and S-methylcysteine sulphoxide on the human faecal microbiome. Eur J Nutr. 2021 Jun;60(4):2141–54.

62. Zumbrun SD, Melton-Celsa AR, Smith MA, Gilbreath JJ, Merrell DS, O'Brien AD. Dietary choice affects Shiga toxin-producing *Escherichia coli* (STEC) O157:H7 colonization and disease. Proc Natl Acad Sci USA. 2013 Jun 4;110(23):E2126–33.

63. Ferrario C, Statello R, Carnevali L, Mancabelli L, Milani C, Mangifesta M, et al. How to Feed the Mammalian Gut Microbiota: Bacterial and Metabolic Modulation by Dietary Fibers. Front Microbiol. 2017 Sep 12;8:1749.

64. Healey G, Murphy R, Butts C, Brough L, Whelan K, Coad J. Habitual dietary fibre intake influences gut microbiota response to an inulin-type fructan prebiotic: a randomised, double-blind, placebo-controlled, cross-over, human intervention study. Br J Nutr. 2018 Jan 28;119(2):176–89.

65. Omori K, Miyakawa H, Watanabe A, Nakayama Y, Lyu Y, Ichikawa N, et al. The Combined Effects of Magnesium Oxide and Inulin on Intestinal Microbiota and Cecal Short-Chain Fatty Acids. Nutrients. 2021 Jan 5;13(1):152.

66. Gelpi M, Vestad B, Hansen SH, Holm K, Drivsholm N, Goetz A, et al. Impact of Human Immunodeficiency Virus–Related Gut Microbiota Alterations on Metabolic Comorbid Conditions. Clinical Infectious Diseases. 2020 Nov 5;71(8):e359–67.

67. Cherbuy C, Bellet D, Robert V, Mayeur C, Schwiertz A, Langella P. Modulation of the Caecal Gut Microbiota of Mice by Dietary Supplement Containing Resistant Starch: Impact Is Donor-Dependent. Front Microbiol. 2019 Jun 6;10:1234.

68. Nelson R, Peterson D, Karp E, Beckham G, Salvachúa D. Mixed Carboxylic Acid Production by Megasphaera elsdenii from Glucose and Lignocellulosic Hydrolysate. Fermentation. 2017 Mar 1;3(1):10.

69. Choi K, Jeon BS, Kim B-C, Oh M-K, Um Y, Sang B-I. In Situ Biphasic Extractive Fermentation for Hexanoic Acid Production from Sucrose by Megasphaera elsdenii NCIMB 702410. Appl Biochem Biotechnol. 2013 Nov;171(5):1094–107.

70. Possemiers S, Bolca S, Verstraete W, Heyerick A. The intestinal microbiome: A separate organ inside the body with the metabolic potential to influence the bioactivity of botanicals. Fitoterapia. 2011 Jan;82(1):53–66.

71. Hur SJ, Lim BO, Decker EA, McClements DJ. In vitro human digestion models for food applications. Food Chemistry. 2011 Mar;125(1):1–12.

72. Pereira D, Valentão P, Pereira J, Andrade P. Phenolics: From Chemistry to Biology. Molecules. 2009 Jun 17;14(6):2202–11.

73. Gawlik-Dziki U. Effect of hydrothermal treatment on the antioxidant properties of broccoli (Brassica oleracea var. botrytis italica) florets. Food Chemistry. 2008 Jul;109(2):393–401.

74. Rosazza JPN, Huang Z, Dostal L, Volm T, Rousseau B. Review: Biocatalytic transformations of ferulic acid: An abundant aromatic natural product. Journal of Industrial Microbiology. 1995 Dec;15(6):457–71.

75. Peppercorn MA, Goldman P. Caffeic Acid Metabolism by Gnotobiotic Rats and Their Intestinal Bacteria. Proceedings of the National Academy of Sciences. 1972 Jun 1;69(6):1413–5.

76. Russell WR, Gratz SW, Duncan SH, Holtrop G, Ince J, Scobbie L, et al. High-protein, reduced-carbohydrate weight-loss diets promote metabolite profiles likely to be detrimental to colonic health. The American Journal of Clinical Nutrition. 2011 May 1;93(5):1062–72.

77. Fernández-Jalao I, Balderas C, Calvo MV, Fontecha J, Sánchez-Moreno C, De Ancos B. Impact of High-Pressure Processed Onion on Colonic Metabolism Using a Dynamic Gastrointestinal Digestion Simulator. Metabolites. 2021 Apr 22;11(5):262.

78. van de Wouw M, Boehme M, Lyte JM, Wiley N, Strain C, O'Sullivan O, et al. Short-chain fatty acids: microbial metabolites that alleviate stress-induced brain-gut axis alterations. J Physiol. 2018 Oct;596(20):4923–44.

79. Parada Venegas D, De la Fuente MK, Landskron G, González MJ, Quera R, Dijkstra G, et al. Short Chain Fatty Acids (SCFAs)-Mediated Gut Epithelial and Immune Regulation and Its Relevance for Inflammatory Bowel Diseases. Front Immunol. 2019 Mar 11;10:277.

80. Lewis K, Lutgendorff F, Phan V, Söderholm JD, Sherman PM, McKay DM. Enhanced translocation of bacteria across metabolically stressed epithelia is reduced by butyrate†: Inflammatory Bowel Diseases. 2010 Jul;16(7):1138–48.

81. He C, Huang L, Lei P, Liu X, Li B, Shan Y. Sulforaphane Normalizes Intestinal Flora and Enhances Gut Barrier in Mice with BBN-Induced Bladder Cancer. Mol Nutr Food Res. 2018 Dec;62(24):1800427.

82. Riemschneider S, Hoffmann M, Slanina U, Weber K, Hauschildt S, Lehmann J. Indol-3-Carbinol and Quercetin Ameliorate Chronic DSS-Induced Colitis in C57BL/6 Mice by AhR-Mediated Anti-Inflammatory Mechanisms. IJERPH. 2021 Feb 25;18(5):2262.

Chapter 4: *In vitro* fecal fermentation of *Moringa oleifera* and pure glucomoringin (GMG): a focus on glucosinolates production

Giulia Gaudioso[1,2], Daniele Perenzoni[3], Kieran Michael Tuohy[1], Fulvio Mattivi[2,3], Renato Iori[3] and Francesca Fava[1].

[1] Nutrition and Nutrigenomics Unit, Department of Food Quality and Nutrition, Research and Innovation Center, Fondazione Edmund Mach, 38098 Trento, Italy

[2] CIBIO – Department of Cellular, Computational and Integrative Biology, University of Trento, 38123 Trento, Italy

[3] Metabolomics Unit, Department of Food Quality and Nutrition, Research and Innovation Center, Fondazione Edmund Mach, 38098 Trento, Italy 1. Introduction

Abstract: *Moringa oleifera* is a plant native to India and an interesting candidate as a sustainable food crop for human health. *Moringa oleifera* leaves are a rich source of polyphenols and glucosinolates (GLS), both widely recognized for their anti-cancer, antioxidant and anti-inflammatory properties. Due to the crucial role of human gut microbiota (GM) in breaking down plant phytochemicals into their bioactive form, we investigated whether and to which extent the human GM metabolizes polyphenols and GLS in Moringa, examining which bacterial taxa might be involved in these biotransformations. We made use of a small volume *in vitro* anaerobic faecal fermentation to determine the ability of faecal bacteria to breakdown Moringa phytochemicals, using as fermentation substrate an *in vitro*-digested *Moringa oleifera* leaf powder (MOR) or glucomoringin (GMG), the main GLS in Moringa. Illumina 16S rRNA gene sequencing was used to analyze GM composition of different faecal donors (n=7) and targeted Liquid Chromatography Triple Quadrupole Mass Spectrometry (LC-MS/MS) metabolomics approach was employed to quantify polyphenols and GLS concentrations over 8 hours of faecal fermentation. Finally, we made use of an *in vitro* trans-epithelial electric resistance (TEER) model with human colorectal adenocarcinoma cells (Caco-2) to investigate the potential of MOR or GMG fermentation supernatants in improving gut epithelial barrier integrity. As expected, GM composition was unique to each faecal donor, showing differences in terms of bacterial richness and composition among volunteers and thus suggesting a personalized response to Moringa metabolites, as highlighted by Spearman's correlation analysis. While no significant TEER improvement was observed after incubation of Caco-2 monolayers with MOR supernatant, GMG supernatants significantly increased TEER, thus suggesting the role of glucomoringin GLS or of the derived glucotropaeolin and sinalbin in stimulating gut barrier function. Our results provide novel insights on the fate of target plant phytochemicals during faecal microbial fermentation and on their potential beneficial activity on gut health.

1. Introduction

Moringa oleifera is one of the thirteen species of plants belonging to the Moringaceae family (1). *M. oleifera*, also known as 'ben tree oil' or 'drumstick tree' (2,3) was originally distributed in South Asia, West, East and South Africa, but it is now broadly dispersed in Europe, Americas and Oceania (4). All parts of this plant – leaves, flowers, nuts, seeds and tubers – are edible and utilized for human consumption (4). In particular, *M. oleifera* leaves are rich in essential amino acids, vitamin C and A, calcium, iron and potassium (5,6) thus supporting the growing interest in the use of this plant as an alternative nutritious food source to fight malnourishment in children and as a functional food to fight chronic diet associated diseases in other age groups (7–9). Several *in vitro* and animal studies reported the anti-inflammatory (10,11), anti-diabetic (12), anti-cancer (13,14) and antimicrobial (15) effects of *M. oleifera* leaves and seeds extracts, thus encouraging further human studies to fully establish the health potential of this plant. Many of the purported health effects of *M. oleifera* have been attributed to its bioactive chemical constituents (16,17). *M. oleifera* leaves are reported to contain huge amounts of glucosinolates and polyphenols (18), both widely recognized for their health promoting activities, including anti-cancer and anti-inflammatory properties (19–22). Glucosinolates (GLS) are secondary metabolites serving as defense compounds in plants (23), and glucosinolate hydrolysis by both plant and gut microbiota myrosinase enzymes generates various derivatives, including isothiocyanates (ITC). The 4(α-L-rhamnosyloxy)-benzyl ITC, also called moringin, has been recently characterized as one of the main bioactive compounds being responsible for *M. oleifera* health properties. Moringin is produced by myrosinase-catalyzed hydrolysis of 4(α-L-rhamnosyloxy)-benzyl GLS or glucomoringin, the main GLS in moringa (24) as described in **Figure 1**.

Figure 1. Moringin production from glucomoringin hydrolysis. Adapted from Borgonovo *et al.* (2020) (25).

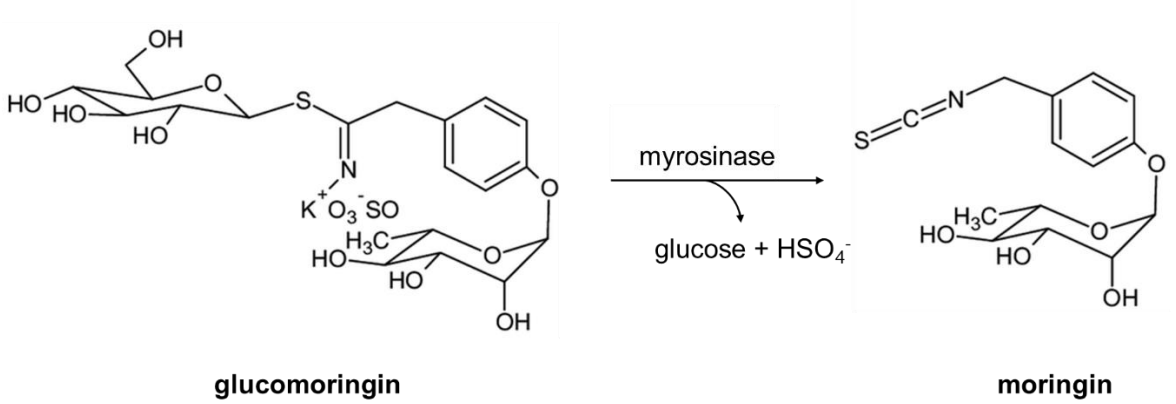

In 2017, Jaja-Chimedza and colleagues (26) demonstrated that moringin at 5 or 10 μM concentration modulated NF-kB and Nrf2 inflammatory pathways *in vitro* when incubated with lipopolysaccharide (LPS)-stimulated murine macrophages, thus significantly reducing the synthesis of pro-inflammatory cytokines IL-1β, IL-6 and TNF-α.

These results confirmed what previously observed by Rajan *et al.* in 2016 (27) and were further supported by an *in vivo* study, where feeding C57Bl/GJ obese mice with a high-fat diet supplemented with 0.25% moringin significantly modulated NADPH quinone oxidoreductase (NQO1) and inducible nitric oxide synthase (iNOS) pathways, both associated with chronic inflammation (28). Youjin and colleagues (2017) investigated wheter the anti-inflammatory activity of moringin derive from its protective action on the intestinal barrier, since it is known that increased intestinal permeability can trigger local and systemic inflammation due to the uncontrolled translocation of potentially pathogenic bacteria (29). The authors employed a mouse model of chronic ulcerative colitis (UC) to investigate the anti-inflammatory activity of *M. oleifera* seed extract enriched in moringin (29). Chronic UC was induced in mice by dextran sulphate sodium (DSS) treatment, a chemical colitogen able to distrupt the integrity of the mucosal barrier, thus increasing gut permeability and resulting in intestinal inflammation (30). Following UC induction, mice were orally administered for 2 weeks with 150 mg/kg moringa seed extract containing 47% (w/w) moringin. Moringa seed extract + moringin supplementation significantly alleviated chronic ulcerative colitis symptoms and increased tigh-junction proteins expression in UC mice (29), thus suggesting a potential effect of *Moringa* metabolites in treating gut barrier dysfunction and gut permeability in UC. Moreover, dietary supplementation of *Moringa* leaves powder significantly reduced inflammatory cytokines IL-1β, IL-6, TNF-α and INF-γ production in a colitis-associated colorectal cancer mouse model (31). These effects were attributed to chlorogenic acid, p-coumaric acid and other phenolic compounds found at high concentration in *Moringa* leaves (31,32).

In vivo biotransformation of polyphenols and glucosinolates strongly involves colonic microbiota. Up to 90%-95% of dietary polyphenols are not absorbed in the small intestine, thus they reach the colon almost intact (33). Here, they interact with the gut microbiota (GM) through a reciprocal interplay whereby microorganisms transform the complex phytochemicals into biologically available and bioactive moieties, and the phytochemicals have the potential to change the relative abundance of GM (34). Both polyphenols and glucosinolates undergo microbial biotransformation, producing several metabolites that exert *in vivo* beneficial activities, both locally in the intestine and systemically, through the bloodstream (35,36). As an example, plant glucosinolates glucomoringin

and glucoraphanin can be hydrolyzed by microbial myrosinases to bioactive isothiocyanates moringin and sulforaphane, respectively (25,35). Liou and colleagues (2020) (37) identified an operon required for glucosinolate metabolism in *Bacteroides thetaiotaomicron*, a prominent human gut symbiont. Moreover, previous *in vivo* and *in vitro* work has demonstrated the myrosinase-like activity of different GM members, such as *Bifidobacterium* spp., *Enterococcus* spp. and *Lactobacillus* spp. (38–41). These results are of a great importance since they provide insight into the mechanism by which GM could process *Brassica* phytochemicals, generating their bioactive metabolites.

To date, there are no *in vitro* studies investigating the fate of *M. oleifera* phytochemical components using mixed cultures of faecal bacteria. The aim of this work was to measure the extent of gut microbiota biotransformation of target polyphenols and glucosinolates in *M. oleifera*, upon fermentation of digested *M. oleifera* leaves and glucomoringin (GMG), making use of a small volume *in vitro* anaerobic fecal fermentation, analytical chemistry and next generation sequencing to investigate the compounds that are produced as a result of bacterial conversion of original plant metabolites, and which bacteria might be involved in this conversion. Illumina 16S rRNA gene sequencing was used to analyze gut microbiota composition of different faecal donors (n=7). A targeted Liquid Chromatography Triple Quadrupole Mass Spectrometry (LC-MS/MS) metabolomics approach was used to quantify glucosinolates and polyphenols concentrations over 8 hours of faecal fermentation. We performed a Spearman's correlation analysis between GM composition and glucosinolates and polyphenols concentration over the fermentation process, in order to understand how individual GM profile drives a personalized biotransformation of plant metabolites, thus generating a unique metabolite signature.

Considering previous studies which highlighted the potential of Moringa and moringin to restore gut barrier function through an increasing of tight-junction proteins expression (29), we employed an *in vitro* moldel of intestinal barrier to investigate whether Moringa and GMG faecal supernatants modulate gut permeability.

2. Materials and methods

2.1 Moringa *in vitro* digestion

Moringa (*Moringa oleifera*) leaf powder was obtained from Impresa Moringa Salento s.r.l, Nociglia, Italy, in January 2021. To simulate human digestion in the stomach and small intestine, the *in vitro* digestion protocol of Minekus *et al.* (2014) was used with some modifications (42). The same

protocol was used to digest *M. oleifera* (MOR) leaf powder, and the control substrates cellulose (CL), a lowly fermented fiber, and inulin (IN), a readily fermented fiber. Both controls did not contain plant polyphenols. 30 g of sample was added to 30 mL of simulated salivary fluid (21 mL saline solution, 5.85 mL milliQ H_2O, 150 µL 0.3 M $CaCl_2(H_2O)_2$, 3 mL 1500 U mL^{-1} α-amylase, Sigma-Aldrich) and incubated for 2 min at 37°C while rotating at 150 rpm. Subsequently, the oral bolus was mixed to 100 mL of simulated gastric fluid (45 mL saline solution containing 10mg/mL lipid vescicles, Sigma Aldrich, 4.17 mL milliQ H_2O, 30 µL 0.3 M $CaCl_2(H_2O)_2$ and 9.6 mL 25000 U mL^{-1} pepsin, Sigma Aldrich) to simulate the gastric phase and pH was decreased to pH 3 with 5 M HCl. This mixture was incubated for 2 hours at 37 °C while rotating at 150 rpm. Finally, the food bolus passed to the intestinal phase, where it was mixed with 200 mL of simulated intestinal fluid (66 mL saline solution, 7.86 mL milliQ H_2O, 240 µL 0.3 M $CaCl_2(H_2O)_2$, 4.8 g porcine bile extract and 30 mL 800 U mL^{-1} pancreatin) and where the pH was increased to pH 7 using 5 M NaOH. This mixture was incubated for 2 hours at 37 °C while rotating at 150 rpm. To simulate passive intestinal absorption of water and hydrolytic products from digestion in the small intestine, *in vitro* dialysis was performed using Spectra/Por® Dialysis Membrane MWCO 1000 KDa (Repligen, Waltham, MA, USA). Samples were collected inside dialysis membranes and sealed at both ends. They were incubated overnight at 4 °C while rotating, inside tanks with a volume 100 times higher than the sample volume and filled with a 10 mM NaCl solution. After incubation, samples were frozen at -80 °C overnight, then freeze-dried. Freeze dried samples were milled using a sterile pestle, divided into portions of 2 g/each and then stored at –80 °C until further analysis.

2.2 Small volumes faecal batch cultures

Fecal samples were collected from seven healthy volunteers (age between 20 and 55 years, no antibiotic treatment in the 3 months preceeding the experiment) and kept anaerobic until inoculation. For each volunteer, five batch fermentations were run in parallel, filling tubes with sterile anaerobic medium and inoculating with 4 mL of 10% (w/v) faecal slurry up to a total volume of 40 mL. All the experiments were carried out in an anaerobic cabinet at 37°C, without pH-control. 50 mL sterile tubes (Sarstedt, Nümbrecht, Germany) were prepared in the anaerobic cabinet the day before the experiment and filled with 36 mL of sterile hot basal nutrient medium according to Sanchez-Patan *et al.* 2012 (43). On the day of the experiment, fresh fecal samples were collected and slurries were prepared by homogenizing faeces in anoxic 1X PBS (pH 7.2) by using a Stomacher® 400 Circulator (Seward Ltd., UK). After inoculation with faecal slurry, 0.4 g of freeze-dried *in vitro*

digested substrate or 19 mg of glucomoringin (GMG) pure compound were added in each tube as follows: tube 1, contained only faecal inoculum and no substrate (blank, BK); tube 2, 1% (w/v) inulin (IN, positive control), tube 3, 1% (w/v) cellulose (CL, negative control), tube 4, 1% (w/v) Moringa (MOR), tube 5 19 mg of GMG. Hydroalcholoic extraction was performed by the Metabolomics Unit in FEM to quantify the content of GMG in Moringa leaf powder. GMG content ranged between 35 and 45 mg/g of Moringa leaf powder. Considering that 0.4 g of *in vitro* digested-Moringa leaf powder corresponded to 0.544 g of Moringa leaf powder pre-digestion, we expected to have a minimum of 19 mg of GMG in 0.4g of *in vitro* digested Moringa leaf powder. Thus, the amount of GMG used in the faecal fermentations was equivalent to the amount of GMG present in 0.4 g of digested Moringa leaves. The amount of digested IN, CL and MOR was estimated in order to reflect colonic proportion of digested food and faecal slurry. Also, this considers that a total amount of approximately 200 g of material (including food particles, water, bacteria and mucus) could be measured at any given time in the large intestine (44). Batch cultures were carried out over 8 hours and samples obtained from each tube at 0 (baseline, after faecal inoculum, T0), 30 minutes (T0.5), 1 (T1), 2 (T2), 5 (T5) and 8 (T8) hours. Selected timepoints were chosen in order to include all phases of microbial metabolism of targeted polyphenols and glucosinolates, thus considering the lag (T0, T0.5 and T1), exponential (T2 and T5) and stationary (T8) phases of bacterial growth. Samples were immediately centrifuged at 18000 *g* for 5 min. Pellets and supernatants were stored at –80 °C for metagenomics and metabolomics analysis respectively.

2.3 Gut microbiota analysis

Total DNA extraction from frozen pellets (10-20 mg) collected at T0 was performed using MP Biomedicals™ FastDNA™ SPIN DNA Isolation Kit for Feces (Thermo Fisher Scientific, Waltham, MA, USA), following manufacturer's instructions. DNA quality and concentration were measured using a NanoDrop® 8000 spectrophotometer (Thermo Fisher Scientific, Waltham, MA, USA). PCR amplification was performed by targeting 16S rRNA gene V3-V4 variable regions with the bacterial primer set 341F (5′-CCTACGGGNGGCWGCAG-3′) and 806R (5′-GACTACNVGGGTWTCTAATCC-3′), as previously reported (45). PCR amplification of each samples was carried out using 25 μL reactions, with 12.5 μL of 2X KAPA Hifi HotStart Ready Mix (Kapa Biosystems Ltd., UK), 0.5 μL of each primer, 2.5 μL DNA (5 ng/μL) and 9 μL. All PCR reactions were carried out using the Verity™ 96-well Thermal Cycler (Thermo Fisher Scientific, Waltham, MA, USA), according to the following protocol: 5 min at 95 °C, 30 cycles of 30 s at 95 °C, 30 s at 55 °C, and

30 s at 72 °C, followed by a final extension of 5 min at 72 °C. PCR products were checked by gel electrophoresis and cleaned using an Agencourt AMPure XP system (Beckman Coulter, Brea, CA, USA), following the manufacturer's instructions. After seven PCR cycles (16S Metagenomic Sequencing Library Preparation, Illumina), Illumina adaptors were attached (Illumina Nextera XT Index Primer). Libraries were purified using Agencourt AMPure XP (Beckman) and then sequenced on an Illumina® MiSeq (PE300) platform (MiSeq Control Software 2.0.5 and Real-Time Analysis software 1.16.18, Illumina, San Diego, CA, USA). Sequences obtained from Illumina sequencing were analyzed using the Quantitative Insights Into Microbial Ecology (QIIME) 2.0 pipeline (46). Unidentified taxa include those whose percentage sequence homology with Silva database (SILVA 138 06-RS202 release) was less than 95% (47). α- diversity (within-sample richness) and β-diversity (between-sample dissimilarity) estimates were determined using the phyloseq R Package (48).

2.4 Supernatants preparation for metabolomic analysis and cell culture experiments

All supernatants were thawed on ice and sterile-filtered using sterile Sartorius 0.22 μm filters (Thermo Fisher Scientific, Waltham, MA, USA). Filtered supernatant were used for metabolomics analysis, performed through Liquid Chromatography Triple Quadrupole Mass Spectrometry (LC-MS/MS) and for TEER experiments.

2.5 LC-MS/MS

Analysis on glucosinolates and polyphenols were performed on a Sciex Triple Quad 6500+ (Sciex, USA) LC-MS/MS system. A protocol was developed to separate 45 compounds divided between polyphenols, glucosinolates, isothiocyanates and indoles through a single chromatographic run of 17 minutes. A complete list of the quantified compounds is provided in the *Results* section (**Table 1**), together with the range of concentration used for the calibration curve. Each compound was identified and quantified in multiple reaction monitoring (MRM) and dosed with its own calibration curve.

2.6 Cell cultures and experimental treatments

Human epithelial colorectal adenocarcinoma Caco-2 cell line (ATCC® HTB-37™, number of passage between 50 and 60) were grown in Dulbecco's Modified Eagle's Medium (DMEM) with high glucose (4.5g/L) (Lonza, Switzerland) supplemented with 20% decomplemented (56°C, 60 minutes) fetal bovine serum (Lonza, Switzerland), 100 units/ml penicillin (Biological Industries, Israel), 100 μg/ml streptomycin (Biological Industries, Israel), 1% non-essential amino acids (Euroclone, Milan), 2 mM glutamine and 0,25 ug/ml Amphotericin B (Biological Industries, Israel). Before and during

treatments, cell cultures were maintained in humidified atmosphere of 5% CO_2 in air at 37 °C. Before the experiment, Caco-2 cells were maintained in T-75 cm^2 flasks (Sarstedt, Nümbrecht, Germany) and passaged when they reached 70% confluence using 0.05% trypsin–0.5 mM EDTA (Lonza, Switzerland). Medium was refreshed every second day. Prior to seeding, transwell inserts were coated with rat tail collagen Type I (Sigma Aldrich), according to the manufacturer's instruction. For the experiment, Caco-2 cells were harvested to obtain a cell suspension of 1 X 10^5 cells/cm^2. 2.5 mL of cell suspension were added in transwell inserts with membrane filters (0.1 μm pore size; Falcon, Sacco s.r.l, Cadorago, Como, Italy) and grown for 13 days until a tight monolayer was formed (TEER measurements stable for two consecutive days). 1.5 mL of medium was added to the basolateral chamber. MOR and GMG supernatants collected after 1 hour of faecal fermentation were thawed on ice and sterile-filtered using Sartorius 0.22 μm filters (Thermo Fisher Scientific, Waltham, MA, USA). Sterile supernatants from different donors were pooled and used as a single treatment for cell culture experiments. All control and test treatments were prepared on the day of the assay. 10 mM propionic acid and 7% ethanol were used as positive and negative controls, respectively. All treatments were added to the culture medium at 10% of the total apical volume (2.5 mL).

2.7 Transepithelial electrical resistance (TEER) measurement

TEER was measured using an epithelial volt-ohm-meter (EVOM, World Precision Instruments Inc., Sarasota, FL, USA). Plates were left at room temperature for exactly 25 minutes prior to TEER measurements. The integrity of cell monolayers was assessed just before the addition of testing substrates ($resistance_{T0}$). The media was then removed from basolateral and apical chambers and the control or test treatments added to the apical layer. Resistance was measured after 24 h ($resistance_{T24}$). The TEER was calculated using the following equation, as described in previous works (49–51):

$$TEER(\Omega\ cm^2) = resistance(\Omega) \times membrane\ area(cm^2)$$

Where area of the semipermeable membrane was 9.6 cm^2. The change in TEER for each insert was calculated using the following formula:

$$\text{Change in TEER (\%)} = TEER_{T24}\ (\Omega\ cm^2) / TEER_{T0}\ (\Omega\ cm^2) \times 100\%$$

Where $TEER_{T24}$ and $TEER_{T0}$ represent TEER after 24 hours treatment and TEER at baseline, respectively. This experiment was repeated three times.

2.8 Statistical analysis

All statistical analysis was performed using R studio version 3.6.2. Normal distribution of data was assessed by Shapiro–Wilk's test. Percentage relative abundance of taxa from different dietary groups was compared using nonparametric Wilcoxon test. Pairwise comparison among groups in terms of α-diversity was performed by Kruskal–Wallis test. Differences in the β-diversity were checked using the non-parametric Permutational Multivariate Analysis of Variance (PERMANOVA) and adonis tests with 999 permutations, via the vegan R Package (52). Correlation between bacterial taxa and microbial metabolites was performed by Spearman's correlation analysis. All p-values were adjusted using Benjamini-Hochberg false discovery rate (FDR) correction. After FDR correction, a p value < 0.05 was considered statistically significant. Statistical significance between TEER results was performed by unpaired t-test. All data are expressed as the mean ± standard deviation, SD.

3. Results

3.1 Gut microbial ecology of different donors at baseline

Illumina MiSeq sequencing of gut microbial 16S rRNA gene amplicons produced a total of 5,857,720 reads, with 167,363 ± 26,873.66 raw reads per sample. After QIIME 2.0 analysis, we removed chimeras, low quality sequences, and sequences that were identified as Cyanobacteria, and the total number of reads was 3,630,828, with 103,737.9 ± 16,306.04 raw reads per sample.

Bacterial α-diversity showed significant differences among donors (n=7). Three different α-diversity estimators were used, namely the observed number of operational taxonomic units (OTUs), the Chao1 index and the Shannon entropy index (**Figure 2**). No significant differences were observed among different samples coming from the same donor at time of inoculation with different fermentation substrates (T0).

Figure 2. Bacterial α-diversity using Observed OTUs, Chao1 and Shannon index, at baseline (T0). Different boxplot colors indicate different faecal donors (n=7). Line inside the box represents the median, whiskers from either side of the box represent the first and the third quartiles, respectively. Different superscript letters indicate statistical significance among gut microbial richness of different donors.

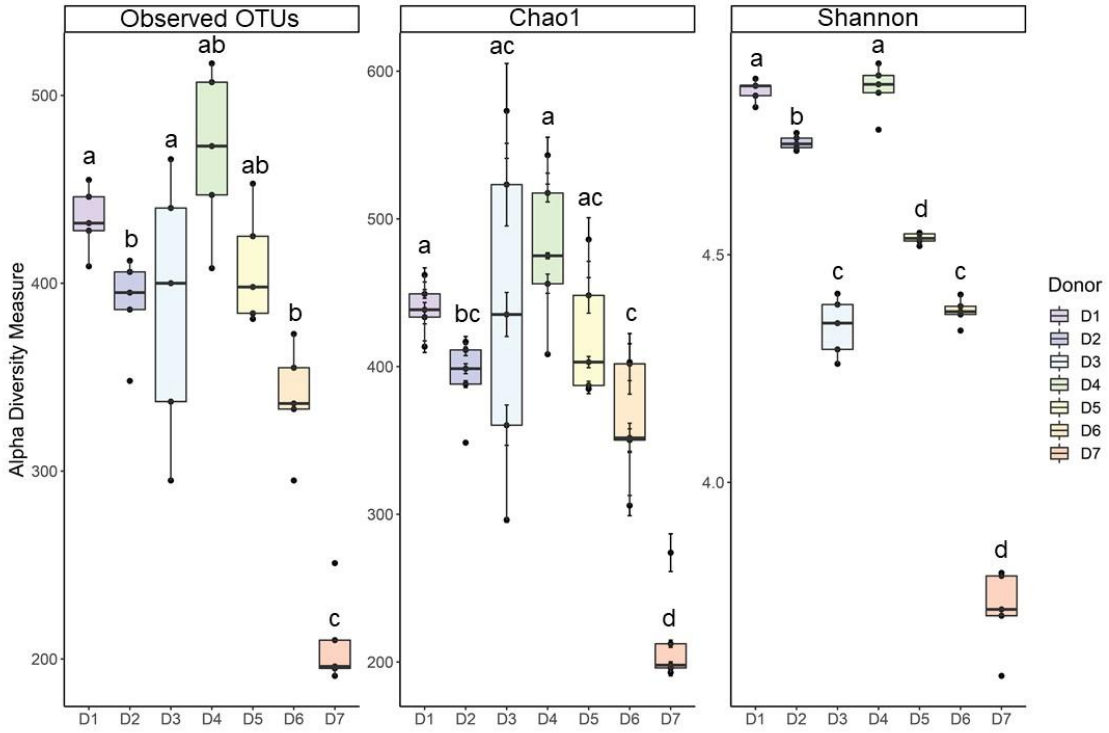

To identify differences between bacterial composition of different faecal donors at T0, we calculated β-diversity using Bray-Curtis dissimilarity, weighted and unweighted UniFrac distances (**Figure 3**A, B and C). As expected, PERMANOVA analysis showed that different donors significantly separated from each other when considering Bray-Curtis dissimilarity, weighted and unweighted UniFrac indexes ($p < 0.05$).

Figure 3. Bacterial β-diversity at time of inoculation (T0) analyzed using Bray-Curtis dissimilarity index (**A**), Unweighted Unifrac (**B**) or Weighted Unifrac distance (**C**). Different colors indicate different fecal donors (D) (n=7).

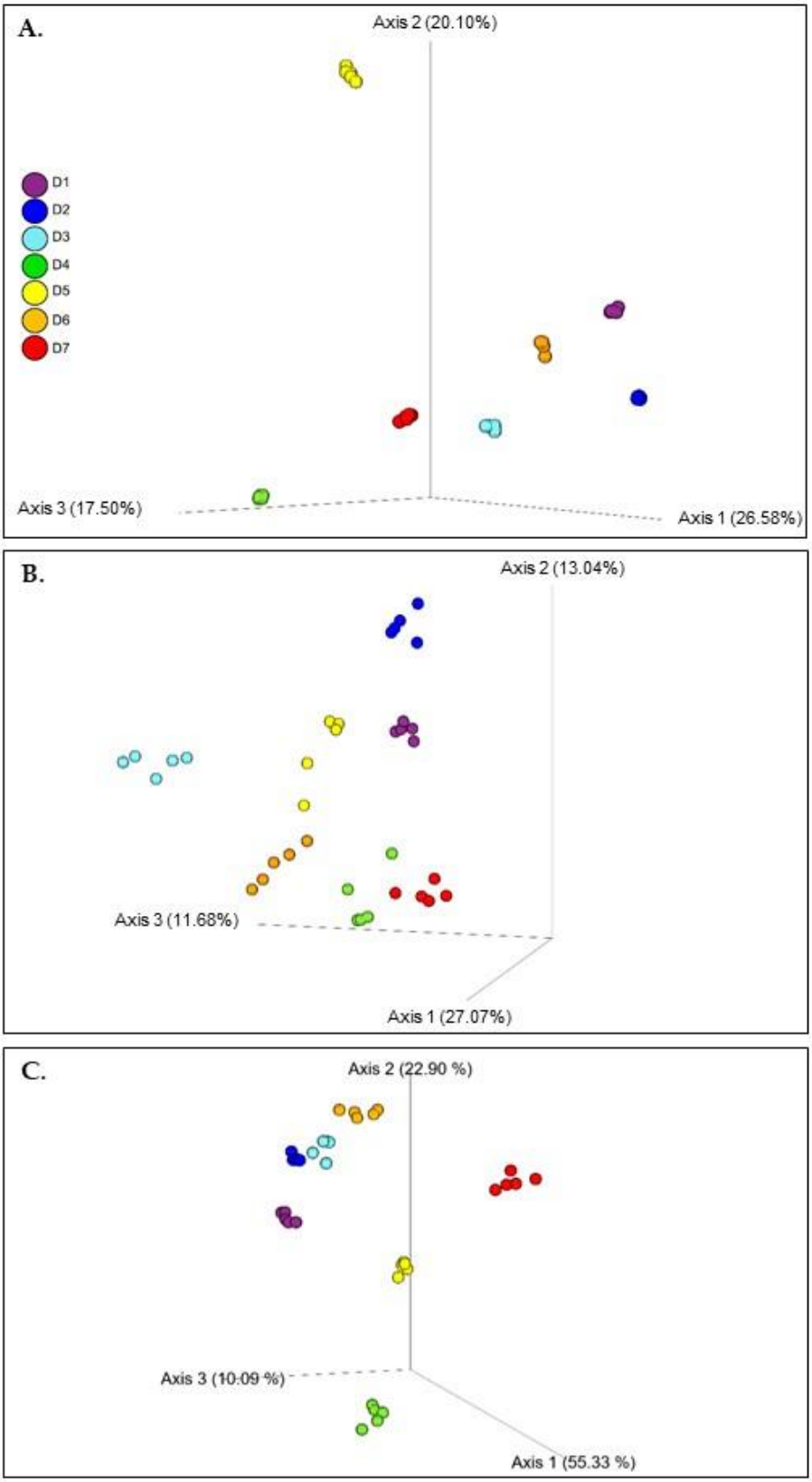

The results of gut microbiota analysis in relative abundance of taxa are illustrated in **Figure 4** and **Table S1** and **S2**. Firmicutes, Bacteroidetes, Actinobacteria and Proteobacteria were the most represented phyla in all samples, regardless of fermentation substrate and donor, covering between 96% and 99% of all identified phyla (**Figure 4**A, **Table S1**). Differences in bacterial relative abundances among the fecal donors are presented as supplementary information in **Table S1** and **S2**.

Figure 4. Percentage bacterial relative abundance of phyla (**A**) and genera (**B**) at time of feces inoculation (T0) (n=7 healthy donors). Fermenters were administrated with inulin (IN), cellulose (CL), Moringa (MOR) or glucomoringin (GMG) as substrates (treatments). Control is represented by fermenters with no substrate inoculum (BK). Values are mean % relative abundance. Less abundant phyla include bacteria with a relative abundance less than 0.01% in fewer than 25% of samples; less abundant genera include bacteria with a relative abundance less than 0.1% in fewer than 25% of samples.

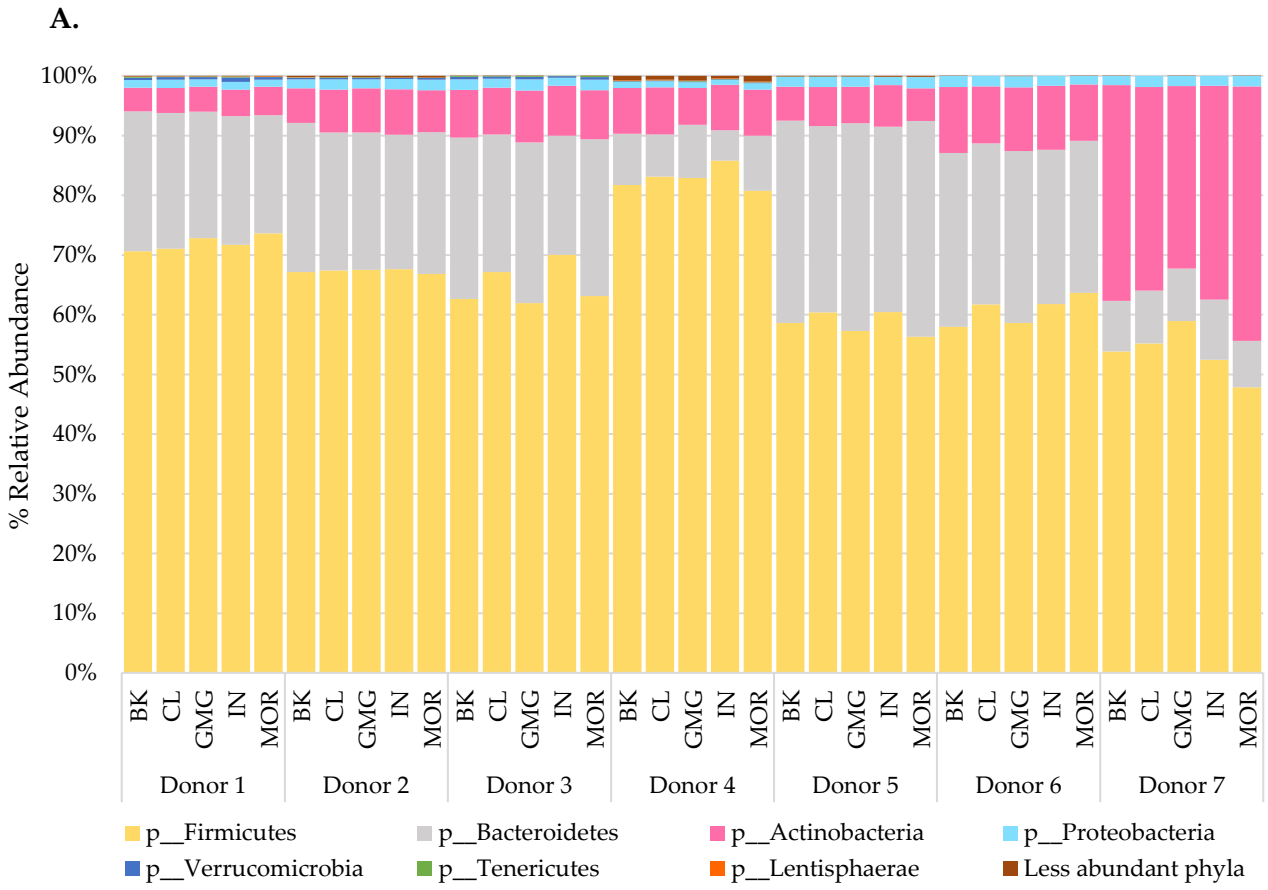

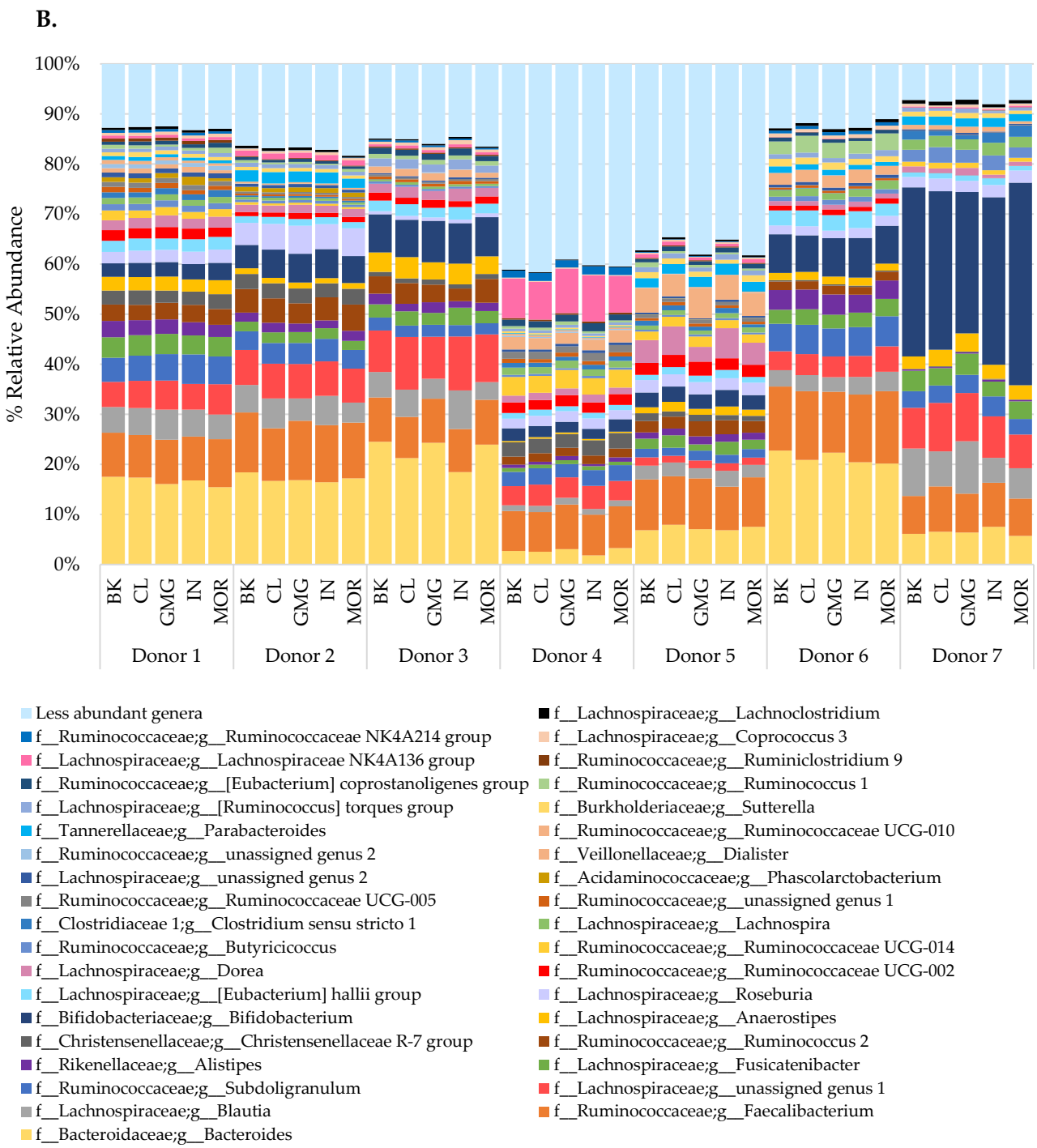

3.2 Microbial metabolites analysis

Table 1 summarizes the target glucosinolates and polyphenols quantified in faecal supernatants by LC-MS/MS. .

Table 1. List of polyphenols, glucosinolates and their derivatives analyzed in faecal supernatant through LC-MS/MS. For each compound the column "Origin" specifies if the compound was present in the plant or if it derived from microbial breakdown (▪) (53).

Glucosinolates	Origin

4- methoxyglucobrassicin	Plant
4-Hydroxyglucobrassicin	Plant
Glucoalyssin	Plant
Glucobrassicanapin	Plant
Glucobrassicin	Plant
Glucocheirolin	Plant
Glucoerucin	Plant
Glucoiberin	Plant
Glucoiberverin	Plant
Gluconapin	Plant
Gluconasturtin	Plant
Glucoraphanin	Plant
Glucotropaeolin	Plant
Glucomoringin	Plant
Neoglucobrassicin	Plant
Progoitrin	Plant
Sinalbin	Plant
Sinigrin	Plant
Moringin▪	Microbial derivative of glucomoringin
Sulforaphane▪	Microbial derivative of glucoraphanin
Polyphenols and indoles	
4-aminobenzoic acid	Plant
Caffeic acid	Plant
Catechin	Plant
Cinnamic acid	Plant
p-coumaric acid	Plant
Ferulic acid	Plant
Isorhamnetin-3-glucoside	Plant
Quercetin-3-glucoside	Plant
Quercetin-3,4-diglucoside	Plant
Sinapic acid	Plant
Synapyl alcohol	Plant
Syringaldehyde	Plant
Syringic acid	Plant
Chlorogenic acid	Plant
Neochlorogenic acid	Plant
Cryptochlorogenic acid	Plant
Indole-3-acetonitrile▪	Microbial derivative of glucobrassicin
Indole-3-carbinol▪	Microbial derivative of glucobrassicin

The results of targeted metabolites are shown in **Figure 5** and **6** and in **Table S4** and **5**. Metabolites that were not detected in ≥ 70% of the samples were excluded from further analysis. Statistical analysis (Kruskal–Wallis test, followed by the post-hoc Dunn's test with FDR p value correction) showed significant differences in glucomoringin concentrations, which significantly decreased

between T1 and T2 when MOR was used as fermentation substrate (T1: 0.029 ± 0.02, T2: 0.002 ± 0.004, mean ± SD, p = 0.0311) (**Table S3**). Significant differences were observed when comparing glucosinolate concentrations between different fermentation substrates at different timepoints. Sinalbin, glucotropaeolin and glucomoringin concentrations were significantly higher in GMG samples when compared to MOR and to BK at T0, after substrate inoculation, and over the 8 h of fermentation (**Table S3**). Changes in glucosinolate concentrations are reported in **Figure 5**. Among target polyphenols, isorhamnetin-3-glucoside concentrations in MOR supernatant significantly decreased after 5 (T5: 0.092 ± 0.238, mean ± SD, p = 0.0325) and after 8 hours of fermentation (T8: 0.054 ± 0.141, mean ± SD, p = 0.0197) when compared to baseline (T0: 1.295 ± 1.099, mean ± SD) (**Figure 6**, **Table S4**). At baseline, immediately after substrate inoculation, both isorhamnetin-3-glucoside and quercetin-3-glucoside were significantly higher in MOR samples compared to all the other substrates (**Figure 6**, **Table S4**). After 1 hour of fermentation (T1), isorhamnetin-3-glucoside was still significantly higher in MOR samples when compared to BK and GMG (**Table S4**). No other statistically significant changes in metabolites measured during MOR or GMG fermentations were observed.

Figure 5. Line plots of glucosinolates concentrations in Moringa (MOR), glucomoringin (GMG) and blank (BK) supernatants at T0 (inoculation time) and after 30 min (T0.5), 1 (T1), 2 (T2), 5 (T5) and 8 (T8) hours of fecal fermentation. Error bars correspond to the positive standard deviation (n=7 faecal donors). Symbols indicate statistical significance between substrates within the same timepoint, as follows:□ BK vs MOR; ◊ BK vs GMG; ▪ GMG and MOR.

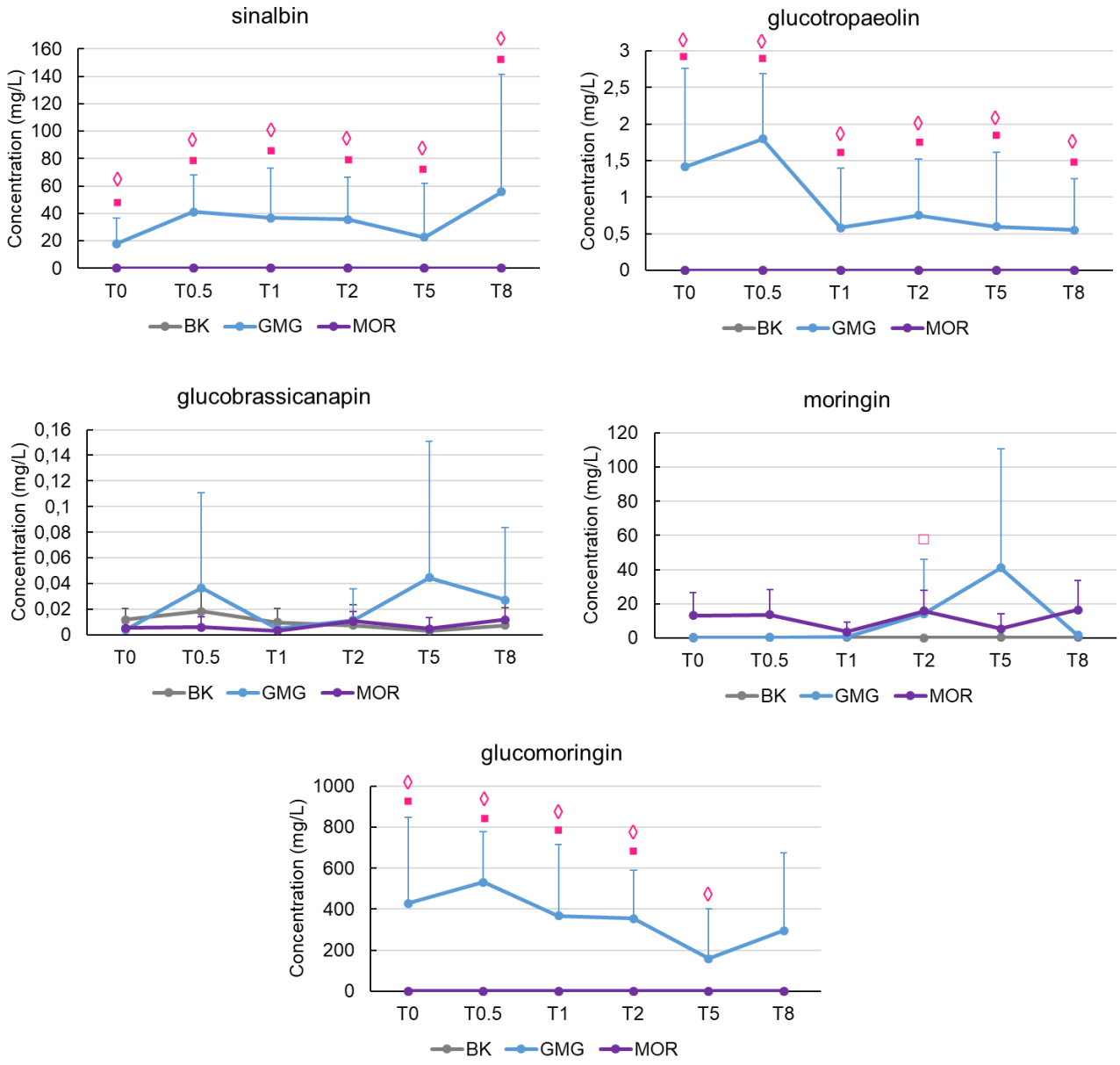

Figure 6. Line plots of polyphenols concentrations in Moringa (MOR), glucomoringin (GMG) and blank (BK) supernatants at T0 (inoculation time) and after 30 min (T0.5), 1 (T1), 2 (T2), 5 (T5) and 8 (T8) hours of fecal fermentation. Error bars correspond to the positive standard deviation (n=7 donors). Symbols indicate statistical significance within the same timepoint, as follows: □ BK vs MOR; ◊ BK vs GMG; ▪ GMG and MOR. Stars * indicate statistical significance when comparing different timepoints with T0 within the same substrate.

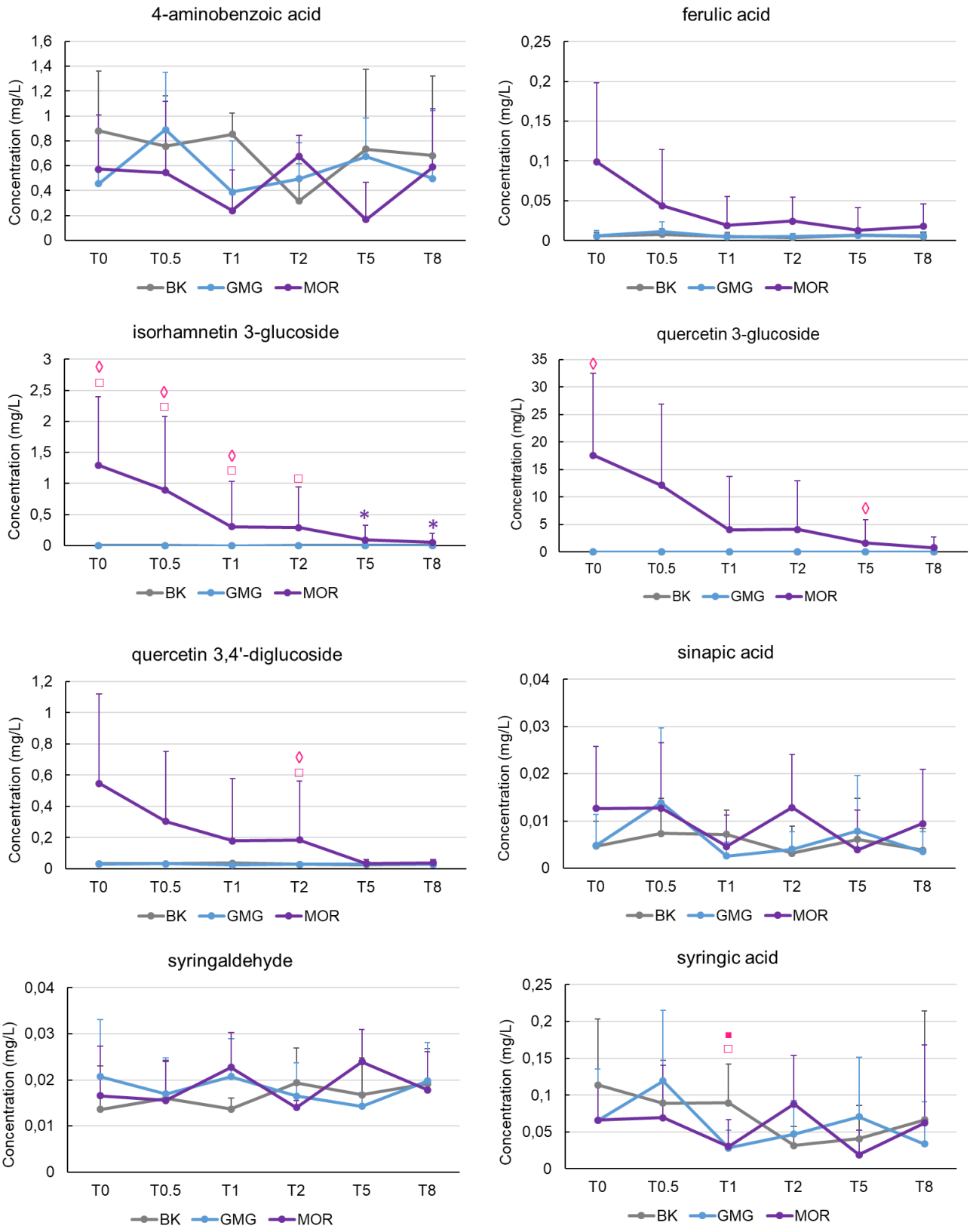

Figure 6. Continues from previous page.

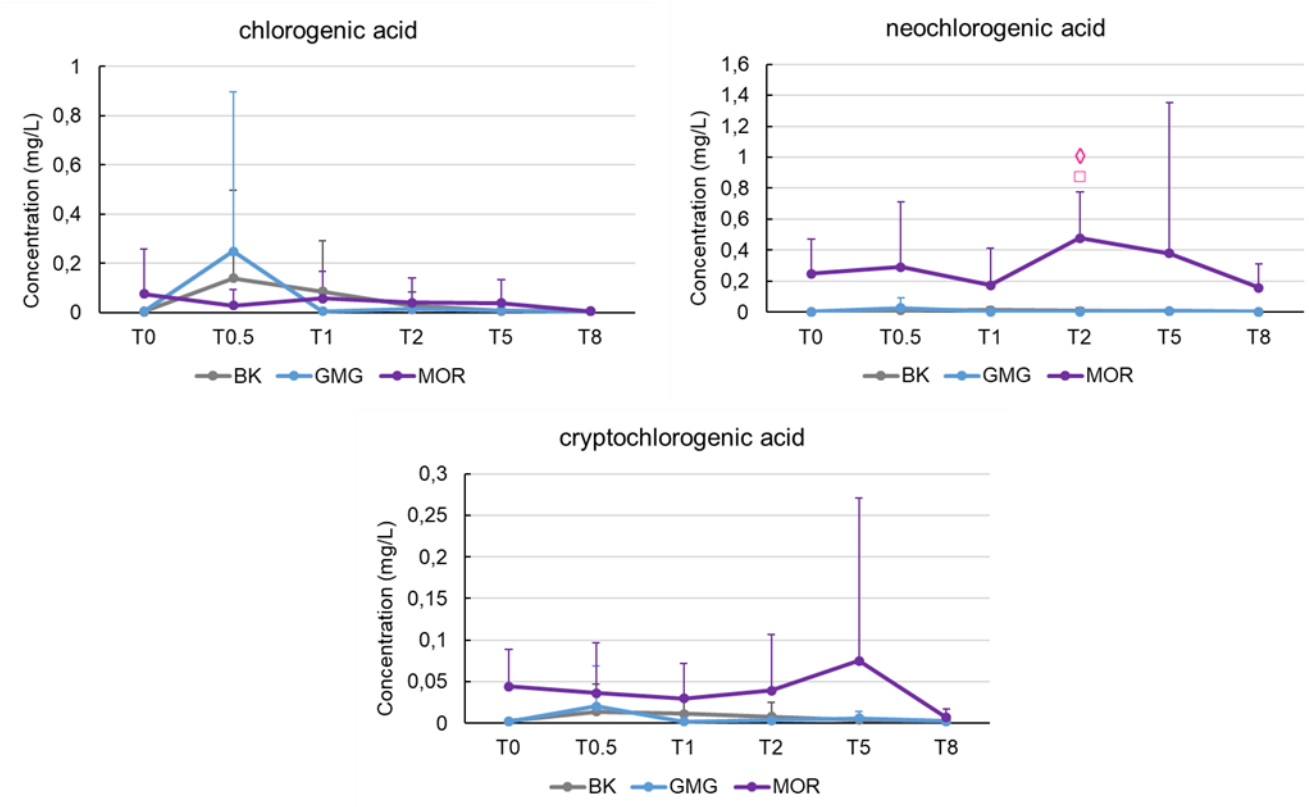

3.3 Correlation analysis between GM and metabolites identified through LC/MS-MS

Spearman's correlation analysis was performed to correlate microbial relative abundances of different donors at baseline with polyphenols and glucosinolates identified in fermentation supernatants using LC/MS-MS. Statistically significant differences were observed between GM taxa at genus level and target compounds (**Figure 7** and **8**). When considering the variation in glucosinolates concentration between T5 and T8 (ΔT8-T5), glucobrassicanapin showed statistically significant negative correlation with *Blautia* and *Fusicatenibacter*, while moringin was negative correlated with *Alistipes, Eubacterium hallii* and *Coprococcus 3* (**Figure 7**). Among polyphenols, syringaldehyde showed statistically significant positive correlation with *Eubacterium hallii* and *Coprococcus 3* (**Figure 8**).

Figure 7. Spearman's correlation between the relative abundance of gut microbial genera and target glucosinolates identified by LC/MS-MS. Changes in glucosinolates concentrations are reported as differences (delta, Δ) between two consecutive timepoints and between T8 and baseline. A positive correlation is indicated by dark green, a negative correlation by dark pink. Stars indicate statistical significance after FDR correction (* $p < 0.05$, ** $p < 0.01$, *** $p < 0.001$). Genera were reported as "Unassigned" when they could not be assigned to any genus (g) within the reference database (https://www.arb-silva.de/download/archive/, accessed on 13 July 2020), at a percentage sequence homology of 95% for genus.

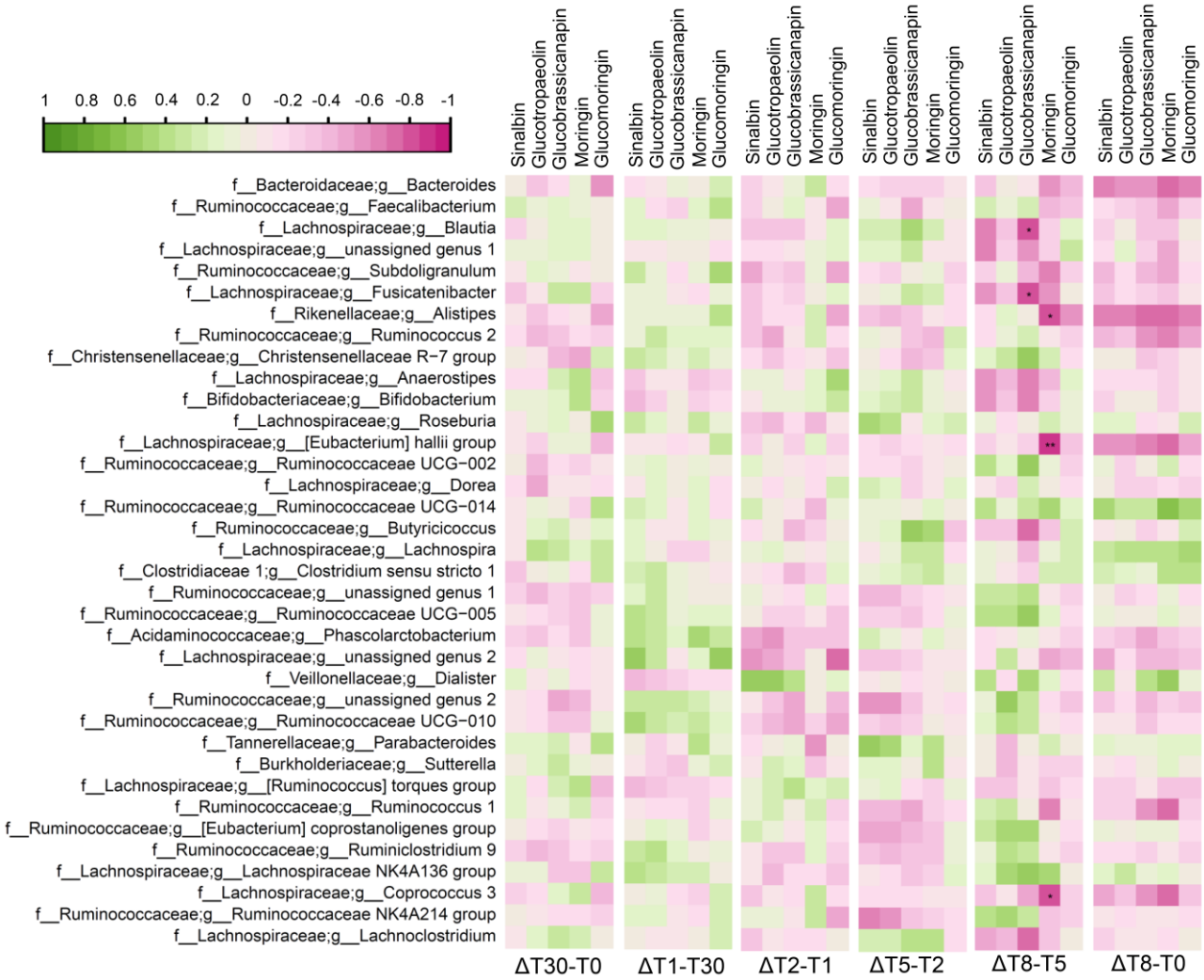

Figure 8. Spearman's correlation between the relative abundance of gut microbial genera and target polyphenols identified by LC/MS-MS. Changes in glucosinolates concentrations are reported as differences (delta, Δ) between two consecutive timepoints and between T8 and baseline. A positive correlation is indicated by dark green, a negative correlation by dark pink. Stars indicate statistical significance after FDR correction (* $p < 0.05$, ** $p < 0.01$, *** $p < 0.001$). Genera were reported as "Unassigned" when they could not be assigned to any genus (g) within the reference database (https://www.arb-silva.de/download/archive/, accessed on 13 July 2020), at a percentage sequence homology of 95% for genus.

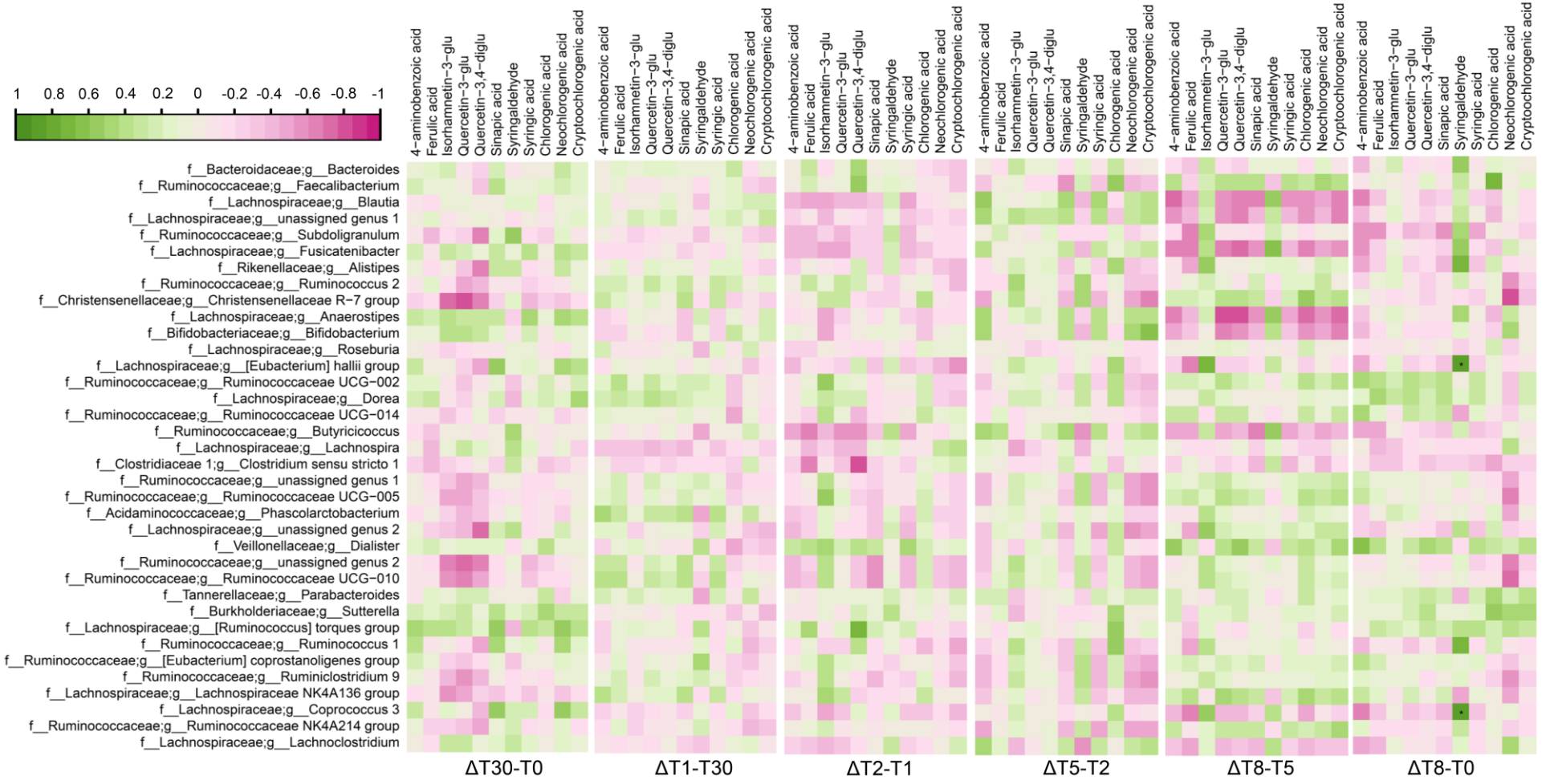

3.4 Effects of MOR and GMG supernatants on TEER measurements

TEER (Ωcm^2) was calculated as described in Section 2.7. **Figure 9** reports changes in TEER expressed as % of increase or decrease after 24 hours incubation with MOR and GMG supernatants, compared to baseline TEER. Compared with monolayers incubated with medium as control, the results showed a clear-cut reduction of TEER after 24 hours exposure to ethanol (medium: 102.94 ± 4.38%, EtOH: 69.93 ± 14.88%, mean ± SD; $p < 0.001$), as well as a clear TEER improvement after 24 hours exposure to propionic acid (propionic acid: 117.00 ± 7.30 %, mean ± SD; $p < 0.0001$). When compared to control medium, monolayer resistance significantly increased after 24 hours of incubation with GMG supernatant (GMG: 108.19 ± 2.77 %, mean ± SD; $p = 0.0035$). Incubation with MOR supernatant showed a small increase of TEER at T24 (MOR: 104.74 ± 3.68 %, mean ± SD), although this result did not reach statistical significance ($p = 0.2599$). 24 h incubation with MOR supernatants did not induce gut permeability, since MOR TEER was significantly higher when compared to ethanol ($p < 0.001$).

Figure 9. Changes in trans-epithelial electrical resistance (TEER) across differentiated Caco-2 monolayers in presence/absence of test substrates. The change in TEER is the percentage (%) change compared to the initial TEER for each monolayer. The values plotted are the means for three experimental replicates + the error bars show the standard deviation (SD). Different superscript letters indicate statistical significance when comparing different substrates. MOR, Moringa supernatants; GMG, glucomoringin supernatants.

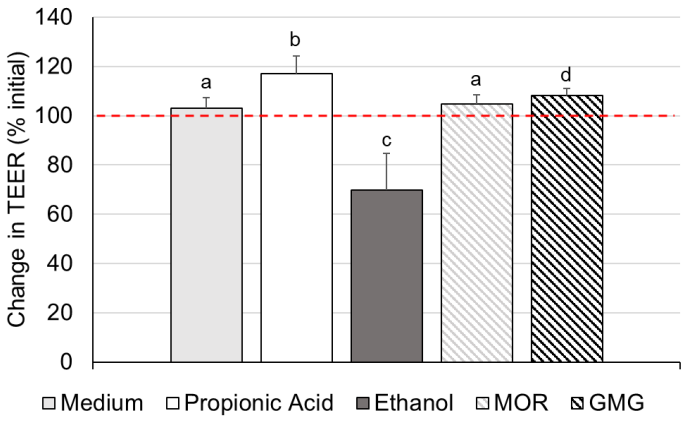

4. Discussion

Moringa is a rich source of protein, vitamins and phytochemicals, making this plant a very interesting candidate as an under-utilised sustainable food crop for human health (7,54,55). Since the human gut microbiota (GM) has a crucial role in breaking down plant phytochemicals into their biologically available and possibly biologically active form (38,39), we investigated whether and to which extent the human GM metabolizes the main phytochemicals in Moringa. We also analyzed which bacteria might be involved in Moringa glucosinolates and polyphenols metabolism and

examined whether fermentation supernatants of Moringa or glucomoringin could improve intestinal barrier function *in vitro*. Anaerobic faecal batch cultures from healthy donors were used to determine the ability of faecal bacteria to breakdown *Moringa oleifera* polyphenols and glucosinolates. We evaluated whether glucomoringin alone, the main glucosinolate in moringa, was able to modulate the GM, by adding glucomoringin pure standard as fermentation substrate.

As expected, the GM from different faecal donors was significantly different in terms of bacterial richness and composition (56,57). Isorhamnetin-3-glucoside, one of the major flavonoid glycosides found in *M. oleifera* leaves (58,59), significantly decreased after 5 hours of Moringa leaf powder fermentation. Previous *in vitro* studies reported the ability of human GM to metabolise isorhamnetin-3-glucoside (60), thus producing its aglycon isorhamnetin, which was previously reported to have anti-inflammatory and antioxidant properties(61).

Glucomoringin was selected and used as single fermentation substrate as it represents the most abundant glucosinolate in Moringa (24). The quantity of glucomoringin per gram of dried moringa was 35-45 mg, and the quantity of moringin per gram of dried moringa was 3.2-3.6 mg, as measured upon hydroalcoholic extraction. However, we found very low concentrations of glucomoringin in MOR supernatants after in vitro digestion and under the acquaeous physiological concentrations of the colon model (T0: 0.009 ± 0.016, mean ± SD). On the other hand, moringin concentrations detected in MOR supernatants at T0 were higher than expected. We thereby speculate that *in vitro* digestion may have activated thermal-, enzymatic/endogenous myrosinases-mediated breakdown (62,63), thus stimulating the conversion of glucomoringin to its stable isothiocyanate moringin, widely studied for its putative anti-inflammatory and anti-cancer activities (26,27,64). Notably, we observed a significant decrease in glucomoringin concentrations after 2 hours of faecal fermentation in GMG samples. In parallel, we observed an increase in moringin concentrations in the same samples over time, but this result did not reach statistical significance after FDR correction. However, the opposite trend was observed between the two compounds over 8 hours of faecal fermentation, which is consistent with the literature, since moringin represents the most frequent isothiocyanate produced by glucomoringin metabolism (25).

From baseline, GMG supernatants showed higher concentration of glucomoringin, sinalbin and glucotropaeolin compared to MOR, BK and to the other fermentation substrates. Although we expected to find high concentrations of glucomoringin in GMG samples, it was unexpected to find also sinalbin and glucotropaeolin. Excluding that these two compounds were originally present in the fermentation medium or in the faecal samples, since they were not detected in BK, CL, IN and

MOR supernatants, we have instead assumed that sinalbin and glucotropaeolin might have been present in the GMG extract. Moreover, while glucomoringin and glucotropaeolin concentrations showed a decreasing trend over time in GMG samples, sinalbin increased from T0 (18.15 ± 18.34) to T8 (55.90 ± 85.36), although these results did not reach statistical significance. As shown in **Figure 10**, sinalbin structure differs from that of glucomoringin only by the absence of a rhamnosyl moiety (65). Interestingly, a human anaerobic gut bacterium, *Bacteroides* JY-6 has been found to metabolize different rhamnoglucosides *in vitro*, including rutin and hesperidin (66). It is therefore possible that faecal bacteria cleave off the rhamnose moiety from glucomoringin, thus producing sinalbin. Also glucotropaeolin is a derivative of sinalbin which can be obtained by anaerobic bacteria via 'Birch-like' reduction (dihydroxylation), catalyzed by the enzyme hydroxybenzoyl-CoA reductase (67).

Figure 10. Glucomoringin, sinalbin and glucotropaeolin structures. Adapted from Jaafaru *et al*. (2018) (65)

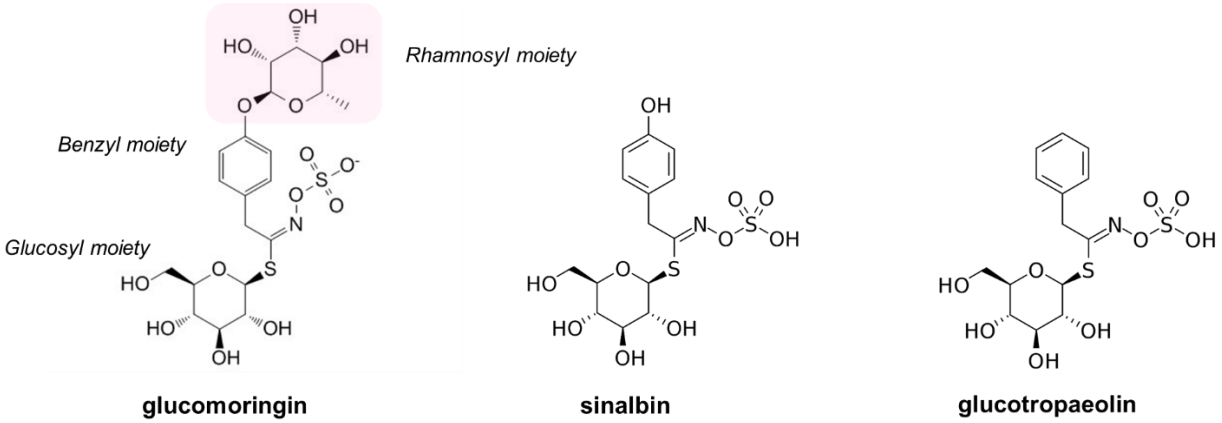

When comparing polyphenols concentrations between different substrates at the same timepoint, some differences were observed. As expected, quercetin-3-glucoside and isorhamnetin-3-glucoside were significantly higher in MOR samples compared to GMG, and to all the other fermentation substrates. Our results are in line with previous studies reporting these compounds as the most abundant in *M. oleifera* leaves (16,25,59,68). Differences in gut microbiota composition between the faecal donors could result in differences in glucosinolate and polyphenol metabolism during faecal fermentations. For this reason, we speculate that the host exposure to these bioactive compounds and to their microbial metabolites strongly depends on the quantity of Moringa consumed and on its processing, but also on the composition of the intestinal microbiota. We also observed a large variability in the concentrations of target metabolites for the same donor at different timepoints. This explains the large standard deviation of the measurements and the lack of statistically significant results. We suppose that these observations could be related to the strong pH fluctuations occurring

during the faecal fermentations. Myrosinase activity on GLS leads to glucosyl moiety cleavage, with the concomitant release of an unstable aglycone (69). Hydrolysis conditions, including pH, strongly influence the fate of these unstable intermediates, which could be converted into different classes of degradation products such as isothiocyanates, thiocyanates, indoles or other related compounds (69). In our study, pH variations due to the microbial fermentative activity, pH differences existing between faecal samples from different donors (70) and the potential hydrolytic activity of the different faecal microbiota themselves, may have contributed to the observed fluctuations concentration of the target metabolites. For these reasons, future *in vitro* studies should be performed using larger fermentation volumes, to facilitate pH control over the fermentation process. In this experiment the fermentation volume was determined by the limited amount of pure GMG substrate available.

We correlated donors' GM composition with metabolite concentrations using Spearman's correlation. Our results highlighted some significant associations between GM composition at genus level at T0 and changes in target metabolites. Among glucosinolates, variations in glucobrassicanapin levels between T5 and T8 showed a significant negative correlation with *Blautia* genus, while moringin concentrations were inversely correlated to *Alistipes, Eubacterium hallii* and *Coprococcus 3* within the same timepoints. To our knowledge, no studies evaluated the role of these bacterial genera in metabolizing glucobrassicanapin or moringin. However, besides significant correlations observed in our work, metabolism of target compounds did not appear to depend on specific bacterial genera. Since β-diversity analysis showed a substantial difference in GM composition among different faecal donors, it is likely that different bacteria have similar metabolic functions associated with glucosinolates and polyphenols biotransformation, as already suggested (71). For this reason, if each faecal donor harbors a unique GM community with its own myrosinase-like activity, it is possible that glucosinolates and polyphenols ingestion could drive a personalized response depending on GM composition, thus partially explaining the different pattern of response observed in Spearman's correlation heatmaps and the standard deviation we observed when looking at metabolite concentration over time. To date, *in vitro* incubation of glucosinolates or polyphenols have confirmed that certain bacterial taxa are able to metabolize these compounds in pure culture, including *Enterococcus* spp., *Bifidobacterium* spp. (40) and *Lactobacillus* spp. (72). However, to our knowledge, no studies have evaluated the impact of human GM composition on the metabolism of Moringa metabolites during mixed culture using *in vitro* faecal fermentations.

Since previous studies have shown that Moringa extracts improve symptoms of ulcerative colitis by improving barrier function, we assessed if MOR or GMG fermentation supernatants improved gut epithelial barrier integrity, using an *in vitro* trans-epithelial electric resistance (TEER) model. The gut epithelium represents a critical barrier limiting microbial translocation, thus protecting the host against chronic systemic inflammation, caused by bacterial endotoxemia (73,74). Our study shows that GMG supernatants collected at T1 (i.e. 1 hour from beginning of fermentation), improved gut barrier function, by significantly changing TEER. On the other hand, no significant TEER improvement was observed after incubation with MOR supernatants. We therefore speculated that the stimulation of TEER may have been brought about by glucomoringin or by the derived glucotropaeolin or sinalbin, which reached the highest concentration at T1.

Although further studies are required to clarify the existing relationship between GM metabolism and *Moringa oleifera* health beneficial effects, our results provide novel insights on the fate of target polyphenols and glucosinolates during faecal fermentation and on their potential biological activity at the intestinal level.

Supplementary material

Table S1. Percentage relative abundance (%) of bacterial OTUs, at phylum level, at T0 in different faecal donors (n=7). Columns names indicate the substrate added at the beginning of faecal fermentations. BK, blank; CL, cellulose; GMG, glucomoringin; IN, inulin; MOR, Moringa.

Donor 1	**BK**	**CL**	**GMG**	**IN**	**MOR**
p__Firmicutes	70.64	71.04	72.84	71.71	73.60
p__Bacteroidetes	23.43	22.77	21.18	21.54	19.82
p__Actinobacteria	3.93	4.17	4.18	4.46	4.77
p__Proteobacteria	1.30	1.40	1.21	1.30	1.18
p__Verrucomicrobia	0.38	0.39	0.37	0.72	0.42
p__Tenericutes	0.14	0.11	0.11	0.15	0.08
p__Lentisphaerae	0.10	0.06	0.06	0.07	0.09
Donor 2	**BK**	**CL**	**GMG**	**IN**	**MOR**
p__Firmicutes	67.15	67.42	67.51	67.61	66.79
p__Bacteroidetes	24.96	23.11	23.02	22.51	23.79
p__Actinobacteria	5.81	7.18	7.38	7.62	7.00
p__Proteobacteria	1.52	1.69	1.52	1.72	1.79
p__Verrucomicrobia	0.26	0.29	0.24	0.24	0.29
p__Tenericutes	0.07	0.08	0.09	0.07	0.10
p__Lentisphaerae	0.01	0.01	0.01	0.01	0.00
Donor 3	**BK**	**CL**	**GMG**	**IN**	**MOR**
p__Firmicutes	62.61	67.14	61.94	70.04	63.13
p__Bacteroidetes	27.05	23.04	26.93	19.95	26.28
p__Actinobacteria	7.99	7.82	8.67	8.35	8.19
p__Proteobacteria	1.77	1.54	1.89	1.36	1.78
p__Verrucomicrobia	0.42	0.36	0.42	0.25	0.42
p__Tenericutes	0.16	0.10	0.13	0.05	0.19
p__Lentisphaerae	0.00	0.00	0.00	0.00	0.00
Donor 4	**BK**	**CL**	**GMG**	**IN**	**MOR**
p__Firmicutes	81.71	83.13	82.90	85.77	80.73
p__Bacteroidetes	8.59	7.05	8.91	5.10	9.25
p__Actinobacteria	7.69	7.88	6.17	7.65	7.71
p__Proteobacteria	1.00	1.00	0.97	0.78	1.07
p__Verrucomicrobia	0.10	0.13	0.10	0.11	0.09
p__Tenericutes	0.06	0.08	0.09	0.09	0.08
p__Lentisphaerae	0.09	0.09	0.09	0.09	0.08
Donor 5	**BK**	**CL**	**GMG**	**IN**	**MOR**
p__Firmicutes	58.63	60.38	57.26	60.43	56.30
p__Bacteroidetes	33.86	31.23	34.82	31.04	36.16
p__Actinobacteria	5.68	6.52	6.10	6.95	5.47
p__Proteobacteria	1.68	1.74	1.64	1.39	1.88
p__Verrucomicrobia	0.00	0.00	0.00	0.00	0.00
p__Tenericutes	0.04	0.05	0.05	0.03	0.03
p__Lentisphaerae	0.00	0.00	0.00	0.00	0.00

Donor 6	BK	CL	GMG	IN	MOR
p__Firmicutes	57.96	61.74	58.60	61.77	63.66
p__Bacteroidetes	29.14	26.98	28.83	25.85	25.48
p__Actinobacteria	11.02	9.52	10.67	10.74	9.41
p__Proteobacteria	1.88	1.76	1.87	1.65	1.45
p__Verrucomicrobia	0.00	0.00	0.00	0.00	0.00
p__Tenericutes	0.00	0.00	0.00	0.00	0.00
p__Lentisphaerae	0.00	0.00	0.00	0.00	0.00
Donor 7	**BK**	**CL**	**GMG**	**IN**	**MOR**
p__Firmicutes	53.84	55.17	58.94	52.42	47.82
p__Bacteroidetes	8.47	8.87	8.76	10.12	7.79
p__Actinobacteria	36.12	34.08	30.60	35.80	42.61
p__Proteobacteria	1.57	1.88	1.69	1.66	1.79
p__Verrucomicrobia	0.00	0.00	0.00	0.00	0.00
p__Tenericutes	0.00	0.00	0.00	0.00	0.00
p__Lentisphaerae	0.00	0.00	0.00	0.00	0.00

Table S2. Percentage relative abundance (%) of bacterial OTUs, at genus level, at T0 in different faecal donors (n=7). Columns names indicate the substrate added at the beginning of faecal fermentations. BK, blank; CL, cellulose; GMG, glucomoringin; IN, inulin; MOR, Moringa.

Donor 1	**BK**	**CL**	**GMG**	**IN**	**MOR**
g__[Eubacterium] coprostanoligenes group	0.65	0.77	0.77	0.76	0.99
g__[Eubacterium] hallii group	2.22	2.45	2.30	2.45	2.51
g__[Ruminococcus] torques group	0.74	0.66	0.69	0.69	0.74
g__Alistipes	3.28	3.00	2.91	2.65	2.43
g__Anaerostipes	2.77	2.68	2.78	2.44	2.79
g__Bacteroides	17.52	17.39	16.07	16.79	15.45
g__Bifidobacterium	2.66	2.84	2.90	3.04	3.45
g__Blautia	5.14	5.37	6.02	5.40	4.96
g__Butyricicoccus	1.26	1.34	1.37	1.25	1.23
g__Christensenellaceae R-7 group	2.82	2.87	2.46	2.64	3.00
g__Clostridium sensu stricto 1	1.14	1.04	1.25	1.10	1.37
g__Coprococcus 3	0.55	0.59	0.64	0.57	0.66
g__Dialister	0.88	0.98	0.81	1.09	0.65
g__Dorea	1.96	2.00	2.31	2.00	2.19
g__Faecalibacterium	8.81	8.49	8.84	8.75	9.57
g__Fusicatenibacter	4.06	4.10	4.05	3.79	3.89
g__Lachnoclostridium	0.50	0.55	0.51	0.53	0.49
g__Lachnospira	1.24	1.26	1.20	1.15	1.25
g__Lachnospiraceae NK4A136 group	0.59	0.53	0.57	0.50	0.58
g__Parabacteroides	0.76	0.77	0.64	0.61	0.57
g__Phascolarctobacterium	0.95	0.90	0.98	1.68	0.58
g__Roseburia	2.29	2.44	2.41	2.51	2.66
g__Ruminiclostridium 9	0.63	0.62	0.63	0.66	0.57
g__Ruminococcaceae NK4A214 group	0.53	0.57	0.52	0.58	0.48
g__Ruminococcaceae UCG-002	2.16	2.07	2.28	2.13	1.89
g__Ruminococcaceae UCG-005	0.99	1.02	0.95	1.00	0.95
g__Ruminococcaceae UCG-010	0.81	0.69	0.61	0.46	0.51
g__Ruminococcaceae UCG-014	1.94	1.48	1.65	1.34	1.46
g__Ruminococcus 1	0.73	0.70	0.41	0.48	1.11
g__Ruminococcus 2	3.24	3.07	3.28	3.47	3.12
g__Subdoligranulum	4.82	5.02	5.31	5.89	5.57
g__Sutterella	0.75	0.98	0.78	0.74	0.71
f__Lachnospiraceae;g__unassigned genus 1	5.05	5.44	5.79	5.15	6.04
f__Lachnospiraceae;g__unassigned genus 2	0.95	0.97	0.96	0.89	0.95
f__Ruminococcaceae;g__unassigned genus 1	1.07	0.90	1.05	0.86	0.83
f__Ruminococcaceae;g__unassigned genus 2	0.83	0.83	0.78	0.78	0.85
Donor 2	**BK**	**CL**	**GMG**	**IN**	**MOR**
g__[Eubacterium] coprostanoligenes group	0.62	0.56	0.63	0.50	0.55
g__[Eubacterium] hallii group	1.32	1.35	1.34	1.38	1.24
g__[Ruminococcus] torques group	0.85	0.76	0.78	0.81	0.72
g__Alistipes	1.84	1.91	1.74	1.58	2.04
g__Anaerostipes	1.15	1.12	1.19	1.05	1.15
g__Bacteroides	18.42	16.69	16.86	16.44	17.21
g__Bifidobacterium	4.65	5.62	5.75	5.80	5.36

g__Blautia	5.49	5.95	4.46	5.86	4.02
g__Butyricicoccus	0.50	0.57	0.51	0.58	0.44
g__Christensenellaceae R-7 group	3.01	2.99	2.96	2.80	3.14
g__Clostridium sensu stricto 1	0.31	0.31	0.34	0.34	0.36
g__Coprococcus 3	0.43	0.45	0.46	0.53	0.50
g__Dialister	0.00	0.00	0.00	0.00	0.00
g__Dorea	1.45	1.39	1.66	1.42	1.60
g__Faecalibacterium	11.93	10.51	11.86	11.40	11.13
g__Fusicatenibacter	1.89	2.11	2.15	2.09	1.83
g__Lachnoclostridium	0.53	0.53	0.53	0.48	0.38
g__Lachnospira	0.52	0.55	0.51	0.50	0.49
g__Lachnospiraceae NK4A136 group	1.08	1.14	1.06	1.07	1.01
g__Parabacteroides	2.28	2.30	2.17	2.26	1.90
g__Phascolarctobacterium	0.92	0.84	0.92	0.93	0.89
g__Roseburia	4.42	5.15	5.61	4.99	5.58
g__Ruminiclostridium 9	0.19	0.14	0.16	0.18	0.16
g__Ruminococcaceae NK4A214 group	0.07	0.06	0.05	0.04	0.07
g__Ruminococcaceae UCG-002	0.84	0.92	1.18	0.86	1.03
g__Ruminococcaceae UCG-005	0.41	0.41	0.46	0.41	0.38
g__Ruminococcaceae UCG-010	0.35	0.26	0.32	0.27	0.28
g__Ruminococcaceae UCG-014	0.54	0.42	0.42	0.41	0.37
g__Ruminococcus 1	0.49	0.36	0.41	0.25	0.57
g__Ruminococcus 2	4.70	4.90	4.02	4.59	5.23
g__Subdoligranulum	3.77	4.17	4.21	4.53	3.71
g__Sutterella	0.69	0.77	0.69	0.64	0.60
f__Lachnospiraceae;g__unassigned genus 1	7.00	6.94	6.87	6.87	6.78
f__Lachnospiraceae;g__unassigned genus 2	0.63	0.62	0.63	0.61	0.54
f__Ruminococcaceae;g__unassigned genus 1	0.35	0.37	0.34	0.35	0.36
f__Ruminococcaceae;g__unassigned genus 2	0.07	0.04	0.06	0.04	0.07
Donor 3	**BK**	**CL**	**GMG**	**IN**	**MOR**
g__[Eubacterium] coprostanoligenes group	1.20	1.17	1.17	1.35	1.05
g__[Eubacterium] hallii group	2.07	2.37	1.91	2.49	1.91
g__[Ruminococcus] torques group	1.58	1.88	1.58	2.05	1.36
g__Alistipes	2.11	1.50	2.13	1.29	1.70
g__Anaerostipes	3.90	4.28	3.41	4.19	3.52
g__Bacteroides	24.52	21.25	24.29	18.44	23.93
g__Bifidobacterium	7.58	7.47	8.28	8.05	7.85
g__Blautia	5.08	5.46	3.99	7.70	3.49
g__Butyricicoccus	0.43	0.43	0.40	0.39	0.33
g__Christensenellaceae R-7 group	0.90	0.93	1.03	0.81	0.97
g__Clostridium sensu stricto 1	0.01	0.00	0.00	0.00	0.00
g__Coprococcus 3	0.53	0.61	0.56	0.84	0.56
g__Dialister	1.25	1.38	1.48	1.43	0.96
g__Dorea	1.76	2.17	1.77	2.51	1.74
g__Faecalibacterium	8.85	8.22	8.83	8.64	9.00
g__Fusicatenibacter	2.65	2.84	2.39	3.46	2.40
g__Lachnoclostridium	0.29	0.29	0.30	0.34	0.29
g__Lachnospira	0.46	0.49	0.46	0.48	0.46

g__Lachnospiraceae NK4A136 group	0.44	0.60	0.49	0.60	0.46
g__Parabacteroides	0.00	0.00	0.00	0.00	0.00
g__Phascolarctobacterium	0.00	0.00	0.00	0.00	0.00
g__Roseburia	0.67	0.74	0.67	0.75	0.76
g__Ruminiclostridium 9	0.26	0.28	0.29	0.23	0.25
g__Ruminococcaceae NK4A214 group	0.33	0.38	0.36	0.34	0.33
g__Ruminococcaceae UCG-002	1.65	1.28	1.63	1.15	1.43
g__Ruminococcaceae UCG-005	0.43	0.36	0.34	0.37	0.43
g__Ruminococcaceae UCG-010	0.04	0.04	0.07	0.03	0.05
g__Ruminococcaceae UCG-014	0.00	0.00	0.00	0.00	0.00
g__Ruminococcus 1	0.91	0.70	0.93	0.79	0.89
g__Ruminococcus 2	3.45	4.15	3.55	2.55	4.75
g__Subdoligranulum	2.60	2.29	2.37	2.27	2.21
g__Sutterella	0.00	0.00	0.00	0.00	0.00
f__Lachnospiraceae;g__unassigned genus 1	8.28	10.51	8.38	10.78	9.57
f__Lachnospiraceae;g__unassigned genus 2	0.28	0.29	0.28	0.39	0.27
f__Ruminococcaceae;g__unassigned genus 1	0.53	0.59	0.58	0.67	0.52
f__Ruminococcaceae;g__unassigned genus 2	0.05	0.06	0.09	0.04	0.05
Donor 4	**BK**	**CL**	**GMG**	**IN**	**MOR**
g__[Eubacterium] coprostanoligenes group	1.27	1.30	1.33	1.62	1.21
g__[Eubacterium] hallii group	1.16	1.24	1.00	1.12	1.07
g__[Ruminococcus] torques group	0.50	0.59	0.57	0.53	0.52
g__Alistipes	0.66	0.57	0.81	0.45	0.84
g__Anaerostipes	0.26	0.32	0.30	0.26	0.25
g__Bacteroides	2.69	2.53	3.08	1.83	3.26
g__Bifidobacterium	2.55	2.20	2.15	1.97	2.51
g__Blautia	1.17	1.25	1.34	1.13	1.21
g__Butyricicoccus	0.41	0.42	0.40	0.45	0.40
g__Christensenellaceae R-7 group	2.84	2.90	2.75	3.07	3.10
g__Clostridium sensu stricto 1	0.92	0.84	0.79	0.90	0.90
g__Coprococcus 3	0.16	0.15	0.17	0.16	0.16
g__Dialister	2.47	2.29	2.20	2.12	2.49
g__Dorea	1.32	1.45	1.35	1.58	1.32
g__Faecalibacterium	7.98	7.95	8.91	8.13	8.35
g__Fusicatenibacter	0.78	0.71	0.77	0.76	0.68
g__Lachnoclostridium	0.17	0.16	0.17	0.21	0.17
g__Lachnospira	1.44	1.35	1.47	1.33	1.34
g__Lachnospiraceae NK4A136 group	7.93	7.58	8.96	9.22	7.35
g__Parabacteroides	0.19	0.14	0.20	0.10	0.18
g__Phascolarctobacterium	0.00	0.00	0.00	0.00	0.00
g__Roseburia	1.90	2.02	2.10	2.10	1.79
g__Ruminiclostridium 9	0.34	0.34	0.30	0.34	0.35
g__Ruminococcaceae NK4A214 group	1.39	1.58	1.47	1.67	1.56
g__Ruminococcaceae UCG-002	2.10	1.94	2.21	2.06	2.14
g__Ruminococcaceae UCG-005	1.38	1.43	1.27	1.58	1.45
g__Ruminococcaceae UCG-010	0.37	0.32	0.32	0.25	0.30
g__Ruminococcaceae UCG-014	3.76	3.38	3.67	3.26	3.56
g__Ruminococcus 1	0.55	0.50	0.67	0.39	0.39

g__Ruminococcus 2	1.64	1.71	1.66	1.69	1.78
g__Subdoligranulum	2.85	3.26	2.67	3.16	3.16
g__Sutterella	0.35	0.27	0.29	0.21	0.28
f__Lachnospiraceae;g__unassigned genus 1	3.82	4.25	4.08	4.61	3.89
f__Lachnospiraceae;g__unassigned genus 2	0.50	0.47	0.48	0.59	0.52
f__Ruminococcaceae;g__unassigned genus 1	0.84	0.76	0.84	0.77	0.86
f__Ruminococcaceae;g__unassigned genus 2	0.24	0.22	0.22	0.16	0.20
Donor 5	**BK**	**CL**	**GMG**	**IN**	**MOR**
g__[Eubacterium] coprostanoligenes group	0.70	0.94	0.73	0.98	0.93
g__[Eubacterium] hallii group	1.06	1.45	1.30	1.66	1.12
g__[Ruminococcus] torques group	0.98	1.02	0.83	1.09	0.96
g__Alistipes	1.23	1.33	1.60	1.50	1.42
g__Anaerostipes	1.22	1.91	1.20	1.71	1.22
g__Bacteroides	6.87	7.96	7.08	6.88	7.51
g__Bifidobacterium	2.93	3.07	2.88	3.33	2.94
g__Blautia	2.72	2.78	2.06	3.12	2.45
g__Butyricicoccus	0.33	0.36	0.44	0.40	0.34
g__Christensenellaceae R-7 group	1.56	1.01	1.27	1.03	1.05
g__Clostridium sensu stricto 1	0.94	0.98	0.77	1.08	0.61
g__Coprococcus 3	0.27	0.38	0.19	0.38	0.33
g__Dialister	4.85	4.37	6.03	4.83	4.60
g__Dorea	4.55	5.71	2.98	6.00	4.38
g__Faecalibacterium	10.14	9.65	10.11	8.70	9.93
g__Fusicatenibacter	2.02	2.48	1.29	2.62	1.86
g__Lachnoclostridium	0.34	0.41	0.30	0.36	0.35
g__Lachnospira	0.88	0.94	0.79	0.97	1.04
g__Lachnospiraceae NK4A136 group	0.78	0.74	0.47	0.54	0.72
g__Parabacteroides	1.87	1.94	2.03	2.22	1.95
g__Phascolarctobacterium	0.03	0.05	0.05	0.04	0.04
g__Roseburia	2.48	2.41	2.46	2.34	2.47
g__Ruminiclostridium 9	0.20	0.21	0.21	0.20	0.22
g__Ruminococcaceae NK4A214 group	0.13	0.09	0.13	0.12	0.11
g__Ruminococcaceae UCG-002	2.40	2.47	2.77	2.32	2.46
g__Ruminococcaceae UCG-005	0.68	0.66	0.74	0.63	0.70
g__Ruminococcaceae UCG-010	0.12	0.08	0.20	0.08	0.20
g__Ruminococcaceae UCG-014	1.71	1.90	2.05	1.63	1.68
g__Ruminococcus 1	0.96	0.41	0.55	0.35	0.39
g__Ruminococcus 2	2.26	2.42	3.00	2.77	2.32
g__Subdoligranulum	1.71	1.60	1.95	1.72	1.73
g__Sutterella	1.20	1.14	1.00	0.79	1.29
f__Lachnospiraceae;g__unassigned genus 1	1.68	1.33	1.53	1.50	1.45
f__Lachnospiraceae;g__unassigned genus 2	0.39	0.43	0.24	0.47	0.41
f__Ruminococcaceae;g__unassigned genus 1	0.55	0.66	0.63	0.52	0.55
f__Ruminococcaceae;g__unassigned genus 2	0.03	0.06	0.04	0.04	0.05
Donor 6	**BK**	**CL**	**GMG**	**IN**	**MOR**
g__[Eubacterium] coprostanoligenes group	0.75	0.69	0.70	0.60	0.69
g__[Eubacterium] hallii group	3.03	3.17	3.13	3.34	2.46
g__[Ruminococcus] torques group	0.94	1.01	0.89	1.03	1.22

g__Alistipes	3.94	3.95	4.04	3.58	3.66
g__Anaerostipes	1.43	1.58	1.59	1.62	1.37
g__Bacteroides	22.73	20.90	22.36	20.43	20.16
g__Bifidobacterium	7.70	7.34	7.67	7.92	7.59
g__Blautia	3.26	3.20	2.88	3.56	3.90
g__Butyricicoccus	0.90	1.00	0.98	1.00	0.87
g__Christensenellaceae R-7 group	0.26	0.25	0.24	0.26	0.24
g__Clostridium sensu stricto 1	0.06	0.09	0.08	0.08	0.06
g__Coprococcus 3	0.70	0.59	0.66	0.67	0.68
g__Dialister	2.35	2.41	2.40	2.65	1.76
g__Dorea	0.88	0.93	0.94	1.03	0.99
g__Faecalibacterium	12.81	13.71	12.17	13.50	14.45
g__Fusicatenibacter	2.79	3.12	2.74	2.91	3.46
g__Lachnoclostridium	0.49	0.55	0.59	0.60	0.66
g__Lachnospira	1.30	1.54	1.30	1.50	1.69
g__Lachnospiraceae NK4A136 group	0.08	0.05	0.07	0.07	0.09
g__Parabacteroides	1.30	1.10	1.12	0.93	0.78
g__Phascolarctobacterium	0.00	0.00	0.00	0.00	0.00
g__Roseburia	1.75	1.79	1.50	1.96	1.93
g__Ruminiclostridium 9	0.05	0.05	0.04	0.04	0.06
g__Ruminococcaceae NK4A214 group	0.58	0.63	0.67	0.68	0.68
g__Ruminococcaceae UCG-002	0.99	0.94	1.09	0.89	1.04
g__Ruminococcaceae UCG-005	0.05	0.04	0.05	0.05	0.04
g__Ruminococcaceae UCG-010	0.00	0.00	0.01	0.00	0.00
g__Ruminococcaceae UCG-014	0.00	0.00	0.00	0.00	0.00
g__Ruminococcus 1	2.56	3.34	3.03	2.50	3.35
g__Ruminococcus 2	1.72	1.66	1.76	1.56	1.78
g__Subdoligranulum	5.54	5.84	5.59	5.74	6.02
g__Sutterella	1.49	1.33	1.44	1.23	1.13
f__Lachnospiraceae;g__unassigned genus 1	3.77	4.23	4.17	4.18	5.07
f__Lachnospiraceae;g__unassigned genus 2	0.53	0.65	0.60	0.63	0.65
f__Ruminococcaceae;g__unassigned genus 1	0.45	0.51	0.44	0.50	0.45
f__Ruminococcaceae;g__unassigned genus 2	0.00	0.01	0.06	0.01	0.01
Donor 7	**BK**	**CL**	**GMG**	**IN**	**MOR**
g__[Eubacterium] coprostanoligenes group	0.00	0.00	0.00	0.03	0.00
g__[Eubacterium] hallii group	0.99	1.13	1.13	1.38	0.94
g__[Ruminococcus] torques group	0.79	0.57	0.87	0.41	0.68
g__Alistipes	0.29	0.24	0.28	0.38	0.28
g__Anaerostipes	2.49	3.33	3.66	2.78	2.83
g__Bacteroides	6.11	6.52	6.39	7.50	5.72
g__Bifidobacterium	33.75	31.64	28.23	33.46	40.48
g__Blautia	9.44	7.01	10.46	5.01	6.08
g__Butyricicoccus	2.39	3.06	2.62	2.93	2.07
g__Christensenellaceae R-7 group	0.10	0.14	0.13	0.16	0.08
g__Clostridium sensu stricto 1	1.78	0.97	0.86	2.03	2.35
g__Coprococcus 3	0.50	0.29	0.52	0.32	0.43
g__Dialister	0.84	0.86	1.23	0.89	0.50
g__Dorea	1.12	0.87	1.43	0.63	0.80

g__Faecalibacterium	7.61	9.09	7.76	8.81	7.43
g__Fusicatenibacter	4.09	3.45	4.24	2.95	3.53
g__Lachnoclostridium	0.76	0.81	0.94	0.63	0.71
g__Lachnospira	2.02	2.32	2.09	2.55	2.13
g__Lachnospiraceae NK4A136 group	0.25	0.18	0.28	0.23	0.30
g__Parabacteroides	1.71	1.70	1.69	1.82	1.45
g__Phascolarctobacterium	0.00	0.00	0.00	0.00	0.00
g__Roseburia	2.07	2.56	2.21	2.42	2.44
g__Ruminiclostridium 9	0.00	0.01	0.01	0.01	0.01
g__Ruminococcaceae NK4A214 group	0.02	0.01	0.03	0.06	0.03
g__Ruminococcaceae UCG-002	0.03	0.03	0.03	0.07	0.03
g__Ruminococcaceae UCG-005	0.01	0.01	0.02	0.02	0.02
g__Ruminococcaceae UCG-010	0.00	0.00	0.00	0.00	0.00
g__Ruminococcaceae UCG-014	0.95	1.14	1.04	0.91	0.75
g__Ruminococcus 1	0.00	0.00	0.00	0.13	0.00
g__Ruminococcus 2	0.00	0.00	0.00	0.08	0.00
g__Subdoligranulum	3.31	3.49	3.61	4.00	3.11
g__Sutterella	0.96	1.16	1.06	0.94	0.68
f__Lachnospiraceae;g__unassigned genus 1	8.16	9.66	9.66	8.25	6.75
f__Lachnospiraceae;g__unassigned genus 2	0.26	0.25	0.36	0.17	0.20
f__Ruminococcaceae;g__unassigned genus 1	0.02	0.01	0.03	0.02	0.02
f__Ruminococcaceae;g__unassigned genus 2	0.00	0.00	0.00	0.00	0.00

Table S3. Glucosinolates concentration (mg/L) in Moringa (MOR, **A**), glucomoringin (GMG, **B**), blank (BK, **C**), cellulose (CL, **D**) and inulin (IN, **E**) supernatants quantified by LC-MS/MS and normalized according to fermentation volume. Data represent the mean and standard deviation (SD) starting from T0 (inoculation time) and after 30 min (T0.5), 1 (T1), 2 (T2), 5 (T5) and 8 (T8) hours of fecal fermentation. Glucoraphanin, sinigrin, gluconapin, glucobrassicin, glucoiberin, glucocherolin, progoitrin, gluconasturtin, glucoiberverin, glucoalysis, 4-hydroxyglucobrassicin, 4-methoxyglucobrassicin, neoglucobrassicin and sulforaphane are not shown, since they were not detected in ≥ 70% of the samples.

A.	**MOR fermentation**					
	T0	**T0.5**	**T1**	**T2**	**T5**	**T8**
Sinalbin						
mean	0.000	0.000	0.000	0.000	0.000	0.000
SD	0.000	0.000	0.000	0.000	0.000	0.000
Glucotropaeolin						
mean	0.000	0.000	0.000	0.000	0.000	0.000
SD	0.000	0.000	0.000	0.000	0.000	0.000
Glucobrassicanapin						
mean	0.005	0.006	0.003	0.011	0.005	0.012
SD	0.008	0.008	0.005	0.008	0.009	0.016
Moringin						
mean	13.094	13.668	3.740	15.853	5.469	16.424
SD	13.293	14.869	5.452	11.859	8.534	17.322
Glucomoringin						
mean	0.009	0.013	0.029	0.002	0.012	0.007
SD	0.016	0.023	0.020	0.004	0.012	0.009
B.	**GMG fermentation**					
	T0	**T0.5**	**T1**	**T2**	**T5**	**T8**
Sinalbin						
mean	18.146	41.083	36.852	35.647	22.744	55.896
SD	18.338	26.908	35.960	30.743	39.060	85.356
Glucotropaeolin						
mean	1.417	1.800	0.582	0.755	0.601	0.555
SD	1.347	0.893	0.816	0.772	1.013	0.702
Glucobrassicanapin						
mean	0.004	0.037	0.005	0.012	0.044	0.027
SD	0.005	0.074	0.007	0.024	0.106	0.056
Moringin						
mean	0.188	0.475	0.831	14.398	41.021	1.728
SD	0.194	0.277	1.288	31.530	69.409	2.028
Glucomoringin						
mean	429.160	531.636	367.713	354.105	159.400	295.433
SD	419.654	245.438	346.867	235.973	241.639	377.222
C.	**BK fermentation**					
	T0	**T0.5**	**T1**	**T2**	**T5**	**T8**
Sinalbin						
mean	0.000	0.000	0.002	0.000	0.000	0.000
SD	0.000	0.000	0.005	0.000	0.000	0.000
Glucotropaeolin						

mean	0.000	0.000	0.000	0.000	0.000	0.000
SD	0.000	0.000	0.000	0.000	0.000	0.000
Glucobrassicanapin						
mean	0.012	0.018	0.010	0.007	0.003	0.007
SD	0.009	0.020	0.011	0.016	0.003	0.014
Moringin						
mean	0.387	0.430	0.354	0.182	0.310	0.429
SD	0.613	0.632	0.608	0.276	0.481	0.695
Glucomoringin						
mean	0.054	0.052	0.026	0.012	0.019	0.005
SD	0.063	0.056	0.040	0.018	0.021	0.008
D.			**CL fermentation**			
	T0	**T0.5**	**T1**	**T2**	**T5**	**T8**
Sinalbin						
mean	0.000	0.000	0.004	0.008	0.000	0.000
SD	0.000	0.000	0.011	0.014	0.000	0.000
Glucotropaeolin						
mean	0.000	0.000	0.000	0.000	0.000	0.000
SD	0.000	0.000	0.000	0.000	0.000	0.000
Glucobrassicanapin						
mean	0.005	0.007	0.002	0.003	0.002	0.002
SD	0.006	0.007	0.003	0.005	0.004	0.004
Moringin						
mean	0.122	0.155	0.187	0.134	0.002	0.085
SD	0.179	0.212	0.245	0.246	0.006	0.211
Glucomoringin						
mean	0.087	0.069	0.091	0.116	0.012	0.020
SD	0.066	0.069	0.085	0.219	0.012	0.011
E.			**IN fermentation**			
	T0	**T0.5**	**T1**	**T2**	**T5**	**T8**
Sinalbin						
mean	0.006	0.007	0.009	0.014	0.022	0.000
SD	0.010	0.018	0.024	0.025	0.042	0.000
Glucotropaeolin						
mean	0.000	0.000	0.000	0.000	0.000	0.000
SD	0.000	0.000	0.000	0.000	0.000	0.000
Glucobrassicanapin						
mean	0.017	0.012	0.008	0.008	0.010	0.002
SD	0.027	0.016	0.013	0.010	0.018	0.005
Moringin						
mean	0.326	0.301	0.169	0.247	0.195	0.010
SD	0.519	0.483	0.250	0.654	0.368	0.025
Glucomoringin						
mean	0.160	0.105	0.086	0.064	0.066	0.021
SD	0.151	0.151	0.098	0.097	0.104	0.009

Table S4. Polyphenols concentration (mg/L) in Moringa (MOR, **A**), glucomoringin (GMG, **B**), blank (BK, **C**), cellulose (CL, **D**) and inulin (IN, **E**) supernatants quantified by LC-MS/MS and normalized according to fermentation volume. Data represent the mean and standard deviation (SD) starting from T0 (inoculation time) and after 30 min (T0.5), 1 (T1), 2 (T2), 5 (T5) and 8 (T8) hours of fecal fermentation. Caffeic acid, catechin, cinnamic acid, p-coumaric acid, synapyl alcohol, syringaldehyde and indole-3-carbinol are not shown, since they were not detected in ≥ 70% of the samples.

A.	**MOR fermentation**					
	T0	**T0.5**	**T1**	**T2**	**T5**	**T8**
4-aminobenzoic acid						
mean	0.573	0.544	0.240	0.677	0.167	0.591
SD	0.434	0.572	0.325	0.169	0.298	0.469
Ferulic acid						
mean	0.099	0.044	0.019	0.024	0.013	0.018
SD	0.099	0.071	0.036	0.030	0.029	0.028
Isorhamnetin-3-glucoside						
mean	1.295	0.898	0.305	0.289	0.092	0.054
SD	1.099	1.178	0.731	0.654	0.238	0.141
Quercetin-3-glucoside						
mean	17.591	12.131	4.023	4.076	1.624	0.790
SD	14.885	14.775	9.705	8.913	4.279	1.977
Quercetin-3,4'-diglucoside						
mean	0.548	0.303	0.179	0.184	0.034	0.039
SD	0.574	0.451	0.399	0.376	0.025	0.021
Sinapic acid						
mean	0.013	0.013	0.005	0.013	0.004	0.009
SD	0.013	0.014	0.007	0.011	0.008	0.011
Syringic acid						
mean	0.066	0.069	0.030	0.088	0.019	0.062
SD	0.049	0.071	0.036	0.066	0.034	0.106
Chlorogenic acid						
mean	0.076	0.029	0.057	0.042	0.040	0.005
SD	0.183	0.064	0.111	0.099	0.094	0.002
Neochlorogenic acid						
mean	0.250	0.292	0.176	0.479	0.379	0.157
SD	0.223	0.421	0.240	0.296	0.974	0.152
Cryptochlorogenic acid						
mean	0.044	0.036	0.030	0.039	0.075	0.007
SD	0.044	0.060	0.042	0.067	0.195	0.010
B.	**GMG fermentation**					
	T0	**T0.5**	**T1**	**T2**	**T5**	**T8**
4-aminobenzoic acid						
mean	0.457	0.889	0.389	0.496	0.674	0.498
SD	0.436	0.461	0.408	0.289	0.310	0.544
Ferulic acid						
mean	0.006	0.011	0.004	0.005	0.006	0.006
SD	0.007	0.012	0.005	0.003	0.007	0.005
Isorhamnetin-3-glucoside						

mean	0.000	0.000	0.000	0.000	0.000	0.000
SD	0.000	0.000	0.000	0.000	0.000	0.000
Quercetin-3-glucoside						
mean	0.002	0.005	0.002	0.002	0.003	0.002
SD	0.002	0.004	0.001	0.001	0.001	0.000
Quercetin-3,4'-diglucoside						
mean	0.030	0.033	0.025	0.028	0.032	0.029
SD	0.004	0.006	0.012	0.003	0.005	0.006
Sinapic acid						
mean	0.005	0.014	0.003	0.004	0.008	0.003
SD	0.007	0.016	0.003	0.004	0.012	0.004
Syringic acid						
mean	0.066	0.119	0.028	0.047	0.070	0.034
SD	0.070	0.096	0.024	0.046	0.081	0.057
Chlorogenic acid						
mean	0.006	0.250	0.006	0.014	0.010	0.006
SD	0.002	0.646	0.002	0.019	0.009	0.002
Neochlorogenic acid						
mean	0.003	0.029	0.004	0.004	0.008	0.003
SD	0.003	0.067	0.003	0.004	0.011	0.005
Cryptochlorogenic acid						
mean	0.002	0.021	0.002	0.004	0.006	0.002
SD	0.001	0.048	0.002	0.003	0.008	0.002
C.	**BK fermentation**					
	T0	**T0.5**	**T1**	**T2**	**T5**	**T8**
4-aminobenzoic acid						
mean	0.880	0.756	0.852	0.317	0.733	0.681
SD	0.482	0.407	0.173	0.298	0.643	0.641
Ferulic acid						
mean	0.006	0.008	0.006	0.004	0.007	0.005
SD	0.004	0.007	0.005	0.005	0.005	0.004
Isorhamnetin-3-glucoside						
mean	0.000	0.000	0.000	0.001	0.001	0.001
SD	0.001	0.001	0.000	0.001	0.001	0.001
Quercetin-3-glucoside						
mean	0.005	0.007	0.005	0.003	0.004	0.003
SD	0.003	0.004	0.004	0.003	0.001	0.001
Quercetin-3,4'-diglucoside						
mean	0.033	0.033	0.036	0.028	0.028	0.029
SD	0.004	0.004	0.002	0.005	0.013	0.005
Sinapic acid						
mean	0.005	0.007	0.007	0.003	0.006	0.004
SD	0.005	0.007	0.005	0.006	0.009	0.004
Syringic acid						
mean	0.114	0.089	0.089	0.032	0.041	0.066
SD	0.090	0.058	0.053	0.026	0.045	0.148
Chlorogenic acid						

mean	0.005	0.140	0.086	0.027	0.007	0.006
SD	0.002	0.358	0.205	0.056	0.003	0.002
Neochlorogenic acid						
mean	0.000	0.012	0.013	0.009	0.005	0.004
SD	0.000	0.026	0.021	0.017	0.010	0.004
Cryptochlorogenic acid						
mean	0.003	0.014	0.011	0.008	0.004	0.002
SD	0.001	0.033	0.019	0.017	0.003	0.001
D.	**CL fermentation**					
	T0	**T0.5**	**T1**	**T2**	**T5**	**T8**
4-aminobenzoic acid						
mean	0.565	0.554	0.242	0.363	0.137	0.165
SD	0.402	0.250	0.294	0.343	0.264	0.250
Ferulic acid						
mean	0.005	0.005	0.002	0.003	0.002	0.003
SD	0.005	0.004	0.002	0.003	0.004	0.003
Isorhamnetin-3-glucoside						
mean	0.001	0.000	0.002	0.001	0.002	0.001
SD	0.001	0.001	0.001	0.001	0.001	0.001
Quercetin-3-glucoside						
mean	0.003	0.003	0.003	0.002	0.003	0.002
SD	0.002	0.001	0.001	0.001	0.001	0.001
Quercetin-3,4'-diglucoside						
mean	0.031	0.030	0.028	0.028	0.026	0.026
SD	0.006	0.004	0.003	0.004	0.005	0.003
Sinapic acid						
mean	0.004	0.004	0.002	0.002	0.003	0.003
SD	0.004	0.004	0.003	0.003	0.008	0.005
Syringic acid						
mean	0.069	0.056	0.024	0.027	0.017	0.013
SD	0.054	0.024	0.023	0.024	0.028	0.016
Chlorogenic acid						
mean	0.198	0.135	0.031	0.006	0.011	0.005
SD	0.508	0.334	0.067	0.003	0.016	0.002
Neochlorogenic acid						
mean	0.010	0.012	0.004	0.003	0.005	0.003
SD	0.021	0.018	0.006	0.004	0.011	0.005
Cryptochlorogenic acid						
mean	0.010	0.012	0.004	0.002	0.005	0.002
SD	0.022	0.023	0.006	0.002	0.009	0.002
E.	**IN fermentation**					
	T0	**T0.5**	**T1**	**T2**	**T5**	**T8**
4-aminobenzoic acid						
mean	0.705	0.495	0.438	0.466	0.429	0.038
SD	0.275	0.403	0.347	0.323	0.396	0.091
Ferulic acid						
mean	0.009	0.005	0.006	0.007	0.011	0.002

SD	0.011	0.006	0.007	0.012	0.020	0.002
Isorhamnetin-3-glucoside						
mean	0.001	0.001	0.001	0.001	0.001	0.002
SD	0.002	0.001	0.001	0.001	0.001	0.001
Quercetin-3-glucoside						
mean	0.003	0.003	0.004	0.003	0.003	0.002
SD	0.001	0.001	0.002	0.001	0.001	0.001
Quercetin-3,4'-diglucoside						
mean	0.036	0.033	0.032	0.030	0.033	0.028
SD	0.006	0.007	0.006	0.007	0.010	0.008
Sinapic acid						
mean	0.008	0.005	0.005	0.008	0.013	0.001
SD	0.010	0.006	0.008	0.014	0.032	0.003
Syringic acid						
mean	0.085	0.053	0.038	0.043	0.021	0.006
SD	0.035	0.039	0.029	0.037	0.031	0.008
Chlorogenic acid						
mean	0.441	0.483	0.484	0.544	0.129	0.115
SD	1.149	1.264	1.268	1.425	0.329	0.293
Neochlorogenic acid						
mean	0.023	0.023	0.022	0.031	0.041	0.023
SD	0.051	0.058	0.050	0.080	0.103	0.062
Cryptochlorogenic acid						
mean	0.028	0.031	0.033	0.038	0.044	0.038
SD	0.067	0.076	0.083	0.095	0.112	0.097

References

1. Abd Rani NZ, Husain K, Kumolosasi E. Moringa Genus: A Review of Phytochemistry and Pharmacology. Front Pharmacol. 2018 Feb 16;9:108.

2. Anwar F, Bhanger MI. Analytical Characterization of *Moringa oleifera* Seed Oil Grown in Temperate Regions of Pakistan. J Agric Food Chem. 2003 Oct 1;51(22):6558–63.

3. Kuete V, editor. Medicinal spices and vegetables from Africa: therapeutic potential against metabolic, inflammatory, infectious and systemic diseases. Amsterdam: Academic Press, an impring of Elsevier; 2017. 669 p.

4. Fahey J. Microbiological Monitoring of Laboratory Mice. In: Sundberg J, editor. Genetically Engineered Mice Handbook [Internet]. CRC Press; 2005 [cited 2021 Oct 1]. p. 157–64. (Research Methods For Mutant Mice; vol. 20051540). Available from: http://www.crcnetbase.com/doi/abs/10.1201/9781420039078.ch12

5. Gopalan C, Rama SBV, Balasubramanian S. Nutritive value of Indian foods. Hyderabad, India: National Institute of Nutrition, Indian Council of Medial Research; 1978.

6. Makkar HPS, Becker K. Nutrional value and antinutritional components of whole and ethanol extracted Moringa oleifera leaves. Animal Feed Science and Technology. 1996 Dec;63(1–4):211–28.

7. Zongo U, Zoungrana SL, Savadogo A, Traoré AS. Nutritional and Clinical Rehabilitation of Severely Malnourished Children with <i>Moringa oleifera Lam</i>. Leaf Powder in Ouagadougou (Burkina Faso). FNS. 2013;04(09):991–7.

8. Thurber MD, Fahey JW. Adoption of *Moringa oleifera* to Combat Under-Nutrition Viewed Through the Lens of the "Diffusion of Innovations" Theory. Ecology of Food and Nutrition. 2009 May 7;48(3):212–25.

9. Sahay S, Yadav U, Srinivasamurthy S. Potential of Moringa oleifera as a functional food ingredient: a review. 2017 Sep;2(5):31–7.

10. Fard M, Arulselvan P, Karthivashan G, Adam S, Fakurazi S. Bioactive extract from moringa oleifera inhibits the pro-inflammatory mediators in lipopolysaccharide stimulated macrophages. Phcog Mag. 2015;11(44):556.

11. Waterman C, Cheng DM, Rojas-Silva P, Poulev A, Dreifus J, Lila MA, et al. Stable, water extractable isothiocyanates from Moringa oleifera leaves attenuate inflammation in vitro. Phytochemistry. 2014 Jul;103:114–22.

12. Villarruel-López A, López-de la Mora DA, Vázquez-Paulino OD, Puebla-Mora AG, Torres-Vitela MR, Guerrero-Quiroz LA, et al. Effect of Moringa oleifera consumption on diabetic rats. BMC Complement Altern Med. 2018 Dec;18(1):127.

13. Syahputri V, Budhy TI, Sumaryono B. The potential of ethanolic extract of Moringa oleifera leaves on HSF1 expression in oral cancer induced by benzo[a]pyrene. Dent J (Maj Ked Gigi). 2020 Jun 30;53(2):107.

14. Luetragoon T, Pankla Sranujit R, Noysang C, Thongsri Y, Potup P, Suphrom N, et al. Anti-Cancer Effect of 3-Hydroxy-β-Ionone Identified from Moringa oleifera Lam. Leaf on Human Squamous Cell Carcinoma 15 Cell Line. Molecules. 2020 Aug 5;25(16):3563.

15. Viera GHF, Mourão JA, Ângelo ÂM, Costa RA, Vieira RHS dos F. Antibacterial effect (in vitro) of Moringa oleifera and Annona muricata against Gram positive and Gram negative bacteria. Rev Inst Med trop S Paulo. 2010 Jun;52(3):129–32.

16. Leone A, Fiorillo G, Criscuoli F, Ravasenghi S, Santagostini L, Fico G, et al. Nutritional Characterization and Phenolic Profiling of Moringa oleifera Leaves Grown in Chad, Sahrawi Refugee Camps, and Haiti. IJMS. 2015 Aug 12;16(8):18923–37.

17. Tumer TB, Rojas-Silva P, Poulev A, Raskin I, Waterman C. Direct and Indirect Antioxidant Activity of Polyphenol- and Isothiocyanate-Enriched Fractions from *Moringa oleifera*. J Agric Food Chem. 2015 Feb 11;63(5):1505–13.

18. Mbikay M. Therapeutic Potential of Moringa oleifera Leaves in Chronic Hyperglycemia and Dyslipidemia: A Review. Front Pharmacol [Internet]. 2012 [cited 2021 Oct 1];3. Available from: http://journal.frontiersin.org/article/10.3389/fphar.2012.00024/abstract

19. Hanlon N, Coldham N, Sauer MJ, Ioannides C. Up-regulation of the CYP1 family in rat and human liver by the aliphatic isothiocyanates erucin and sulforaphane. Toxicology. 2008 Oct;252(1–3):92–8.

20. McWalter GK, Higgins LG, McLellan LI, Henderson CJ, Song L, Thornalley PJ, et al. Transcription Factor Nrf2 Is Essential for Induction of NAD(P)H:Quinone Oxidoreductase 1, Glutathione S-Transferases, and Glutamate Cysteine Ligase by Broccoli Seeds and Isothiocyanates. The Journal of Nutrition. 2004 Dec 1;134(12):3499S-3506S.

21. Szliszka E, Krol W. The role of dietary polyphenols in tumor necrosis factor-related apoptosis inducing ligand (TRAIL)-induced apoptosis for cancer chemoprevention. European Journal of Cancer Prevention. 2011 Jan;20(1):63–9.

22. Du L, Li J, Zhang X, Wang L, Zhang W, Yang M, et al. Pomegranate peel polyphenols inhibits inflammation in LPS-induced RAW264.7 macrophages via the suppression of TLR4/NF-κB pathway activation. Food & Nutrition Research [Internet]. 2019 Apr 23 [cited 2021 Aug 18];63(0). Available from: http://www.foodandnutritionresearch.net/index.php/fnr/article/view/3392

23. Mahn A, Castillo A. Potential of Sulforaphane as a Natural Immune System Enhancer: A Review. Molecules. 2021 Feb 1;26(3):752.

24. Galuppo M, Nicola G, Iori R, Dell'Utri P, Bramanti P, Mazzon E. Antibacterial Activity of Glucomoringin Bioactivated with Myrosinase against Two Important Pathogens Affecting the Health of Long-Term Patients in Hospitals. Molecules. 2013 Nov 20;18(11):14340–8.

25. Borgonovo G, De Petrocellis L, Schiano Moriello A, Bertoli S, Leone A, Battezzati A, et al. Moringin, A Stable Isothiocyanate from Moringa oleifera, Activates the Somatosensory and Pain Receptor TRPA1 Channel In Vitro. Molecules. 2020 Feb 22;25(4):976.

26. Jaja-Chimedza A, Graf BL, Simmler C, Kim Y, Kuhn P, Pauli GF, et al. Biochemical characterization and anti-inflammatory properties of an isothiocyanate-enriched moringa (Moringa oleifera) seed extract. Hsieh Y-H, editor. PLoS ONE. 2017 Aug 8;12(8):e0182658.

27. Rajan TS, De Nicola GR, Iori R, Rollin P, Bramanti P, Mazzon E. Anticancer activity of glucomoringin isothiocyanate in human malignant astrocytoma cells. Fitoterapia. 2016 Apr;110:1–7.

28. Jaja-Chimedza A, Zhang L, Wolff K, Graf BL, Kuhn P, Moskal K, et al. A dietary isothiocyanate-enriched moringa (Moringa oleifera) seed extract improves glucose tolerance in a high-fat-diet mouse model and modulates the gut microbiome. Journal of Functional Foods. 2018 Aug;47:376–85.

29. Kim Y, Wu AG, Jaja-Chimedza A, Graf BL, Waterman C, Verzi MP, et al. Isothiocyanate-enriched moringa seed extract alleviates ulcerative colitis symptoms in mice. Hsieh Y-H, editor. PLoS ONE. 2017 Sep 18;12(9):e0184709.

30. Chassaing B, Aitken JD, Malleshappa M, Vijay-Kumar M. Dextran Sulfate Sodium (DSS)-Induced Colitis in Mice. Current Protocols in Immunology [Internet]. 2014 Feb [cited 2021 Oct 16];104(1). Available from: https://onlinelibrary.wiley.com/doi/10.1002/0471142735.im1525s104

31. Cuellar-Núñez ML, Gonzalez de Mejia E, Loarca-Piña G. Moringa oleifera leaves alleviated inflammation through downregulation of IL-2, IL-6, and TNF-α in a colitis-associated colorectal cancer model. Food Research International. 2021 Jun;144:110318.

32. Cuellar-Nuñez ML, Luzardo-Ocampo I, Campos-Vega R, Gallegos-Corona MA, González de Mejía E, Loarca-Piña G. Physicochemical and nutraceutical properties of moringa (Moringa oleifera

) leaves and their effects in an in vivo AOM/DSS-induced colorectal carcinogenesis model. Food Research International. 2018 Mar;105:159–68.

33. Monagas M, Urpi-Sarda M, Sánchez-Patán F, Llorach R, Garrido I, Gómez-Cordovés C, et al. Insights into the metabolism and microbial biotransformation of dietary flavan-3-ols and the bioactivity of their metabolites. Food Funct. 2010;1(3):233.

34. Ozdal T, Sela DA, Xiao J, Boyacioglu D, Chen F, Capanoglu E. The Reciprocal Interactions between Polyphenols and Gut Microbiota and Effects on Bioaccessibility. Nutrients. 2016 Feb 6;8(2):78.

35. Manach C, Scalbert A, Morand C, Rémésy C, Jiménez L. Polyphenols: food sources and bioavailability. The American Journal of Clinical Nutrition. 2004 May 1;79(5):727–47.

36. Barba FJ, Nikmaram N, Roohinejad S, Khelfa A, Zhu Z, Koubaa M. Bioavailability of Glucosinolates and Their Breakdown Products: Impact of Processing. Front Nutr [Internet]. 2016 Aug 16 [cited 2021 Oct 26];3. Available from: http://journal.frontiersin.org/Article/10.3389/fnut.2016.00024/abstract

37. Liou CS, Sirk SJ, Diaz CAC, Klein AP, Fischer CR, Higginbottom SK, et al. A Metabolic Pathway for Activation of Dietary Glucosinolates by a Human Gut Symbiont. Cell. 2020 Feb;180(4):717-728.e19.

38. Luang-In V, Albaser AA, Nueno-Palop C, Bennett MH, Narbad A, Rossiter JT. Glucosinolate and Desulfo-glucosinolate Metabolism by a Selection of Human Gut Bacteria. Curr Microbiol. 2016 Sep;73(3):442–51.

39. Luang-In V, Narbad A, Nueno-Palop C, Mithen R, Bennett M, Rossiter JT. The metabolism of methylsulfinylalkyl- and methylthioalkyl-glucosinolates by a selection of human gut bacteria. Mol Nutr Food Res. 2014 Apr;58(4):875–83.

40. Cheng D-L, Hashimoto K, Uda Y. In vitro digestion of sinigrin and glucotropaeolin by single strains of Bifidobacterium and identification of the digestive products. Food and Chemical Toxicology. 2004 Mar;42(3):351–7.

41. Liu X, Wang Y, Hoeflinger J, Neme B, Jeffery E, Miller M. Dietary Broccoli Alters Rat Cecal Microbiota to Improve Glucoraphanin Hydrolysis to Bioactive Isothiocyanates. Nutrients. 2017 Mar 10;9(3):262.

42. Minekus M, Alminger M, Alvito P, Ballance S, Bohn T, Bourlieu C, et al. A standardised static *in vitro* digestion method suitable for food – an international consensus. Food Funct. 2014;5(6):1113–24.

43. Sánchez-Patán F, Cueva C, Monagas M, Walton GE, Gibson GRM, Quintanilla-López JE, et al. In vitro fermentation of a red wine extract by human gut microbiota: changes in microbial groups and formation of phenolic metabolites. J Agric Food Chem. 2012 Mar 7;60(9):2136–47.

44. Frayn KN. Metabolic Regulation: a Human Perspective. [Internet]. Somerset: Wiley; 2013 [cited 2022 Feb 3]. Available from: http://public.ebookcentral.proquest.com/choice/publicfullrecord.aspx?p=4037568

45. Klindworth A, Pruesse E, Schweer T, Peplies J, Quast C, Horn M, et al. Evaluation of general 16S ribosomal RNA gene PCR primers for classical and next-generation sequencing-based diversity studies. Nucleic Acids Research. 2013 Jan 1;41(1):e1–e1.

46. Bolyen E, Rideout JR, Dillon MR, Bokulich NA, Abnet CC, Al-Ghalith GA, et al. Reproducible, interactive, scalable and extensible microbiome data science using QIIME 2. Nat Biotechnol. 2019 Aug;37(8):852–7.

47. Quast C, Pruesse E, Yilmaz P, Gerken J, Schweer T, Yarza P, et al. The SILVA ribosomal RNA gene database project: improved data processing and web-based tools. Nucleic Acids Research. 2012 Nov 27;41(D1):D590–6.

48. McMurdie PJ, Holmes S. phyloseq: An R Package for Reproducible Interactive Analysis and Graphics of Microbiome Census Data. Watson M, editor. PLoS ONE. 2013 Apr 22;8(4):e61217.

49. Anderson RC, Cookson AL, McNabb WC, Park Z, McCann MJ, Kelly WJ, et al. Lactobacillus plantarum MB452 enhances the function of the intestinal barrier by increasing the expression levels of genes involved in tight junction formation. BMC Microbiol. 2010;10(1):316.

50. Coates EM, Popa G, Gill CI, McCann MJ, McDougall GJ, Stewart D, et al. Colon-available raspberry polyphenols exhibit anti-cancer effects on in vitro models of colon cancer. J Carcinog. 2007;6(1):4.

51. Srinivasan B, Kolli AR, Esch MB, Abaci HE, Shuler ML, Hickman JJ. TEER Measurement Techniques for In Vitro Barrier Model Systems. J Lab Autom. 2015 Apr;20(2):107–26.

52. Oksanen J, Blanchet G, Kindt R, Legendre P, Minchin P, O'Hara B, et al. Vegan: Community Ecology Package. R Package Version 22-1. 2015;2:1–2.

53. Lopez-Rodriguez NA, Gaytán-Martínez M, de la Luz Reyes-Vega M, Loarca-Piña G. Glucosinolates and Isothiocyanates from Moringa oleifera: Chemical and Biological Approaches. Plant Foods Hum Nutr. 2020 Dec;75(4):447–57.

54. Sultana S. Nutritional and functional properties of Moringa oleifera. Metabolism Open. 2020 Dec;8:100061.

55. Masih LP, Singh S, Elamathi S, Anandhi P, Abraham T. Moringa: A multipurpose potential crop – A review. PINSA [Internet]. 2019 May 24 [cited 2021 Oct 22]; Available from: http://insa.nic.in/writereaddata/UpLoadedFiles/PINSA/PINSA_2019_Art31.pdf

56. Walker AW, Ince J, Duncan SH, Webster LM, Holtrop G, Ze X, et al. Dominant and diet-responsive groups of bacteria within the human colonic microbiota. ISME J. 2011 Feb;5(2):220–30.

57. Salonen A, Lahti L, Salojärvi J, Holtrop G, Korpela K, Duncan SH, et al. Impact of diet and individual variation on intestinal microbiota composition and fermentation products in obese men. ISME J. 2014 Nov;8(11):2218–30.

58. Rodríguez-Pérez C, Quirantes-Piné R, Fernández-Gutiérrez A, Segura-Carretero A. Optimization of extraction method to obtain a phenolic compounds-rich extract from Moringa oleifera Lam leaves. Industrial Crops and Products. 2015 Apr;66:246–54.

59. Nizioł-Łukaszewska Z, Furman-Toczek D, Bujak T, Wasilewski T, Hordyjewicz-Baran Z. *Moringa oleifera L* . Extracts as Bioactive Ingredients That Increase Safety of Body Wash Cosmetics. Dermatology Research and Practice. 2020 Jul 1;2020:1–14.

60. Du L, Zhao M, Xu J, Qian D, Jiang S, Shang E, et al. Analysis of the Metabolites of Isorhamnetin 3 -*O* -Glucoside Produced by Human Intestinal Flora in Vitro by Applying Ultraperformance Liquid Chromatography/Quadrupole Time-of-Flight Mass Spectrometry. J Agric Food Chem. 2014 Mar 26;62(12):2489–95.

61. Sun J, Sun G, Meng X, Wang H, Luo Y, Qin M, et al. Isorhamnetin Protects against Doxorubicin-Induced Cardiotoxicity In Vivo and In Vitro. Kukreja R, editor. PLoS ONE. 2013 May 28;8(5):e64526.

62. Rungapamestry V, Duncan AJ, Fuller Z, Ratcliffe B. Effect of cooking brassica vegetables on the subsequent hydrolysis and metabolic fate of glucosinolates. Proc Nutr Soc. 2007 Feb;66(1):69–81.

63. Oliviero T, Verkerk R, Dekker M. Isothiocyanates from *Brassica* Vegetables-Effects of Processing, Cooking, Mastication, and Digestion. Mol Nutr Food Res. 2018 Sep;62(18):1701069.

64. Jaafaru MS, Nordin N, Shaari K, Rosli R, Abdull Razis AF. Isothiocyanate from Moringa oleifera seeds mitigates hydrogen peroxide-induced cytotoxicity and preserved morphological features of human neuronal cells. Gallyas F, editor. PLoS ONE. 2018 May 3;13(5):e0196403.

65. Jaafaru M, Abd Karim N, Mohamed Eliaser E, Maitalata Waziri P, Ahmed H, Mustapha Barau M, et al. Nontoxic Glucomoringin-Isothiocyanate (GMG-ITC) Rich Soluble Extract Induces Apoptosis and Inhibits Proliferation of Human Prostate Adenocarcinoma Cells (PC-3). Nutrients. 2018 Aug 27;10(9):1174.

66. Jang I-S, Kim D-H. Purification and Characterization of .ALPHA.-L-Rhamnosidase from Bacteroides JY-6, a Human Intestinal Bacterium. Biological & Pharmaceutical Bulletin. 1996;19(12):1546–9.

67. Boll M. Key enzymes in the anaerobic aromatic metabolism catalysing Birch-like reductions. Biochimica et Biophysica Acta (BBA) - Bioenergetics. 2005 Feb;1707(1):34–50.

68. Makita C, Chimuka L, Steenkamp P, Cukrowska E, Madala E. Comparative analyses of flavonoid content in Moringa oleifera and Moringa ovalifolia with the aid of UHPLC-qTOF-MS fingerprinting. South African Journal of Botany. 2016 Jul;105:116–22.

69. Parchem K, Piekarska A, Bartoszek A. Enzymatic activities behind degradation of glucosinolates. In: Glucosinolates: Properties, Recovery, and Applications [Internet]. Elsevier; 2020 [cited 2021 Oct 22]. p. 79–106. Available from: https://linkinghub.elsevier.com/retrieve/pii/B9780128164938000032

70. Robinson CS. THE HYDROGEN ION CONCENTRATION OF HUMAN FECES. Journal of Biological Chemistry. 1922 Jun;52(2):445–66.

71. Li F, Hullar MAJ, Schwarz Y, Lampe JW. Human Gut Bacterial Communities Are Altered by Addition of Cruciferous Vegetables to a Controlled Fruit- and Vegetable-Free Diet. The Journal of Nutrition. 2009 Sep 1;139(9):1685–91.

72. Palop MLl, Smiths JP, ten Brink B. Degradation of sinigrin by Lactobacillus agilis strain R16. International Journal of Food Microbiology. 1995 Jul;26(2):219–29.

73. Ghosh SS, Wang J, Yannie PJ, Ghosh S. Intestinal Barrier Dysfunction, LPS Translocation, and Disease Development. Journal of the Endocrine Society. 2020 Feb 1;4(2):bvz039.

74. Ghosh S, Whitley CS, Haribabu B, Jala VR. Regulation of Intestinal Barrier Function by Microbial Metabolites. Cellular and Molecular Gastroenterology and Hepatology. 2021;11(5):1463–82.

Chapter 5: Could fermented food boost our gut health? A study of Sauerkraut fermentation water.

Giulia Gaudioso[1,2], Tobias Weil[1], Giulia Marzorati[1], Pavel Solovyev[3], Luana Bontempo[3], Elena Franciosi[1], Kieran Michael Tuohy[1] and Francesca Fava[1].

[1] Nutrition and Nutrigenomics Unit, Department of Food Quality and Nutrition, Research and Innovation Center, Fondazione Edmund Mach, 38098 Trento, Italy

[2] CIBIO – Department of Cellular, Computational and Integrative Biology, University of Trento, 38123 Trento, Italy

[3] Traceability Unit, Department of Food Quality and Nutrition, Research and Innovation Center, Fondazione Edmund Mach, 38098 Trento, Italy.

Abstract

Sauerkraut is a traditionally fermented *Brassica* and recent evidence suggests it has beneficial properties for human health. In this work, we employed a multi-disciplinary approach to first characterize the fermentation process of locally produced, artisanal sauerkraut and then to measure the potential of sauerkraut water to improve gut health. Physicochemical measurements showed that temperature and pH were both dependent on microbial metabolism over the fermentation process. NMR analysis revealed significant changes in microbial metabolite profiles overall the fermentation process, with acetic and lactic acid being the dominant end-products of microbial fermentation. Viable bacterial count (CFU/mL) showed increased abundance of lactic acid bacteria (LAB) and 16S rRNA metagenomics results showed that bacterial diversity gradually decreased as the fermentation progressed, with microbial communities being shaped by the acidic and salty environmental conditions. A biobank of 88 different LAB isolates representing different biotypes was created for future evaluation of their biotechnological and probiotic potential. Moreover, we made use of an *in vitro* preclinical model of the intestinal mucosa to investigate the potential anti-inflammatory role of sauerkraut water and its ability to influence intestinal permeability. Although no differences were observed in gut barrier function as measured by trans-epithelial electrical potential of Caco-2 cell monolayers, sauerkraut water significantly modulated the inflammatory response in PBMCs cells under LPS stimulation. Sauerkraut water supported a robust inflammatory response to LPS, increasing TNF-α and IL-6 production while also stimulating the anti-inflammatory IL-10, thereby resolving the inflammatory response after 24 hours. This work suggests that sauerkraut water therefore may have potential to regulate intestinal immune function, supporting appropriate response to LPS/pathogen challenge but also contributing to switching off inflammation once mounted. This *in vitro* finding should be confirmed in human intervention trials in target populations at risk of intestinal inflammation, in order to get a better understanding of the role of sauerkraut water *in vivo*.

Authors contributions: Pavel Solovyev: NMR analysis, Tobias Weil: DNA extraction, sequencing and joint analysis with Giulia Gaudioso.

1. Introduction

Fermented foods and beverages are now estimated to account for 1/3 of human foods , regardless of culture and lifestyle and have been used for millennia as a means of food preservation and to improve the digestibility and nutritional content of foods (1,2). Food fermentation is a transformative process whereby starting raw materials are progressively modified by microbial consortia during their fermentative growth, producing organic acids, gasses (carbon dioxide, CO_2, and hydrogen) and resulting in energy production for the microorganisms involved. The organisms responsible for food fermentations can be spontaneously present in the starting raw materials or added as starter cultures for a more controlled food transformation (1–4). Fermentation of raw foods can lead to an enrichment of their nutritional properties by degrading anti-nutrients like phytates or breaking down recalcitrant food macromolecules. The end products of fermentation and other microbial metabolic reactions can enhance flavor and aroma in foods, and acid production during fermentation can inhibit acid sensitive spoilage or pathogenic microorganisms, thus increasing food safety and extending shelf-life (4). Amongst fermentative bacteria, lactic acid bacteria (LAB) especially *Lactobacillus*, *Leuconostoc*, *Pediococcus* and *Streptococcus* genera have been identified as the most important bacteria involved in food fermentations (5,6). Notably, some strains of these bacteria are potential probiotics as they fulfill the definition established by the Food and Agriculture Organization (FAO) and by the World Health Organization (WHO) as 'live microorganisms which when administered in adequate amounts confer a health benefit on the host' (7).

Although human clinical trials are still scarce, consumption of fermented foods has been linked to improved immune and metabolic function, protection against inflammation and decrease of fasting glycaemia in people with type 2 diabetes mellitus (8,9) in ways not always attributable to the starting food material. In fact, during food fermentation, bacterial metabolism converts fermentable substrates, mainly carbohydrates and proteins, into biologically active metabolites, including secondary metabolites generated by the fermentation process, such as short chain fatty acids (SCFAs) and biogenic amines. Microorganisms can also convert other macromolecules present in the raw food into more biologically available or biologically active moieties, for example releasing small phenolic acids from polyphenols. Microbial growth can also result in production of vitamins and other bioactive compounds like bacteriocins, which can act as human nutrients or regulate the microbiota associated with the fermented food inhibiting spoilage and pathogenic bacteria (10). Besides affecting organoleptic properties, some of these molecules demonstrate antioxidant, anti-

inflammatory and anti-cancer effects (1,6,11,12), thus resulting in modification of health-related properties of the final food product. This is especially true for fermented fruits and vegetables, which as raw materials, are rich in bioactive phytochemicals and micronutrients.

Sauerkraut represents the most important European fermented vegetable, deriving from malolactic fermentation of fresh white cabbage (*Brassica oleracea* L. var. *capitata*) salted with 2-3% (w/w) sodium chloride (13,14). While large-scale industrial production of sauerkraut is supported by the use of bacterial starter cultures, homemade and small-scale artisanal products are traditionally obtained by spontaneous fermentation by bacteria naturally present on the fresh cabbage or in the food processing environment (14). *Weissella* spp., *Leuconostoc mesenteroides*, *Lactobacillus brevis*, *Lactobacillus plantarum* and *Pediococcus pentosaceus* have been identified as the main hetero- and homo-fermentative LAB involved in sauerkraut spontaneous fermentation and in the production of lactic acid, SCFA and several amino acids found at high concentrations in sauerkraut (14–16).

Ingestion of certain probiotics, including those present in fermented foods, has been shown to induce significant positive improvements in gut barrier function (17–19). The gut barrier forms a tight barrier preventing bacteria from translocating the gut wall and being absorbed into the blood stream where they can induce inflammation (20). An unbalanced diet, including our modern Western diet, low in fiber and high in sugar, saturated fats and ultra-processed foods, could alter gut barrier function, thus leading to augmented gut permeability (often referred to as 'leaky gut'). Increased permeability of the intestinal mucosa leads to uncontrolled microbial translocation from the intestinal lumen across the gut wall. Translocation of microorganisms or their inflammatory cell wall components, such as lipopolysaccharides (LPS) leads to an inflammatory response, and where this translocation persists unchecked, it can lead to chronic systemic low-grade inflammation (20,21). This condition, which has been described by Cani and colleagues (2007) (21) as 'metabolic endotoxemia', has frequently been reported in patients with inflammatory bowel disease (IBD) (22,23), irritable bowel syndrome (IBS) (24), diabetes, obesity and other chronic diseases (25). Chronic systemic low-grade inflammation differs from a physiologic inflammatory response in its chronicity and magnitude, being characterized by sustained elevation of circulating inflammatory mediators, including IL-6 and C-reactive protein (CRP) which render this condition a powerful risk factor for cardiovascular diseases, type 2 diabetes mellitus, cancer and other chronic conditions (26). Gut barrier represents a complex multilayer system including a surrounding mucus layer, a monolayer of epithelial cells connected by tight junctions (TJ) and a basal *lamina propria* rich in immune cells regulating microbial tolerance and immune function (20,27). Abnormalities in this

complex barrier, and especially in TJ function lead to increased gut permeability, with a concomitant absorption of inflammatory bacterial lipopolysaccharide (LPS) (20). Since diet is one of the major factors influencing gut barrier integrity, several studies investigated the role of microbial metabolites provided by diet in regulating intestinal permeability. Some evidence suggest that lactic acid and other organic acids in fermented products might positively affect gut barrier integrity, thus lowering inflammation. For example, SCFAs significantly improved epithelial barrier function in several *in vitro* and animal studies, by increasing the levels of colonic mucus proteins (28) and/or by upregulating TJ proteins expression (29,30). Butyrate has been shown to recover the gut barrier function by modulating claudin-1 and occludin expression in Caco-2 cells, thus increasing TEER (29,31). SCFAs have also been reported to regulate immune response by binding to G protein-coupled receptors (GPCRs), thus regulating the activity of inflammatory cells, including neutrophils and macrophages. Acetate GPR43 activation suppresses colonic inflammation in ulcerative colitis mouse models (32). Moreover, acetate binding to GPR43 suppressed LPS-induced TNF-α secretion in mouse PBMCs, confirming the role of SCFA in mediating anti-inflammatory effects through GPCRs (33). Recently, different bioactive capacities have also been addressed to lactic acid, including immunomodulation (34). Interestingly, Okada *et al.* (2013) demonstrated that luminal lactic acid stimulated enterocytes proliferation in a murine model, thus maintaining intestinal barrier function (35).

Hence, the inclusion of fermented foods in diet has potential to improve gut health, preventing intestinal permeability and thus improving intestinal immune function. Recently, sauerkraut juice increased its commercial popularity as a potential functional food, although it has received little scientific attention (36). This beverage consists of the liquid in which sauerkraut is cured, and is made up of the mixture of pickling brine and cabbage juice itself. Early studies are supporting an anti-cancer potential of sauerkraut water (37). Considering the nutritional and health potential of this beverage and the lack of scientific evidences related to its consumption, we decided to focus our study on the analysis of sauerkraut juice.

In this study, we conduct an in-depth and multi-disciplinary analysis to first characterize the fermentation of locally produced, artisanal sauerkraut and to measure the potential of sauerkraut juice to improve gut health. Specifically, we used both culture dependent and culture independent microbiological methodologies to characterize sauerkraut fermentation, we used untargeted NMR based metabolomics to characterize metabolite production during fermentation and pre-clinical models to examine the ability of sauerkraut water to improve gut permeability and immune

function. Five replicate fermentations were characterized from two artisanal organic producers in Val di Gresta, Trento, Northern Italy. Samples for microbiological and metabolomics analysis were taken at day 1, 2, 3, 7, 14, 21, 28 and 35 to characterize the microbiological succession of the sauerkraut microbiota and their associated metabolites. Finally, sauerkraut juice was collected at the end of the fermentative process (35 days) to investigate whether sauerkraut fermentation water was capable of enhancing gut barrier function as determined by trans-epithelial electrical resistance (TEER) of human colorectal adenocarcinoma (Caco-2) cell monolayers and immune function using a co-culture of Caco-2 differentiated as intestinal monolayer and peripheral blood mononuclear cells (PBMCs) as a model of the gut immune system. The overall experimental layout is presented in **Figure 1**.

Figure 1. Summary of the experimental layout.

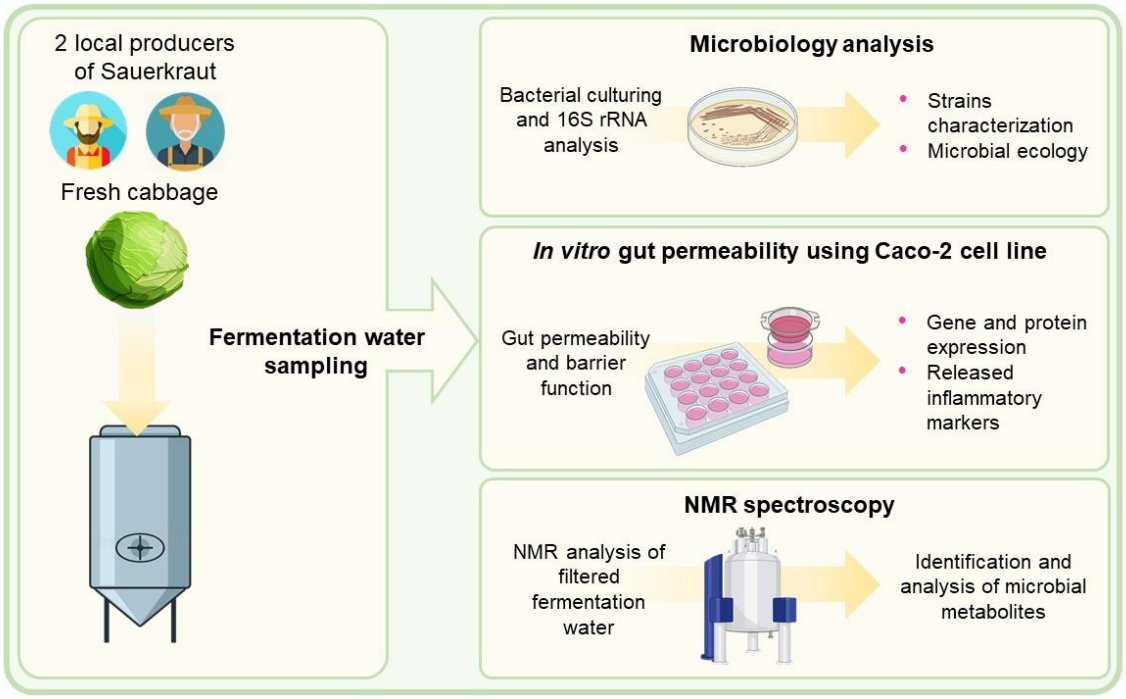

2. Materials and methods

2.1 Sauerkraut fermentation and water sampling

Sauerkraut fermentation were studied in two organic producers (SK1 and SK2) in Val di Gresta, Trentino (Northern East Italy), between October and November 2019. The sauerkraut fermentation was performed using fresh white cabbage (*Brassica oleracea* L. var. *capitata*) chopped, shredded and layered in five separated 500 kg tanks with approximately 3% sodium chloride. The top of each tank was covered with nylon coating, covered with a layer of water to keep pressure on the head of the fermenter and maintain it anaerobic. Fermentation water samples for the analysis were collected

from the lower part of the tank using a tap every 24 hours for the first 3 days of fermentation (day 1, day 2, day 3) and then after 7 (day 7), 14 (day 14), 21 (day 21), 28 (day 28) and 35 (day 35) days of fermentation. The samples were taken each time from five different tanks using aseptic technique. Temperature was measured each day using a probe inside each tank and an external probe to monitor the temperature of the room where the tanks were stored. pH of fermentation water was measured for each sample using laboratory pH-meter.

2.2 Microbiological analysis

2.2.1 Viable count of lactic acid bacteria and collection of bacterial isolates

Sauerkraut water samples were decimally diluted in sterile peptone water and plated onto de Man, Rogosa and Sharpe (MRS), for viable count of lactic acid bacteria and isolation of putative lactobacilli. Bacteria were incubated under anaerobic conditions (using jars with AnaeroGen™ anaerobic system) and in aerobic conditions at 30°C for 48 h. All culture media and anaerobic systems were purchased from Oxoid (Milan, Italy). Viable cells count (CFU/mL) were determined by colony formation on MRS agar using the standard spread plate method. For each different colony morphology, one to three colonies were randomly picked up from countable MRS agar plates for bacterial isolation and purified by subsequent culturing and Gram staining. Each purified isolate was subsequently cultured in MRS and stored at –80°C in 40% glycerol stocks.

2.2.2 DNA extraction and genotypic identification of sauerkraut water bacteria

1 mL of bacterial culture from putative LAB isolates grown overnight in MRS broth was centrifuged at 13.000 *g* for 3 min, supernatant was discarded and pellet was used to prepare bacterial DNA using by Instagene Matrix (Bio-Rad, Hercules, CA, USA) extraction, following the manufacturer's instruction. RAPD–PCRs were carried out using the primer M13 (38). PCR amplification of each samples was carried out using 25 μL reactions, with 2.5 μL of Buffer 10X, 1.5 μL $MgCl_2$ 50 mM, 2 μL dNTPs 10 mM, 0.1 μL primer M13 100 μM, 0.2 μL Taq (5 U/mL) and 13.7 μL H_2O and 5 μL DNA. All PCR reagents were purchased from Invitrogen (Thermo Fisher Scientific, Waltham, MA, USA). PCR reactions were carried out using the Verity™ 96-well Thermal Cycler (Thermo Fisher Scientific, Waltham, MA, USA), according to the following protocol: 2 min at 94 °C, 40 cycles of 1 min at 94 °C, 30 s at 42 °C, and 2 min at 72 °C, followed by a final extension of 10 min at 72 °C (39). PCR products were separated by electrophoresis on 2 % (w/v) agarose gel (Gibco BRL, Cergy Pontoise, France) and stained with ethidium bromide (0.5 μg/L). DNA patterns were analysed through the Unweighted Pair Group Method Arithmetic averages (UPGMA) using the GelCompar

II-BioNumerics® software (package version 6.0; Applied Maths, Belgium). Calculation of similarity of the PCR fingerprinting profiles was based on the Pearson product–moment correlation coefficient. Isolates with a similarity coefficient higher than 90% were considered belonging to the same biotype, as described by Gatti *et al.* (2008) (40).

2.3 Metagenomic analysis of sauerkraut water microbiota

Total DNA extraction from frozen sauerkraut water was performed using the DNA Blood and tissue kit (Qiagen, Hilden, Germany) according to manufacturer's recommendations following the protocol 'Pretreatment for Gram-Positive Bacteria'. DNA quality was assessed by gel-electrophoresis and UV/Vis spectrophotometry. PCR amplification was performed by targeting 16S rRNA gene V3-V4 variable regions with the bacterial primer set 341F (5′-CCTACGGGNGGCWGCAG-3′) and 806R (5′-GACTACNVGGGTWTCTAATCC-3′), as previously reported (25). PCR amplification of each samples was carried out using 25 μL reactions, with 12.5 μL of 2X KAPA Hifi HotStart Ready Mix (Kapa Biosystems Ltd., UK), 0.5 μL of each primer, 2 μL DNA (10 ng/μL) and 9.5 μL. All PCR reactions were carried out using the Verity™ 96-well Thermal Cycler (Thermo Fisher Scientific, Waltham, MA, USA), according to the following protocol: 95°C for 5 min and 25 cycles of 95°C for 30 s, 55°C for 30 s, 72°C for 40 s, with a final elongation step of 72°C for 5 min. PCR products were checked by gel electrophoresis and cleaned using an Agencourt AMPure XP system (Beckman Coulter, Brea, CA, USA), following the manufacturer's instructions. After seven PCR cycles (16S Metagenomic Sequencing Library Preparation, Illumina), Illumina adaptors were attached (Illumina Nextera XT Index Primer). Libraries were purified using Agencourt AMPure XP (Beckman) and then sequenced on an Illumina® MiSeq (PE300) platform (MiSeq Control Software 2.0.5 and Real-Time Analysis software 1.16.18, Illumina, San Diego, CA, USA). Sequences obtained from Illumina sequencing were imported, filtered, denoised, merged, and chimaeras removed using the DADA2 package (version 1.16) in R at different sequence lengths according to the quality results observed for reads 1 and 2 (41). Taxonomy was assigned to amplicon sequence variants (ASVs) using the Silva reference database (version 138.1). Multiple sequence alignment (MSA) was created using the DECIPHER package (v2.16.1) (42) and the phylogenetic tree was inferred using the packages ape (version 5.4) (43) and phangorn (version 2.5.5) (44). The phylogenetic tree, read count data, assigned ASVs and sample metadata were imported into the phyloseq package (v1.32) (45) for downstream analysis.

2.4 NMR analysis of sauerkraut water metabolites

900 μL of the each sauerkraut water sample was mixed with 100 μL of deuterium oxide and vortexed for 15 sec, then filtered using sterile Sartorius 0.22 μm PVDF syringe filters (Thermo Fisher Scientific, Waltham, MA, USA) and transferred to the 5 mm NMR tube. NMR spectra were recorded on Bruker Avance Neo 600 (base frequency 600 MHz for 1H nuclei), equipped with a broadband Z-gradient probe (5 mm sample tubes) and SampleCase 24-position autosampler. The spectra were acquired and processed using Topspin 4.1.1 software in the automation mode with Icon NMR 5.2.1. The deuterium lock signal was optimised for the 9:1 mixture of H2O and D2O (v/v). All proton NMR spectra were recorded using the noesygppr1d pulse sequence with automatic adjustment of water signal suppression frequency (o1p) and power level utilized for pulse was 47.10 dB (25 hZ suppression window). The size of the spectrum (sweep width, SW) was 20.8 ppm, time domain (TD) consisted of 65536 (64K) data points, number of scans (NS) was 64 and the number of dummy scans (DS) was 4, the time for relaxation delay (D1) was 10 sec, receiver gain (RG) for all spectra was fixed at 101, and baseopt digitization mode was used. Acquisition of each spectrum was preceded by automatic adjustment of the probe (ATMA routine) and automatic shimming (TOPSHIM). Spectra were processed in the TopSpin software with the size of real spectrum (SI) set to 131072 (128K, 2xTD) data points, and apk0.noe phase correction au program was applied automatically to each spectrum.

Quantitative analysis were performed using AssureNMR software with the external standard technique (ERETIC or Electronic REference To access In vivo Concentrations) (46), with the 2 mmol sucrose reference solution in 9:1 mixture of H2O and D2O (v/v) used as the external standard.

2.5 In vitro model of intestinal epithelium

2.5.1 Cell culture

Peripheral blood mononuclear cells (PBMCs) were isolated from buffy coat blood sample from healthy donors (n=3), donated by the Transfusion Unit of Santa Chiara Hospital, Trento, Italy, by Lymphoprep™ density gradient centrifugation (Thermo Fisher Scientific, Waltham, MA, USA). The experimental plan was approved by the local Ethical Committee of Azienda Provinciale dei Servizi Sanitari (APSS, Santa Chiara Hospital, Italy; approval document n. 401/2015). The study was designed in conformity with the international recommendation (Dir. EU 2001/20/EC) and its Italian counterpart (DM 15 Luglio 1997; D.Lvo 211/2003; D.L.vo 200/2007) for clinical trial and following the Declaration of Helsinki, to assure protection and care of subjects involved. Briefly, fresh human blood was diluted 1:1 in PBS 1X and then gently aliquoted in sterile 50 mL tubes (Sarstedt, Germany)

containing Lymphoprep™ in 2:1 proportion (Thermo Fisher Scientific, Waltham, MA, USA). Samples were centrifuged at 400 x *g* without break at room temperature for 20 min. PBMCs were collected from the ring surrounding the Lymphoprep™ layer and then washed twice in RPMI 1640 and once in PBS 1X. Human PBMCs were collected on the day before the experiment and 1.5 mL (2 x 10^6 cells/mL) were put in the basolateral compartment of the co-culture (see Section *2.5.3*). RPMI 1640 Dutch modification (RPMI; Sigma-Aldrich), supplemented with 10% decomplemented (56°C, 60 minutes) fetal bovine serum (Lonza, Switzerland), 1% penicillin (100 U)-streptomycin (100 µg)/mL, 1% 200 mM L-glutamine, and 1% 100 mM sodium pyruvate (Biological Industries, Israel) was used as culture medium. Cells were maintained in humidified atmosphere of 5% CO_2 in air at 37 °C for one night before using them in Caco2 co-culture assays upon LPS exposure.

Human epithelial colorectal adenocarcinoma Caco-2 cell line (ATCC® HTB-37™, number of passage between 50 and 60) were grown in Dulbecco's Modified Eagle's Medium (DMEM) with high glucose (4.5g/L) (Lonza, Switzerland) supplemented with 20% decomplemented (56°C, 60 minutes) fetal bovine serum (Lonza, Switzerland), 1% penicillin (100 U)-streptomycin (100 µg)/mL (Biological Industries, Israel), 1% 10 mM non-essential amino acids (Euroclone, Milan), 1% 200 mM of L-glutamine and 0.1% amphotericin 0.25 µg/mL (Biological Industries, Israel). Before and during treatments, cell cultures were maintained in humidified atmosphere of 5% CO_2 in air at 37 °C. Before the experiment, Caco-2 cells were maintained in T-75 cm^2 flasks (Sarstedt, Nümbrecht, Germany) and passaged when they reached 70% confluence using 0.05% trypsin–0.5 mM EDTA (Lonza, Switzerland). Medium was refreshed every second day. Prior to seeding, transwell inserts were coated with rat tail collagen Type I (Sigma Aldrich), according to the manufacturer's instruction. For both the experiments (**Figure 2**), Caco-2 cells were harvested to obtain a cell suspension of 1 X 10^5 cells/cm^2. 2.5 mL of cell suspension were added to transwell inserts with membrane filters (0.1 µm pore size; Falcon, Sacco s.r.l, Cadorago, Como, Italy) and grown for 13 days until a tight monolayer was formed (TEER measurements stable for two consecutive days). 1.5 mL of medium was added to the basolateral chamber. Sauerkraut water samples from both producers (SK1 and SK2) collected from tank 1 at 35 days of fermentation were thawed on ice and filter-sterilized using Sartorius 0.22 µm filters (Thermo Fisher Scientific, Waltham, MA, USA). All control and test treatments were prepared on the day of the assay. 10 mM propionic acid and 7% ethanol were used as positive and negative controls, respectively. All treatments were diluted in culture medium and added at 10% of the total apical volume (2.5 mL). All investigated experimental conditions are schematically illustrated in **Figure 2**.

Figure 2. Schematic illustration of investigated experimental conditions. Human adenocarcinoma cells (Caco-2) were grown to confluence to mimic the intestinal epithelial barrier. Trans epithelial electric resistance (TEER) results were obtained from Caco-2 alone incubated with sauerkraut fermentation water from both producers (SK1 and SK2), in order to assess the effects of sauerkraut water in modulating gut barrier function (**A**). To evaluate anti-inflammatory effects of sauerkraut water, Caco-2 were further co-incubated with peripheral blood mononuclear cells (PBMCs) isolated from human blood upon lipopolysaccharide (LPS) exposure (**B**).

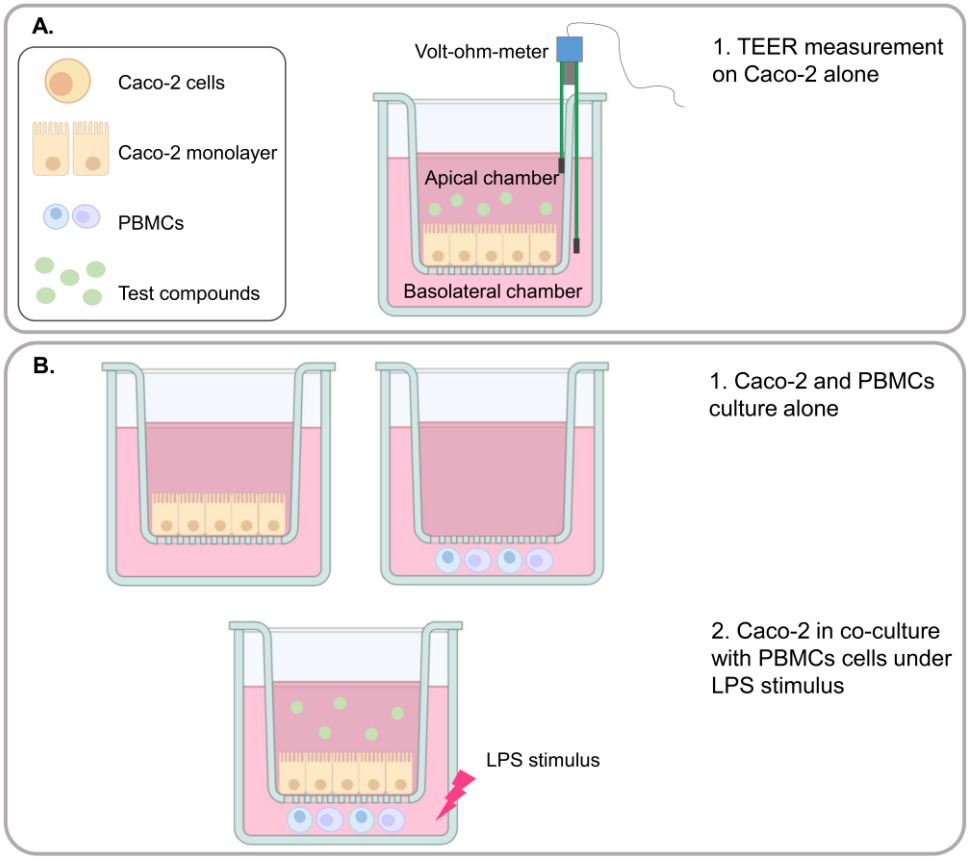

2.5.2 Trans epithelial electrical resistance (TEER) measurement on Caco-2 monolayer

TEER was measured using an epithelial volt-ohm-meter (EVOM, World Precision Instruments Inc., Sarasota, FL, USA). Plates were left at room temperature for exactly 25 minutes prior to TEER measurements. The integrity of cell monolayers was assessed just before the addition of testing substrates ($resistance_{0h}$). The media was then removed from basolateral and apical chambers and the control or test treatments added to the apical layer. Resistance was measured after 24 h ($resistance_{24h}$). The TEER was calculated using the following equation, as described in previous works (47–49):

$$TEER(\Omega\ cm^2) = resistance(\Omega) \times membrane\ area(cm^2)$$

Where area of the semipermeable membrane was 9.6 cm^2. The change in TEER for each insert was then calculated using the following formula:

$$\text{Change in TEER (\%)} = TEER_{24h}\ (\Omega\ cm^2) / TEER_{0h}\ (\Omega\ cm^2) \times 100\%$$

Where $TEER_{24h}$ and $TEER_{0h}$ represent TEER after 24 hours treatment and TEER at baseline, respectively. This experiment was repeated three times.

2.5.3 Co-culture system

To evaluate anti-inflammatory effects of sauerkraut fermentation water, an *in vitro* assay using a Caco-2/PBMCs co-culture model was performed (**Figure 2**B), according to previous studies (50–52). Briefly, Caco-2 cells were harvested to obtain a cell suspension of 1 X 10^5 cells/cm^2. 2.5 mL of cell suspension were added to the apical side of transwell inserts with membrane filters (0.1 μm pore size; Falcon, Sacco s.r.l, Cadorago, Como, Italy) and grown for 13 days until a tight monolayer was formed (TEER measurements stable for two consecutive days). 2 x 10^6 PBMCs/mL were then seeded in the basolateral compartment of the co-culture in 1.5 mL and ensured complete adherence to the well over night before being used. On the day of the experiment, basolateral medium was refreshed and apical medium was replaced with complete RMPI 1640 in the presence or absence of test compounds. Transwell inserts containing Caco-2 were added to the multiple plate wells preloaded with PBMCs. This co-culture system was incubated for 2 h. 10 ng/mL of lipopolysaccharide (LPS) was then added to the basolateral side of this co-culture model. Sauerkraut water samples from both producers (SK1 and SK2) collected from tank 1 at 35 days of fermentation were thawed on ice and filter-sterilized using Sartorius 0.22 μm filters (Thermo Fisher Scientific, Waltham, MA, USA). All control and test treatments were prepared on the day of the assay. 10 mM propionic acid and 7% ethanol were used as positive and negative controls, respectively. All treatments were diluted in culture medium and added at 10% of the total apical volume (2.5 mL). This experiment was repeated three times with three different PBMCs donors.

2.5.4 Cytokines quantification using Magpix®

For the analysis, both the apical and basolateral supernatants were collected after 0 and 24 h of co-culture. Supernatants were then centrifuged for 5 min at 18,000 x *g* to pellet cell debris and stored at –80 °C. The release of IL-1β, IL-6, IL-10 and TNF-α was quantified in apical and basolateral chambers supernatants using a cytokine magnetic bead-based panel (Milliplex MAP kit, Millipore Corp., Billerica, MA, USA) and measured by a Magpix® instrument (Luminex, Texas, USA) and xponent software (version 4.2, Luminex Corp, Austin, Texas, US) according to manufacturer's instruction. Blanks and standard curves were included on each plate. The overall intra- and inter-assay precision is reported by the manufacturer as 2–19%, and accuracy as 87–107% over the calibration range of 3.2–10'000 pg/mL cytokine concentration (53).

2.5.5 RNA isolation and gene expression analysis

Caco-2 and PBMCs cells were collected from the co-culture system after 0, 3 and 6 hours of co-culture. Briefly, medium was removed from both apical and basolateral chambers, then covered with 500 µL of TRIzol reagent (Thermo Fisher Scientific, Waltham, MA, USA). Samples were collected in Eppendorf tubes and stored at –80 °C. Total RNA was isolated from cultured cells according to the manufacturer's recommendations (Thermo Fisher Scientific, Waltham, MA, USA). Extracted total RNA was quantified using a Nanodrop 8000 Spectrophotometer (Thermo Fisher Scientific, Waltham, MA, USA) and RNA quality was assessed using a 2200 TapeStation (Agilent Technologies, Santa Clara, CA, USA). mRNA samples with high quality (RNA Integrity Number, RIN > 8) were used for retrotranscription. Reverse transcription was performed with a High-Capacity cDNA Reverse Transcription Kit (Applied Biosystems™, Thermo Fisher Scientific, Waltham, MA, USA) in a 20 µL reaction volume containing 10 µL template RNA (5 ng/µL), 2.0 µL of 10X RT Buffer, 0.8 µL of 25X dNTP Mix (100 mM), 2.0 µL of 10X RT Random Primers, 1.0 µL of MultiScribe™ Reverse Transcriptase, and 4.2 µL of DEPC-treated water. After transcription, cDNA was stored at −20 °C until quantitative Real-Time PCR (RT-PCR).

The expression level of inflammatory genes was determined by RT-PCR using ViiA™ 7 System (Thermo Fisher Scientific, Waltham, MA, USA). Pairs of primers and TaqMan probes were obtained from Applied Biosystems (TaqMan® Gene Expression Assays). RT-PCR was carried out in 20 µL reactions prepared following the manufacturer's instruction and containing 10 µL of KAPA PROBE FAST qPCR Master Mix 2x Universal (Kapa Biosystems, Sigma-Aldrich, Germany), 0.4 µL 50x Rox Low (10 ng/µL), 1 µL TaqMan Assay, 2 µL of cDNA (10 ng/µL) and 6.6 µL H_2O. Reactions were carried out in triplicate under the following conditions: 95 °C for 1 min, followed by 40 cycles at 95 °C for 1 s, 60 °C for 20 s. Ct values for each sample were normalized against the geometric mean Ct values obtained for two housekeeping genes, 18S and GAPDH. Gene expression was therefore expressed as the relative fold change $2^{-\Delta\Delta Ct}$, where ΔCt was obtained by subtracting the geometric mean Ct for the two reference housekeeping genes 18S and GAPDH from the Ct of the tested gene, and ΔΔCt represented the difference between ΔCt of cells incubated with sauerkraut water compared to the ΔCt of control samples (medium with no treatment, Ctrl).

2.5.6 Western blot quantification of tight junction proteins

The analyses were performed on the Caco-2 cells from the co-culture system, following the method described by Bianchi *et al.* (2019) (54) with some modifications. Briefly, the monolayers were

rinsed two times with ice-cold PBS and then covered with 350 μL of Lysis buffer (20 mM Tris–HCl, pH 7.5, 150 mM NaCl, 1 mM EDTA, 1 mM EGTA, 1% Triton, 2.5 mM sodium pyrophosphate, 1 mM β-glycerophosphate, 1 mM Na_3VO_4, 1 mM NaF, 2 mM imidazole) supplemented with a protease inhibitor cocktail (Complete, Mini, EDTA-free, Roche, Monza, Italy). Total cell lysates were collected in Eppendorf tubes, sonicated and centrifuged at 14,000 x g for 10 min at 4 °C to eliminate cell debris. Protein concentration was determined by performing a Bicinchoninic Acid (BCA) protein assay using Pierce™ BCA Protein Assay Kit (Thermo Fisher, Waltham, MA, USA).

Before using samples for Western blot (WB) analysis, acetone protein precipitation was performed. Four volumes of cold acetone (Sigma-Aldrich, Germany) were added to each samples and samples were incubated overnight at 4 °C. Samples were centrifuged at 18,000 x *g* for 10 minutes and supernatant was removed. Dry pellets were finally resuspended in 15 μL of Loading buffer 1X (63 mM Tris–HCl, pH 6.8, 2% SDS, 10% glycerol, 0.1% 2-mercapto-ethanol and 0.005% Bromophenol blue) to a final concentration of 35 μg protein/15μL. This mixture was boiled at 85 °C for 15 min for soluble protein or at 70 °C for 5-10 min for multi-pass membrane proteins. Samples were then loaded on 12% SDS-polyacrylamide gel (35 μg proteins/well), and proteins were separated for 1.30 h at 100 V. Proteins were then blotted on PVDF membrane (Immobilon-P, Millipore, Millipore Merck Corporation, Burlington, MA, USA) for 1 h at 100 V, at 4 °C. After transfer, PVDF membrane was rinsed using TRIS-Buffered Saline (TBS) and then incubated in TBS 0.05%Tween (TBS-T) with 5% skim milk powder (Oxoid, Milan, Italy) solution for 1 h at room temperature (RT). Membrane was washed three times in TBS-T an then exposed overnight at 4 °C to primary monoclonal antibodies (Santa Cruz Biotechnology, Texas, USA) (initial concentration 200 μg/ml) diluted 1:1000 in TBS-T with a 1% skim milk powder solution. After three washes of 10 min each in TBS-T, membranes were exposed to the HRP-conjugated secondary antibodies in TBS-T with 0.5% skim milk powder solution for 1 hour at RT. After three washes of 10 min each in TBS-T and one wash in PBS-T, visualization of protein bands was performed combining 10X CN/DAB Concentrate with the Stable Peroxide Substrate (1:10 proportion). Development reaction was stopped by rinsing the membrane with H_2O.

Quantification of band intensity was done by employing the ImageJ Software (designed at the National Institutes of Health, https://imagej.nih.gov/ij), as previously described by Gallo-Oller *et al.* (2018) (55). Each band was individually selected and circumscribed with the Region of Interest (ROI) selection under 'Gels' function, followed by quantification of the acquired data. Pixel density was inverted for all data and background noise was removed, following the manufacturer's instructions (https://imagej.nih.gov/ij/docs/guide/user-guide.pdf). Data were expressed as normalized ratio

(fold-changes) to β-actin and to control samples (cells incubated with complete DMEM medium as control).

2.6 Statistical analysis

All statistical analysis was performed using R studio version 3.6.2. Normal distribution of data was assessed by Shapiro–Wilk's test. Differences in microbial metabolites over fermentation time within the same producer were checked by Kruskal–Wallis test, followed by the post-hoc Dunn's test with Benjamini–Hochberg false discovery rate (FDR) p value correction. 16S rRNA metagenomic data were analyzed as detailed in the relative method section. Statistical significance between TEER measures, Magpix® citokine quantification, gene expression and Western blot data was performed by unpaired t-test. After FDR correction, a p value < 0.05 was considered statistically significant. All data are expressed as the mean ± standard deviation, SD.

3. Results

3.1 Temperature, pH and viable count of lactic acid bacteria (LAB) variation over 35 days of fermentation

Changes in temperature, pH and viable counts of LAB are reported in **Figure 3** and **4**. Temperature inside all tanks changed over the fermentation process, ranging from 18.5 °C to 22.5 °C for SK1 and from 13.5 °C to 16 °C for SK2 (**Figure 3**). As expected, temperature increased rapidly during the first week of fermentation and gradually decreased after day 18 in both producers. Notably, temperature recorded in the room where tanks were stored underwent many more shifts both daily and weekly, without affecting the temperature inside fermentation tanks.

For both producers, the viable counts of LAB increased rapidly after the first days of fermentation and reached the maximum density by day 3 (10^8 CFU/mL), when inside-tank temperature was 19.44 °C for SK1 and 14 °C for SK2. On day 35, the LAB counts were around 10^6 for SK1 and around 10^8 for SK2 (**Figure 4**). The decline in viable LAB count observed after day 3 might be due to the high acidity (**Figure 4**). The huge drop down observed in SK2 viable LAB count was due to the effect of two tanks, which explains the large SD. Acid production was rapid during the first 7 days of fermentation (day 7) in all tanks, dropping from 5.7 at day 1 in both producers to 3.82 and 3.99 at day 7 for SK1 and SK2, respectively (**Figure 4**). Thereafter, pH reduced at a slower rate and remained unchanged after day 21. Similar pH profiles were obtained for samples from both producers.

Figure 3. Temperature changes inside (Tank mean) and outside (out) fermentation tanks over 35 days. The values plotted for internal temperature are the means between tanks (n=5 tanks/each producer) ± the error bars showing the standard deviation (SD).

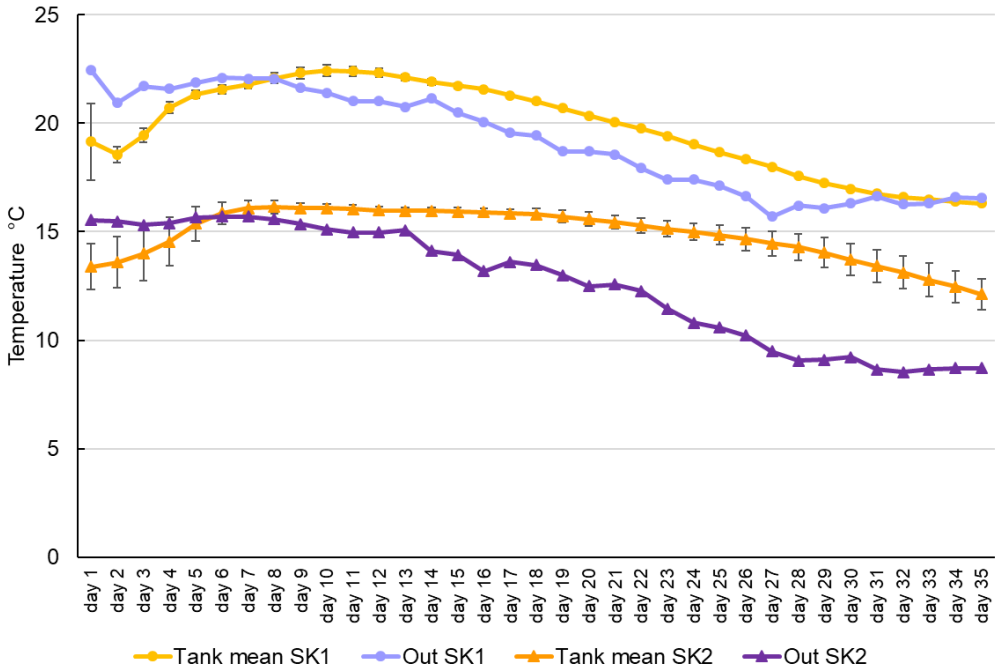

Figure 4. Changes of pH and viable LAB count (expressed in Log_{10}(CFU/mL) over 35 days of sauerkraut fermentation. The values plotted are the means of viable counts from each tank (n=5 tanks/producer) ± the error bars showing the standard deviation (SD).

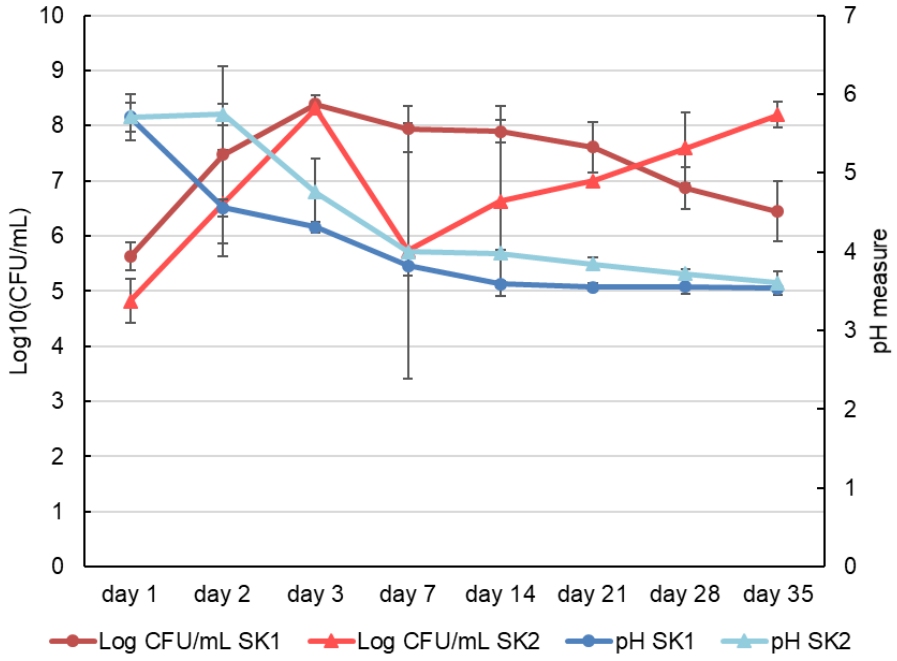

3.2 RAPD PCR and biotyping

Two hundred and fifty one colonies were isolated from sauerkraut water samples after 35 days of fermentation from both producers. The RAPD-PCR analysis through M13 primer successfully

generated 220 fingerprints, observed using agarose gel electrophoresis. The Bionumerics® analysis clustered the isolates into 133 biotypes having 90% of similarity index. Of these, 88 biotypes in total from both producers were selected for Sanger sequencing, in order to characterize the main species driving sauerkraut fermentation. Strain taxonomic identification and characterization for biotechnological and probiotic potential is ongoing and not presented in this thesis.

3.3 Gut microbial ecology

Observed OTUs, Chao1 and Shannon index were used to analyze changes in bacterial α-diversity (**Figure 5**A**)**. In SK1, bacterial richness significantly decreased over 35 days of fermentation, according to Observed OTUs and Chao1 index (Observed OTUs: day 1 vs day 7, $p = 0.018$; day 1 vs day 21, $p = 0.003$; day 1 vs day 35, $p = 0.001$; Chao1: day 1 vs day 7, $p = 0.019$; day 1 vs day 21, $p = 0.003$; day 1 vs day 35, $p = 0.001$). In SK2, bacterial richness significantly increased between day 1 and day 2 (Observed OTUs: $p = 0.047$; Chao1: $p = 0.048$) and then significantly decreased until day 35 (day 2 vs day 35; Observed OTUs: $p = 0.0195$; Chao1: $p = 0.0199$). Shannon index significantly decreased during the first 3 and 7 days of fermentation in SK1 (day 1 vs day 3, $p = 0.0079$) and SK2 (day 1 vs day 7, $p = 0.0079$), respectively. After day 3, a slight increase in α-diversity was observed for SK1, but this result did not reach statistical significance. Similarly, an increase in bacterial evenness was observed for SK2 after day 7, being significantly higher at day 14 when compared to day 7 ($p = 0.0079$). These results also coincided with a drop in viable LAB count observed for SK2 at day 7. In order to highlight differences in bacterial composition following sauerkraut fermentation over time, β-diversity was plotted using Bray-Curtis dissimilarity matrix (**Figure 5**B). We observed significant changes in sauerkraut water microbiota composition with a significant shift from day 1 to day 35 ($p < 0.01$). The same trend was observed for both producers. Genera % relative abundance in sauerkraut water is shown in **Figure 6**. We observed that the number of identified genera dramatically decreased from day 1 to day 2, and then slowly decreased until day 35, when the lowest number of genera was observed for both producers. As expected, *Lactiplantibacillus* (SK1: 56.19 ± 15.21%; SK2: 47.75 ± 12.68%; mean ± SD), *Leuconostoc* (SK1: 29.00 ± 12.61 %; SK2: 8. 05 ± 2.85%; mean ± SD), *Pediococcus* (SK2: 24.16 ± 8.12%; mean ± SD), *Levilactobacillus* (SK2: 8.67 ± 5.86%; mean ± SD), *Paucilactobacillus* (SK1: 11.66 ± 5.04%; mean ± SD) and *Secundilactobacillus* (SK2: 4.95 ± 2.18%; mean ± SD) represent the dominant genera at day 35. In SK1, LAB become predominant at day 7 as shown by the relative abundance results (**Figure 6**), thus explaining the separation between day 3 and day

7 observed in Bray-Curtis analysis (**Figure 5**B). These results confirm LAB intrinsically resistance to acid environments and the main drivers of the sauerkraut fermentation.

Figure 5. Bacterial α-diversity using Observed OTUs, Chao1 and Shannon index from day 1 to day 35 of sauerkraut fermentation from both producers (SK1 and SK2). Line inside the box represents the median, whiskers from either side of the box represent the first and the third quartiles, respectively. °=outliers. Different superscript letters indicate statistical significance within the same producer (**A**). Principal Component Analysis (PCoA) representing the bacterial β-diversity according to Bray-Curtis dissimilarity index. Different colors indicate different timepoints and different shapes indicate different producers, as described in the legend (**B**).

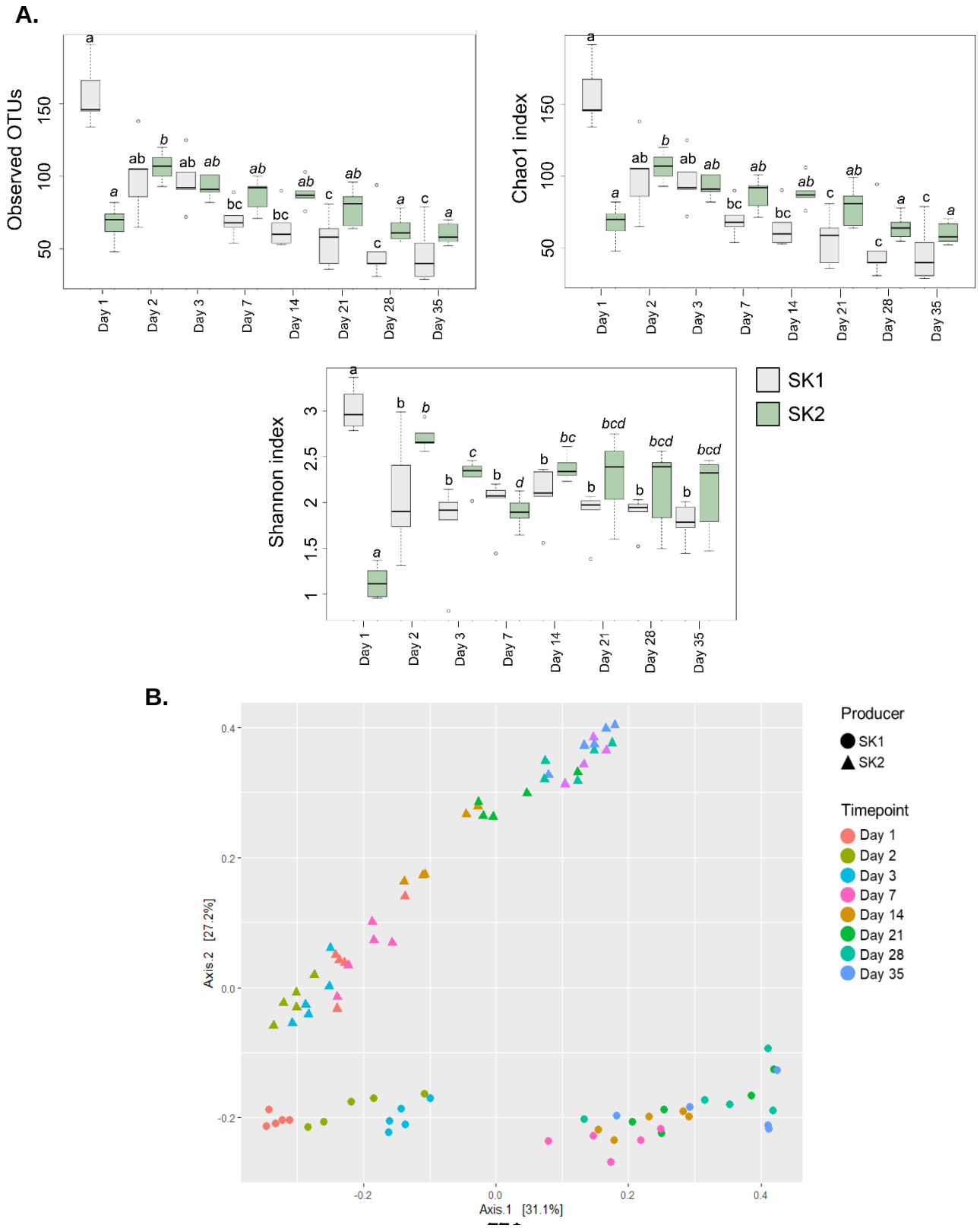

Figure 6. Percentage bacterial relative abundance of genera after 1, 2, 3, 7, 14, 21, 28 and 35 days of fermentation. Low abundance genera (< 2%) have been filtered. Values are mean percentage relative abundance between different tanks (n=5 for each producer).

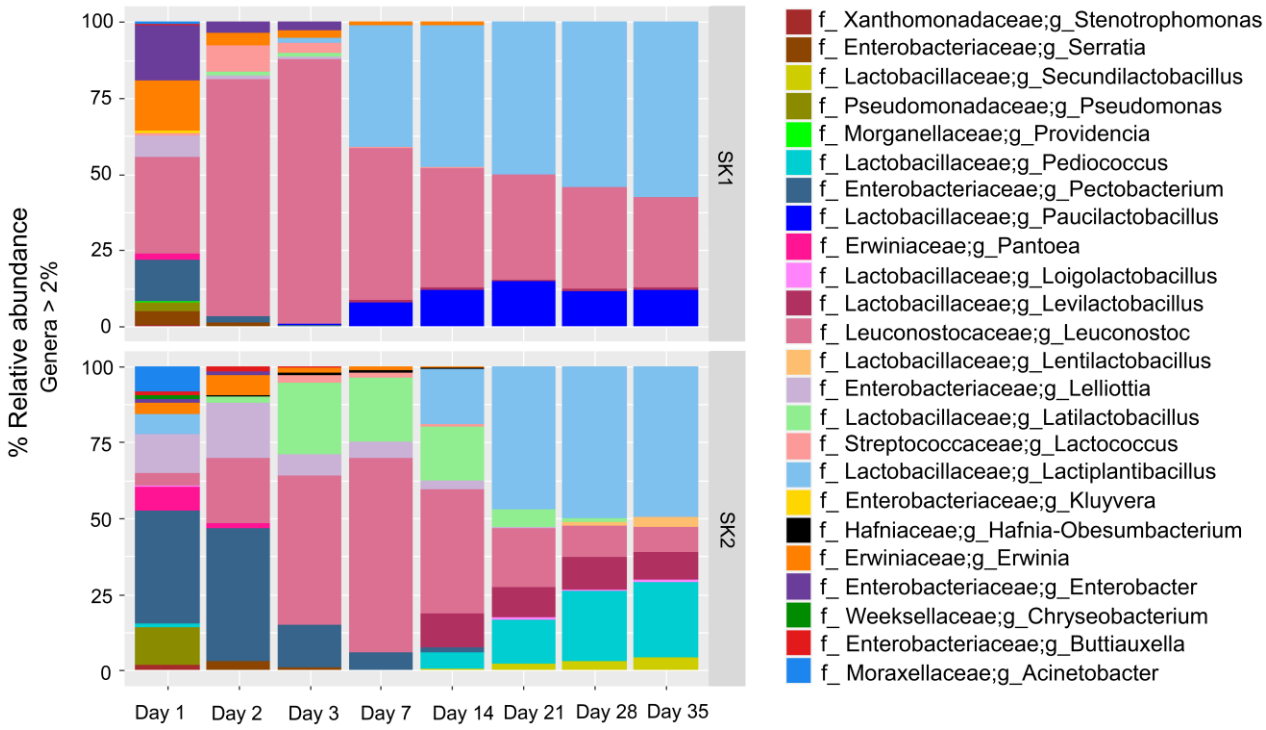

3.4 Microbial metabolite analysis

NMR was performed by the Traceability Unit at Fondazione Edmund Mach to quantify microbial metabolites in sauerkraut water samples from both producers (SK1 and SK2). The results of metabolites quantifications are shown in **Figure 7** and **Table S1**. Metabolites that were below the detection limit in 70% of total samples were excluded from further analysis.

After the NMR analysis, a total of 29 compounds, including organic acids, amino acids and sugars, were identified in sauerkraut water samples over 35 days of fermentation (**Table S1**). Seven organic acids were identified, including lactic acid, acetic acid, malic acid, propionic acid, butyric acid and formic acid (**TableS1**, **Figure 7**A) and their amount significantly varied over time. Among SCFA, acetic acid significantly increased over sauerkraut fermentation, reaching its maximum concentration at day 28 for SK2 (2340.99 ± 297.64 mg/L, mean ± SD) and at day 35 for SK1 (1923.64 ± 298.16 mg/L). Similarly, lactic acid significantly increased overall the fermentation process, both in SK1 and SK2, reaching its maximum concentration at day 35 (SK1: 9418.22 ± 953.14 mg/L; SK2: 6121.66 ± 3554.43 mg/L). A total of 5 amino acids, including alanine (Ala), leucine (Leu), phenylalanine (Phe), tyrosine (Tyr) and valine (Val) were identified (**Table S1**, **Figure 7**B). Aromatic

amino acids Phe and Tyr significantly increased during sauerkraut fermentation (SK1: day 1 vs day 35, Phe $p < 0.001$; Tyr $p < 0.001$; SK2: day 1 vs day 28, Phe $p = 0.0047$; Tyr $p = 0.006$) reaching their maximum concentration at day 28 for SK2 (Phe = 39.98 ± 2.15 mg/L, Tyr = 47.47 ± 4.51 mg/L) and at day 35 for SK1 (Phe = 56.83 ± 7.16 mg/L, Tyr 56.53 ± 5.19 mg/L). On the other hand, most of the sugars, including D-fructose, alpha-D-glucose and beta-D-glucose showed decreasing concentrations over time (**Table S1**, **Figure 7**C). However, only D-fructose changes over time were statistically significant after FDR correction. In samples from both producers, we observed a significant increase in D-mannitol levels after 7 days of fermentation. Another 13 compounds were found in sauerkraut water samples, including acetaldehyde, dimethyl sulfoxide (DMSO), deoxyuridine monophosphate, ethanol, 2,3-butanediol, gamma-aminobutyric acid (GABA), D-mannose, methanol, putrescine, succinamide, succinimide, trimethylamine N-oxide (TMAO) and uracil (**Table S1**, **Figure 7**D). We observed several diversified patterns for these compounds. Ethanol, 2,3'-butanediol, methanol, putrescine and uracil significantly increased over time, in both producers. GABA levels strongly decreased after 3 or 7 days of fermentation in both producers (SK1, day 1: 52.80 ± 7.23, day 3: 0.00 ± 0.00; SK2, day1: 74.25 ± 14.27, day 7: 0.00 ± 0.00).

Figure 7. Individual line plots of microbial metabolites identified by NMR analysis, divided in organic acids (**A**), amino acids (**B**), sugars (**C**) and other compounds (**D**). The plots compare the concentration (mg/L) changes between all experimental timepoints, after 1, 2, 3, 7, 14, 21, 28 and 35 days of fermentation. Different colors and line shapes indicate different producers: —●— SK1; - -●- - SK2. The error bars correspond to the standard deviation. Different superscript letters indicate statistical significance among different timepoints, within the same producer ($p < 0.05$) and capital letters indicate a p value < 0.001. Grey-colored letters refer to SK1, black underlined letters refer to SK2. No letter indicates the absence of statistical significance after FDR correction.

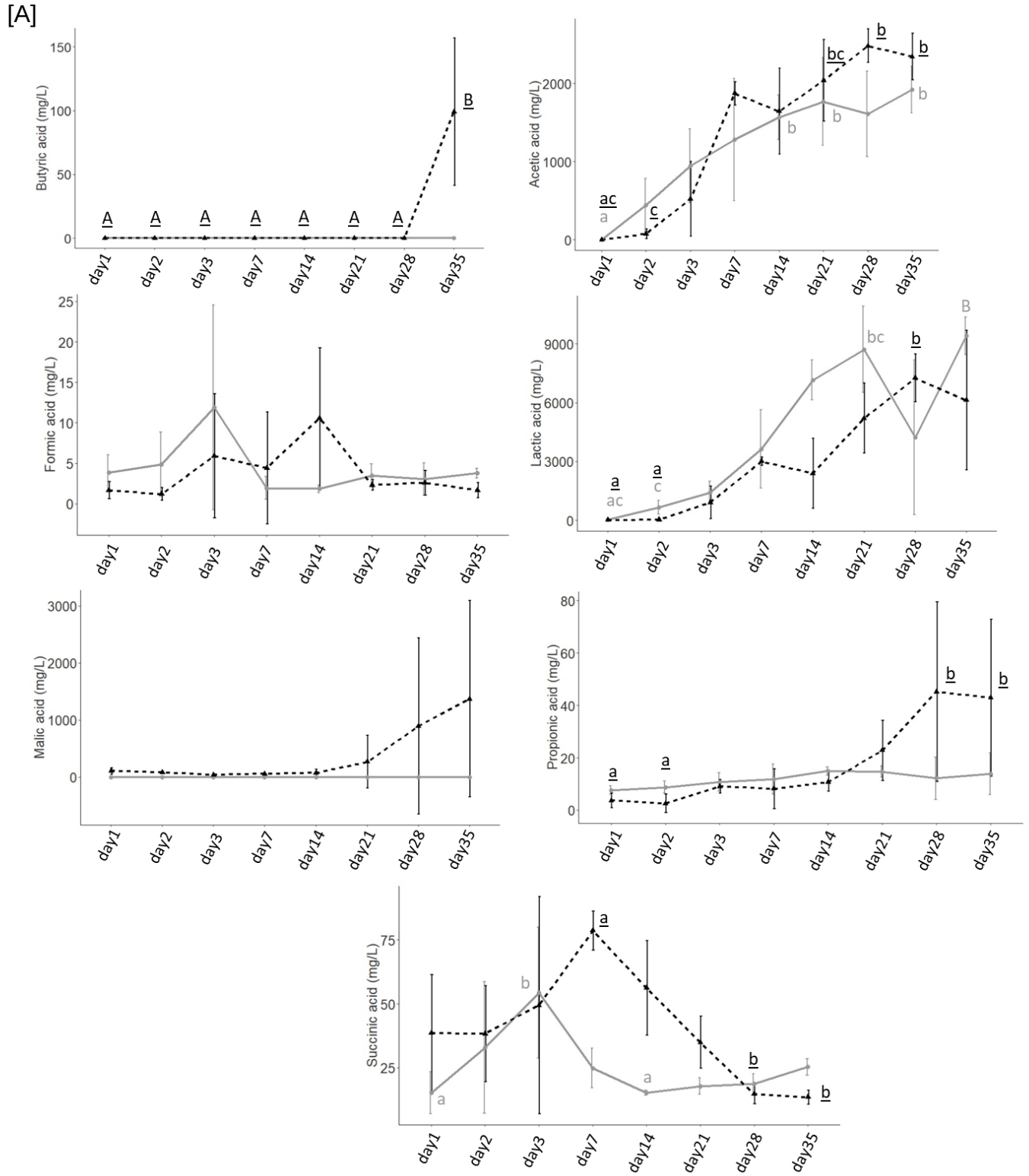

Figure 7B. Continues form Figure 7.

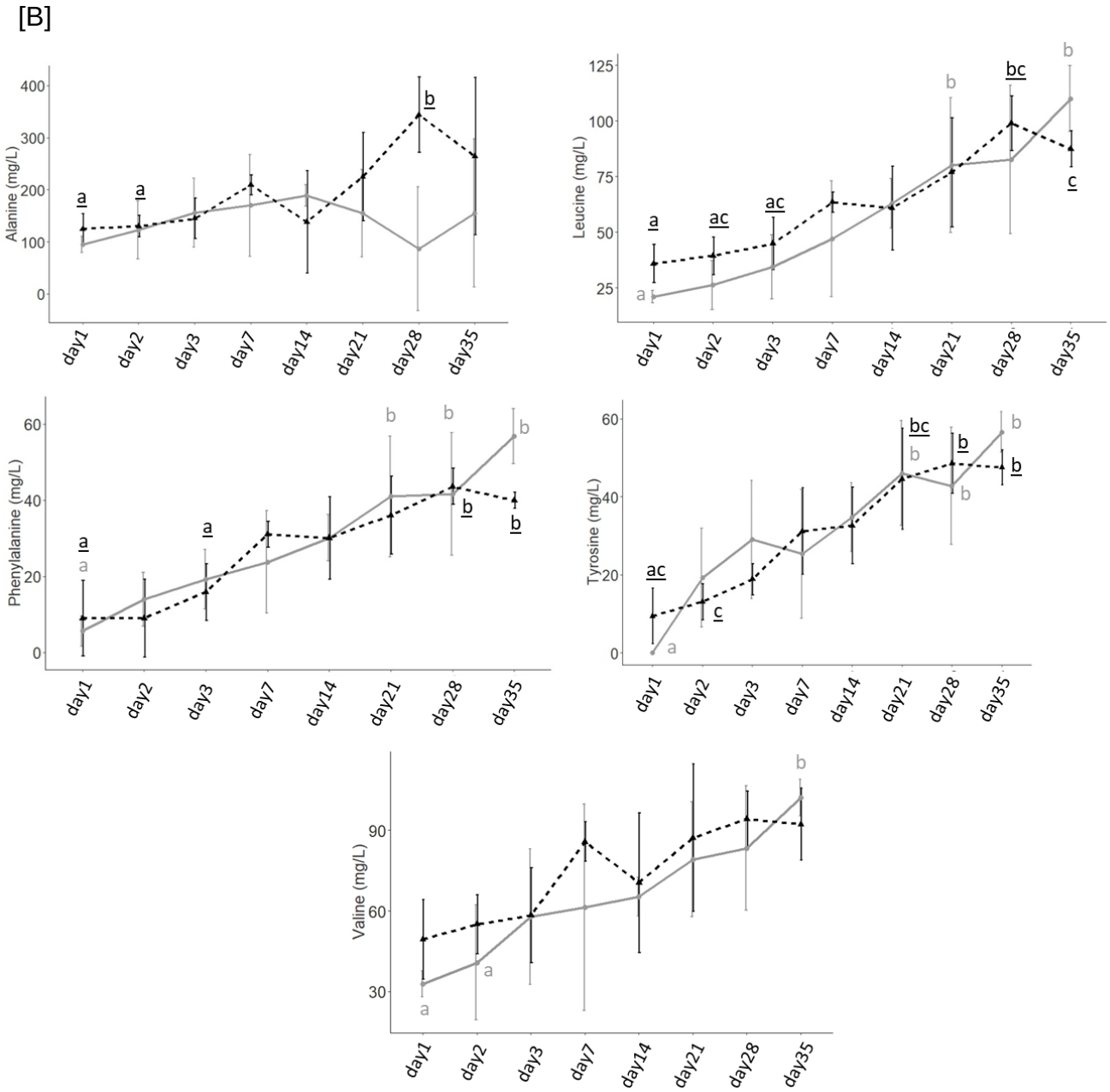

Figure 7C. Continues from Figure 7.

[C]

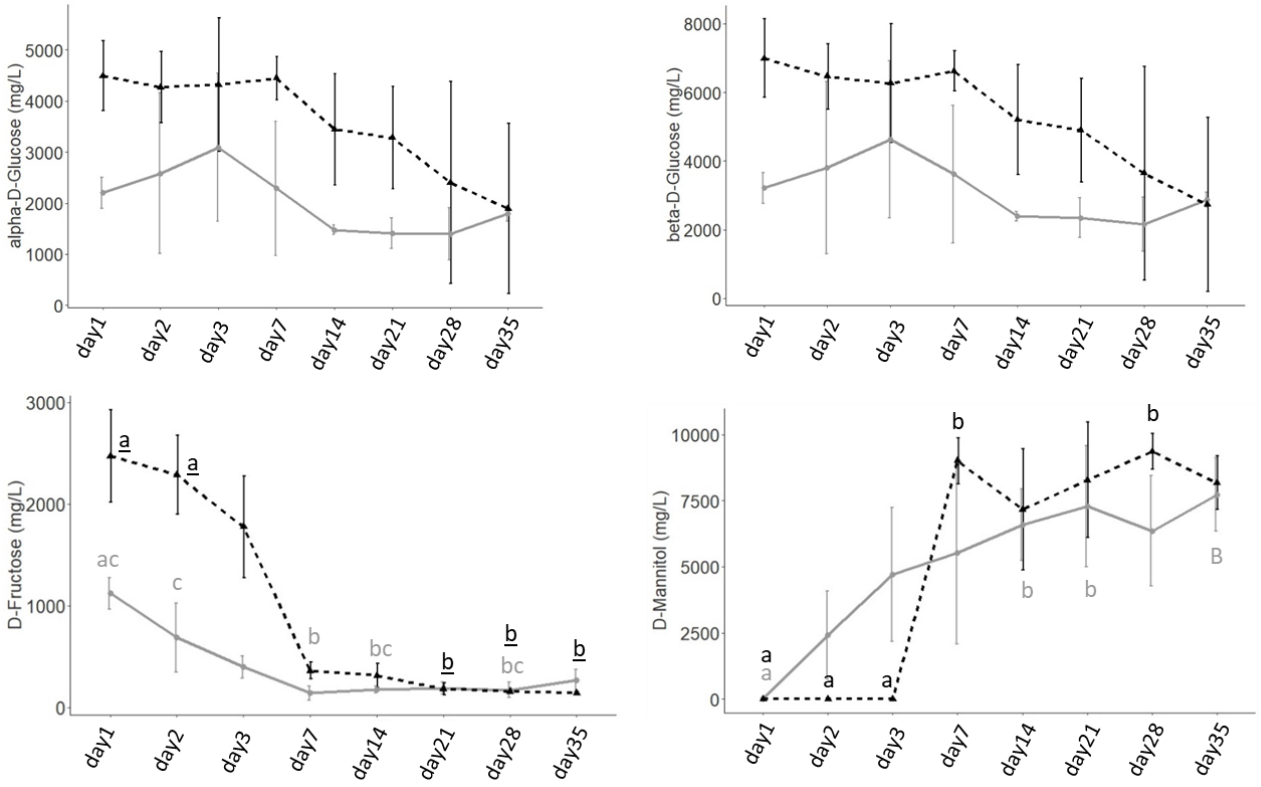

Figure 7D. Continues from Figure 7.

[D]

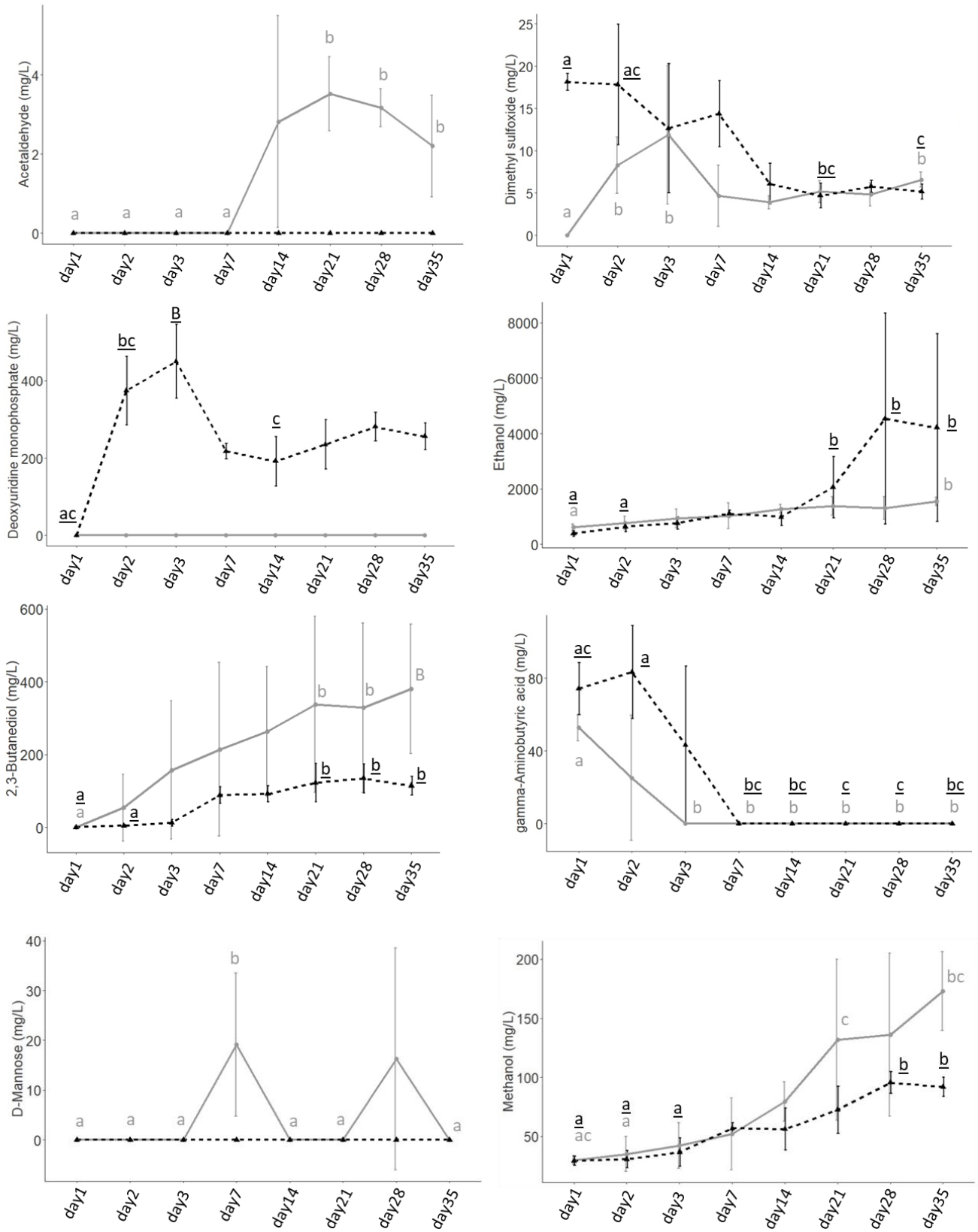

Figure 7D. Continues from previous page.

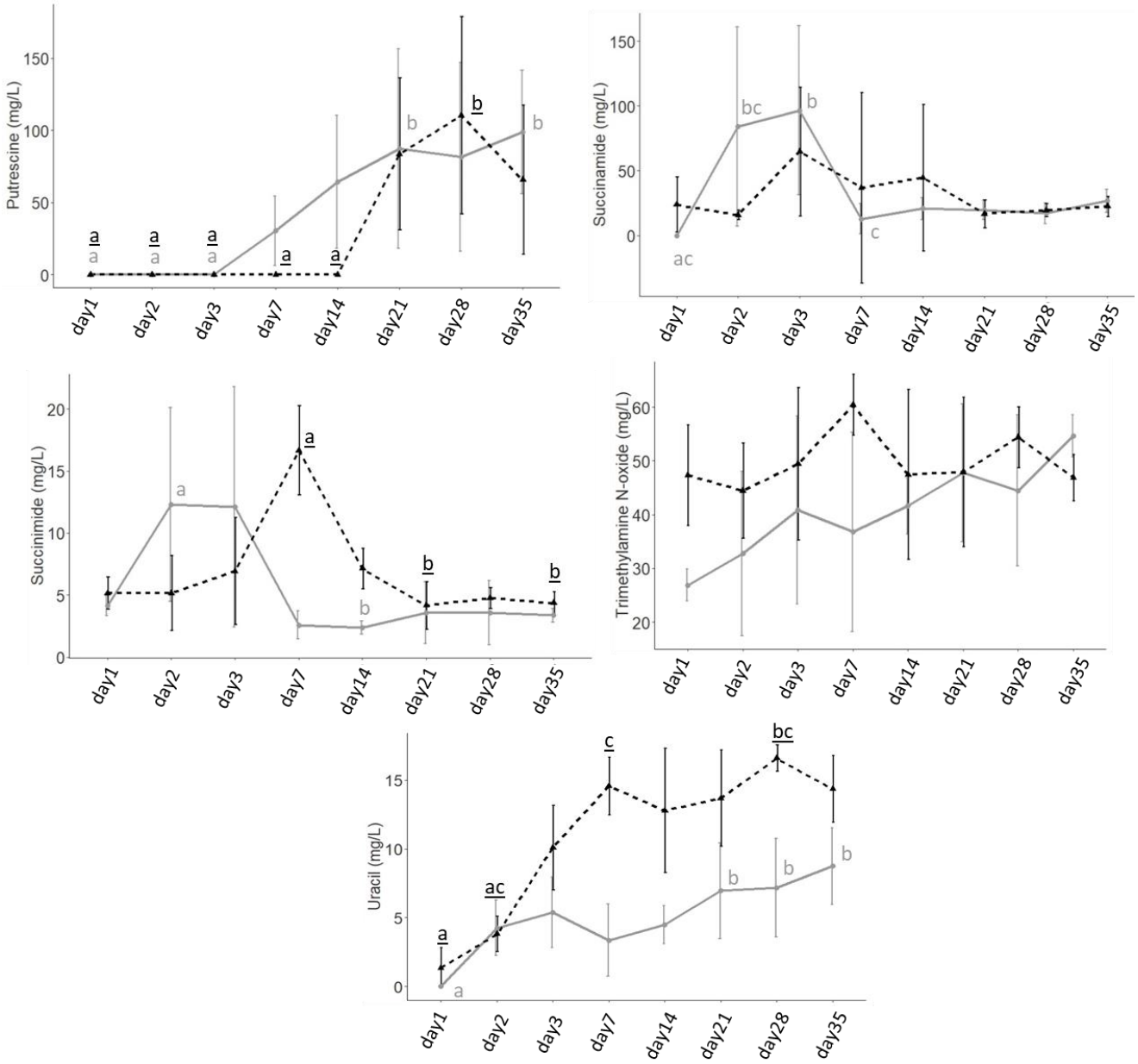

3.5 Effects of sauerkraut water supernatants on TEER measurements

TEER (Ωcm^2) was calculated as described in Section *2.5.2*. **Figure 8** reports changes in TEER expressed as percentage (%) of increase or decrease after 24 hours incubation with test substrates, compared to baseline TEER for each monolayer. The threshold (100%) indicates no changes after 24 h treatment, while higher or lower percentages indicate an increase or a decrease in TEER, respectively. Ethanol is known to decrease TEER inducing tight junction dysfunction (56), while propionic acid plays a crucial role in maintenance and protection of intestinal gut barrier (57), thus they were selected as negative and positive control, respectively. As expected, compared with monolayers incubated with complete DMEM medium as control, the results obtained showed a

clear-cut reduction of TEER after 24 hours exposure to ethanol, as well as a clear TEER improvement after 24 hours exposure to propionic acid (Ctrl: 105.52 ± 10.38 %; ethanol: 57.36 ± 32.76 % ; propionic acid: 122.35 ± 9.64%; p = 0.0274 Ctrl vs ethanol; p = 0.0126 Ctrl vs propionic acid). 24 h exposure to SK1 and SK2 supernatants (SK1: 109.34 ± 9.50 %, SK2: 108.44 ± 7.25 %) did not significantly improve TEER. However, sauerkraut treatment also did not decrease epithelial barrier function when compared to control medium ($p > 0.05$). Both SK1 and SK2 showed significantly lower TEER values when compared to positive control (SK1 vs propionic acid: p = 0.0466; SK2 vs propionic acid: p = 0.0291), and significantly higher values when compared to negative control (SK1 vs ethanol: p = 0.0218; SK2 vs ethanol: p = 0.0239). This does not support the hypothesis that sauerkraut water improves gut barrier function, but showed that SK1 and SK2 did not disrupt barrier integrity.

Figure 8. Changes in trans-epithelial electrical resistance (TEER) across differentiated Caco-2 monolayers in presence/absence of test substrates ($TEER_{24h}$ (Ω cm²)/ $TEER_{0h}$ (Ω cm²) × 100%). The change in TEER is the percentage (%) change after 24 h incubation compared to the initial TEER (0h) for each monolayer. The threshold (100%) indicate no change between baseline and 24 h. The values plotted are the means for three experimental replicates ± the error bars showing the standard deviation (SD). Stars indicate statistical significance when comparing different treatments to control medium, within the same timepoint. SK1, producer 1; SK2, producer 2.

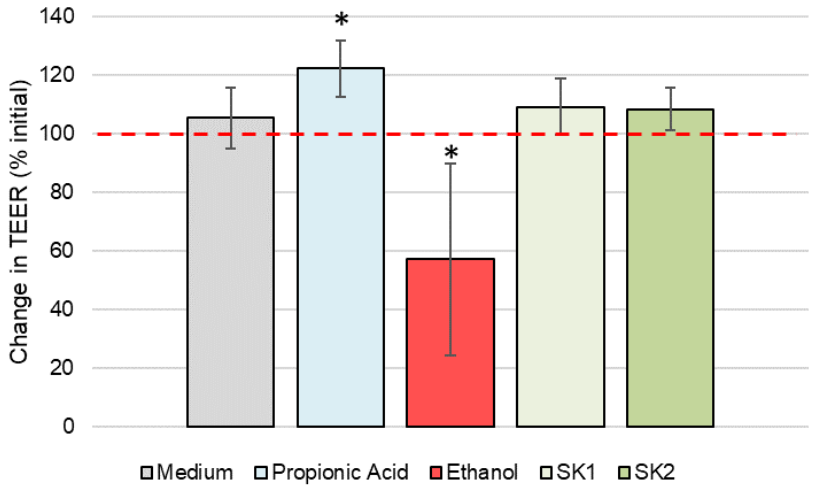

3.6 Cytokine quantification in co-culture supernatants using Magpix®

Both apical and basolateral supernatants from co-culture experiments were analyzed at baseline and after 24 hours of incubation with sauerkraut fermentation water. The median values for the production of each cytokine on either side of the co-culture model (n= 3) are presented in **Figure 9**. In general, the data show high variability of the concentration of each of the cytokines quantified by the assay. This large variability has been previously observed in *in vitro* cell culture experiments that employ PBMCs from different healthy donors, as already suggested by Katial and colleagues (1998) (58). The median values (Median Fluorescent Intensity, MFI) demonstrated no significant

differences in cytokine secretion both from PBMCs and from Caco-2 cells at baseline. As expected, LPS stimulus induced a dramatic increase in all cytokines levels, both in the apical side and in the basolateral, as shown in 24 h panels (**Figure 10**). However, no differences were observed between cytokine concentrations in the apical side when comparing Caco-2 cells incubated with control (CTRL) or with sauerkraut water. Statistically significant changes were observed when considering the basolateral side. Sauerkraut water from both producers stimulated IL-6 (SK1: 40,190.10 ± 1,170.24 MFI; SK2: 40,136.50 ± 2,001.52 MFI; Ctrl: 26,971.2 ± 3,660.37 MFI; mean ± SD; SK1 vs Ctrl, $p = 0.0002$; SK2 vs Ctrl, $p < 0.0001$) production, while IL-10 (SK2: 12,115.3 ± 2,525.93; Ctrl: 8,656.67 ± 1,357.85 MFI, SK2 vs Ctrl, $p = 0.0192$) and TNF-α levels significantly increased after SK2 treatment (SK2: 16,092.90 ± 5,173.35 MFI; Ctrl: 8,338.58 ± 2,328.42 MFI; SK2 vs Ctrl, $p = 0.0124$).

Figure 9. IL-10, IL-1β, IL-6 and TNF-α production by co-cultured Caco-2 (apical side) and PBMCs (basolateral side) under LPS stimulation at baseline (0h) and after 24 h of incubation with sauerkraut water. CTRL is cell culture medium without treatment. Bar plots represent median values of Median Fluorescent Intensity (MFI) and the error bars represent standard deviation. Note the different scales on the y-axis. Different superscript letters indicate statistical significant differences within each cytokine.

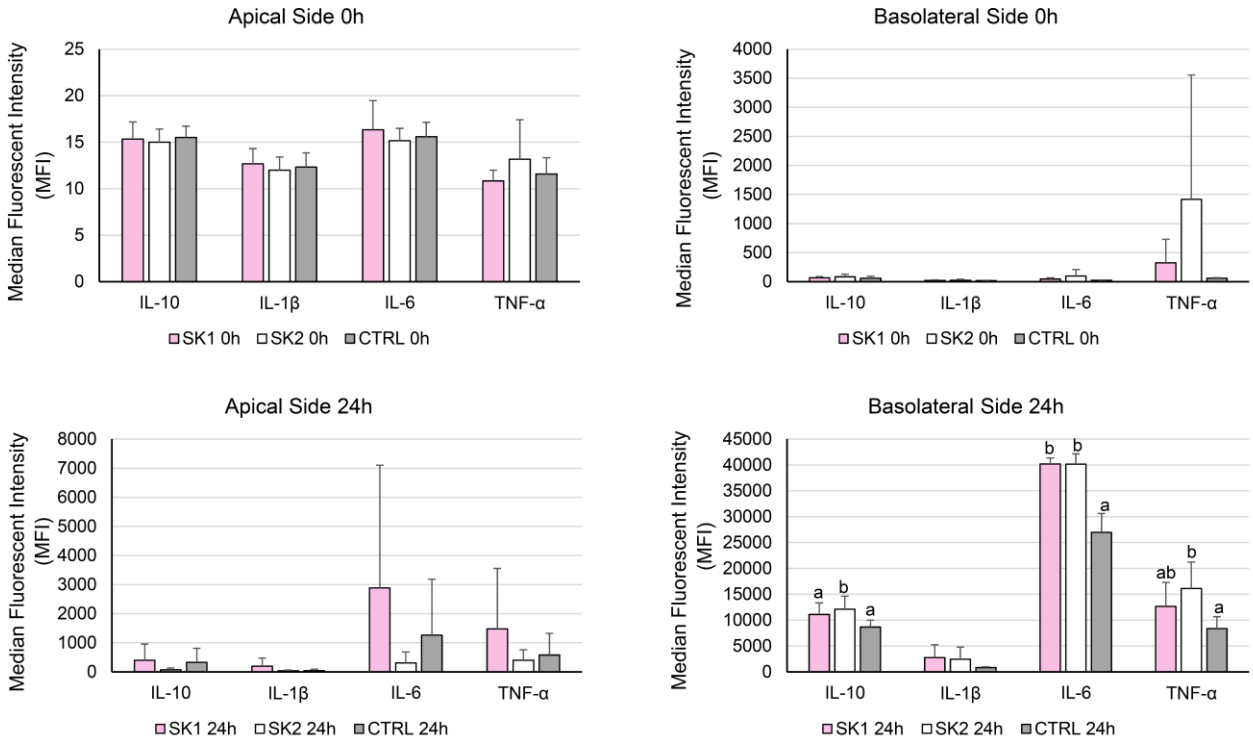

3.7 Effect of sauerkraut water incubation on inflammatory and tight junction (TJ) genes expression

To support the quantification of pro- and anti-inflammatory cytokines in PBMCs supernatants after 24 h incubation with sauerkraut water, gene expression was investigated by RT-PCR. As shown in **Figure 10**A, no significant changes were observed in IL-10 and IL-6 expression after 3 h and 6 h

of incubation with sauerkraut water. To support the results obtained from TEER measurements, expression of tight junction (TJ) genes was investigated in Caco-2 cells before and after incubation with SK1, SK2 and Ctrl. Occludin showed increased expression from 0h to 6h, although not statistically significant. No significant changes were observed in claudin-1 and claudin-4 after incubation with the different treatments (**Figure 10**B).

Figure 10. Gene expression of inflammatory cytokines IL-6 and IL-10 in PBMCs cells (**A**) and of TJ proteins occludin, claudin-1 and claudin-4 in Caco-2 cells (**B**) (n=3 co-culture experiments). Bar plots show mean relative fold change ($2^{-\Delta\Delta Ct}$) compared to Ctrl medium. Error bars represent the standard deviation.

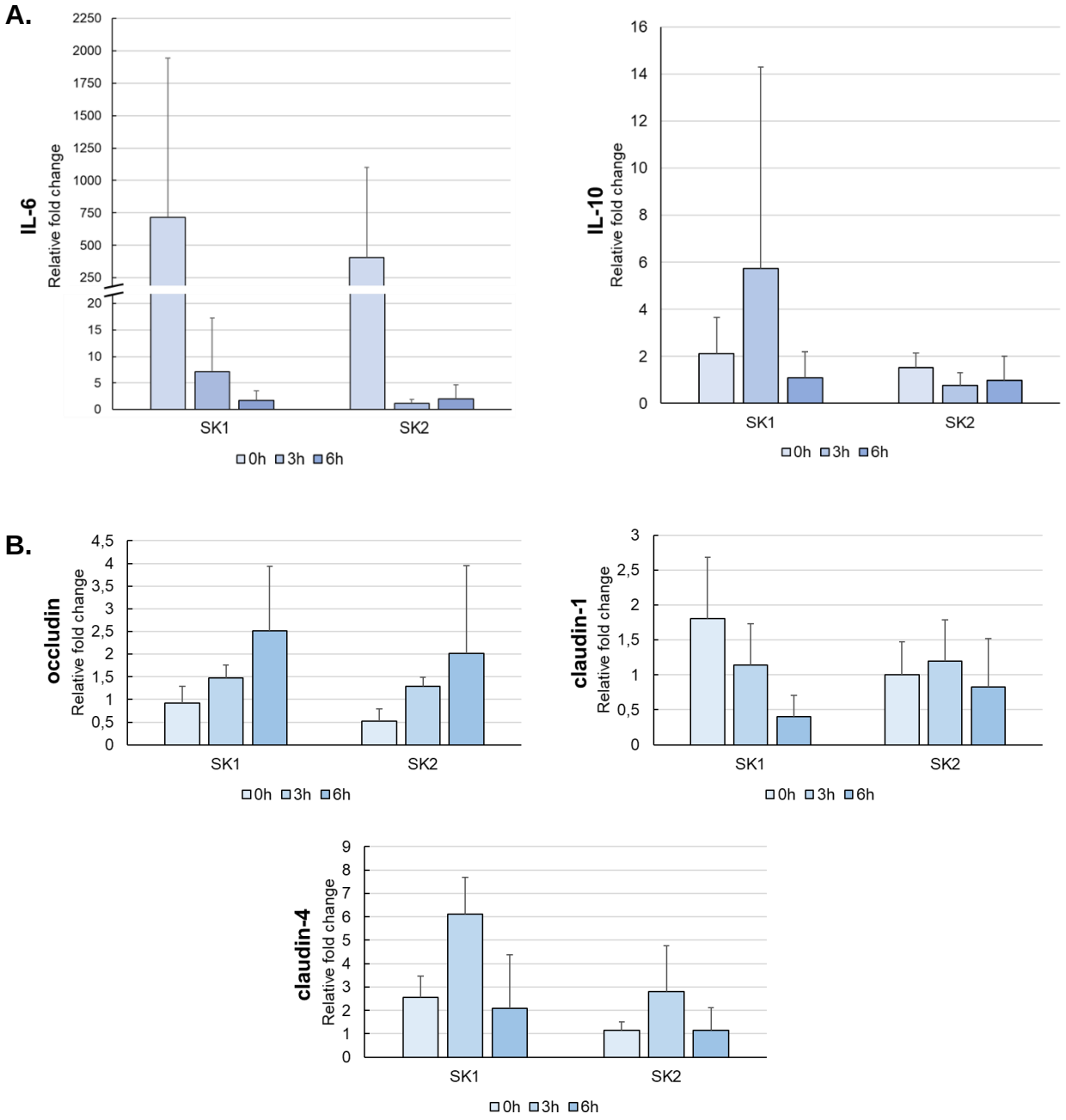

3.8 Effect of sauerkraut water on cytokines and TJ proteins in Caco-2 cells.

To further confirm the effect of sauerkraut water on gut barrier function, the quantity of TJ proteins in Caco-2 cells was analyzed by western blot (**Figure 11**). We found no significant enhancement of occludin and claudin-1 protein expression after 24 h incubation with SK1 or SK2. A slight increase in claudin-4 protein, although not statistically significant, was observed 24 h after incubation with SK1 and SK2 in all experimental replicates (n=3).

Figure 11. Western blot in co-cultured Caco-2 cells at baseline (0h) and after 24 h incubation with sauerkraut water from both producers (SK1 and SK2) (n=3). Molecular weight of each protein is described on the left side of the image. β-actin was used as control protein (**A**). Densitometric analysis was performed with ImageJ software. Values are expressed as fold change normalized to medium control (Ctrl) samples (**B**). No significant differences were observed between different treatments and between different timepoints.

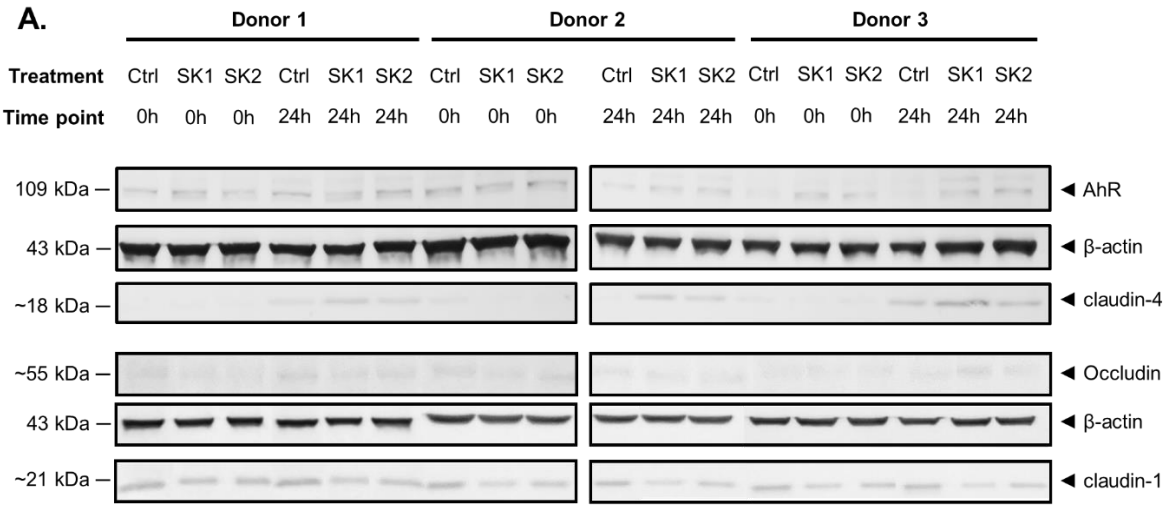

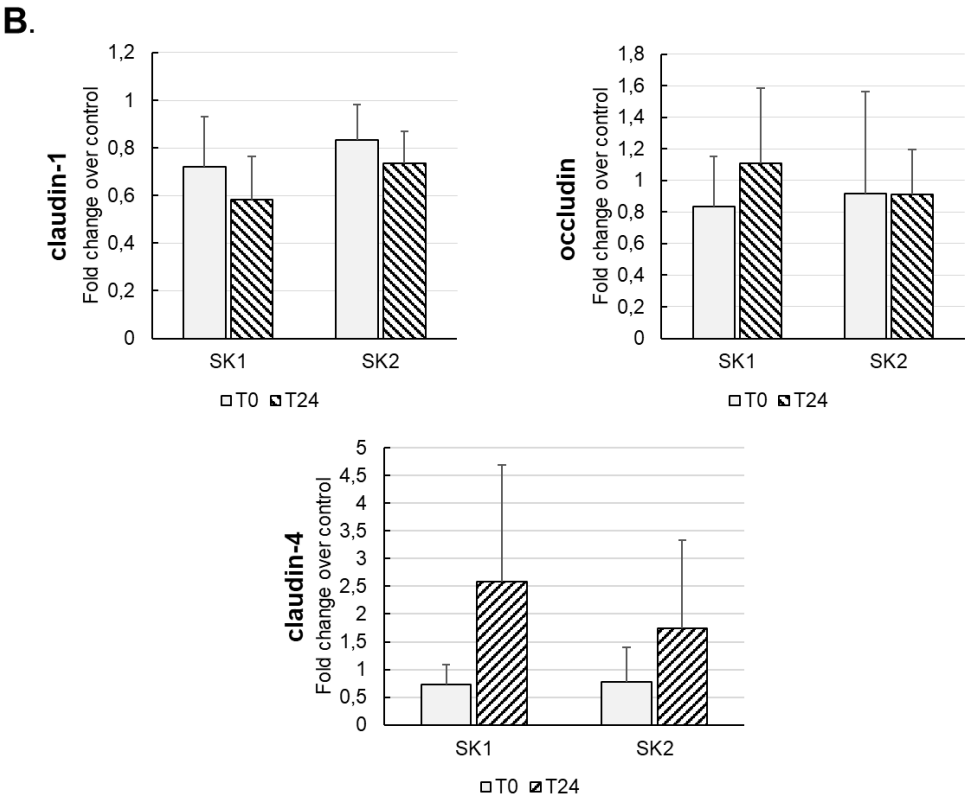

4. Discussion

The aim of this study was to characterize the sauerkraut-associated microbiome, its successional development over the course of the fermentation and its metabolic output. Further, we aimed to evaluate the protective role of sauerkraut water on gut permeability and inflammation using a preclinical *in vitro* model of the intestinal barrier and immune function.

Our current study characterized the sauerkraut fermentation process in two local organic sauerkraut products. Temperature, pH and the succession of fermentative microbiota were assessed over 35 days of fermentation. Temperature increased over the first week of fermentation, reaching the maximum value around day 10 (SK1: 22.42 °C ± 0.27, SK2: 16.15 °C ± 0.30, mean ± SD) and then decreasing until approaching room temperature. This is consistent with previous reports with similar fermented foods (59). The increase in temperature levels occurred at the same time as rapid acid production, thus reducing the pH, between the beginning of fermentation and day 14. In this period pH dropped from 5.7 at day 1 in both products, to 3.82 and 3.99 at day 14. The increase in acidity levels over time is attributable to organic acids production by fermentative bacteria. This was confirmed by NMR results, since pH drop-down went hand in hand with the increase in organic acids production, mainly lactic and acetic acid. We measured changes in viable bacterial counts (CFU/mL) in each tank during the sauerkraut fermentation. From our results, it appears that changes

in acidity and temperature proceeded in parallel with bacterial counts variation. As the fermentation proceeded, the microbial diversity gradually decreased and LAB became the dominant bacteria, as confirmed by the 16S rRNA amplicon-based microbiota profiling. This change was analogous to pH variation over time, thus suggesting that organic acids accumulation inhibited the growth of bacteria which were not tolerant to a higher acidic environment, as previously observed (16). The microbial composition on day 1 included microorganisms from cabbage itself, but also from the environment, including the materials used, the operator and the floor of the storage room, such as *Enterobacter, Serratia, Pseudomonas, Pectobacterium, Pantoea, Lelliottia, Buttiauxella* and *Acinetobacter*. While both observed OTUs and Chao1 index significantly decreased over the fermentation process, thus indicating lower bacterial richness with LAB becoming the predominant taxa, the Shannon diversity index showed a successive increase in α-diversity from day 7 (SK1) or day 14 (SK2) until day 35. As previously suggested by Zabat and colleagues (15), and in agreement with the reduction in bacterial genera observed for the same timepoints through 16S rRNA sequencing, we believe that increased Shannon index reflects increased evenness amongst LAB actively involved in the fermentation while also reflecting a reduced richness of less dominant, rare phylotypes as the fermentation progressed. Results from 16S rRNA analysis showed a clear separation in sauerkraut water microbiota at different fermentation timepoints. After 35 days of fermentation, LAB *Lactiplantibacillus*, *Leuconostoc*, *Pediococcus*, *Levilactobacillus*, *Paucilactobacillus* and *Secundilactobacillus* were the predominant genera. Our findings are in line with previous descriptions of sauerkraut microbiota, which used both culture-based (60) and culture-independent methods (15,16,61) and identified *Leuconostoc, Lactobacillus* and *Pediococcus* as the primary microorganisms in sauerkraut. Our 16S rRNA results were also consistent with pH and NMR results, confirming that acidity levels, lactic acid concentration and LAB abundances are strictly correlated showing an increasing trend until the end of the fermentation. Other than being the most important bacteria involved in the fermentation process, some of these LAB are known for their potential probiotic properties (5,6,62). However, since only specific LAB strains are able to act as probiotic, it is difficult to speculate without knowing these details. For this reason, bacterial biotypes isolated from sauerkraut water and then analyzed using RAPD PCR and Bionumerics® will be characterized using Sanger sequencing. These strains will form the basis of a sauerkraut biobank at FEM of LAB of potential biotechnological and probiotic interest. Future analysis will allow a better understanding of the bacterial strains responsible for the fermentation process, the metabolites they produce, and their

potential to drive vegetable fermentations and/or express probiotic traits such as anti-pathogen, anti-inflammatory or anti-cancer activities.

In the present study, NMR analysis was used for high-throughput and highly-reproducible (63) characterization of metabolites in sauerkraut water samples. An accumulation of organic acids was observed over the fermentation process, with a significant production of acetic and lactic acid. Butyric and propionic acid significantly increased only in SK2 producer reaching the highest levels at day 35, while their concentration did not vary in SK1. The increase in organic acids was paralleled pH variations. Together with acidification, proteolysis is considered a key feature of food fermentation, since it influences the production of flavor compounds, but also increases polypeptides digestibility (64,65). In this study, we observed a significant increase in the concentration of aromatic amino acids Phe and Tyr, which may have contributed to the typical aroma and flavor of fermented cabbage, as previously suggested (66,67). During the fermentation process we also observed a significant increase of the hydrophobic amino acid Leu, which has been suggested to be responsible for bitter taste in different fermented foods (68). γ-aminobutyric acid (GABA), a non-protein amino acid serving as the major inhibitory neurotransmitter in the brain and in the spinal cord (69), showed a pattern of decrease with the fermentation period. This is consistent with previous studies, where GABA was converted to other metabolites, such as succinate, during fermentation (68,70). Over 35 days of fermentation, we observed a significant increase in uracil concentration in sauerkraut water from both producers. Uracil has been previously identified as a metabolic product of LAB fermentation and especially of *Lactobacillus plantarum* metabolism (71).

Changes in metabolites are also key indicators reflecting the activity of bacteria during sauerkraut fermentation. For example, the consumption of D-fructose we observed during the fermentation process, together with the increase in mannitol concentrations which may be attributed to *Leuconostoc*. *Leuconostoc* have been shown to utilize fructose as alternative electron acceptor to produce mannitol by Harth and colleagues (2016) (67).

By employing a Caco-2 cell monolayer grown in a trans-well system, we demonstrated that sauerkraut water did not significantly improve barrier function, as measured by TEER. However, we also confirmed that sauerkraut water did not cause intestinal permeability, since TEER values after 24 h incubation were significantly higher in both SK1 and SK2 compared to ethanol. Gene and protein expression of TJ did not reveal significant changes after Caco-2 monolayer incubation with sauerkraut water. TJ proteins claudin-1, claudin-4 and occludin were selected to assess gut barrier function, since they have been demonstrated to play a key role in maintaining intestinal barrier

integrity (72,73). Moreover, downregulation of claudin-1 and occludin has been observed after LPS-stimulation in Caco-2 cells, together with an increase in gut permeability (72). Downregulation of claudin-4 has been observed after TNF-α inflammatory stimulus in T84 cells monolayers, together with increased paracellular permeability (74). These studies further support the role of these TJ proteins in gut barrier function maintenance, which is disrupted during inflammation. In our work, no changes were observed in claudin-1, claudin-4, occludin mRNA or protein expression in Caco-2 To further investigate possible immune modulatory effects of sauerkraut water we employed an *in vitro* co-culture model, based on Caco-2 cells differentiated as a monolayer and PBMC under LPS stimulus. We found no significant changes in inflammatory interleukin IL-6 and anti-inflammatory IL-10 mRNA expression in PBMCs after 3 and 6 hours incubation with sauerkraut water. However, cytokine quantification in basolateral supernatants revealed a significant increase in IL-6, IL-10 and TNF-α levels after 24 hours incubation with sauerkraut water. IL-6 and TNF-α are pro-inflammatory cytokines typically released by various cell types, including intestinal mucosal immune cells, during LPS stimulation (75–77), while IL-10 is an anti-inflammatory mediator crucial in maintaining an adequate balance of the inflammatory response and is involved in resolving inflammation after an inflammatory trigger (78). The results from the present study indicated that sauerkraut water has the potential to improve immune function, supporting an appropriate immune response to LPS challenge (increased IL-6 and TNF-α) and importantly, modulating the inflammatory response through IL-10 production. The fact that sauerkraut water induced IL-10 production suggests that sauerkraut water might promote a resolution of inflammation and re-establishment of normal inflammatory status after an inflammatory challenge. This is important in chronic inflammatory diseases both within the gastrointestinal tract and at extra-gastrointestinal sites, since unresolved inflammation has been identified as a risk factor for metabolic derangement associated with cardiovascular disease and type 2 diabetes, and may also play an aetiological role in autoimmune diseases. In the present study, the anti-inflammatory role of sauerkraut water may be driven by acetic acid and lactic acid, both present at high concentrations after 35 days of fermentation and both identified as immune response mediators due to their ability to bind GPCRs (35,79). Latham and colleagues highlighted the role of lactic acid in inhibiting the histone deacetylases HDAC11, a suppressor of IL-10 expression, thus suggesting that lactic acid may act as a transcriptional regulator, linking microbial metabolism to immunomodulation (80). In our experiments we did not observe a change in IL-10 gene expression at 3 h and at 6 h after incubation with sauerkraut water, but we did

detect higher concentrations of IL-10 in PBMCs supernatants after 24 h incubation with SK water in presence of an inflammatory stimulus.

In this study, we characterized spontaneous fermentation of white cabbage by the autochthonous microbiota of the plant and we measured the production of different microbial metabolites, including organic acids, amino acids, amines and sugars, as a result of this fermentation. Physicochemical measurements showed that temperature and pH were indicative of the heterolactic fermentation carried out by LAB (59). In line with outcomes from similar studies (16,59) viable bacterial count (CFU/mL) and 16S rRNA amplicon based profiling showed that bacterial diversity gradually decreased as the fermentation progressed, with microbial communities being shaped by the acidic, salty, anaerobic, LAB-dominated environmental conditions. We then investigated how sauerkraut water might impact on gut health, by using an *in vitro* Caco-2 intestinal epithelial cells-PBMCs co-culture model. Although no differences were observed in gut barrier function, sauerkraut water significantly modulated the inflammatory response in PBMCs under LPS stimulation, by resolving inflammation via IL-10 production after an initial LPS-induced inflammatory trigger. Findings from this *in vitro* study regarding the potential role of sauerkraut water in resolving LPS-induced inflammation should be confirmed in human intervention trials, in order to investigate whether daily consumption of sauerkraut water may reduce chronic systemic inflammation in diabetic or obese subjects or intestinal inflammation in patients with irritable bowel syndrome or inflammatory bowel disease.

Supplementary material

Table S1. Metabolites concentration (mg/L) in sauerkraut water quantified by NMR. Data represent the mean and standard deviation (SD) after 1, 2, 3, 7, 14, 21, 28 and 35 days of fermentation. Producer 1 (SK1) (**A**), producer 2 (SK2) (**B**). DMSO, dimethyl sulfoxide; dUMP, deoxyuridine monophosphate; GABA, gamma-aminobutyric acid.

A. SK1	**Day 1**	**Day 2**	**Day 3**	**Day 7**	**Day 14**	**Day 21**	**Day 28**	**Day 35**
Organic acids								
Acetic acid								
mean	0.00	441.25	944.35	1281.35	1568.03	1767.27	1610.06	1923.64
SD	0.00	339.46	472.53	784.27	287.08	562.87	546.43	298.16
Butyric acid								
mean	0.00	0.00	0.00	0.00	0.00	0.00	0.00	0.00
SD	0.00	0.00	0.00	0.00	0.00	0.00	0.00	0.00
Formic acid								
mean	3.87	4.88	11.88	1.93	1.84	3.50	3.04	3.77
SD	2.17	3.97	12.65	1.40	0.46	1.40	2.02	0.60
Lactic acid								
mean	17.66	650.02	1397.50	3634.37	7148.75	8713.62	4228.90	9418.22
SD	3.16	348.11	579.28	1994.91	1018.56	2193.76	3939.70	953.14
Malic acid								
mean	0.00	0.00	0.00	0.00	0.00	0.00	0.00	0.00
SD	0.00	0.00	0.00	0.00	0.00	0.00	0.00	0.00
Propionic acid								
mean	7.62	8.75	10.73	11.86	14.97	14.68	12.14	13.84
SD	1.61	2.32	3.54	5.79	1.61	2.14	8.02	8.01
Succinic acid								
mean	15.12	32.83	54.32	24.80	15.12	17.71	18.66	25.27
SD	8.20	25.78	25.68	7.70	0.99	3.23	3.95	3.19
Amino acids								
Alanine								
mean	95.33	122.41	156.09	170.16	189.05	154.48	86.42	155.19
SD	15.50	55.83	65.80	97.64	20.88	83.80	118.79	142.26
Leucine								
mean	20.99	26.23	34.37	46.96	62.96	80.01	82.64	109.92
SD	2.78	11.05	14.35	25.96	11.09	30.25	33.34	14.71
Phenylalanine								
mean	5.62	13.88	19.16	23.79	30.06	40.97	41.63	56.83
SD	3.98	7.07	7.80	13.45	6.11	15.90	16.16	7.16
Tyrosine								
mean	0.00	19.21	28.99	25.37	34.79	46.02	42.76	56.53
SD	0.00	12.66	15.16	16.56	8.82	13.47	15.03	5.19
Valine								
mean	32.80	40.77	57.87	61.39	65.37	79.19	83.41	102.15
SD	4.76	21.37	25.26	38.47	7.24	21.34	23.23	6.80
Sugars								
alpha-D-Glucose								
mean	2201.56	2584.58	3093.71	2288.03	1474.43	1409.93	1398.76	1799.80
SD	301.24	1567.87	1452.38	1307.72	93.40	293.67	504.74	151.32
beta-D-Glucose								
mean	3214.05	3800.30	4635.16	3616.89	2385.68	2343.88	2149.31	2869.59

SD	448.57	2512.57	2289.34	2004.13	132.50	578.54	786.52	227.60
D-Fructose								
mean	1122.40	688.21	398.15	141.61	176.56	191.69	172.59	265.56
SD	154.91	339.92	108.01	71.13	32.97	59.68	74.62	111.22
D-Mannose								
mean	0.00	0.00	0.00	19.10	0.00	0.00	16.21	0.00
SD	0.00	0.00	0.00	14.39	0.00	0.00	22.28	0.00
Other compounds								
2,3-Butanediol								
mean	0.00	53.53	157.35	213.94	262.97	337.41	329.12	380.85
SD	0.00	92.18	190.09	238.50	179.05	241.85	232.92	178.00
Acetaldehyde								
mean	0.00	0.00	0.00	0.00	2.82	3.52	3.17	2.20
SD	0.00	0.00	0.00	0.00	2.67	0.93	0.48	1.28
DMSO								
mean	0.00	8.28	11.88	4.69	3.91	5.16	4.84	6.56
SD	0.00	3.34	8.18	3.62	0.78	1.31	1.40	0.89
D-Mannitol								
mean	0.00	2418.49	4712.37	5516.47	6587.63	7293.36	6359.92	7734.94
SD	0.00	1672.67	2531.59	3430.65	1341.11	2287.44	2078.10	1393.15
dUMP								
mean	0.00	0.00	0.00	0.00	0.00	0.00	0.00	0.00
SD	0.00	0.00	0.00	0.00	0.00	0.00	0.00	0.00
Ethanol								
mean	607.21	768.34	927.90	1023.51	1275.55	1385.11	1308.00	1541.07
SD	123.49	243.38	339.28	465.98	155.13	333.47	404.74	150.73
GABA								
mean	52.80	25.16	0.00	0.00	0.00	0.00	0.00	0.00
SD	7.23	34.46	0.00	0.00	0.00	0.00	0.00	0.00
Methanol								
mean	29.86	35.12	42.29	52.23	79.65	131.94	136.30	172.95
SD	3.67	14.79	19.12	30.50	16.73	68.09	68.99	33.22
Putrescine								
mean	0.00	0.00	0.00	30.32	64.35	87.44	81.45	98.73
SD	0.00	0.00	0.00	23.94	46.21	69.12	65.41	42.75
Succinamide								
mean	0.00	83.90	96.45	12.78	20.68	19.52	16.97	26.73
SD	0.00	76.90	65.27	11.82	8.36	7.59	7.91	9.00
Succinimide								
mean	4.16	12.29	12.09	2.58	2.38	3.57	3.57	3.37
SD	0.83	7.82	9.67	1.13	0.54	2.49	2.58	0.54
Trimethylamine N-oxide								
mean	26.89	32.74	40.85	36.80	41.61	47.76	44.46	54.67
SD	2.98	15.33	17.54	18.56	5.22	12.80	14.08	3.92
Uracil								
mean	0.00	4.26	5.38	3.36	4.48	6.95	7.17	8.74
SD	0.00	2.01	2.56	2.63	1.37	3.49	3.60	2.79
B. SK2	**Day 1**	**Day 2**	**Day 3**	**Day 7**	**Day 14**	**Day 21**	**Day 28**	**Day 35**
Organic acids								
Acetic acid								
mean	0.00	75.66	522.56	1873.56	1643.09	2037.38	2480.19	2340.99
SD	0.00	62.99	477.37	148.62	551.08	522.57	214.00	297.64

Butyric acid								
mean	0.00	0.00	0.00	0.00	0.00	0.00	0.00	99.04
SD	0.00	0.00	0.00	0.00	0.00	0.00	0.00	57.79
Formic acid								
mean	1.66	1.20	5.89	4.42	10.59	2.30	2.58	1.66
SD	1.06	0.77	7.66	6.94	8.67	0.65	1.51	0.95
Lactic acid								
mean	9.91	29.91	904.58	3003.45	2388.74	5211.31	7255.58	6121.66
SD	13.02	33.95	838.63	220.67	1777.28	1778.69	1229.59	3554.43
Malic acid								
mean	108.07	85.81	40.76	56.05	75.35	270.57	893.51	1370.30
SD	55.81	20.38	17.75	8.91	62.10	464.02	1542.25	1720.16
Propionic acid								
mean	3.67	2.54	9.04	8.19	10.73	22.87	45.18	42.92
SD	2.75	3.52	2.57	7.56	3.54	11.49	34.25	30.00
Succinic acid								
mean	38.50	38.26	49.36	78.65	56.21	34.95	14.64	13.46
SD	22.83	18.79	42.46	7.63	18.44	10.25	3.88	2.72
Amino acids								
Alanine								
mean	124.73	130.07	144.86	209.18	138.27	225.22	343.71	264.60
SD	29.33	20.64	38.73	18.91	98.29	85.14	72.22	150.65
Leucine								
mean	35.94	39.35	44.86	63.49	60.86	76.87	98.90	87.36
SD	8.63	8.55	11.71	4.60	18.82	24.50	12.33	8.01
Phenylalanine								
mean	8.92	8.92	15.86	31.06	30.06	36.01	43.61	39.98
SD	9.95	10.22	7.44	3.39	10.86	10.21	4.76	2.15
Tyrosine								
mean	9.42	13.05	18.84	31.16	32.61	44.57	48.56	47.47
SD	7.06	4.69	3.97	11.13	9.84	12.98	7.73	4.51
Valine								
mean	49.44	55.06	58.34	85.75	70.52	87.16	94.19	92.31
SD	14.80	10.99	17.62	7.38	26.03	27.42	10.40	13.39
Sugars								
alpha-D-Glucose								
mean	4493.91	4266.55	4317.35	4447.79	3446.10	3279.27	2401.89	1891.32
SD	685.64	694.80	1302.40	421.22	1087.34	997.68	1979.30	1664.51
beta-D-Glucose								
mean	6993.09	6465.58	6266.69	6626.28	5203.02	4897.11	3645.00	2733.75
SD	1143.96	948.68	1723.83	590.56	1604.05	1514.98	3113.00	2540.08
D-Fructose								
mean	2469.99	2287.31	1776.74	361.76	315.64	183.04	158.18	143.41
SD	451.93	390.67	499.02	82.74	118.43	59.35	16.28	14.78
D-Mannose								
mean	0.00	0.00	0.00	0.00	0.00	0.00	0.00	0.00
SD	0.00	0.00	0.00	0.00	0.00	0.00	0.00	0.00
Other compounds								
2,3-Butanediol								
mean	0.00	4.51	12.62	88.50	91.74	122.56	134.46	114.27
SD	0.00	2.55	9.45	22.59	21.83	52.88	39.78	25.97
Acetaldehyde								

mean	0.00	0.00	0.00	0.00	0.00	0.00	0.00	0.00
SD	0.00	0.00	0.00	0.00	0.00	0.00	0.00	0.00
DMSO								
mean	18.13	17.81	12.66	14.38	6.09	4.69	5.78	5.16
SD	1.02	7.11	7.66	3.93	2.43	1.46	0.70	0.89
D-Mannitol								
mean	0.00	0.00	0.00	9009.76	7162.92	8279.26	9361.35	8179.80
SD	0.00	0.00	0.00	865.01	2292.56	2182.12	668.02	1006.09
dUMP								
mean	0.00	374.13	449.95	217.58	191.69	235.45	281.06	255.79
SD	0.00	88.21	95.26	20.16	64.11	64.37	37.58	34.59
Ethanol								
mean	385.42	627.27	761.60	1103.45	980.41	2057.37	4534.17	4209.72
SD	107.59	170.53	226.04	126.81	308.06	1107.45	3808.75	3389.78
GABA								
mean	74.25	83.32	43.31	0.00	0.00	0.00	0.00	0.00
SD	14.27	25.47	43.24	0.00	0.00	0.00	0.00	0.00
Methanol								
mean	29.28	30.69	36.65	56.84	56.13	72.47	95.54	91.95
SD	3.78	7.22	11.81	4.65	17.88	20.05	9.07	8.00
Putrescine								
mean	0.00	0.00	0.00	0.00	0.00	83.57	110.36	65.58
SD	0.00	0.00	0.00	0.00	0.00	52.52	68.11	51.70
Succinamide								
mean	23.70	15.80	64.61	36.72	44.62	16.50	19.52	22.31
SD	21.20	3.45	49.88	73.66	56.60	10.69	4.89	7.77
Succinimide								
mean	5.15	5.15	6.94	16.65	7.13	4.16	4.76	4.36
SD	1.29	3.01	4.32	3.60	1.63	1.91	0.83	0.89
Trimethylamine N-oxide								
mean	47.31	44.46	49.42	60.38	47.46	47.91	54.37	46.86
SD	9.33	8.88	14.15	5.64	15.78	13.94	5.66	4.33
Uracil								
mean	1.35	3.81	10.09	14.57	12.78	13.67	16.59	14.35
SD	1.46	1.28	3.07	2.10	4.53	3.49	0.94	2.43

References

1. Marco ML, Heeney D, Binda S, Cifelli CJ, Cotter PD, Foligné B, et al. Health benefits of fermented foods: microbiota and beyond. Current Opinion in Biotechnology. 2017 Apr;44:94–102.

2. Carvalho NM de, Costa EM, Silva S, Pimentel L, Fernandes TH, Pintado ME. Fermented Foods and Beverages in Human Diet and Their Influence on Gut Microbiota and Health. Fermentation. 2018 Oct 28;4(4):90.

3. García-Díez J, Saraiva C. Use of Starter Cultures in Foods from Animal Origin to Improve Their Safety. IJERPH. 2021 Mar 4;18(5):2544.

4. Battcock M, Azam-Ali S. Fermented fruits and vegetables: a global perspective. Rome: Food and Agriculture Organization of the United Nations; 1998. 96 p. (FAO agricultural services bulletin).

5. Shahbazi R, Sharifzad F, Bagheri R, Alsadi N, Yasavoli-Sharahi H, Matar C. Anti-Inflammatory and Immunomodulatory Properties of Fermented Plant Foods. Nutrients. 2021 Apr 30;13(5):1516.

6. Dimidi E, Cox S, Rossi M, Whelan K. Fermented Foods: Definitions and Characteristics, Impact on the Gut Microbiota and Effects on Gastrointestinal Health and Disease. Nutrients. 2019 Aug 5;11(8):1806.

7. Food and Agriculture Organization of the United Nations, World Health Organization, editors. Probiotics in food: health and nutritional properties and guidelines for evaluation. Rome: Food and Agriculture Organization of the United Nations : World Health Organization; 2006. 50 p. (FAO food and nutrition paper).

8. Higashikawa F, Noda M, Awaya T, Nomura K, Oku H, Sugiyama M. Improvement of constipation and liver function by plant-derived lactic acid bacteria: A double-blind, randomized trial. Nutrition. 2010 Apr;26(4):367–74.

9. Moroti C, Souza Magri LF, de Rezende Costa M, Cavallini DC, Sivieri K. Effect of the consumption of a new symbiotic shake on glycemia and cholesterol levels in elderly people with type 2 diabetes mellitus. Lipids Health Dis. 2012 Dec;11(1):29.

10. Septembre-Malaterre A, Remize F, Poucheret P. Fruits and vegetables, as a source of nutritional compounds and phytochemicals: Changes in bioactive compounds during lactic fermentation. Food Research International. 2018 Feb;104:86–99.

11. Guan Q, Ding X-W, Zhong L-Y, Zhu C, Nie P, Song L-H. Beneficial effects of *Lactobacillus* -fermented black barley on high fat diet-induced fatty liver in rats. Food Funct. 2021;10.1039.D1FO00290B.

12. Bhattacharya S, Gachhui R, Sil PC. Effect of Kombucha, a fermented black tea in attenuating oxidative stress mediated tissue damage in alloxan induced diabetic rats. Food and Chemical Toxicology. 2013 Oct;60:328–40.

13. Satora P, Skotniczny M, Strnad S, Ženišová K. Yeast Microbiota during Sauerkraut Fermentation and Its Characteristics. IJMS. 2020 Dec 18;21(24):9699.

14. Di Cagno R, Filannino P, Gobbetti M. Fermented Foods: Fermented Vegetables and Other Products. In: Encyclopedia of Food and Health [Internet]. Elsevier; 2016 [cited 2021 May 26]. p. 668–74. Available from: https://linkinghub.elsevier.com/retrieve/pii/B9780123849472002841

15. Zabat M, Sano W, Wurster J, Cabral D, Belenky P. Microbial Community Analysis of Sauerkraut Fermentation Reveals a Stable and Rapidly Established Community. Foods. 2018 May 12;7(5):77.

16. Yang X, Hu W, Xiu Z, Jiang A, Yang X, Saren G, et al. Microbial Community Dynamics and Metabolome Changes During Spontaneous Fermentation of Northeast Sauerkraut From Different Households. Front Microbiol. 2020 Aug 5;11:1878.

17. Hiippala K, Jouhten H, Ronkainen A, Hartikainen A, Kainulainen V, Jalanka J, et al. The Potential of Gut Commensals in Reinforcing Intestinal Barrier Function and Alleviating Inflammation. Nutrients. 2018 Jul 29;10(8):988.

18. Bell V, Ferrão J, Pimentel L, Pintado M, Fernandes T. One Health, Fermented Foods, and Gut Microbiota. Foods. 2018 Dec 3;7(12):195.

19. Lamprecht M, Bogner S, Schippinger G, Steinbauer K, Fankhauser F, Hallstroem S, et al. Probiotic supplementation affects markers of intestinal barrier, oxidation, and inflammation in trained men; a randomized, double-blinded, placebo-controlled trial. J Int Soc Sports Nutr. 2012 Dec;9(1):45.

20. Ghosh SS, Wang J, Yannie PJ, Ghosh S. Intestinal Barrier Dysfunction, LPS Translocation, and Disease Development. Journal of the Endocrine Society. 2020 Feb 1;4(2):bvz039.

21. Cani PD, Amar J, Iglesias MA, Poggi M, Knauf C, Bastelica D, et al. Metabolic Endotoxemia Initiates Obesity and Insulin Resistance. Diabetes. 2007 Jul 1;56(7):1761–72.

22. Oriishi T, Sata M, Toyonaga A, Sasaki E, Tanikawa K. Evaluation of intestinal permeability in patients with inflammatory bowel disease using lactulose and measuring antibodies to lipid A. Gut. 1995 Jun 1;36(6):891–6.

23. Petit CSV, Barreau F, Besnier L, Gandille P, Riveau B, Chateau D, et al. Requirement of Cellular Prion Protein for Intestinal Barrier Function and Mislocalization in Patients With Inflammatory Bowel Disease. Gastroenterology. 2012 Jul;143(1):122-132.e15.

24. Liebregts T, Adam B, Bredack C, Röth A, Heinzel S, Lester S, et al. Immune Activation in Patients With Irritable Bowel Syndrome. Gastroenterology. 2007 Mar;132(3):913–20.

25. Creely SJ, McTernan PG, Kusminski CM, Fisher ff. M, Da Silva NF, Khanolkar M, et al. Lipopolysaccharide activates an innate immune system response in human adipose tissue in obesity and type 2 diabetes. American Journal of Physiology-Endocrinology and Metabolism. 2007 Mar;292(3):E740–7.

26. Chen Y, Liu S, Leng SX. Chronic Low-grade Inflammatory Phenotype (CLIP) and Senescent Immune Dysregulation. Clinical Therapeutics. 2019 Mar;41(3):400–9.

27. Groschwitz KR, Hogan SP. Intestinal barrier function: Molecular regulation and disease pathogenesis. Journal of Allergy and Clinical Immunology. 2009 Jul;124(1):3–20.

28. Nielsen ES, Garnås E, Jensen KJ, Hansen LH, Olsen PS, Ritz C, et al. Lacto-fermented sauerkraut improves symptoms in IBS patients independent of product pasteurisation – a pilot study. Food Funct. 2018;9(10):5323–35.

29. Peng L, Li Z-R, Green RS, Holzman IR, Lin J. Butyrate Enhances the Intestinal Barrier by Facilitating Tight Junction Assembly via Activation of AMP-Activated Protein Kinase in Caco-2 Cell Monolayers. The Journal of Nutrition. 2009 Sep 1;139(9):1619–25.

30. Wang H-B, Wang P-Y, Wang X, Wan Y-L, Liu Y-C. Butyrate Enhances Intestinal Epithelial Barrier Function via Up-Regulation of Tight Junction Protein Claudin-1 Transcription. Dig Dis Sci. 2012 Dec;57(12):3126–35.

31. Miao W, Wu X, Wang K, Wang W, Wang Y, Li Z, et al. Sodium Butyrate Promotes Reassembly of Tight Junctions in Caco-2 Monolayers Involving Inhibition of MLCK/MLC2 Pathway and Phosphorylation of PKCβ2. IJMS. 2016 Oct 10;17(10):1696.

32. Maslowski KM, Vieira AT, Ng A, Kranich J, Sierro F, Di Yu, et al. Regulation of inflammatory responses by gut microbiota and chemoattractant receptor GPR43. Nature. 2009 Oct;461(7268):1282–6.

33. Masui R, Sasaki M, Funaki Y, Ogasawara N, Mizuno M, Iida A, et al. G Protein-Coupled Receptor 43 Moderates Gut Inflammation Through Cytokine Regulation from Mononuclear Cells: Inflammatory Bowel Diseases. 2013 Dec;19(13):2848–56.

34. Iraporda C, Romanin DE, Rumbo M, Garrote GL, Abraham AG. The role of lactate on the immunomodulatory properties of the nonbacterial fraction of kefir. Food Research International. 2014 Aug;62:247–53.

35. Okada T, Fukuda S, Hase K, Nishiumi S, Izumi Y, Yoshida M, et al. Microbiota-derived lactate accelerates colon epithelial cell turnover in starvation-refed mice. Nat Commun. 2013 Jun;4(1):1654.

36. Hallmann E, Kazimierczak R, Marszałek K, Drela N, Kiernozek E, Toomik P, et al. The Nutritive Value of Organic and Conventional White Cabbage (*Brassica Oleracea* L. Var. *Capitata*) and Anti-Apoptotic Activity in Gastric Adenocarcinoma Cells of Sauerkraut Juice Produced Therof. J Agric Food Chem. 2017 Sep 20;65(37):8171–83.

37. Szaefer H, Krajka-Kuźniak V, Bartoszek A, Baer-Dubowska W. Modulation of Carcinogen Metabolizing Cytochromes P450 in Rat Liver and Kidney by Cabbage and Sauerkraut Juices: Comparison with the Effects of Indole-3-carbinol and Phenethyl Isothiocyanate: CABBAGE AND CYTOCHROME P450 IN RAT LIVER AND KIDNEY. Phytother Res. 2012 Aug;26(8):1148–55.

38. Huey B, Hall J. Hypervariable DNA fingerprinting in Escherichia coli: minisatellite probe from bacteriophage M13. J Bacteriol. 1989 May;171(5):2528–32.

39. Giraffa G, Rossetti L, Neviani E. An evaluation of chelex-based DNA purification protocols for the typing of lactic acid bacteria. Journal of Microbiological Methods. 2000 Oct;42(2):175–84.

40. Gatti M, De Dea Lindner J, De Lorentiis A, Bottari B, Santarelli M, Bernini V, et al. Dynamics of Whole and Lysed Bacterial Cells during Parmigiano-Reggiano Cheese Production and Ripening. Appl Environ Microbiol. 2008 Oct;74(19):6161–7.

41. Callahan BJ, McMurdie PJ, Rosen MJ, Han AW, Johnson AJA, Holmes SP. DADA2: High-resolution sample inference from Illumina amplicon data. Nat Methods. 2016 Jul;13(7):581–3.

42. Wright ES. DECIPHER: harnessing local sequence context to improve protein multiple sequence alignment. BMC Bioinformatics. 2015 Dec;16(1):322.

43. Studier JA, Keppler KJ. A note on the neighbor-joining algorithm of Saitou and Nei. Mol Biol Evol. 1988 Nov;5(6):729–31.

44. Schliep KP. phangorn: phylogenetic analysis in R. Bioinformatics. 2011 Feb 15;27(4):592–3.

45. McMurdie PJ, Holmes S. phyloseq: An R Package for Reproducible Interactive Analysis and Graphics of Microbiome Census Data. Watson M, editor. PLoS ONE. 2013 Apr 22;8(4):e61217.

46. Hong, Ran Seon, Hwang, Kyunghwa, Cho, Hwang Eui, Lee, Hun Joo, Hong, Jin Tae, Moon, Dong Cheul. Survey of ERETIC2 NMR for quantification. 한국자기공명학회논문지. 2013 Dec 20;17(2):98–104.

47. Srinivasan B, Kolli AR, Esch MB, Abaci HE, Shuler ML, Hickman JJ. TEER Measurement Techniques for In Vitro Barrier Model Systems. J Lab Autom. 2015 Apr;20(2):107–26.

48. Coates EM, Popa G, Gill CI, McCann MJ, McDougall GJ, Stewart D, et al. Colon-available raspberry polyphenols exhibit anti-cancer effects on in vitro models of colon cancer. J Carcinog. 2007;6(1):4.

49. Anderson RC, Cookson AL, McNabb WC, Park Z, McCann MJ, Kelly WJ, et al. Lactobacillus plantarum MB452 enhances the function of the intestinal barrier by increasing the expression levels of genes involved in tight junction formation. BMC Microbiol. 2010;10(1):316.

50. Borsci G, Barbieri S, Guardamagna I, Lonati L, Ottolenghi A, Ivaldi GB, et al. Immunophenotyping Reveals No Significant Perturbation to PBMC Subsets When Co-cultured With Colorectal Adenocarcinoma Caco-2 Cells Exposed to X-Rays. Front Immunol. 2020 Jun 2;11:1077.

51. Nishitani Y, Yamamoto K, Yoshida M, Azuma T, Kanazawa K, Hashimoto T, et al. Intestinal anti-inflammatory activity of luteolin: Role of the aglycone in NF-κB inactivation in macrophages co-cultured with intestinal epithelial cells: Intestinal Anti-Inflammatory Activity of Iuteolin. BioFactors. 2013 Sep;39(5):522–33.

52. Kämpfer AAM, Urbán P, Gioria S, Kanase N, Stone V, Kinsner-Ovaskainen A. Development of an in vitro co-culture model to mimic the human intestine in healthy and diseased state. Toxicology in Vitro. 2017 Dec;45:31–43.

53. Millipore M. Product information on HCYTOMAG-60K/MILLIPLEX MAP HumanCytokine/Chemokine Magnetic Bead Panel [Internet]. Available from: http://www.merckmillipore.com/CH/en/product/MILLIPLEX-MAP-Human-Cytokine/Chemokine-Magnetic-Bead-Panel-Immunology-Multiplex-Assay,MM_NF-HCYTOMAG-60K

54. Bianchi MG, Chiu M, Taurino G, Brighenti F, Del Rio D, Mena P, et al. Catechin and Procyanidin B2 Modulate the Expression of Tight Junction Proteins but Do Not Protect from Inflammation-Induced Changes in Permeability in Human Intestinal Cell Monolayers. Nutrients. 2019 Sep 21;11(10):2271.

55. Gallo-Oller G, Ordoñez R, Dotor J. A new background subtraction method for Western blot densitometry band quantification through image analysis software. Journal of Immunological Methods. 2018 Jun;457:1–5.

56. Elamin E, Jonkers D, Juuti-Uusitalo K, van IJzendoorn S, Troost F, Duimel H, et al. Effects of Ethanol and Acetaldehyde on Tight Junction Integrity: In Vitro Study in a Three Dimensional Intestinal Epithelial Cell Culture Model. Butterworth M, editor. PLoS ONE. 2012 Apr 19;7(4):e35008.

57. Suzuki T. Regulation of the intestinal barrier by nutrients: The role of tight junctions. Anim Sci J [Internet]. 2020 Jan [cited 2021 Oct 25];91(1). Available from: https://onlinelibrary.wiley.com/doi/10.1111/asj.13357

58. Katial RK, Sachanandani D, Pinney C, Lieberman MM. Cytokine production in cell culture by peripheral blood mononuclear cells from immunocompetent hosts. Clin Diagn Lab Immunol. 1998 Jan;5(1):78–81.

59. Parmele HB, Fred EB, Peterson WH. Relation of temperature to rate and type of fermentation and to quality of commercial sauerkraut. Journal of Agricultural Research. 1927;35(11):1021–38.

60. Pederson CS, Albury MN. The Sauerkraut Fermentation. New York: New York State Agricultural Experiment Station; 1969 p. 87. Report No.: 824.

61. Plengvidhya V, Breidt F, Lu Z, Fleming HP. DNA Fingerprinting of Lactic Acid Bacteria in Sauerkraut Fermentations. Appl Environ Microbiol. 2007 Dec;73(23):7697–702.

62. Marco ML, Sanders ME, Gänzle M, Arrieta MC, Cotter PD, De Vuyst L, et al. The International Scientific Association for Probiotics and Prebiotics (ISAPP) consensus statement on fermented foods. Nat Rev Gastroenterol Hepatol. 2021 Mar;18(3):196–208.

63. Nicholson JK, Lindon JC, Holmes E. "Metabonomics": understanding the metabolic responses of living systems to pathophysiological stimuli via multivariate statistical analysis of biological NMR spectroscopic data. Xenobiotica. 1999 Jan;29(11):1181–9.

64. Rizzello CG, Coda R, Wang Y, Verni M, Kajala I, Katina K, et al. Characterization of indigenous Pediococcus pentosaceus, Leuconostoc kimchii, Weissella cibaria and Weissella confusa for faba bean bioprocessing. International Journal of Food Microbiology. 2019 Aug;302:24–34.

65. Zhao N, Zhang C, Yang Q, Guo Z, Yang B, Lu W, et al. Selection of Taste Markers Related to Lactic Acid Bacteria Microflora Metabolism for Chinese Traditional Paocai: A Gas Chromatography-Mass Spectrometry-Based Metabolomics Approach. J Agric Food Chem. 2016 Mar 23;64(11):2415–22.

66. Jagannath A, Raju PS, Bawa AS. A TWO-STEP CONTROLLED LACTIC FERMENTATION OF CABBAGE FOR IMPROVED CHEMICAL AND MICROBIOLOGICAL QUALITIES*: A TWO-STEP CONTROLLED LACTIC FERMENTATION OF CABBAGE. Journal of Food Quality. 2012 Feb;35(1):13–20.

67. Harth H, Van Kerrebroeck S, De Vuyst L. Community dynamics and metabolite target analysis of spontaneous, backslopped barley sourdough fermentations under laboratory and bakery conditions. International Journal of Food Microbiology. 2016 Jul;228:22–32.

68. Baek JG, Shim S-M, Kwon DY, Choi H-K, Lee CH, Kim Y-S. Metabolite Profiling of *Cheonggukjang* , a Fermented Soybean Paste, Inoculated with Various *Bacillus* Strains during Fermentation. Bioscience, Biotechnology, and Biochemistry. 2010 Sep 23;74(9):1860–8.

69. Kondziella D. The Top 5 Neurotransmitters from a Clinical Neurologist's Perspective. Neurochem Res. 2017 Jun;42(6):1767–71.

70. Shelp B. Metabolism and functions of gamma-aminobutyric acid. Trends in Plant Science. 1999 Nov 1;4(11):446–52.

71. Liu Y-Y, Zeng S-Y, Leu Y-L, Tsai T-Y. Antihypertensive Effect of a Combination of Uracil and Glycerol Derived from *Lactobacillus plantarum* Strain TWK10-Fermented Soy Milk. J Agric Food Chem. 2015 Aug 26;63(33):7333–42.

72. Gao Y, Li S, Wang J, Luo C, Zhao S, Zheng N. Modulation of Intestinal Epithelial Permeability in Differentiated Caco-2 Cells Exposed to Aflatoxin M1 and Ochratoxin A Individually or Collectively. Toxins. 2017 Dec 27;10(1):13.

73. Wu J, He C, Bu J, Luo Y, Yang S, Ye C, et al. Betaine attenuates LPS-induced downregulation of Occludin and Claudin-1 and restores intestinal barrier function. BMC Vet Res. 2020 Dec;16(1):75.

74. Prasad S, Mingrino R, Kaukinen K, Hayes KL, Powell RM, MacDonald TT, et al. Inflammatory processes have differential effects on claudins 2, 3 and 4 in colonic epithelial cells. Lab Invest. 2005 Sep;85(9):1139–62.

75. Meng F, Lowell CA. Lipopolysaccharide (LPS)-induced Macrophage Activation and Signal Transduction in the Absence of Src-Family Kinases Hck, Fgr, and Lyn. Journal of Experimental Medicine. 1997 May 5;185(9):1661–70.

76. Zhou S, Chen G, Qi M, El-Assaad F, Wang Y, Dong S, et al. Gram Negative Bacterial Inflammation Ameliorated by the Plasma Protein Beta 2-Glycoprotein I. Sci Rep. 2016 Dec;6(1):33656.

77. Dittel LJ, Dittel BN, Brod SA. Ingested ACTH blocks Th17 production by inhibiting GALT IL-6. Journal of the Neurological Sciences. 2020 Feb;409:116602.

78. Cavalcanti YVN, Brelaz MCA, Lemoine Neves JK de A, Ferraz JC, Pereira VRA. Role of TNF-Alpha, IFN-Gamma, and IL-10 in the Development of Pulmonary Tuberculosis. Pulmonary Medicine. 2012;2012:1–10.

79. Parada Venegas D, De la Fuente MK, Landskron G, González MJ, Quera R, Dijkstra G, et al. Short Chain Fatty Acids (SCFAs)-Mediated Gut Epithelial and Immune Regulation and Its Relevance for Inflammatory Bowel Diseases. Front Immunol. 2019 Mar 11;10:277.

80. Latham T, Mackay L, Sproul D, Karim M, Culley J, Harrison DJ, et al. Lactate, a product of glycolytic metabolism, inhibits histone deacetylase activity and promotes changes in gene expression. Nucleic Acids Research. 2012 Jun;40(11):4794–803.

Chapter 6: Processed animal proteins from insect and poultry by-products in a fish meal-free diet for rainbow trout: impact on intestinal microbiota and inflammatory markers

Giulia Gaudioso[1,2], Giulia Marzorati[1], Filippo Faccenda[3], Tobias Weil[1], Fernando Lunelli[3], Gloriana Cardinaletti[4], Giovanna Marino[5], Ike Olivotto[6], Giuliana Parisi[7], Emilio Tibaldi[4], Kieran Michael Tuohy[1] and Francesca Fava[1]

[1] Nutrition and Nutrigenomics Unit, Department of Food Quality and Nutrition, Research and Innovation Center, Fondazione Edmund Mach, 38098 Trento, Italy

[2] CIBIO – Department of Cellular, Computational and Integrative Biology, University of Trento, 38123 Trento, Italy

[3] Aquaculture and Hydrobiology Unit, Technology Transfer Centre, Experiment and Technological Services Department, Fondazione Edmund Mach, 38098 Trento, Italy

[4] Department of Agricultural, Food, Environmental and Animal Science, University of Udine, 33100 Udine, Italy

[5] Institute for Environmental Protection and Research (ISPRA), 00144 Roma, Italy

[6] Department of Life and Environmental Sciences, Polytechnic University of Marche, 60131 Ancona, Italy

[7] Department of Agriculture, Food, Environment and Forestry, University of Florence, 50144 Florence, Italy

This chapter has been reprinted from:

Gaudioso, G.; Marzorati, G.; Faccenda, F.; Weil, T.; Lunelli, F.; Cardinaletti, G.; Marino, G.; Olivotto, I.; Parisi, G.; Tibaldi, E.; Tuohy, K.M.; Fava, F. Processed Animal Proteins from Insect and Poultry By-Products in a Fish Meal-Free Diet for Rainbow Trout: Impact on Intestinal Microbiota and Inflammatory Markers. *Int. J. Mol. Sci.* **2021**, 22, 5454. https://doi.org/10.3390/ijms22115454

A sustainable diet can only be achieved by eating sustainable and nutritious food. The healthy and sustainable reference diet from EAT Lancet Commission suggests to consume 2 portions of fish per week, thanks to its omega-3 fatty acids and protein content (1). The global demand for fish and seafood is predicted to double by 2050, due to the dramatic increase in the world population (2). However, captured wild fish is no longer able to support fish demands, due to excessive exploitation of wild fish stocks (2). To date, fish supply is largely provided by aquaculture, which surpassed wild caught fish in terms of global annual production (1,2). In order to decrease the environmental footprint of aquaculture, we investigated the use of more sustainable ingredients for rainbow trout (*Oncorhynchus mykiss*), their impact on the fish GM, links between gut microbiota modulation and fish health, especially regulation of inflammation, and aquaculture productivity. The work presented in the next chapter was focused on analyzing the role of microbiota in sustainable food production, connecting animal health and environmental sustainability. Experiments were carried out inside the AGER SUSHIN project, investigating farmed rainbow trout (*Oncorhynchus mykiss*) response to innovative feeds containing poultry by-products and insect meal (*Hermetia illucens* larvae) as protein sources to replace the unsustainable fishmeal and to improve vegetable base fish-feed formulations. The effects of alternative fish meal-free formulations were evaluated by determining fish growth performance, changes in GM composition and inflammatory and immune biomarkers. My personal contribution to this work concerned methods validation, data curation, data analysis and paper writing. I participated in animal sampling and in the collection of biological samples (intestinal content, blood and tissue biopsies). I validated the primers used to investigate gene expression in midgut and head kidney biopsies, I optimized and performed RNA extractions, RT-PCR and results analysis. I examined high-throughput 16S rRNA sequencing data from Illumina MiSeq by applying QIIME2.0 pipeline, both on fish GM and on feed microbiota. Moreover, I made use of different statistical tests in R studio (version 3.6.2) to analyze metagenomic results and to perform Spearman's correlation analysis between GM composition and ingredients of experimental diets. Finally, I wrote and reviewed the original manuscript.

References

1. Willett W, Rockström J, Loken B, Springmann M, Lang T, Vermeulen S, et al. Food in the Anthropocene: the EAT–Lancet Commission on healthy diets from sustainable food systems. The Lancet. 2019 Feb;393(10170):447–92.

2. FAO. The State of World Fisheries and Aquaculture 2020 [Internet]. 2020 [cited 2021 May 20]. Available from: http://www.fao.org/documents/card/en/c/ca9229en

International Journal of
Molecular Sciences

MDPI

Article

Processed Animal Proteins from Insect and Poultry By-Products in a Fish Meal-Free Diet for Rainbow Trout: Impact on Intestinal Microbiota and Inflammatory Markers

Giulia Gaudioso [1,2], Giulia Marzorati [1], Filippo Faccenda [3], Tobias Weil [1], Fernando Lunelli [3], Gloriana Cardinaletti [4], Giovanna Marino [5], Ike Olivotto [6], Giuliana Parisi [7], Emilio Tibaldi [4], Kieran Michael Tuohy [1] and Francesca Fava [1,*]

1 Nutrition and Nutrigenomics Unit, Department of Food Quality and Nutrition, Research and Innovation Center, Fondazione Edmund Mach, 38098 Trento, Italy; giulia.gaudioso@fmach.it (G.G.); giulia.marzorati@fmach.it (G.M.); tobias.weil@fmach.it (T.W.); kieran.tuohy@fmach.it (K.M.T.)
2 CIBIO—Department of Cellular, Computational and Integrative Biology, University of Trento, 38123 Trento, Italy
3 Aquaculture and Hydrobiology Unit, Technology Transfer Centre, Experiment and Technological Services Department, Fondazione Edmund Mach, 38098 Trento, Italy; filippo.faccenda@fmach.it (F.F.); fernandolunelli@gmail.com (F.L.)
4 Department of Agricultural, Food, Environmental and Animal Science, University of Udine, 33100 Udine, Italy; gloriana.cardinaletti@uniud.it (G.C.); emilio.tibaldi@uniud.it (E.T.)
5 Institute for Environmental Protection and Research (ISPRA), 00144 Roma, Italy; giovanna.marino@isprambiente.it
6 Department of Life and Environmental Sciences, Polytechnic University of Marche, 60131 Ancona, Italy; i.olivotto@univpm.it
7 Department of Agriculture, Food, Environment and Forestry, University of Florence, 50144 Florence, Italy; giuliana.parisi@unifi.it
* Correspondence: francesca.fava@fmach.it; Tel.: +39-0461-615-566

Abstract: Sustainability of aquaculture is tied to the origin of feed ingredients. In search of sustainable fish meal-free formulations for rainbow trout, we evaluated the effect of *Hermetia illucens* meal (H) and poultry by-product meal (P), singly (10, 30, and 60% of either H or P) or in combination (10% H + 50% P, H10P50), as partial replacement of vegetable protein (VM) on gut microbiota (GM), inflammatory, and immune biomarkers. Fish fed the mixture H10P50 had the best growth performance. H, P, and especially the combination H10P50 partially restored α-diversity that was negatively affected by VM. Diets did not differ in the Firmicutes:Proteobacteria ratio, although the relative abundance of Gammaproteobacteria was reduced in H and was higher in P and in the fishmeal control. H had higher relative abundance of chitin-degrading *Actinomyces* and *Bacillus*, *Dorea*, and *Enterococcus*. *Actinomyces* was also higher in H feed, suggesting feed-chain microbiome transmission. P increased the relative abundance of protein degraders *Paeniclostridium* and Bacteroidales. IL-1β, IL-10, TGF-β, COX-2, and TCR-β gene expression in the midgut and head kidney and plasma lipopolysaccharide (LPS) revealed that the diets did not compromise the gut barrier function or induce inflammation. H, P, and H10P50 therefore appear valid protein sources in fishmeal-free aquafeeds.

Keywords: rainbow trout; aquaculture; sustainability; gut microbiota; inflammation; *Hermetia illucens*; poultry by-products; feed-borne microbiota

Citation: Gaudioso, G.; Marzorati, G.; Faccenda, F.; Weil, T.; Lunelli, F.; Cardinaletti, G.; Marino, G.; Olivotto, I.; Parisi, G.; Tibaldi, E.; et al. Processed Animal Proteins from Insect and Poultry By-Products in a Fish Meal-Free Diet for Rainbow Trout: Impact on Intestinal Microbiota and Inflammatory Markers. *Int. J. Mol. Sci.* **2021**, *22*, 5454. https://doi.org/10.3390/ijms22115454

Academic Editor: Carlo C. Lazado

Received: 26 April 2021
Accepted: 18 May 2021
Published: 21 May 2021

1. Introduction

Fish is recommended as a nutritious source of dietary protein for human health, and farmed fish have great potential for environmental sustainability according to the EAT Lancet Commission on Healthy Diets from Sustainable Food Systems [1]. Aquaculture is also currently the fastest growing food production sector, surpassing wild caught fish in terms of global annual production [1,2]. In order to decrease the future environmental

footprint of aquaculture, several studies are evaluating alternative and more sustainable sources of feed protein-rich ingredients, able to ensure fish health while retaining nutritional and organoleptic quality for the consumer.

In the past, searching for high-performance fishmeal (FM)-free formulations led to the development of innovative aquafeeds comprising new sustainable alternative ingredients. Vegetable protein-rich feeds (VM) have been used as sustainable alternatives to high-performance fishmeal (FM) [3], although VM often suffer from inferior growth performance [4] and changes in immune function [5]. Endogenous anti-nutritional factors and complex indigestible carbohydrates present in VM, together with low levels of essential amino acids and insufficient n-3 PUFA, lead to adverse effects on fish health and the nutritional quality of the final product. Moreover, intestinal barrier integrity as a consequence of VM diets leads to impaired nutrient absorption, alterations in the gut-associated immune system, and changes in resident gut microbiota composition [5]. Alternative animal-based protein sources therefore may offer considerable advantages over plant-derived protein. Poultry by-product meal (P) is a candidate animal-sourced alternative protein source that was re-authorized for use by the European Union in 2013 [6]. P is obtained from rendered and clean by-products of the poultry processing industry; it has an energy content similar to that of FM, with a well-balanced amino acid profile and good palatability, which are key attributes for carnivorous fish diets [7]. In addition, animal by-products have a lower carbon footprint compared to FM or vegetable alternatives [3,8]. Previous studies showed that replacement of high amounts of dietary proteins from FM or VM with P gave good results in terms of growth performance in salmonids [9–11]. However few studies have examined the growth performance and animal health effects of increasing percentages of P in FM-free, VM-based feeds in rainbow trout (*Oncorhynchus mykiss*) [12]. Insect meal (IM) also represents a valid alternative protein source to VM and possibly FM for aquaculture formulations. Compared to poultry by-products, insects have high/medium protein levels. In addition, certain insect meals have been shown to contain biologically active compounds, such as chitin, antimicrobial peptides, and short–medium fatty acids (FAs) [13], which have been associated with improved fish innate immune function (promoting immunomodulatory effects) and modulation of gut microbiome composition [14–16]. Interestingly, employment of *Hermetia illucens* meal (H) at a low percentage in fish feed resulted in immunostimulation (up-regulation of genes encoding for IL-1β, IL-17F, and TNF- α), probably due to its chitin, antimicrobial peptides, and fatty acids content. Immunomodulatory and antimicrobial effects of H seem to be dependent on both the insect species and the diet of the insect [17]. Insects also have the advantage of growing on a wide range of substrates, and it is possible to improve their nutritional profile simply by changing their growth substrate. They have also a low-environmental impact since insects can grow on waste derived from the vegetable food industry [18].

Fish health deeply influences growth performance, and, in turn, fish wellbeing is influenced by gut health. Absorption of nutrients, immune function, and the inflammatory state are strongly linked to gut health and the composition of the resident gut microbiota. Previous studies highlighted how the gut microbiota (GM) and the diet are strictly interconnected and influence the inflammatory, immune, and nutritional status of fish [19,20]. GM could mediate the host immune response by stimulating the production of several soluble mediators of inflammation and immune cell recruitment. Fish GM plays a crucial role in gut-associated lymphoid tissue (GALT) maturation and development, also protecting the fish from infection [21–23]. The gut microbiota and its metabolites (such as short-chain fatty acids, SCFAs) are directly involved in maintaining intestinal barrier function and integrity, thus supporting fish growth rates [24]. The composition of the gut microbiota and relative abundances of different members of the gut microbiota respond to the nutritional composition and ingredients used in aquafeeds [25].

Rainbow trout is the most commonly farmed teleost fish species in Italy, with 36.800 tons produced in 2019 [26]. Its gut microbial community is mainly dominated by Actinobacteria, Firmicutes, and Proteobacteria, whose proportions are strongly influenced by dietary

proteins. A higher Firmicutes:Proteobacteria ratio seems to be promoted by vegetable ingredients, particularly soybean proteins but also pea and canola proteins [27]. The effect of partial replacement of FM with a mixture of animal by-products and plant proteins on gut microbial populations of rainbow trout has been recently studied [28]. However, while Rimoldi and colleagues employed a mixture of P, animal proteins, including swine blood, and vegetable proteins to substitute part of FM, and soybean oil to replace fish oil, in this current study, we examine the effect of adding different percentages of P to a VM-based FM-free diet. Replacement of fish proteins with alternative animal and vegetable proteins was previously shown to significantly change the abundance of Fusobacteriaceae, Bacteroidetes phyla, and several families and genera within the Proteobacteria and Firmicutes phyla, with variability between diets [28]. However, there is lack of knowledge on the impact of P in sustainable, FM-free, vegetable formulations on the gut microbiota. Insect meal inclusion (up to 30%) in rainbow trout feed was also shown to significantly affect dominant gut bacterial phyla such as Firmicutes, Tenericutes, Actinobacteria, and Proteobacteria and to promote the growth of *Mycoplasma* and Actinomycetales genera, specifically *Actinomyces* and *Corynebacterium*, as well as *Enterococcus*, *Lactobacillus*, and *Staphylococcus*, whilst decreasing *Bacillaceae*, especially *Bacillus* and *Oceanobacillus* genera [16]. The magnitude of differences in bacterial abundance reflected the percentage of insect proteins in the diet [15]. Insect-derived ingredients also increased the abundance of lactic acid bacteria within the Firmicutes phylum in trout intestinal contents [14]. There is some evidence from other fish species that a combination of H and P might promote fish growth and immune defense against pathogens, although no studies in trout have investigated the mixture H + P in rainbow trout microbiota in an FM-free vegetable aquafeed [29].

In this study, which is part of a larger investigation [30], we studied the effects of including a commercial insect meal (H) from *Hermetia illucens*, poultry by-product meal (P), and their combination (H + P) on the gut microbiota composition and biomarkers of inflammation and gut barrier integrity in rainbow trout fed a fish meal-free plant-based diet.

2. Results

2.1. Growth Parameters

The fish readily accepted the experimental diets, and all feeds were consumed without rejection or loss. In all dietary treatments, the average body weight of fish fed over three months (69 meals) more than tripled at the end of the feeding trials, and the survival rate of the fish was 100% for all the experimental groups. Fish fed the diet coined H10P50 showed a higher final body weight than fish fed either CV or CF ($p < 0.001$), and their weight did not differ ($p > 0.05$) from the other dietary treatments (Table 1). In addition, fish fed H10P50 showed a higher total length compared to fish fed CF or CV diets. The corresponding Fulton's condition factor (K) was found to indicate well-proportioned growth under all experimental conditions. CV showed higher K values than CF and comparable K to all H groups. Insect meal groups had significantly higher K than P groups, while the mixed H + P meal had a significantly higher K factor than both P groups (Table 1). All other zootechnical parameters, such as the specific growth rate (SGR), feed intake (FI), and feed conversion ratio (FCR), were already reported and discussed elsewhere by Randazzo and colleagues [30].

Table 1. Final body weight, total length, and Fulton's condition factor, K = Weight (g) × 100/Total Length (cm^3) of rainbow trout fed the test diets. Within each column, means with different superscript letters are significantly different ($p < 0.05$).

Diet	Final Weight (g)	Total Length (cm)	K (g/cm^3)
CF	231.18 ± 32.11 ^{b}	25.53 ± 1.35 ^{d}	1.39 ± 0.11 ^{cd}
CV	227.92 ± 35.22 ^{b}	25.01 ± 1.30 ^{e}	1.45 ± 0.11 ^{a}
H10	235.02 ± 30.41 ^{ab}	25.46 ±1.24 ^{d}	1.42 ± 0.11 ^{abc}
H30	239.1 ± 36.26 ^{ab}	25.48 ± 1.42 ^{d}	1.44 ± 0.11 ^{ab}
H60	241.07 ± 35.58 ^{ab}	25.78 ± 1.31 ^{c}	1.40 ± 0.10 ^{bcd}
P30	240.03 ± 37.82 ^{ab}	25.81 ± 1.45 ^{bc}	1.39 ± 0.10 ^{cd}
P60	244.06 ± 36.02 ^{ab}	26.02 ± 1.25 ^{ab}	1.38 ± 0.09 ^{d}
H10P50	254.81 ± 36.82 ^{a}	26.13 ± 1.14 ^{a}	1.42 ± 0.12 ^{abc}

2.2. Gut Microbial Ecology

Illumina MiSeq sequencing of gut microbial 16S rRNA gene amplicons produced a total of 8,798,863 reads, with 129,395 ± 28,897.18 raw reads per sample. Raw sequences were submitted to the European Nucleotide Archive (PRJEB43152). After QIIME2 analysis, we removed sequences that were identified as Cyanobacteria, and the total number of reads was 2,023,741, with an average of 29,760.89 ± 30,730.25 reads per sample. Fish feed was also sequenced and generated a total of 3,960,358.98 raw reads, with 141,441.39 ± 38,974.52 reads per sample. After QIIME2 quality filtering and removal of reads identified as Cyanobacteria, the total number of reads of fish feeds was 2,018,291, with 29,680.75 ± 30,762.37 reads per sample.

The fish feed composition had a strong impact on the microbial composition in terms of α-diversity indexes, particularly showing that vegetable-based diets drastically reduced microbiota complexity. CF had the highest bacterial richness in terms of observed features and the Chao1 index of all the experimental groups (Figure 1A,B). On the other hand, CV showed the lowest values for both indexes (observed OTUs 73.67 ± 28.97 and Chao1 77 ± 32.30). When insect and poultry meal ingredients were introduced in the feed, α-diversity was partially restored, and the difference with CF tapered. Amongst tested feeds, dietary inclusion of 23% and 45% of *Hermetia illucens* (H30 and H60, respectively) did not differ in bacterial α-diversity compared to CF ($p = 0.565$ and $p = 0.585$, H30 vs. CF; $p = 0.511$ and $p = 0.503$, H60 vs. CF, Chao1, and number of features, respectively). In addition, the community evenness of the feed containing insect meal was similar to that of fishmeal, although the difference in the Shannon index did not reach statistical significance (Figure 1C). β-diversity (Bray Curtis dissimilarity, weighted and unweighted Unifrac analysis) showed a clear separation between diets, with H diets and P diets clustering together (Figure 1D).

The results of gut microbiota analysis and the significant differences in relative abundance of taxa are illustrated in Figure 2 and Table 2.

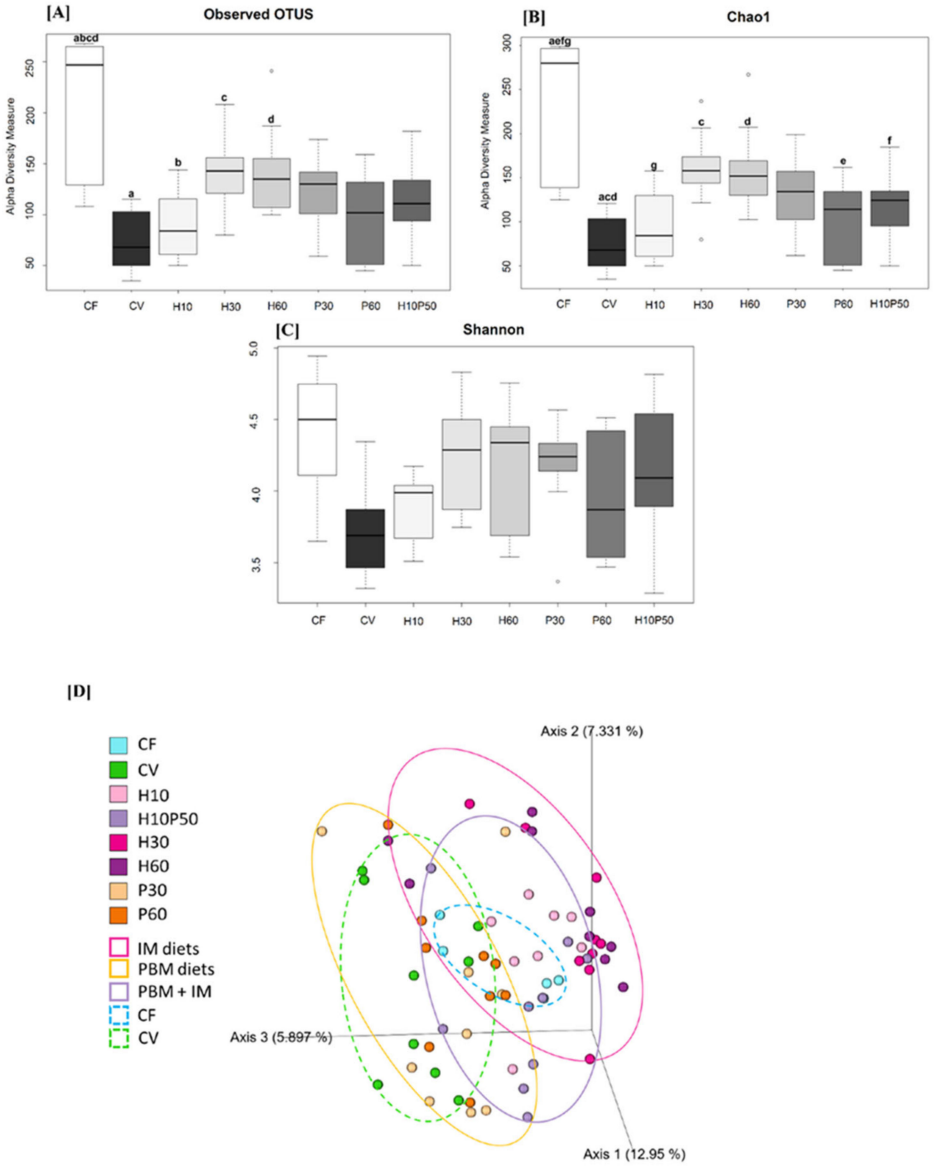

Figure 1. Intestinal bacterial α-diversity (Observed features (**A**), Chao1 (**B**) and Shannon index (**C**)), and β-diversity (Unweighted Unifrac PCoA plot (**D**)) in rainbow trout fed fish-meal (CF), vegetable meal (CV), increasing percentage of *Hermetia illucens* insect meal (H10, H30, H60), increasing percentage of poultry by-product meal (P30, P60), and a combination of insect meal and poultry by product meal (H10P50) (n = nine fish per group). Within each panel, identical superscript letters indicate statistically significant differences (FDR $p < 0.05$).

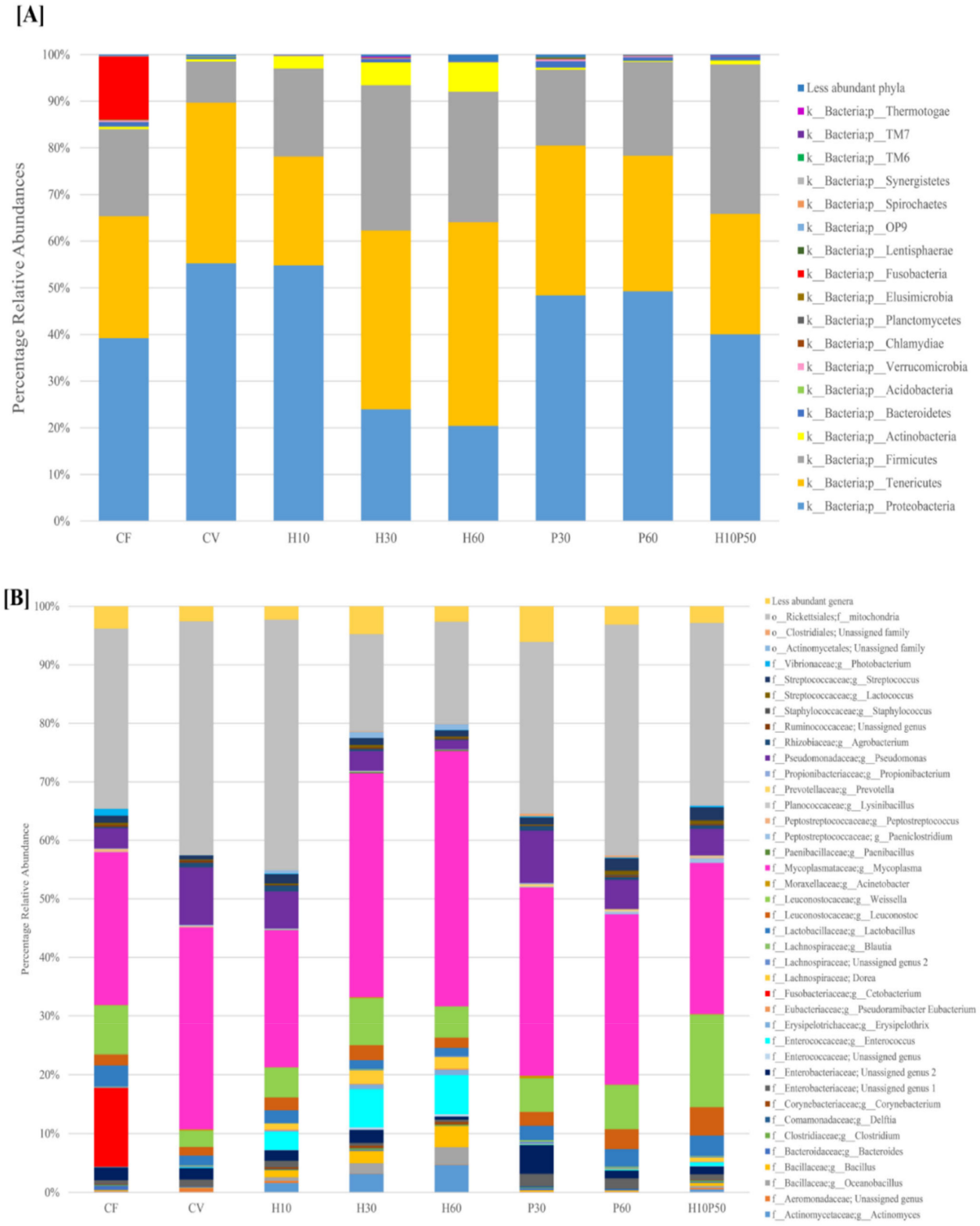

Figure 2. Percentage relative abundance of phyla (**A**) and genera (**B**) in the intestinal contents. Less abundant phyla or genera include bacteria with a relative abundance less than 0.01% in fewer than 25% of samples.

Table 2. (**A**–**B**) Bacterial relative abundances (mean ± SD) of taxonomic groups that were significantly different between diet groups. Identical superscript letters indicate significant differences among treatments according to Benjamini-Hochberg FDR correction. Individual *p* values are reported in the text and in Table S2.

[A]	Diet							
	CF	**CV**	**H10**	**H30**	**H60**	**P30**	**P60**	**H10P50**
Phylum								
Actinobacteria	0.51 ± 0.67	0.52 ± 0.46	2.62 ± 4.26	4.89 ± 4.23	6.29 ± 5.49 ^{a}	0.48 ± 0.53	0.23 ± 0.32 ^{a}	0.87 ± 0.65
Bacteroidetes	1.00 ± 1.22	0.41 ± 0.69	0.03 ± 0.06	0.72 ± 1.11	0.09 ± 0.09 ^{a}	1.35 ± 1.26 ^{a}	0.75 ± 0.82	0.77 ± 0.91
Fusobacteria	13.50 ± 29.88 $^{a–g}$	<0.0001^{a}	<0.0001 ^{b}	<0.0001^{c}	<0.0001 ^{d}	<0.0001 ^{e}	<0.0001 ^{f}	0.002 ± 0.01 ^{g}
				Class				
Erysipelotrichi	0.04 ± 0.06	0.002 ± 0.01 ^{ab}	0.34 ± 0.37	0.91 ± 0.80 ^{a}	1.11 ± 1.07 ^{b}	0.58 ± 0.17	0.04 ± 0.10	0.18 ± 0.31
Fusobacteriia	13.50 ± 29.88 ^{a}	<0.0001	<0.0001 ^{a}	<0.0001	<0.0001	<0.0001	<0.0001	0.002 ± 0.01
Gammaproteobacteria	7.72 ± 7.05	14.02 ± 14.53^{a}	10.76 ± 10.82	6.47 ± 6.36	2.61 ± 2.74 ^{a}	17.20 ± 15.41	8.52 ± 5.00	7.59 ± 6.12
Order								
Actinomycetales	0.49 ± 0.66	0.31 ± 0.29	2.50 ± 4.29 ^{a}	4.83 ± 4.14 ^{b}	6.25 ± 5.46	0.45 ± 0.52	0.20 ± 0.33 ^{ab}	0.85 ± 0.65
Bacteroidales	1.00 ± 1.22	0.25 ± 0.55	0.03 ± 0.06	0.69 ± 1.13	0.04 ± 0.05 ^{a}	1.14 ± 1.05 ^{a}	0.69 ± 0.83	0.47 ± 0.52
Erysipelotrichales	0.04 ± 0.06	0.002 ± 0.001 ^{abc}	0.34 ± 0.37 ^{a}	0.91 ± 0.80 ^{bde}	1.11 ± 1.07 ^{cf}	0.06 ± 0.17 ^{df}	0.04 ± 0.10 ^{e}	0.18 ± 0.31
Fusobacteriales	13.50 ± 29.88 ^{abc}	<0.0001	<0.0001 ^{a}	<0.0001 ^{b}	<0.0001	<0.0001 ^{c}	<0.0001 ^{d}	0.002 ± 0.01
Pseudomonadales	3.61 ± 2.94	10.08 ± 11.47^{a}	7.17 ± 7.51	3.56 ± 3.40	1.54 ± 1.88 ^{a}	9.40 ± 8.19	5.06 ± 3.65	4.72 ± 3.73
				Family				
Actinomycetaceae	0.10 ± 0.19	0.05 ± 0.16^{abcd}	1.57 ± 2.70 ^{aef}	3.16 ± 2.86 ^{bgh}	4.66 ± 3.93 ^{cil}	0.02 ± 0.06 ^{egim}	<0.0001 ^{fhln}	0.52 ± 0.40 ^{dmn}
Corynebacteriaceae	0.10 ± 0.20	0.002 ± 0.007	0.32 ± 0.40 ^{a}	0.41 ± 0.53	0.47 ± 0.63	<0.0001 ^{a}	0.004 ± 0.01	0.09 ± 0.12
Bacillaceae	0.31 ± 0.33	0.35 ± 0.70	1.79 ± 2.73 ^{a}	3.83 ± 3.28	6.59 ± 5.60	0.30 ± 0.35	0.18 ± 0.26 ^{a}	0.94 ± 0.74
Paenibacillaceae	<0.0001	<0.0001 ^{a}	0.06 ± 0.11	0.21 ± 0.26	0.20 ± 0.28 ^{a}	0.02 ± 0.07	<0.0001	0.02 ± 0.06
Clostridiaceae	0.16 ± 0.18	<0.0001 ^{a}	0.09 ± 0.23	0.31 ± 0.29	0.24 ± 0.28 ^{a}	0.22 ± 0.42	0.26 ± 0.49	0.34 ± 0.62
Eubacteriaceae	<0.0001	<0.0001 ^{a}	0.16 ± 0.31	0.12 ± 0.18 ^{bc}	0.19 ± 0.22 ^{a}	<0.0001 ^{b}	<0.0001 ^{c}	0.02 ± 0.05
Erysipelotrichaceae	0.04 ± 0.06	0.002 ± 0.01 ^{ab}	0.34 ± 0.37 ^{a}	0.91 ± 0.81 ^{cd}	1.11 ± 1.07 ^{b}	0.06 ± 0.17 ^{c}	0.04 ± 0.10 ^{d}	0.18 ± 0.31
Fusobacteriaceae	13.49 ± 29.88 ^{a}	<0.0001	<0.0001 ^{a}	<0.0001	<0.0001	<0.0001	<0.0001	<0.0001

Table 2. *Cont.*

[B]	Diet							
	CF	**CV**	**H10**	**H30**	**H60**	**P30**	**P60**	**H10P50**
				Genus				
Actinomyces	0.10 ± 0.18	0.05 ± 0.16 ^{abcd}	1.58 ± 2.70 ^{aef}	3.16 ± 2.86 ^{bgh}	4.66 ± 3.98^{cil}	0.02 ± 0.06 ^{egi}	<0.0001 ^{fhlm}	0.52 ± 0.39 ^{dm}
Oceanobacillus	0.06 ± 0.14	0.04 ± 0.11 ^{ab}	0.63 ± 1.03 ^{cd}	1.75 ± 1.54 ^{aef}	2.94 ± 2.58 ^{bgh}	<0.0001 ^{ceg}	<0.0001 ^{dfh}	0.35 ± 0.37
Bacillus	0.16 ± 0.14	0.07 ± 0.14 ^{a}	1.16 ± 1.75	2.08 ± 1.96	3.60 ± 3.09 ^{a}	0.25 ± 0.27	0.18 ± 0.26	0.51 ± 0.44
Pseudoramibacter Eubacterium	<0.0001	<0.0001 ^{a}	0.16 ± 0.31	0.12 ± 0.18	0.19 ± 0.22 ^{bc}	<0.0001^{b}	<0.0001 ^{ac}	0.02 ± 0.05
Dorea	0.03 ± 0.04	<0.0001 ^{abcd}	1.05 ± 1.72 ^{ae}	2.26 ± 1.89 ^{bf}	1.99 ± 1.71 ^{cg}	0.08 ± 0.25	0.09 ± 0.26 ^{efgh}	0.71 ± 0.79 ^{dh}
Paeniclostridium	0.05 ± 0.05	<0.0001 ^{a}	0.05 ± 0.13	0.04 ± 0.08	0.02 ± 0.07	0.05 ± 0.10	0.36 ± 0.39	0.77 ± 1.35 ^{a}
Erysipelothrix	0.04 ± 0.06	<0.0001 ^{ab}	0.21 ± 0.41	0.80 ± 0.63 ^{acd}	0.89 ± 0.79 ^{bef}	<0.0001 ^{ce}	0.01 ± 0.03 ^{df}	0.13 ± 0.30
Enterococcus	0.06 ± 0.09	0.15 ± 0.27 ^{ab}	3.09 ± 4.70 ^{bfg}	6.48 ± 5.12 ^{cdf}	6.68 ± 5.45 ^{eg}	0.10 ± 0.21 ^{c}	0.17 ± 0.20 ^{ade}	0.62 ± 0.81
Cetobacterium	13.44 ± 29.91 ^{a}	<0.0001	<0.0001 ^{a}	<0.0001	<0.0001	<0.0001	<0.0001	<0.0001
Pseudomonas	3.48 ± 2.85	9.80 ± 11.06 ^{a}	6.36 ± 6.69	3.38 ± 3.10	1.53 ± 1.89 ^{a}	8.94 ± 7.85	4.99 ± 3.67	4.56 ± 3.65

Proteobacteria, Firmicutes, and Tenericutes were the most represented phyla in all the fish, regardless of diet, covering between 84% and 98% of all identified phyla (Figure 2A). No significant differences were observed in the relative abundances of Proteobacteria, Firmicutes or Tenericutes between diets. In addition, no differences ($p > 0.05$) were observed in the Firmicutes:Proteobacteria ratio between the dietary groups. We observed fewer Gammaproteobacteria in all diets including the insect meal (H) compared to CV, with lower abundance in those diet groups with a high percentage of *Hermetia* in the feed. Gammaproteobacteria abundance in the P30 and P60 dietary groups was not different ($p > 0.05$) from that of CF (Table 2A). Actinobacteria were a less dominant member of the gut microbiota of all trout, mainly colonizing *Hermetia*-fed animals, where they constituted 3–6% of all phyla. The Actinobacteria phylum was affected by the concentration of the *Hermetia* meal in a dose-dependent manner, with significantly higher abundance in H60 compared to P60 (Figure 2A and Table 2, $p = 0.037$). Bacteroidetes were less prevalent, with an average relative abundance of 0.6 ± 0.4% across all samples. Bacteroidetes were significantly higher in the P30 group compared to H60 (1.35 ± 1.26% vs. 0.09 ± 0.09%, P30 vs. H60 relative abundance respectively; $p = 0.016$, Table 2 and Table S2). Fusobacteria were only observed in CF, with a noteworthy percentage of relative abundance, but also with high inter-individual variability (13.5 ± 29.91%; $p < 0.05$). This was due exclusively to the presence of the *Cetobacterium* genus, which was a dominant member of the microbiota in three specimens fed CF (13.44 ± 29.91%). *Weissella*, *Enterococcus*, *Lactobacillus*, *Leuconostoc*, *Streptococcus,* and *Lactococcus* of the Lactobacillales order were the most represented genera within the Firmicutes phylum, regardless of diet. The *Weissella* genus was present in all animals, with the highest relative abundance in the CF and H10P50 group and the lowest in CV (Figure 2B). Within Lactobacillales, the *Enterococcus* genus was found at significantly higher relative abundance in *Hermetia* diets (Table 2). In addition, *Dorea* was mainly present in H-fed trout, with significantly higher relative abundance in H10, H30, H60, and H10P50 compared to CV and to P60 (Figure 2B, Table 2; $p < 0.05$, Table S2). All insect-fed trout had higher intestinal relative abundance of the *Actinomyces* genus compared to CV and to both P groups (Figure 2B, Table 2; $p < 0.05$, Table S2). In addition, the group fed the insect and poultry protein mixture (H10P50) had higher intestinal levels of *Actinomyces* than CV animals (Figure 2B; $p = 0.04$). Trout fed increasing percentages of *Hermetia* meal had progressively lower relative abundance of *Pseudomonas,* and this was statistically significant for H60 compared to CV (H60: 1.53 ± 1.89%, CV: 9.80 ± 11.06%; $p = 0.04$, Figure 2B, Table 2). An opposite trend was observed for the *Bacillus* genus, which was significantly higher in H60 compared to CV (H60: 3.60 ± 3.09%, CV: 0.07 ± 0.14%, relative abundance mean ± SD; $p = 0.036$). Similarly, *Oceanobacillus* was mainly recovered from intestinal contents of H-fed trout, and its relative abundance was significantly higher than that in CV and P, but not compared to CF (Table 2).

The *Erysipelothrix* genus was almost absent in animals fed CV or P, while its relative abundance increasing with an increasing percentage of *Hermetia* meal in the diet. A similar trend was observed for *Pseudoramibacter Eubacterium*, a member of the *Eubacteriaceae* family, within the Firmicutes phylum, which was present in *Hermetia* groups but not in Ps and CV (Figure 2A,B, Table S2).

2.3. Microbiota Composition of Fish Feed

β-diversity showed a good separation of microbiota isolated from feed pellets ($p < 0.001$; Figure 3C), but no statistically significant differences were observed in relative abundances, probably due to the fact that only three replicates of feed pellet for each diet were sequenced. However, 16S rRNA sequencing of fish feed pellets revealed that Bacteroidetes, Firmicutes, and Proteobacteria were the dominant phyla in all the experimental feeds (Figure 3C). The relative abundance of Actinobacteria increased with increasing percentage of insect meal from 2.27 ± 0.44% in H10 feed to 3.38% ± 0.81% in H30 and 5.94 ± 1.14% in H60. Within the Actinobacteria, the *Actinomyces* genus was mainly present in insect meal-enriched

feeds (H10: 1.12 ± 0.26%; H30: 2.03 ± 0.57%; H60: 3.50 ± 0.72%) (Figure 3C). The relative abundance of Bacteroidetes in the feed increased proportionally with the insect meal content (3.36 ± 0.27% in H10, 6.04 ± 0.93% in H30, 9.77 ± 1.22% in H60, 3.16 ± 0.29% in H10P50), while it was present at a much lower relative abundance in the other feeds (0.38 ± 0.27% in CF, 1.16 ± 1.00% in CV, 0.61 ± 0.31% in P30, 1.45% ± 1.18% in P60) (Figure 3A). This was mainly due to a higher presence of genera *Bacteroides* (1.43 ± 0.18% in H10, 2.28 ± 0.19% in H30, 4.05 ± 0.37% in H60) and *Dysgonomonas* (0.47 ± 0.31% in H10, 1.83 ± 0.43% in H30, 2.64 ± 0.24% in H60) (Figure 3C). An opposite trend was observed for the Proteobacteria phylum, which decreased both with increasing percentage of *Hermetia* meal (65.45 ± 1.08% in H10, 61.06 ± 1.57% in H30, 52.33 ± 1.55% in H60) and of the poultry by-product meal (70.65 ± 1.49% in P30, 68.62 ± 1.76% in P60, and 64.12 ± 0.60% in H10P50). Within Firmicutes, *Lactobacillus* and *Weissella* represented the genera at the highest relative abundance in H and P feeds (Figure 3C). *Weissella* relative abundance decreased with increasing quantity of insect meal in the feed (9.90 ± 2.21% in H30, 7.25 ± 0.69% in H60), and it was also higher in CF compared to CV (12.91 ± 2.63% vs. 10.66 ± 3.52%, respectively). The highest relative abundance of Lactobacillus was found in CF (11.43 ± 0.95%), while the lowest in H60 (5.78 ± 0.69%). Proteobacteria was the most abundant phylum in CF feed, mainly represented by the Rickettsiales order (62.08 ± 3.09%). Within Proteobacteria, CF had the highest relative abundance of the *Photobacterium* genus (4.07 ± 1.19%). Conversely, this genus decreased in concomitance with a higher content of *Hermetia* in feeds (0.84 ± 1.29% in H10, 0.56 ± 0.85% in H30 and 0.30 ± 0.49% in H60).

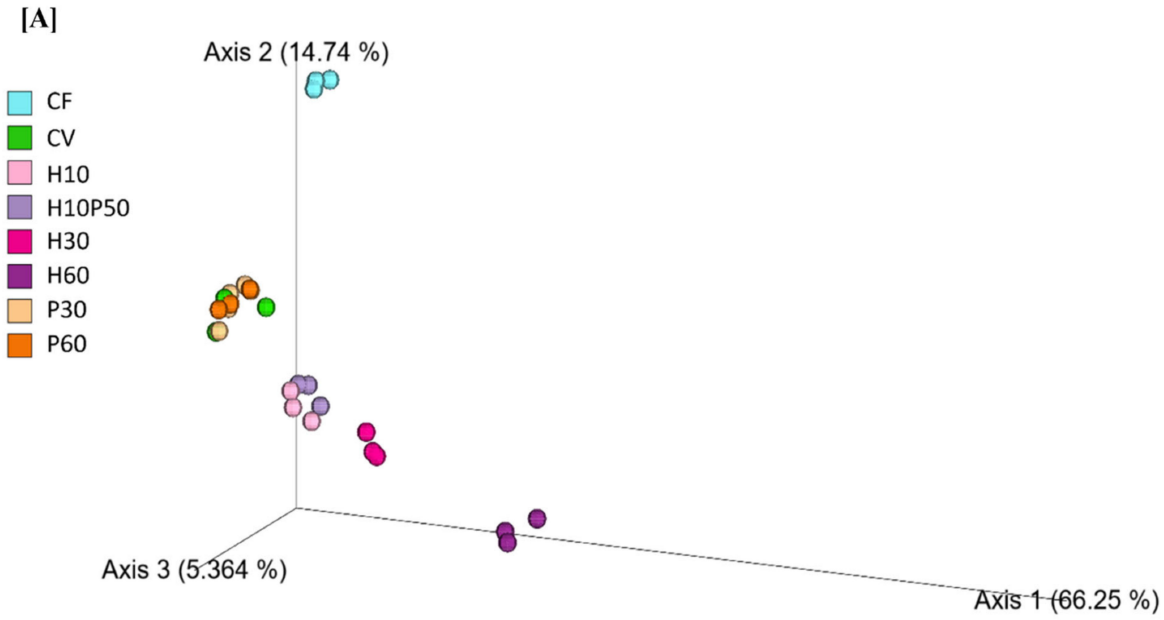

Figure 3. *Cont.*

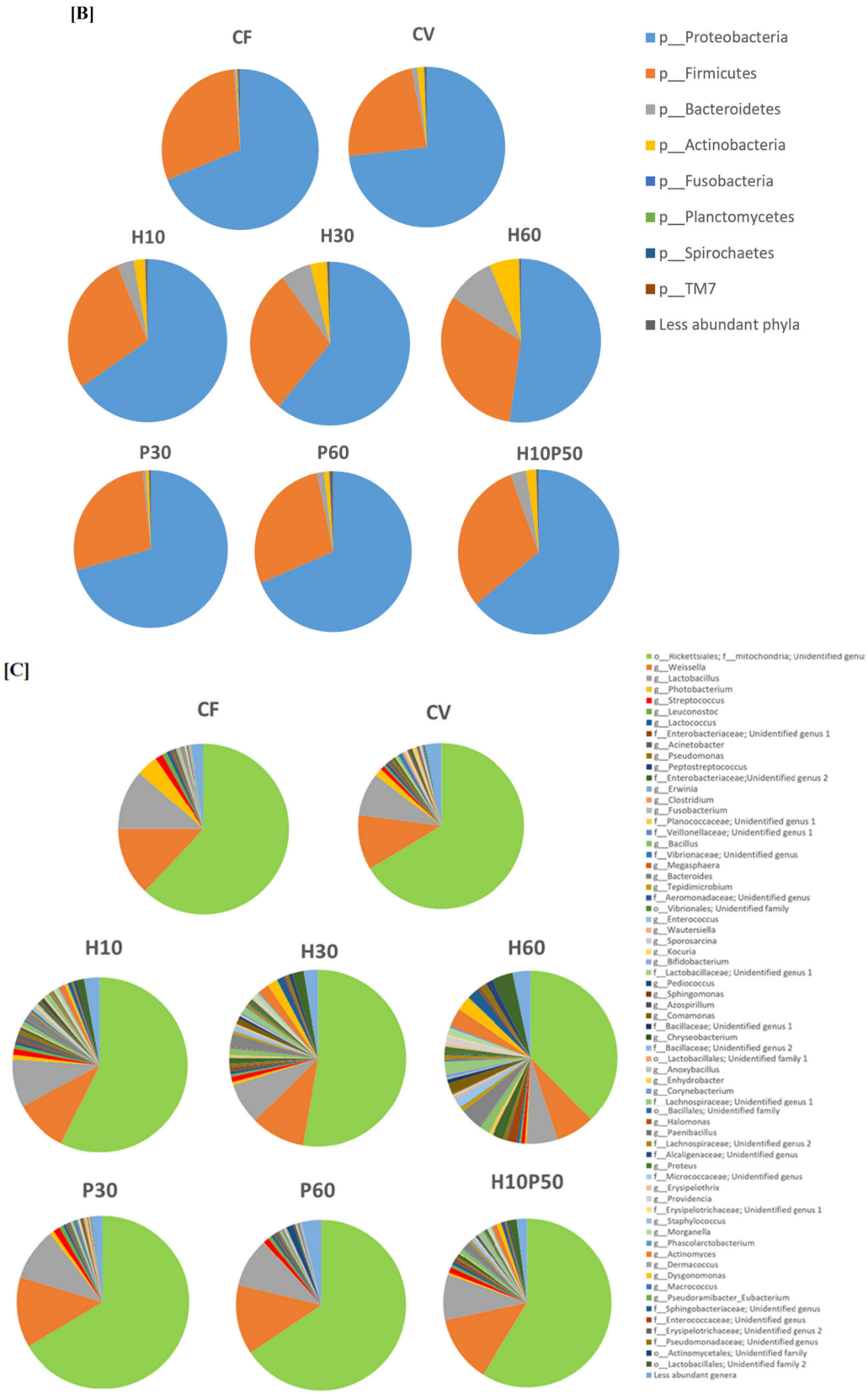

Figure 3. (**A**) PCoA representing the β-diversity of microbial populations in fish feed, according to Bray–Curtis dissimilarity ($p < 0.001$). Percentage relative abundance of phyla (**B**) and genera (**C**) in fish feed. Unassigned phyla or genera include those with percentage sequence homology less than 95% with the Greengenes database. Less abundant phyla or genera include bacteria with a relative abundance less than 0.01% in fewer than 25% of samples.

2.4. Correlation Analysis between GM and Ingredients

Spearman's correlation analysis was performed to correlate microbial relative abundances with dietary ingredients. Statistically significant differences were observed between GM taxa and dietary ingredients (Figure 4). *Hermetia* meal showed a strong positive correlation with *Actinomyces*, *Bacillus*, *Corynebacterium*, *Dorea*, *Enterococcus*, *Erysipelothrix*, *Oceanobacillus*, *Paenibacillus*, and *Pseudoramibacter Eubacterium* ($p < 0.001$ for all correlations). An opposite trend was observed between the L-Tryptophan concentration and the same genera ($p < 0.01$). The presence of poultry by-product meal showed a significant ($p < 0.05$) negative correlation with *Actinomyces*, *Erysipelothrix*, *Enterococcus*, *Pseudoramibacter Eubacterium* and with *Oceanobacillus*. P was positively correlated with *Paeniclostridium* within the *Peptostreptococcaceae* family ($p < 0.01$), while genus *Peptostreptococcus* showed a significant positive correlation with fish meal ($p < 0.05$). No other statistically significant differences were observed when correlating bacterial taxa with growth parameters, gene expression or plasma lipopolysaccharide (LPS) concentration results (Supplementary Information Figures S1–S8.)

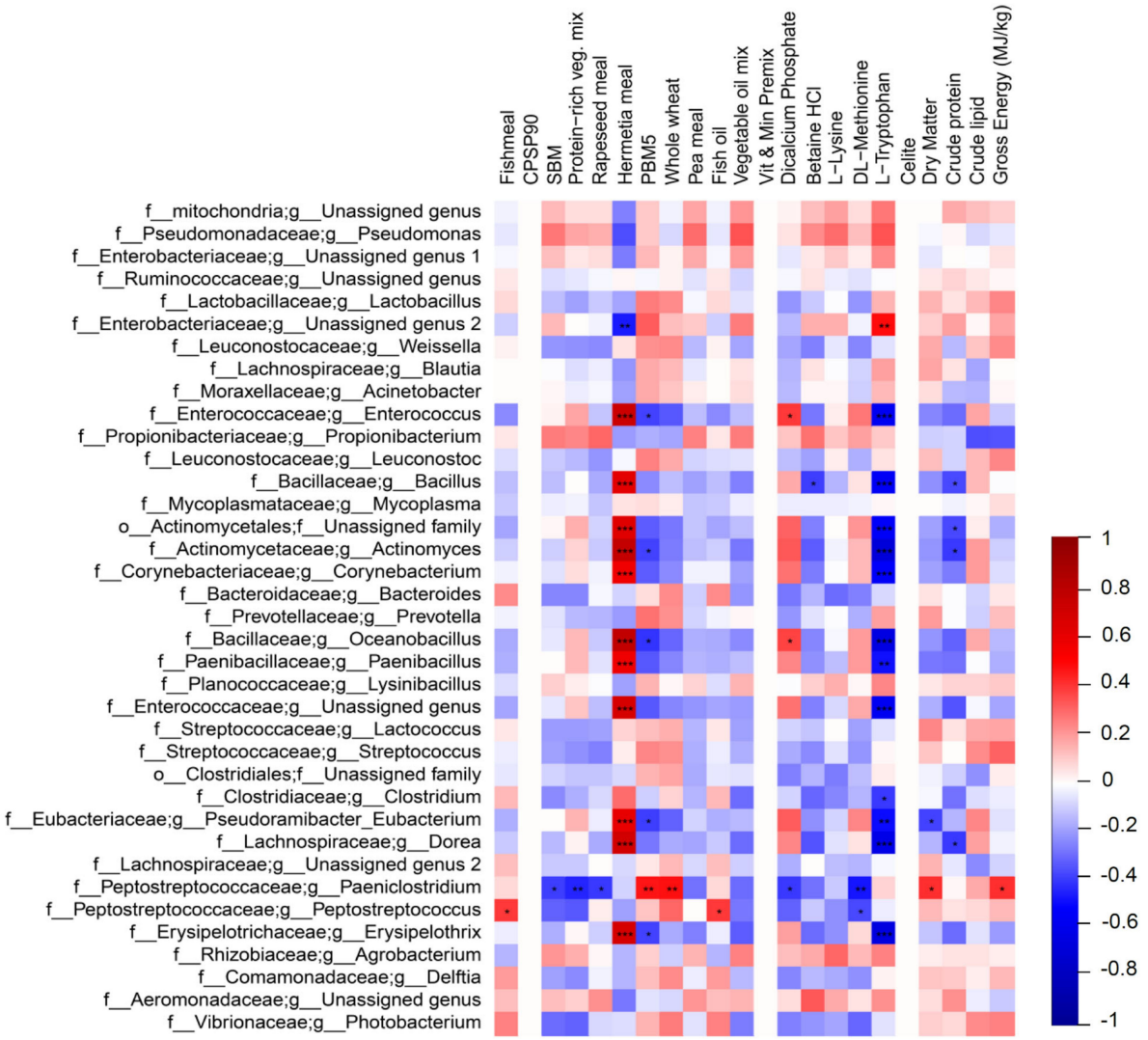

Figure 4. Spearman's correlation between the relative abundance of gut microbial genera and ingredient composition. A positive correlation is indicated by dark red, a negative correlation by dark blue. Stars indicate statistical significance after FDR correction (* $p < 0.05$, ** $p < 0.01$, *** $p < 0.001$). Families and genera were reported as "Unassigned" when they could not be assigned to any genus (g) or family (f) within the reference database (http://greengenes.lbl.gov, accessed on 13 July 2020), at a percentage sequence homology of 95% or 90% for genus and family, respectively.

2.5. Gene Expression in the Midgut and Head Kidney

The midgut and head kidney showed different expression patterns of selected markers. Significantly higher levels of the pro-inflammatory cytokine IL-1β were observed in head kidney biopsies of fish fed with H10, H30, H60, and P30 compared with CV (H10 vs. CV, $p = 0.016$; H30 vs. CV, $p = 0.016$; H60 vs. CV, $p = 0.016$; P30 vs. CV, $p = 0.016$) (Figure 5B). An opposite trend was observed in midgut biopsies, with lower IL-1β in *Hermetia* diets compared to CV, although not statistically significant (Figure 5A). A similar pattern for TGF-β was found in both midgut and head kidney biopsies, with higher levels of expression in H60, P30, and H10P50 than in CV, even if not statistically significant (Figure 5E,F). No significant changes were observed in IL-10 (Figure 5C,D), COX-2 (Figure 5G,H), and TCR-β (Figure 5I,J) among dietary groups.

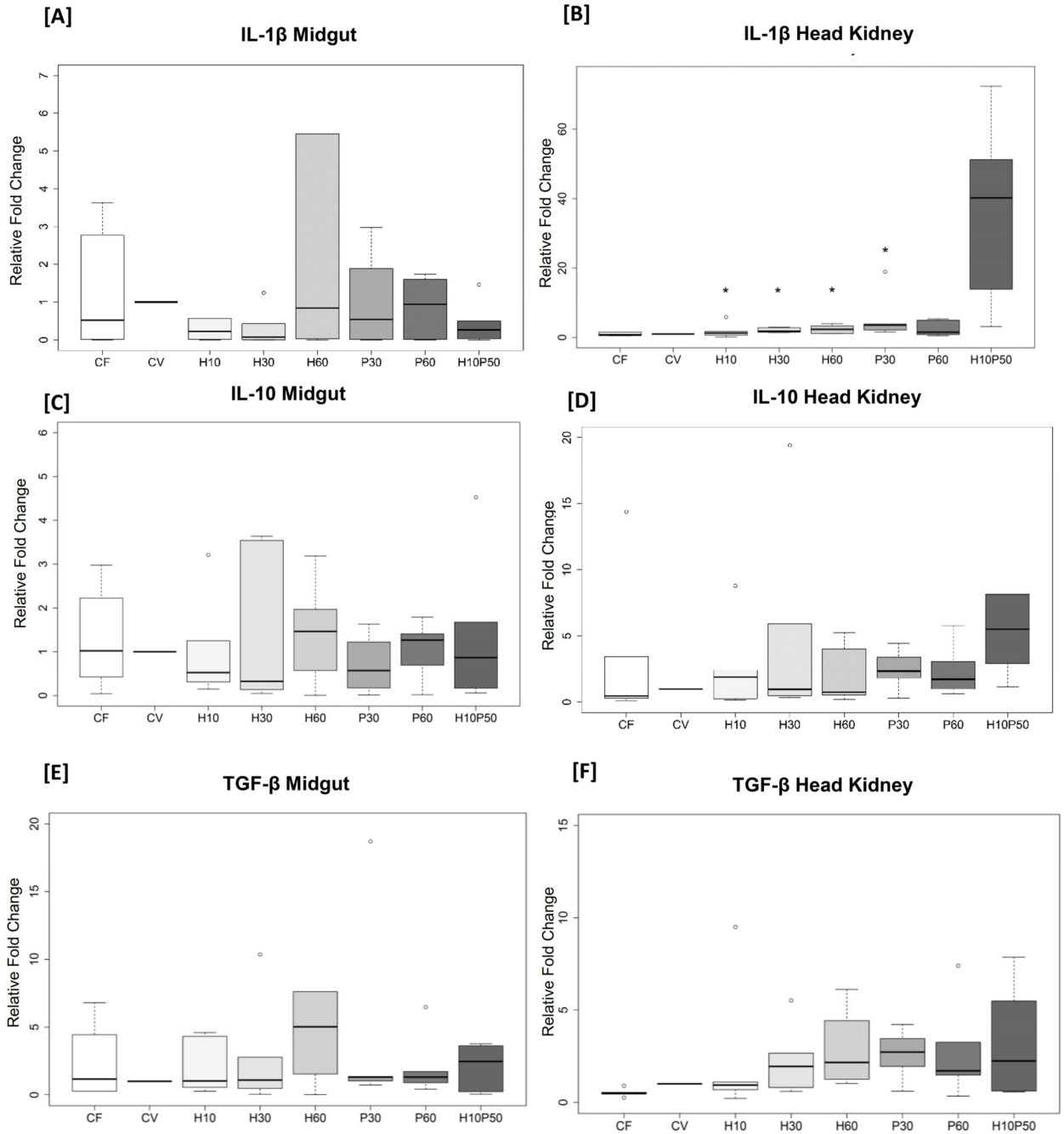

Figure 5. *Cont.*

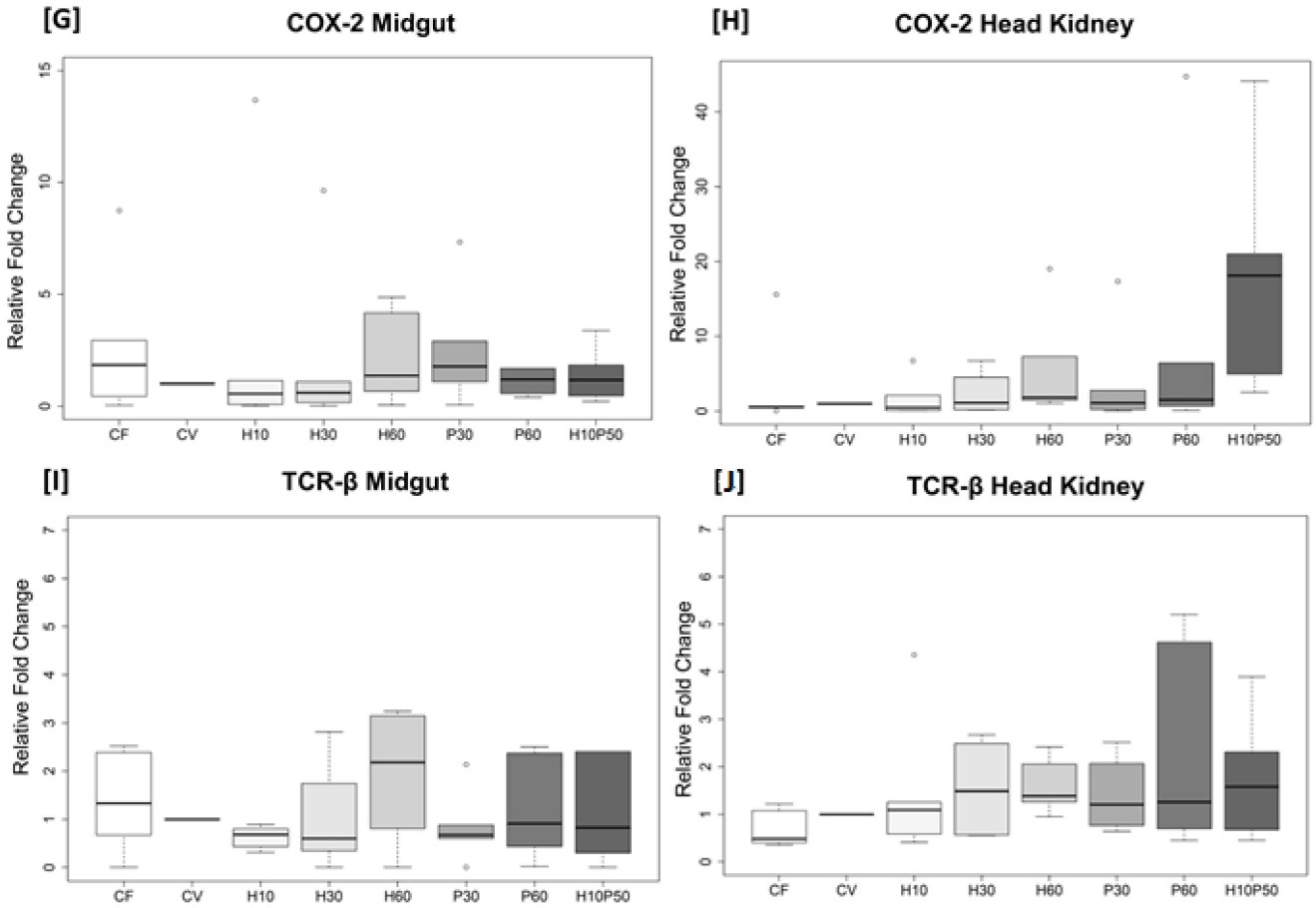

Figure 5. (**A**–**J**). Gene expression of IL-1β, IL-10, TGF-β, COX-2m and TCR-β in midgut and head kidney biopsies (n = 6 per diet) expressed as relative fold change $2^{-\Delta\Delta Ct}$ (CV = reference diet). The confidence interval box shows the 95% confidence interval for the median. ° = outliers. * $p < 0.05$ when compared with CV. Note the different scales on the y-axis.

2.6. Plasma LPS as an Intestinal Permeability Marker

No significant differences in LPS were observed between experimental groups (Table 3).

Table 3. Plasma LPS concentration (ng/µL), mean ± standard deviation (SD).

Diet	LPS Concentration (ng/µL)
CF	240.13 ± 150.13
CV	130.22 ± 111.60
H10	160.23 ± 163.10
H30	117.72 ± 175.90
H60	297.22 ± 347.59
P30	139.84 ± 130.44
P60	176.33 ± 215.96
H10P50	210.21 ± 178.07

3. Discussion

Replacement of fishmeal with vegetable plant protein meal was previously shown to affect the growth and general wellbeing of carnivorous fish [27]. The gut microbiota is strongly involved in digestion and absorption of nutrients and is markedly modulated by dietary composition [31,32]. In the search for sustainable protein sources to improve VM-based FM-free formulations, this study investigated the effect of including different percentages of *Hermetia illucens* meal (H) and poultry by-product meal (P) on gut microbial composition, as well as gut and systemic biomarkers of inflammation.

Overall, at the end of the feeding trial, fish showed a good performance in response to the test diets containing H or P meal, both singly and in combination, when compared to the vegetable or fish meal control formulations, as already reported and discussed elsewhere by Randazzo and colleagues (2021) [30]. The lower growth rate observed in trout fed the CV diet is in line with a previous study performed on the same fish species with similar size [33], where the FM substitution that ranged from 75% to 100% with the vegetable counterpart negatively affected the fish growth performance by up-regulating the gene involved in the white muscle lysosomal proteolysis, thus affecting its growth. In the present study, the observed improvements in the growth and feed efficiency (data not shown) of trout fed the FM-free diet combining H and P (H10P50) compared to both controls diets (CV and CF) are not easily comparable to other studies on different or the same fish species. In fact, in previous studies, *Hermetia illucens* or poultry by-product meals were mainly evaluated as FM substitutes in diets containing variable, but low levels of vegetable proteins [10,34,35]; while in the present study, the alternative ingredients were used to replace vegetable protein meals from the CV diet preparation lacking fish meal. Since all diets have been formulated to fit the rainbow trout nutrient requirements, the better final body weight and feed conversion efficiency observed mostly in all FM-free diets could possibly result from either a better overall digestible amino acid balance or improved gut health and nutrient digestibility, or even both. Fulton's condition factor is an easy key performance index used to compare the condition, fatness, or wellbeing of fish, based on the assumption that heavier fish of a given length are in better condition [36]; K values less than 1 imply that fish are not in good state of well-being within their habitat, while values greater than 1 imply that fish are in good physiological state of well-being. The Fulton's K values reported in the present study, independently from the dietary treatments, were all greater than 1 and were similar to those recorded in rainbow trout with a comparable final size fed a plant protein mixture diet [37].

The detrimental effect of high VM diets in salmonids has been widely demonstrated [27,38,39]. Anti-nutritional factors (ANF) are thought to be the main culprits inducing mucosal inflammation, disruption of the intestinal barrier, inhibition of digestive enzymes, and/or reduced nutrient uptake [38]. Few studies in rainbow trout have employed exclusively vegetable diets and also monitored changes in GM. Modulation of the gut microbiota may be exploited to potentially taper the observed undesirable effects of VM. Inclusion of ingredients such as P and H might potentially act in synergy with gut bacteria to stimulate gut functions and reduce inflammation. In fact recent studies have highlighted increased feed efficiency parameters when poultry by-product meal or insect meal were used to partially replace FM [28,40], but fewer studies have investigated the impact of P or H in a totally FM-free vegetable formulation. Here, we analyzed the specific impact of P and/or H as sole sources of animal protein replacing vegetable protein with increasing doses in a FM-free diet (CV).

Gut microbiota analysis through 16S rRNA sequencing revealed that the test diets induced significant differences in intestinal bacterial profiles. A marked reduction of gut microbiota α-diversity in terms of species richness and evenness was observed for all the vegetable-based diets compared to the fishmeal diet (CF). High gut microbial richness and biodiversity were previously suggested as gut health indicators since low-diversity or alterations of gut microbial ecosystems have often been related to acute bacterial infections in rainbow trout [41]. The analysis of α-diversity showed that the GM of trout fed CV had the lowest bacterial richness, both in terms of observed features and the Chao1 index, while animals fed CF had the highest bacterial richness (Figure 1A,B). Interestingly, the inclusion of different percentages of *Hermetia* meal positively influenced the alpha diversity and partly restored the loss of bacterial diversity in fishmeal-free diets, thus reaching values close to those obtained with CF. Insect meal also influenced community evenness, even if no significant differences were observed using the Shannon index (Figure 1C). Notably, these results are in agreement with recent studies where bacterial richness and evenness increased with increasing percentages of *Hermetia* meal in the diet [14,40,42].

Chitin was previously suggested as the major driver of this increase of alpha-diversity. Chitin is a structural polysaccharide and a primary component of the insect exoskeleton that behaves as an insoluble fiber since it reaches the distal part of the intestine almost undigested. Fermentation of chitin and its derivative chitosan leads to the production of several beneficial compounds, such as short-chain fatty acids (SCFAs), in particular acetate, a precursor of the synthesis of butyrate, which exerts a well-known positive effect on gut and overall fish health, nutrient utilization, and disease resistance [43–48]. Several species of *Lactobacillus* and other non-lactic bacteria such as *Bacillus* have been used as chitin fermenters [49], and this suggests that they may have a similar role in the fish gut. In our study, the chitinase producer *Bacillus* genus was found at high concentration in trout fed the highest H feed, as discussed later. Chitin may therefore act as a prebiotic by supporting the growth of beneficial chitin degraders, thus increasing gut bacterial richness and biodiversity and possibly stimulating intestinal fermentation.

The gut microbial community of all experimental groups was dominated by Tenericutes, Proteobacteria, Firmicutes, Actinobacteria, Bacteroidetes, and Fusobacteria phyla, regardless of diet. These results are in line with previous analysis of rainbow trout GM [28,41]. Tenericutes represented the most abundant phylum in trout microbiota, followed by Proteobacteria and Firmicutes. Previous analysis of trout GM in response to FM substitution with vegetable proteins or with *Hermetia* meal highlighted a shift in the Firmicutes:Proteobacteria ratio due to lower Proteobacteria in the presence of high VM or high H in the feed [27]. However, in our feeding trial we did not observe significant differences in the overall abundance of Firmicutes or Proteobacteria or the Firmicutes:Proteobacteria ratio between the diets. Our results might be explained by the high quality of the vegetable protein used in our diets (Table S1). As already suggested, purified and processed plant proteins might induce smaller impairments of gut microbiota, probably due to lower ANF and increased protein availability [27]. An increase in Firmicutes was previously observed after feeding fish with diets including insect meal [14], and we also found slightly higher Firmicutes in H groups, although this was not significant compared to other diets (Table 3). The aundance of Proteobacteria in *Hermetia*-fed animals was slightly lower than that in CF and CV, while in poultry by-product meal, the dietary abundance of Proteobacteria was more similar to both CF and CV (Figure 2A). In particular, Gammaproteobacteria of trout fed the highest *Hermetia* concentration were significantly lower than in CV, while all the other diets had comparable levels of Gammaproteobacteria between each other and similar to CF (Table 3, Table S2). Within Gammaproteobacteria we did not detect any potential pathogens, such as Vibrionales or Aeromonadales, different from previous reports [28]. Within Gammaproteobacteria, the *Pseudomonas* genus was a dominant member. *Pseudomonas* was significantly lower in H60 compared to CV. The highest relative abundance of *Pseudomonas* was found in CV, while H30- and all P-fed animals harboured similar levels to CF. *Pseudomonas*, together with *Bacillus*, *Serratia*, *Cetobacterium,* and *Lactobacillus* are common dominant members of the gut microbiota of healthy farmed trout [41]. High abundance of Rickettsiales within Alphaproteobacteria was also found in all the samples, ranging between 17% and 43% of all identified orders and apparently not affected by diet. This intracellular bacterium has been seen to have both a symbiotic as well as a pathogenic relationship with its host and it appears not to be necessarily linked to disease, similar to what we observed in this study [50].

Fish fed H10, H30, and H60 showed an increase in the relative abundance of bacteria belonging to the *Mycoplasma* genus, within the Tenericutes phylum, although not significant after FDR. This observation agrees with previous studies, where *Mycoplasma* was found as one of the most abundant genera in rainbow trout and Atlantic salmon intestines [40,42,51]. *Mycoplasma* uses dietary substrates to produce lactic acid and acetic acid as the main fermentation end-products [52]. Moreover, a decrease in *Mycoplasma* abundance in rainbow trout intestine has recently been related to a higher susceptibility to disease and inflammation [53]. *Mycoplasma* was previously seen to colonize the GM of

farmed salmonids and to be less affected by diet. Nevertheless, it has an essential role in maintaining gut homeostasis in rainbow trout.

We observed a significant increase of Actinobacteria in the GM of animals fed different percentages of *Hermetia* meal in the diet. The abundance of Actinobacteria ranged from about 3% in H10 to 5% in H30 and reached 6% in H60, while the same animals showed a proportional decrease in Proteobacteria, with 55% in H10, 24% in H30, and 20% in H60 (Figure 2A). This is consistent with other studies where a similar shift in these two dominant phyla was observed with a partial substitution of fish meal with insect meal [16,42]. Our results showed that all insect meal-including diets had significantly higher relative abundances of the *Actinomyces* genus, within the Actinobacteria phylum, compared to CV (H10: 1.58%, H30: 3.16%, H60: 4.66%, H10P50: 0.52%, CV: 0.05%; Table 3). Bacteria belonging to this genus were previously identified as active chitin degraders, which were seen to increase fish growth and efficiency proportionally to the quantity of chitin in the diet [43]. The chitinolytic activity of *Actinomyces* leads to the production of chitosan, a partial-deacetylated derivative of chitin [54]. In support of this hypothesis, a positive Spearman's correlation was observed between *Actinomyces* and insect meal (Figure 4). Another chitinase-producing genus, *Bacillus,* within the Firmicutes phylum, was significantly increased in relative abundance in H-fed trout. *Bacillus* is commonly used as a probiotic in aquaculture industries and is reported as one of the core taxa in the fish gut microbiome [55–57]. Several recent studies reported an increase in *Bacillus* in the GM of fish fed insect meal [14,40,42] and its increased relative abundance in the current study is probably related to the chitin content of the H diets (Table S1). In support of this, we observed a strong positive Spearman correlation between *Bacillus* and insect meal. Microbiota analysis of feed pellets revealed that feed formulations containing *Hermetia illucens* carry both *Actinomyces* sequences and *Bacillus* sequences (Figure 3). These results suggest that on the one hand, the H diet may promote the growth of specific autochthonous bacteria that constitute the natural gut microbial community, and on the other, that such diets may also contribute to enrich allochthonous bacteria via microbiota transfer from insect feed to the fish gut, possibly impacting feed conversion and animal health. Microbiota transfer from feed has been previously reported. Li et al. (2021) [42] suggested that the increased *Actinomyces* relative abundance in rainbow trout fed black soldier fly may be explained by feed-borne microbiota. Similarly, in our study, *Photobacterium* had the highest abundance in CF-fed trout, while it was nearly absent in all the other experimental groups. A similar distribution was observed in the microbial composition of the feed, with *Photobacterium* being higher in CF than in all the other feeds. In accordance with a previous study [58], it appears that both *Actinomyces* and *Photobacterium* may transit from feed to the gut. The fish gut microbiota therefore behaves as a dynamic ecosystem which appears to be modelled by feed-associated bacteria and nutrient composition providing the host with acquired digestive functions [59]. Microbial transfer from feed to fish could therefore be exploited as a strategy to enhance fish capability to absorb nutrients.

Fish fed H10, H30, and H60 showed higher relative abundance of the *Erysipelothrix* genus. Moreover, Spearman's correlation analysis showed a positive correlation between *Erysipelothrix* and the presence of insect meal in the diet. Rimoldi and collaborators (2021) [40] recently observed higher abundance of *Erysipelotrichaceae*, and especially *Erysipelothrix*, in the GM of trout fed an H-enriched diet. High relative abundance of *Erysipelothrix* was also previously found in animals fed high poultry by-product proteins (55%) in addition to FM, together with high abundance of *Enterococcaceae*, *Streptococcaceae*, and *Enterobacteriaceae* [28]. On the other hand, in our study, *Erysipelothrix* was almost absent in trout fed P and CV. Although the role of this genus in the fish intestine is not fully understood, some species belonging to *Erysipelothrix* such as *E. piscisicarius* cause systemic disease in several fish with necrotizing dermatitis and orofacial ulceration [60]. Further studies are required to fully understand the role of *Erysipelothrix* in rainbow trout metabolism and health. In addition, we reported a higher abundance of the *Enterococcus* genus, within *Enterococcaceae*, in H diets compared to the other diet groups. This is in

contrast with Rimoldi et al. (2018) [28], who reported higher abundance of *Enterococcaceae* and, specifically, of the *Enterococcus* genus, together with high values of *Eryspelothrix* after feeding a high poultry by-product and animal protein commercial diet. However, in the study by Rimoldi et al. (2018) [28], the diet that showed the highest abundance of *Enterococcus* is not comparable to any of our P diets, due to a much higher animal protein content from various sources (poultry, swine) as well as FM content. In our study, *Enterococcus* abundance in H diets was much higher than that observed by Rimoldi and colleagues (2018) [28], while *Erysipelothrix*, on the other hand, had a much lower relative abundance.

Dorea genus, within the *Lachnospiraceae* family, was significantly higher in all H diets, including H10P50, compared to CV and to P60. The *Paeniclostridium* genus was significantly higher in H10P50 compared to CV (Table 3). Interestingly, two different genera within the *Peptostreptococcaceae* family correlated positively with fishmeal and with poultry meal, respectively (Figure 4). *Peptostreptococcaceae* was reported as one of the dominant members of the GM after P feeding in salmonids and, specifically, in rainbow trout [28,61]. *Peptostreptococcaceae* and *Lachnospiraceae* are fast protein degraders; therefore, distinctive microbial genera within the same family might be specialized in the digestion of different protein structures present in FM and P [62]. Both *Lachnospiraceae* and *Peptostreptococcaceae* were previously reported as indicator taxa for fast-growing fish [63]. Considering the good growth performance we observed when feeding trout with a mixture of insect and poultry meal, there may be a role for *Lachnospiraceae* and *Peptostreptococcaceae* in helping digestion and promoting animal growth.

In addition to the characterization of the gut microbial community, we performed a gene expression analysis of immune and inflammatory biomarkers in midgut and head kidney tissues. Different patterns of expression of the cytokines IL-1β, IL-10, TGF-β, and the inflammatory markers COX-2 and TCR-β were observed in the analyzed tissue biopsies. IL-1β is a pro-inflammatory cytokine and plays a central role in generating and controlling the immune response in rainbow trout during infection and inflammatory processes [64,65]. The early activation of IL-1β stimulates the recruitment of other cytokines and the activation of lymphocytes and macrophages [66]. Our results showed an overexpression of IL-1β in the head kidney of fish fed P30 and H10P50 diets compared to CV. An opposite trend of expression, even if not statistically significant, was reported in midgut biopsies. The expressions of the others selected biomarkers (i.e., IL-10, TGF-β, COX-2, and TCR-β) were not affected by dietary treatment. Interestingly, the anti-inflammatory cytokine IL-10 had a pattern of expression resembling that of IL-1β. This was observed in all dietary treatments, both in midgut and head kidney tissues, even if not statistically significant. IL-10 has a crucial role in controlling autoimmune and inflammatory reactions in fish [67] and its expression is commonly induced together with pro-inflammatory cytokines [68]. According to these considerations, we presume that the expression of IL-10 could have a role in modulating the immune response in trout limiting excessive inflammatory reactions, as already hypothesized by Heinecke and Buchmann in 2013 [69]. Nevertheless, since no significant changes were reported in the expression of all the other selected markers and given that changes in IL-1β expression were only observed in the head kidney of two dietary groups, we can conclude that none of the experimental diets had a deleterious impact on the overall immune health of the animals. Plasma LPS analysis supported this result. Circulating LPS is a marker of intestinal barrier integrity, since increased gut permeability may induce translocation of inflammatory bacterial LPS from the lumen to the blood circulation [70]. In this study, no significant differences in LPS concentration were observed between diets, thus suggesting maintenance of intestinal barrier integrity in response to the experimental diets.

4. Materials and Methods

4.1. Animal Ethics Statement

All the experiments were performed following directive 2010/63/UE on the protection of animals used for scientific purposes and in line with Italian legislation and approved

by the Ethics Committee of the Edmund Mach Foundation (n. 99F6E.0). The study protocol was authorized by the Italian Ministry of Health (530/2018-PR). In order to avoid animal suffering, fish were euthanized by immersion in a lethal dose solution of tricaine methanesulfonate (MS-222, 1 g L^{-1}) before tissue sampling.

4.2. Fish, Experimental Diets, and Culture Conditions

A total number of 1200 juvenile rainbow trout (*Oncorhynchus mykiss*) with an average weight of 54.2 g (±9.94) were randomly distributed into 24 square fiberglass tanks (1.6 m^3) and assigned to eight different dietary treatments for three months. The growth trial was performed at the indoor experimental facility at the Technology Transfer Center (CTT), Edmund Mach Foundation (FEM), San Michele all'Adige, TN, Italy, as reported in Randazzo et al., 2021 [30]. Briefly, eight iso-proteic (N × 6.25, 42% dry matter), iso-lipidic (24% DM) and iso-energetic (approximately 23 MJ/kg) diets were manufactured at SPAROS Lda. (Olhão, Portugal) by extrusion. A diet rich in vegetable protein derivatives (control vegetable, CV) was prepared to have a 10:90 and 20:80 fish-to-vegetable protein and lipid ratios, respectively. By contrast, a fish-based diet (control fish, CF) was formulated with opposite fish-to-vegetable protein and lipid ratios. Six more diets were obtained by replacing graded levels of protein (10, 30, and 60%) of diet CV, by protein from partially defatted *Hermetia illucens* pre-pupae meal (H10, H30, and H60) or poultry by-product meal (P30, P60), while maintaining the same vegetable-to-fish lipid ratio as in the CV diet. An additional diet that replaced 60% vegetable protein with a combination of 10% and 50% of protein from *Hermetia illucens* and poultry by-product meal (H10P50) respectively, was also formulated. The ingredient composition and proximate analysis of the test diets are shown as supplementary material (Table S1). During the feeding trial, a visual inspection of tanks was carried out daily to check feeding behavior and mortalities. The rearing conditions were monitored every week to maintain optimal environment control for rainbow trout growth. The mean dissolved oxygen (DO), measured after the daily meal in the tank water outlet, was 9.43 ± 0.42 mg/L, and the water temperature fluctuated close to 13.3 ± 0.23 °C. Fish were fed by hand twice a day, six days a week, at apparent visual satiety over 91 days. Feed ingested was recorded daily for each tank, recovering and weighing uneaten feed pellets at the end of each meal. Mortality was also monitored.

4.3. Tissue Sampling and Calculation

After a 3-month feeding trial, all fish were subjected to stage three anaesthesia with 300 mg L^{-1} of MSS-222 (Finquel®MS-222, Argent Laboratories, Redmont-VI, USA). Biometry measurements (total length, cm and body weight, g) were recorded for the subsequent Fulton's condition factor calculation [K = fish weight (g) × 100/fish total length $(cm)^3$]. After that, three fish in each tank (nine fish/diet) were sacrificed by a lethal dose of the same anesthetic (Finquel®MS-222 1 g L^{-1}). Blood samples (2 mL) were collected from the caudal vein in S-Monovette® heparin-containing tubes (Sarstedt, Nümbrecht, Germany) and stored in ice and, subsequently, plasma was obtained by blood centrifugation. After the sacrifice, the ventral side of the animals was opened to remove the gastrointestinal tract and the head kidney. The intestinal content, obtained by squeezing the gastrointestinal tract, was collected in sterile cryovials (Eppendorf, USA) and frozen in liquid nitrogen. Subsequently, tissue biopsies from the midgut and head kidney were collected in sterile cryogenic vials CryoTubes® (Merck, Darmstadt, Germany), immediately frozen in liquid nitrogen, and all samples were then stored at −80 °C until assays were performed.

4.4. Gut Microbiota Analysis

Total genomic DNA extraction from intestinal contents (90–120 mg) and animal feed was carried out using the DNeasy® PowerSoil® kit (Qiagen, Milan, Italy) following the manufacturer's instructions but adding Proteinase K after C1 solution, incubating at 70 °C for 10 min and lysing samples in a PowerBead Tube using TissueLyser II (Qiagen, Italy) at maximum power for 10 min. A double elution of the Spin column tube was then made

with DEPC-treated water to a final volume of 100 µL. DNA quality and concentration were measured using a NanoDrop 8000 spectrophotometer (Thermo Fisher, Waltham, MA, USA). High-quality DNA was stored at −20 °C.

PCR amplification was performed by targeting 16S rRNA gene V3-V4 variable regions with the bacterial primer set 341F (5′-CCTACGGGNGGCWGCAG-3′) and 806R (5′-GACTACNVGGGTWTCTAATCC-3′), as previously reported [71]. PCR reactions were carried out using 2X KAPA Hifi HotStart Ready Mix (Kapa Biosystems Ltd., UK) according to the following protocol: 5 min at 95 °C, 30 cycles of 30 s at 95 °C, 30 s at 55 °C, and 30 s at 72 °C, followed by a final extension of 5 min at 72 °C. PCR products were checked by gel electrophoresis and cleaned using an Agencourt AMPure XP system (Beckman Coulter, Brea, CA, USA), following the manufacturer's instructions. After seven PCR cycles (16S Metagenomic Sequencing Library Preparation, Illumina), Illumina adaptors were attached (Illumina Nextera XT Index Primer). Libraries were purified using Agencourt AMPure XP (Beckman) and then sequenced on an Illumina® MiSeq (PE300) platform (MiSeq Control Software 2.0.5 and Real-Time Analysis software 1.16.18, Illumina, San Diego, CA, USA). Sequences obtained from Illumina sequencing were analyzed using the Quantitative Insights Into Microbial Ecology (QIIME) 2.0 pipeline [72]. Unidentified taxa include those whose percentage sequence homology with Greengenes database was less than 95% [73]. α- and β-diversity estimates were determined using the *phyloseq* R Package [74].

4.5. Gene Expression in the Midgut and Head Kidney

Total RNA was extracted from 10–30 mg frozen tissue using the TRIzol reagent (Thermo Fisher Scientific, Waltham, MA, USA) according to the manufacturer's recommendations with the following modifications. Briefly, the tissue was first homogenized in 300 µL Trizol reagent using a sterile plastic pestle, and then 700 µL Trizol reagent was added to a final volume of 1 mL. After homogenization, all steps (including optional steps) were performed as suggested but adding 40 µL of 3 M sodium acetate, 5.5 pH, and 1 mL of cold ethanol 96% to the aqueous phase. Samples were stored overnight at −20 °C and then centrifuged at 13.200× *g* for 30 min at 4 °C. Two washing steps with 500 µL cold 70% ethanol were performed, each followed by 5 min and 6 min centrifugation at 13.000× *g*. Dry pellets were finally resuspended with 50 µL of DEPC-treated water and stored at −80 °C. Extracted total RNA was quantified using a Nanodrop 8000 Spectrophotometer (Thermo Fisher Scientific, Waltham, MA, USA), and RNA quality was assessed using a 2200 TapeStation (Agilent Technologies, Santa Clara, CA, USA). mRNA samples with high quality (RINe > 8) were used for retrotranscription. Reverse transcription was performed with a High-Capacity cDNA Reverse Transcription Kit (Applied Biosystems™, Thermo Fisher Scientific, Waltham, MA, USA) in a 20 µL reaction volume containing 10 µL template RNA (5 ng/µL), 2.0 µL of 10X RT Buffer, 0.8 µL of 25X dNTP Mix (100 mM), 2.0 µL of 10X RT Random Primers, 1.0 µL of MultiScribe™ Reverse Transcriptase, and 4.2 µL of DEPC-treated water. After transcription, cDNA was stored at −20 °C until quantitative Real-Time PCR (RT-PCR).

The expression level of inflammatory genes was determined by RT-PCR using a LightCycler® 480 SW 1.5.1.62 (Roche). RT-PCR was carried out in 20 µL reactions prepared following the manufacturer's instruction and containing 10 µL of 2x qPCRBIO SyGreen Mix Separate-ROX (PCR BioSystems, UK), 0.4 µL of each primer (10 ng/µL), 5.2 µL of DEPC-treated water, and 4 µL of cDNA (10 ng). Reactions were carried out in triplicate under the following conditions: 95 °C for 15 s, followed by 45 cycles at 95 °C for 15 s, 63 °C for 30 s, 72 °C for 10 s, one cycle at 95 °C for 10 s, 65 °C for 15 s, 97 °C continuous and a final step at 40 °C for 30 s. Ct values for each sample were normalized against the geometric mean Ct values obtained for two housekeeping genes, 18S and EF-1α. Accurate calculation of primer efficiency was evaluated from the standard curve and since it was between 1.96 and 2.0, it was approximated to 100% efficiency for all the target and reference genes. Gene expression was therefore expressed as the relative fold change $2^{-\Delta\Delta Ct}$, where ΔCt was obtained by subtracting the geometric mean Ct for the two reference housekeeping genes

18S and EF-1α from the Ct of the tested gene, and ΔΔCt represented the difference between ΔCt of the test diet compared to the ΔCt of CV as the reference diet. Primers and relative accession numbers are shown in Table 4.

Table 4. Primers used to evaluate gene expression by RT-PCR.

Gene	Accession Number	Forward Primer (5′-3′)	Reverse Primer (5′-3′)	References
IL-1β	AJ557021	ACATTGCCAACCTCATCATCG	TTGAGCAGGTCCTTGTCCTTG	[75]
IL-10	NM001246350	CGACTTTAAATCTCCCATCGAC	GCATTGGACGATCTCTTTCTT	[76]
COX-2	AJ238307	ATCCTTACTCACTACAAAGG	GCTGGTCCTTTCATGAAGTCTG	[77]
TGF-β	X99303	AGATAAATCGGAGAGTTGCTGTG	CCTGCTCCACCTTGTGTTGT	[78]
TCR-β	AF329700	TCACCAGCAGACTGAGAGTCC	AAGCTGACAATGCAGGTGAATC	[79]
EF-1α	AF498320	ACCCTCCTCTTGGTCGTTTC	TGATGACACCAACAGCAACA	[79]
18S	AF308735	GATCCATTGGAGGGCAAGTCT	CGAGCTTTTTAACTGCAGCAACTTT	[80]

4.6. Plasma LPS Concentration

The quantity of 50 µL of plasma was analysed in duplicate. Detection of LPS was performed using an ELISA Kit for Lipopolysaccharide (LPS) (Cloud-Clone Corp, CCC, Katy, TX, USA) according to the manufacturer's recommendations. Absorbance analysis was carried out using a PowerWave 340 (BioTek) and Gen5™ software.

4.7. Statistical Analysis

All statistical analysis was performed using R studio. Percentage relative abundance of taxa from different dietary groups was compared using a nonparametric Wilcoxon statistical test. Normal distribution of data was assessed by Shapiro–Wilk's test. Pairwise comparison among groups in terms of α-diversity was calculated by the Kruskal–Wallis test, followed by the post-hoc Dunn's test with Benjamini–Hochberg false discovery rate (FDR) p value correction. Differences in the β-diversity were checked using the non-parametric Permutational Multivariate Analysis of Variance (PERMANOVA) and adonis tests with 999 permutations, via the vegan R Package [81]. Correlation between bacterial taxa and experimental ingredients was performed by Spearman's correlation analysis. After FDR correction, a p value < 0.05 was considered statistically significant. All data are expressed as the mean ± standard deviation, SD.

5. Conclusions

In summary, our findings suggest that none of the experimental diets negatively affected fish health in terms of growth parameters and inflammatory status. Both poultry by-product and insect meals could be considered valid alternatives to vegetable protein ingredients and may be useful for improving FM-free diets. Changes in bacterial α-diversity after feeding animals with *Hermetia* clearly indicated that a percentage of insect meal in fish feed ranging from 8% to 45% positively modifies the fish gut microbiota. Experimental diets H10, H30, and H60 increased gut bacterial community richness, ameliorating the low diversity profile induced by the vegetable diet and reaching values close to those obtained with the fish meal diet. In addition, according to existing data and to our results, we believe that fermentable chitin should be considered the major driver of positive changes in gut bacterial populations, acting as a prebiotic in trout. However, uptake of insect meal by the aquafeed industry faces cost-effectiveness challenges. For this reason, the combination of insect meal with other alternatives to fish meal such as poultry by-product meal represents a viable alternative in terms of cost, environmental sustainability, and fish health. P addition to VM-based formulations sustained the growth of the animals and maintained a microbiota composition more similar to that of FM-fed animals. In particular, P supported the growth of Proteobacteria, particularly non-pathogenic Gammaproteobacteria, as demonstrated by a comparable relative abundance to that observed in trout fed fish meal. Both *Hermetia*

and poultry by-products contributed to increase GM α-diversity, thus rendering it more similar to the GM of fish fed the control fishmeal. GM specifically responded to inclusion of *Hermetia* in vegetable feed with an increase in chitin degraders, i.e., *Actinomyces* and *Bacillus* genera, as well as some Lactobacillales. Similarly, the presence of poultry by-products in the feed promoted the growth of specific proteolytic *Peptostreptococcaceae* and non-pathogenic Proteobacteria. *Weissella* and *Actinomyces* were directly transferred from *Hermetia* feed to trout GM. In other words, the GM of tested animals was able to change dynamically in response to the diet of the host and may play a key role in nutrient digestion.

Supplementary Materials: The following are available online at https://www.mdpi.com/article/10.3390/ijms22115454/s1, Table S1: Diet formulation and proximate composition of the tested diets (modified from Randazzo et al., 2021); Table S2: (A-B) p values of statistically significant differences in percentage relative abundance of gut microbial taxa after pairwise comparisons between diets with Benjamini–Hochberg FDR correction. Figure S1: Spearman's correlation between the relative abundance of gut microbial genera and gene expression in midgut biopsies. Figure S2: Spearman's correlation between the relative abundance of gut microbial genera and gene expression in head kidney biopsies. Figure S3: Spearman's correlation between the relative abundance of gut microbial genera and LPS measures. Figure S4: Spearman's correlation between the relative abundance of gut microbial genera and growth parameters. Figure S5: Spearman's correlation between gene expression in midgut biopsies and growth parameters. Figure S6: Spearman's correlation between gene expression in head kidney biopsies and growth parameters. Figure S7: Spearman's correlation between gene expression in midgut biopsies and proximate composition of the tested diets. Figure S8: Spearman's correlation between gene expression in head kidney biopsies and proximate composition of the tested diets.

Author Contributions: Conceptualization: F.F. (Filippo Faccenda), F.L., G.C., G.M. (Giovanna Marino), I.O., G.P., E.T., K.M.T., F.F. (Francesca Fava); Data curation; G.G., G.M. (Giulia Marzorati), F.F. (Francesca Fava), F.F. (Filippo Faccenda), G.C.; Formal Analysis: G.G., G.M. (Giulia Marzorati), F.F. (Filippo Faccenda), F.F. (Francesca Fava); Funding acquisition: F.F. (Filippo Faccenda), F.L., G.C., G.M. (Giovanna Marino), I.O., G.P., E.T., K.M.T., F.F. (Francesca Fava); Investigation: G.G., G.M. (Giulia Marzorati), T.W., F.F. (Francesca Fava); Methodology: F.F. (Filippo Faccenda), G.C., T.W., E.T., F.L., F.F. (Francesca Fava); Project Administration: F.F. (Francesca Fava), F.F. (Filippo Faccenda), F.L., I.O., G.C., E.T.; Supervision: I.O., F.F. (Francesca Fava), K.M.T., F.F. (Filippo Faccenda), G.C., E.T.; Validation: G.G., F.F. (Francesca Fava), F.F. (Filippo Faccenda), CG, TE, LF; Writing—Original draft: G.G., F.F. (Francesca Fava); Writing—review & editing: G.G., F.F. (Francesca Fava), G.C., K.M.T., F.F. (Filippo Faccenda), G.P., G.M. (Giovanna Marino). All authors have read and agreed to the published version of the manuscript.

Funding: This work was funded by AGER Network Foundation project SUSHIN (SUstainable fiSH feeds INnovative ingredients), AGER2, Cod 2016-0112; 2). This work was also supported by the EFH-Environment, Food and Health project approved by GECT EUREGIO (ref. doc Nr. 19/2017) and funded by the Autonomous Provinces of Trento and Bolzano in Italy and Tyrol in Austria.

Institutional Review Board Statement: The experiment was performed following directive 2010/63/UE. The study was approved by the Ethics Committee of the Edmund Mach Foundation (n. 99F6E.0), and the protocol was authorized by the Italian Ministry of Health (530/2018-PR).

Informed Consent Statement: Not applicable.

Data Availability Statement: The data for this study have been deposited in the European Nucleotide Archive (ENA) at EMBL-EBI under accession number PRJEB43152 (https://www.ebi.ac.uk/ena/browser/view/PRJEB43152, accessed on 10 May 2021).

Acknowledgments: The authors thank Massimo Pindo and the members of the Sequencing Platform at Fondazione Edmund Mach for sequencing; Matthias Scholz at Fondazione Edmund Mach for bioinformatic advice; Maria Messina, Patrizia Di Marco, Basilio Randazzo, Leonardo Bruni, Matteo Fontana, Camilla Diotallevi, and the SUSHIN team for their help during sampling and analysis.

Conflicts of Interest: The authors declare no conflict of interest.

References

1. Willett, W.; Rockström, J.; Loken, B.; Springmann, M.; Lang, T.; Vermeulen, S.; Garnett, T.; Tilman, D.; DeClerck, F.; Wood, A.; et al. Food in the Anthropocene: The EAT—Lancet Commission on healthy diets from sustainable food systems. *Lancet* **2019**, *393*, 447–492. [CrossRef]
2. FAO. *The State of World Fisheries and Aquaculture 2020. Sustainability in Action*; FAO: Rome, Italy, 2020. [CrossRef]
3. Den Hartog, L.A.; Sijtsma, S.R. Sustainable feed ingredients. In Proceedings of the 12th International Symposium of Australian Renderers Association "Rendering for Sustainability", Victoria, Australia, 23–26 July 2013.
4. Nasopoulou, C.; Zabetakis, I. Benefits of fish oil replacement by plant originated oils in compounded fish feeds. A review. *LWT Food Sci. Technol.* **2012**, *47*, 217–224. [CrossRef]
5. Montero, D.; Izquierdo, M. Welfare and health of fish fed vegetable oils as alternative lipid sources to fish oil. In *Fish Oil Replacement and Alternative Lipid Sources in Aquaculture Feeds*; CRC Press: Boca Raton, FL, USA, 2010; pp. 439–485. [CrossRef]
6. Jędrejek, D.; Levic, J.; Wallace, J.; Oleszek, W. Animal by-products for feed: Characteristics, European regulatory framework, and potential impacts on human and animal health and the environment. *J. Anim. Feed Sci.* **2016**, *25*, 189–202. [CrossRef]
7. Hernández, C.; Osuna-Osuna, L.; Benitez-Hernandez, A.; Sanchez-Gutierrez, Y.; González-Rodríguez, B.; Dominguez-Jimenez, P. Replacement of fish meal by poultry by-product meal, food grade, in diets for juvenile spotted rose snapper (*Lutjanus guttatus*). *Lat. Am. J. Aquat. Res.* **2014**, *42*, 111–120. [CrossRef]
8. Maiolo, S.; Parisi, G.; Biondi, N. Fishmeal partial substitution within aquafeed formulations: Life cycle assessment of four alternative protein sources. *Int. J. Life Cycle Assess* **2020**, *25*, 1455–1471. [CrossRef]
9. Badillo, D.; Herzka, S.Z.; Viana, M.T. Protein Retention Assessment of Four Levels of Poultry By-Product Substitution of Fishmeal in Rainbow Trout (*Oncorhynchus mykiss*) Diets Using Stable Isotopes of Nitrogen (δ15N) as Natural Tracers. *PLoS ONE* **2014**, *9*, e107523. [CrossRef]
10. Hatlen, B.; Jakobsen, J.V.; Crampton, V.; Alm, M.; Langmyhr, E.; Espe, M.; Hevrøy, E.M.; Torstensen, B.E.; Liland, N.; Waagbø, R. Growth, feed utilization and endocrine responses in Atlantic salmon (*Salmo salar*) fed diets added poultry by-product meal and blood meal in combination with poultry oil. *Aquac. Nutr.* **2015**, *21*, 714–725. [CrossRef]
11. Doughty, K.H.; Garner, S.R.; Bernards, M.A.; Heath, J.W.; Neff, B.D. Effects of dietary fishmeal substitution with corn gluten meal and poultry meal on growth rate and flesh characteristics of Chinook salmon (*Oncorhynchus tshawytscha*). *Int. Aquat. Res.* **2019**, *11*, 325–334. [CrossRef]
12. Barreto-Curiel, F.; Parés-Sierra, G.; Correa-Reyes, G.; Durazo-Beltrán, E.; Viana, M.T. Total and partial fishmeal substitution by poultry by-product meal (pet food grade) and enrichment with acid fish silage in aquafeeds for juveniles of rainbow trout *Oncorhynchus mykiss*. *Lat. Am. J. Aquat. Res.* **2016**, *44*, 327–335. [CrossRef]
13. Nogales-Mérida, S.; Gobbi, P.; Jozefiak, D.; Mazurkiewicz, J.; Dudek, K.; Rawski, M.; Kieronczyk, B.; Jozefiak, A. Insect meal in fish nutrition. *Rev. Aquacult.* **2018**, *11*, 1080–1103. [CrossRef]
14. Bruni, L.; Pastorelli, R.; Viti, C.; Gasco, L.; Parisi, G. Characterisation of the intestinal microbial communities of rainbow trout (*Oncorhynchus mykiss*) fed with *Hermetia illucens* (black soldier fly) partially defatted larva meal as partial dietary protein source. *Aquaculture* **2018**, *487*, 56–63. [CrossRef]
15. Rimoldi, S.; Gini, E.; Iannini, F.; Gasco, L.; Terova, G. The effects of dietary insect meal from *Hermetia illucens* prepupae on autochthonous gut microbiota of rainbow trout (*Oncorhynchus mykiss*). *Animals* **2019**, *9*, 143. [CrossRef]
16. Terova, G.; Rimoldi, S.; Ascione, C.; Gini, E.; Ceccotti, C.; Gasco, L. Rainbow trout (*Oncorhynchus mykiss*) gut microbiota is modulated by insect meal from *Hermetia illucens* prepupae in the diet. *Rev. Fish Biol. Fish.* **2019**, *29*, 465–486. [CrossRef]
17. Mousavi, S.; Zahedinezhad, S.; Loh, J. A review on insect meals in aquaculture: The immunomodulatory and physiological effects. *Int. Aquat. Res.* **2020**, *12*, 100–115. [CrossRef]
18. St-Hilaire, S.; Cranfill, K.; Mcguire, M.A.; Mosley, E.E.; Tomberlin, J.K.; Newton, L.; Sealey, W.; Sheppard, C.; Irving, S. Fish offal recycling by the black soldier fly produces a foodstuff high in omega-3 fatty acids. *J. World Aquac. Soc.* **2007**, *38*, 309–313. [CrossRef]
19. Cebra, J.J. Influences of microbiota on intestinal immune system development. *Am. J. Clin. Nutr.* **1999**, *69*, 1046S–1051S. [CrossRef]
20. Pérez, T.; Balcazar, J.L.; Ruiz-Zarzuela, I.; Halaihel, N.; Vendrell, D.; de Blas, I.; Muzquiz, J.L. Host-microbiota interactions within the fish intestinal ecosystem. *Mucosal. Immunol.* **2010**, *3*, 355–360. [CrossRef]
21. Wang, A.R.; Ran, C.; Ringø, E.; Zhou, Z.G. Progress in fish gastrointestinal microbiota research. *Rev. Aquacult.* **2018**, *10*, 626–640. [CrossRef]
22. Kim, S.; Covington, A.; Pamer, E.G. The intestinal microbiota: Antibiotics, colonization resistance, and enteric pathogens. *Immunol. Rev.* **2017**, *279*, 90–105. [CrossRef]
23. Sakata, T. Microflora in the digestive tract of fish and shellfish, Microbiology in Poecilotherms. *Elsevier* **1990**, 171–176.
24. Estensoro, I.; Ballester-Lozano, G.; Benedito-Palos, L.; Grammes, F.; Martos-Sitcha, J.A.; Mydland, L.T.; Calduch-Giner, J.A.; Fuentes, J.; Karalazos, V.; Ortiz, A.; et al. Dietary Butyrate Helps to Restore the Intestinal Status of a Marine Teleost (*Sparus aurata*) Fed Extreme Diets Low in Fish Meal and Fish Oil. *PLoS ONE* **2016**, *11*, e0166564. [CrossRef]
25. Wu, S.; Wang, G.; Angert, E.R.; Wang, W.; Li, W.; Zou, H. Composition, diversity and origin of the bacterial community in grass carp intestine. *PLoS ONE* **2012**, *7*, e30440. [CrossRef]
26. *FEAP Report. FEAP European Aquaculture Report 2014–2019*; FEAP Secretariat: Brussels, Belgium, 2020.

27. Desai, A.R.; Links, M.; Collins, S.A.; Mansfield, G.S.; Drew, M.; Kessel, A.; Hill, J. Effects of plant-based diets on the distal gut microbiome of rainbow trout (*Oncorhynchus mykiss*). *Aquaculture* **2012**, *350*, 134–142. [CrossRef]
28. Rimoldi, S.; Terova, G.; Ascione, C.; Giannico, R.; Brambilla, F. Next generation sequencing for gut microbiome characterization in rainbow trout (*Oncorhynchus mykiss*) fed animal by-product meals as an alternative to fishmeal protein sources. *PLoS ONE* **2018**, *13*, e0193652. [CrossRef]
29. Chaklader, M.R.; Siddik, M.A.B.; Fotedar, R.; Howieson, J. Insect larvae, *Hermetia illucens* in poultry by-product meal for barramundi, *Lates calcarifer* modulates histomorphology, immunity and resistance to *Vibrio harveyi*. *Sci. Rep.* **2019**, *9*, 16703. [CrossRef]
30. Randazzo, B.; Zarantoniello, M.; Gioacchini, G.; Cardinaletti, G.; Belloni, A.; Giorgini, E.; Faccenda, F.; Cerri, R.; Tibaldi, E.; Olivotto, I. Physiological response of rainbow trout (*Oncorhynchus mykiss*) to graded levels of *Hermetia illucens* or poultry by-product meals as single or combined substitute ingredients to dietary plant proteins. *Aquaculture* **2021**, *538*, 736550. [CrossRef]
31. Gómez, G.D.; Balcázar, J.L. A review on the interactions between gut microbiota and innate immunity of fish. *FEMS Immunol Med. Microbiol.* **2008**, *52*, 145–154. [CrossRef]
32. Ringø, E.; Zhou, Z.; Vecino, J.; Wadsworth, S.; Romero, J.; Krogdahl, Å.; Olsen, R.; Dimitroglou, A.; Foey, A.; Davies, S.; et al. Effect of dietary components on the gut microbiota of aquatic animals. A never-ending story? *Aquacult. Nutr.* **2016**, *22*, 219–282. [CrossRef]
33. Alami-Durante, H.; Médale, F.; Cluzeaud, M.; Kaushik, S.J. Skeletal muscle growth dynamics and expression of related genes in white and red muscles of rainbow trout fed diets with graded levels of a mixture of plant protein sources as substitutes for fishmeal. *Aquaculture* **2010**, *303*, 50–58. [CrossRef]
34. Burr, G.S.; Wolters, W.R.; Barrows, F.T.; Hardy, R.W. Replacing fishmeal with blends of alternative proteins on growth performance of rainbow trout (*Oncorhynchus mykiss*), and early or late stage juvenile Atlantic salmon (*Salmo salar*). *Aquaculture* **2012**, *334–337*, 110–116. [CrossRef]
35. Renna, M.; Schiavone, A.; Gai, F.; Dabbou, S.; Lussiana, C.; Malfatto, V.; Prearo, M.; Capucchio, M.T.; Biasato, I.; De Marco, M.; et al. Evaluation of the suitability of a partially defatted black soldier fly (*Hermetia illucens* L.) larvae meal as ingredient for rainbow trout (*Oncorhynchus mykiss* Walbaum) diets. *J. Anim. Sci. Biotechnol.* **2017**, *8*, 57. [CrossRef]
36. Muddasir, J.; Imtiaz, A. Length weight relationship and condition factor of snow trout, *Schizothorax plagiostomus* (Heckel, 1838) from Lidder River, Kashmir. *Int. J. Fish Aquat. Stud.* **2016**, *4*, 131–136.
37. Le Boucher, R.; Quillet, E.; Vandeputte, M.; Lecalvez, J.M.; Goardon, L.; Chatain, B.; Médale, F.; Dupont-Nivet, M. Plant-based diet in rainbow trout (*Oncorhynchus mykiss* Walbaum): Are there genotype-diet interactions for main production traits when fish are fed marine vs. plant-based diets from the first meal? *Aquaculture* **2011**, *321*, 41–48, ISSN 0044-8486. [CrossRef]
38. Krogdahl, Å.; Penn, M.; Thorsen, J.; Refstie, S.; Bakke, A.M. Important antinutrients in plant feedstuffs for aquaculture: An update on recent findings regarding responses in salmonids. *Aquac. Res.* **2010**, *41*, 333–344. [CrossRef]
39. Hu, H.; Kortner, T.M.; Gajardo, K.; Chikwati, E.; Tinsley, J. Intestinal Fluid Permeability in Atlantic Salmon (*Salmo salar* L.) Is Affected by Dietary Protein Source. *PLoS ONE* **2016**, *11*, e0167515. [CrossRef]
40. Rimoldi, S.; Antonini, M.; Gasco, L.; Moroni, F.; Terova, G. Intestinal microbial communities of rainbow trout (*Oncorhynchus mykiss*) may be improved by feeding a *Hermetia illucens* meal/low-fishmeal diet. *Fish Physiol. Biochem.* **2021**. [CrossRef]
41. Parshukov, A.N.; Kashinskaya, E.N.; Simonov, E.P.; Hlunov, O.V.; Izvekova, G.I.; Andree, K.B.; Solovyev, M.M. Variations of the intestinal gut microbiota of farmed rainbow trout, *Oncorhynchus mykiss* (Walbaum), depending on the infection status of the fish. *J. Appl. Microbiol.* **2019**, *127*, 379–395. [CrossRef]
42. Li, Y.; Bruni, L.; Jaramillo-Torres, A.; Gajardo, K.; Kortner, T.M.; Krogdahl, Å. Differential Response of Digesta- and Mucosa-Associated Intestinal Microbiota to Dietary Black Soldier Fly (*Hermetia illucens*) Larvae Meal in Seawater Phase Atlantic Salmon (*Salmo salar*). *Anim. Microbiome* **2021**, *3*, 8. [CrossRef]
43. Beier, S.; Bertilsson, S. Bacterial chitin degradation-mechanisms and ecophysiological strategies. *Front. Microbiol.* **2013**, *4*, 149. [CrossRef] [PubMed]
44. Ng, W.K.; Koh, C.B. The utilization and mode of action of organic acids in the feeds of cultured aquatic animals. *Rev Aquacult.* **2017**, *9*, 342–368. [CrossRef]
45. Oushani, A.K.; Soltani, M.; Sheikhzadeh, N.; Mehrgan, M.S.; Islami, H.R. Effects of dietary chitosan and nano-chitosan loaded clinoptilolite on growth and immune responses of rainbow trout (*Oncorhynchus mykiss*). *Fish Shellfish. Immunol.* **2020**, *98*, 210–217, ISSN 1050-4648. [CrossRef]
46. Nawaz, A.; Javaid, A.B.; Irshad, S.; Hoseinifar, S.H.; Xionga, H. The functionality of prebiotics as immunostimulant: Evidences from trials on terrestrial and aquatic animals. *Fish Shellfish. Immunol.* **2018**, *76*, 272–278. [CrossRef]
47. Zhou, Z.; Karlsen, Ø.; He, S.; Olsen, R.E.; Yao, B.; Ringø, E. The effect of dietary chitin on the autochthonous gut bacteria of Atlantic cod (*Gadus morhua* L.). *Aquac. Res.* **2013**, *44*, 1889–1900. [CrossRef]
48. Esteban, M.A.; Cuesta, A.; Ortuño, J.; Meseguer, J. Immunomodulatory effects of dietary intake of chitin on gilthead seabream (*Sparus aurata* L.) innate immune system. *Fish Shellfish. Immunol.* **2001**, *11*, 303–315. [CrossRef] [PubMed]
49. Casadidio, C.; Peregrina, D.V.; Gigliobianco, M.R.; Deng, S.; Censi, R.; Di Martino, P. Chitin and Chitosans: Characteristics, Eco-Friendly Processes, and Applications in Cosmetic Science. *Mar. Drugs* **2019**, *17*, 369. [CrossRef]

50. Gonçalves, A.T.; Gallardo-Escarate, C. Microbiome dynamic modulation through functional diets based on pre- and probiotics (mannan-oligosaccharides and *Saccharomyces cerevisiae*) in juvenile rainbow trout (*Oncorhynchus mykiss*). *J. Appl. Microbiol.* **2017**, *122*, 1333–1347. [CrossRef]
51. Lyons, P.P.; Turnbull, J.F.; Dawson, K.A.; Crumlish, M. Effects of low-level dietary microalgae supplementation on the distal intestinal microbiome of farmed rainbow trout *Oncorhynchus mykiss* (Walbaum). *Aquac. Res.* **2017**, *48*, 2438–2452. [CrossRef]
52. Pollack, J.D.; Williams, M.V.; McElhaney, R.N. The comparative metabolism of the mollicutes (Mycoplasmas): The utility for taxonomic classification and the relationship of putative gene annotation and phylogeny to enzymatic function in the smallest free-living cells. *Crit. Rev. Microbiol.* **1997**, *23*, 269–354. [CrossRef]
53. Brown, R.M.; Wiens, G.D.; Salinas, I. Analysis of the gut and gill microbiome of resistant and susceptible lines of rainbow trout (*Oncorhynchus mykiss*). *Fish Shellfish. Immunol.* **2019**, *86*, 497–506, ISSN 1050-4648. [CrossRef]
54. Lacombe-Harvey, M.È.; Brzezinski, R.; Beaulieu, C. Chitinolytic functions in actinobacteria: Ecology, enzymes, and evolution. *Appl. Microbiol. Biotechnol.* **2018**, *102*, 7219–7230. [CrossRef]
55. Kim, D.H.; Brunt, J.; Austin, B. Microbial diversity of intestinal contents and mucus in rainbow trout (*Oncorhynchus mykiss*). *J. Appl. Microbiol.* **2007**, *102*, 1654–1664. [CrossRef]
56. Tarnecki, A.M.; Wafapoor, M.; Phillips, R.N. Benefits of a *Bacillus* probiotic to larval fish survival and transport stress resistance. *Sci. Rep.* **2019**, *9*, 4892. [CrossRef]
57. Veliz, E.A.; Martínez-Hidalgo, P.; Hirsch, A.M. Chitinase-producing bacteria and their role in biocontrol. *AIMS microbiology* **2017**, *3*, 689–705. [CrossRef]
58. Parris, D.J.; Morgan, M.M.; Stewart, F.J. Feeding rapidly alters microbiome composition and gene transcription in the clownfish gut. *Appl. Environ. Microbiol.* **2019**, *23*, 85. [CrossRef]
59. Jin, X.; Chen, Z.; Shi, Y.; Gui, J.F.; Zhao, Z. Response of gut microbiota to feed-borne bacteria depends on fish growth rate: A snapshot survey of farmed juvenile *Takifugu Obscurus*. *Microb. Biotechnol.* 2021. [CrossRef] [PubMed]
60. Pomaranski, E.K.; Griffin, M.J.; Camus, A.C.; Armwood, A.R.; Shelley, J.; Waldbieser, G.C.; LaFrentz, B.R.; García, J.C.; Yanong, R.; Soto, E. Description of *Erysipelothrix piscisicarius* sp. nov., an emergent fish pathogen, and assessment of virulence using a tiger barb (*Puntigrus tetrazona*) infection model. *Int. J. Syst. Evol. Microbiol.* **2020**, *70*, 857–867. [CrossRef]
61. Hartviksen, M.; Vecino, J.L.G.; Ringo, E.; Bakke, A.M.; Wadsworth, S.; Krogdahl, A.; Ruohonen, K.; Kettunen, A. Alternative dietary protein sources for Atlantic salmon (*Salmo salar* L.) effect on intestinal microbiota, intestinal and liver histology and growth. *Aquac. Nutr.* **2014**, *20*, 381–398. [CrossRef]
62. Amaretti, A.; Gozzoli, C.; Simone, M.; Raimondi, S.; Righini, L.; Pérez-Brocal, V.; García-López, R.; Moya, A.; Rossi, M. Profiling of Protein Degraders in Cultures of Human Gut Microbiota. *Front Microbiol.* **2019**, *10*, 2614. [CrossRef]
63. Chapagain, P.; Arivett, B.; Cleveland, B.M.; Walker, D.M.; Salem, M. Analysis of the fecal microbiota of fast- and slow-growing rainbow trout (*Oncorhynchus mykiss*). *BMC Genom.* **2019**, *20*, 788. [CrossRef]
64. Sigh, J.; Lindenstrøm, T.; Buchmann, K. Expression of pro-inflammatory cytokines in rainbow trout (*Oncorhynchus mykiss*) during an infection with *Ichthyophthirius multifiliis*. *Fish Shellfish. Immunol.* **2004**, *17*, 75–86. [CrossRef] [PubMed]
65. Secombes, C.J.; Wang, T.; Hong, S.; Peddie, S.; Crampe, M.; Laing, K. Cytokines and innate immunity of fish. *Dev. Comp. Immunol.* **2001**, *25*, 713–723. [CrossRef]
66. Low, C.; Wadsworth, S.; Burrells, C.; Secombes, C.J. Expression of immune genes in turbot (*Scophthalmus maximus*) fed a nucleotide-supplemented diet. *Aquaculture* **2003**, *221*, 23–40. [CrossRef]
67. Wang, X.; Lupardus, P.; Laporte, S.L.; Garcia, K.C. Structural biology of shared cytokine receptors. *Annu. Rev. Immunol.* **2009**, *27*, 29–60. [CrossRef]
68. Harun, N.O.; Costa, M.M.; Secombes, C.J.; Wang, T. Sequencing of a second interleukin-10 gene in rainbow trout *Oncorhynchus mykiss* and comparative investigation of the expression and modulation of the paralogues in vitro and in vivo. *Fish Shellfish. Immunol.* **2011**, *31*, 107–117, ISSN 1050-4648. [CrossRef]
69. Heinecke, R.D.; Buchmann, K. Inflammatory response of rainbow trout *Oncorhynchus mykiss* (Walbaum, 1792) larvae against *Ichthyophthirius multifiliis*. *Fish Shellfish. Immunol.* **2013**, *34*, 521–528. [CrossRef]
70. Ghosh, S.S.; Wang, J.; Yannie, P.J.; Ghosh, S. Intestinal Barrier Dysfunction, LPS Translocation, and Disease Development. *J. Endocr. Soc.* **2020**, *4*, bvz039. [CrossRef]
71. Klindworth, A.; Pruesse, E.; Schweer, T.; Peplies, J.; Quast, C.; Horn, M.; Glockner, F.O. Evaluation of general 16S ribosomal RNA gene PCR primers for classical and next-generation sequencing-based diversity studies. *Nucleic Acids Res.* **2013**, *41*, e1. [CrossRef]
72. Bolyen, E.; Rideout, J.R.; Dillon, M.R.; Bokulich, N.A.; Abnet, C.C.; Al-Ghalith, G.A.; Alexander, H.; Alm, E.J.; Arumugam, M.; Asnicar, F.; et al. Reproducible, interactive, scalable and extensible microbiome data science using QIIME 2. *Nat. Biotechnol.* **2019**, *37*, 852–857. [CrossRef]
73. De Santis, T.Z.; Hugenholtz, P.; Larsen, N.; Rojas, M.; Brodie, E.L.; Keller, K.; Huber, T.; Dalevi, D.; Hu, P.; Andersen, G.L. Greengenes, a Chimera-Checked 16S rRNA Gene Database and Workbench Compatible with ARB. *Appl. Environ. Microbiol.* **2006**, *72*, 5069–5072. [CrossRef]
74. McMurdie, P.J.; Holmes, S. phyloseq: An R Package for Reproducible Interactive Analysis and Graphics of Microbiome Census Data. *PLoS ONE* **2013**, *8*, e61217. [CrossRef]

75. Tacchi, L.; Lowrey, L.; Musharrafieh, R.; Crossey, K.; Larragoite, E.T.; Salinas, I. Effects of transportation stress and addition of salt to transport water on the skin mucosal homeostasis of rainbow trout (*Oncorhynchus mykiss*). *Aquaculture* **2015**, *435*, 120–127, ISSN 0044-8486. [CrossRef]
76. Inoue, Y.; Kamota, S.; Ito, K.; Yoshiura, Y.; Ototake, M.; Moritomo, T.; Nakanishi, T. Molecular cloning and expression analysis of rainbow trout (*Oncorhynchus mykiss*) interleukin-10 cDNAs. *Fish Shellfish. Immunol.* **2005**, *18*, 335–344. [CrossRef]
77. Zou, J.; Neuman, N.; Holland, J.; Belosevic, M.; Cunningham, C.; Secombes, C.J.; Rowley, A.F. Fish macrophages express a cyclooxygenase-2 homologue following activation. *Biochem. J.* **1999**, *340*, 153–159. [CrossRef] [PubMed]
78. Kim, D.H.; Austin, B. Cytokine expression in leukocytes and gut cells of rainbow trout, *Oncorhynchus mykiss* Walbaum, induced by probiotics. *Vet. Immunol. Immunopathol.* **2006**, *114*, 297–304. [CrossRef]
79. Henriksen, M.M.M.; Kania, P.W.; Buchmann, K.; Dalsgaard, I. Effect of hydrogen peroxide and/or *Flavobacterium psychrophilum* on the gills of rainbow trout, *Oncorhynchus mykiss* (Walbaum). *J. Fish Dis.* **2014**, *38*, 259–270. [CrossRef]
80. Zhang, Z.; Swain, T.; Bøgwald, J.; Dalmo, R.A.; Kumari, J. Bath immunostimulation of rainbow trout (*Oncorhynchus mykiss*) fry induces enhancement of inflammatory cytokine transcripts, while repeated bath induce no changes. *Fish Shellfish. Immunol.* **2009**, *26*, 677–684. [CrossRef]
81. Oksanen, J.; Blanchet, F.G.; Friendly, M.; Kindt, R.; Legendre, P.; McGlinn, D.; Minchin, P.R.; O'Hara, R.B.; Simpson, G.L.; Solymos, P.; et al. Vegan: Community Ecology Package. R package version 2.5–2.6. 2019. Available online: https://CRAN.R-project.org/package=vegan (accessed on 13 July 2020).

General discussion

Providing a definition for a healthy reference diet is a pressing challenge. With dramatic coexistence of undernutrition along with overweight and obesity, together with the global burden of diet-related non-communicable diseases predicted to increase and global food production still representing one of the largest environmental pressures caused by humans on the planet (1–4), it is now becoming increasingly evident that unhealthy and unsustainably-produced food endangers both people and the stability of Earths ecological system (5). In 2017, the Global Burden of Disease Collaborators provided that the shift from current dietary habits to a healthier balanced diet, rich in plant-based foods and low in red meat, would likely reduce adult deaths per year by 22.4% (6). Two years later, the EAT-Lancet Commission summarized existing evidence describing healthy diets, providing quantitative targets to define a healthy and sustainable reference diet (5). According to EAT-Lancet guidelines, a healthy diet should mainly consist of vegetables and fruits, whole grains, nuts, legumes and unsaturated oils, moderate fish and dairy, together with low quantity of highly processed foods, simple sugars, red meat and starchy vegetables (5). In the search for a sustainable and healthy food system, one potential emerging modulator of food production and human health is the food chain microbiome, a complex network of microbial communities and their genomes colonizing soil, food and also the human gastrointestinal tract (7). In this thesis, we adopted an interdisciplinary approach, employing both *in vitro* and *in vivo* animal models to understand how sustainable, health-promoting and nutritious foods and diets could be achieved by exploiting and modulating the food chain microbiome, focusing on gut microbiomes.

Our modern Western-style diet (MWD) lacks in fresh and plant-based foods, while it is enriched in simple sugars and saturated fats as well as high intakes of red meat and salt (8,9). Moreover, MWD often includes highly processed foods, whose consumption has risen sharply over the last decades because of their relatively low cost and availability across retailers (10). Compared to the healthy reference diet (5), MWD is related to higher incidence of metabolic and inflammatory diseases (9,11). Moreover, the lack of fiber and the high content of high- and ultra-processed ingredients both negatively impact on gut health, dysregulating intestinal barrier function and gut microbiota (GM) composition and function and contributing to inflammation both within the gut and at other body sites (12). Since microbial metabolism relies on the availability of dietary substrates in the colon, GM has been proposed as a mediator through which foods and nutrients can exert their

pro- or anti-inflammatory effects (13). Changes to the gut intestinal mucosal equilibrium with increased intestinal permeability in response to MWD and reduced intestinal concentrations of short chain fatty acids (SCFA) from fiber fermentation typically corresponds with an altered gut microbial environment and has been proposed as a pathological feature of obesity, metabolic syndrome, type 2 diabetes and dementia (13). On the contrary, high consumption of vegetable foods exert a positive effect on gut health, thanks to microbial fermentation of complex undigested polysaccharides releasing biologically active SCFA and plant phytochemicals biotransformation releasing biologically available and biologically active smaller phenolic acids (14,15). These microbially produced metabolites have been shown to reduce intestinal inflammation and induce expression of tight junction proteins between mucosal epithelial cells, increasing intestinal integrity and also to induce production of mucins, which serve to improve the intestinal barrier and promote the growth of commensal microorganisms, including *Akkermansia muciniphila*, a microorganism depleted within the obese type microbiota.

Studying the effects of both beneficial and detrimental foods on gut microbiota populations could be a useful tool in investigating the underlying mechanisms of how diet:microbe interactions may determine host metabolic health and risk of inflammatory diseases. For this reason, the first part of my PhD was dedicated to investigating how specific foods could modulate host metabolic health and inflammatory status through GM metabolism. Advanced glycation end-products (AGE) represent an example of pro-inflammatory compounds present at significant concentrations in highly processed modern foods. Given that dietary AGE have been implicated in the development of metabolic inflammation and since it has been estimated that a consistent fraction of unabsorbed dietary AGE may reach the colon (16), I decided to assess whether AGE exerted some of their effects by negatively modulating the gut microbiota. AGE have been previously shown to alter colonic microbiota composition *in vitro*, promoting the growth of sulphate-reducing bacteria clostridia and Bacteroidetes and decreasing putatively beneficial lactobacilli and bifidobacteria (17). Thus, the effects of an AGE-enriched diet were investigated in mice identifying a possible role for microbial populations in determining some of the AGE-related metabolic and inflammatory imbalances (**Chapter 2**). We demonstrated that a single AGE-enrichment in diet was sufficient to induce significant shifts in GM composition, resulting in a microbiota community structure similar to that previously observed in diabetic and obese mice. Specifically, mice fed the AGE enriched diet (AGE-D) had lower relative abundance of murine commensal and SCFA-producing bacteria such as S24-

7, *Candidatus Arthromitus* and *Anaerostipes* together with increased abundance of microbial taxa typically associated to high-fat or diabetogenic diets in mice, including *Parabacteroides*, *Ruminococcus* (within Lachnospiraceae family) and *Oscillospira*. We also demonstrated that GM profile of AGE-D mice correlated with impaired systemic measures of metabolic/cardiovascular disease markers, including plasma IL-1β, IL-17 and PAI-1 levels and negatively correlated to circulating incretins GIP and GLP-1. GIP and GLP-1 are protective against metabolic disease in laboratory animals and in humans. In AGE-D mice, the increase in blood concentrations of pro-inflammatory cytokines IL-1β and IL-17, and of PAI-1, a key regulator of vascular remodeling involved in various thrombotic diseases, highlighted the role of dietary AGE in inducing inflammation and vascular integrity impairment. Moreover, the reduction in incretins levels following AGE-D linked dietary AGE with the development of metabolic disorders, since both GIP and GLP-1 are the two primary gut hormones involved in the modulation of glucose metabolism (18). These results suggest that a modern AGE-enriched diet, even if isocaloric, could induce detrimental changes in the host inflammatory state and metabolism. Our findings support recent evidence describing the deleterious effects of high- and ultra-processed food consumption on waist circumference and risk of chronic diseases in both animal and human studies (19–21), thus highlighting the importance of limiting their consumption whatever dietary habits are followed. Moreover, we provide new findings linking diet, inflammation and gut microbiota, demonstrating that some of the physiological effects of dietary AGE chronic exposure can be mediated by reshaping GM community structure.

Diet-GM interactions are also suspected to be involved in some of the health associations of whole plant foods. Vegetable foods represent a key element of the healthy reference diet. There is considerable evidence supporting the association between regular fruit and vegetable consumption to reduced risk of CVD disease, obesity and all-cause mortality (22–25). The gut microbiota plays a major role in the metabolism of whole plant foods. The GM uses complex dietary fibers as their main carbon and energy source through fermentation, and metabolize other phytochemicals generating a range of bioactive compounds, such as SCFA, small phenolic acids and isothiocyanates (26). *Brassicaceae* is a plant family of particular interest because of its high content of glucosinolates and polyphenols, both considered to possess anti-cancer and anti-inflammatory properties (27). Up to 90% of these phytochemicals is not digested nor absorbed in the small intestine, and thus reach the colon where they are biotransformed by GM in their bioavailable and bioactive moieties (28–31).

After highlighting the effects that an unhealthy AGE-enriched diet had on host metabolism, inflammation and GM in mice **(Chapter 2),** I aimed to investigate whether and to what extent a regional *Brassica* vegetable could modulate the gut microbiota, its metabolic output and potential to influence gut health (**Chapter 3**). I selected Broccolo of Torbole (*Brassica oleracea* var. *botrytis*), an original broccoli ecotype from Trentino and investigated its impact on gut health using a combination of *in vitro* anaerobic fecal fermentation, metabolomic analysis and *in vitro* model of intestinal permeability. Data from the *in vitro* fermentation batch culture model showed that both Broccolo of Torbole (BR) and inulin (IN), used as a readily fermentable fiber and prebiotic, significantly affected bacterial evenness and richness across the 24 hours fermentation. Fiber is known to be beneficial for gut health, particularly leading to the production of SCFA (acetate, propionate and butyrate) upon fermentation by the gut microbiota (32), as confirmed by GC-MS/MS analysis, since BR and IN faecal supernatants had the highest concentrations of total SCFA when compared to blank (no substrate) and to methylcellulose (CL), a poorly fermentable fiber used as negative control in our *in vitro* colonic fermentation model. Different fibers can be distinguished based on their degree of polymerization, monomeric unit composition and the type/strength of bonds between monomers which shapes the physicochemical properties of fiber itself and the extent of its fermentation by the GM (33). This explains why different fermentable materials, BR, IN and CL, may have selected for specific taxa capable of using available nutrients as growth substrates, thus prevailing over those species that were unable to use BR, CL or IN as energy or carbon sources, and thus explaining the observed reduction in bacterial richness and evenness at the end of the fermentation. In this work, I demonstrated that Broccolo of Torbole *in vitro* faecal fermentation affects the composition of human GM, by modulating the growth of specific taxa. Specifically, bacterial genera previously shown to be decreased by dietary polyphenols or fiber, including *Alistipes* and *Ruminococcus 1* had significantly lower relative abundance after 24 hours of BR fermentation, while *Escherichia-Shigella*, recently associated with high-fiber and high-glucosinolates environment (33,34), significantly increased over the fermentation process. The increased abundance of *Escherichia-Shigella* might not necessarily be seen as a beneficial modulation of the GM by BR, since this genus includes many potential pathogens (35). However, *Escherichia-Shigella* also comprises common intestinal commensal strains, including the probiotic *Escherichia coli* Nissle 1917 (36) and 16S rRNA metagenomic analysis at genus level is not sufficient to tell the difference between pathogenic, commensal or health promoting/probiotic strains of any bacterial species. Moreover,

targeted LC-MS/MS analysis on BR supernatants confirmed that GM plays a key role in the metabolism of *Brassica* phytochemicals as previously suggested (37,38). In particular, polyphenolic compounds commonly found in *Brassica* crops as defense or pigmentation molecules, including caffeic acid, ferulic acid, sinapic acid and quercetin 3-4'-diglucoside decreased over time during fermentation, confirming the role of GM in their breakdown. I also performed a Spearman's correlation analysis to understand which taxa might have mediated BR phytochemical biotransformation, finding that certain compounds increased together with the increase of certain microbes and vice versa. *Prevotella, Lactobacillus, Streptococcus, Negativibacillus, Acidaminococcus, Dialister, Allisonella, Megasphaera, Parasutterella* and *Akkermansia* showed a strong positive correlation with syringaldehyde, syringic acid and chlorogenic acid, and a strong negative correlation with 4-aminobenzoic acid. On the other hand, *Roseburia, Veillonella, Turicibacter, Olsenella,* different genera belonging to Lachnospiraceae, Ruminococcaceae and Erysipelotrichaceae Family were positively correlated with 4-aminobenzoic acid while showed a strong negative correlation with syringaldehyde, syringic acid, chlorogenic acid and cryptochlorogenic acid. Due to small significant changes observed in both GM composition and in target glucosinolates and polyphenols concentrations over 24 hours of BR fermentation, it was difficult to link GM and metabolites into a clear metabolic pathway. However, to our knowledge this is one of the few works employing *in vitro* anaerobic faecal fermentation techniques, coupled to metagenomic and metabolomic analysis to investigate the role of *Brassica* in modulating human gut microbiota composition and metabolism. We suggested that the lack of statistical significance may be related to GM variation among faecal donors, and this is why further *in vitro* analysis involving higher numbers of faecal donors is warranted to further explore the correlation between GM, their metabolites and *Brassica*-related benefits.

The intestinal epithelium plays a crucial role in the absorption of nutrients and bioactive compounds deriving from microbial metabolism. The intestinal epithelial cells, together with the sourronding mucus layer and the mucosal immune system, constitute a physical barrier which protects against uncontrolled bacterial translocation through the epithelial mucosa to blood stream (39). Alterations of the gut barrier integrity lead to augmented gut permeability (i.e. 'leaky gut') with a concomitant absorption of bacterial lipopolysaccharide A (LPS), a component of outer membrane in gram-negative bacteria known to promote local or systemic inflammation, including the chronic low-grade systemic inflammation characteristic of obesity and related diseases (40,41). Dietary SCFA

and metabolites deriving from microbial breakdown of plant phytochemicals have a key role in protecting gut barrier function by supporting the growth of colonocyte, reducing inflammation and by upregulating tight-junctions proteins supporting the integrity of the epithelial layer (42,43). Trans epithelial electric resistance (TEER) measurement is a reference technique used to measure gut barrier integrity in cell culture models of epithelial monolayers. For this reason, I employed TEER measurement to assess the role of BR microbial metabolites in modulating gut permeability, using an *in vitro* model of intestinal epithelium formed by human colorectal adenocarcinoma cells (Caco-2). 24 h incubation of BR faecal supernatants on Caco-2 monolayers did not improve nor decrease trans-epithelial electric resistance (TEER), thus suggesting mechanism other than barrier strengthening may be involved in the anti-inflammatory effects of *Brassica*.

After highlighting the effects of a local variety of broccoli on GM structure and activity, I conducted an investigation on *Moringa oleifera*, an innovative crop with great potential for both human health and as an environmentally friendly, high value new crop suitable for improving the resilience of the local production chain to the effects of climate change (**Chapter 4**). In recent years, *Moringa oleifera* has attracted increasing attention because of its high nutritional value (44,45). Moringa leaves are a rich source of vitamins, minerals and highly digestible proteins (44), which render this plant a potential functional food to be used as dietary supplement to improve nutritional status of malnourished children (46), as a source of nutraceutical ingredients or extracts, and as an alternative protein source for animal feeds (47,48). Several commercial varieties of Moringa can be grown on marginal and degraded lands, with high temperatures (it can survive up to 48°C for a limited period of time) and low water availability (49). For these reasons, Moringa could be considered a new potential multipurpose, nutritious and sustainable crop, with particular resilience to the local effects of climate change in Italy. Moreover, *Moringa oleifera* is still under studied for its potential benefits for human health (50–53). Preliminary observations in pre-clinical models show that anti-cancer, anti-inflammatory and antioxidant properties of this plant might be attributed to its content in bioactive phytochemicals, including polyphenols and glucosinolates (GLS) (54,55). Due to the crucial role of human gut microbiota (GM) in breaking down plant phytochemicals into their bioactive forms, we investigated the role of the human GM in metabolizing polyphenols and GLS in Moringa, examining which bacterial taxa might be involved in these biotransformations. I employed *in vitro* anaerobic faecal fermentation to determine the ability of human faecal bacteria to breakdown Moringa phytochemicals, using as fermentation substrates an *in vitro*-digested *Moringa oleifera* leaf

powder (MOR) or glucomoringin (GMG), the main GLS in Moringa. Targeted Liquid Chromatography Triple Quadrupole Mass Spectrometry (LC-MS/MS) revealed a significant decrease in glucomoringin concentrations after 2 hours of fermentation in GMG samples, accompanied by a parallel increase over time in moringin, the most frequent isothiocyanate produced by glucomoringin metabolism (56). To our knowledge, this is the one of the few studies evaluating the impact of human GM in breaking down Moringa metabolites using an *in vitro* model of colonic fermentation. Hence, this work provides new insights about the fate of glucomoringin in the human intestine, highlighting the role of GM in mediating its biotransformation to moringin. Illumina 16S rRNA gene sequencing revealed the uniqueness of the GM of each faecal donor (supporting what previously observed in **Chapter 3**), both in terms of richness and composition. These differences underpinned the great variability in the metabolism of target polyphenols and GLS, thus suggesting a personalized response to Moringa metabolites, as highlighted by Spearman's correlation analysis. Among glucosinolates, glucobrassicanapin variation between 5 and 8 hours of fermentation showed strong negative correlation with *Blautia* genus, while moringin concentrations were inversely correlated to *Alistipes*, *Eubacterium hallii* and *Coprococcus 3* within the same timepoints. These are the first results correlating changes in Moringa phytochemicals during *in vitro* colonic fermentation to specific bacterial taxa. Due to recent observations highlighting the effect of Moringa extract in improving symptoms of ulcerative colitis by improving barrier function in mouse models, we also decided to assess whether MOR or GMG fermentation supernatants improved gut epithelial barrier integrity, using *in vitro* trans-epithelial electric resistance (TEER) model with Caco-2 monolayers. While no significant TEER improvement was observed after incubation of Caco-2 monolayers with MOR supernatant, while GMG supernatants significantly increased TEER, thus suggesting the role of glucomoringin GLS or of the derived glucotropaeolin and sinalbin in stimulating gut barrier function and reducing gut permeability and undue inflammation. Our results provide novel insight into the fate of target Moringa phytochemicals during faecal microbial fermentation and on their potential beneficial activity on gut health. In order to better explore the great potential of this plant, human dietary intervention trials investigating the role of GM in mediating anti-inflammatory role of Moringa are needed, including an appropriate sample size as well as a well-defined target population to reduce the variation. In order to assess whether Moringa consumption could reduce both local and systemic inflammation, subjects affected by chronic low-grade inflammation should be in the subject of future *in vivo* investigations.

After having investigated the role of GM in driving some of beneficial or detrimental effects related to specific dietary habits or foods, I aimed to investigate the role of microbial communities in healthy and sustainable food production. Food fermentation has long been used to store foods and beverages for long periods, enhancing their taste, safety and nutritional properties (57). In **Chapter 5** I described an in-depth and multi-disciplinary analysis of artisanal, locally produced sauerkraut, from two organic producers (SK1 and SK2). Using both culture-based and culture-independent methods, I demonstrated how sauerkraut-associated microbiome developed over the course of the fermentation, being shaped by salinity, temperature and increasing acidity. We confirmed the role of lactic acid bacteria (LAB) *Lactobacillus*, *Leuconostoc*, *Pediococcus* and other genera belonging to *Lactobacillaceae* family as the main microrganisms responsible for the fermentation process, as previously described (58,59). In our experiment, the ability of LAB to convert fermentable carbohydrates and proteins into a wide range of metabolites was measured by an NMR based metabolomics analysis, which gave us high-throughput and highly-reproducible measurements of microbial metabolites produced in sauerkraut during fermentation and in the final sauerkraut water used to investigate the ability of sauerkraut to improve gut health. We observed that the fermentation process significantly increased the levels of aromatic amino acids and of organic acids, all responsible for the particular taste and flavor of sauerkraut compared to the fresh non fermented cabbage. Besides increasing the organoleptic quality of the fermented food product, the organic acids were found at significantly higher levels after 35 days of fermentation, comprising mainly acetic acid (SK1: 1923.64 ± 298.16 mg/L; SK2: 2340.99 ± 297.64 mg/L; mean ± SD) and lactic acid (SK1: 9418.22 ± 953.14 mg/L; SK2: 6121.66 ± 3554.43 mg/L). These organis acids have long been studied for their potential beneficial properties on gut health. In particular, *in vitro* and animal studies demonstrated that both acetic and lactic acid could stimulate enterocyte proliferation and suppress secretion of inflammatory mediators (43,60,61). Using two different precininal models of gut health, measurement of TEER upon sauekraut challenge in monolayers of Caco-2 cells as a model of intestinal permeability, and cytokine production from co-cultured Caco-2 and peripheral blood mononuclear cells (PBMCs) stimulated with LPS, we examined whether SK water could improve intestinal barrier function and regulate the inflammatory response. Potential anti-inflammatory and anti-cancer effects of sauerkraut consumption have been investigated *in vitro* (62–64) and a limited number of human dietary intervention studies have started to explore the role of sauerkraut in ameliorating irritable bowel syndrome (IBS) severity score (65). However, this is the first study

evaluating the effects of sauerkraut water on gut barrier function. I demonstrated that sauerkraut water did not improve intestinal barrier function, according to TEER measurements, but we could also conclude that it did not cause intestinal permeability, since TEER values after 24 hours incubation were significantly higher in both SK1 and SK2 when compared to ethanol, the control used to induce intestinal permeability. Moreover, although in our experiment sauerkraut water did not improve gut barrier function, it appeared to improve immune response to inflammatory challenge in our *in vitro* model of the gut associated lymphoid tissue (GALT). In particular, cytokine quantification in basolateral supernatants after 24 hours incubation with sauerkraut water revealed a significant increase in pro-inflammatory cytokines IL-6 and TNF-α, typically released by GALT cells during LPS stimulation (66–68), together with an increase in the anti-inflammatory interleukin IL-10, a crucial mediator involved in resolving inflammation after an inflammatory trigger (69). These findings indicated the potential immunomodulatory activity of sauerkraut juice, supporting an improved immune response to LPS stimulus by increasing IL-6 and TNF-α mediators, and at the same time promoting the resolution or switching off of inflammation and the re-establishment of normal inflammatory status through IL-10 production. The capacity of sauerkraut water to modulate immune function may be driven by its high concentration in acetic acid and lactic acid**,** known ligands of G-protein coupled receptors (GPCRs), GPR-43 and GPR-41 for acetate and GPR-81 for lactate (70), all involved in the activation of signaling pathways which lead to the secretion of both pro- and anti-inflammatory factors (43,61). These results have to be confirmed in human intervention studies, but they provide new insights on how certain fermented foods could improve human health at the population level. Fermented foods represent an example of how microbiomes and their metabolic end-products contribute to high-quality nutrition, safety and flavors in our diet, thus representing a key element in the food chain sustainability and nutritional value (57). Future studies should investigate to what extent the health beneficial properties of these foods can be attributed to the microbial communities they host, since fermented food consumption has parallels with the 'One Health concept', linking humans, environment, foods and microbiota which modifies nutritional and physicochemical characteristics of fermented foods as well as our health.

Together with high intake of fruit and vegetables, the healthy and sustainable reference diet should include 2 portions per week of fish (5). Fish is rich in omega-3 fatty acids, proteins and micronutrients which make this food of particular interest from a nutritional point of view (71). The global demand for fish and seafood increased by 122% from 1990 to 2018, and is projected to double

by 2050 due to the dramatic increase in the worlds population (1). However, captured wild fish is no longer able to support fish demands due to excessive exploitation and potential collapse of wild fish stocks (1). For this reason, future supply of fish should be provided by aquaculture. Since feeds for aqua-cultured species have historically relied upon the use of fish meal from wild fisheries, we investigated the use of more sustainable ingredients to improve health and yield of rainbow trout (*Oncorhynchus mykiss*), their impact on the fish GM, links between gut microbiota modulation and fish immune function (**Chapter 6**). Our results were encouraging regarding the possible use of waste products from the poultry industry and insect meal to replace fish meal, which is no longer sustainable. In fact, when compared to vegetable proteins (CV), to date the most studied alternative but also the least advantageous from a fish health (productivity) and environmental point of view, our test ingredients proved to be more performing. In particular, I demonstrated that a combination of poultry by-products and insect meal induced better growth performance in animals compared to trout fed CV diet. Nutrient absorption, immune function and inflammatory state strongly depend on gut health and on the composition of the resident GM (72). Here, I employed 16S rRNA Illumina sequencing to analyze both fish gut microbiota and the microbial composition of the fish feeds. Trout gut microbiota community was strongly influenced by diet composition and CV fed animals showed the lowest richness in terms of bacterial α-diversity. Since CV fed animals also showed the lowest growth performances, while increasing percentages of *Hermetia* meal in the diet increased both bacterial α-diversity and growth parameters, we suggested that certain dietary ingredients and especially chitin, may act as prebiotics increasing gut bacterial richness and biodiversity and possibly stimulating nutrient utilization and fish overall health. This was also supported by differences in GM composition observed in animals fed diet enriched in *Hermetia illucens* (H) or in poultry-by products (P). In particular, fish fed H diets had higher relative abundance of chitin-degraders *Actinomyces* and *Bacillus*. This study also provides new observations regarding feed-chain microbiome transmission, since *Actinomyces* was also found in H feed, with significantly higher relative abundance than in the other feeds used for this investigation. On the other hand, P increased the relative abundance of protein-degraders *Paeniclostridium* and Bacteroidales. In summary, these data support the hypothesis that alterations in gut microbial ecosystems or bacterial richness could be reliable indicators of gut health and, in turn, in this case, of fish growth (73,74). Moreover, characterizing the microbiota of the different fish feeds revealed some analogies between trout GM and feed microbial composition, thus supporting the idea that some bacteria, such as *Actinomyces*

may transit from feed to gut. Our study provides new insights connecting food chain microbiomes to fish production, confirming the potential of both fish and feed microbiomes to improve production yields, animal welfare and nutritional quality of farmed fish.

To conclude, this PhD thesis demonstrates how the exploitation of food chain microbiomes and in particular the gut microbiomes of both humans and production animals could have a great potential in improving the environmental sustainability of food production chains and for improving human (and animal) nutrition related welfare. The analysis of gut microbiomes could represent an innovative strategy to define a healthy reference modern diet, to characterize potential beneficial effects of local and traditionally consumed foods, to investigate new sustainable and nutritious crops and to drive the urgently needed transformation of the global food system. In order to obtain more sustainable, healthy and nutritious food production systems a better understanding and management of microbiomes along the food chain has never been more important.

References

1. FAO. The State of World Fisheries and Aquaculture 2020 [Internet]. 2020 [cited 2021 May 20]. Available from: http://www.fao.org/documents/card/en/c/ca9229en

2. WHO. Obesity and overweight. Updated February 2018. [Internet]. 2018. Available from: https://www.who.int/en/news-room/fact-sheets/detail/obesity-and-overweight

3. Koohafkan P, FAO, editors. The state of the world's land and water resources for food and agriculture: managing systems at risk. Abingdon: Earthscan [u.a.]; 2011. 285 p.

4. The Lancet. A future direction for tackling malnutrition. The Lancet. 2020 Jan;395(10217):2.

5. Willett W, Rockström J, Loken B, Springmann M, Lang T, Vermeulen S, et al. Food in the Anthropocene: the EAT–Lancet Commission on healthy diets from sustainable food systems. The Lancet. 2019 Feb;393(10170):447–92.

6. Stanaway JD, Afshin A, Gakidou E, Lim SS, Abate D, Abate KH, et al. Global, regional, and national comparative risk assessment of 84 behavioural, environmental and occupational, and metabolic risks or clusters of risks for 195 countries and territories, 1990–2017: a systematic analysis for the Global Burden of Disease Study 2017. The Lancet. 2018 Nov;392(10159):1923–94.

7. Marchesi JR, Ravel J. The vocabulary of microbiome research: a proposal. Microbiome. 2015 Dec;3(1):31, s40168-015-0094–5.

8. Hu FB. Dietary pattern analysis: a new direction in nutritional epidemiology: Current Opinion in Lipidology. 2002 Feb;13(1):3–9.

9. Odermatt A. The Western-style diet: a major risk factor for impaired kidney function and chronic kidney disease. American Journal of Physiology-Renal Physiology. 2011 Nov;301(5):F919–31.

10. Cordain L, Eaton SB, Sebastian A, Mann N, Lindeberg S, Watkins BA, et al. Origins and evolution of the Western diet: health implications for the 21st century. The American Journal of Clinical Nutrition. 2005 Feb 1;81(2):341–54.

11. Schnabel L, Kesse-Guyot E, Allès B, Touvier M, Srour B, Hercberg S, et al. Association Between Ultraprocessed Food Consumption and Risk of Mortality Among Middle-aged Adults in France. JAMA Intern Med. 2019 Apr 1;179(4):490.

12. Sánchez-Tapia M, Miller AW, Granados-Portillo O, Tovar AR, Torres N. The development of metabolic endotoxemia is dependent on the type of sweetener and the presence of saturated fat in the diet. Gut Microbes. 2020 Nov 9;12(1):1801301.

13. Bolte LA, Vich Vila A, Imhann F, Collij V, Gacesa R, Peters V, et al. Long-term dietary patterns are associated with pro-inflammatory and anti-inflammatory features of the gut microbiome. Gut. 2021 Jul;70(7):1287–98.

14. Chen K, Zhao H, Shu L, Xing H, Wang C, Lu C, et al. Effect of resveratrol on intestinal tight junction proteins and the gut microbiome in high-fat diet-fed insulin resistant mice. International Journal of Food Sciences and Nutrition. 2020 Nov 16;71(8):965–78.

15. Singh R, Chandrashekharappa S, Bodduluri SR, Baby BV, Hegde B, Kotla NG, et al. Enhancement of the gut barrier integrity by a microbial metabolite through the Nrf2 pathway. Nat Commun. 2019 Dec;10(1):89.

16. Qu W, Nie C, Zhao J, Ou X, Zhang Y, Yang S, et al. Microbiome–Metabolomics Analysis of the Impacts of Long-Term Dietary Advanced-Glycation-End-Product Consumption on C57BL/6 Mouse Fecal Microbiota and Metabolites. J Agric Food Chem. 2018 Aug 22;66(33):8864–75.

17. Mills DJS, Tuohy KM, Booth J, Buck M, Crabbe MJC, Gibson GR, et al. Dietary glycated protein modulates the colonic microbiota towards a more detrimental composition in ulcerative colitis patients and non-ulcerative colitis subjects. Journal of Applied Microbiology. 2008 Sep;105(3):706–14.

18. Kim W, Egan JM. The Role of Incretins in Glucose Homeostasis and Diabetes Treatment. Pharmacol Rev. 2008 Dec;60(4):470–512.

19. Stanhope KL, Schwarz JM, Keim NL, Griffen SC, Bremer AA, Graham JL, et al. Consuming fructose-sweetened, not glucose-sweetened, beverages increases visceral adiposity and lipids and decreases insulin sensitivity in overweight/obese humans. J Clin Invest. 2009 May 1;119(5):1322–34.

20. Oikonomou E, Psaltopoulou T, Georgiopoulos G, Siasos G, Kokkou E, Antonopoulos A, et al. Western Dietary Pattern Is Associated With Severe Coronary Artery Disease. Angiology. 2018 Apr;69(4):339–46.

21. Rauber F, Steele EM, Louzada ML da C, Millett C, Monteiro CA, Levy RB. Ultra-processed food consumption and indicators of obesity in the United Kingdom population (2008-2016). Meyre D, editor. PLoS ONE. 2020 May 1;15(5):e0232676.

22. Oyebode O, Gordon-Dseagu V, Walker A, Mindell JS. Fruit and vegetable consumption and all-cause, cancer and CVD mortality: analysis of Health Survey for England data. J Epidemiol Community Health. 2014 Sep;68(9):856–62.

23. Crowe FL, Roddam AW, Key TJ, Appleby PN, Overvad K, Jakobsen MU, et al. Fruit and vegetable intake and mortality from ischaemic heart disease: results from the European Prospective Investigation into Cancer and Nutrition (EPIC)-Heart study. European Heart Journal. 2011 May 2;32(10):1235–43.

24. Lock K, Pomerleau J, Causer L, Altmann DR, McKee M. The global burden of disease attributable to low consumption of fruit and vegetables: implications for the global strategy on diet. Bull World Health Organ. 2005 Feb;83(2):100–8.

25. He FJ, Nowson CA, Lucas M, MacGregor GA. Increased consumption of fruit and vegetables is related to a reduced risk of coronary heart disease: meta-analysis of cohort studies. J Hum Hypertens. 2007 Sep;21(9):717–28.

26. Martel J, Ojcius DM, Ko Y-F, Young JD. Phytochemicals as Prebiotics and Biological Stress Inducers. Trends in Biochemical Sciences. 2020 Jun;45(6):462–71.

27. Favela-González KM, Hernández-Almanza AY, De la Fuente-Salcido NM. The value of bioactive compounds of cruciferous vegetables (*Brassica*) as antimicrobials and antioxidants: A review. J Food Biochem [Internet]. 2020 Oct [cited 2021 May 21];44(10). Available from: https://onlinelibrary.wiley.com/doi/10.1111/jfbc.13414

28. Monagas M, Urpi-Sarda M, Sánchez-Patán F, Llorach R, Garrido I, Gómez-Cordovés C, et al. Insights into the metabolism and microbial biotransformation of dietary flavan-3-ols and the bioactivity of their metabolites. Food Funct. 2010;1(3):233.

29. Ozdal T, Sela DA, Xiao J, Boyacioglu D, Chen F, Capanoglu E. The Reciprocal Interactions between Polyphenols and Gut Microbiota and Effects on Bioaccessibility. Nutrients. 2016 Feb 6;8(2):78.

30. Barba FJ, Nikmaram N, Roohinejad S, Khelfa A, Zhu Z, Koubaa M. Bioavailability of Glucosinolates and Their Breakdown Products: Impact of Processing. Front Nutr [Internet]. 2016 Aug 16 [cited 2021 Oct 26];3. Available from: http://journal.frontiersin.org/Article/10.3389/fnut.2016.00024/abstract

31. Michaelsen S, Otte J, Simonsen L-O, Sørensen H. Absorption and Degradation of Individual Intact Glucosinolates in the Digestive Tract of Rodents. Acta Agriculturae Scandinavica, Section A - Animal Science. 1994 Feb;44(1):25–37.

32. Miller TL, Wolin MJ. Pathways of acetate, propionate, and butyrate formation by the human fecal microbial flora. Appl Environ Microbiol. 1996 May;62(5):1589–92.

33. Chen M, Fan B, Liu S, Imam KMSU, Xie Y, Wen B, et al. The in vitro Effect of Fibers With Different Degrees of Polymerization on Human Gut Bacteria. Front Microbiol. 2020 May 15;11:819.

34. Zhu Y, Wang C, Li F. Impact of dietary fiber/starch ratio in shaping caecal microbiota in rabbits. Can J Microbiol. 2015 Oct;61(10):771–84.

35. Pettengill EA, Pettengill JB, Binet R. Phylogenetic Analyses of Shigella and Enteroinvasive Escherichia coli for the Identification of Molecular Epidemiological Markers: Whole-Genome Comparative Analysis Does Not Support Distinct Genera Designation. Front Microbiol. 2016 Jan 19;6:1573.

36. Wang H, Bastian SE, Cheah KY, Lawrence A, Howarth GS. *Escherichia coli* Nissle 1917-derived factors reduce cell death and late apoptosis and increase transepithelial electrical resistance in a model of 5-fluorouracil-induced intestinal epithelial cell damage. Cancer Biology & Therapy. 2014 May;15(5):560–9.

37. Roopchand DE, Carmody RN, Kuhn P, Moskal K, Rojas-Silva P, Turnbaugh PJ, et al. Dietary Polyphenols Promote Growth of the Gut Bacterium Akkermansia muciniphila and Attenuate High-Fat Diet-Induced Metabolic Syndrome. Diabetes. 2015 Aug;64(8):2847–58.

38. Possemiers S, Bolca S, Verstraete W, Heyerick A. The intestinal microbiome: A separate organ inside the body with the metabolic potential to influence the bioactivity of botanicals. Fitoterapia. 2011 Jan;82(1):53–66.

39. Madsen K, Park H. Immunologic Response in the Host. In: The Microbiota in Gastrointestinal Pathophysiology [Internet]. Elsevier; 2017 [cited 2021 Aug 4]. p. 233–41. Available from: https://linkinghub.elsevier.com/retrieve/pii/B9780128040249000264

40. Mohammad S, Thiemermann C. Role of Metabolic Endotoxemia in Systemic Inflammation and Potential Interventions. Front Immunol. 2021 Jan 11;11:594150.

41. Cani PD, Amar J, Iglesias MA, Poggi M, Knauf C, Bastelica D, et al. Metabolic Endotoxemia Initiates Obesity and Insulin Resistance. Diabetes. 2007 Jul 1;56(7):1761–72.

42. He C, Huang L, Lei P, Liu X, Li B, Shan Y. Sulforaphane Normalizes Intestinal Flora and Enhances Gut Barrier in Mice with BBN-Induced Bladder Cancer. Mol Nutr Food Res. 2018 Dec;62(24):1800427.

43. Parada Venegas D, De la Fuente MK, Landskron G, González MJ, Quera R, Dijkstra G, et al. Short Chain Fatty Acids (SCFAs)-Mediated Gut Epithelial and Immune Regulation and Its Relevance for Inflammatory Bowel Diseases. Front Immunol. 2019 Mar 11;10:277.

44. Sultana S. Nutritional and functional properties of Moringa oleifera. Metabolism Open. 2020 Dec;8:100061.

45. Anwar F, Latif S, Ashraf M, Gilani AH. Moringa oleifera: a food plant with multiple medicinal uses. Phytother Res. 2007 Jan;21(1):17–25.

46. Zongo U, Zoungrana SL, Savadogo A, Traoré AS. Nutritional and Clinical Rehabilitation of Severely Malnourished Children with <i>Moringa oleifera Lam</i>. Leaf Powder in Ouagadougou (Burkina Faso). FNS. 2013;04(09):991–7.

47. Shi H, Su B, Chen X, Pian R. Solid state fermentation of *Moringa oleifera* leaf meal by mixed strains for the protein enrichment and the improvement of nutritional value. PeerJ. 2020 Nov 18;8:e10358.

48. Su B, Chen X. Current Status and Potential of Moringa oleifera Leaf as an Alternative Protein Source for Animal Feeds. Front Vet Sci. 2020 Feb 26;7:53.

49. Masih LP, Singh S, Elamathi S, Anandhi P, Abraham T. Moringa: A multipurpose potential crop – A review. PINSA [Internet]. 2019 May 24 [cited 2021 Oct 22]; Available from: http://insa.nic.in/writereaddata/UpLoadedFiles/PINSA/PINSA_2019_Art31.pdf

50. Fahey J. Microbiological Monitoring of Laboratory Mice. In: Sundberg J, editor. Genetically Engineered Mice Handbook [Internet]. CRC Press; 2005 [cited 2021 Oct 1]. p. 157–64. (Research Methods For Mutant Mice; vol. 20051540). Available from: http://www.crcnetbase.com/doi/abs/10.1201/9781420039078.ch12

51. Gopalan C, Rama SBV, Balasubramanian S. Nutritive value of Indian foods. Hyderabad, India: National Institute of Nutrition, Indian Council of Medial Research; 1978.

52. Fard M, Arulselvan P, Karthivashan G, Adam S, Fakurazi S. Bioactive extract from moringa oleifera inhibits the pro-inflammatory mediators in lipopolysaccharide stimulated macrophages. Phcog Mag. 2015;11(44):556.

53. Villarruel-López A, López-de la Mora DA, Vázquez-Paulino OD, Puebla-Mora AG, Torres-Vitela MR, Guerrero-Quiroz LA, et al. Effect of Moringa oleifera consumption on diabetic rats. BMC Complement Altern Med. 2018 Dec;18(1):127.

54. Leone A, Fiorillo G, Criscuoli F, Ravasenghi S, Santagostini L, Fico G, et al. Nutritional Characterization and Phenolic Profiling of Moringa oleifera Leaves Grown in Chad, Sahrawi Refugee Camps, and Haiti. IJMS. 2015 Aug 12;16(8):18923–37.

55. Tumer TB, Rojas-Silva P, Poulev A, Raskin I, Waterman C. Direct and Indirect Antioxidant Activity of Polyphenol- and Isothiocyanate-Enriched Fractions from *Moringa oleifera*. J Agric Food Chem. 2015 Feb 11;63(5):1505–13.

56. Borgonovo G, De Petrocellis L, Schiano Moriello A, Bertoli S, Leone A, Battezzati A, et al. Moringin, A Stable Isothiocyanate from Moringa oleifera, Activates the Somatosensory and Pain Receptor TRPA1 Channel In Vitro. Molecules. 2020 Feb 22;25(4):976.

57. Marco ML, Heeney D, Binda S, Cifelli CJ, Cotter PD, Foligné B, et al. Health benefits of fermented foods: microbiota and beyond. Current Opinion in Biotechnology. 2017 Apr;44:94–102.

58. Plengvidhya V, Breidt F, Lu Z, Fleming HP. DNA Fingerprinting of Lactic Acid Bacteria in Sauerkraut Fermentations. Appl Environ Microbiol. 2007 Dec;73(23):7697–702.

59. Yang X, Hu W, Xiu Z, Jiang A, Yang X, Saren G, et al. Microbial Community Dynamics and Metabolome Changes During Spontaneous Fermentation of Northeast Sauerkraut From Different Households. Front Microbiol. 2020 Aug 5;11:1878.

60. Iraporda C, Romanin DE, Rumbo M, Garrote GL, Abraham AG. The role of lactate on the immunomodulatory properties of the nonbacterial fraction of kefir. Food Research International. 2014 Aug;62:247–53.

61. Okada T, Fukuda S, Hase K, Nishiumi S, Izumi Y, Yoshida M, et al. Microbiota-derived lactate accelerates colon epithelial cell turnover in starvation-refed mice. Nat Commun. 2013 Jun;4(1):1654.

62. Szaefer H, Licznerska B, Krajka-Kuźniak V, Bartoszek A, Baer-Dubowska W. Modulation of CYP1A1, CYP1A2 and CYP1B1 Expression by Cabbage Juices and Indoles in Human Breast Cell Lines. Nutrition and Cancer. 2012 Aug;64(6):879–88.

63. Peñas E, Frias J, Sidro B, Vidal-Valverde C. Chemical Evaluation and Sensory Quality of Sauerkrauts Obtained by Natural and Induced Fermentations at Different NaCl Levels from Brassica oleracea Var. *capitata* Cv. Bronco Grown in Eastern Spain. Effect of Storage. J Agric Food Chem. 2010 Mar 24;58(6):3549–57.

64. Martinez-Villaluenga C, Peñas E, Sidro B, Ullate M, Frias J, Vidal-Valverde C. White cabbage fermentation improves ascorbigen content, antioxidant and nitric oxide production inhibitory activity in LPS-induced macrophages. LWT - Food Science and Technology. 2012 Apr;46(1):77–83.

65. Nielsen ES, Garnås E, Jensen KJ, Hansen LH, Olsen PS, Ritz C, et al. Lacto-fermented sauerkraut improves symptoms in IBS patients independent of product pasteurisation – a pilot study. Food Funct. 2018;9(10):5323–35.

66. Meng F, Lowell CA. Lipopolysaccharide (LPS)-induced Macrophage Activation and Signal Transduction in the Absence of Src-Family Kinases Hck, Fgr, and Lyn. Journal of Experimental Medicine. 1997 May 5;185(9):1661–70.

67. Zhou S, Chen G, Qi M, El-Assaad F, Wang Y, Dong S, et al. Gram Negative Bacterial Inflammation Ameliorated by the Plasma Protein Beta 2-Glycoprotein I. Sci Rep. 2016 Dec;6(1):33656.

68. Dittel LJ, Dittel BN, Brod SA. Ingested ACTH blocks Th17 production by inhibiting GALT IL-6. Journal of the Neurological Sciences. 2020 Feb;409:116602.

69. Cavalcanti YVN, Brelaz MCA, Lemoine Neves JK de A, Ferraz JC, Pereira VRA. Role of TNF-Alpha, IFN-Gamma, and IL-10 in the Development of Pulmonary Tuberculosis. Pulmonary Medicine. 2012;2012:1–10.

70. Lee Y-S, Kim T-Y, Kim Y, Kim S, Lee S-H, Seo S-U, et al. Microbiota-derived lactate promotes hematopoiesis and erythropoiesis by inducing stem cell factor production from leptin receptor+ niche cells. Exp Mol Med. 2021 Sep;53(9):1319–31.

71. HLPE. Sustainable fisheries and aquaculture for food security and nutrition. A report by the High Level Panel of Experts on Food Security and Nutrition of the Committee on World Food Security. Rome; 2014.

72. Cebra JJ. Influences of microbiota on intestinal immune system development. Am J Clin Nutr. 1999;69:1046S-1051S.

73. Bozzi D, Rasmussen JA, Carøe C, Sveier H, Nordøy K, Gilbert MTP, et al. Salmon gut microbiota correlates with disease infection status: potential for monitoring health in farmed animals. anim microbiome. 2021 Dec;3(1):30.

74. Butt RL, Volkoff H. Gut Microbiota and Energy Homeostasis in Fish. Front Endocrinol. 2019 Jan 24;10:9.

Appendix

nutrients

MDPI

Article

Effects of Exogenous Dietary Advanced Glycation End Products on the Cross-Talk Mechanisms Linking Microbiota to Metabolic Inflammation

Raffaella Mastrocola [1,*,†], Debora Collotta [2,†], Giulia Gaudioso [3], Marie Le Berre [4], Alessia Sofia Cento [1], Gustavo Ferreira Alves [2], Fausto Chiazza [2], Roberta Verta [2], Ilaria Bertocchi [5], Friederike Manig [6], Michael Hellwig [6], Francesca Fava [3], Carlo Cifani [7], Manuela Aragno [1], Thomas Henle [6], Lokesh Joshi [4], Kieran Tuohy [3] and Massimo Collino [2,*]

1 Department of Clinical and Biological Sciences, University of Turin, 10125 Turin, Italy; alessiasofia.cento@unito.it (A.S.C.); manuela.aragno@unito.it (M.A.)
2 Department of Drug Science and Technology, University of Turin, 10125 Turin, Italy; debora.collotta@unito.it (D.C.); gustavo.ferreiraalves@unito.it (G.F.A.); fausto.chiazza@uniupo.it (F.C.); roberta.verta@edu.unito.it (R.V.)
3 Fondazione Edmund Mach, 38010 San Michele all'Adige, Italy; giulia.gaudioso@fmach.it (G.G.); francesca.fava@fmach.it (F.F.); kieran.tuohy@fmach.it (K.T.)
4 Biomedical Sciences, National University of Ireland, H91 TK33 Galway, Ireland; marie.leberre@nuigalway.ie (M.L.B.); lokesh.joshi@nuigalway.ie (L.J.)
5 Department of Neuroscience, University of Turin, 10124 Turin, Italy; ilaria.bertocchi@unito.it
6 Chair of Food Chemistry, Technische Universität Dresden, 01062 Dresden, Germany; friederike.manig@tu-dresden.de (F.M.); michael.hellwig@tu-dresden.de (M.H.); thomas.henle@tu-dresden.de (T.H.)
7 Pharmacology Unit, School of Pharmacy, University of Camerino, 62032 Camerino, Italy; carlo.cifani@unicam.it
* Correspondence: raffaella.mastrocola@unito.it (R.M.); massimo.collino@unito.it (M.C.); Tel.: +39-011-6707758 (R.M.); +39-011-6706861 (M.C.)
† Both authors contributed equally.

Received: 29 July 2020; Accepted: 17 August 2020; Published: 19 August 2020

Abstract: Heat-processed diets contain high amounts of advanced glycation end products (AGEs). Here we explore the impact of an AGE-enriched diet on markers of metabolic and inflammatory disorders as well as on gut microbiota composition and plasma proteins glycosylation pattern. C57BL/6 mice were allocated into control diet (CD, $n = 15$) and AGE-enriched diet (AGE-D, $n = 15$) for 22 weeks. AGE-D was prepared replacing casein by methylglyoxal hydroimidazolone-modified casein. AGE-D evoked increased insulin and a significant reduction of GIP/GLP-1 incretins and ghrelin plasma levels, altered glucose tolerance, and impaired insulin signaling transduction in the skeletal muscle. Moreover, AGE-D modified the systemic glycosylation profile, as analyzed by lectin microarray, and increased Nε-carboxymethyllysine immunoreactivity and AGEs receptor levels in ileum and submandibular glands. These effects were associated to increased systemic levels of cytokines and impaired gut microbial composition and homeostasis. Significant correlations were recorded between changes in bacterial population and in incretins and inflammatory markers levels. Overall, our data indicates that chronic exposure to dietary AGEs lead to a significant unbalance in incretins axis, markers of metabolic inflammation, and a reshape of both the intestinal microbiota and plasma protein glycosylation profile, suggesting intriguing pathological mechanisms underlying AGEs-induced metabolic derangements.

Keywords: advanced glycation end products; proteins glycosylation; gut microbiota; metabolic inflammation; insulin signal pathway

1. Introduction

The progressive ageing of world population and the rapid changes in the lifestyle occurred in recent decades have contributed to the rising of chronic metabolic and inflammatory diseases [1]. In particular, nowadays nutrition is considered the main beneficial or harmful tool able to either prevent or cause metabolic inflammation (known as "metaflammation"), which is strictly related to the pathogenesis of many chronic diseases, exerting an enormous socioeconomic impact. A widely studied class of diet-derived substances with possible impact on inflammatory processes is the heterogeneous group of advanced glycation end products (AGEs). These highly reactive compounds are derived from a first reaction between a reducing sugar and the amino group of proteins and give rise, through a sequence of dehydration, cyclization, fragmentation, and oxidation reactions, to final AGE-modified proteins, which are non-degradable and functionally compromised [2]. A growing body of evidence is demonstrating the pivotal role of AGEs in several pathogenic mechanisms involving oxidative stress, inflammatory response and endothelial dysfunction, responsible for chronic diseases onset such as insulin resistance, diabetes, atherosclerosis, cardiovascular diseases, and renal dysfunction [3].

AGEs can be endogenously formed in conditions of hyperglycemia and dyslipidemia [4]. However, AGEs can also be contained in foods as a product of cooking or food processing. Indeed, particular conditions of cooking (high temperatures for long time, low level of hydration and high pH) generate large amounts of different classes of AGEs [5]. Several databases reporting AGEs quantification in the most common ingredients and popular prepared foods have been published, however, data are often contrasting and AGEs chemical characterization is limited [6,7]. Very recently, the Senate Commission on Food Safety of the German Research Foundation has published quality criteria for studies dealing with dietary glycation compounds and human health [8]. Accordingly, the best methods available for quantification of AGEs rely on chromatographic analyses, and by using these methods, a daily intake of AGEs between 25 and 75 mg was estimated [7]. Even though dietary interventions aimed to reduce AGEs intake have been demonstrated to be effective in reducing markers of oxidative stress, inflammation, and endothelial dysfunction in patients with diabetes or cardiometabolic diseases [9], it is still controversial whether, and in which amount, dietary AGEs contribute to the physiological pool of AGEs; and how they can modify systemic and tissue proteins, including their post-translational modification such as glycosylation, and affect the overall metabolism mainly in the absence of pre-existing cardiometabolic disorders. It has been estimated that a fraction of ingested AGEs, that are not absorbed and not defecated, may be metabolized intraluminally by the microbiota [10]. We have recently shown that AGEs such as N-ε-carboxymethyllysine (CML) can be metabolized by the human microbiota [11] and that E. coli is able to convert CML to mainly one metabolite, the biogenic amine N-carboxymethylcadaverine [12].

Hence, the present study aimed at investigating the effects of an AGE-enriched diet (AGE-D) on gut microbiota composition and function, as well as on the development of metabolic inflammation, focusing on the molecular pathways activated by AGEs chronic exposure at organ and tissue levels.

2. Materials and Methods

2.1. Materials

All reagents were of the highest grade of purity available and were obtained from Sigma-Aldrich (Milan, Italy). Antibodies were from Cell-Signaling Technology (Beverly, MA, USA).

2.2. Animals and Experimental Design

The in vivo experimental procedures here described were approved by the local Animal Use and Care Committee and the Ministry of Health (approval n°. 42/2017-PR) and are in keeping with the European Directive 2010/63/EU on the protection of animals used for scientific purposes as well as the Guide for the Care and Use of Laboratory Animals. This study was carried out using 4-weeks old C57BL/6 male mice, housed in a controlled environment at 25 ± 2 °C. Mice were randomly allocated to two experimental groups (n = 15 per group): mice fed with a control not-irradiated standard diet

(CD) and mice fed with an AGE-enriched diet (AGE-D) for 22 weeks. AGE-D was prepared replacing casein in the CD (200 g/kg of diet) by an equal amount of modified casein where 80.5% of arginine and 41.5% of lysine were modified. The diet contained 15 µmol of MG-H1 (methylglyoxal-derived 5-hydro-5-methylimidazolone) per g of diet. MG-H1 was enriched in casein as follows: A 10% solution of sodium caseinate was mixed with MGO (40% solution, Sigma), heated for 4 h, and then lyophilized after casein precipitation. Casein and methylglyoxal were left to react in aqueous medium, whereupon casein was precipitated in order to remove methylglyoxal. Thereby, 80.5% of arginine residues were modified together with 41.5% of lysine residues, which is an unavoidable side-reaction during reaction of proteins with MGO. After lyophilization, the MGO-modified casein was used as an ingredient for the preparation of the AGEs diet (AGE-D). The fraction of arginine and lysine that had been modified was replaced in the diet by the addition of the respective amounts of free lysine and arginine, so that any effect elicited by the diet may not be due to a deficiency in these essential amino acids. This preparation contained 17.4 ± 1.5 g/kg MG-H1 as analyzed by HPLC-MS/MS after enzymatic hydrolysis [13].

All groups received water and food *ad libitum*. Body weight and food/water intake were recorded weekly, whereas fasting glucose was recorded monthly. After 22 weeks of dietary manipulation, one day before the end of the experiment, feces were collected using metabolic cages (18 h starving) after which oral glucose tolerance test (OGTT) was performed. The day after, mice (fasted for 4 h) were anesthetized using isoflurane (IsoFlo, Abbott Laboratories) and killed by cardiac exsanguination. Blood samples were collected and plasma was isolated. Submandibular salivary glands and a portion of the ileum tract of intestine were fixed in neutral buffered formalin and embedded in paraffin for histological slides preparation. The gastrocnemius muscle was isolated, frozen in liquid nitrogen and stored at −80 °C.

2.3. Oral Glucose Tolerance Test (OGTT)

OGTT was performed after an overnight fasting period by administering glucose (2 g/kg) by oral gavage. Once before administration and 15, 30, 60 and 120 min afterward, blood was obtained from the saphenous vein and glucose concentration was measured with a conventional glucometer (GlucoMen LX kit, Menarini Diagnostics, Italy).

2.4. Biochemical Analysis

The plasma lipid profile was determined by measuring the content of triglycerides (TGs), total cholesterol, high-density-lipoprotein (HDL) and low density-lipoprotein (LDL) by standard enzymatic procedures using reagent kits (Hospitex Diagnostics, Florence, Italy). Plasma insulin, ghrelin, glucose-dependent insulinotropic polypeptide (GIP), glucagon like peptide (GLP-1), plasminogen activator inhibitor (PAI)-1, IL-1β, TNF-α, IFN-γ, IL-6, IL-10 and IL-17 levels were measured by using Bio-Plex Multiplex Immunoassay System (Bio-Rad Laboratories, Hercules, CA, USA). Intestinal alkaline phosphatase (IAP) activity was detected in plasma with SensoLite pNPP Alkaline Phosphatase colorimetric assay kit (AnaSpec Inc, Fremont, CA, USA) following manufacturer's instructions for kinetic reading.

2.5. Fecal Microbiota Analysis

Total genomic DNA extraction from frozen feces was carried out using QIAamp® PowerFecal® DNA Isolation kit (MoBio Laboratories, Inc., Carlsbad, CA, USA) and then subjected to PCR amplification by targeting 16S rRNA V3-V4 variable regions with specific bacterial primer set 341F (5′ CCTACGGGNGGCWGCAG 3′) and 806R (5′ GACTACNVGGGTWTCTAATCC 3′), as previously reported [14]. PCR products were checked by gel electrophoresis and cleaned using Agencourt AMPure XP system (Beckman Coulter, Brea, CA, USA), following manufacturer's instructions. After 7 PCR cycles, (16S Metagenomic Sequencing Library Preparation, Illumina), Illumina adaptors were attached (Illumina Nextera XT Index Primer). Libraries were purified using Agencourt AMPure XP (Beckman) and then sequenced on an Illumina® MiSeq (PE300) platform (MiSeq Control Software 2.0.5 and Real-Time Analysis software 1.16.18). Sequences obtained from Illumina sequencing were analyzed using Quantitative Insights

Into Microbial Ecology (QIIME) 2.0 pipeline [15]. Percentage relative abundance of taxa from different dietary groups were compared using nonparametric Wilcoxon statistical test. Alpha and beta-diversity estimates were determined using phyloseq R Package [16]. Correlation between bacterial genera and systemic parameters in CD and AGE-D groups was performed by Spearman correlation analysis. Unidentified genera include those whose percentage sequence homology with Greengenes database was below 95% (http://greengenes.lbl.gov) [17].

2.6. Plasma Glycosylation Profile by Lectin Microarray

Sera from 5 mice from the CD and AGE-D were pooled and pre-cleared prior to IgG purification by centrifugation at 10,000× *g* for 15 min. IgGs were purified by protein G affinity chromatography using a protein G chromatography (Biosciences, ThermoFisher, Dublin, Ireland) following manufacturer's instructions. Both fractions, IgGs and IgG-depleted blood, were buffered exchanged with PBS and directly fluorescently labelled with Alexa Fluor® 555 (Biosciences, ThermoFisher, Dublin, Ireland) following manufacturer's instructions, in the dark.

Lectin microarray were prepared by dilution of lectins of known specificities in phosphate buffered saline (PBS), pH 7.4, containing 1 mM concentrations of their respective haptenic sugar to ensure preservation of their binding site (Supplementary Table S1) and printed on Nexterion® H (Schott, Mainz, Germany) amine-reactive, N-hydroxysuccinimide ester functionalized, hydrogel-coated glass slides using a SciFlexArrayer S3 piezoelectric spotter (Scienion, Berlin, Germany) under constant 62% (+/−2%) humidity at 20 °C. Each feature was printed with approximately 1 nL of probe using an uncoated 90 mm glass piezoelectric dispenser capillary in replicates of 6 features per probe. Eight replicate subarrays, each consisting of 52 probes in replicates of 6 features, were printed per slide. Slides were incubated in a humidity chamber overnight after printing to ensure complete conjugation. The remaining functional groups on the slide surface were then deactivated by incubation with 100 mM ethanolamine in 50 mM sodium borate, pH 8, for 1 h at room temperature. Slides were washed with PBS, pH 7.4 with 0.05% Tween-20 (PBS-T) three times for 2 min each wash and once with PBS prior to drying by centrifugation (470× *g*, 5 min). The printed lectin microarrays were stored at 4 °C with desiccant until use.as previously described [18]. Labelled IgG and D fractions were incubated on microarray slides and data extracted as described elsewhere [19]. In brief, raw intensity values were extracted from the image *.tif files using GenePix Pro v6.1.0.4 (Molecular Devices, Berkshire, UK) and a proprietary *.gal file (containing feature spot address and identity) using adaptive diameter (70–130%) circular alignment based on 230 um features and were exported as text to Excel (Version 2007, Microsoft). Local background-corrected median feature intensity data (F543median-B543) were analyzed. The median of 6 replicate spots per subarray was handled as a single data point for graphical and statistical analysis. Data were normalized to the median total intensity value of 6 replicate. Unsupervised hierarchical clustering of sample binding intensity data was performed with Hierarchical Clustering Explorer v3.0 (http://www.cs.umd.edu/hcil/hce/hce3.html). Mean total intensity, normalized by rescaling lectin binding data to 65,000 RFU, was clustered with the following parameters: no pre-filtering, complete linkage, and Euclidean distance. The significance of binding data was evaluated using a standard Student's t test (paired, two-tailed).

2.7. Tissue Extracts

Gastrocnemius protein extracts were prepared as previously described [20]. Briefly, tissues were homogenized and centrifuged at 15,000× *g* for 40 min at 4 °C. Supernatants were collected and the protein content was determined using a BCA protein assay (Pierce Biotechnology Inc., Rockford, IL, USA) following manufacturer's instructions.

2.8. Western Blot Analysis

About 60 µg of total proteins were loaded for Western blot experiments. Proteins were separated by 8% sodium dodecyl sulphate-polyacrylamide gel electrophoresis (SDS-PAGE) and transferred to a polyvinyldenedifluoride (PVDF) membrane, which was then incubated with primary antibodies (dilution 1:1000). The antibodies used were: rabbit anti-Ser307 IRS-1 (#2381); mouse anti-total IRS-1 (#3194); rabbit anti-Ser473 Akt (#4060); rabbit anti-total Akt (#9272); rabbit anti-Ser9 GSK–3β (#9332); and rabbit anti-total GSK–3β (#9315). Blots were then incubated with secondary antibodies conjugated with horseradish peroxidase (HRP) (dilution 1:20,000) and developed using the ECL detection system. The immunoreactive bands were analyzed by the Bio-Rad Image Lab SoftwareTM 6.0.1 and results were normalized to CD.

2.9. Immunohistochemistry

CML and receptor for AGEs (RAGE) immunopositivity was analyzed by immunohistochemistry on 7 µm paraffin-embedded sections of ileum and submandibular salivary glands. Slides were deparaffinized, rehydrated, and antigens were retrieved by 5 min boiling in 10 mM sodium citrate buffer, pH 6.0. After blocking, sections were incubated overnight with primary antibodies (CML, R&D, #MAB3247, dilution 1:50; RAGE, Invitrogen, #PA1-075, dilution 1:50) and subsequently for 1 h with HRP-conjugated secondary antibodies (dilution 1:200) and nuclei were counterstained with hematoxylin.

2.10. Statistical Analysis

All values in both the text and figures are expressed as mean ± S.E.M. for n observations. Statistical significance between CD and AGE-D values was performed by unpaired t test. OGTTs were analyzed using the area under the receiver operating characteristic (ROC) curve.

A p value <0.05 was considered to be statistically significant. Statistical analysis was carried out using GraphPad Prism 5.03 (GraphPad Software, La Jolla, CA, USA).

3. Results

3.1. General Parameters

Most commonly, AGEs are ingested by humans in a protein-bound form within a food matrix. Therefore, we intended to apply AGEs to mice in a protein-bound form and decided to enrich casein, an important food protein, with MG-H1, which is the predominating derivative of modification of arginine residues with methylglyoxal (MGO). HPLC-MS/MS analysis revealed that the MGO-modified casein contained 17.4 ± 1.5 g/kg of MG-H1 which, with a fraction of 20% casein in the diet, corresponds to a concentration of 3.5 g/kg or 15 µmol/g. The highest concentrations of MG-H1 in food have been found in cakes and biscuits (up to 360 mg/kg, [6]). Hence, the diet of the present study contains far more MG-H1 than may normally be ingested.

After 22 weeks of dietary intervention, the mice exposed to AGE-D showed a robust increase in blood insulin level, associated with decreased levels of GIP and GLP-1, the two primary incretins secreted from the intestine, and ghrelin, and a significant impairment in OGTT (Figure 1), when compared to mice fed with CD. However, these effects were not associated with significant changes in body weight gain, fasting blood glucose, and lipid profile (Table 1).

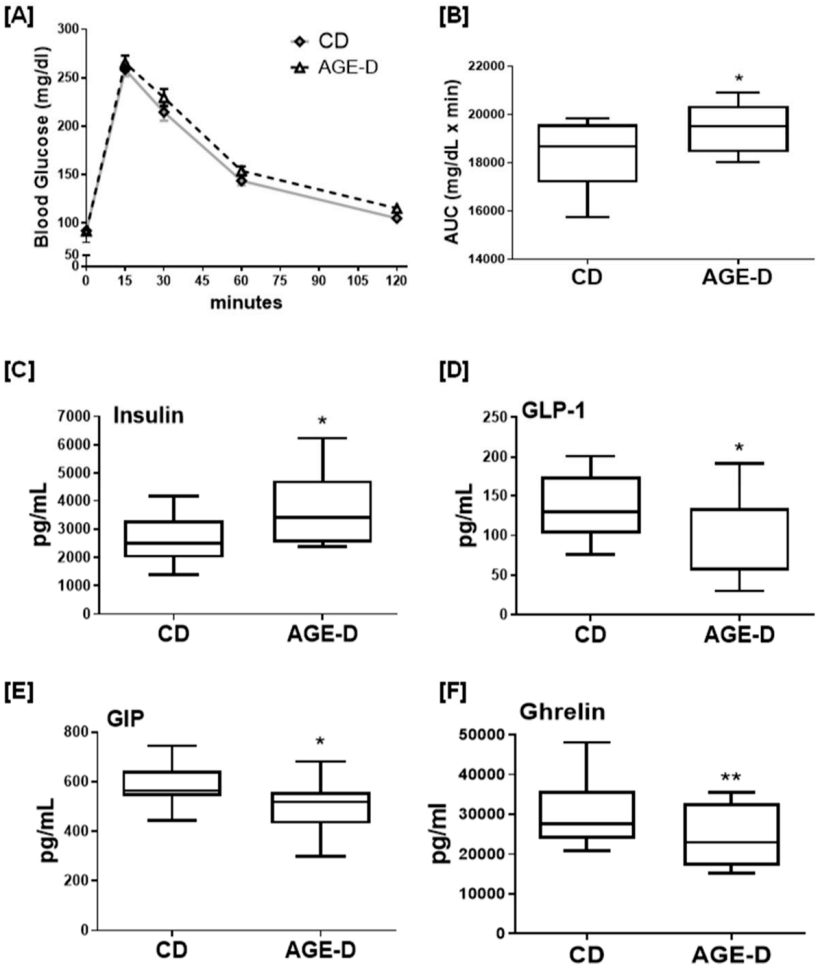

Figure 1. (**A**) Oral glucose tolerance test (OGTT) performed after 22 weeks of dietary manipulation on control not-irradiated standard diet (CD) and advanced glycation end products-enriched diet (AGE-D) mice. (**B**) Area under the curve showing altered OGTT in AGE-D mice indicating glucose intolerance. (**C**–**F**) Plasma levels of insulin, GLP-1, GIP, and ghrelin in CD and AGE-D mice measured by luminex suspension bead-based multiplexed Bio-Plex 3D system. Data are means ± S.E.M. (n = 15 per group). Statistical significance: ** $p < 0.01$, * $p < 0.05$ vs. CD.

Table 1. Effects on mice body weight and systemic lipid/glucose profile at 22 weeks of the AGE-enriched diet (AGE-D) in comparison to the control diet (CD).

	CD	AGE-D
Body weight (g)	29.3 ± 2.5	27.5 ± 2.1
Body weight gain	0.83 ± 2.30	0.62 ± 2.23
Food intake (g/day)	3.60 ± 0.36	3.30 ± 0.25
Water intake (mL/day)	4.81 ± 0.15	4.82 ± 0.20
Caloric intake (cal/day)	13.9 ± 1.4	11.9 ± 1.0
Triglyceride (mg/dL)	75 ± 5	79 ± 2
Total cholesterol (mg/dL)	110 ± 6	118 ± 4
HDL cholesterol (mg/dL)	63 ± 10	60 ± 3
Glucose (mg/dL)	86 ± 3	89 ± 4

Data are means ± S.E.M. (n = 15). No statistically significant differences were recorded for the tested marker.

3.2. Impact of an AGE-Enriched Diet on CML and RAGE Amounts in Salivary Glands and Intestine

The AGE-enriched diet evoked CML accumulation and increased RAGE expression in both submandibular salivary glands and the ileum tract of intestine detected by immunohistochemistry analysis. Specifically, in the submandibular salivary glands of AGE-D mice, we detected increased CML immunopositivity in the extracellular spaces among serous and mucous acini and in the cytoplasm of duct cells (Figure 2A), while RAGE was mainly expressed in the ducts of myoepithelial cells and basal lamina (Figure 2B), compared to the CD mice. Similarly, CML accumulation was higher in the villi epithelium of the ileum of AGE-D mice when compared to CD mice (Figure 3A) and RAGE expression was maximally expressed at the basal membrane and muscularis mucosae of AGE-D mice (Figure 3B).

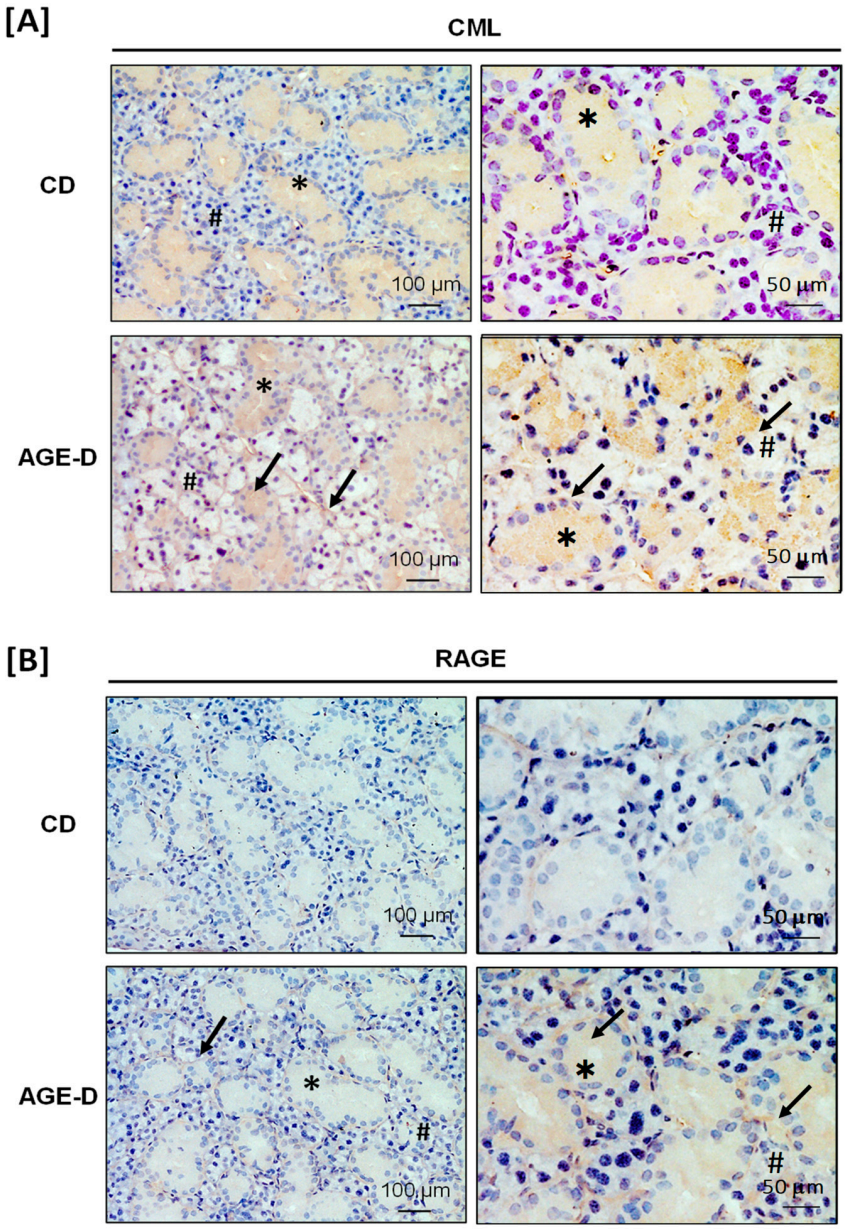

Figure 2. Immunohistochemistry performed on paraffin-embedded submandibular salivary glands. (**A**) Photomicrographs at 20× and 40× magnification for carboxymethyllysine (CML) immunopositivity, showing increased amounts in acini (#) and ducts (⁎), as indicated by arrows, of the AGE-D mice. (**B**) Photomicrographs at 20× and 40× magnification for receptor for AGEs (RAGE) immunopositivity, which was increased in the myoepithelial and basal lamina of ducts as indicated by arrows.

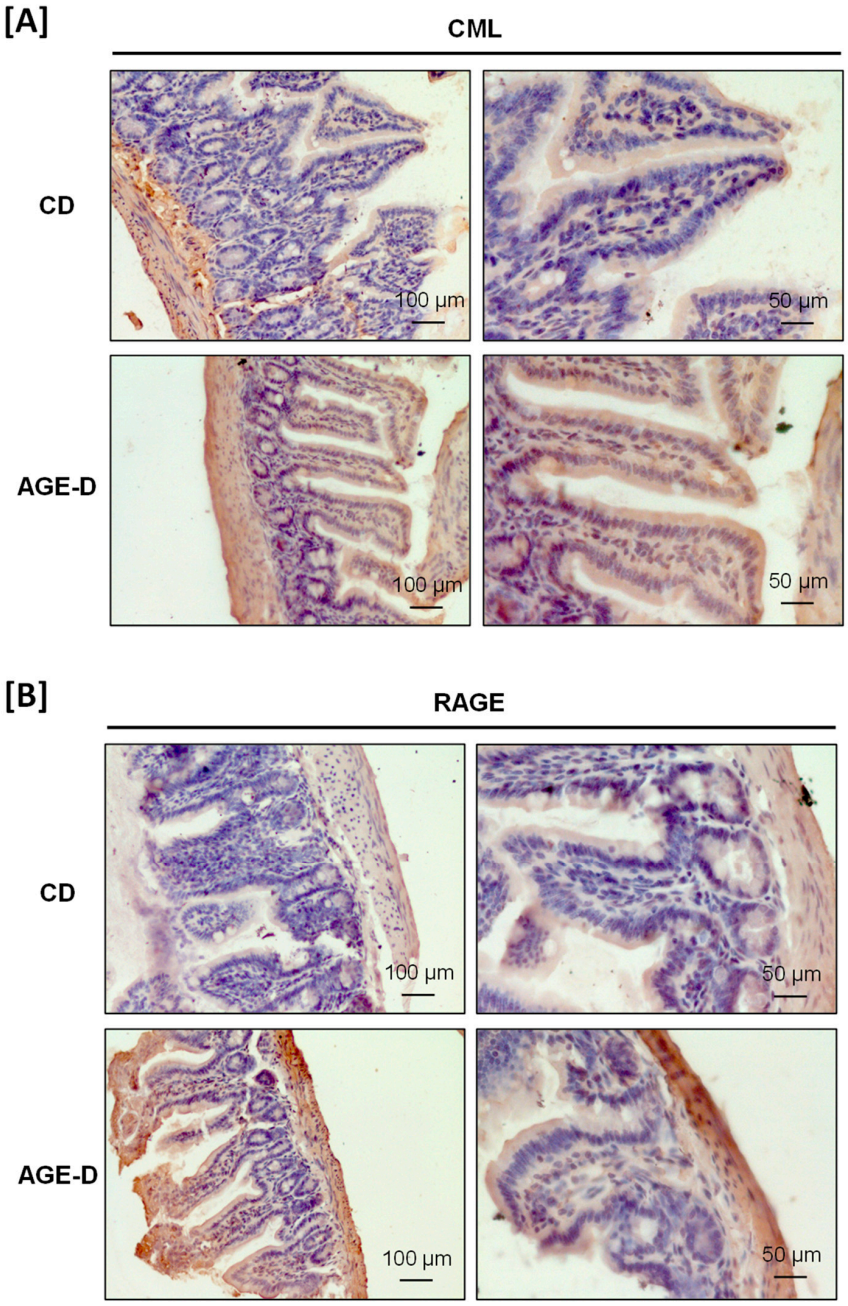

Figure 3. Immunohistochemistry performed on paraffin-embedded ileum portion of intestine. (**A**) Photomicrographs at 20× and 40× magnification for CML immunopositivity, showing increased amounts in villi epithelium of the AGE-D mice. (**B**) Photomicrographs at 20× and 40× magnification for RAGE immunopositivity, mostly increased in the basal membrane and muscularis mucosae.

3.3. Chronic AGEs Exposure Evokes Changes in Plasma Glycosylation

Glycosylation differences between feeding groups were investigated. Plasma samples were fractionated into two components, IgG and IgG-depleted fractions (DP), and fluorescently labelled. Glycosylation profiles of labelled fractions were compared by lectin microarray. Binding to a broad range of lectin was observed, suggesting the presence of multiple glycosylation structures (Figure 4). Similar structures were present in both fractions, albeit with diverse distribution, suggesting different glycosylation profiles between IgG and DP fractions (Figure 4A,B). The profile across CD and AGE-D in both fractions were closely comparable, with a similar glycosylation profile, despite a different distribution (Figure 4).

Comparative analysis for individual lectins showed significant differences between CD and AGE-D groups. Binding on AIA, WGA, and SNA-I with labelled IgG fractions was significantly increased in the AGE-D group (Figure 4A), suggesting an increase in galactose (AIA binding), presence of N-acetylglucosamine residues (WGA binding) and sialylation which would most likely be terminal α-(2,6) linked sialic acid (WGA and SNA-I binding). On the other hand, binding on AIA and PHA-E was significantly decreased in the AGE-D group in the DP fractions (Figure 4B), implying a decrease in galactose (AIA binding) and N-linked complex type structures with β-linked Gal or Gal-β-(1,4)GlcNAc termini, with or without bisecting GlcNAc (PHA-E binding).

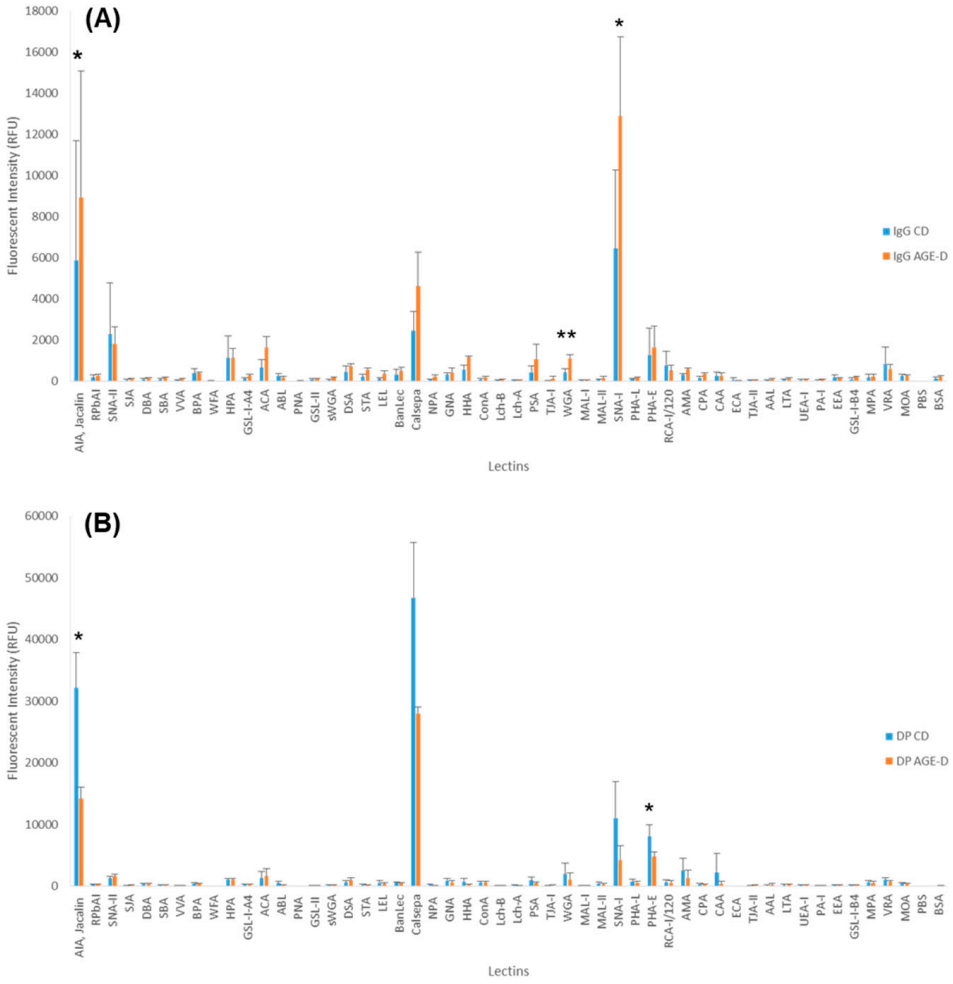

Figure 4. Glycosylation profiles of (**A**) immunoglobulin fractions, control diet (IgG CD) and control diet enriched in AGEs (IgG AGE-D) and (**B**) plasma glycoproteins depleted from IgG fractions, control diet (DP CD) and control diet enriched in AGEs (DP AGE-D). Bars represent the average binding intensity of fluorescently labelled samples from three technical replicate experiments and error bars represent +/− standard deviation. Statistical significance: ** $p < 0.01$, * $p < 0.05$ vs. CD, determined by two-tailed, paired Student's t-test.

3.4. AGE-Enriched Diet Evoked Systemic Inflammatory Response

As shown in Figure 5, the local AGEs over-accumulation was paralleled by increased plasma levels of the pro-inflammatory cytokines IL-1β, IL-17, and TNFα and reduced levels of anti-inflammatory factors IL-6 and IL-10, with no significant effects on INF-γ. Interestingly, chronic AGE-D exposure was associated with a robust increase in blood concentrations of PAI-1, a marker of diabetes vascular complications and prothrombotic state [21], as well as with a significant decrease in the levels of IAP, a sign of impaired intestinal homeostasis and inflammation [22].

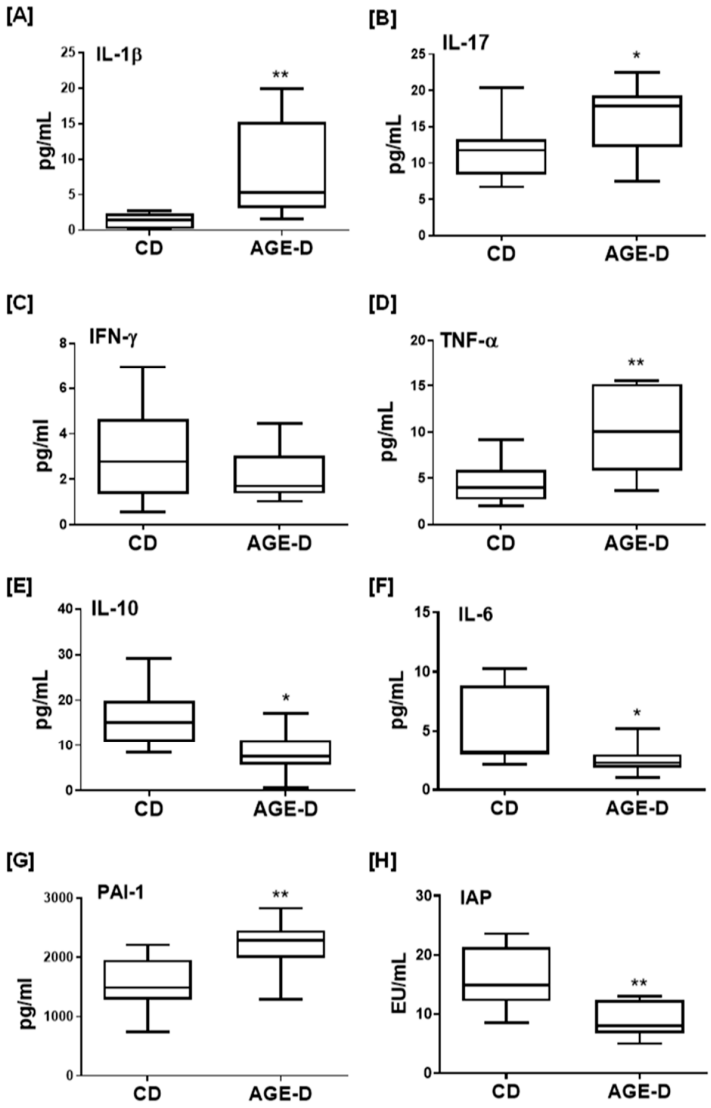

Figure 5. (**A**–**G**) Systemic inflammation markers evaluated in plasma of CD and AGE-D mice by multiplexed Bio-Plex 3D system, indicating increased pro-inflammatory (IL-1β, IL-17, IFN-γ, TNF-α, and PAI-1) and decreased IL-6 and IL-10. (**H**) Activity of intestinal alkaline phosphatase (IAP) evaluated in plasma by kinetic assay, indicating reduced ability of AGE-D mice to maintain microbiota homeostasis and loss of detoxifying potential in intestine. Data are means ± S.E.M. (n = 15 per group). Statistical significance: * $p < 0.05$, ** $p < 0.01$ vs. CD.

3.5. Chronic AGEs Exposure Altered Microbial Community Profile

The analysis of microbiota revealed differences in relative abundance of fecal microbial populations (Figure 6A), with a general decreasing trend of the Bacteroidetes/Firmicutes ratio in the AGE-D group at T22 (n = 10) compared to CD (n = 8) (0.73 vs. 1.16, $p = 0.07$). No differences were observed in gut microbial composition at T0 (baseline) among the two groups. AGE-D mice differed significantly from CD in fecal microbial β-diversity at T22 weeks using Weighted UniFrac analysis (Figure 6B), but not in α-diversity (data not shown). Specifically, at family level, AGE-D mice had significantly lower S24-7 bacteria (Muribaculaceae, within the Bacteroidetes phylum, $p < 0.05$) and doubled amount of Lachnospiraceae ($p < 0.01$), in comparison to CD mice; while at the genus level, AGE-D mice had lower *Lactobacillus* ($p < 0.001$), *Prevotella* ($p < 0.01$), *Anaerostipes* ($p < 0.01$), and *Candidatus Arthromitus* ($p < 0.01$) and higher *Parabacteroides* ($p < 0.001$), *Ruminococcus* (Lachnospiraceae family, $p < 0.001$) and *Lawsonia* ($p = 0.01$) (Figure 6A).

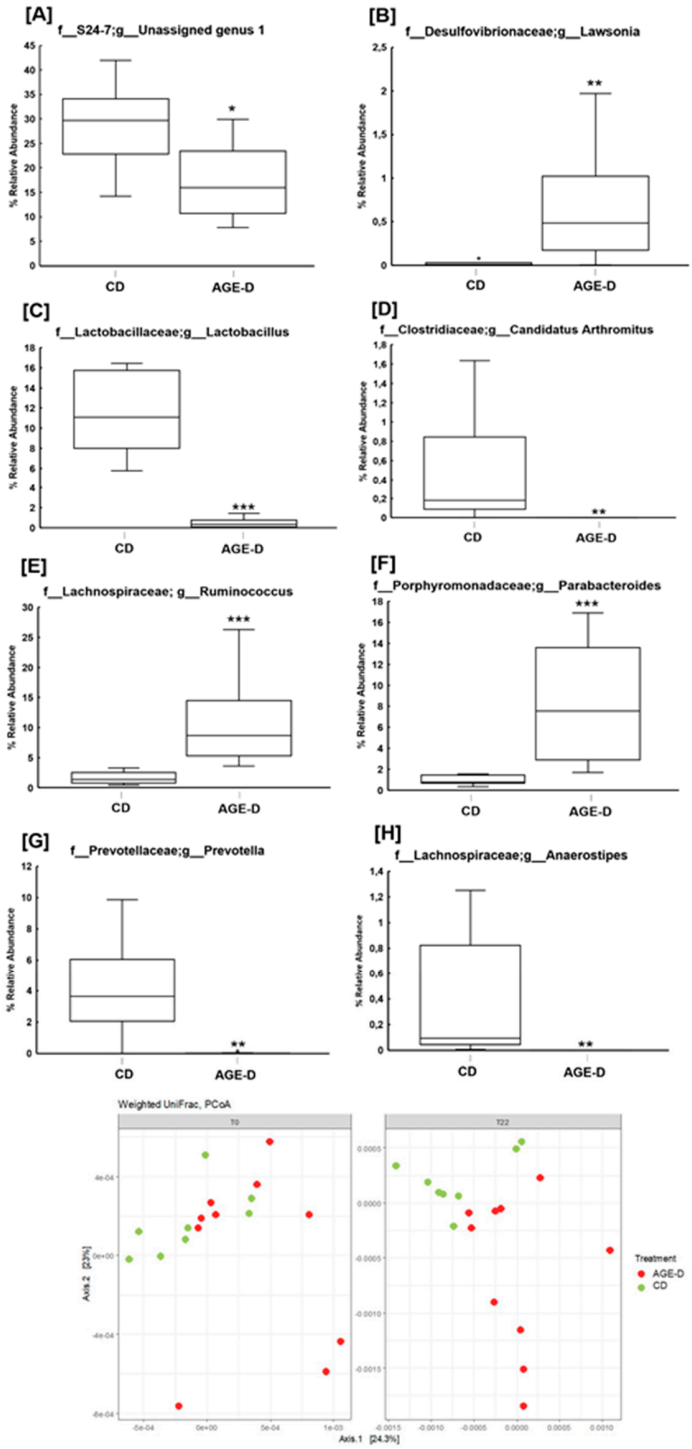

Figure 6. (**A**–**H**) Boxplots of percentage relative abundance of fecal microbial genera in CD (n = 8) and AGE-D (n = 10) mice at 22 weeks (T22) of dietary intervention after 16SrRNA sequencing using V3-V4 targeted primers. "Unidentified genus 1": a genus within the Family S 24-7 which could not be assigned at a percentage sequence homology of at least 95% to any existing genera within the reference database (http://greengenes.lbl.gov). (**I**) Beta-diversity of microbial populations in CD and AGE-D at T0 and T22, according with Weighted UniFrac analysis. Statistical significance: * $p < 0.05$, ** $p < 0.01$, *** $p < 0.001$.

The heatmap of Spearman's rank correlation coefficients in Figure 7 indicate significant correlation between relative abundance of bacterial families/genera and systemic measurements. Indeed, the overall results obtained in CD and AGE-D groups showed that Lachnospiraceae, *Parabacteroides*, *Lawsonia*

and *Ruminococcus* (Lachnospiraceae family) are all positively correlated to PAI-1, IL-1β, and IL-17 levels and negatively correlated to GIP and GLP-1. Furthermore, *Prevotella*, *Lactobacillus*, *Anaerostipes*, and *Candidatus Arthromitus* have a significant positive correlation with GIP and GLP-1, and a negative correlation with systemic inflammatory blood parameters.

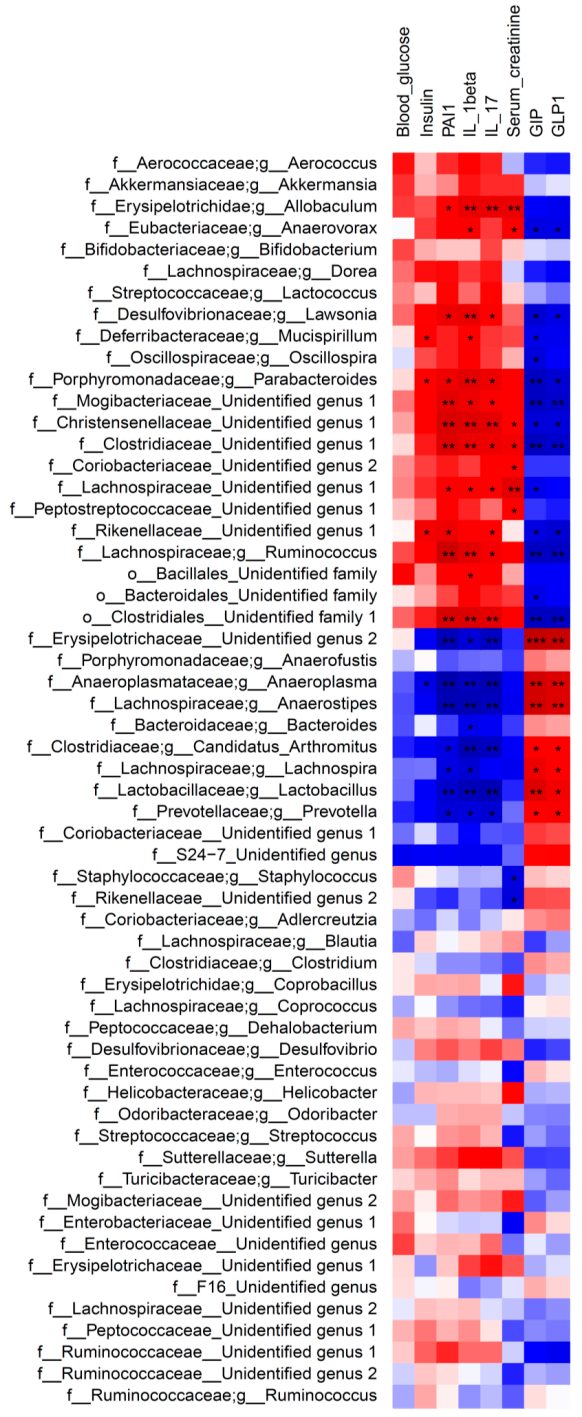

Figure 7. Heatmap of Spearman's correlation between the fecal bacteria genera and systemic measurements in CD and AGE-D groups. Dark red indicates positive correlation, while dark blue represents negative correlation. Statistical significance: * $p < 0.05$, ** $p < 0.01$. Genera and families were reported as "Unidentified" when they could not be assigned to any genera/family within a given family/order at a percentage sequence homology of 95% and 90%, respectively, to existing genera and families in the reference database (http://greengenes.lbl.gov).

3.6. Chronic AGEs Exposure Impaired Insulin Signal Transduction in the Skeletal Muscle

Changes in the activity of the insulin signal transduction pathway were evaluated by immunoblotting experiments on homogenates from gastrocnemius muscles (Figure 8). The AGE-D did not alter the protein expression of the insulin receptor substrate-1 (IRS-1), protein kinase B (Akt), or glycogen synthase kinase-3β (GSK-3β) in muscles, when compared to muscles from CD mice. In contrast, mice fed an AGE-enriched diet exhibited a significant increase in the degree of phosphorylation of IRS-1 on Ser307 (Figure 8A) in parallel with a reduction in the phosphorylation of downstream effectors of the insulin signaling pathway, Akt on Ser473 (Figure 8B) and a significant decrease in the phosphorylation of GSK-3β on Ser9 (Figure 8C). These alterations in protein phosphorylation, and hence activation status of the respective proteins are suggestive of an impairment in insulin signaling evoked by the AGE-enriched diet.

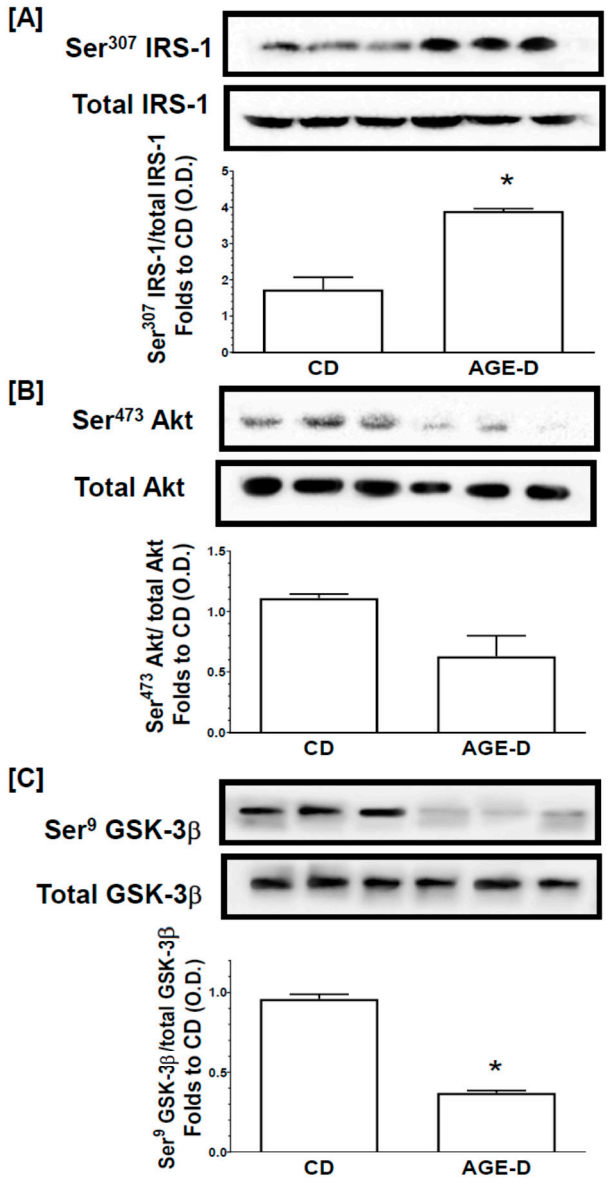

Figure 8. Assessment of insulin signal transduction in the gastrocnemius muscle through the Western blotting analysis of the phosphorylation rate of (**A**) IRS-1, (**B**) Akt, (**C**) GSK-3β. Histograms report the densitometric analysis represented as the ratio between phosphorylated-to-total protein amount and expressed as fold of CD value. Data are means ± S.E.M. (n = 15 per group). Statistical significance: * $p < 0.05$ vs. CD.

4. Discussion

In the present study we reported for the first time that the enrichment of a standard diet with MG-H1, a common dietary AGEs found in highly processed foods [23], is sufficient to evoke AGEs tissue accumulation. These effects were associated with a pro-inflammatory state and changes in early markers of dysmetabolism, more likely through alterations in microbiota homeostasis. We used a non-irradiated standard diet enriched in only MG-H1 to investigate the effective causal contribution of a well-characterized AGE in metabolic derangements, excluding the effect of other factors such as food processing products or alternative sources of AGEs. Interestingly, the significant changes recorded in the blood levels of key master hormonal regulators of metabolism were associated with local impairment of the insulin signaling pathway, which is a crucial regulator of glucose transportation, glycogen synthesis and glycolysis. However, these modifications were not associated with changes in body weight gain, fasting blood glucose, and lipid profile, suggestive of a condition of early metabolic derangement. Longer kinetics of dietary manipulation and/or more severe dietary insult would be requested to confirm the clinical relevance of AGEs exposure in vivo. Our findings are in accordance with previously in vitro studies demonstrating that cellular exposure to AGEs resulted in impaired secretion and activity of GIP and GLP-1, the two primary incretin hormones [24,25] and increased expression of dipeptidyl peptidase-4 (DPP-4), the main enzyme degrading incretins [26,27]. Therefore, it is conceivable that dietary AGEs impair the effects of incretins, further promoting the development of metabolic disorders. The AGE-D-induced reduction in incretin levels along with the well-known AGEs ability to induce activation of inflammatory transcription factors through interaction with RAGE [28], may account for the here recorded increase in blood concentrations of pro-inflammatory cytokines and PAI-1. In fact, GLP-1 plays a vital role in modulating cytokines function and their production by CD4+ T cells via GLP-1 receptors [29] and, in keeping with our findings, the GLP-1 analogue exenatide has been demonstrated to reduce the levels of IL-1β, IL-17 and TNF-α in human islet supernatants [30]. Interestingly, among the panel of cytokines we tested, IL-10 and IL-6 were the ones whose systemic concentrations were significantly reduced following AGE-D. IL-6 is a pro-inflammatory cytokine. However, at the local level, it may exert several anti-inflammatory actions, including downregulation of IFN-γ, IL-1β, and TNF-α [31]. Most notably, GLP-1 secretion is regulated by IL-6 [32]; thus, offering a further insight on the molecular mechanism linking dietary AGEs exposure to impairment in incretin levels. Ghrelin signaling is another key mediator linking nutrient-sensing signals with insulin resistance, and ablation of ghrelin has been reported to worsen diet-induced insulin resistance and adipose inflammation [33]. As previously documented [34,35], ghrelin may contribute to the physiological anti-AGEs system, counteracting the deleterious effects exerted by AGEs on vascular endothelium. The decrease in ghrelin concentration following AGE-D in this study was paralleled by a massive increase in the plasma levels of PAI-1, a key regulator of vascular remodeling, involved in various thrombotic diseases such as deep vein thrombosis, ischemic heart disease and diabetic vascular complications. AGEs may induce a RAGE-mediated functional synthesis of PAI-1 in human microvascular endothelial cells [36], and blood AGEs levels in either non-diabetic and diabetic populations are one of the most important independent determinants of PAI-1 [37,38]. We may therefore speculate that the changes in ghrelin and PAI-1 concentrations induced by AGE-D may contribute to early cellular senescence and impaired vascular integrity. However, the lack of investigation on the effects of the AGE-D at vascular level on thrombogenic and anti-fibrinolytic changes, does not allow us to confirm a significant impact of AGE-D on cardiovascular risk factors in our experimental model.

Our study also offers an interesting insight on the relative contribution of exogenous dietary AGEs to the impairment of metabolic homeostasis. Maillard reaction, commonly known as protein glycation, normally occurs in vivo as well as during the preparation of foods at high temperatures. Here, AGEs diet was enriched in MG-H1, which is one of the most important Maillard reaction product identified and quantified in food and biological matrices [23], and the most abundant in body fluids of diabetes patients [39,40]. The AGE-D differed from the control diet only for the presence of MG-H1 instead of a

part of the arginine residues in the casein; thus, indicating that all the systemic and tissue alterations here recorded have to be related to this dietary modification.

Several cross-sectional and intervention studies have shown positive correlations between AGEs intake and their circulating levels, as measured by food databases [2,6,41]. Isocaloric restrictions of dietary AGEs have been shown to decrease circulating AGEs levels and inflammatory biomarkers, and to improve endothelial dysfunction [42]. However, the mechanisms linking dietary AGEs exposure to their absorption and their effective bioavailability, are still largely unknown. Here we recorded an important local accumulation of AGEs and overexpression of RAGE not only in the ileum tract of intestine but also in submandibular salivary glands; thus, confirming the potential correlation between dietary AGEs and periodontal pathology, recently suggested by several studies [43]. Interestingly, the specific Maillard reaction product we detected was CML, which is a chemical entity different from MG-H1 and not included in the modified diet. These results imply that AGEs found in salivary glands originate, at least in part, from blood. This hypothesis has been recently confirmed in an intervention study on healthy subjects exposed to diets with different amount and quality of AGEs [13]. Nevertheless, the specific mechanisms of transports of AGEs from blood to saliva remains to be elucidated. Interestingly, CML fecal excretion does not exceed the 50% [44], suggesting that some of the ingested AGEs are neither absorbed nor defecated and could be metabolized intraluminally by the microbiota. Thus, it is likely that protein-bound dietary AGEs are processed at the consumption of an MG-H1-enriched diet, resulting in accumulation of a different class of AGEs, such as CML, in both proximal (ileum) and distal (salivary glands) organs/tissues. The intestinal AGEs processing is due to specific microorganisms and local AGEs accumulation may affect gut microbiota through negative selection for direct toxic effects, or positive selection favoring bacterial species that use AGEs as source of energy [45]. Here, for the first time, we demonstrated that a diet enrichment with a single AGEs is sufficient to induce significant changes in the microbiota composition. Notably, the MG-H1 enriched diet here used was neither heated nor irradiated; thus, offering an appropriate experimental approach to detect the impact of AGEs on gut microbiota. Indeed, many contradictory data have been reported on the effect of heated foods on microbiota due to the heterogeneity of compounds that are formed during thermal treatment [46–48]. Our results showed marked differences in gut microbiota population of AGE-D mice, characterized by a depletion of commensal bacteria such as S24-7, *Candidatus Arthromitus* and *Anaerostipes*. Among them, *Candidatus Arthromitus* plays a key role in mouse intestinal immune function control and its downregulation may be associated with intestinal inflammatory imbalance [49]. In addition, AGE-D mice showed a decrease of a butyrate-producing bacterial genus, *Anaerostipes*, that is inversely related to inflammation and insulin resistance, since butyrate is reported as one of the most important short-chain fatty acids (SCFAs) in the maintenance of colonic health [50]. Moreover, we also found an increase of *Parabacteroides*, *Ruminococcus* (Lachnospiraceae family) and *Lawsonia* in the AGE-D group. An abnormal increase in Lachnospiraceae has been recently proposed as one of the factors involved in metabolic diseases such as diabetes and obesity [50], but the mechanism through which these bacteria affect these conditions is still unclear. It has been proposed that members of Lachnospiraceae may be involved in intestinal lipopolysaccharide translocation in blood, thus becoming one of the causes of the inflammatory processes which characterize these metabolic diseases [51]. Our results support previous studies where *Lactobacillus* spp. ameliorate Type 2 diabetes by acting on GLP-1 mechanism [52]. *Prevotella* is a dietary fiber fermenter bacterium, known to increase after a high fiber intake [53] and to produce SCFAs [54], which affect satiety regulation and glucose metabolism by increasing GLP-1 and other gut hormones production [55]. This mechanism may provide a link between *Prevotella* reduction in AGE-D mice and incretin production. Diet induced shifts in gut microbial population by modulating SCFAs production: we can speculate that AGE-enriched diet may affect incretins production by a microbiota-driven mechanism, in which *Prevotella* and other fiber-fermenting and SCFAs-producing bacteria are decreased. The rise of *Lawsonia* abundance was previously observed in diabetic mice fed with high-fat chow and was seen to decrease after metformin treatment, which normally acts by increasing GLP-1 production and glucose utilization [56–58]. Since

AGEs seem to reduce GLP-1 levels as described above, we speculated that *Lawsonia* increase in AGE-D mice may be caused by incretins unbalance and systemic changes induced by MG-H1. Many of the microbial alterations observed in AGE-D group were significantly related to incretins and inflammatory markers levels and have been associated in previous studies with obesogenic and/or diabetogenic environments. Interestingly, compared to CD, the AGE-D was not characterized by a higher fat content, and mice fed with AGE-D did not show an increase in body weight gain and feeding behavior. This suggests that the simple enrichment of MG-H1 in the diet caused a reshaping of the microbiota that is normally observed in high-fat diets or in the presence of inflammatory conditions such as diabetes. Our results showed that systemic unbalance caused by AGEs enrichment in diet, mainly in the pro-inflammatory profile, incretins axis, and glucose control, induced significant changes in gut microbial populations. Furthermore, these shifts resemble what has previously been seen in obesity, diabetes, and metabolic disorders.

Moreover, our glycomic analysis using lectin microarray indicates for the first time that even one specific class of AGEs contained in food (i.e., MG-H1) can trigger modification of the post-translational glycosylation profile of peripheral blood proteins. Alteration in the glycosylation profile of plasma and blood cell surface proteins, including IgGs, can impact on their conformation and functionality; thus, interfering with key physiological processes. The observed alteration of blood protein glycosylation is most likely associated with changes in the plasma level of acute phase proteins, with circulating cytokines and hormones [59], diet, and lifestyles known to affect glycosylation level [60]. IgG glycosylation is known to be altered by environmental and in vivo status, and, in turn, to influence the immune response, acting therefore as a potential dynamic biomarker for disease or therapeutics [61]. Significant increase in galactosylation and IgG sialylation, most likely α-(2,6)-linked, were observed in mice fed with AGE-enriched diet compared to the control group. Level of sialylation is known to correlate to level of galactosylation [62]. Our feeding study showed an increase in circulatory pro-inflammatory cytokines; therefore, suggesting an activation of inflammation transcription factors. Decrease in sialylation and galactosylation is often associated with poor metabolic health [63,64] and with chronic inflammatory disease [65]. Whereas the opposite has been shown to be linked with anti-inflammatory response, with α-(2,6)-linked sialylation playing a key role in mediating the response [66,67]. However, in agreement with the cytokine profile here evoked by the AGE-D, it has been reported that the sialylated IgG fraction reduces phagocytosis by monocytes and induces a switch of the cytokine profile from IL-6/IL-8 to TNF-α/IL-1β [68]. We could thus hypothesize that in the acute body response to the AGE-D, the IgG glycosylation is altered in an attempt to counteract or attenuate the effect of the circulatory proinflammatory cytokines.

Our study has several limitations. First, the dietary content of MG-H1, which is far more than the amount that may normally be ingested. In addition, no significant changes in systemic lipid and glucose profile were recorded, despite the significant changes in the blood levels of key master hormonal regulators of metabolism; thus, suggesting that longer kinetics of dietary manipulation and/or more severe dietary insult are requested to obtain clinically relevant metabolic derangements. Our study shows that chronic MG-H1 exposure results in local (submandibular glands, ileum, and skeletal muscle) and systemic toxicity. However further organs and tissues involved in cardiometabolic derangements, including adipose tissue, liver, and vascular endothelium, should be analyzed to offer a better elucidation of the MG-H1 on-target toxicity.

5. Conclusions

In conclusion, the present work provides original findings linking the presence of a specific AGEs in the diet to alterations in the microbiota homeostasis and the related incretins axis that lead to a systemic pro-inflammatory profile responsible for compromised glucose control and endothelial dysfunction. Overall, these findings help to elucidate the pivotal role of AGEs as a striking link between modern diet and health, moving from correlation toward causation. Further experimental and clinical studies are needed to highlight the importance of specific AGEs in human metabolism and disease,

as well as data revealing how AGEs can elicit specific signaling functions, in the perspective to prevent the progression of diet-related metabolic derangements.

Supplementary Materials: The following are available online at http://www.mdpi.com/2072-6643/12/9/2497/s1, Table S1: lectin microarray composition list and lectin specificities

Author Contributions: Conceptualization, R.M., T.H., M.H., and M.C.; methodology, R.M., D.C., M.H., F.C., and L.J.; validation, M.H., K.T., M.A., and M.C.; formal analysis, R.M., M.L.B., and F.C.; investigation, R.M., D.C., G.G., A.S.C., G.F.A., I.B., R.V., and F.M.; resources, C.C., K.T., L.J., and M.C.; data curation, L.J., K.T., and M.C.; writing—original draft preparation, R.M. and M.C.; writing—review and editing, D.C., M.L.B., F.F., C.C., M.A., T.H., L.J., and K.T.; supervision, L.J., K.T., and M.C.; funding acquisition, T.H., C.C., L.J., and M.C. All authors have read and agreed to the published version of the manuscript.

Funding: This research was funded by the Italian Ministry of Agricultural, Alimentary and Forestry Policies (grant ID 777 HDHL INTIMIC-Knowledge Platform, grant ID 1170 HDHL INTIMIC METADIS and grant ID CABALA_diet&health, ERA HDHL), and by the Italian Ministry of Education, University and Research (grant ID SALIVAGES, ERA HDHL and grant ID CABALA_diet&health, ERA HDHL). The authors acknowledge the German Federal Ministry for Research and Education (BMBF) for support of the project (grant number 01EA1703). Authors are responsible for the contents of the present work.

Conflicts of Interest: The authors declare no conflict of interest.

References

1. Singh, R.; Barden, A.; Mori, T.; Beilin, L. Advanced glycation end-products: A review. *Diabetologia* **2001**, *44*, 129–146. [CrossRef] [PubMed]
2. Poulsen, M.W.; Hedegaard, R.V.; Andersen, J.M.; de Courten, B.; Bügel, S.; Nielsen, J.; Skibsted, L.H.; Dragsted, L.O. Advanced glycation endproducts in food and their effects on health. *Food Chem. Toxicol.* **2013**, *60*, 10–37. [CrossRef]
3. Cepas, V.; Collino, M.; Mayo, J.C.; Sainz, R.M. Redox Signaling and Advanced Glycation Endproducts (AGEs) in Diet.-Related Diseases. *Antioxidants* **2020**, *9*, 142. [CrossRef] [PubMed]
4. Vistoli, G.; De Maddis, D.; Cipak, A.; Zarkovic, N.; Carini, M.; Aldini, G. Advanced glycoxidation and lipoxidation end products (AGEs and ALEs): An overview of their mechanisms of formation. *Free Radic. Res.* **2013**, *47* (Suppl. 1), 3–27.
5. Luévano-Contreras, C.; Gómez-Ojeda, A.; Macías-Cervantes, M.H.; Garay-Sevilla, M.E. Dietary Advanced Glycation End Products and Cardiometabolic Risk. *Curr. Diab. Rep.* **2017**, *17*, 63. [CrossRef]
6. Scheijen, J.L.; Clevers, E.; Engelen, L.; Dagnelie, P.C.; Brouns, F.; Stehouwer, C.D.; Schalkwijk, C.G. Analysis of advanced glycation endproducts in selected food items by ultra-performance liquid chromatography tandem mass spectrometry: Presentation of a dietary AGE database. *Food Chem.* **2016**, *190*, 1145–1150. [CrossRef]
7. Henle, T. AGEs in foods: Do they play a role in uremia? *Kidney Int. Suppl.* **2003**, *63*, S145–S147. [CrossRef] [PubMed]
8. Hellwig, M.; Humpf, H.U.; Hengstler, J.; Mally, A.; Vieths, S.; Henle, T. Quality Criteria for Studies on Dietary Glycation Compounds and Human Health. *J. Agric. Food Chem.* **2019**, *67*, 11307–11311. [CrossRef]
9. Kellow, N.J.; Savige, G.S. Dietary advanced glycation end-product restriction for the attenuation of insulin resistance, oxidative stress and endothelial dysfunction: A systematic review. *Eur. J. Clin. Nutr.* **2013**, *67*, 239–248. [CrossRef]
10. Qu, W.; Nie, C.; Zhao, J.; Ou, X.; Zhang, Y.; Yang, S.; Bai, X.; Wang, Y.; Wang, J.; Li, J. Microbiome-Metabolomics Analysis of the Impacts of Long-Term Dietary Advanced-Glycation-End-Product Consumption on C57BL/6 Mouse Fecal Microbiota and Metabolites. *J. Agric. Food Chem.* **2018**, *66*, 8864–8875. [CrossRef]
11. Hellwig, M.; Bunzel, D.; Huch, M.; Franz, C.M.; Kulling, S.E.; Henle, T. Stability of Individual Maillard Reaction Products in the Presence of the Human Colonic Microbiota. *J. Agric. Food Chem.* **2015**, *63*, 6723–6730. [CrossRef] [PubMed]
12. Hellwig, M.; Auerbach, C.; Müller, N.; Samuel, P.; Kammann, S.; Beer, F.; Gunzer, F.; Henle, T. Metabolization of the Advanced Glycation End Product N-ε-Carboxymethyllysine (CML) by Different Probiotic *E. coli* Strains. *J. Agric. Food Chem.* **2019**, *67*, 1963–1972. [CrossRef] [PubMed]
13. Manig, F.; Hellwig, M.; Pietz, F.; Henle, T. Quantitation of free glycation compounds in saliva. *PLoS ONE* **2019**, *14*, e0220208. [CrossRef] [PubMed]

14. Basso, N.; Soricelli, E.; Castagneto-Gissey, L.; Casella, G.; Albanese, D.; Fava, F.; Donati, C.; Tuohy, K.; Angelini, G.; La Neve, F.; et al. Insulin Resistance, Microbiota, and Fat Distribution Changes by a New Model. of Vertical Sleeve Gastrectomy in Obese Rats. *Diabetes* **2016**, *65*, 2990–3001. [CrossRef]
15. Bolyen, E.; Rideout, J.R.; Dillon, M.R.; Bokulich, N.A.; Abnet, C.C.; Al-Ghalith, G.A.; Alexander, H.; Alm, E.J.; Arumugam, M.; Asnicar, F.; et al. Reproducible, interactive, scalable and extensible microbiome data science using QIIME 2. *Nat. Biotechnol.* **2019**, *37*, 852–857. [CrossRef]
16. McMurdie, P.J.; Holmes, S. phyloseq: An. R package for reproducible interactive analysis and graphics of microbiome census data. *PLoS ONE* **2013**, *8*, e61217. [CrossRef]
17. DeSantis, T.Z.; Hugenholtz, P.; Larsen, N.; Rojas, M.; Brodie, E.L.; Keller, K.; Huber, T.; Dalevi, D.; Hu, P.; Andersen, G.L. Greengenes, a Chimera-Checked 16S rRNA Gene Database and Workbench Compatible with ARB. *Appl. Environ. Microbiol.* **2006**, *72*, 5069–5072. [CrossRef]
18. Gerlach, J.Q.; Krüger, A.; Gallogly, S.; Hanley, S.A.; Hogan, M.C.; Ward, C.J.; Joshi, L.; Griffin, M.D. Surface glycosylation profiles of urine extracellular vesicles. *PLoS ONE* **2013**, *8*, e74801. [CrossRef]
19. Kilcoyne, M.; Sharma, S.; McDevitt, N.; O'Leary, C.; Joshi, L.; McMahon, S.S. Neuronal glycosylation differentials in normal, injured and chondroitinase-treated environments. *Biochem. Biophys. Res. Commun.* **2012**, *420*, 616–622. [CrossRef]
20. Mastrocola, R.; Nigro, D.; Chiazza, F.; Medana, C.; Dal Bello, F.; Boccuzzi, G.; Collino, M.; Aragno, M. Fructose-derived advanced glycation end-products drive lipogenesis and skeletal muscle reprogramming via SREBP-1c dysregulation in mice. *Free Radic. Biol. Med.* **2016**, *91*, 224–235. [CrossRef]
21. Domingueti, C.P.; Dusse, L.M.; das Graças Carvalho, M.; de Sousa, L.P.; Gomes, K.B.; Fernandes, A.P. Diabetes mellitus: The linkage between oxidative stress, inflammation, hypercoagulability and vascular complications. *J. Diabetes Complicat.* **2016**, *30*, 738–745. [CrossRef] [PubMed]
22. Estaki, M.; DeCoffe, D.; Gibson, D.L. Interplay between intestinal alkaline phosphatase, diet, gut microbes and immunity. *World J. Gastroenterol.* **2014**, *20*, 15650–15656. [CrossRef] [PubMed]
23. Ahmed, N.; Mirshekar-Syahkal, B.; Kennish, L.; Karachalias, N.; Babaei-Jadidi, R.; Thornalley, P.J. Assay of advanced glycation endproducts in selected beverages and food by liquid chromatography with tandem mass spectrometric detection. *Mol. Nutr. Food Res.* **2005**, *49*, 691–699. [CrossRef] [PubMed]
24. Puddu, A.; Sanguineti, R.; Montecucco, F.; Viviani, G.L. Effects of High. Glucose Levels and Glycated Serum on GIP Responsiveness in the Pancreatic Beta Cell Line HIT-T15. *J. Diabetes Res.* **2015**, *2015*, 326359. [CrossRef]
25. Wang, Z.; Wang, X.; Zhang, L.; Wang, B.; Xu, B.; Zhang, J. GLP-1 inhibits PKCβ2 phosphorylation to improve the osteogenic differentiation potential of hPDLSCs in the AGE microenvironment. *J. Diabetes Complicat.* **2020**, *34*, 107495. [CrossRef]
26. Schlatter, P.; Beglinger, C.; Drewe, J.; Gutmann, H. Glucagon-like peptide 1 receptor expression in primary porcine proximal tubular cells. *Regul. Pept.* **2007**, *141*, 120–128. [CrossRef]
27. Tahara, N.; Yamagishi, S.I.; Takeuchi, M.; Tahara, A.; Kaifu, K.; Ueda, S.; Okuda, S.; Imaizumi, T. Serum levels of advanced glycation end products (AGEs) are independently correlated with circulating levels of dipeptidyl peptidase-4 (DPP-4) in humans. *Clin. Biochem.* **2013**, *46*, 300–303. [CrossRef]
28. Xie, J.; Méndez, J.D.; Méndez-Valenzuela, V.; Aguilar-Hernández, M.M. Cellular signalling of the receptor for advanced glycation end products (RAGE). *Cell Signal* **2013**, *25*, 2185–2197. [CrossRef]
29. Sha, S.; Liu, X.; Zhao, R.; Qing, L.; He, Q.; Sun, L.; Chen, L. Effects of glucagon-like peptide-1 analog liraglutide on the systemic inflammation in high-fat-diet-induced mice. *Endocrine* **2019**, *66*, 494–502. [CrossRef]
30. Cechin, S.R.; Perez-Alvarez, I.; Fenjves, E.; Molano, R.D.; Pileggi, A.; Berggren, P.O.; Ricordi, C.; Pastori, R.L. Anti-inflammatory properties of exenatide in human pancreatic islets. *Cell Transplant* **2012**, *21*, 633–648. [CrossRef]
31. Opal, S.M.; DePalo, V.A. Anti-inflammatory cytokines. *Chest* **2000**, *117*, 1162–1172. [CrossRef] [PubMed]
32. Ellingsgaard, H.; Seelig, E.; Timper, K.; Coslovsky, M.; Soederlund, L.; Lyngbaek, M.P.; Albrechtsen, N.J.; Schmidt-Trucksäss, A.; Hanssen, H.; Frey, W.O.; et al. GLP-1 secretion is regulated by IL-6 signalling: A randomised, placebo-controlled study. *Diabetologia* **2020**, *63*, 362–373. [CrossRef]
33. Ma, X.; Lin, L.; Yue, J.; Wu, C.S.; Guo, C.A.; Wang, R.; Yu, K.J.; Devaraj, S.; Murano, P.; Chen, Z.; et al. Suppression of Ghrelin Exacerbates HFCS-Induced Adiposity and Insulin Resistance. *Int. J. Mol. Sci.* **2017**, *18*, 1302. [CrossRef] [PubMed]

34. Li, P.; Liu, Y.; Xiang, Y.; Lin, M.; Gao, J. Ghrelin protects human umbilical vein endothelial cells against advanced glycation end products-induced apoptosis via NO/cGMP signaling. *Int. J. Clin. Exp. Med.* **2015**, *8*, 15269–15275.
35. Xiang, Y.; Li, Q.; Li, M.; Wang, W.; Cui, C.; Zhang, J. Ghrelin inhibits AGEs-induced apoptosis in human endothelial cells involving ERK1/2 and PI3K/Akt pathways. *Cell Biochem. Funct.* **2011**, *29*, 149–155. [CrossRef] [PubMed]
36. Yamagishi, S.; Fujimori, H.; Yonekura, H.; Yamamoto, Y.; Yamamoto, H. Advanced glycation endproducts inhibit prostacyclin production and induce plasminogen activator inhibitor-1 in human microvascular endothelial cells. *Diabetologia* **1998**, *41*, 1435–1441. [CrossRef]
37. Yamagishi, S.; Adachi, H.; Takeuchi, M.; Enomoto, M.; Furuki, K.; Matsui, T.; Nakamura, K.; Imaizumi, T. Serum level of advanced glycation end-products (AGEs) is an independent determinant of plasminogen activator inhibitor-1 (PAI-1) in nondiabetic general population. *Horm. Metab. Res.* **2007**, *39*, 845–848. [CrossRef] [PubMed]
38. Matsui, T.; Takeuchi, M.; Yamagishi, S. Involvement of aldosterone-mineralocorticoid receptor system in advanced glycation end product (AGE)-elicited plasminogen activator inhibitor-1 (PAI-1) expression in diabetes. *Int. J. Cardiol.* **2010**, *145*, 566–567. [CrossRef]
39. Van Eupen, M.G.; Schram, M.T.; Colhoun, H.M.; Scheijen, J.L.; Stehouwer, C.D.; Schalkwijk, C.G. Plasma levels of advanced glycation endproducts are associated with type 1 diabetes and coronary artery calcification. *Cardiovasc. Diabetol.* **2013**, *12*, 149. [CrossRef]
40. Ahmed, N.; Babaei-Jadidi, R.; Howell, S.K.; Beisswenger, P.J.; Thornalley, P.J. Degradation products of proteins damaged by glycation, oxidation and nitration in clinical type 1 diabetes. *Diabetologia* **2005**, *48*, 1590–1603. [CrossRef]
41. Uribarri, J.; Woodruff, S.; Goodman, S.; Cai, W.; Chen, X.; Pyzik, R.; Yong, A.; Striker, G.E.; Vlassara, H. Advanced glycation end products in foods and a practical guide to their reduction in the diet. *J. Am. Diet. Assoc.* **2010**, *110*, 911–916. [CrossRef] [PubMed]
42. Uribarri, J.; Cai, W.; Ramdas, M.; Goodman, S.; Pyzik, R.; Chen, X.; Zhu, L.; Striker, G.E.; Vlassara, H. Restriction of advanced glycation end products improves insulin resistance in human type 2 diabetes: Potential role of AGER1 and SIRT1. *Diabetes Care* **2011**, *34*, 1610–1616. [CrossRef] [PubMed]
43. Ilea, A.; Băbţan, A.M.; Boşca, B.A.; Crişan, M.; Petrescu, N.B.; Collino, M.; Sainz, R.M.; Gerlach, J.Q.; Câmpian, R.S. Advanced glycation end products (AGEs) in oral pathology. *Arch. Oral. Biol.* **2018**, *93*, 22–30. [CrossRef] [PubMed]
44. Delgado-Andrade, C.; Tessier, F.J.; Niquet-Leridon, C.; Seiquer, I.; Navarro, M.P. Study of the urinary and faecal excretion of Nε-carboxymethyllysine in young human volunteers. *Amino Acids* **2012**, *43*, 595–602. [CrossRef]
45. Ames, J.M.; Wynne, A.; Hofmann, A.; Plos, S.; Gibson, G.R. The effect of a model melanoidin mixture on faecal bacterial populations in vitro. *Br. J. Nutr.* **1999**, *82*, 489–495. [CrossRef]
46. Zinöcker, M.K.; Lindseth, I.A. The Western Diet-Microbiome-Host Interaction and Its Role in Metabolic Disease. *Nutrients* **2018**, *10*, 365. [CrossRef]
47. Delgado-Andrade, C.; de la Cueva, S.P.; Peinado, M.J.; Rufián-Henares, J.Á.; Navarro, M.P.; Rubio, L.A. Modifications in bacterial groups and short chain fatty acid production in the gut of healthy adult rats after long-term consumption of dietary Maillard reaction products. *Food Res. Int.* **2017**, *100 Pt 1*, 134–142. [CrossRef]
48. Helou, C.; Anton, P.M.; Niquet-Leridon, C.; Spatz, M.; Tessier, F.J.; Gadonna-Widehem, P. Fecal excretion of Maillard reaction products and the gut microbiota composition of rats fed with bread crust or bread crumb. *Food Funct.* **2017**, *8*, 2722–2730. [CrossRef]
49. Bolotin, A.; De Wouters, T.; Schnupf, P.; Bouchier, C.; Loux, V.; Rhimi, M.; Jamet, A.; Dervyn, R.; Boudebbouze, S.; Blottière, H.M.; et al. Genome Sequence of "*Candidatus Arthromitus*" sp. Strain SFB-Mouse-NL, a Commensal Bacterium with a Key Role in Postnatal Maturation of Gut Immune Functions. *Genome Announc.* **2014**, *2*. [CrossRef]
50. Ma, Q.; Li, Y.; Wang, J.; Li, P.; Duan, Y.; Dai, H.; An, Y.; Cheng, L.; Wang, T.; Wang, C.; et al. Investigation of gut microbiome changes in type 1 diabetic mellitus rats based on high-throughput sequencing. *Biomed. Pharmacother.* **2020**, *124*, 109873. [CrossRef]

51. Kameyama, K.; Itoh, K. Intestinal colonization by a Lachnospiraceae bacterium contributes to the development of diabetes in obese mice. *Microbes Environ.* **2014**, *29*, 427–430. [CrossRef] [PubMed]
52. Wang, Z.; Saha, S.; Van Horn, S.; Thomas, E.; Traini, C.; Sathe, G.; Rajpal, D.K.; Brown, J.R. Gut microbiome differences between metformin- and liraglutide-treated T2DM subjects. *Endocrinol. Diabetes Metab.* **2018**, *1*, e00009. [CrossRef] [PubMed]
53. De Filippo, C.; Cavalieri, D.; Di Paola, M.; Ramazzotti, M.; Poullet, J.B.; Massart, S.; Collini, S.; Pieraccini, G.; Lionetti, P. Impact of diet in shaping gut microbiota revealed by a comparative study in children from Europe and rural Africa. *Proc. Natl. Acad. Sci. USA* **2010**, *107*, 14691–14696. [CrossRef] [PubMed]
54. Chen, T.; Long, W.; Zhang, C.; Liu, S.; Zhao, L.; Hamaker, B.R. Fiber-utilizing capacity varies in Prevotella- versus Bacteroides-dominated gut microbiota. *Sci. Rep.* **2017**, *7*, 2594. [CrossRef]
55. Cani, P.D.; Van Hul, M.; Lefort, C.; Depommier, C.; Rastelli, M.; Everard, A. Microbial regulation of organismal energy homeostasis. *Nat. Metab.* **2019**, *1*, 34–46. [CrossRef]
56. Zhang, C.; Zhang, M.; Pang, X.; Zhao, Y.; Wang, L.; Zhao, L. Structural resilience of the gut microbiota in adult mice under high-fat dietary perturbations. *ISME J.* **2012**, *6*, 1848–1857. [CrossRef]
57. Shin, N.R.; Lee, J.C.; Lee, H.Y.; Kim, M.S.; Whon, T.W.; Lee, M.S.; Bae, J.W. An increase in the *Akkermansia* spp. population induced by metformin treatment improves glucose homeostasis in diet-induced obese mice. *Gut* **2014**, *63*, 727–735. [CrossRef]
58. Whang, A.; Nagpal, R.; Yadav, H. Bi-directional drug-microbiome interactions of anti-diabetics. *EBioMedicine* **2019**, *39*, 591–602. [CrossRef]
59. Saldova, R.; Huffman, J.E.; Adamczyk, B.; Mužinić, A.; Kattla, J.J.; Pučić, M.; Novokmet, M.; Abrahams, J.L.; Hayward, C.; Rudan, I.; et al. Association of medication with the human plasma N-glycome. *J. Proteome Res.* **2012**, *11*, 1821–1831. [CrossRef]
60. Knežević, A.; Gornik, O.; Polašek, O.; Pučić, M.; Redžić, I.; Novokmet, M.; Rudd, P.M.; Wright, A.F.; Campbell, H.; Rudan, I. Effects of aging, body mass index, plasma lipid profiles, and smoking on human plasma N-glycans. *Glycobiology* **2010**, *20*, 959–969. [CrossRef]
61. Russell, A.; Adua, E.; Ugrina, I.; Laws, S.; Wang, W. Unravelling Immunoglobulin G Fc N-Glycosylation: A Dynamic Marker Potentiating Predictive, Preventive and Personalised Medicine. *Int. J. Mol. Sci.* **2018**, *19*, 390. [CrossRef] [PubMed]
62. Plomp, R.; Ruhaak, L.R.; Uh, H.W.; Reiding, K.R.; Selman, M.; Houwing-Duistermaat, J.J.; Slagboom, P.E.; Beekman, M.; Wuhrer, M. Subclass-specific IgG glycosylation is associated with markers of inflammation and metabolic health. *Sci. Rep.* **2017**, *7*, 12325. [CrossRef] [PubMed]
63. Gudelj, I.; Lauc, G.; Pezer, M. Immunoglobulin G glycosylation in aging and diseases. *Cell Immunol.* **2018**, *333*, 65–79. [CrossRef] [PubMed]
64. Reily, C.; Stewart, T.J.; Renfrow, M.B.; Novak, J. Glycosylation in health and disease. *Nat. Rev. Nephrol.* **2019**, *15*, 346–366. [CrossRef] [PubMed]
65. Arnold, J.N.; Saldova, R.; Hamid, U.M.; Rudd, P.M. Evaluation of the serum N-linked glycome for the diagnosis of cancer and chronic inflammation. *Proteomics* **2008**, *8*, 3284–3293. [CrossRef] [PubMed]
66. Kaneko, Y.; Nimmerjahn, F.; Ravetch, J.V. Anti-inflammatory activity of immunoglobulin G resulting from Fc sialylation. *Science* **2006**, *313*, 670–673. [CrossRef]
67. Jennewein, M.F.; Alter, G. The Immunoregulatory Roles of Antibody Glycosylation. *Trends Immunol.* **2017**, *38*, 358–372. [CrossRef]
68. Biermann, M.H.; Griffante, G.; Podolska, M.J.; Boeltz, S.; Stürmer, J.; Munoz, L.E.; Bilyy, R.; Herrmann, M. Sweet but dangerous-the role of immunoglobulin G glycosylation in autoimmunity and inflammation. *Lupus* **2016**, *25*, 934–942. [CrossRef]